Design and Mechanistic Understanding of New Boronic Acid Catalyst Systems

by

Jason Peter Gregory Rygus

A thesis submitted in partial fulfillment of the requirements for the degree of

Doctor of Philosophy

Department of Chemistry
University of Alberta

Abstract

Catalysis is essential to the modern chemical industry. Catalytic strategies can enable new synthetic methods with improved atom economy and reduced chemical waste under mild conditions, representing an indispensable approach to the development of green chemical processes with improved sustainability. New advances in catalysis can facilitate the discovery of new bond-forming reactions using ubiquitous starting materials for which direct activation has otherwise proven challenging. In this context, boronic acid catalysis has emerged as a promising strategy for the direct activation of hydroxy-containing functional groups under mild conditions, allowing for conversion of these common motifs into functionalized products without the need for wasteful pre-activation steps. In this thesis, advances towards the development and understanding of new catalytic systems in boronic acid catalysis are presented.

The modification of catalyst activity *in situ* using suitable additives has rarely been explored as a reactivity-enabling strategy in boronic acid catalysis. In Chapter 2, the use of perfluoropinacol as a co-catalyst in the boronic acid-catalyzed Friedel-Crafts benzylation of electron-deficient benzylic alcohols for the synthesis of triarylmethanes is described. Mechanistic studies reveal that condensation of perfluoropinacol with the boronic acid catalyst leads to generation of a hydronium boronate species, which is likely responsible for C–O activation through indirect Brønsted acid catalysis.

Although boron-containing heterocycles have found wide ranging application in drug discovery and materials science, their application in catalysis has been hindered by a poor understanding of their inherent acidity, stability, and reactivity. Chapter 3 of this thesis details a systematic study on a series of model pseudoaromatic benzoxazaborine and benzodiazaborine heterocycles. While all

compounds are unambiguously demonstrated to act as Lewis acids, their acidity and boranol (B–OH) exchangeability with exogenous alcohols is highly dependent on the nature of the endocyclic heteroatom. Dynamic crossover experiments reveal that *N*-sulfonyl substituted benzodiazaborines are unstable towards ring-opening in methanol, while computational studies suggested that the boron-containing rings retain little aromaticity of their all-carbon analogs.

Chapter 4 presents the rational application of the benzoxazaborine scaffold in two mechanistically divergent modes of boronic acid catalysis. The parent heterocycle is found to be an effective catalyst for the nucleophilic activation of vicinal diols towards monophosphorylation, while a cationic hemiboronic acid is found to be highly active for the electrophilic activation of alcohols and ketones towards reductive deoxygenation in the presence of a silane. Mechanistic investigations of both transformations reveal the contrasting nature of crucial tetravalent boron species in the two catalytic manifolds and demonstrated that mechanistically guided structure-activity relationships can be employed in the design of new hemiboronic acid catalysts.

Preface

Chapter 2 of this thesis has been published as Ang, H. T.,[#] Rygus, J. P. G.,[#] Hall, D. G. "Two-Component Boronic Acid Catalysis for Increased Reactivity in Challenging Friedel-Crafts Alkylations with Deactivated Benzylic Alcohols", *Org. Biomol. Chem.* **2019**, *17*, 6007–6014 ([#]authors contributed equally). I was responsible for all experimental studies with diarylmethanol substrates, including reaction optimization, substrate scope exploration, kinetic studies and mechanistic studies on the effect of 2,6-di-*tert*-butylpyridine and of anhydrous conditions. I was also responsible for the additive study on the benzylation of primary alcohols. The project was a collaboration with Dr. Hwee Ting Ang, who performed initial co-catalyst identification, substrate scope exploration for primary alcohols and 1-arylethanols, and mechanistic studies involving catalyst speciation under the reaction conditions. Her contributions are identified in the chapter. I assisted with the writing of the manuscript which was done primarily by Dr. Hwee Ting Ang and Prof. D. G. Hall, who was the supervisory author and involved with concept development. I wrote the supporting information along with Dr. Hwee Ting Ang.

Chapter 3 of this thesis has been published as Kazmi, M. Z. H.,[#] Rygus, J. P. G.,[#] Ang, H. T., Paladino, M., Johnson, M. A., Ferguson, M. J., Hall, D. G. "Lewis or Brønsted? A Rectification of the Acidic and Aromatic Nature of Boranol-Containing Naphthoid Heterocycles", *J. Am. Chem. Soc.* **2021**, *143*, 10143–10156 ([#]authors contributed equally). I was responsible for the synthesis and characterization of all boron heterocycles, alcohol exchange experiments, and crossover experiments performed in methanol. The contributions of M. Z. H. Kazmi, H. T. Ang, M. Paladino and M. Johnson are specified throughout the chapter. M. J. Ferguson was responsible for X-ray crystallographic analyses. I assisted in the writing of the manuscript, which was done primarily by

Prof. D. G. Hall, who was the supervisory author and involved with concept development as well as computational studies. I wrote the supporting information with contributions from co-authors.

Chapter 4 of this thesis has been submitted for publication as Rygus, J. P. G., Hall, D. G. "Direct Nucleophilic and Electrophilic Activation of Alcohols Using a Common Organocatalyst Scaffold" and is currently under review. I was responsible for all experimental contributions. I wrote the manuscript and supporting information with assistance from Prof D. G. Hall, who was the supervisory author and involved with concept formation.

Acknowledgements

I am deeply grateful to my supervisor, Prof. Dennis Hall. His passion for teaching permeates all aspects of the group, and I am extremely thankful to have worked for a supervisor that cares as much about the chemist as he does the chemistry. He has always put the education and well-being of his students above everything else, and we are all better for having worked with him. His endless patience, his limitless knowledge, and his unwavering support have made the completion of this degree possible. I am eternally thankful for all his efforts to aid in my development as a scientist in every way, and I feel extremely fortunate to have learned from him over the last five years.

I would like to extend my sincere appreciation to my supervisory committee and examining committee members: Professor Rik Tykwinski, Professor Steven Bergens, Professor John Vederas, Professor Sheref Mansy, Professor RB Jordan and Professor Alex Speed. Their insightful questions, suggestions and advice during annual report meetings and the candidacy examination were always appreciated.

I owe a sincere thanks to all the administrative and research service staff in the department. Thank you to Mark Miskolzie, Ryan McKay and Nupur Dabral for their assistance with NMR, to Jing Zheng and Angelina Morales-Izquierdo for their assistance with mass spec, to Ryan Lewis and Mike Barteski for making the storeroom so welcoming, to Jennifer Jones and Jack Worden for analytical services, and to Anita Weiler for always answering my questions about the graduate program.

I cannot begin to express my gratitude to all the past and present members of the Hall Group that I have crossed path with during my time here. They have created a tremendous environment to work in every day and I feel lucky to have worked with and learned from all of them. I am

particularly grateful to those I have collaborated with: Dr. Hwee Ting Ang, Zain Kazmi, Dr. Marco Paladino and Daniel Boateng. A special thanks to those I have spent the most time with: Carl Estrada, Dr. Helen Clement, Dr. Hwee Ting Ang, Rory McDonald, Dr. Mohamad Estaitie, Ashley Ponich, Jake Blackner, Dawson Konowalchuk and Martin Lessard. Thank you all for your helpful discussion and continued support. A special thanks to Dr. Hayley Wan for her friendship and her mentorship as a teaching assistant.

I am grateful to Steve, Bruce, Adrian, Dave, Nicko, Janick, Vince and Peter for being continuous sources of inspiration. I would like to thank my closest friends outside of the work for their friendship during my graduate studies, including Maria, Dan, Sarah, Hwee Ting and Ashley. Thank you for letting me learn to be myself, for the comfort of shared quietness, and for helping me climb mountains. Thank you to my high school chemistry teacher, Sandra Warren, without whom none of this would be possible. Finally, thank you to my mother–my star, my perfect silence.

Table of Contents

List of Figures

List of Tables

List of Schemes

List of Abbreviations

Å	Angstrom
Ac	Acetyl
ACS	American Chemical Society
AIBN	Azobisisobutyronitrile
app	Apparent
aq	Aqueous
Ar	Aryl
ATP	Adenosine triphosphate
BAC	Boronic acid catalysis
BINAP	(1,1'-Binaphthalene-2,2'-diyl)bis(diphenylphosphine)
Bn	Benzyl
Bz	Benzoyl
calcd	Calculated
cat.	Catalytic
cm^{-1}	Wavenumbers
d	Doublet
dd	Doublet of doublets
dr	Diastereomeric ratio
DBU	1,8-Diazabicyclo[5.4.0]undec-7-ene
DCM	Dichloromethane
DFT	Density functional theory
DIPEA	*N,N*-Diisopropylethylamine
DMF	*N,N*-Dimethylformamide
DMSO	Dimethylsulfoxide
DNB	1,4-Dinitrobenzene

ee	Enantiomeric excess
EI	Electron impact
equiv	Equivalents
Et	Ethyl
EtOAc	Ethyl acetate
FC	Friedel-Crafts
FG	Functional group
GTP	Guanosine triphosphate
h	Hour
Hex	Hexanes
HFIP	1,1,1,3,3,3-hexafluoroisopropanol
HOMO	Highest occupied molecular orbital
HRMS	High-resolution mass spectrometry
Hz	Hertz
*i*Pr	*iso*-Propyl
IR	Infrared
IUPAC	International Union of Pure and Applied Chemistry
K_a	Acid dissociation constant
L	Litre
LCMS	Liquid chromatography–mass spectrometry
LG	Leaving group
LUMO	Lowest unoccupied molecular orbital
M	Molarity
m	Multiplet
Me	Methyl
MHz	Megahertz
min	Minute

mg	Milligram
mol	Mole
MTBE	Methyl *tert*-butyl ether
NICS	Nucleus-independent chemical shifts
NMR	Nuclear magnetic resonance
n-Bu	*n*-Butyl
NHC	N-Heterocyclic carbene
Nu	Nucleophile
ORTEP	Oak Ridge thermal ellipsoid plot
Pin	Pinacol
Ph	Phenyl
PMA	Phosphomolybdic acid
q	Quartet
rt	Room temperature
s	Singlet
sep	Septet
sex	Sextet
S_N	Nucleophilic substitution
TADDOL	α,α,α',α'-Tetraaryl-2,2-disubstituted 1,3-dioxolane-4,5-dimethanol
TBPP	Tetrabenzylpyrophosphate
TBS	*tert*-Butyldimethyl
t-Bu	*tert*-Butyl
Temp	Temperature
TES	Triethylsilyl
Tf	Triflyl
TFA	Trifluoroacetic acid
TFE	2,2,2-Trifluoroethanol

THF	Tetrahydrofuran
TLC	Thin layer chromatography
TMB	1,3,5-Trimethoxybenzene
TMDSO	1,1,3,3-Tetramethyldisiloxane
TFE	2,2,2-Trifluoroethanol
Ts	Tosyl
μ	Micro
UV	Ultraviolet

Chapter 1 Introduction: Boronic Acid Catalysis for Direct Hydroxy-Group Functionalization

1.1 Introduction to Catalysis and Hydroxy Groups

The development of new strategies in catalysis is fundamental to the implementation of sustainable processes in the chemical industry. With approximately 85% of all industrial chemical processes estimated to involve at least one catalytic step, catalysis plays an essential role in the production of raw materials and fine chemicals alike.[1] Catalysis refers to the acceleration of a chemical transformation through the involvement of a species, known as a catalyst, that is regenerated with each equivalent of product that is formed.[2] The addition of a catalyst may reduce the activation barrier that must be overcome to promote a chemical reaction or offer alternative mechanisms by which the desired transformation can be achieved. Catalytic strategies can thus enable the development of new transformations that would otherwise be prohibitively slow or can afford increasingly selective synthetic protocols under mild conditions. New advances in catalysis can facilitate the design of unprecedented bond-forming processes or expand the scope of existing reactions beyond their current limitations.[2]

The use of a substoichiometric amount of catalyst allows for the promotion of chemical transformations with minimal waste, placing catalysis at the heart of the green chemistry revolution.[3] In an effort to spearhead the integration of green chemistry principles in drug discovery and medicinal chemistry, the ACS Green Chemistry Institute has identified several key research areas in which there is an urgent need to develop methods with improved sustainability.[4] Among these, improved strategies for the direct activation of hydroxy groups with improved atom economy represents a significant challenge that could have far-reaching impact.

The hydroxy group refers to an –OH unit in which the oxygen is bonded to an additional atom. The hydroxy moiety can be found in a diverse assortment of functional groups, including water, alcohols, phenols, carboxylic acids, and oximes. Additionally, it has been estimated that approximately 65% of biologically relevant natural products and 40% of synthetic pharmaceutical compounds contain at least one hydroxy group.[5,6] Accordingly, reactions involving the transformation of hydroxy groups are fundamental to synthetic chemistry, and the development of new strategies for the manipulation and functionalization of this ubiquitous functional group have the potential to be widely utilized in synthesis.

Methods for the functionalization of hydroxy-containing functional groups, particularly with respect to substitution reactions, often require stoichiometric pre-functionalization to convert the hydroxy group into an activated intermediate (Figure 1-1).[5] This can lead to the generation of excessive chemical waste, additional purification steps, or the use of hazardous activating reagents. This limitation is exemplified in several widely used reactions for the derivatization of alcohols, including the Appel reaction,[7] Mitsunobu reaction,[8] and Grieco elimination.[9] It has been estimated that nearly 2% of all reactions used in the manufacturing of active pharmaceutical ingredients are directly related to the conversion of alcohols into activated intermediates.[10]

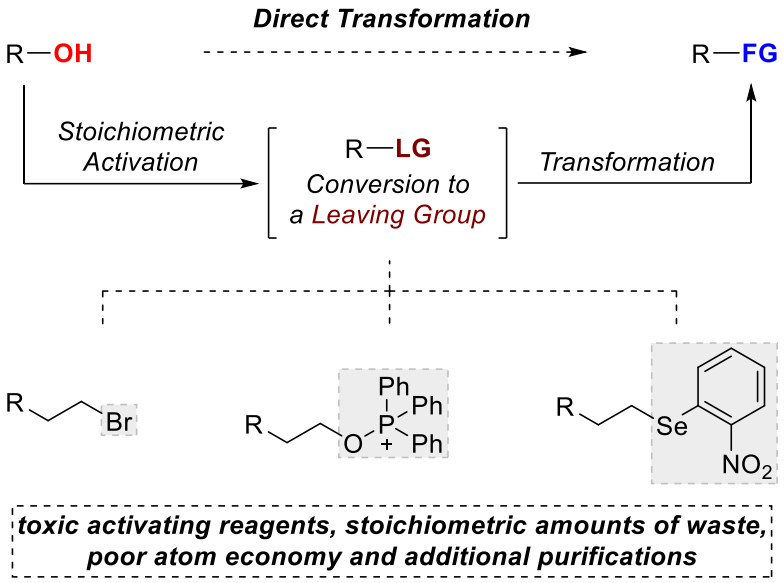

Figure 1-1 Stoichiometric activation of hydroxy-containing compounds.

Despite these drawbacks, reactions involving stoichiometric pre-activation of hydroxy-containing compounds are still widely used in synthesis owing to their high yields and broad generality of scope. Accordingly, in order to reduce the reliance of synthetic chemists on these wasteful procedures, it is necessary to develop new strategies for the direct catalytic activation of hydroxy groups. In this context, boronic acid catalysis (BAC) has emerged as a promising strategy for the direct activation and functionalization of hydroxy-containing compounds.[11] The fundamentals of boronic acid derivatives and their use as reaction catalysts will be described in Sections 1.2 and 1.3.

1.2 Introduction to Boronic Acids

1.2.1 Background of Boronic Acids

Boronic acids have emerged as essential compounds in a variety of chemical applications. These ubiquitous reagents have no natural source, and therefore must be accessed through chemical synthesis.[12] The first synthetic preparation of a boronic acid was described by Frankland and

Duppa in 1860, who reported the synthesis of ethylboronic acid (**1-02)** from the reaction of diethylzinc and triethylborate after oxidation of the intermediate triethylborane (**1-01**) under ambient conditions (Scheme 1-1a).[13] Two decades later, the first synthesis of an arylboronic acid was reported by Michaelis and Becker (Scheme 1-1b).[14] The reaction of gaseous BCl_3 with diphenylmercury at high temperatures was found to generate aryldichloroborane **1-03**, which was readily hydrolyzed to phenylboronic acid (**1-04**) in aqueous solution. The same group reported a similar discovery twenty years later using BBr_3 as an alternative boron source.[15]

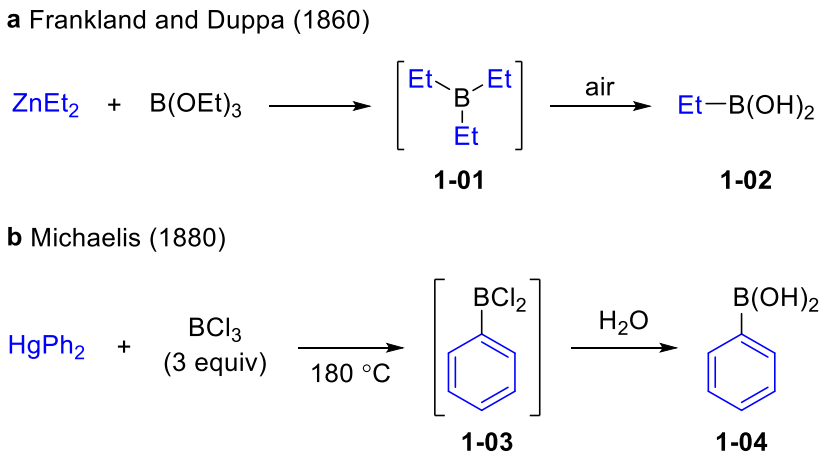

Scheme 1-1 First reported syntheses of alkyl and arylboronic acids.

Nearly a century after these initial discoveries, the widespread adoption of boronic acids as versatile reagents in organic synthesis has been encouraged by developments in transition metal-catalyzed cross-coupling reactions. Decades of study have established the ability of organoboron derivatives to undergo transmetalation with suitable metal complexes under basic conditions, forming new organometallic species that are intermediates in innumerable catalytic processes.[16] This advancement has been most notable in the development of the Suzuki-Miyaura reaction, which refers to the palladium-catalyzed cross-coupling of an organoboron reagent with a halide or pseudohalide under basic conditions.[17] This reaction has become an essential tool in the formation

of carbon-carbon bonds in both academic and industrial settings.[18] Boronic acids and their derivatives have also been employed in other metal-catalyzed reactions, such as the Chan-Evans-Lam reaction,[19–21] Liebeskind-Srogl coupling[22] or Rh-catalyzed conjugate addition[23] (Scheme 1-2), and in metal-free transformations including the Petasis reaction,[24] Matteson homologation,[25] carbonyl allylboration[26] and Zweifel olefination.[27]

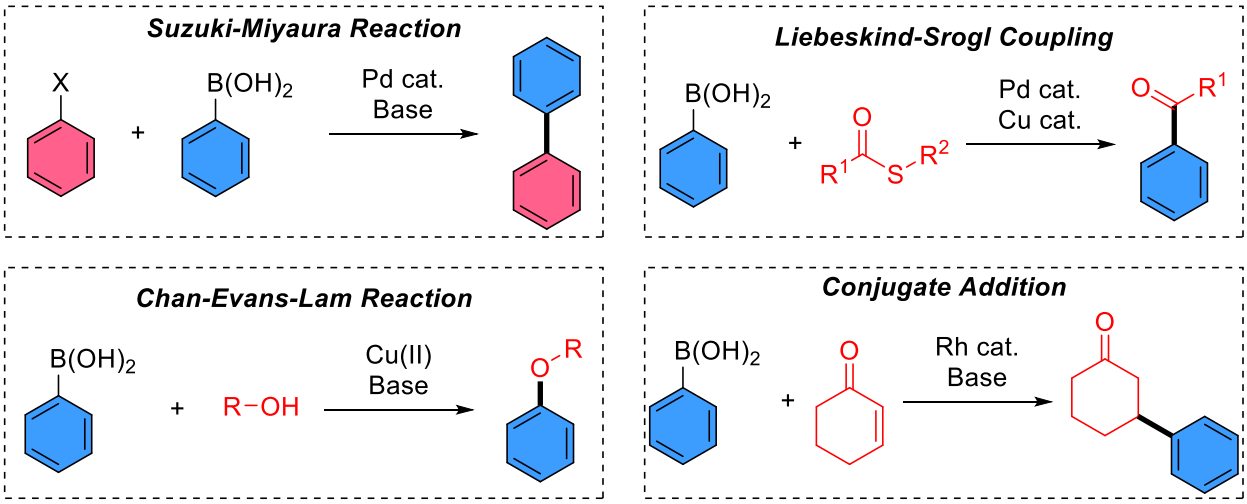

Scheme 1-2 Applications of boronic acids in transition metal-catalyzed cross-coupling reactions.

Advances in borylation methods to access boronic acid derivatives,[28–30] particularly in the expanding chemistry of diboryl reagents,[31,32] as well as the increasing commercial availability of organoboron compounds have enabled new applications of boronic acids outside of the realm of organic synthesis. Several boronic acid derivatives have been developed as therapeutic agents, pioneered by the disclosure of bortezomib (a proteasome inhibitor) in 2003.[33,34] The incorporation of a boronic acid can serve as a valuable prodrug strategy to enable release of a phenol-containing drug upon reaction with a radical oxygen species,[35] while boronic ester formation is a widely used technique in bioconjugation.[36] The incorporation of boronic acids into hydrogels can introduce self-healing properties,[37] while the dynamic nature of B–O bonds has been utilized in the

development of cross-linked polymers.[38] Boronic acids have been used as chemical sensors for carbohydrates[39] or fluoride anions[40] and have found other applications in nanomaterials,[41] functionalized chromatography stationary phases,[42] and the construction of covalent organic frameworks.[43] These diverse applications are related to the unique structural and electronic properties of boronic acids and their derivatives.

1.2.2 Structure and Properties of Boronic Acids

Boronic acids are trivalent organoboron compounds with one carbon-based substituent and two hydroxy groups (Figure 1-2a).[12] The central boron atom contains only six valence electrons and is thus sp^2-hybridized with a vacant p-orbital that is orthogonal to the plane of the three substituents (Figure 1-2b). In the solid state, boronic acids generally exist as hydrogen bonded dimers (Figure 1-2c).[44] For arylboronic acids, the degree of coplanarity between the aromatic ring and sp^2-hybridized boron atom is highly dependent on arene substitution, although they are generally substantially coplanar in the absence of a destabilizing steric or electronic interaction.[45]

Owing to their vacant p-orbital and electron-deficient nature, boronic acids have been widely demonstrated to act as mild organic Lewis acids.[12] Coordination to a Lewis basic moiety generates a tetravalent, sp^3-hybridized boron atom. The acidity of boronic acids in water can be attributed to an indirect proton transfer between two equivalents of water, in which the Lewis acidic boron atom forms a tetravalent trihydroxyboronate conjugate base (Figure 1-2d).[46] The pK_a values of arylboronic acids in water are generally on the order of 5–9, although significant changes in acidity can be conferred with suitable substituents on the aromatic ring.[12]

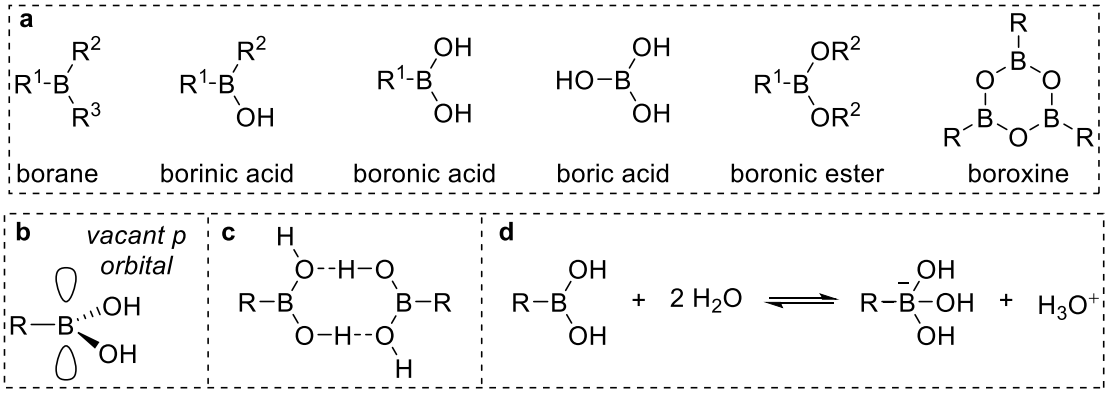

Figure 1-2 Fundamentals of boronic acids. **a** Types of organoboron compounds. **b** Structure. **c** Solid state hydrogen-bonding. **d** Acidity.

The boranol (B–OH) units of boronic acids have been well-established to undergo reversible covalent exchange with hydroxy-containing compounds. The resulting trivalent alkoxy, aryloxy or carboxy-containing boron compounds are referred to as boronic esters (Figure 1-3a). This dynamic exchange process is facilitated by the Lewis acidity of boron and is believed to occur through an associative mechanism involving rapid proton transfer between hydroxy substituents (Figure 1-3b). Boronic acids are also known to form trimeric cyclic anhydrides, known as boroxines, upon dehydration.[12]

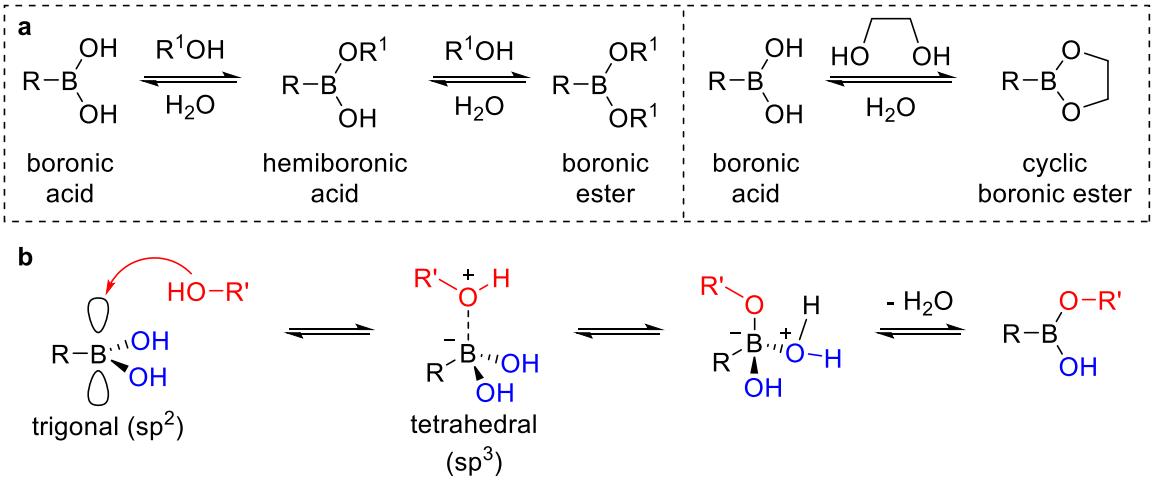

Figure 1-3 a Formation of boronic esters. **b** Associative mechanism of esterification.

1.3 Boronic Acid Catalysis

1.3.1 Early Reports and Fundamentals

Boronic acids have emerged as promising catalysts for the direct functionalization of hydroxy-containing compounds, a field known as boronic acid catalysis (BAC).[11] The first example of a boronic acid-catalyzed transformation was reported by Letsinger and co-workers in 1963, who described the use of 8-quinolineboronic acid (**1-05**) to promote the hydrolysis of 2-chloroethanol (Scheme 1-3a).[47] Hydroxy-group exchange between substrate and catalyst was believed to generate boronic ester **1-06**, facilitating the substitution reaction by temporary pseudo-intramolecularity with a coordinated water nucleophile. Additionally, the endocyclic nitrogen atom was believed to facilitate nucleophilic attack through hydrogen bonding or a cooperative base effect.[47] The bifunctional nature of catalyst **1-05** highlights the ability to tune the activity of a boronic acid catalyst with remote substitutions to facilitate secondary interactions. The concept of temporary intramolecularity in boronic acid catalysis was further explored by Philipp and co-workers, who reported the ability of boronic acid **1-04** to catalyze the hydrolysis of salicylaldehyde imine under mild conditions (Scheme 1-3b).[48] In addition to the templating effect provided by B–O exchange, the formal negative charge on boron was proposed to enhance oxygen nucleophilicity to facilitate hydrolysis through tetravalent intermediate **1-07**.

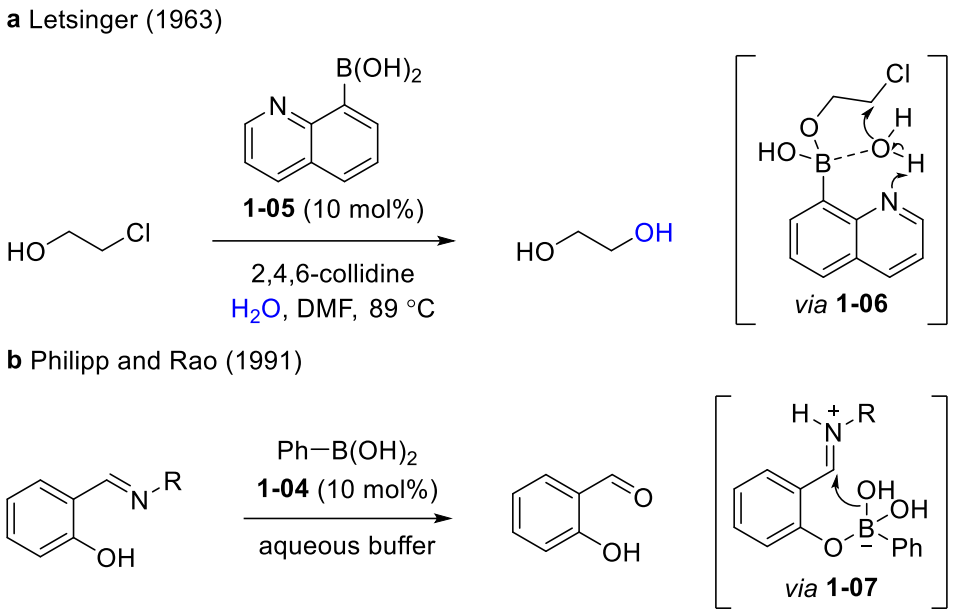

Scheme 1-3 Early boronic acid-catalyzed hydrolysis reactions promoted through templating effects.

Boronic acid catalysis is founded upon the ability of these compounds to undergo reversible covalent exchange with alcohols, carboxylic acids, or other hydroxy-containing compounds. This interaction is facilitated by the Lewis acidity of boron, which can be readily tuned through modification of the arene core. Additionally, a suitably placed *ortho*-substituent may facilitate exchange or substrate activation through hydrogen bonding interactions or coordination (Scheme 1-4).[12] Hydroxy-group exchange with a boronic acid can provide activation towards subsequent functionalization by way of several different mechanisms depending on the nature of the substrate, the catalyst, and the reaction conditions. Several detailed reviews have been published on this topic in the past decade.[11,49] Accordingly, only representative examples to illustrate the fundamental mechanisms of activation in boronic acid catalysis will be described here.

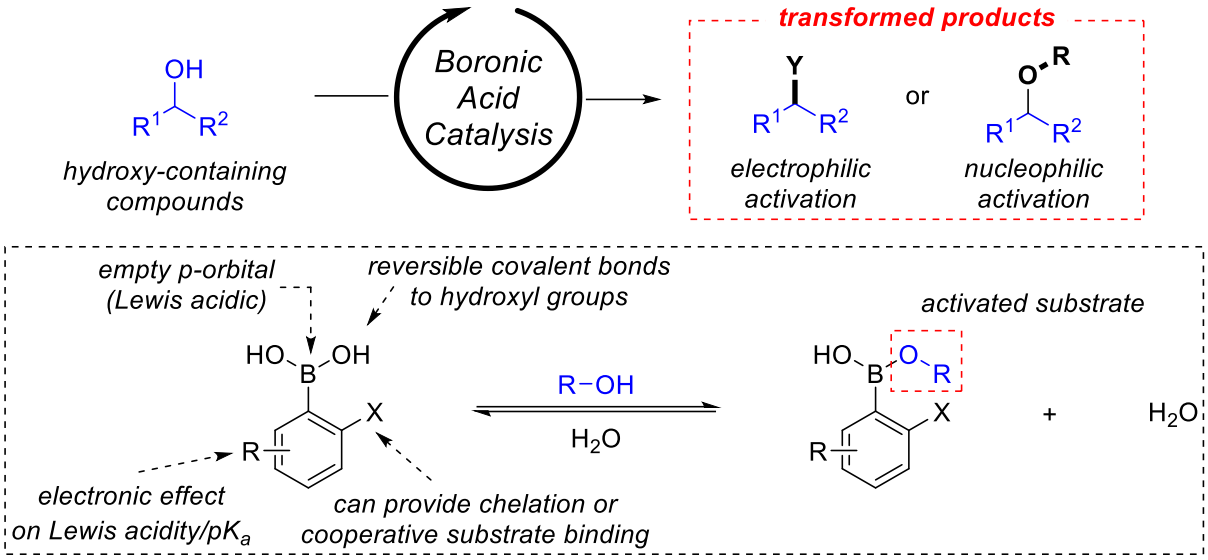

Scheme 1-4 Fundamentals of boronic acid catalysis.

1.3.2 Electrophilic Activation of Carboxylic Acids

The development of new methods to form amide bonds with improved atom economy was highlighted by the ACS Green Chemical Institute as an essential research area due to the ubiquity of amide units in medicinal chemistry.[4] A 2006 analysis of drug candidates prepared by GlaxoSmithKline, AstraZeneca and Pfizer revealed that approximately 65% of compounds surveyed contained an amide bond formation in their synthesis. Within these compounds, approximately 36% of amidation reactions were conducted using stoichiometric coupling reagents, such as carbodiimides, which generate significant quantities of chemical waste.[50,51] Accordingly, significantly improved atom economy in synthesis could be achieved with the development of catalytic strategies for carboxylic acid activation. Along these lines, the use of boronic acid catalysts to promote electrophilic activation of free carboxylic acids has received significant interest in the past several decades, with direct amidation reactions being a particular focus.

The application of boronic acid catalysis towards the direct amidation of carboxylic acids with amines was first reported by Yamamoto and co-workers in 1996, who disclosed the use of electron-deficient boronic acid catalysts for this process (Scheme 1-5a).[52] Under azeotropic removal of water, boronic acid **1-08** was demonstrated to be an active catalyst for this transformation in non-polar solvents. This process was initially hypothesized to occur through formation of monoacyl boronic ester **1-09**, where the combination of an internal hydrogen bond and B–O bond polarization can serve to activate the carbonyl moiety towards nucleophilic attack.[52]

The mechanism of these reactions was examined further by Whiting and co-workers, who proposed that activation occurs through dimeric intermediate **1-11** rather than monoacylboronate **1-09** as previously proposed (Scheme 1-5b).[53] The dimeric B–O–B linkage of intermediate **1-11** was proposed to facilitate delivery of the amine nucleophile to form bridged B–N–B species **1-12**. Boronic acid catalysts with *ortho*-substituents were found to be most effective under Whiting's conditions, which was rationalized by their preference for the formation of dimeric anhydrides rather than trimeric cyclic boroxines.[53] Stoichiometric reaction between carboxylic acids and boronic acid **1-10** in the absence of amine failed to provide evidence for monoacyl boron species **1-09**.

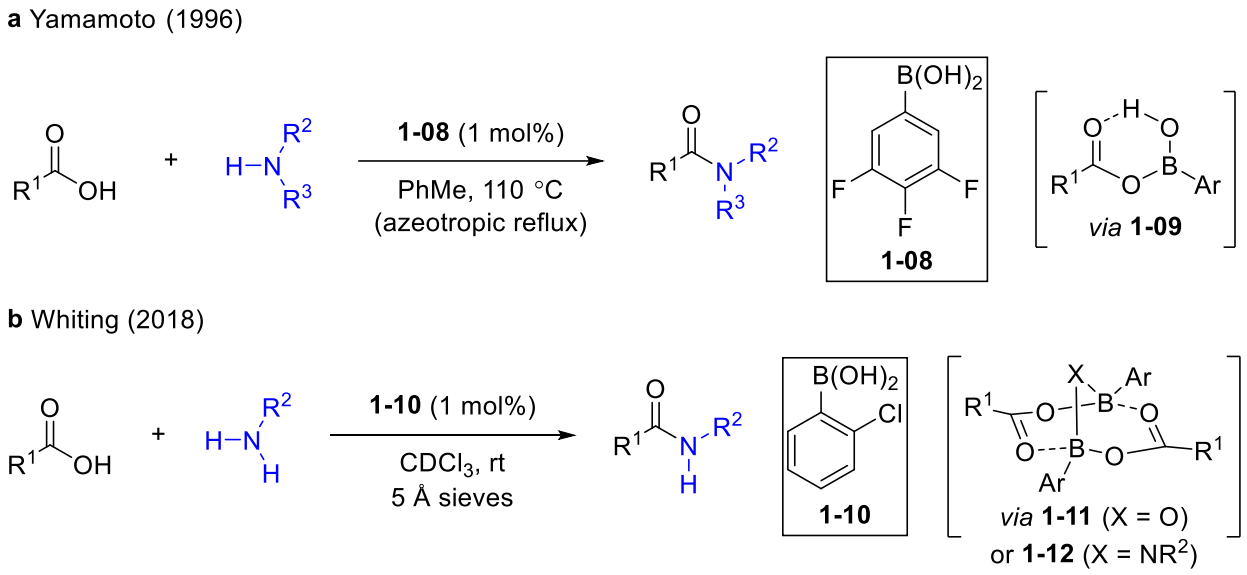

Scheme 1-5 Boronic acid-catalyzed direct amidation of carboxylic acids.

Electrophilic activation of carboxylic acids has been extended beyond amidation reactions to include other nucleophiles such as azides,[54] borohydride,[55] ureas[56] and alcohols,[57] leading to diverse products directly from carboxylic acids. The intramolecular dehydration of *ortho*-dicarboxylic acids has also been reported by Ishihara and co-workers using bifunctional boronic acid catalyst **1-15** (Scheme 1-6).[58] The bifunctional catalyst was believed to promote anhydride formation through a twofold activation mechanism via intermediate **1-16**, in which one carboxylic acid is activated as a nucleophile upon deprotonation by the amine while the other is activated as an electrophile through formation of a monoacyl boronic ester and internal hydrogen bonding.[58]

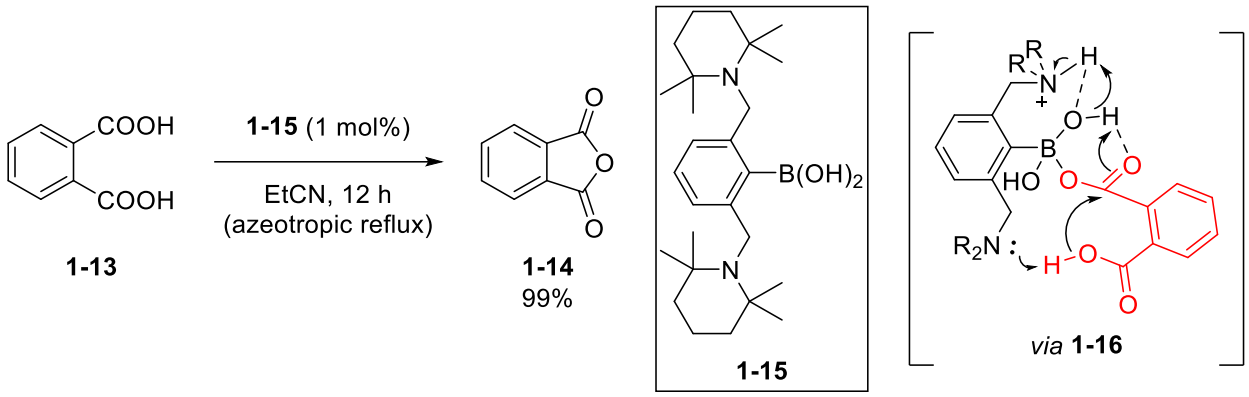

Scheme 1-6 Boronic acid-catalyzed intramolecular anhydride formation.

Activation of carboxylic acids was further extended in the application of boronic acid catalysis to α,β-unsaturated carboxylic acids. Boronic acid **1-20** was demonstrated by Hall and co-workers to be an efficient catalyst for the direct [4+2] cycloaddition of acrylic acid, which was believed to occur through the LUMO-lowering activation of monoacyl boronic ester **1-21** (Scheme 1-7a).[59] The use of free carboxylic acids directly removes the need to add additional protection and deprotection steps that may be required when using traditional Lewis acid catalysts. Subsequent reports extended this mechanism of activation to other cycloaddition reactions, including Huisgen, nitrile oxide and nitrone [3+2] cycloadditions.[60]

Electrophilic activation of unsaturated carboxylic acids was further demonstrated in the enantioselective intramolecular oxa-Michael reaction of acrylic acid **1-22** reported by Takemoto and co-workers (Scheme 1-7b).[61] A two-component catalyst system was used, where boronic acid **1-25** was believed to provide electrophilic activation while chiral base **1-24** was responsible for stereoinduction through hydrogen bonding interactions to activated acyl boron intermediate **1-26**. The same group later reported an arylboronic acid catalyst with a pendant chiral aminothiourea moiety for enantioselective intermolecular conjugate additions, combining the features of catalysts **1-24** and **1-25** into a single reagent.[62]

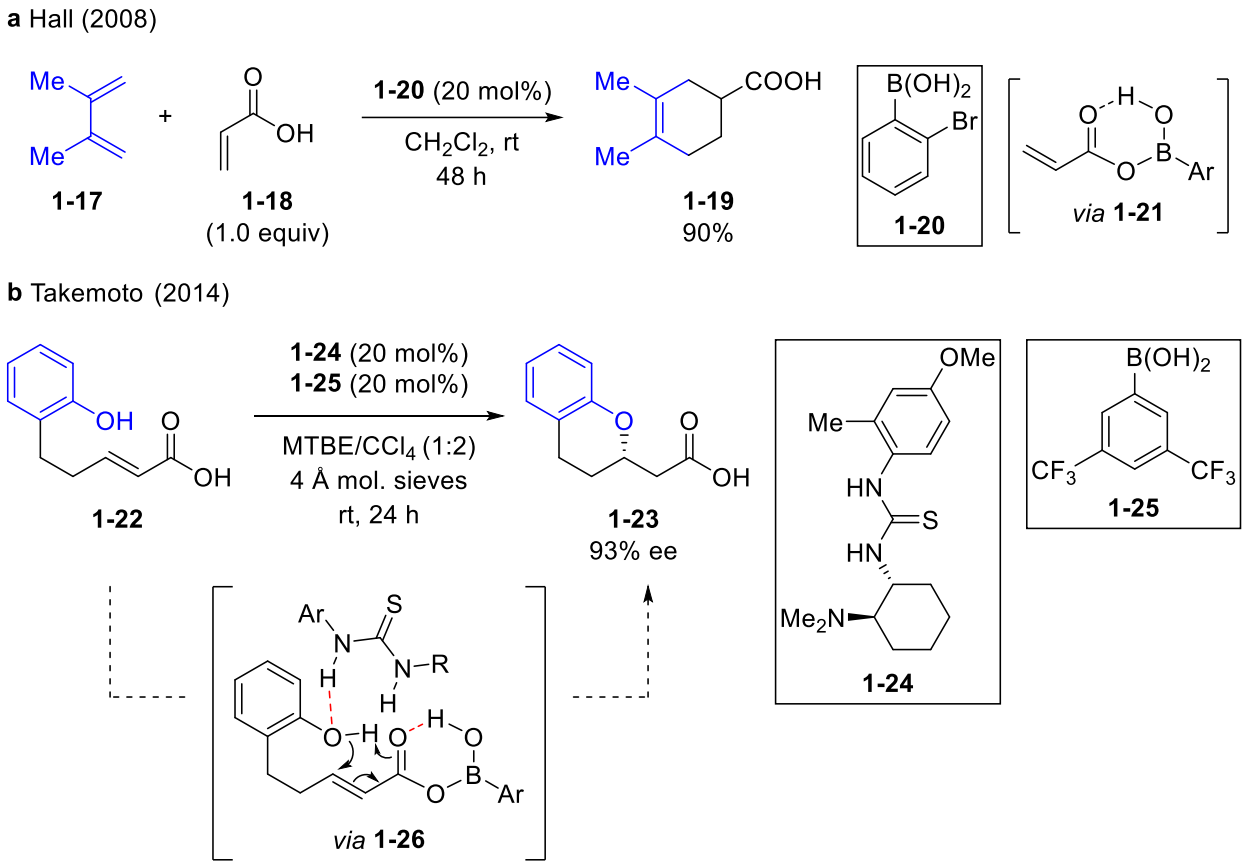

Scheme 1-7 Boronic acid-catalyzed activation of α,β-unsaturated carboxylic acids.

1.3.3 Electrophilic Activation of Alcohols

Arguably the most widely used application of boronic acid catalysis is in the direct electrophilic activation of alcohols.[11] As discussed previously, boronic acids can undergo reversible covalent exchange with alcohol substrates, providing a boronic ester intermediate. Polarization of the B–O bond facilitates partial or complete ionization of the C–O bond, providing transient activation of the alcohol towards nucleophilic substitution or rearrangements (Scheme 1-8). The extent of bond polarization is related to the Lewis acidity of the boronic acid catalyst, and consequently highly Lewis acidic boronic acids are often employed.[11]

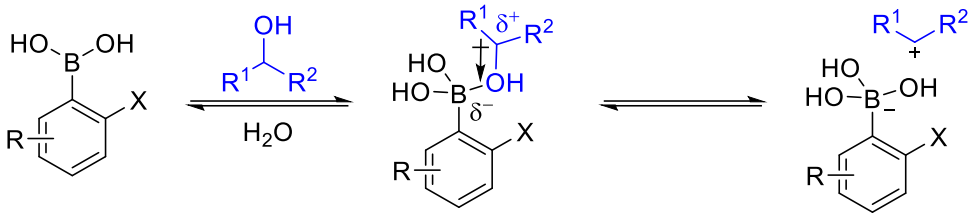

Scheme 1-8 Electrophilic activation of alcohols using boronic acids.

Electrophilic alcohol activation in boronic acid catalysis was first described by McCubbin and co-workers in 2010, who demonstrated that fluorinated boronic acid **1-30** was sufficiently Lewis acidic to promote Friedel-Crafts allylation of electron-rich arenes with highly activated allylic alcohols (Scheme 1-9a).[63] This transformation was believed to occur via an S_N1 mechanism involving intermediate **1-31**, followed by nucleophilic addition to the least hindered terminus of the allylic carbocation. The use of boronic acid catalysis for the related 1,3-transposition of allylic or propargylic alcohols was subsequently reported by the Hall Group (Scheme 1-9b).[64] Meyer-Schuster rearrangement of ^{18}O-labelled propargylic alcohol **1-32** using stoichiometric boronic acid **1-34** was found to proceed with 33% retention of the isotopic label, consistent with an S_N1 mechanism through stabilized allylic carbocation/hydroxyboronate anion ion pair **1-35**. In contrast, 1,3-transposition of allylic alcohol **1-36** showed only 10% retention of the ^{18}O-label, suggesting that two competitive pathways are operating in parallel through both S_N1 and S_N2' mechanisms.[64] For enantiomerically enriched allylic alcohols, migration of electron-deficient substrates proceeded with significantly improved stereospecificity, suggesting that the degree of ionization is highly substrate dependent.[64] The dramatic change in mechanism of these rearrangements for different substrates serves as a cautionary tale in the mechanistic analysis of boronic acid-catalyzed reactions. Mechanistic conclusions from probe compounds cannot be

applied to all substrates, particularly for reactions that are believed to proceed through S_N1 mechanisms.

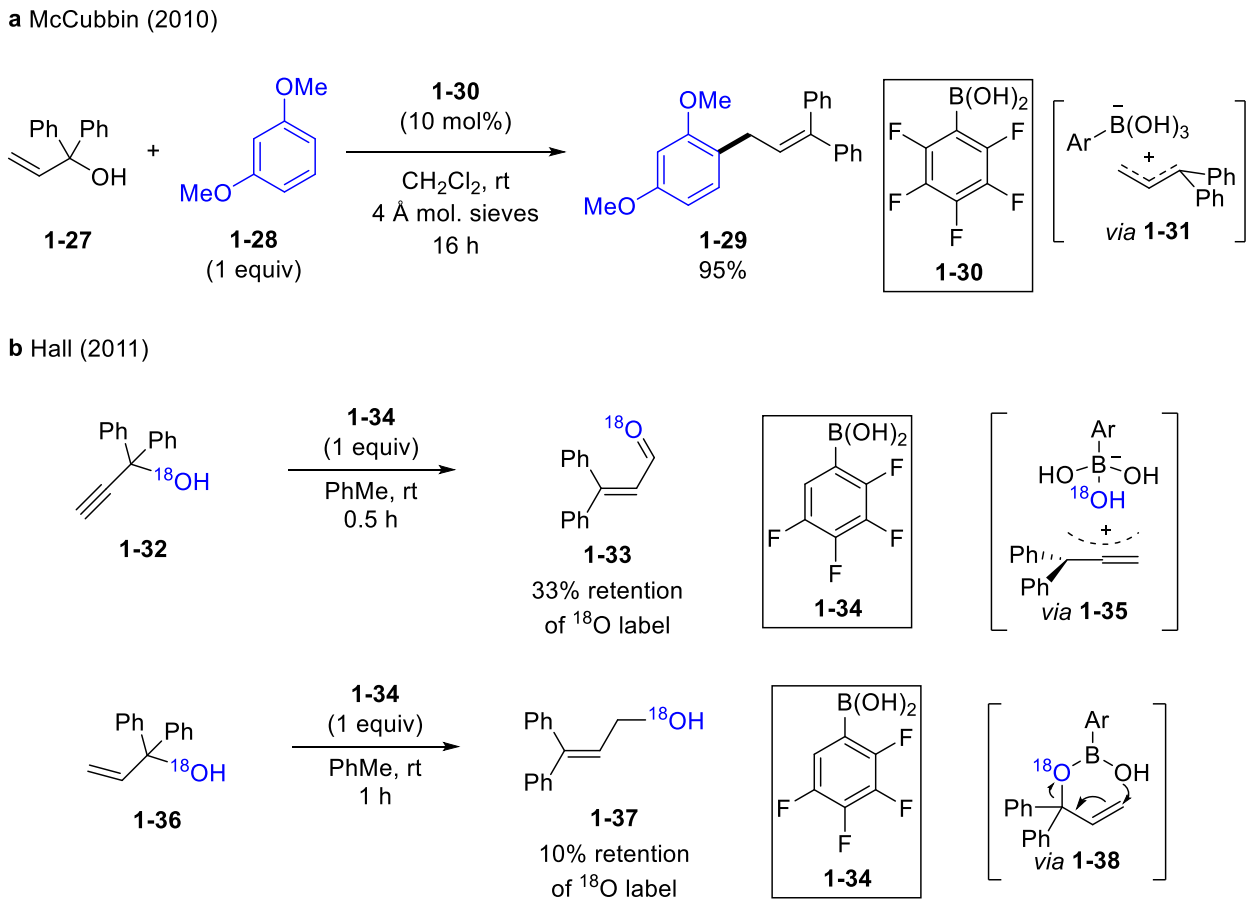

Scheme 1-9 Boronic acid-catalyzed electrophilic activation of alcohols. **a** Friedel-Crafts benzylation. **b** Transposition of allylic and propargylic alcohols.

Fluorinated boronic acids **1-34** and **1-39** were subsequently reported to catalyze intramolecular cyclization reactions of activated allylic alcohols using pendant aliphatic alcohols, phenols, or arenes as nucleophiles as highlighted in the syntheses of **1-40** through **1-42** (Scheme 1-10a).[65] Boronic acid **1-34** has also been reported as a catalyst for the Nazarov-type cycloaddition of 1,4-pentadienol substrates,[66] or the aza-Piancatelli reaction of furanyl alcohols.[67] In the latter, substrate ionization was proposed to afford cation intermediate **1-43**, which was converted to

pentadienyl cation **1-44** (Scheme 1-10b). Subsequent conrotatory electrocyclization ring closure afforded the enone products with high *trans*-selectivity. The application of boronic acid catalysis to cationic rearrangements highlights the utility of this strategy for C–O bond activation beyond the substitution reactions that dominated initial reports.

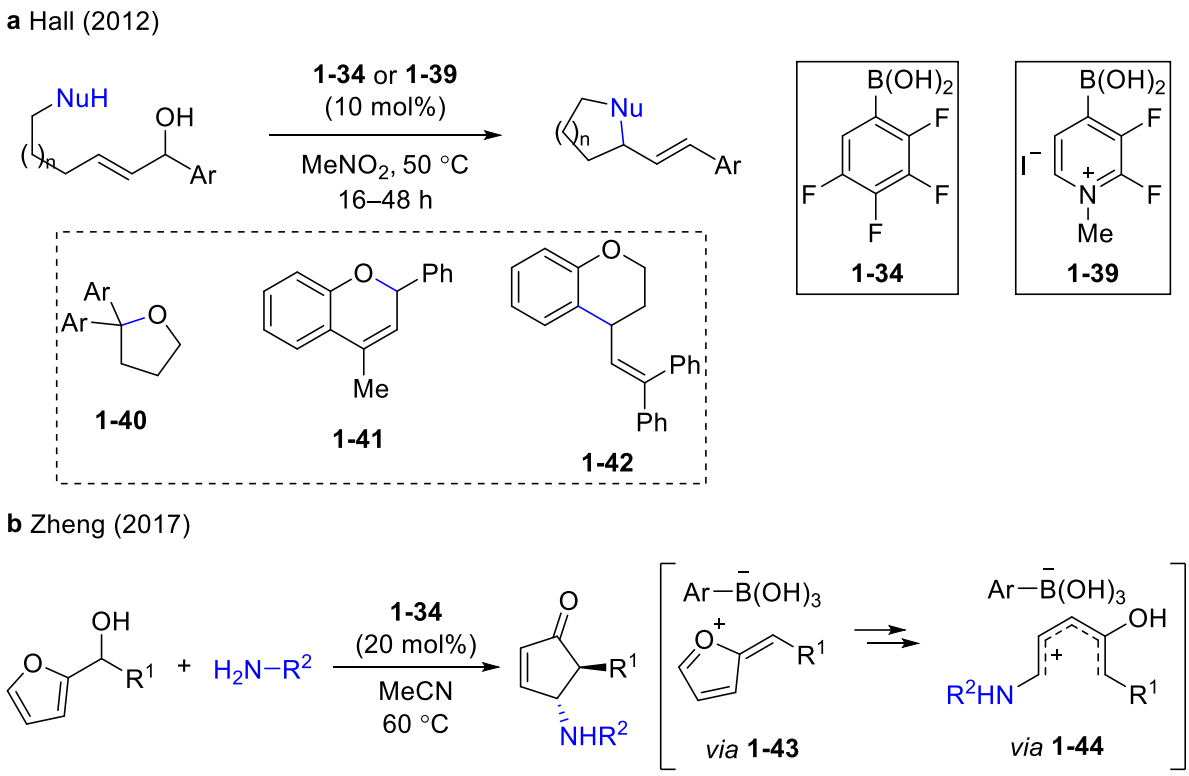

Scheme 1-10 Boronic acid-catalyzed alcohol activation. **a** Intramolecular cyclization. **b** Aza-Piancatelli rearrangement.

1.3.4 Nucleophilic Activation of Carbonyl Compounds

Boronic acids can also be used for the nucleophilic activation of carbonyl compounds, where the Lewis acidity of boron can be exploited to facilitate enolate formation and subsequent addition to electrophiles.[11] By circumventing the need for strong bases, boronic acid catalysis may offer milder reaction conditions or improved functional group tolerance in the reactions of carbonyl compounds. An early example of this mode of activation was reported by Carboni and co-workers

in 2006, who described the use of phenylboronic acid as a catalyst for the three-component Biginelli reaction of ethyl acetoaceteate, urea and benzaldehyde derivatives (Scheme 1-11a).[68] A dual catalytic function of the boronic acid was postulated (**1-45**). Formation of a boron enolate was proposed to provide nucleophilic activation of the acetoacetate, while B–N coordination was proposed to increase the electrophilicity of the *N*-acylimine intermediate formed though condensation of urea and the aldehyde.[68] Tetravalent boronate **1-49** was subsequently reported by Whiting and co-workers as an effective catalyst for the crossed aldol reaction of aldehydes and α-hydroxyketone **1-46** in water, which was proposed to involve two simultaneous modes of activation (Scheme 1-11b).[69] The boronic acid moiety was proposed to promote formation of the boron enolate, while the benzimidazole nitrogen was believed to increase the electrophilicity of the aldehyde through solvent-mediated hydrogen bonding (**1-50**).[69]

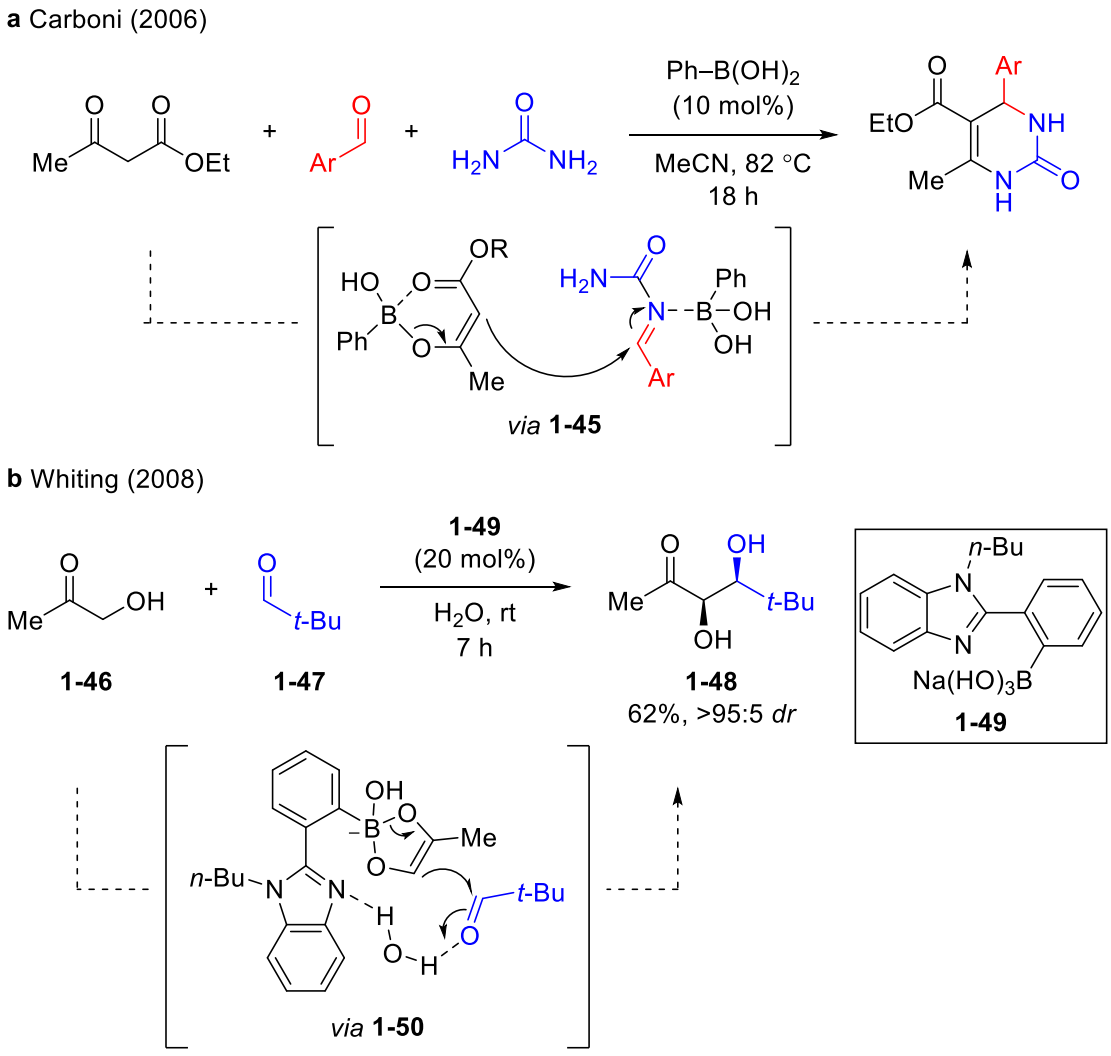

Scheme 1-11 Nucleophilic activation of carbonyls: **a** Biginelli reaction. **b** Aldol reaction.

1.3.5 Nucleophilic Activation of Diols

Under basic conditions, boronic acids can also induce nucleophilic activation of polyol substrates through the formation of a tetravalent anionic boronate species (Scheme 1-12).[11] The formal negative charge on boron results in increased electron density on the more electronegative oxygen atoms, increasing their nucleophilicity. This type of activation has been widely demonstrated using diarylborinic acids (Ar_2BOH), which will not be discussed here.[49]

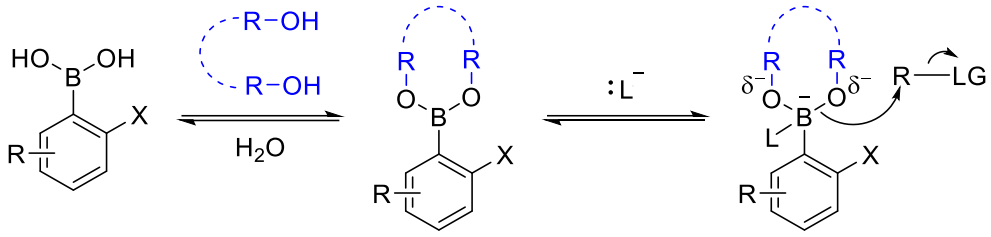

Scheme 1-12 Fundamentals of nucleophilic polyol activation via boronic acid catalysis.

Regioselective silylation of pyranosides was reported by Taylor and co-workers in 2013 using a co-catalytic system of boronic acid **1-53** and tributylphosphine oxide (Scheme 1-13a).[70] Complexation of the *cis*-diol moiety with boronic acid **1-53** was believed to result in a neutral trivalent boronic ester. Accordingly, coordination of the Lewis basic phosphine oxide was necessary to form tetravalent boronate **1-54** and provide sufficient nucleophilic activation.[70] Similarly, boronic acid **1-58** was reported by Toshima and co-workers as a catalyst for the α-selective glycosylation of 1α,2α-epoxyglycosyl donor **1-56** with glycosyl acceptor **1-55** containing a *cis*-diol unit (Scheme 1-13b).[71] After complexation to the *cis*-diol of the acceptor, electrophilic activation of the epoxide was believed to afford zwitterionic oxonium boronate intermediate **1-59**, in which the hydroxy groups are sufficiently nucleophilic to promote intramolecular glycosylation with high regio- and stereoselectivity. The enhanced nucleophilicity of tetravalent boronate esters was further exploited by Onomura and co-workers for the selective oxidation of vicinal diols to the corresponding α-hydroxyketones (Scheme 1-13c).[72] Selectivity for mono-oxidation was believed to arise from the enhanced nucleophilicity of boronate **1-63** towards the electrophilic halogen source. The oxidation of cyclic *trans*-diols was unsuccessful for small ring sizes, consistent with the proposed cyclic boronate intermediate.[72]

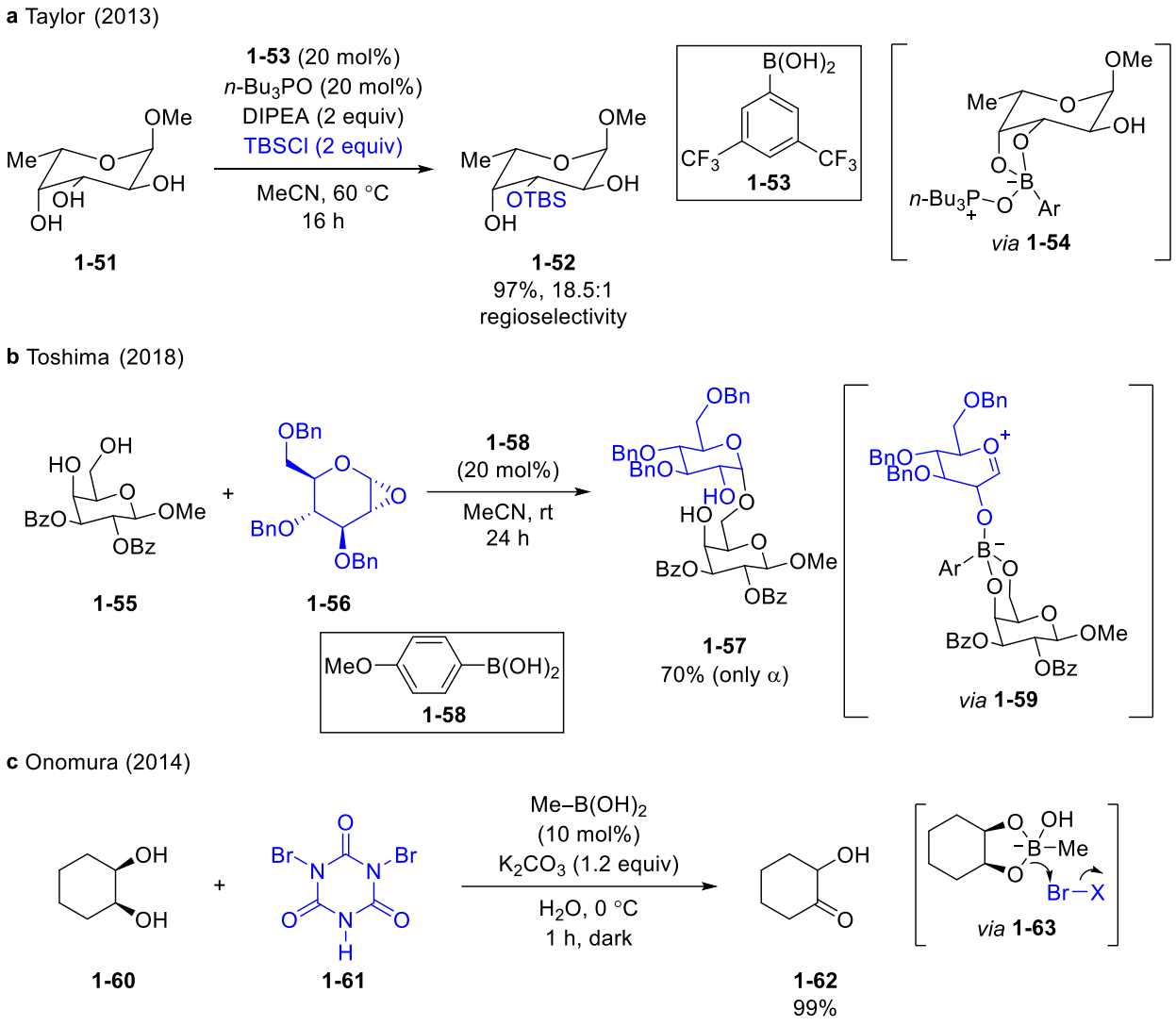

Scheme 1-13 Boronic acid-catalyzed nucleophilic activation of diols.

1.4 Challenges and Limitations in Boronic Acid Catalysis

1.4.1 Mechanistic Ambiguities

The modes of activation described in Section 1.3 are largely founded upon the Lewis acidity of boronic acids. The formation of temporary covalent interactions between hydroxy-containing substrates and the boron atom has been widely proposed in mechanisms of both nucleophilic and electrophilic activation. However, new considerations have recently been reported that call into question previous mechanistic proposals, particularly in the electrophilic activation. Moran and

co-workers demonstrated that boronic acid **1-67**, reported by Hall and co-workers for the Friedel-Crafts benzylation with benzylic alcohols, is an active catalyst for the arylative ring-opening of activated cyclopropane **1-64** to afford diarylalkane **1-66** when 1,1,1,3,3,3-hexafluoroisopropanol (HFIP) is used as the solvent (Scheme 1-14).[73] Given the absence of a hydroxy group in the substrate, Lewis acid catalysis involving covalent B–O bond exchange with substrate is precluded.

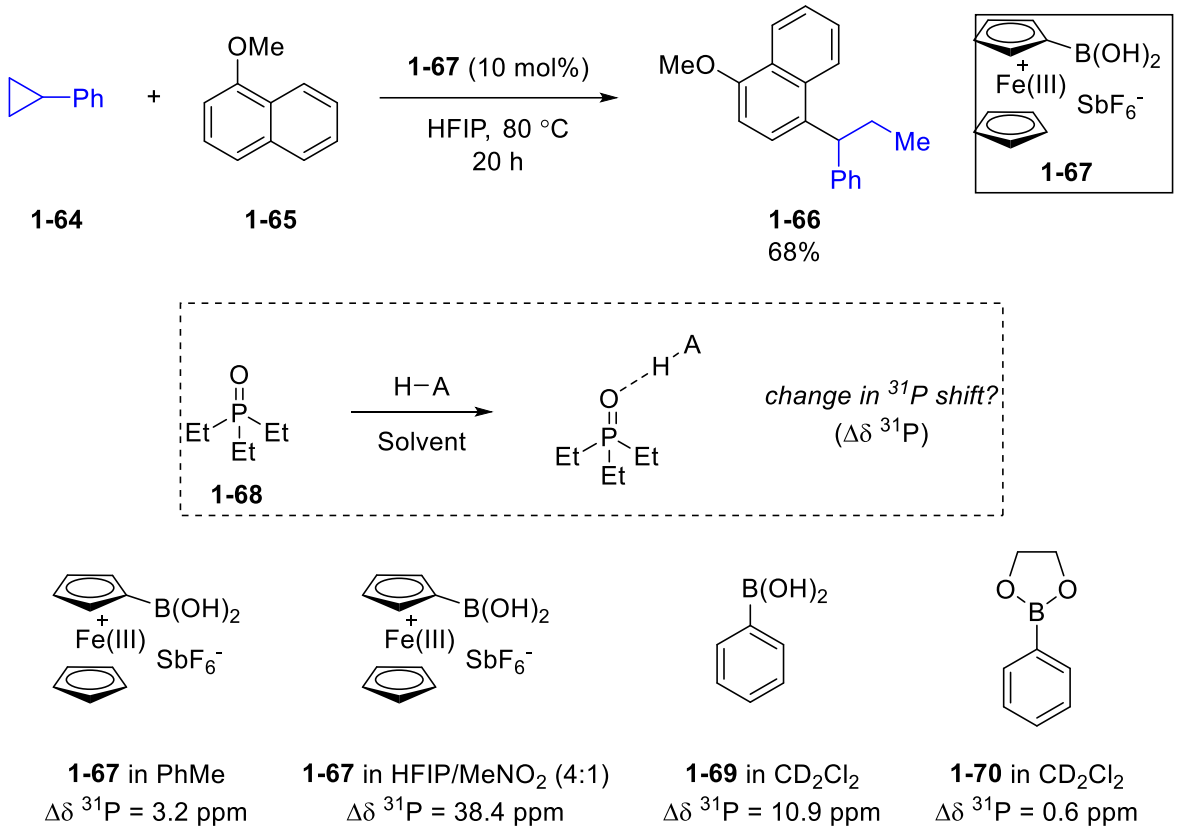

Scheme 1-14 Evidence for Brønsted acidity and hydrogen bonding in boronic acid catalysis.

Catalytic efficiency in this system was found to be highly solvent dependent, suggesting that proposed mechanisms and catalytic intermediates do not necessarily hold in different solvents. Control reactions suggested that the combination of electron-deficient boronic acids with HFIP solvent can lead to the formation of strong Brønsted acids or hydrogen bonding networks *in situ*, which are likely responsible for catalytic activity.[73] These observations were further supported by

Guttman-Beckett analysis, in which the change in ^{31}P chemical shift ($\Delta\delta\ ^{31}P$) of triethylphosphine oxide (**1-68**) is examined upon addition of an acidic species.[74] A large $\Delta\delta\ ^{31}P$ was observed for boronic acid **1-67** in HFIP, while a dramatically reduced $\Delta\delta\ ^{31}P$ was reported in toluene. Although this study could not unambiguously differentiate between Brønsted acid catalysis or hydrogen bonding catalysis, it was clear that the mechanism of electrophilic alcohol activation in acidic solvents is more complicated than initially believed.[73] A systematic investigation of the hydrogen bonding ability of boronic acids was subsequently conducted by Franz and Diemoz (Scheme 1-14).[75] Using similar ^{31}P NMR experiments, a significantly larger $\Delta\delta\ ^{31}P$ was observed upon reaction with arylboronic acid **1-69** relative the corresponding ethylene glycol ester **1-70**. Furthermore, the change in ^{11}B NMR chemical shift upon reaction of phenylboronic acid with triethylphosphine oxide was found to be less than 1 ppm, inconsistent with the formation of a tetravalent boron compound.[75] Taken together, these results provide renewed evidence for the importance of hydrogen bonding interactions in boronic acid catalysis.

Further mechanistic support for electrophilic activation without direct substrate-catalyst interaction was reported by Judeh and co-workers, who described the use of electron-deficient boronic acid **1-30** as a catalyst for the direct α-selective addition of alcohols to peracetylated D-galactal **1-71** (Scheme 1-15).[76] Supplementary ^{1}H NMR experiments revealed that the chemical shifts of the olefinic protons of substrate **1-71** were unchanged upon addition of the catalyst, suggesting that direct Lewis acid activation of the substrate is not operative in this process. An alternative mechanism was proposed in which indirect proton transfer between two equivalents of alcohol mediated by the Lewis acidic catalyst generates alkyloxonium species **1-73**, which serves as a Brønsted acid to promote formation of cyclic oxocarbenium intermediate **1-72**.[76] These results demonstrate that the combination of electron-deficient boronic acids with alcohols can serve as a

mild source of *in situ* Brønsted acids. In many boronic acid-catalyzed transformations, strong protic acid catalysts such as camphorsulfonic acid or *p*-toluenesulfonic acid have afforded decreased yields or increased formation of undesired side products.[65,77]

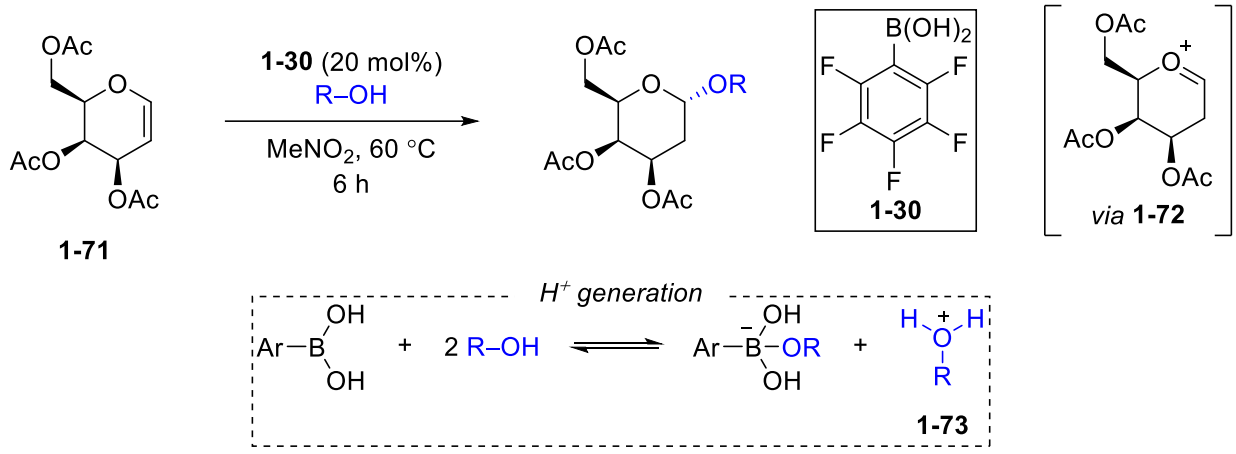

Scheme 1-15 Boronic acid-catalyzed synthesis of 2-deoxygalactosides.

1.4.2 Catalyst Specificity and Lack of Universal Frameworks

Boronic acid catalysts are often highly specific to a given transformation. Even within the realm of electrophilic activation, a wide range of arylboronic acids have proven optimal for different reactions.[11] This was highlighted in a tandem reaction sequence reported by Hall and co-workers, in which three sequential boronic acid-catalyzed reactions were conducted using three different catalysts (Scheme 1-16).[64] Allylic alcohol **1-74** was transformed into diene **1-75** through a tandem 1,3-transposition and elimination, followed by [4+2] cycloaddition with acrylic acid and direct amidation with benzyl amine to afford amide **1-77**. As evidenced by the use of three different catalysts in this tandem reaction, the discovery of new boronic acid-catalyzed transformations often requires the synthesis of new catalysts or exploration of a variety of catalytic species in initial optimization. The development of broadly applicable catalyst frameworks could significantly accelerate the development of new boronic acid-catalyzed reactions.

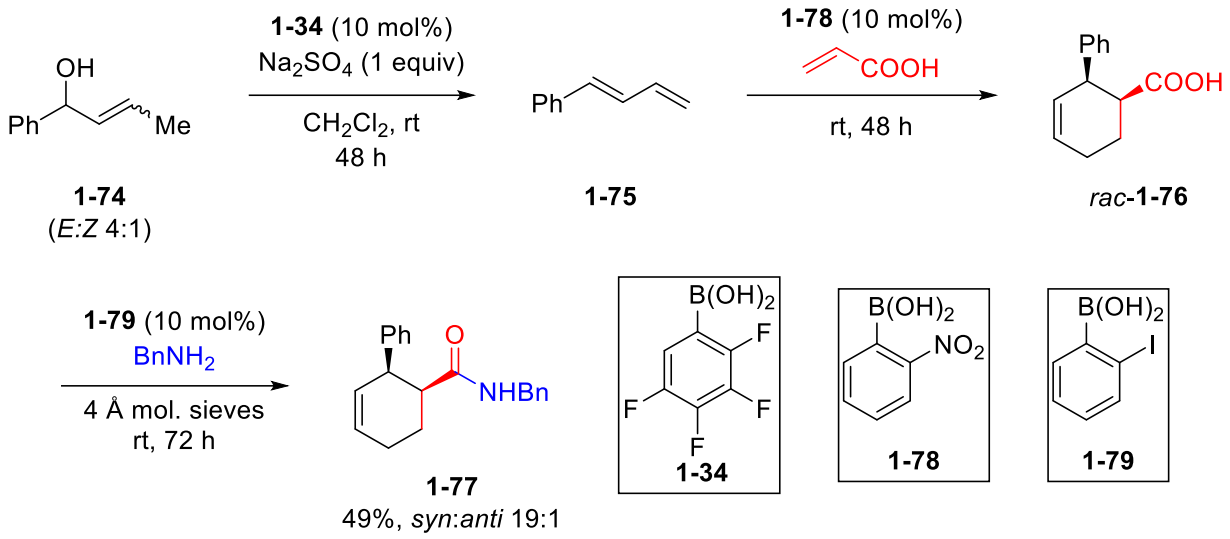

Scheme 1-16 Tandem boronic acid catalysis sequence using three different catalysts.

1.4.3 Modulation of Catalyst Activity

1.4.3.1 Diol Additives

The inability to apply boronic acid catalyst scaffolds across multiple transformations stems in part from an inability to modify catalyst reactivity *in situ* using additives. In transition metal catalysis, catalyst activity can be effectively tuned through the addition of ligands.[2] Metal-ligand bonding interactions can be used to modulate the electronic properties of the metal catalyst and can significantly alter the steric environment of the metal coordination sphere. The combined electron and steric effect of the ligand can be instrumental in determining the reactivity or selectivity of transition-metal catalysts.[2] Furthermore, the use of chiral ligands to promote stereoselective metal-catalyzed reactions is an essential strategy in asymmetric synthesis. The formation of metal-ligand complexes generally proceeds effectively *in situ*, allowing a single metal pre-catalyst to be rapidly modified in catalytic reactions.[2]

In contrast, the use of diol ligands in boronic acid catalysis has been poorly examined, and modification of catalyst steric and electronic properties generally requires the use of a different

catalyst altogether rather than diversification of a common pre-catalyst *in situ* (Figure 1-4). Although boronic acids are well known to undergo rapid condensation reactions with diols to form boronic esters,[12] a reluctance towards the use of hydroxy-containing additives likely stems from outdated mechanistic proposals in boronic acid catalysis, where the formation of hydroxy-exchange products with covalent B–O bonds has long been proposed. Accordingly, trivalent boronic esters lacking an exchangeable boranol moiety may have been expected to be catalytically inactive. Given the recent studies demonstrating the importance of new mechanistic paradigms in boronic acid catalysis, a re-investigation of the use of chelating dihydroxy-containing additives is warranted.

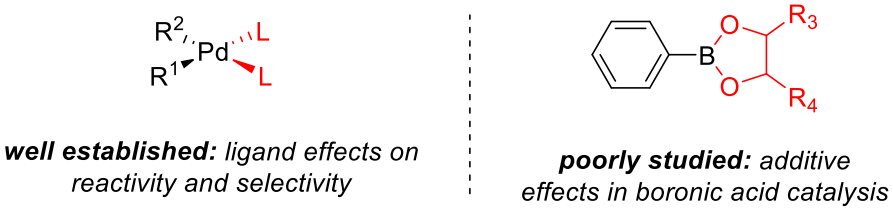

Figure 1-4 Ligand effects in transition metal catalysis and boronic acid catalysis.

A boronic acid-catalyzed variant of the asymmetric aldol reaction was reported by Whiting and co-workers in 2008.[78] When free boronic acid **1-82** was employed as a catalyst, β-hydroxyketone **1-81** was formed in only 38% ee (Scheme 1-17a). Addition of co-catalytic (*R,R*)-diisopropyl tartrate (**1-83**) led to significant increase in enantioselectivity, which was further enhanced by the addition of molecular sieves to promote diol condensation.[78] Notably, the same enantioselectivity and absolute stereochemistry was observed with either enantiomer of the tartrate additive, suggesting that stereoselectivity is controlled by the boronic acid rather than the diol. It was proposed that complexation to the electron-deficient diol additive led to an increasingly Lewis acidic boron center, improving stereoinduction in the nucleophilic attack of the catalyst-derived

enamine through transition state **1-84**. The use of catechol as an additive under the same conditions was found to increase the enantiomeric excess from 38% to 70%, consistent with the proposal that the diol effect at boron is largely electronic in nature.[78]

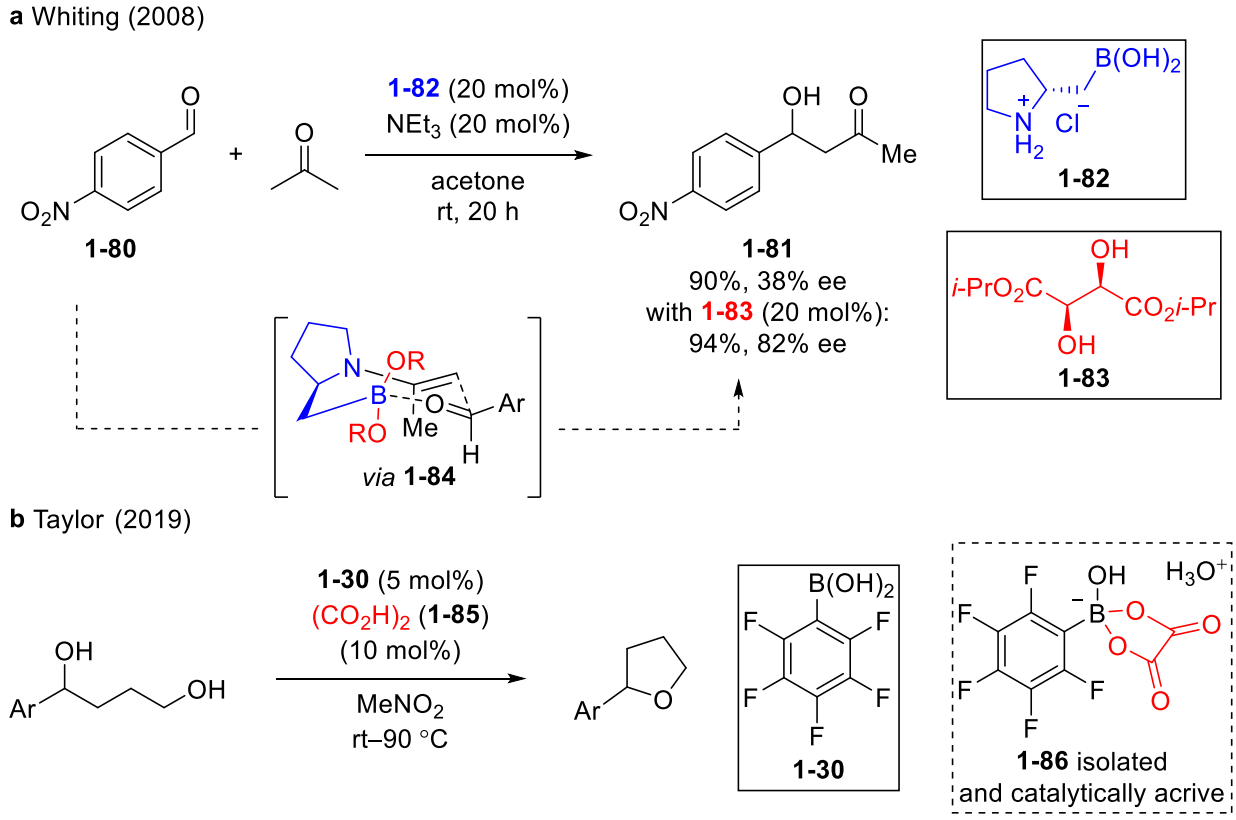

Scheme 1-17 Diol additives in boronic acid catalysis: **a** Asymmetric aldol reaction. **b** Dehydrative substitution.

A mechanistically distinct process involving a dihydroxy-containing additive was described by Taylor and co-workers, who reported the co-catalyst system of perfluorinated boronic acid **1-30** and oxalic acid (**1-85**) for the dehydrative substitution of benzylic alcohols via inter- or intramolecular ether formation (Scheme 1-17b).[79] An S_N1 mechanism was proposed based on erosion of stereochemistry from enantiomerically enriched substrates. Reaction of the two catalyst components in the absence of substrate was found to afford hydronium boronate species **1-86**,

which was demonstrated to be a competent catalyst for the reaction in comparable yields to *in situ* catalyst formation. It was proposed that complexation between catalysts **1-30** and **1-85** results in an increasingly electron-deficient boron atom that is sufficiently Lewis acidic to promote ionization of water, and that activation occurs through Brønsted acid catalysis.[79]

These reports by Whiting and Taylor demonstrate that significant advances in boronic acid catalysis can be realized with the use of dihydroxy-containing additives for electronic modulation of the boron atom. As new mechanistic proposals emerge in boronic acid catalysis to suggest that formation of a covalent substrate-catalyst adduct may not be required, further investigations into the use of diol additives and *in situ*-formed boronic esters catalysts are encouraged. It is worth noting that the use of oxalic acid (**1-85**) as an additive in boronic acid catalysis had been previously reported by Hall and co-workers for the direct sulfonamidation of benzylic alcohols,[80] and by Moran and co-workers for the Friedel-Crafts benzylation with benzylic alcohols.[81] However, neither of these reports provided experimental support for the nature of the catalytic intermediate. The isolation of boronate **1-86** by Taylor was instrumental in obtaining a thorough mechanistic understanding of the reaction.[79] To advance the understanding of boronic acid-catalyzed mechanisms for hydroxy group activation, a renewed focus on the synthesis, characterization and study of catalytic intermediates is essential.

1.4.3.2 Hemiboronic Acid Catalysts

A survey of the boronic acid catalysts described in this chapter reveals that the field has been extremely reliant on free boronic acids, species containing a discrete $B(OH)_2$ moiety. However, the poor solubility of these compounds in organic media, and their solvent-dependent equilibrium with the corresponding trimeric cyclic anhydrides, can complicate the unambiguous characterization of free boronic acids in solution.[12] New mechanistic paradigms that have been

uncovered in boronic acid catalysis suggest that the presence of two exchangeable B–OH units may not be necessary for effective substrate activation, and that successful development of new boronic acid-catalyzed transformations will require an exploration of other classes of boron-containing catalysts.

One such class of compounds are cyclic hemiboronic acids. Hemiboronic acids contain a boron atom at the same oxidation state as that in a boronic acid with one carbon substituent and two oxygen substituents. However, hemiboronic acids contain only a single free B–OH unit, while the other oxygen is part of an ester linkage that may confer increased solubility in organic solvents. The term cyclic hemiboronic acid specifically refers to compounds in which the boronic ester contains an intramolecular alkoxy or aryloxy tether.[12]

Among cyclic hemiboronic acids, the most well studied scaffold is benzoxaborole (Scheme 1-18a). First synthesized by Torssell in 1957 via the benzylic bromination of *ortho*-tolylboronic acid,[82] benzoxaborole has emerged as an important boron-containing pharmacophore, with several derivatives of this scaffold now marketed as therapeutic agents including crisaborole and tavaborole.[83–85] Benzoxaborole has demonstrated high affinity for pyranosides, offering effective sugar binding in aqueous solution at neutral pH.[86] Incorporation of the oxoborole ring has a significant impact on the acidity of benzoxaborole (pK_a 7.3) relative to phenylboronic acid (pK_a 8.8), a difference believed to be due to relief of strain in the five-membered heterocyclic ring upon ionization.[81] Experiments by Hall and co-workers have established that benzoxaborole exists in a dynamic rapid equilibrium between the open and closed forms in aqueous solution.[88]

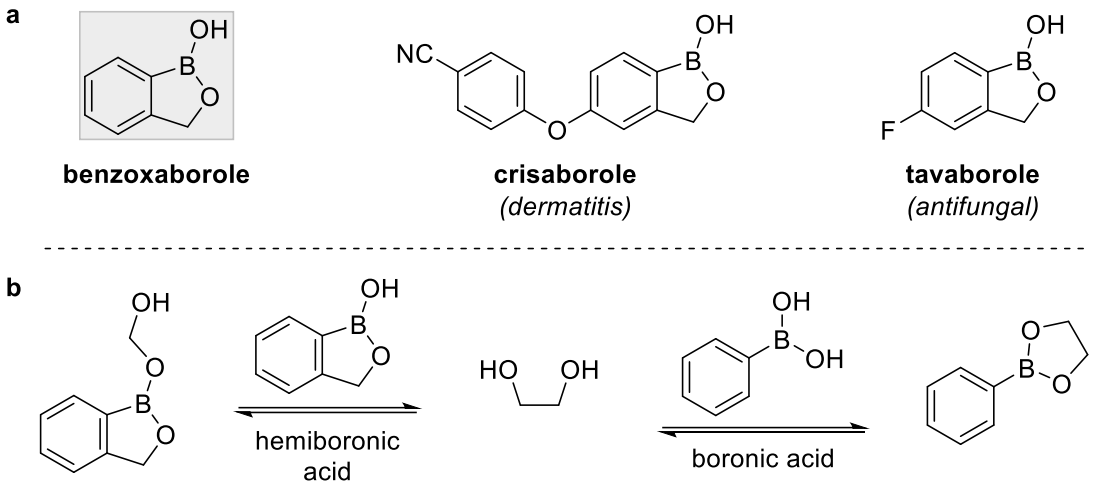

Scheme 1-18 a The benzoxaborole scaffold **b** Binding of a diol to boronic acids versus cyclic hemiboronic acids.

Cyclic hemiboronic acids contain only a single exchangeable B–OH unit in their closed form. Accordingly, reaction with a diol under neutral conditions does not lead to a cyclic boronic ester as it does in the reaction of conventional boronic acids. Instead, cyclic hemiboronic acids can readily form tetravalent adducts with diols under basic conditions (Scheme 1-18b). By combining the oxidative stability of a boronic acid with the single exchangeable site of a borinic acid, cyclic hemiboronic acids may offer new strategies in the development of boronic acid-catalyzed transformations.

However, catalytic applications of cyclic hemiboronic acids in hydroxy-group activation are rare. Diboronic acid anhydride **1-87** was employed by Shimada and co-workers as an active catalyst for the direct amidation of β-hydroxyacids through carboxylate-bridged reactive intermediate **1-88** (Scheme 1-19a),[89] consistent with the dimeric intermediate proposed previously by Whiting (*cf.* Scheme 1-5b).[53] The single exchangeable site of each boron atom may be essential to facilitating formation of the bridged intermediate. The following year, the same catalyst was highlighted for the direct amidation of serine or threonine derivatives with minimal

epimerization.[90] *Gem*-diboronic acid **1-89** was reported to catalyze direct dehydrative peptide bond formation between a range of protected amino acids, which was believed to occur through bridged intermediate **1-90** (Scheme 1-19b).[91] This study represented a notable advance in boronic acid-catalyzed amidation, as direct peptide bond formation in these systems is often difficult due to catalyst inhibition by way of a stable five-membered chelate.[92]

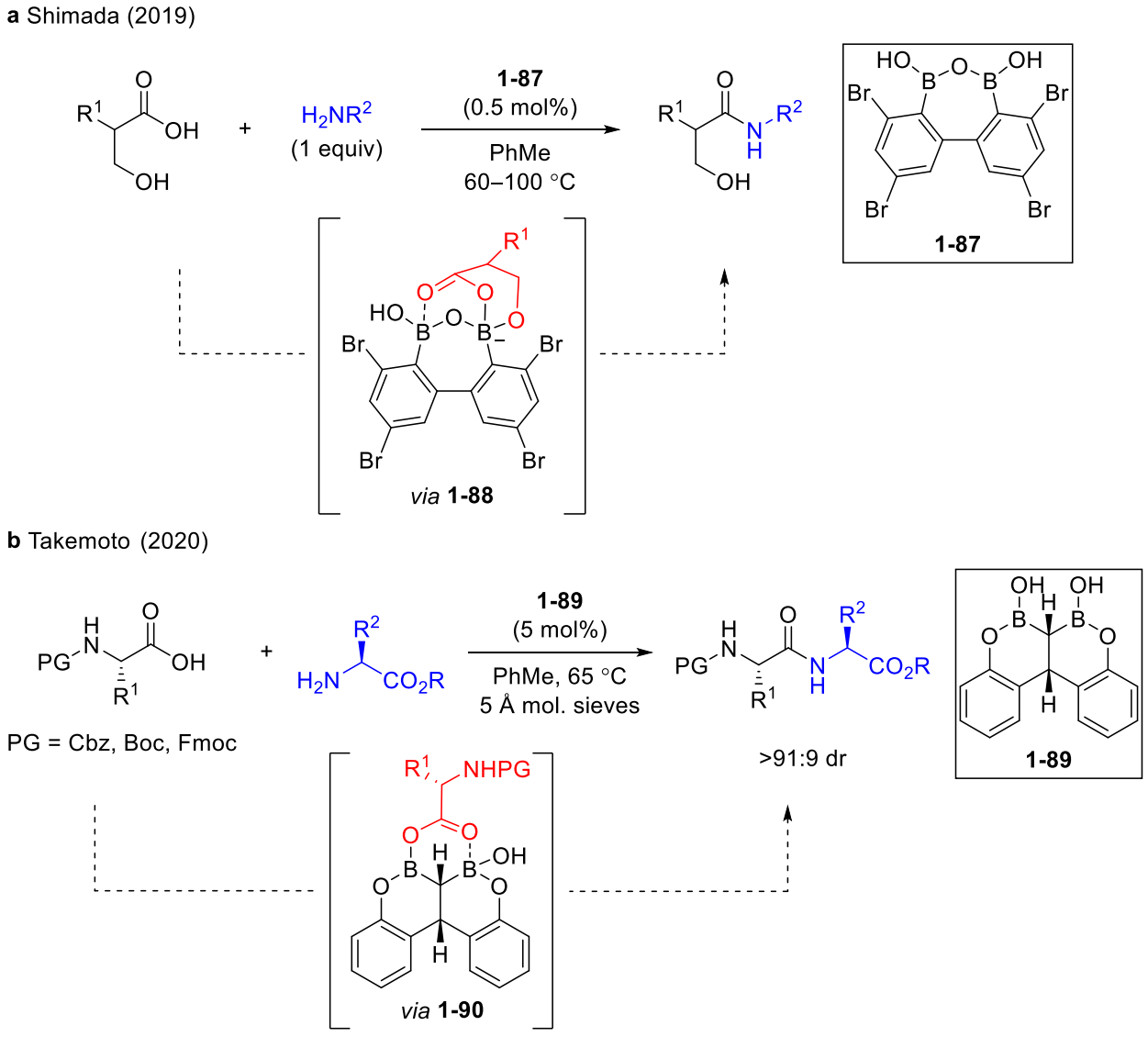

Scheme 1-19 Hemiboronic acids in the direct amidation of carboxylic acids.

The first application of the benzoxaborole scaffold in catalysis was reported by Hayashida and co-workers in 2020, who described the regioselective benzoylation, tosylation and benzylation of vicinal diols using hemiboronic acid **1-91** (Scheme 1-20a).[93] This transformation was proposed to occur through nucleophilic activation of the diol moiety via tetravalent boronate intermediate **1-92**. High selectivity for *cis*-diols over *trans*-diols was observed in cyclic substrates, consistent with the relative ability of these diols to form the key tetravalent boronate adduct.[93] Similarly, chiral benzazaborole **1-93** was reported as a catalyst for the enantioselective sulfonylation of vicinal diols by Arai and co-workers (Scheme 1-20b).[94] Lewis base **1-94** was employed as a co-catalyst to generate a reactive *N*-sulfonylimidazolium electrophile. In the absence of electrophile, reaction of catalyst **1-94** with substrate was found to form condensation product **1-95**, in which the second diol remains protonated and uncoordinated to boron. Upon addition of base, adduct **1-95** was converted to tetravalent boronate **1-96**, which undergoes nucleophilic attack on the activated electrophile. The authors found that use of phenylboronic acid as a catalyst afforded only trace sulfonylated product under comparable conditions, highlighting the utility of the hemiboronic acid scaffold in promoting formation of the tetravalent catalytic intermediate **1-96**.[94]

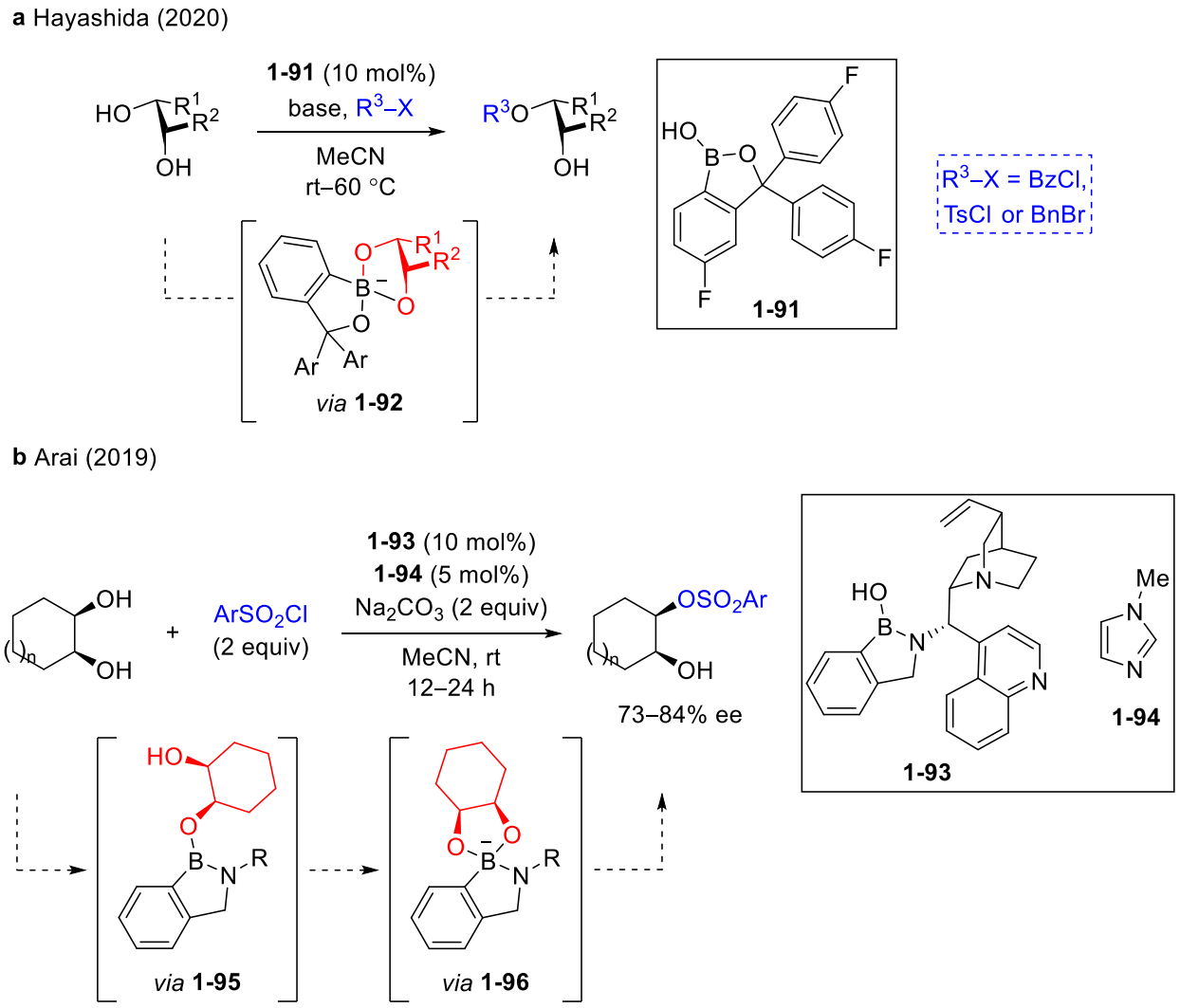

Scheme 1-20 Catalytic applications of cyclic hemiboronic acids.

1.5 Thesis Objectives

As described above, the development of new catalysts for boronic acid-catalyzed transformations has largely remained limited to the synthesis of new arylboronic acids. While strategic functionalization of the arene core can be used to tailor boronic acid acidity, the ability to unlock new catalytic intermediates and access new mechanisms of activation with existing catalyst scaffolds remains unaddressed. This thesis will aim to address these limitations in two ways.

In light of scattered reports regarding the ability of co-catalytic diol additives to modulate reactivity in boronic acid catalysis, it was envisioned that the use of an electron-deficient diol may be used to increase the reactivity of electron-poor catalysts in the direct electrophilic activation of alcohols. Chapter 2 will describe efforts to develop a two-component catalyst system for challenging Friedel-Crafts benzylation reactions of benzylic alcohols. Mechanistic studies will be described to elucidate the role of the co-catalyst and to identify catalytic intermediates.

The lack of reported examples of cyclic hemiboronic acids as reaction catalysts may arise from a poor understanding of the fundamental properties of these compounds. A rigorous knowledge of their stability, acidity and reactivity towards hydroxy-containing compounds is required in order to facilitate their use as reaction catalysts, and to bring catalyst development out of the "black box" in which optimization is often done. In this regard, Chapter 3 will describe studies towards a systematic understanding of the benzoxazaborine and benzodiazaborine classes of cyclic hemiboronic acids. The relationship between pseudoaromaticity, acidity, hydrolytic stability and reactivity towards alcohols will be examined through a rigorous experimental approach, where dramatic differences between structurally related heterocycles will be rationalized.

With an improved understanding of the fundamental properties of cyclic hemiboronic acids, Chapter 4 will detail efforts towards the application of these scaffolds in boronic acid catalysis. Two mechanistically divergent transformations will be described in which the catalysts differ only in the introduction of a single methyl group. The mechanism of both transformations will be discussed, and evidence will be provided for key intermediates in both pathways to explore the interconversion of trivalent and tetravalent boron species during catalysis. The results of Chapters 3 and 4 will facilitate the discovery of new hemiboronic acid-catalyzed transformations.

1.6 References

1) Catlow, C. R., Davidson, M., Hardacre, C., Hutchings, G. J. *Phil. Trans. R. Soc. A* **2016**, *374*, 20150089.
2) Hartwig, J. *Organotransition Metal Chemistry: From Bonding to Catalysis*; University Science Books: Sausalito, CA, **2010**.
3) Clark, J. H. *Green Chem.* **1999**, *1*, 1–8.
4) Constable, D. J. C., Dunn, P. J., Hayler, J. D., Humphrey, G. R., Leazer Jr., J. L., Linderman, R. J., Lorenz, K. L., Manley, J., Pearlman, B. A., Wells, A., Zaks, A., Zhang, T. Y. *Green Chem.* **2007**, *9*, 411–420.
5) Trader, D. J., Carlson, E. E. *Mol. Biosyst.* **2012**, *8*, 2484–2493.
6) Henkel, T., Brunne, R. M., Müller, H., Reichel, F. *Angew. Chem. Int. Ed.* **1999**, *38*, 643–647.
7) Appel, R. *Angew. Chem. Int. Ed.* **1975**, *14*, 801–811.
8) Kumara Swamy, K. C., Bhuvan Kumar, N. N., Balaraman, E., Pavan Kumar, K. V. P. *Chem. Rev.* **2009**, *109*, 2551–2561.
9) Grieco, P. A., Gilman, S., Nishizawa, M. *J. Org. Chem.* **1976**, *41*, 1485–1486.
10) Carey, J. S., Laffan, D., Thomson, C., Williams, M. T. *Org. Biomol. Chem.* **2006**, *4*, 2337–2347.
11) Hall, D. G. *Chem. Soc. Rev.* **2019**, *48*, 3475–3496.
12) Hall, D. G., Ed. *Boronic Acids: Preparation and Applications in Organic Synthesis,* 2nd edn., Wiley-VCH: Weinheim, **2011**.
13) Frankland, E., Duppa, B. F. *Liebigs Ann.* **1860**, *115*, 319–322.
14) Michaelis, A., Becker, P. *Ber. Dtsch. Chem. Ges.* **1880**, *13*, 58–61.
15) Michaelis, A. *Liebigs Ann. Chen.* **1901**, *315*, 19–43.
16) Partyka, D. V. *Chem. Rev.* **2011**, *111*, 1529–1595.
17) Miyaura, N., Yamada, K., Suzuki, A. *Tetrahedron Lett.* **1979**, *20*, 3437–3440.
18) Suzuki, A. *Angew. Chem. Int. Ed.* **2011**, *50*, 6722–6737.
19) Chan, D., Monaco, K., Wang, R., Winter, M. *Tetrahedron Lett.* **1998** *39*, 2933–2936.
20) Evans, D., Katz, J., West, T. *Tetrahedron Lett.* **1998**, *39*, 2937–2940.
21) Lam, P., Clark, C., Saubern, S., Adams, J., Winters, M., Chan, D., Combs, A. *Tetrahedron Lett.* **1998**, *39*, 2941–2944.

22) Liebeskind, L., Srogl, J. *J. Am. Chem. Soc.* **2000**, *122*, 11260–11261.

23) Hayashi, T., Takahashi, M., Takaya, Y., Ogasawara, M. *J. Am. Chem. Soc.* **2002**, *124*, 5052–5058.

24) Petasis, N. A., Akritopoulou, I. *Tetrahedron Lett.* **1993**, *34*, 583–586.

25) Matteson, D. S., Mah, R. W. H. *J. Am. Chem. Soc.* **1963**, *85*, 2599–2603.

26) Lachance, H., Hall, D. G. Allylboration of Carbonyl Compounds. In *Organic Reactions*, **2009**, 1–574.

27) Armstrong, R. J., Aggarwal, V. K. *Synthesis* **2017**, *49*, 3323–3336.

28) Xu, L., Wang, G., Zhang, S., Wang, H., Wang, L., Liu, L., Jiao, J., Li, P. *Tetrahedron* **2017**, *73*, 7123–7157.

29) Yadagiri, B., Daipule, K., Singh, S. P. *Asian J. Chem.* **2020**, *10*, 7–37.

30) Hu, J., Ferger, M., Shi, Z., Marder, T. B. *Chem. Soc. Rev.* **2021**, *50*, 13129–13188.

31) Neeve, E. C., Geier, S. J., Mkhalid, I. A. I., Westcott, S. A., Marder, T. B. *Chem. Rev.* **2016**, *116*, 9091–9161.

32) Chow, W. K., Yuen, O. Y., Choy, P. Y., So, C. M., Lau, C. P., Wong, W. T., Kwong, F. Y. *RSC Adv.* **2013**, *3*, 12518–12539.

33) Silva, M. P., Saraiva, L., Pinto, M., Sousa, M. E. *Molecules* **2020**, *25*, 4323–4362.

34) Messner, K., Vuong, B., Tranmer, G. K. *Pharmaceuticals* **2022**, *15*, 2, 264–296.

35) Cadahía, J. P., Previtali, V., Troelsen, N. S., Clausen, M. H. *Med. Chem. Commun.* **2019**, *10*, 1531–1549.

36) António, J. P. M., Russo, R., Carvalho, C. P., Cal, P. M. S. D., Gois, P. M. P. *Chem. Soc. Rev.* **2019**, *48*, 3513–3536.

37) Cho, S., Hwang, S. Y., Oh, D. X., Park, J. *J. Mater. Chem. A.* **2021**, *9*, 14630–14655.

38) Brooks, W. L. A., Sumerlin, B. S. *Chem. Rev.* **2016**, *116*, 1375–1397.

39) Williams, G. T., Kedge, J. L., Fossey, J. S. *ACS Sens.* **2021**, *6*, 1508–1528.

40) Wu, X., Chen, X.-X., Song, B.-N., Huang, Y.-J., Ouyang, W.-J., Li, Z., James, T. D., Jiang, Y.-B. *Chem. Commun.* **2014**, *50*, 13987–13989.

41) Aung, Y.-Y., Kristani, A. N., Lee, H. V., Fahmi, M. Z. *ACS Omega,* **2021**, *6*, 17750–17765.

42) Li, H., Zhang, X., Zhang, L., Wang, X., Kong, F., Fan, D., Li, L., Wang, W. *Anal. Chim. Acta* **2017**, *15*, 104–113.

43) Frey, L., Jarju, J. J., Salonen, L. M., Medina, D. D. *New J. Chem.* **2021**, *45*, 14879–14907.

44) Rettig, S. J., Trotter, T. *Can. J. Chem.* **1997**, *55*, 3071–3075.
45) Soundararajan, S., Duesler, E. N., Hageman, J. H. *Acta Crystallogr.* **1993**, *C49*, 690–693.
46) Lorand, J. P., Edwards, J. O. *J. Org. Chem.* **1959**, *24*, 769–774.
47) Letsinger, R. L., Dandegaonker, S., Vullo, W. J., Morrison, J. D. *J. Am. Chem. Soc.* **1963**, *85*, 2223–2227.
48) Rao, G., Philipp, M. *J. Org. Chem.* **1991**, *56*, 1505–1512.
49) Taylor, M. S. *Acc. Chem. Res.* **2015**, *48*, 295–305.
50) Carey, J. S., Laffan, D., Thomson, C., Williams, M. T. *Org. Biomol. Chem.* **2006**, *4*, 2337–2347.
51) Dugger, R. W., Ragan, J. A., Ripin, D. H. B. *Org. Process Res. Dev.* **2005**, *9*, 253–258.
52) Ishihara, K., Ohara, S., Yamamoto, H. *J. Org. Chem.* **1996**, *61*, 4196–4197.
53) Arkhipenko, S., Sabatini, M. T., Batsanov, A. S., Karaluka, V., Sheppard, T. D., Rzepa, H. S., Whiting, A. *Chem. Sci.* **2018**, *9*, 1058–1072.
54) Tale, R. H., Patil, K. M. *Tetrahedron Lett.* **2002**, *43*, 9715–9716.
55) Tale, R. H., Patil, K. M., Dapurkar, S. E. *Tetrahedron Lett.* **2003**, *44*, 3427–3428.
56) Maki, T., Ishihara, K., Yamamoto, H. *Synlett* **2004**, 1355–1358.
57) Maki, T., Ishihara, K., Yamamoto, H. *Org. Lett.* **2005**, *7*, 5047–5050.
58) Sakakura, A., Ohkubo, T., Yamashita, R., Akakura, M., Ishihara, K. *Org. Lett.* **2011**, *13*, 892–895.
59) Al-Zoubi, R. M., Marion, O., Hall, D. G. *Angew. Chem. Int. Ed.* **2008**, *47*, 2876–2879.
60) Zheng, H., McDonald, R., Hall, D. G. *Chem. Eur. J.* **2010**, *16*, 5454–5460.
61) Azuma, T., Murata, A., Kobayashi, Y., Inokuma, T., Takemoto, Y. *Org. Lett.* **2014**, *16*, 4256–4259.
62) Ayama, N., Azuma, T., Kobayashi, Y., Takemoto, Y. *Chem. Pharm. Bull.* **2016**, *64*, 704–717.
63) McCubbin, J. A., Hosseini, H., Krokhin, O. V. *J. Org. Chem.* **2010**, *75*, 959–962.
64) Zheng, H., Lejkowski, M., Hall, D. G. *Chem. Sci.* **2011**, *2*, 1305–1310.
65) Zheng, H., Ghanbari, S., Nakamura, S., Hall, D. G. *Angew. Chem. Int. Ed.* **2012**, *51*, 6187–6190.
66) Zheng, H., Lejkowski, M., Hall, D. G. *Tetrahedron Lett.* **2013**, *54*, 91–94.
67) Tang, W.-B., Cao, K.-S., Meng, S.-S., Zheng, W.-H. *Synthesis* **2017**, 3670–3675.

68) Debache, A., Boumoud, B., Armimour, M., Belfaitah, A., Rhouati, S., Carboni, B. *Tetrahedron Lett.* **2006**, *47*, 5697–5699.

69) Aelvoet, K., Batsanov, A. S., Blatch, A. J., Grosjean, C., Patrick, L. G. F., Smethurst, C. A., Whiting, A. *Angew. Chem. Int. Ed.* **2008**, *47*, 768–770.

70) Lee, D., Taylor, M. S. *Org. Biomol. Chem.* **2013**, *11*, 5409–5412.

71) Tanaka, M., Nakagawa, A., Nishi, N., Ijima, K., Sawa, R., Takahashi, D., Toshima, K. *J. Am. Chem. Soc.* **2018**, *140*, 3644–3651.

72) William, J. M., Kuriyama, M., Onomura, O. *Adv. Synth. Catal.* **2014**, *356*, 934–940.

73) Zhang, S., Leboeuf, D., Moran, J. *Chem. Eur. J.* **2020**, *26*, 9883–9888.

74) Pires, E., Fraile, J. S. *Phys. Chem. Chem. Phys.* **2020**, *22*, 24351–24358.

75) Diemoz, K. M., Franz, A. K. *J. Org. Chem.* **2019**, *84*, 1126–1138.

76) Tatina, M. B., Moussa, Z., Xia, M., Judeh, Z. M. A. *Chem. Commun.* **2019** *55*, 12204–12207.

77) Cao, K.-S., Bian, H.-X., Zheng, W.-H. *Org. Biomol. Chem.* **2015**, *13*, 6449–6452.

78) Arnold, K., Batsanov, A. S., Davies, B., Grosjean, C., Schütz, T., Whiting, A., Zawatsky, K. *Chem. Commun.* **2008**, *33*, 3879–3881.

79) Estopiñá-Durán, S., Donnelly, L. J., Mclean, E. B., Hockin, B. M., Slawin, A. M. Z., Taylor, J. E. *Chem. Eur. J.* **2019**, *25*, 3950–3956.

80) Verdelet, T., Ward, R. M., Hall, D. G. *Eur. J. Org. Chem.* **2017**, 5729–5738.

81) Wolf, E., Richmond, E., Moran, J. *Chem. Sci.* **2015**, *6*, 2501–2505.

82) Torssell, K. *Arkiv foer Kemi* **1957**, *10*, 507–511.

83) Baker, S. J., Zhang, Y.-K., Akama, T., Lau, A., Zhou, H., Hernandez, V., Mao, W., Alley, M. R. K., Sanders, V., Plattner, J. J. *J. Med. Chem.* **2006**, *49*, 4447–4450.

84) Liu, C. T., Tomsho, J. W., Benkovic, S. J. *Bioorg***.** *Med. Chem.* **2014**, *22*, 4462–4473.

85) Adamczyk-Woźniak, A., Borys, K. M., Sporzyński, A. *Chem. Rev.* **2015**, *115*, 5224–5247.

86) Dowlut, M., Hall, D. G. *J. Am. Chem. Soc.* **2006**, *128*, 4226–4227.

87) Adamczyk-Woźniak, A., Borys, K. M., Madura, I. D., Pawełko, A., Tomecka, E., Żukowski, K. *New J. Chem.* **2013**, *37*, 188–194.

88) Vshyvenko, S., Clapson, M. L., Suzuki, I., Hall, D. G. *ACS Med. Chem. Lett.* **2016**, *7*, 1097–1101.

89) Shimada, N., Hirata, M., Koshizuka, M., Ohse, N., Kaito, R., Makino, K. *Org. Lett.* **2019**, *21*, 4303–4308.
90) Koshizuka, M., Makino, K., Shimada, N. *Org. Lett.* **2020**, *22*, 8658–8664.
91) Michigami, K., Sakaguchi, T., Takemoto, Y. *ACS Catal.* **2020**, *10*, 683–688.
92) Wang, K., Lu, Y., Ishihara, K. *Chem. Commun.* **2018**, *54*, 5410–5413.
93) Kusano, S., Miyamoto, S., Matsuoka, A., Yamada, Y., Ishikawa, R., Hayashida, O. *Eur. J. Org. Chem.* **2020**, *11*, 1598–1602.
94) Kuwano, S., Hosaka, Y., Arai, T. *Org. Biomol. Chem.* **2019**, *17*, 4475–4482.

Chapter 2 Boronic Acid/Perfluoropinacol-Catalyzed Friedel-Crafts Alkylations with Benzhydryl Alcohols[‡]

2.1 Introduction

Substituted di- and triarylalkanes are an important structural motif in bioactive natural products and pharmaceutical compounds.[1–3] Furthermore, the triarylmethane core represents an essential lynchpin in the design of organic dyes (Figure 2-1).[4] In both biological and optical applications alike, the properties of multiply-arylated alkanes can be tuned by modifying the steric and electronic parameters of the aromatic substituents. In order to properly explore structure-activity relationships of these ubiquitous units in their diverse applications, general synthetic methods to access multiply arylated alkanes from simple starting materials are necessary.

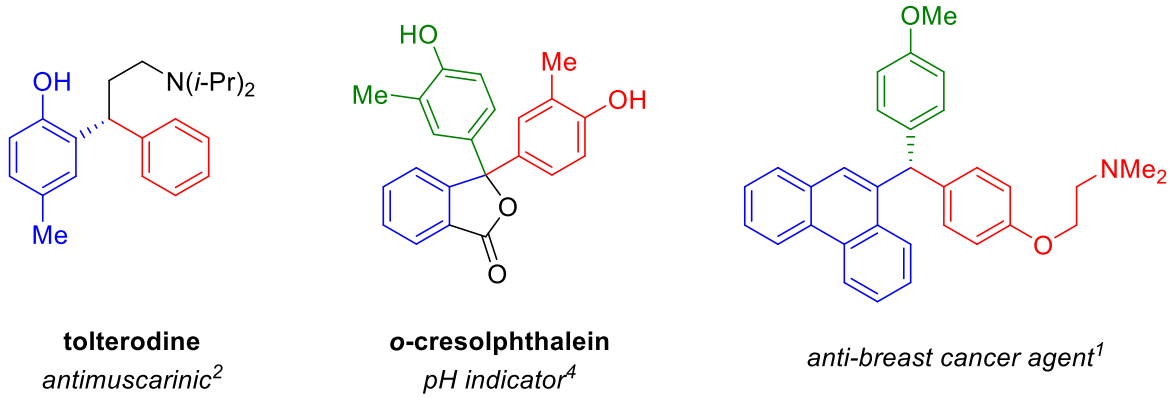

tolterodine
antimuscarinic[2]

***o*-cresolphthalein**
pH indicator[4]

anti-breast cancer agent[1]

Figure 2-1 Examples of multiply arylated alkanes with applications as bioactive compounds and organic dyes.

The functionalization of aromatic compounds is an essential strategy in many areas of chemical synthesis ranging from the production of commodity chemicals to bioactive

[‡]A version of this chapter has been published as Ang, H. T., Rygus, J. P. G., Hall, D. G. *Org. Biomol. Chem.* **2019**, *17*, 6007–6014.

pharmaceutical agents. While transition metal-catalyzed cross-coupling reactions have been widely employed in the synthesis of multiply arylated alkanes,[5] the Friedel-Crafts reaction has remained arguably the most widely used transformation for the construction of carbon-carbon bonds to aromatic rings since it was first reported over 100 years ago.[6] In their pioneering 1877 report, Friedel and Crafts demonstrated the alkylation of benzene with 1-chloropentane (**2-01**) using unspecified amounts of $AlCl_3$ as a Lewis acid (Scheme 2-1).[7]

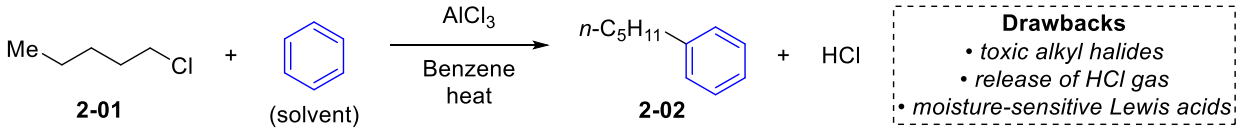

Scheme 2-1 The first electrophilic aromatic alkylation reaction reported by Friedel and Crafts.

Over a century later, the classical Friedel-Crafts reaction remains predominant in this field. Reaction conditions employing toxic alkyl halides and stoichiometric amounts of moisture sensitive Lewis acids, with the generation of strongly Brønsted acidic byproducts, are commonplace.[6] Despite their widespread use, there is no doubt that these methods require improvement for the modern age from the perspective of atom economy, green chemistry and environmental awareness. These limitations were highlighted by the ACS Green Chemistry Institute *Pharmaceutical Roundtable* in 2007, who identified the Friedel-Crafts reaction as a priority research area and stressed the need to develop new methods with improved atom economy for the catalytic activation of less toxic substrates.[8]

In this light, the use of readily accessible benzylic alcohol derivatives in Friedel-Crafts alkylation represents a promising strategy (Scheme 2-2). Relative to their analogous benzyl halides, alcohols are less toxic and more synthetically accessible. In addition, Friedel-Crafts

reactions with alcohol substrates produce only water as a stoichiometric byproduct, offering a more environmentally friendly process and simplifying reaction work-up and waste processing.

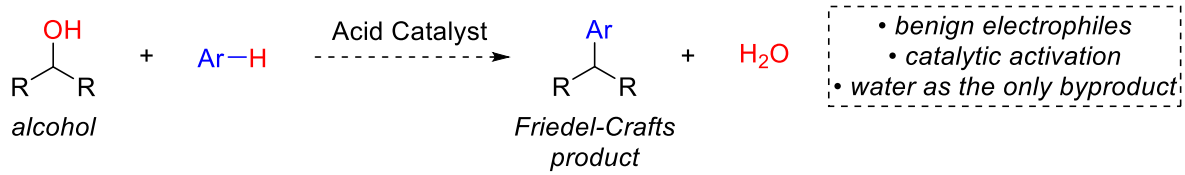

Scheme 2-2 Friedel-Crafts benzylation reaction using alcohols as electrophiles.

The first Friedel-Crafts alkylation using benzylic alcohols was reported by Uemura and co-workers in 1986.[9] While investigating the $TeCl_4$-mediated chlorination of benzylic alcohol **2-03**, an unexpected side reaction was observed when toluene was used as the solvent, affording 1,1-diarylalkane **2-04** in good yield (Scheme 2-3a). This transformation was proposed to occur through a Friedel-Crafts alkylation of the *in situ* formed benzyl chloride intermediate. Surprisingly, good yields could also be obtained when $TeCl_4$ was used in a catalytic fashion rather than stoichiometrically.[9]

In contrast to the serendipitous discovery by Uemura, the first systematic studies on the use of benzylic alcohols in Friedel-Crafts alkylations were reported by the Fukuzuma and Yamamoto groups nearly a decade later employing $Sc(OTf)_3$ (Scheme 2-3b) and $Mo(CO)_6$ (Scheme 2-3c) as catalysts respectively.[10,11] While the latter catalyst was used under strictly anhydrous conditions, the scandium-catalyzed transformation described by Fukuzuma proved tolerant to ambient conditions. The use of large excesses of the nucleophilic arene as the solvent were necessary to obtain high yields in both processes.

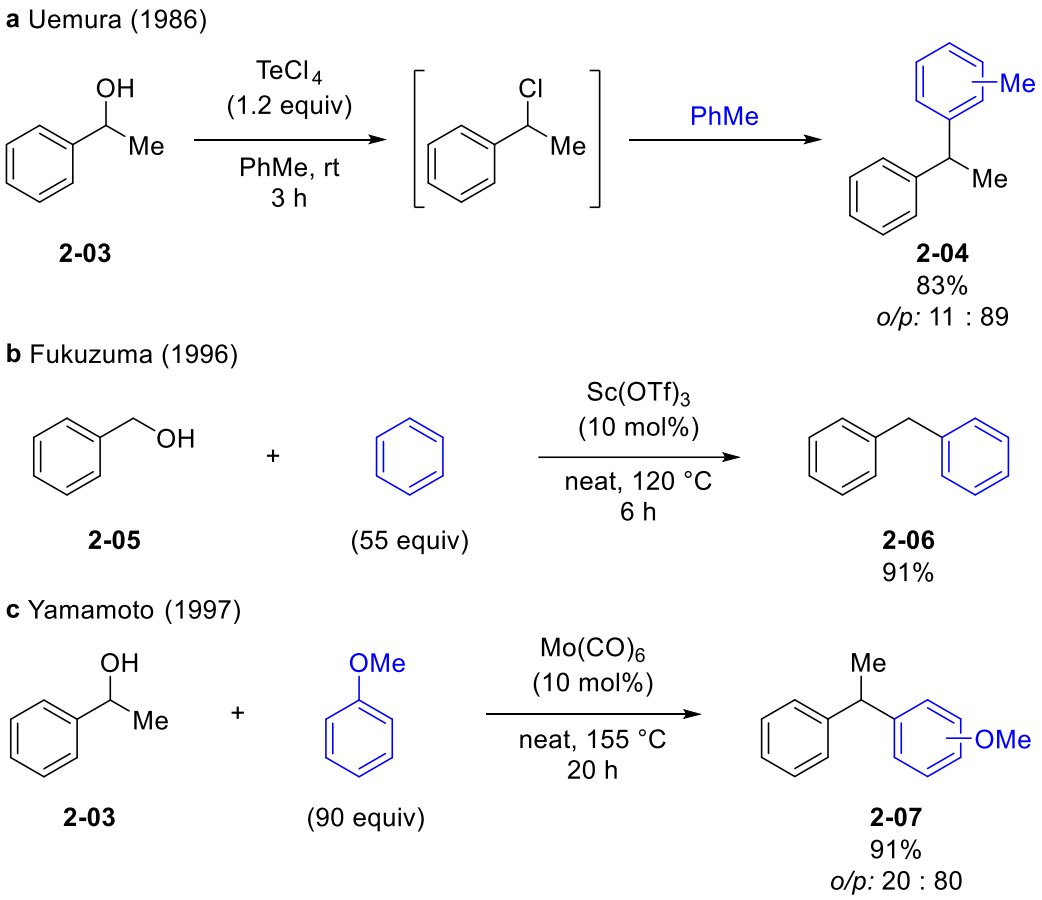

Scheme 2-3 First reported examples of catalytic Friedel-Crafts alkylation using benzylic alcohols.

After these pioneering early reports, a variety of other catalytic systems were examined for the Friedel-Crafts alkylation using benzyl alcohols. Numerous rare-earth or main group metal Lewis acids (including Si, Hf, Yb, La, and In)[12–14] were shown to be effective catalysts, as well as supramolecular catalysts,[15] heterobimetallic Ir-Sn systems,[16] and even molecular iodine.[17] The catalytic activity of various transition metal chlorides was studied by Beller and co-workers in 2005, where metals such as Au(III), Ir(II), Rh(III), Pt(IV) and Fe(III) were all shown to be effective catalysts.[18–20]. The use of a Re_2O_7 as a catalyst was recently described by Floreancig and co-workers.[21] Mechanistic studies demonstrated the formation of an activated perrhenate ester (–$OReO_3$) intermediate, which was a superior Friedel-Crafts substrate than the analogous chloride

or bromide.[21] Strong Brønsted acids have also been reported as catalysts in this transformation, including the use of triflic acid at high temperatures by Moran and co-workers.[22]

Despite the significant advances that have been made in the direct Friedel-Crafts alkylation with benzyl alcohols, many limitations remain in this field. Namely, these protocols often require the use of toxic, rare or expensive metal catalysts, and are often limited to electron-rich or activated substrates. Additionally, harsh reaction conditions or high temperatures are often required which may limit functional group tolerance, and large excesses of the nucleophilic arene are often required. Considering these limitations, the development of mild and direct catalytic systems remains of great interest to synthetic chemists.

In this regard, Boronic Acid Catalysis (BAC) offers a promising new strategy for the direct catalytic activation of alcohols towards a metal-free Friedel-Crafts alkylation (Scheme 2–4).[23] As described in Section 1.3, the reversible interaction between alcohol substrates and boronic acids provides transient C–O bond activation through an electron-withdrawing effect, as well as promoting ionization of the C–O bond to the corresponding carbocation by formation of a stabilized hydroxyboronate counterion. Due to their mild acidity, boronic acid-catalyzed Friedel-Crafts methods may offer improved functional group tolerance and substrate compatibility relative to strong Brønsted or Lewis acids commonly employed as catalysts in the Friedel-Crafts reaction.[23]

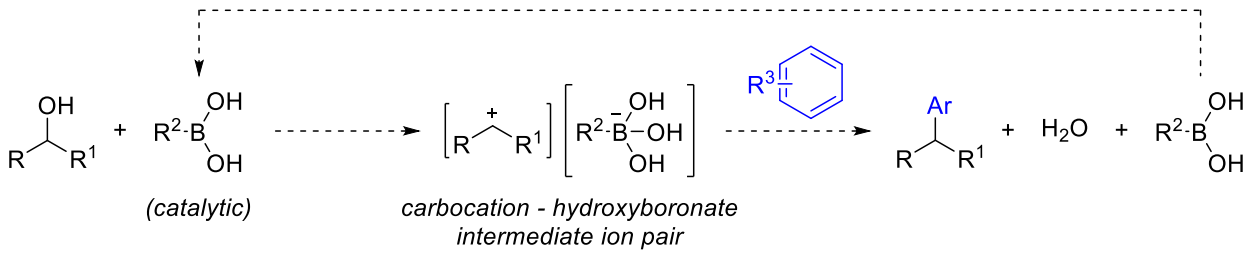

Scheme 2-4 Boronic acid-catalyzed Friedel-Crafts benzylation using benzylic alcohols.

The first boronic acid-catalyzed Friedel-Crafts reaction was described in a seminal paper by McCubbin and co-workers in 2010, who reported the allylation of electron-rich aromatics with highly activated allylic alcohols using pentafluorophenylboronic acid (**2-10**) in the presence of molecular sieves (Scheme 2-5a).[24] The boronic acid-catalyzed system was demonstrated to afford allylated products in improved yield relative to previously reported Friedel-Crafts catalysts, such as TsOH, $BF_3{\cdot}OEt_2$ and $FeCl_3$. Mechanistic studies and substrate limitations were consistent with a delocalized carbocation intermediate. While the catalyst system was subsequently also applied to both benzylic and propargylic alcohols, these methods were consistently limited in substrate scope to strongly activated alcohol partners and highly electron-rich arene nucleophiles.[24]

The Hall group later identified 2,3,4,5-tetrafluorophenylboronic acid (**2-13**) as a superior catalyst and demonstrated that intramolecular Friedel-Crafts allylations of less activated substrates proceed smoothly in nitromethane as a solvent under mild conditions (Scheme 2-5b).[25] Furthermore, a joint study by the Hall and McCubbin groups in 2015 identified an optimal solvent mixture for this transformation containing hexafluoroisopropanol (HFIP) and nitromethane ($MeNO_2$) in a 4:1 ratio (Scheme 2-5c).[26] It was believed that the use of large proportions of HFIP are instrumental in facilitating substrate ionization due to the high ionizing power ($Y_{OTs} = 3.79$) and low nucleophilicity ($N_{OTs} = –4.23$) of this polar solvent, making it effective for stabilizing carbocation intermediates and allowing for facile allylation or benzylation of electronically neutral arenes under mild conditions.[27,28]

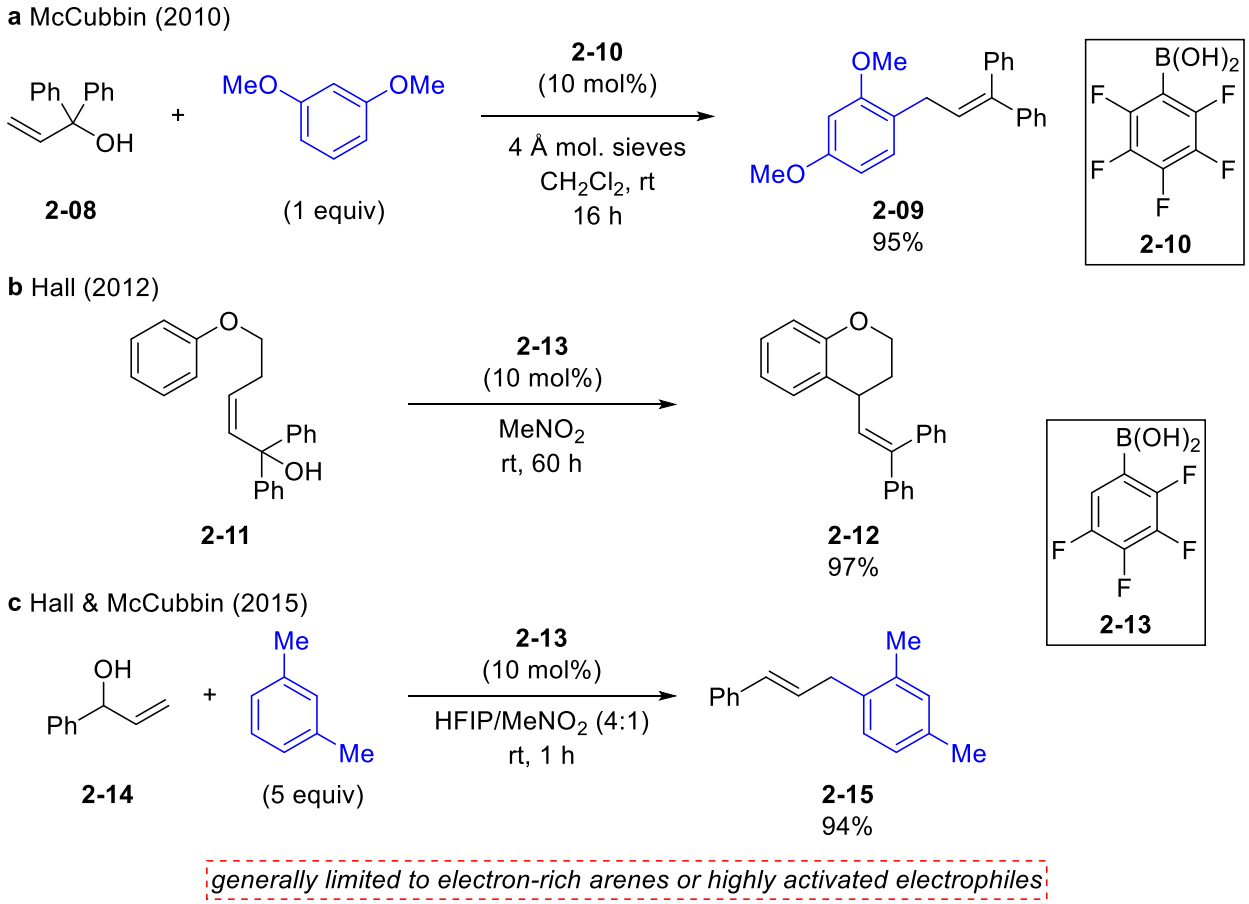

Scheme 2-5 Advances in boronic acid-catalyzed Friedel-Crafts alkylation using benzylic alcohols.

A significant advance in catalyst design was described by Hall and co-workers in 2015, who reported the use of ferrocenium boronic acid hexafluoroantimonate salt (**2-16**) as a highly active catalyst for Friedel-Crafts benzylations (Scheme 2-6).[29] By employing this novel catalyst with the previously detailed HFIP/$MeNO_2$ solvent mixture, a variety of diarylmethanes were synthesized under mild conditions through direct Friedel-Crafts alkylation of primary benzylic alcohols with weakly activated or neutral arenes. Mechanistic studies suggested that the ionic nature of the catalyst was essential and demonstrated that cationic catalyst **2-16** was significantly more reactive than neutral boronic acid catalysts with comparable pK_a. An S_N1 mechanism was proposed, in which substrate ionization affords a zwitterionic ferrocenium boronate species along

with a more reactive carbocation paired with the weakly coordinating hexafluoroantimonate anion.[29]

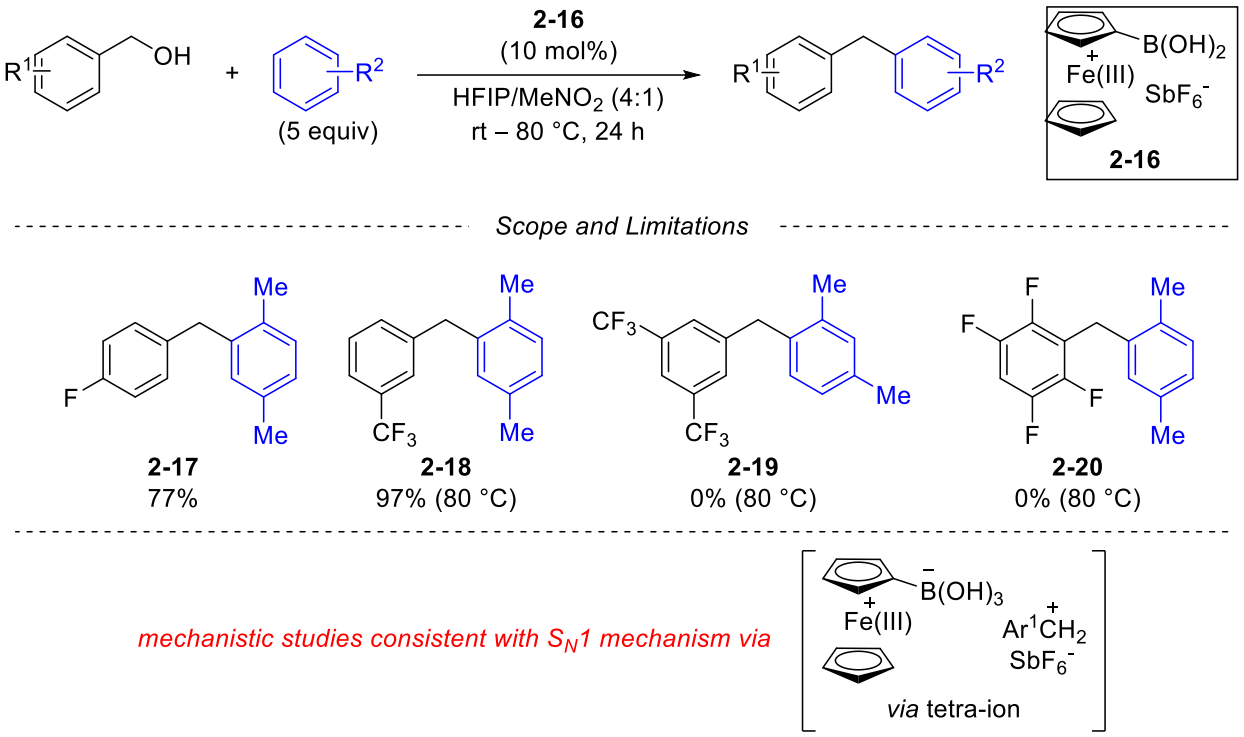

Scheme 2-6 Synthesis of diarylmethanes via Friedel-Crafts benzylation of primary benzylic alcohols catalyzed by ferrocenium boronic acid hexafluoroantimonate salt **(2-16)** reported by the Hall Group.

While this catalyst system was effective for the synthesis of a variety of unsymmetrical diarylmethanes, highly electron-deficient alcohols were poor substrates even at elevated temperatures and the corresponding diarylmethanes (**2-19** and **2-20**) were not obtained. This likely stems from the increased barrier to C–O bond activation arising from destabilization of the carbocation intermediate.[29] Due to the use of hexafluoroisopropanol as a reaction solvent, it was suspected that catalysis may be promoted by transient formation of a mono- or di-hexafluoroisopropoxy boronic ester *in situ*, with the electron-withdrawing fluorine groups increasing the Lewis acidity of boron. Accordingly, a suitable diol-co-catalyst could be designed

to promote formation of a catalytically active boronic ester, allowing for modulation of catalyst reactivity analogous to the use of a ligand for transition metal catalysts.

Along these lines, Moran and co-workers reported in 2015 the use of oxalic acid (**2-23**) as an effective co-catalyst in Friedel-Crafts reaction catalyzed by pentafluorophenylboronic acid (**2-10**) (Scheme 2-7a),[30] suggesting that proper choice of diol co-catalyst could be a promising strategy to increasing catalyst reactivity. We became interested in examining the effect of a co-catalytic diol additive to expand the scope of boronic acid-catalyzed Friedel-Crafts benzylation reactions. Our group has also recently demonstrated the use of perfluoropinacol (**2-27**) as a highly active co-catalyst in the boronic acid-catalyzed Beckmann rearrangement of ketoximes (Scheme 2-7b), where mechanistic studies revealed that its activating effect originates from the formation of Lewis acidic boronic ester **2-28** *in situ*.[31] This served as an important confirmation that identification of a suitable co-catalytic additive can have a remarkable impact on the efficiency of boronic acid-catalyzed transformations.

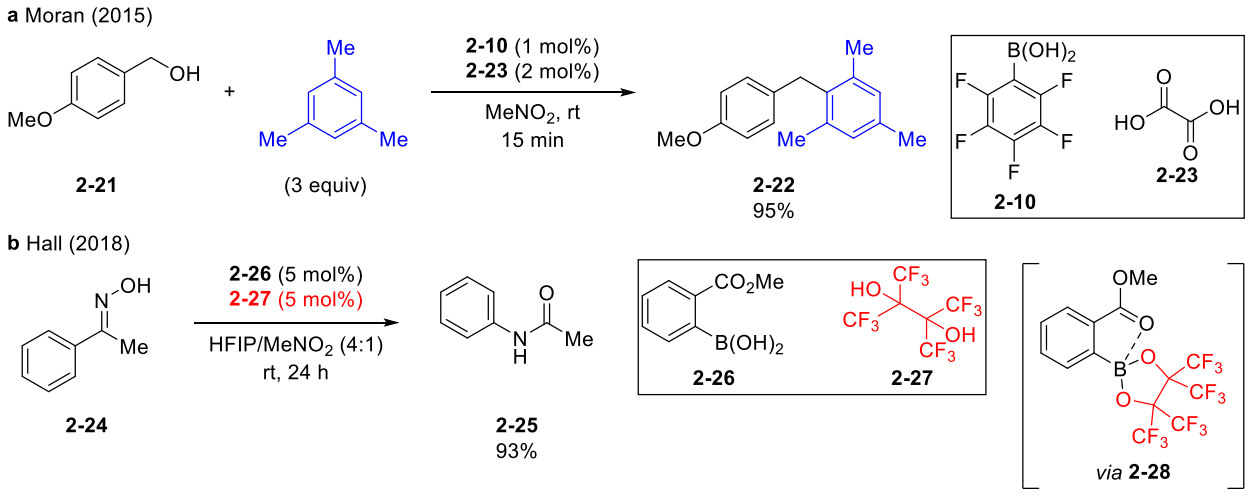

Scheme 2-7 Examples of the use of co-catalytic diol additives in a boronic acid-catalyzed Friedel-Crafts reaction and Beckmann rearrangement.

2.2 Objectives

Evidence has increasingly emerged in recent years that chiral molecules, containing tunable three-dimensional structures and stereochemistry, are often improved drug candidates with fewer off-target effects relative to "flat" molecules composed predominantly of biaryl motifs or sp^2-hyridized units.[32] Accordingly, we were interested in expanding the scope of boronic acid-catalyzed Friedel-Crafts reactions to encompass a wider range of secondary alcohol substrates, particularly those which are electronically deactivated. Furthermore, the ability of co-catalytic diol additives to mediate reactivity in boronic acid-catalyzed Friedel-Crafts reactions warranted further examination.

This chapter will describe research undertaken towards a more general boronic acid-catalyzed benzylation reaction of secondary alcohols through the discovery of a two-component catalyst system. Identification of a diol additive that can afford significantly improved reactivity for challenging substrates will be examined, as well as the ability to use increasingly mild boronic acids to promote alcohol activation in the presence of an activating diol. Additionally, mechanistic studies will be carried out to gain an improved understanding of C–O bond activation in boronic acid-catalyzed systems, and the role of the co-catalytic diol additive will be examined.

2.3 Results and Discussion

2.3.1 Background and Preliminary Results

The identification of an effective co-catalytic diol additive was performed by fellow graduate student Hwee Ting Ang. The reaction between *p*-nitrobenzyl alcohol (**2-29**) and *p*-xylene (**2-30**) was chosen as a model reaction under previously optimized conditions,[29] as substrate **2-29** had previously demonstrated sluggish reactivity presumably due to the increased barrier towards C–O bond activation brought on by the electron-withdrawing nitro group. A variety of diols were

screened for their ability to enhance this reaction using boronic acid **2-16** as a catalyst (Table 2–1).

In the absence of a diol additive, the desired diarylmethane **2-31** was obtained in low yield (Entry 1). The use of 10 mol% perfluoropinacol (**2-27**) as a co-catalyst, which had previously proven useful in the boronic acid-catalyzed Beckmann rearrangement,[31] gave a notable increase in yield (Entry 2) and outperformed the other diols that were examined (Entries 3-6). Using perfluoropinacol, no improvement in yield was obtained by increasing the temperature (Entry 7), the reaction time (Entry 8) or the equivalents of co-catalyst (Entry 9). A control experiment in the absence of boronic acid **2-16** showed that perfluoropinacol alone does not catalyze the reaction, suggesting a synergistic interaction between co-catalysts **2-16** and **2-27**.

Table 2-1 Screening of co-catalytic additives for the Friedel-Crafts benzylation of alcohol **2-29** catalyzed by **2-16** performed by Hwee Ting Ang.

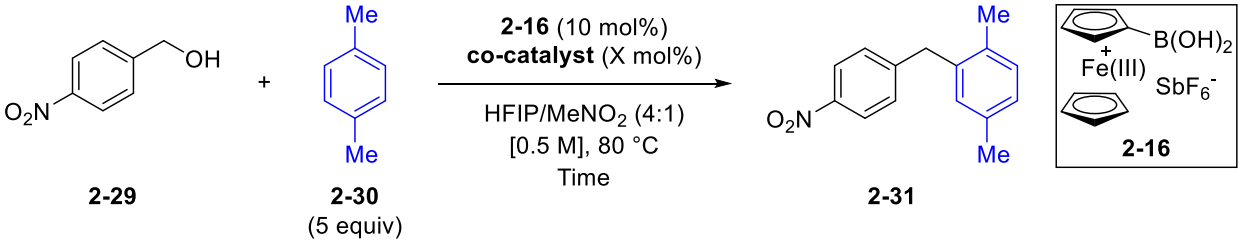

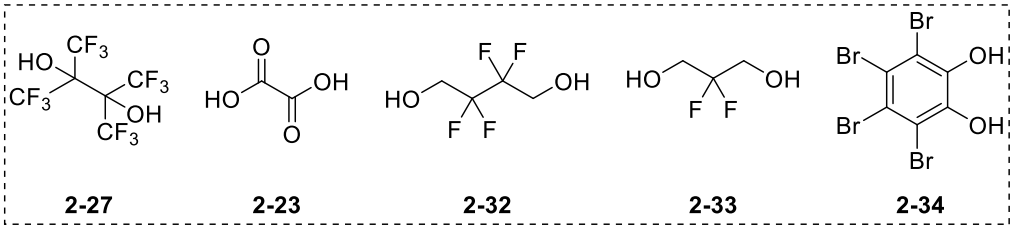

Entry	Co-catalyst	X mol%	Time	Yield **2-31**[a]
1	-	-	24 h	10
2	**2-27**	10	24 h	26
3	**2-23**	10	24 h	10
4	**2-32**	10	24 h	4
5	**2-33**	10	24 h	1
6	**2-34**	10	24 h	6
7[b]	**2-27**	10	24 h	24
8	**2-27**	10	7 days	30
9	**2-27**	100	24 h	28
10[c]	**2-27**	10	24 h	0

Reactions were performed on 0.15 mmol scale of **2-29.** [a]Yield determined by ^{1}H NMR spectroscopy relative to 1,4-dinitrobenzene as an internal standard. [b]Reaction conducted at 100 °C. [c]Reaction conducted without **2-16.**

2.3.2 Synthesis of Triarylmethanes: Optimization of Reaction Conditions

Following identification of an effective co-catalytic additive by Dr. Ang, I examined the use of perfluoropinacol (**2-27**) to promote Friedel-Crafts reactions of secondary benzylic alcohols. The synthesis of triarylmethanes from benzhydryl alcohols was chosen as an area of focus as these substrates had not been examined in our group's previous efforts in boronic acid-catalyzed Friedel-

Crafts reactions. Furthermore, with the enhanced reactivity afforded by perfluoropinacol in mind, subsequent reaction development was performed using shelf-stable boronic acid **2-13** in place of **2-16**, highlighting the ability to use more accessible, stable, and synthetically tunable catalysts in conjunction with a suitable co-catalytic additive.[26]

The Friedel-Crafts reaction between diphenylmethanol **2-35a** and p-xylene **2-30** was examined as an initial model reaction for triarylmethane synthesis using 2,3,4,5-tetrafluorophenylboronic acid (**2-13**) as a catalyst due to its successful use in other Friedel-Crafts reactions (see Section 2.1). In the absence of a diol additive, boronic acid **2-13** was an ineffective catalyst and did not promote formation of the desired triarylmethane **2-36a** (Table 2–2, Entries 1-3). However, good conversion of the starting alcohol to symmetrical ether **2-37** was observed, arising from dehydrative dimerization of the starting alcohol. Conversion of alcohol **2-35a** to ether **2-37** proceeded more effectively at higher temperatures, but triarylmethane **2-36a** was not observed even at 80 °C. The use of perfluoropinacol (**2-27**) as an additive had a dramatic effect on the reaction outcome and resulted in successful formation of triarylmethane **2-36a** even at room temperature (Entry 4). Improved yields were obtained at elevated temperatures, with virtually complete conversion and 85% yield obtained at 80 °C (Entry 6).

Table 2-2 Reaction optimization for the synthesis of triarylmethane **2-36a** through boronic acid-catalyzed Friedel-Crafts benzylation with diphenylmethanol **2-35a**.

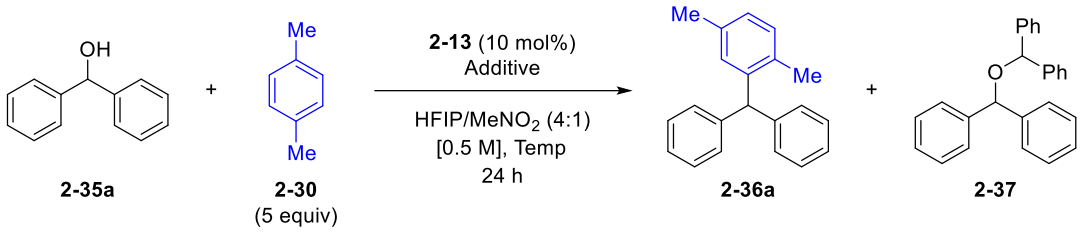

2-35a | **2-30** (5 equiv) | **2-36a** | **2-37**

Entry	Temperature	Additive	Yield **2-35a**[a]	Yield **2-36a**[a]	Yield **2-37**[a]
1	rt	-	27%	0%	47%
2	50 °C	-	0%	0%	79%
3	80 °C	-	0%	0%	80%
4	rt	**2-27** (10 mol%)	10%	20%	55%
5	50 °C	**2-27** (10 mol%)	15%	60%	0%
6	80 °C	**2-27** (10 mol%)	7%	85%	0%

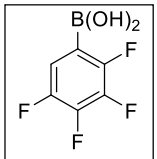

2-13

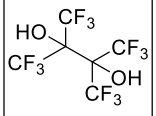

2-27

Reactions were performed on 0.15 mmol scale of **2-35a.** [a]Yield determined by ^{1}H NMR relative to 1,3,5-trimethoxybenzene or dibromomethane as an internal standard.

The use of a hexafluoroisopropanol/nitromethane (4:1) solvent mixture gave improved yield of Friedel-Crafts product **2-36a** relative to either of the component solvents alone (Table 2-3, Entries 1-3). Employing perfluoropinacol as a catalyst in the absence of boronic acid resulted in no formation of triarylmethane **2-36a**, but ether **2-37** was detected in good yield (Entry 4). A control reaction in the absence of both co-catalysts gave quantitative recovery of the starting material, confirming that the Brønsted acidic HFIP solvent does not catalyze the reaction (Entry 5).

Table 2-3 Continued reaction optimization for the synthesis of triarylmethane **2-36a** through boronic acid-catalyzed Friedel-Crafts benzylation with diphenylmethanol **2-35a**.

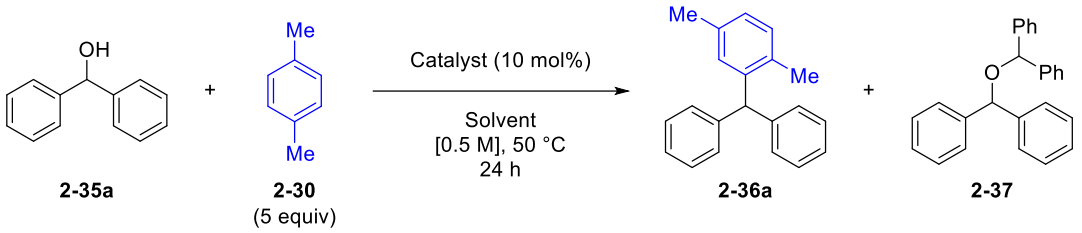

2-35a **2-30** (5 equiv) **2-36a** **2-37**

Entry	Solvent	Catalyst	Yield **2-35a**[a]	Yield **2-36a**[a]	Yield **2-37**[a]
1	HFIP/$MeNO_2$ (4:1)	**2-13** + **2-27**	15%	60%	0%
2	HFIP	**2-13** + **2-27**	11%	19%	66%
3	$MeNO_2$	**2-13** + **2-27**	4%	29%	57%
4[b]	HFIP/$MeNO_2$ (4:1)	**2-27**	18%	0%	80%
5[b]	HFIP/$MeNO_2$ (4:1)	None	96%	0%	0%

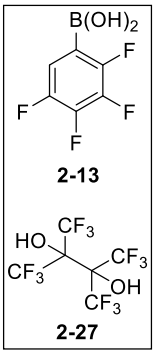

2-13 **2-27**

Reactions were performed on 0.15 mmol scale of **2-35a.** [a]Yield determined by ^{1}H NMR relative to 1,3,5-trimethoxybenzene or dibromomethane as an internal standard. [b]Reaction conducted at 80 °C.

Thus, optimized conditions employed 10 mol% of 2,3,4,5-tetrafluorophenylboronic acid (**2-13**) and perfluoropinacol (**2-27**) as co-catalysts with 5 equivalents of *p*-xylene (**2-30**) in HFIP/$MeNO_2$ (4:1) at 80 °C for 24 hours.

2.3.3 Substrate Scope

With optimized conditions in hand, the scope of diarylmethanol derivatives was then evaluated using the **2-13**/**2-27** co-catalytic system (Scheme 2-8). Triarylmethane **2-36a** was isolated in good yield comparable to the NMR yields determined during reaction optimization. A variety of halogenated benzhydryl alcohols were successfully converted to the corresponding triarylmethanes (**2-36b–d**) in good yield. An increasingly electron-deficient alcohol containing a 3,5-bis(trifluoromethyl)phenyl moiety gave low yield of the corresponding triarylmethane (**2-36e**) under the standard conditions, but dramatically improved yield of 88% was obtained by increasing the temperature to 100 °C and doubling the catalyst loading (experiment with increased catalyst

loading done by Hwee Ting Ang). In all cases, the desired triarylmethanes were not formed in the absence of the co-catalytic diol and mixtures of unreacted starting material and symmetrical ethers were obtained.

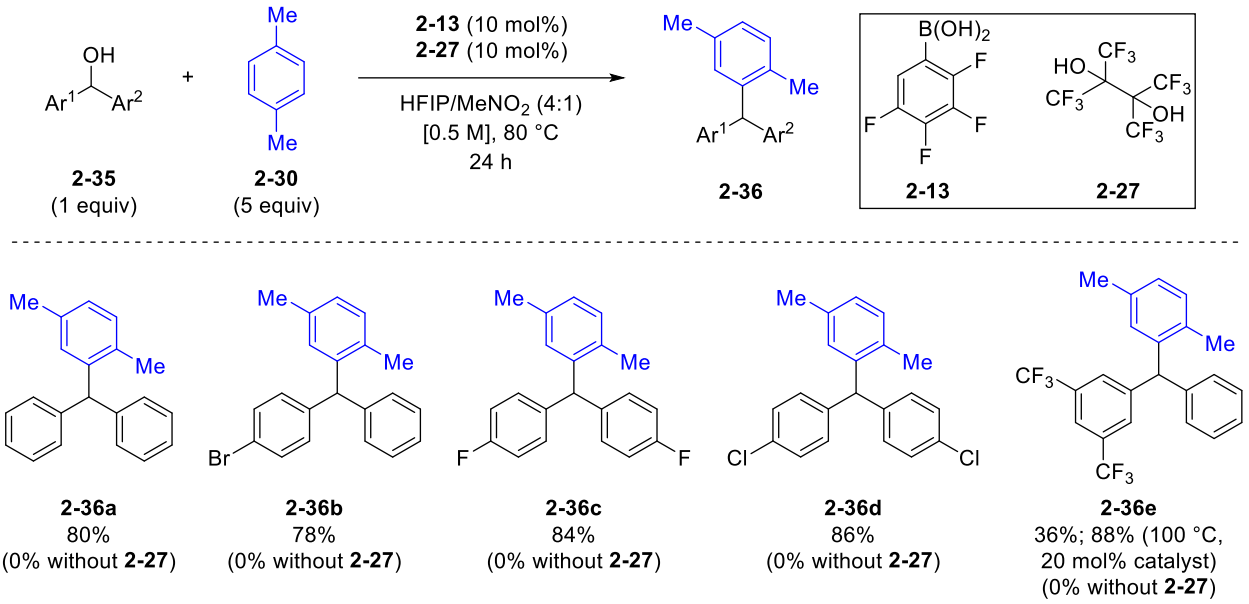

Scheme 2-8 Substrate scope of the direct boronic acid-catalyzed Friedel-Crafts benzylation with diarylmethanol substrates catalyzed by **2-13** and **2-27**.

Concurrently, the scope of the Friedel-Crafts benzylation of 1-arylethanol derivatives using the **2-13**/**2-27** co-catalytic system was investigated by Hwee Ting Ang (Scheme 2-9). In all cases, dramatically improved yield of the corresponding 1,1-diarylalkane was observed with the use of co-catalyst **2-27**. A variety of electronically deactivated alcohol substrates were effective coupling partners in this reaction, including those bearing halogen (**2-39c**), ester (**2-39d**), trifluoromethyl (**2-39e**) and sulphonyl (**2-39f**) moieties. Nitro-substituted diarylethanes **2-39g** and **2-39h** were synthesized in good yield by increasing the reaction temperature to 100 °C, demonstrating that even substrates bearing strongly electron-withdrawing groups can be functionalized using the co-catalytic system of **2-13** and **2-27**.

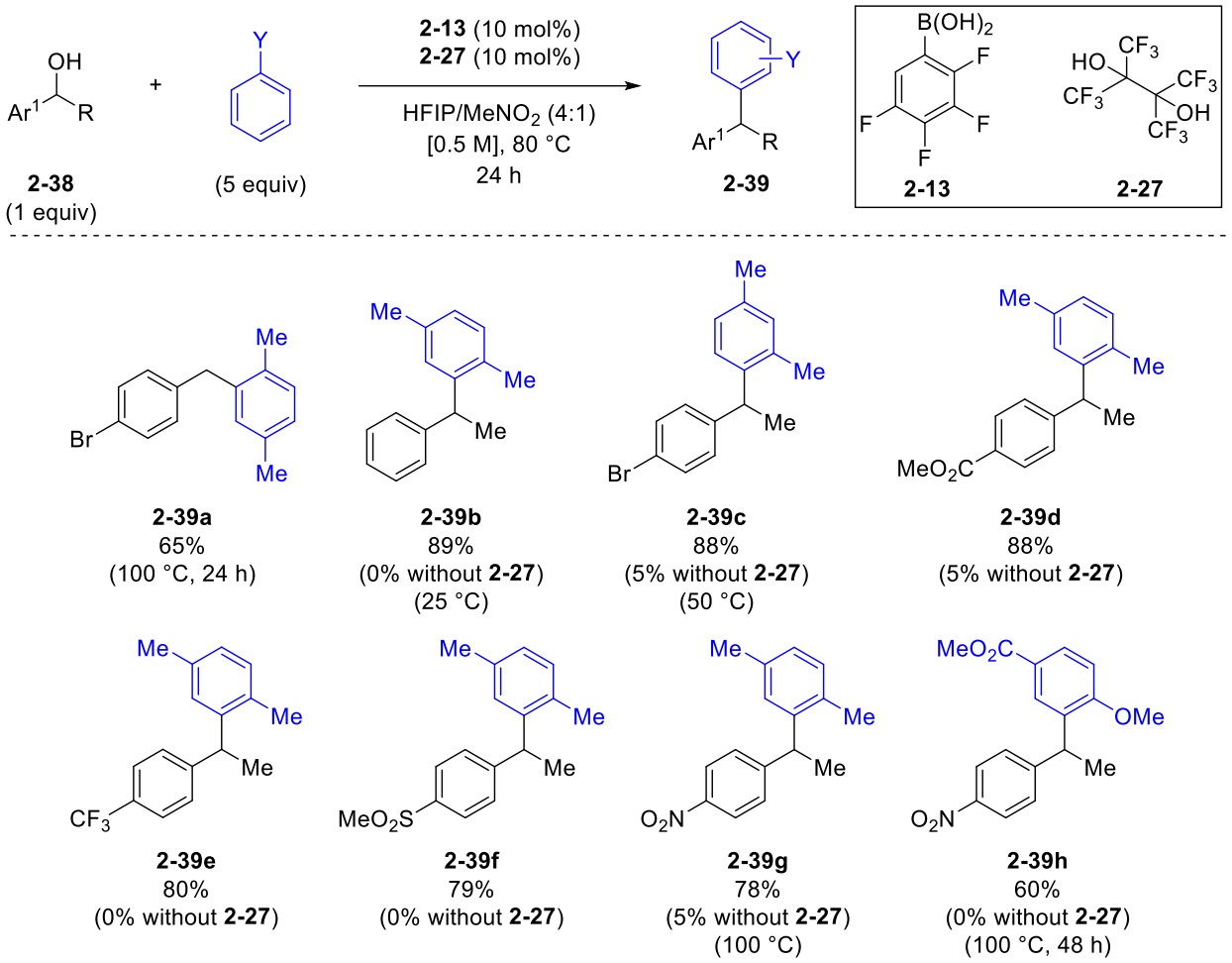

Scheme 2-9 Substrate scope of the direct boronic acid-catalyzed Friedel-Crafts benzylation with 1-arylethanol derivatives catalyzed by **2-13** and **2-27** performed by Hwee Ting Ang.

Having conducted a preliminary investigation of the scope of the boronic acid-catalyzed Friedel-Crafts benzylation, further studies were carried out to elucidate the identity of any reaction intermediates and to understand the mechanism of C–O bond activation.

2.3.4 Mechanistic Studies

2.3.4.1 Kinetic Studies

A key observation during reaction optimization was that ether **2-37** was the major product of the reaction at lower temperatures, or when perfluoropinacol was not used. However, ether **2-37** was

not detected at higher temperatures when the diol additive was used in conjunction with the boronic acid. When isolated ether **2-37** was subjected to the reaction conditions employing both boronic acid catalyst and perfluoropinacol, triarylmethane **2-36a** was obtained in 74% yield (Scheme 2-10), suggesting that the ether may be an intermediate along the reaction pathway that can be further consumed. A yield greater than 50% indicated that both benzhydryl moieties in ether **2-37** were ultimately consumed to form triarylmethane **2-36a**.

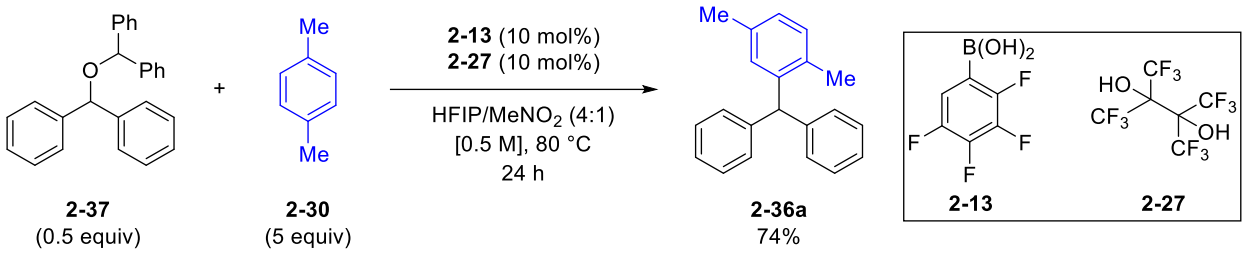

Scheme 2-10 Conversion of ether **2-37** to triarylmethane **2-36a** under optimized conditions.

To further probe the formation of ether **2-37** as an intermediate in this process, reaction monitoring experiments were conducted. The conversion of alcohol **2-35a** to triarylmethane **2-36a** was monitored by ^{1}H NMR through sequential aliquots (Figure 2-2). Rapid formation of ether **2-37** was observed in the initial phase of the reaction, with approximately 80% conversion within the first 15 minutes. Formation of triarylmethane **2-36a** did not occur during this initial period. After most of the starting material was converted to ether **2-37**, further consumption of ether **2-37** occurred to ultimately form the desired triarylmethane **2-36a** in good yield at the end of the reaction. Consumption of ether **2-37** to form triarylmethane **2-36a** proceeds with concomitant release of alcohol **2-35a**. Accordingly, a relatively steady, non-zero concentration of alcohol **2-35a** was observed throughout the reaction as it was continuously reformed during consumption of the rapidly formed ether **2-37** or through capture of the carbocation intermediate by water formed as a by-product of the Friedel-Crafts reaction.

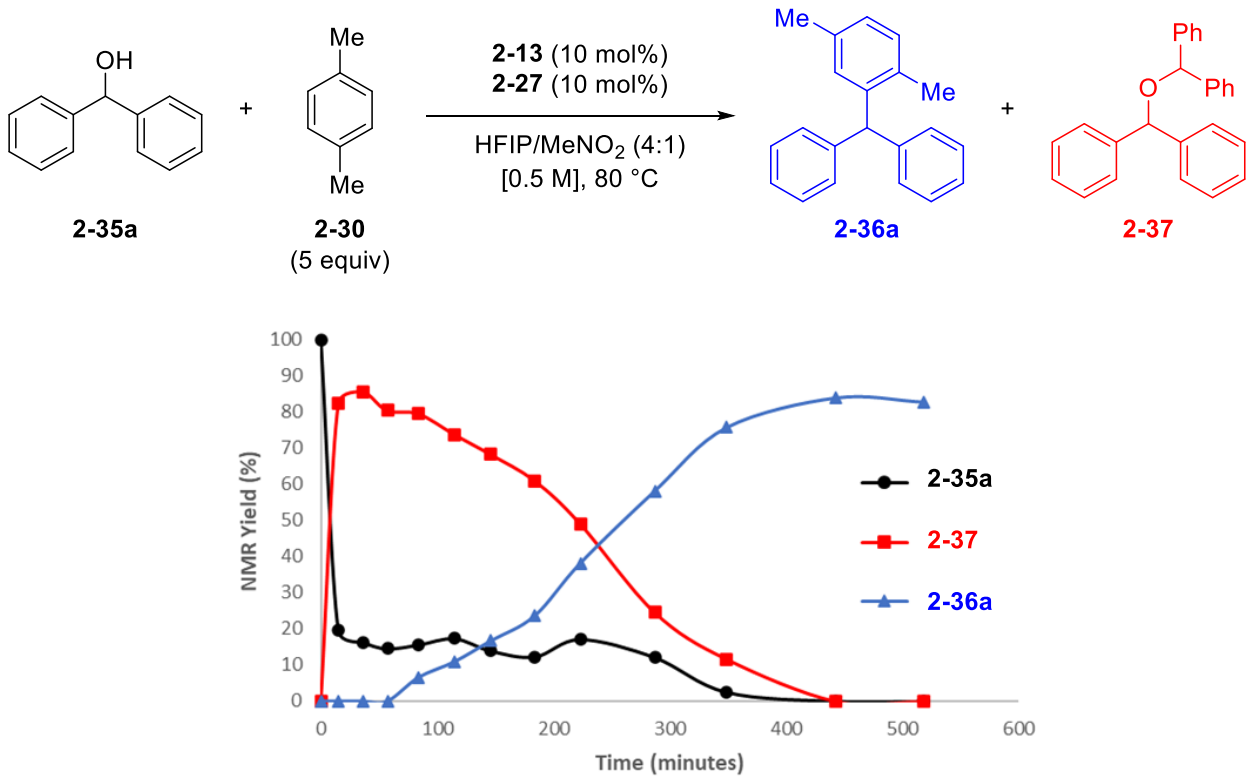

Figure 2-2 Reaction profile for the Friedel-Crafts benzylation of alcohol **2-35a** with *p*-xylene catalyzed by **2-13** and **2-27**.

Several conclusions can be made from the kinetics experiment. For one, ether **2-37** is a viable intermediate in the reaction that itself can be further consumed, rather than an off-cycle side product that is formed irreversibly. Furthermore, it is evident that ether **2-37** is the kinetic product of the reaction and is formed more rapidly than triarylmethane **2-36a**, particularly at low conversion when the concentration of free alcohol is high. This is likely due to the increased nucleophilicity of oxygen relative to the aromatic ring of *p*-xylene. Ultimately, formation of the Friedel-Crafts product **2-36a** appears to be irreversible, and triarylmethane **2-36a** can be obtained in good yield provided a sufficiently long reaction time is used.

The course of the reaction in the absence of perfluoropinacol was also examined to better understand its role as a catalytic additive (Figure 2-3). Accordingly, the reaction monitoring

experiment described above was repeated using **2-13** as a catalyst alone for 24 hours, at which point perfluoropinacol was added (indicated by the dashed vertical line in the plot) and the reaction was run for an additional 24 hours. Clean conversion of alcohol **2-35a** to ether **2-37** was observed in the absence of perfluoropinacol. Notably, starting material consumption occurred significantly more slowly in the absence of additive **2-27** relative to the optimized conditions employing the two-component catalyst system (*cf.* Figure 2-2). Additionally, formation of triarylmethane **2-36a** was not observed in the absence of the diol additive. Upon addition of perfluoropinacol, the reaction profile begins to resemble that which was observed in Figure 2-2, with a dramatic increase in the rate of conversion of alcohol **2-35a** to ether **2-37** and eventual consumption of ether **2-37** to ultimately form triarylmethane **2-36a**.

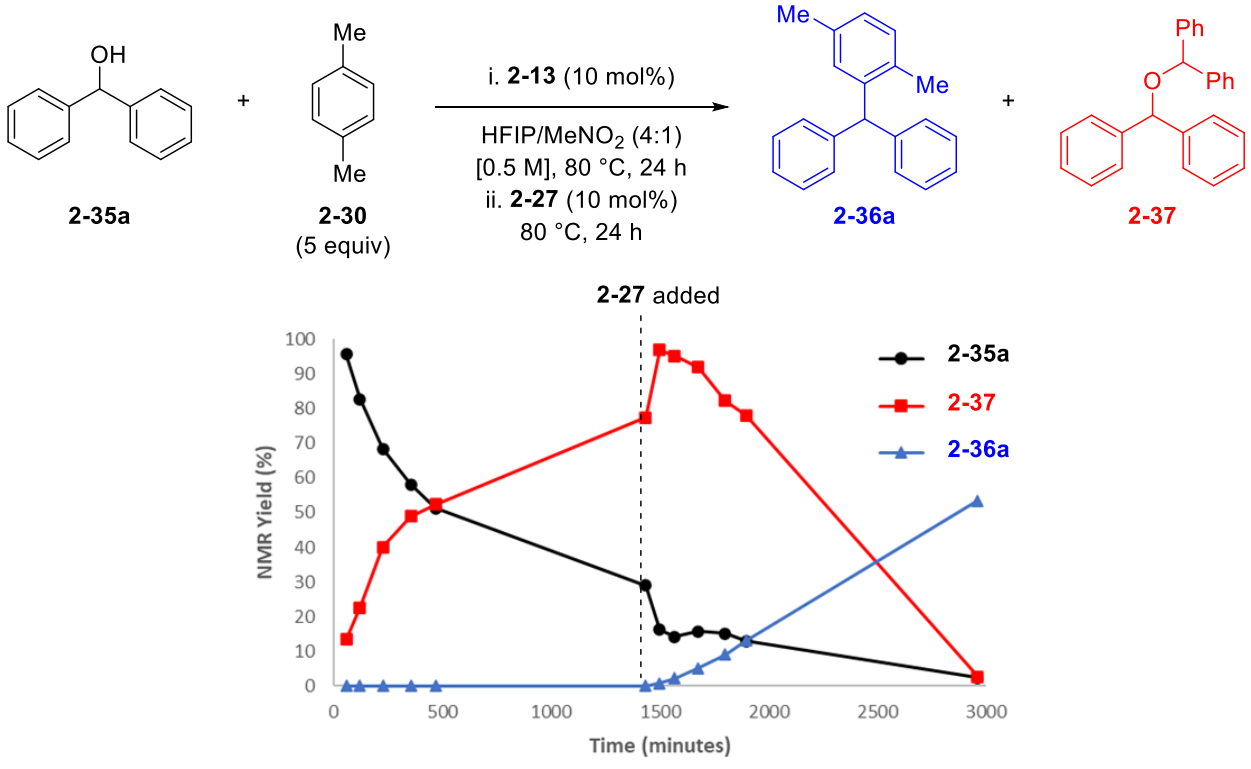

Figure 2-3 Reaction profile for the Friedel-Crafts benzylation of alcohol **2-35a** with *p*-xylene catalyzed by **2-13** alone for 24 hours prior to addition of perfluoropinacol (**2-27**).

Comparison of these two reaction monitoring experiments suggest that boronic acid **2-13** alone is a sufficiently reactive catalyst to promote C–O bond activation of the starting alcohol, but not of the corresponding ether. Under these conditions, formation of ether **2-37** appears essentially irreversible. However, addition of perfluoropinacol appears to generate a catalyst that is sufficiently active to promote C–O bond activation of the ether, with reversible ether formation ultimately driving the reaction toward irreversible formation of the Friedel-Crafts product **2-36a**.

From these observations, it was clear that further studies were necessary to better understand the nature of the catalytically active species that are formed under the reaction conditions in the presence of perfluoropinacol. These studies are described in the following section.

2.3.4.2 Characterization of Catalytic Intermediates

As mentioned in Section 2.1, the role of perfluoropinacol as an additive was previously studied by our group in the boronic acid-catalyzed Beckmann rearrangement.[31] Mechanistic studies revealed that condensation between boronic acid **2-26** and perfluoropinacol occurred to form boronic ester **2-28** (Scheme 2-11). Boronic ester formation also led to internal coordination of the neighboring carbonyl oxygen, suggesting that complexation with the highly electron-deficient diol results in an increasingly Lewis acidic boron center. This internal coordination was proposed to increase the electrophilicity of the carbonyl, promoting transesterification with the oxime substrate to generate acyl oxime **2-40**.[31]

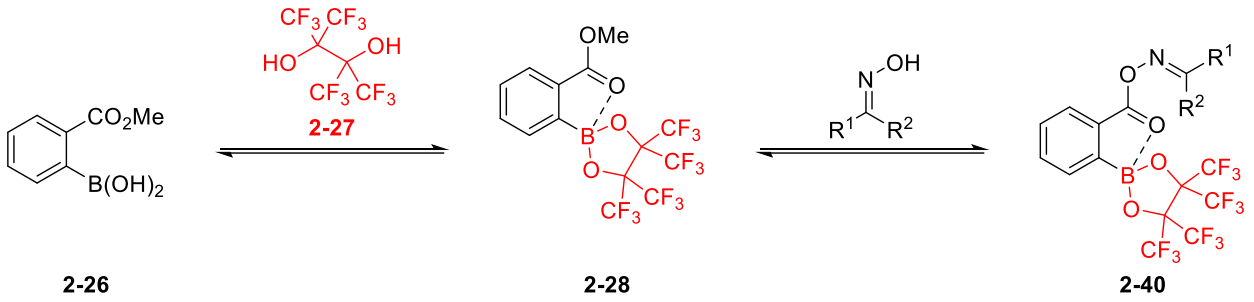

Scheme 2-11 The role of perfluoropinacol (**2-27**) as a co-catalyst in the boronic acid-catalyzed Beckmann rearrangement.

The interaction between boronic acid **2-13** and perfluoropinacol was examined by NMR spectroscopy and mass spectrometry by Hwee Ting Ang (Figure 2-4). An equimolar mixture of **2-13** and perfluoropinacol was stirred in HFIP/$MeNO_2$ (4:1) for 24 hours prior to analysis. Surprisingly, the expected three-coordinate boronic ester **2-42** was not detected by ^{11}B NMR or by mass spectrometry. Instead, a mixture of unreacted **2-13** and four-coordinate boronate **2-41** was observed. The structure of boronate **2-41** was proposed based on the molecular formula obtained from the molecular ion, while an upfield shift was observed by ^{11}B NMR consistent with a four-coordinate boron species.

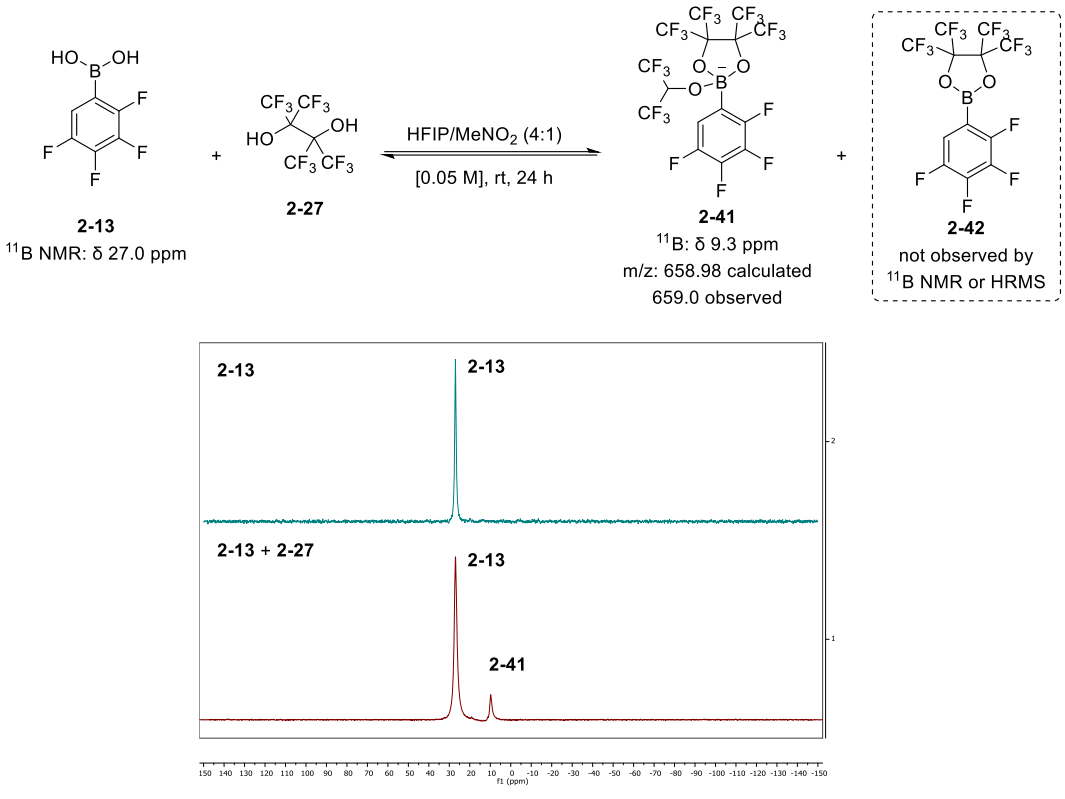

Figure 2-4 Control experiments to elucidate the interaction between boronic acid **2-13** and perfluoropinacol (**2-27**) performed by Hwee Ting Ang. ^{11}B NMR (128 MHz) experiments were run in 4:1:2 HFIP/$MeNO_2$/CD_3CN.

Boronate **2-41** presumably arises first through diol condensation to form transient three-coordinate boronic ester **2-42** (Scheme 2-12). The increase in Lewis acidity of boron upon complexation with the electron-deficient diol appears to be sufficient to promote deprotonation or auto-ionization of bound hexafluoroisopropanol solvent, resulting in a four-coordinate boron species bound to the hexafluoroisopropoxide anion (**2-41**). Due to the absence of a Brønsted basic additive to mediate the deprotonation, boronate **2-41** likely exists with a hydronium (H_3O^+) counterion.[33]

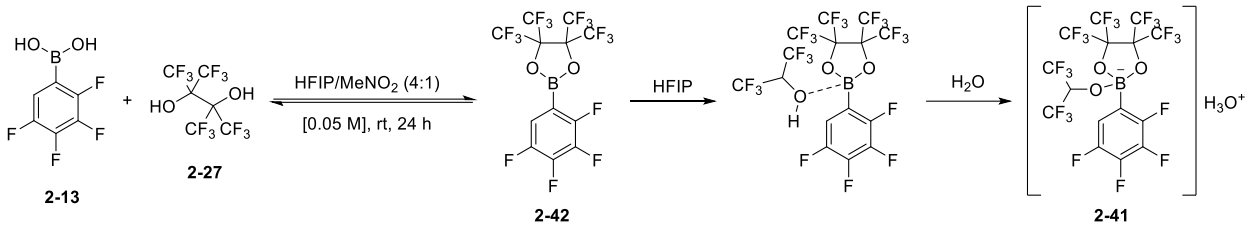

Scheme 2-12 Mechanism of formation of hydronium boronate **2-41** from boronic acid **2-13** in the presence of perfluoropinacol (**2-27**) and HFIP.

To support the hypothesis that the increased Lewis acidity of the perfluoropinacol boronic ester is responsible for formation of the tetrahedral boronate, two control experiments were performed by Hwee Ting Ang. In the absence of perfluoropinacol, the corresponding anionic hexafluoroisopropylborate complexes (**2-43**, **2-44**, and **2-45**) of boronic acid **2-13** were not observed (Scheme 2-13a). Similarly, in the presence of pinacol, the three-coordinate pinacol boronic ester **2-46** was observed by NMR, and the corresponding anionic complex **2-47** was not detected (Scheme 2-13b). These results are consistent with the increased Lewis acidity as a result of perfluoropinacol coordination and show that perfluoropinacolate formation is necessary in order to promote four-coordinate boronate complexation.

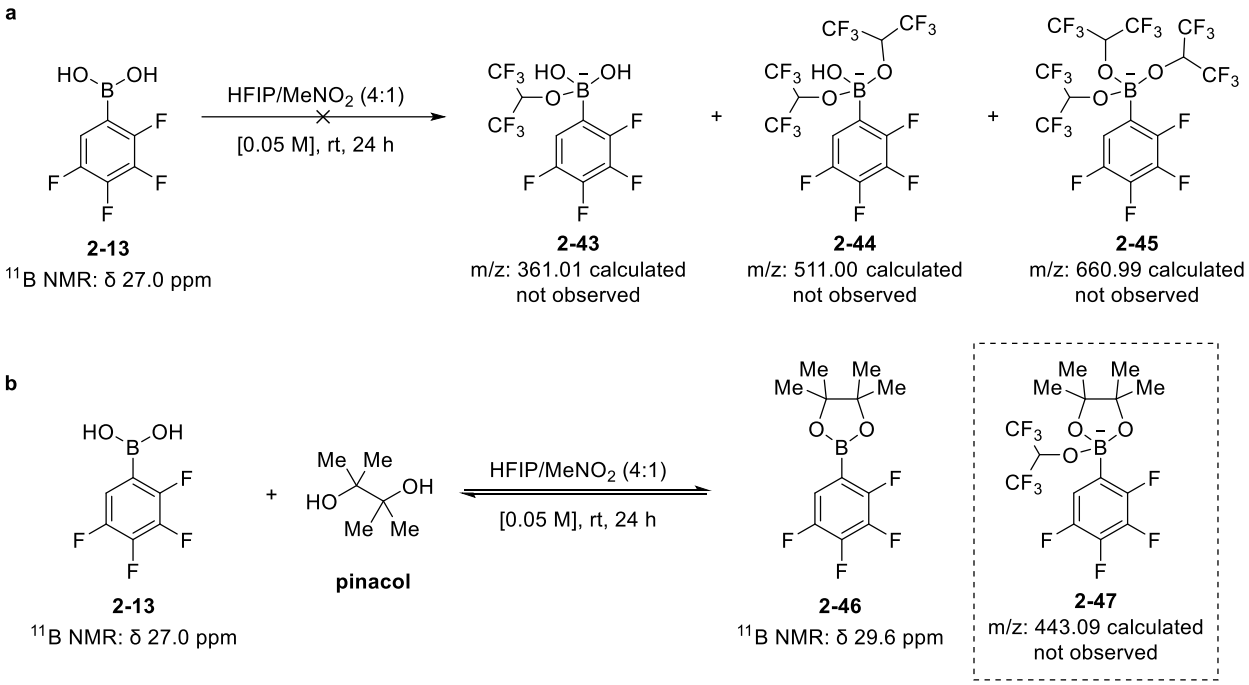

Scheme 2-13 Control experiments to probe four-coordinate boronate formation from boronic acid **2-13** in the absence of perfluoropinacol (**2-27**) performed by Hwee Ting Ang.

2.3.4.3 Additives and Inhibition Studies

A functional group robustness screen[34] was conducted for the synthesis of model diarylmethane **2-39a** catalyzed by ferrocenium boronic acid **2-10** and perfluoropinacol to gain a better understanding of the generality of the reaction (Table 2-4). The reaction was moderately tolerant to various nucleophilic functionalities, including phenol (Entry 3), benzoic acid (Entry 4) thiophenol (Entry 5) and aliphatic alcohols (Entries 6 and 7). However, it was revealed that the reaction was inhibited by basic amines, including pyridine (Entry 2), glycine (Entry 8) and 2,6-di-*tert*-butylpyridine (Entry 12).

Table 2-4 Study of the effect of additives on the synthesis of diarylmethane **2-39a** catalyzed by ferrocenium boronic acid **2-13** and perfluoropinacol (**2-27**).

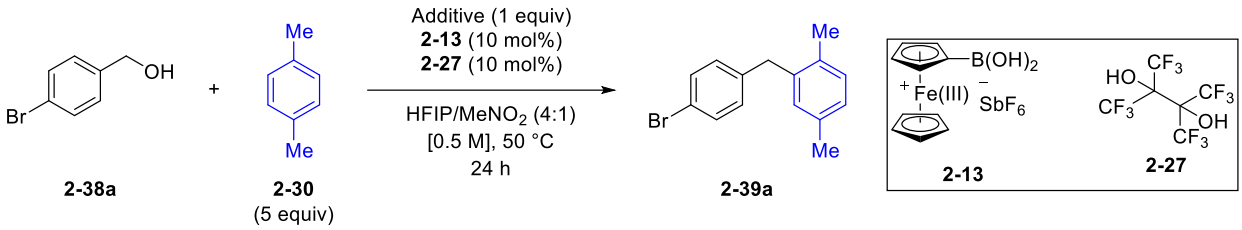

Entry	Additive	Yield **2-39a**[a]	Entry	Additive	Yield **2-39a**[a]
1	None	99%	7	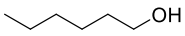	70%
2		0%	8	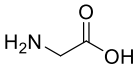	0%
3	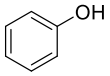	66%	9	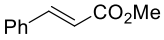	79%
4	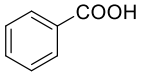	80%	10	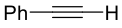	74%
5	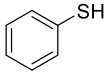	55%	11	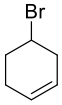	94%
6	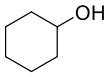	72%	12	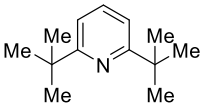	0%

2-48

Reactions were performed on 0.15 mmol scale of **2-39a.** [a]Yield determined by ^{1}H NMR relative to 1,3,5-trimethoxybenzene or dibromomethane as an internal standard.

Inhibition by 2,6-di-*tert*-butylpyridine (**2-48**) is regarded as strong evidence for a protic acid-dependent reaction mechanism rather than Lewis acid. It has been demonstrated by H.C. Brown and co-workers that this highly sterically hindered base is unlikely to coordinate to boron Lewis acids due to steric hindrance, as even the relatively unhindered boron trifluoride showed no complexation with this bulky Lewis base (Scheme 2-14).[35] However, 2,6-di-*tert*-butylpyridine is protonated by Brønsted acids such as HCl to form the corresponding pyridinium salt **2-49**.[35] Thus, 2,6-di-*tert*-butylpyridine can function as a mechanistic probe to differentiate between Brønsted acid- and Lewis acid-dependent mechanisms in acid-catalyzed processes.

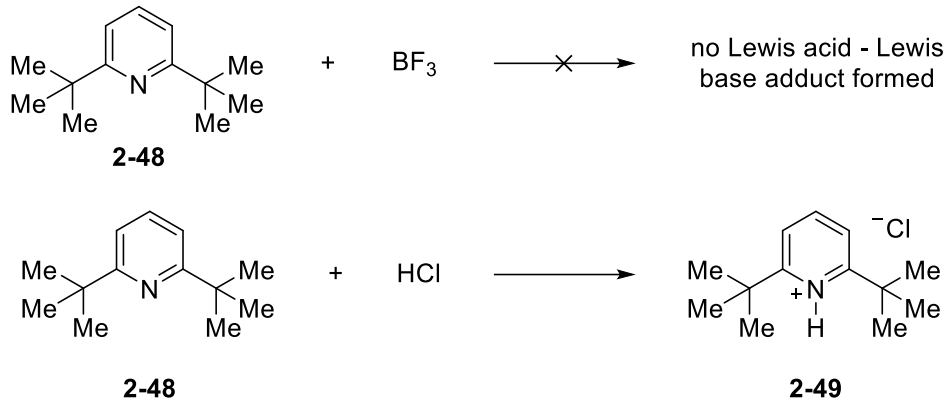

Scheme 2-14 The differing reactivity of 2,6-di-*tert*-butylpyridine (**2-48**) with respect to Lewis acids and Brønsted acids as described by Brown and co-workers.

Furthermore, while these studies were being performed in our group, Taylor and co-workers reported the dehydrative substitution of benzylic alcohols using pentafluorophenylboronic acid and oxalic acid as catalysts and proposed that the reaction proceed via a protic-acid dependent mechanism (Scheme 2-15).[33] Hydronium boronate species **2-52** was isolated and successfully used as a catalyst for the reaction in comparable yield to *in situ* catalyst formation, while complete inhibition was observed by 2,6-di-*tert*-butylpyridine. These results demonstrated the catalytic relevancy of these hydronium boronate species and suggested that Brønsted-acid dependent mechanisms may be operative in boronic acid-catalyzed transformations that involve similar intermediates.

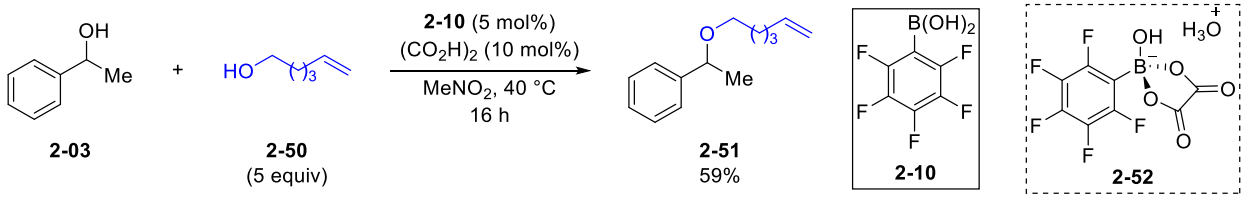

Scheme 2-15 Intermolecular dehydrative substitution of benzylic alcohols catalyzed by pentafluorophenylboronic acid (**2-10**) and oxalic acid reported by Taylor.

The effect of 2,6-di-*tert*-butylpyridine on the synthesis of triarylmethane **2-36a** was examined at different equivalents relative to the two-component catalyst system of boronic acid **2-13** and perfluoropinacol (Table 2-5). Using 10 mol% of **2-13** and perfluoropinacol, the use of a slight excess of the bulky pyridine (12 mol%) led to complete inhibition of the Friedel-Crafts reaction, but ether **2-37** was obtained in moderate yield along with recovered starting alcohol **2-35a** (Entry 2). However, when the pyridine additive was increased beyond the combined catalyst loading of **2-13** and **2-27**, quantitative recovery of the starting alcohol was observed (Entries 3 and 4). Taken together, these results suggest that C–O bond activation of the starting alcohol may proceed through several mechanisms or a combination of Lewis acid and Brønsted acid catalysis mediated by numerous catalytically active species. However, further activation of ether **2-37** to ultimately form triarylmethane **2-36a** is completely inhibited by addition of 2,6-di-*tert*-butylpyridine and thus likely proceeds through the action of a Brønsted-acidic hydronium boronate species.

Table 2-5 The effect of 2,6-di-*tert*-butylpyridine (**2-48**) on the Friedel-Crafts reaction of alcohol **2-35a** catalyzed by boronic acid **2-13** and perfluoropinacol (**2-27**).

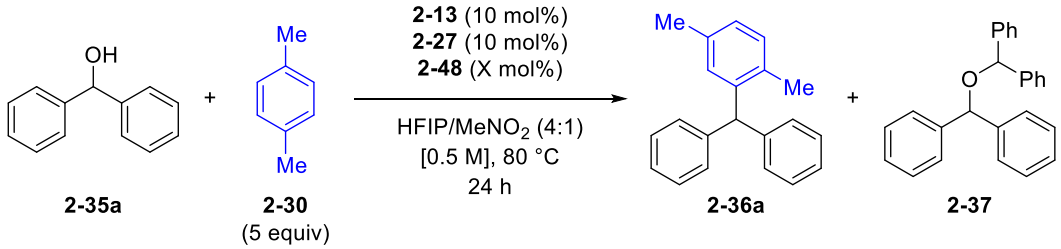

Entry	Equiv. **2-48**	Yield **2-35a**[a]	Yield **2-36a**[a]	Yield **2-37**[a]
1	7.9 mol%	23%	0%	77%
2	12 mol%	58%	0%	42%
3	21 mol%	98%	0%	0%
4	41 mol%	99%	0%	0%

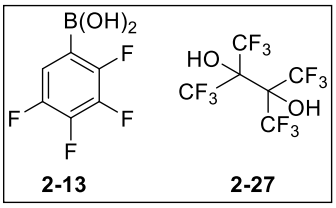

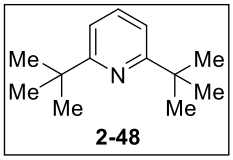

Reactions were performed on 0.15 mmol scale of **2-35a**. [a]Yield determined by ^{1}H NMR relative to 1,3,5-trimethoxybenzeneas an internal standard.

The influence of 2,6-di-*tert*-butylpyridine was further examined on the two-component catalyst system by ^{11}B NMR to elucidate its inhibitory effect on the Friedel-Crafts reaction (Figure 2-4). As shown previously (*cf.* Figure 2-3), reaction of equimolar **2-13** and perfluoropinacol resulted in a mixture of free boronic acid and a four-coordinate boron species that was assigned as hydronium boronate **2-41** (Figure 2-4a). The addition of 1.5 equivalents of 2,6-di-*tert*-butylpyridine under otherwise identical conditions led to a dramatic shift in the equilibrium and virtually complete conversion to the four-coordinate boronate species (Figure 2-4b). Furthermore, the protonated pyridinium cation was observed by ESI mass spectrometry in positive mode (ESI analysis performed by Hwee Ting Ang). These two observations suggest that pyridinium boronate **2-53** is the major component of this mixture in the presence of 2,6-di-*tert*-butylpyridine.

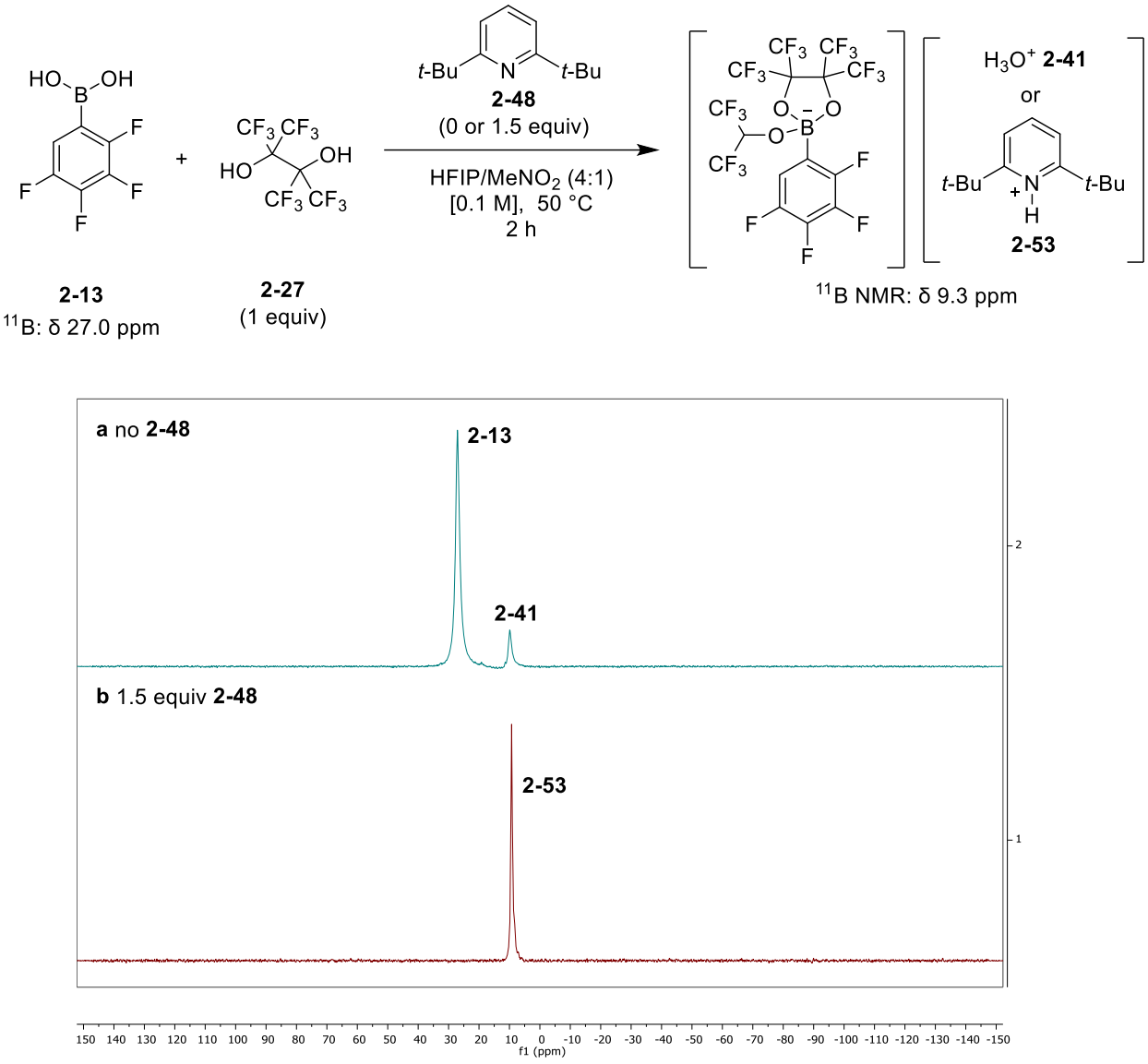

Figure 2-5 The effect of 2,6-di-tert-butylpyridine (**2-48**) on catalyst speciation for the two-component catalyst system of boronic acid **2-13** and perfluoropinacol (**2-27**). ^{11}B NMR (128 MHz) experiments performed in 4:1:2 HFIP/$MeNO_2$/CD_3CN.

Formation of complex **2-53** under these conditions is consistent with an increase in acidity of hexafluoroisopropanol upon coordination to the highly Lewis acidic perfluoropinacol boronic ester that is formed *in situ*, leading to deprotonation of HFIP by the basic pyridine and a complete shift of the boron equilibrium towards the four-coordinate species. Moreover, inhibition of the Friedel-Crafts reaction by 2,6-di-*tert*-butylpyridine suggests that pyridinium boronate species **2-**

53 is an ineffective Brønsted acid catalyst for this transformation. In contrast, hydronium boronate species **2-41** appears to be a highly active catalyst based on the rapid initial rate of alcohol consumption and further C–O bond activation of the less reactive ether intermediate under standard reaction conditions. Complexes **2-53** and **2-41** differ only in their countercation, suggesting that the nature and Brønsted acidity of the countercation are a key factor in the reaction.

Two possible mechanisms for a Brønsted acid-dependent C–O activation process are shown in Scheme 2.16. In Brønsted acid catalysis (water-mediated protonation), the hydronium cation of ion pair **A** can act as a strong protic acid to protonate the benzylic alcohol substrate, leading to species **B** and ultimately carbenium boronate ion pair **C** after C–O bond dissociation (Scheme 2.16a). In contrast, Lewis acid-assisted Brønsted acid catalysis may be operative, in which the acidity of HFIP is sufficiently enhanced upon coordination to the *in situ* formed boronic ester that proton transfer occurs directly from coordinated HFIP to the substrate, ultimately leading to C–O bond cleavage through the same ion pairs **B** and **C** (Scheme 2.16b). The difference between the two mechanisms lies in the importance of water, which is not necessary to generate the active protic acid in Lewis acid-assisted Brønsted acid catalysis. Accordingly, the importance of water to the reaction was investigated to further probe the possibility of a hydronium boronate catalyst.

a *Brønsted Acid Catalysis (water-mediated protonation)*

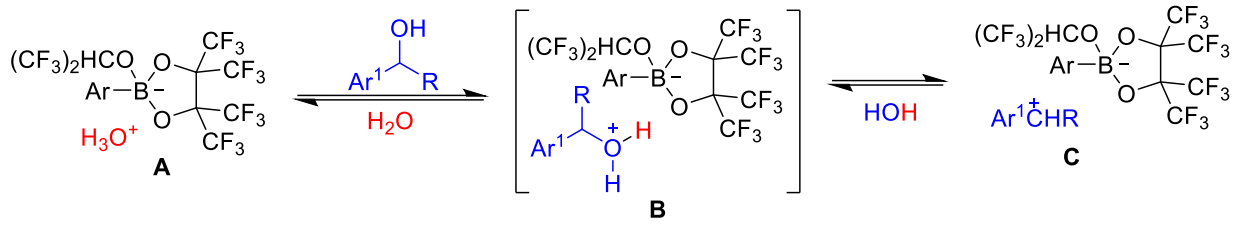

b *Lewis Acid-Assisted Brønsted Acid Catalysis (solvent-mediated protonation)*

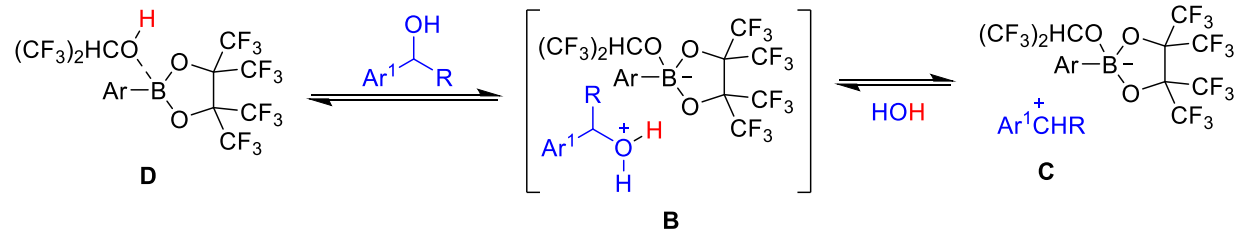

Scheme 2-16 Possible mechanisms of C–O bond activation involving a hydronium boronate intermediate.

2.3.4.4 Investigating Anhydrous Conditions and the Importance of Water

In order to study the importance of water to the Friedel-Crafts reaction catalyzed by boronic acid **2-13** and perfluoropinacol, and to the potential formation of hydronium boronate species **2-41**, a series of reactions were performed using dried glassware and solvents (Table 2-6). Additionally, the use of 3 Å molecular sieves as a desiccant was examined to further remove water from the reaction, including the water that is released upon boronic acid-diol condensation. If hydronium boronate species **2-41** is the catalytically active species under standard reaction conditions, diminished reactivity would be expected when water is removed from this reaction and formation of complex **2-41** is inhibited.

Table 2-6 The effect of anhydrous solvents and molecular sieves on the Friedel-Crafts reaction of alcohol **2-35a** catalyzed by boronic acid **2-13** and perfluoropinacol (**2-27**).

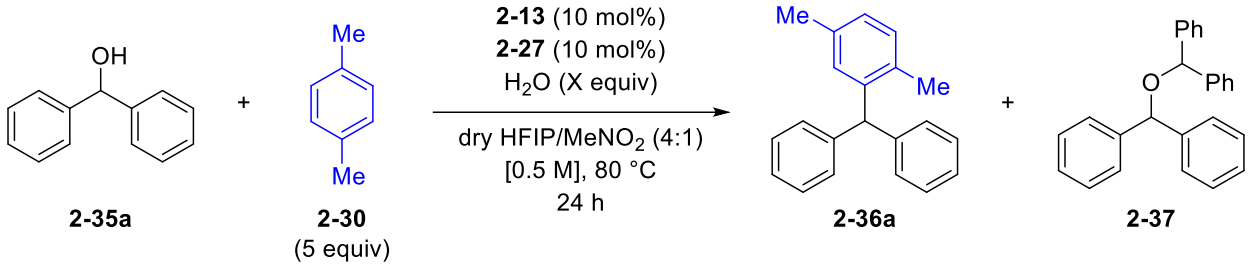

2-35a + **2-30** (5 equiv) → **2-36a** + **2-37**

Entry	Equiv. H_2O	Yield **2-35a**[a]	Yield **2-36a**[a]	Yield **2-37**[a]
1	None	17%	61%	0%
2	None (sieves added)	0%	0%	89%
3	0.37 equiv	0%	71%	27%
4	1.11 equiv	28%	52%	20%
5	20 equiv	77%	0%	22%

Reactions were performed on 0.15 mmol scale of **2-35a**. [a]Yield determined by ^{1}H NMR relative to 1,3,5-trimethoxybenzeneas an internal standard.

When the reaction was conducted using dried reagents and glassware, triarylmethane **2-36a** was still obtained in moderate 61% yield (Entry 1). However, when the same reaction was repeated with the addition of molecular sieves to capture water released during boronic acid-diol condensation, formation of the triarylmethane **2-36a** was completely suppressed and only ether **2-37** was observed in good yield (Entry 2). The addition of 37 mol% water to the reaction when carried out using dry solvents and glassware was found to restore catalytic activity and triarylmethane **2-36a** was again formed in 71% yield (Entry 3). Addition of increased amounts of water had a deleterious effect and led to decreased conversion of starting alcohol **2-35a**, likely due to competing nucleophilic addition of water (Entries 4 and 5). Furthermore, the equilibrium between boronic acid **2-13** and boronate complex **2-41** was found to be shifted towards a greater proportion of complex **2-41** when using dry solvents along with molecular sieves, but no

previously unidentified catalytic species were observed under these conditions that would account for the drastic change in reactivity (Figure 2-6).

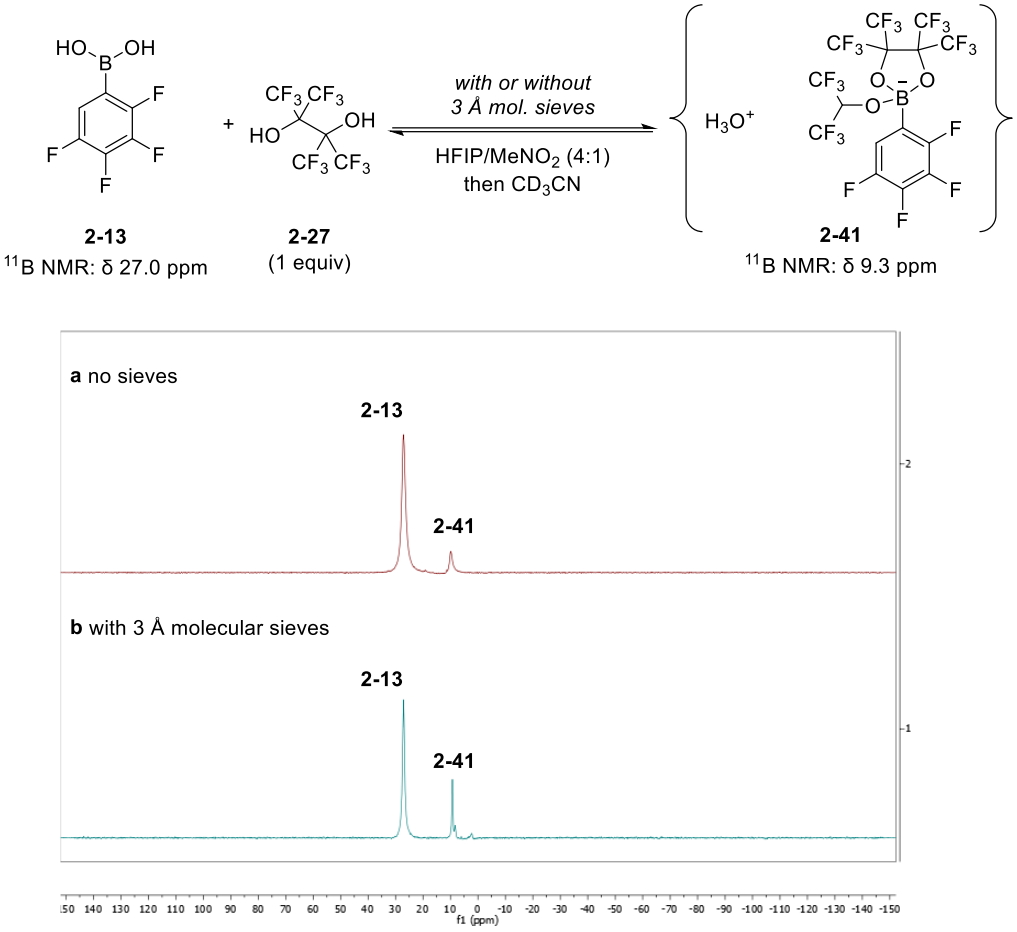

Figure 2-6 The effect of molecular sieves on the equilibrium between boronic acid **2-13** and hydronium boronate **2-41** in the presence of perfluoropinacol (**2-27**). ^{11}B NMR (128 MHz) experiments performed in 4:1:2 HFIP/$MeNO_2$/CD_3CN.

These results establish that while free alcohol **2-35a** can undergo C–O bond activation under anhydrous conditions, further activation of ether **2-37** requires small amounts of water either remaining in commercial solvents or released through condensation between the boronic acid and perfluoropinacol. This suggests that consumption of ether **2-37** does not proceed in the absence of a hydronium boronate species that is sufficiently acidic to promote C–O bond activation of the more hindered ether C–O bonds. In this vein, the Friedel-Crafts benzylation reaction with benzyl

ethers was previously reported by Yang and co-workers using $BF_3 \cdot OEt_2$ as a stoichiometric promoter, where they found that residual water was necessary to generate $BF_3 \cdot H_2O$ as the active Brønsted acid promoter of the reaction.[36]

In addition to the role of water in generating a hydronium boronate catalyst, the formation of water as the reaction proceeds may influence the polarity of the solvent mixture. It is unclear how the rate of reaction is altered when anhydrous solvents are employed. The hydrogen bond donor and acceptor properties of water may accelerate C–O activation through hydrogen bonding to the alcohol substrate or HFIP solvent, although competing nucleophilic addition of water to the carbocation ultimately appears to lower the rate of formation of the Friedel-Crafts product.

2.3.4.5 Proposed Mechanism

Based on the experiments described herein, a plausible mechanism for this reaction can be proposed (Scheme 2-17). Boronic acid catalyst **2-13** reacts with perfluoropinacol and hexafluoroisopropanol solvent in equilibrium to form hydronium boronate complex **2-41** as the catalytically active species. Formation of complex **2-41** is supported by high resolution mass spectrometry and ^{11}B NMR studies. This hydronium boronate is sufficiently acidic to promote C–O bond activation of the alcohol substrate, generating ion pair **A** with the reactive benzylic carbocation electrophile and non-nucleophilic borate anion. This carbocation can be trapped by a second equivalent of alcohol to form ether **B** and regenerate the hydronium cation through proton transfer. This appears to be the kinetically favored pathway, as rapid build-up of the ether was observed in the early stages of the reaction.

Ether formation, however, is reversible under the reaction conditions, and C–O bond activation of sterically hindered ether **B** promoted by complex **2-41** can reversibly regenerate ion pair **A**. Friedel-Crafts benzylation can occur from ion pair **A** by nucleophilic attack of the arene to

form Wheland intermediate **C**, which may be stabilized by the weakly-coordinating boronate counteranion. Subsequent rearomatization via deprotonation with the boronate anion generates the final benzylated product **D**, and hydronium boronate catalyst **2-41** can be regenerated in the presence of HFIP and water through solvent exchange and proton transfer reactions from Lewis acid/base complex **E**.

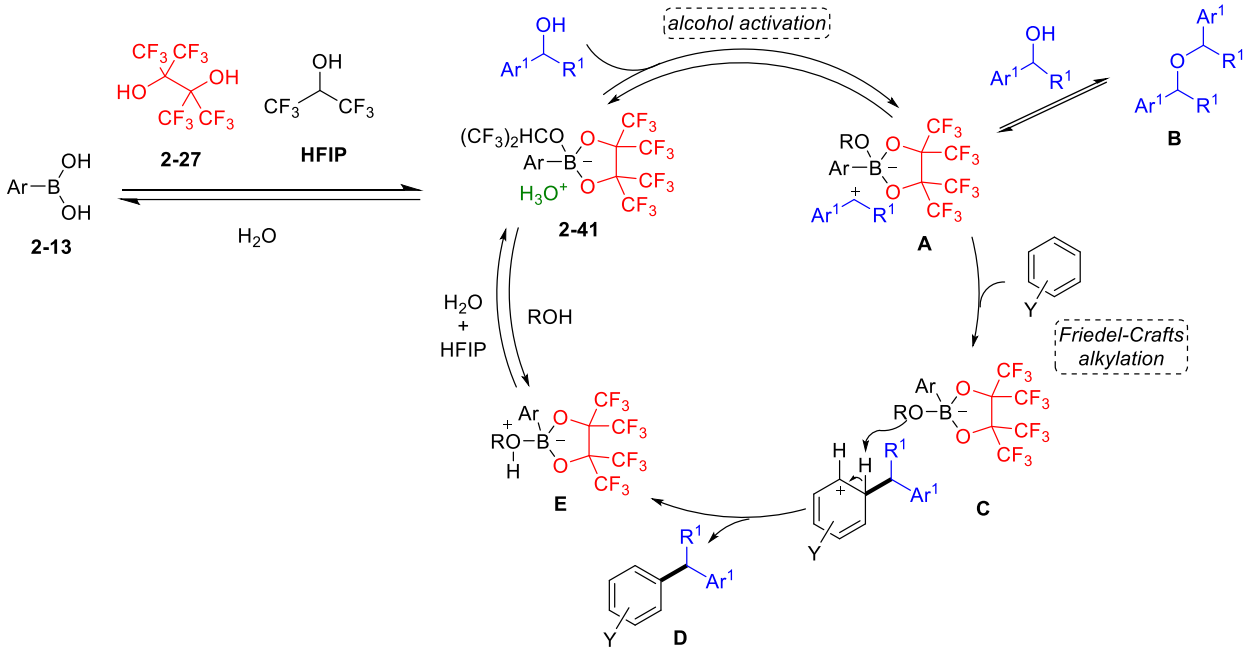

Scheme 2-17 Proposed mechanism for the Friedel-Crafts benzylation reaction catalyzed by **2-13** and perfluoropinacol (**2-27**).

2.3.4.6 Comparison to Other Brønsted Acid Catalysts

To compare the chemoselectivity of the **2-13**/perfluoropinacol catalytic system with other common Brønsted acids catalysts, the Friedel-Crafts reaction of substrate **2-38i**, bearing an acid- and hydrolytically labile acetate moiety, was then examined by Hwee Ting Ang (Table 2-7). Full consumption of alcohol **2-38i** was observed in all cases, and the **2-13**/perfluoropinacol co-catalytic system afforded diarylethane **2-39i** in good yield (Entry 1). Other strong Brønsted acid catalysts gave reduced yield of the desired product (Entries 3-5), while *p*-toluenesulfonic acid resulted in a

complex mixture with no product formation (Entry 2). Similar results were observed using Moran's previously reported Friedel-Crafts conditions of triflic acid in HFIP (Entry 6)[22] or when dichloroethane, a common solvent for Brønsted acid-catalyzed transformations,[37] was employed (Entries 7-9). Reactions that produced a low yield of diarylethane **2-39i** were accompanied by mixtures of by-products.

Table 2-7 Comparison of the boronic acid **2-13**/perfluoropinacol (**2-27**) co-catalytic system with other Brønsted acids for the Friedel-Crafts reaction of acid-labile alcohol **2-39i**. Experiments performed by Hwee Ting Ang.

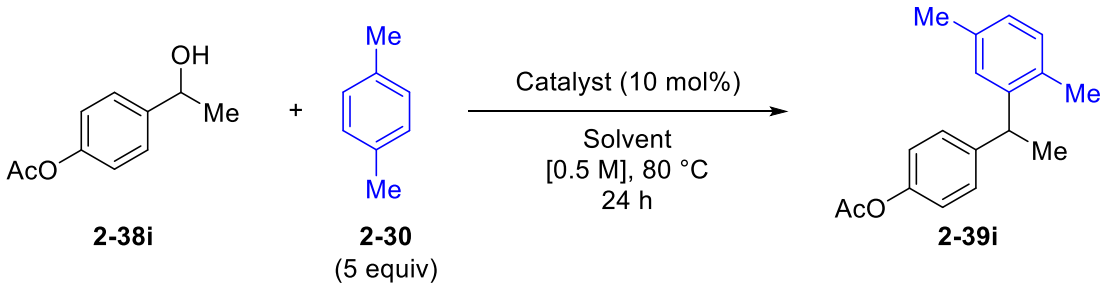

2-38i **2-30** (5 equiv) **2-39i**

Entry	Catalyst	Solvent	Conversion[a]	Yield **2-39i**[a]
1	**2-13** + **2-27**	HFIP/$MeNO_2$ (4:1)	>98%	80%
2	*p*-TsOH·H_2O	HFIP/$MeNO_2$ (4:1)	>98%	0%
3	HCl (4.0 M in dioxane)	HFIP/$MeNO_2$ (4:1)	>98%	50%
4	TFA	HFIP/$MeNO_2$ (4:1)	>98%	56%
5	Oxalic Acid	HFIP/$MeNO_2$ (4:1)	>98%	52%
6	TfOH	HFIP	>98%	0%
7	*p*-TsOH·H_2O	DCE	>98%	0%
8	TFA	DCE	28%	0%
9	Oxalic Acid	DCE	81%	0%

Reactions were performed on 0.50 mmol scale of **2-38i**. [a]Yield and conversion determined by ^1H NMR relative to 1,4-dinitrobenzene as an internal standard.

These results support our group's previous observations regarding the mild reaction conditions and increased chemoselectivity of boronic acid catalysis relative to traditional Brønsted

acid-catalysts,[25] even when the boronic acid-catalyzed reaction appears to follow a Brønsted acid-dependent mechanism as it does here. The large difference in reactivity between **2-13**/perfluoropinacol and other Brønsted acids may be due to the different nature of their counteranions. A boronate counteranion, such as that in hydronium boronate species **2-41**, displays low basicity and nucleophilicity relative to other anions, which may help to minimize the side-reactions that could be proceeding with conventional Brønsted acid catalysts, such as elimination or acetate hydrolysis.

2.4 Summary

This chapter reports the successful application of boronic acid catalysis to the Friedel-Crafts benzylation reaction of secondary diarylmethanol derivatives, providing an efficient synthesis of the triarylmethane scaffold which has shown diverse applications in medicinal and materials chemistry. The use of perfluoropinacol (**2-27**), a highly electron-deficient diol, as a catalytic additive was found to be key to the development of a successful two-component catalyst system. A variety of halogenated or electron-deficient alcohols were successfully applied to this reaction, overcoming the traditionally limited applicability of electron-poor substrates in Friedel-Crafts chemistry.

Kinetic analysis revealed that the reaction rapidly proceeds through a symmetrical ether intermediate formed by dehydrative dimerization of the starting material. Ether formation was shown to be reversible, however, and eventual conversion to the final Friedel-Crafts product was observed. Mechanistic studies showed formation of a hydronium boronate species under the reaction conditions through boronic acid-diol condensation and trapping of the resultant Lewis acidic perfluoropinacol boronic ester by acidic hexafluoroisopropanol solvent. A Brønsted acid-dependent mechanism for C–O bond activation by the hydronium boronate catalyst was proposed,

which was supported by 2,6-di-*tert*-butylpyridine inhibition and a lack of reaction under anhydrous conditions. The results presented herein demonstrate a new synthetic application of boronic acid catalysis and progress towards a mechanistic understanding of the role of co-catalytic additives that may be used to guide the development of new reactions.

2.5 Experimental

2.5.1 General Information

The following section contains representative experimental procedures and details for the isolation of compounds. Partial characterization of known compounds and full characterization of novel compounds presented in this chapter are described. All reactions were performed in regular glassware without any precautions to remove air or moisture, unless otherwise indicated. Unless otherwise noted, all chemicals were purchased from commercial sources and used as received. All solvents were purchased as ACS reagent grade and were used without further purification. 1,1,1,3,3,3-Hexafluoro-2-propanol (HFIP) was purchased and used as received from Oakwood Chemical. Hexafluoro-2,3-bus(trifluoromethyl)-2,3-butanediol (perfluoropinacol, **2-27**) was purchased from Matrix Scientific and used as received. Catalysts **2-13**[26] and **2-16**[29] were synthesized according to literature procedures. Column chromatography was performed on silica gel 60 using ACS grade hexanes and ethyl acetate as eluents. Thin layer chromatography (TLC) analysis was performed on Silicycle silica gel 60 F254 plates, which were visualized under UV light and with phosphomolybdic acid (PMA) or potassium permanganate ($KMnO_4$) stains.

^{1}H, ^{11}B, ^{13}C and ^{19}F NMR spectra were recorded in $CDCl_3$ or CD_3CN at ambient temperature using Varian DD2 MR two-channel 400 MHz, Varian INOVA-400 MHz, Bruker Avance III 400, Varian VNMRS two-channel 500 MHz or Varian INOVA-600 MHz spectrometers at 400/500/600 MHz respectively for ^{1}H NMR. All chemical shifts are reported in

ppm units with residual solvent peaks used as an internal standard. NMR data is reported using the following abbreviations: s, singlet; d, doublet; t, triplet; q, quartet; sept, septet; dd, doublet of doublets; dt, doublet of triplets; tt, triplet of triplets; ddd, doublet of doublet of doublets; m, multiplet. High-resolution mass spectra were obtained by the University of Alberta Mass Spectrometry Services Laboratory using either electrospray (ESI) or electron impact (EI) techniques. Infrared (IR) spectra were obtained using a Nicolet Magna-IR Spectrometer with frequencies expressed in cm^{-1}.

Safety caution: Perfluoropinacol (**2-27**) has demonstrated acute toxicity through skin contact or inhalation, and should be handled with care.[38]

2.5.2 Preparation of Alcohols

General Procedure for the synthesis of diarylmethanol derivatives via reduction (GP2-1)

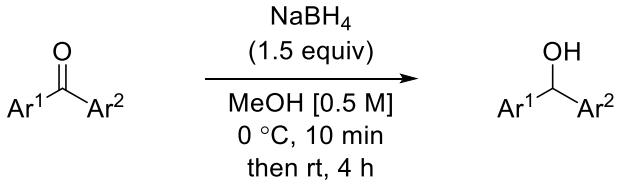

A round bottom flask equipped with a stir bar was charged with ketone (1.0 equiv) and MeOH (0.5 M). The flask was cooled in an ice bath to 0 °C, after which $NaBH_4$ (1.5 equiv) was added in two portions. The reaction mixture was stirred at this temperature for 10 minutes, before removing the ice bath and stirring for an additional 4 hours. The reaction was quenched by addition of saturated $NH_4Cl_{(aq)}$, and methanol was removed by rotary evaporation. The mixture was extracted with EtOAc (3 × 25 mL). The combined organic phases were washed with H_2O (35 mL) and brine (35 mL), dried over Na_2SO_4, filtered, and concentrated by rotary evaporation. Purification by column chromatography was conducted to afford the desired alcohol.

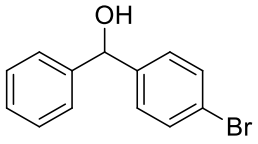

(4-Bromophenyl)(phenyl)methanol (2-35b): Prepared according to **GP2-1** from 4-bromobenzophenone (2.61 g, 10.0 mmol). Purification by flash column chromatography (5:1 hexane/EtOAc) afforded the title compound (2.21 g, 84%) as a white solid. **^{1}H NMR** (600 MHz, $CDCl_3$): δ 7.40 (d, *J* = 8.4 Hz, 2 H), 7.31 – 7.26 (m, 4 H), 7.25 – 7.21 (m, 1 H), 7.18 (d, *J* = 8.4 Hz, 2 H), 5.70 (d, *J* = 3.2 Hz, 1 H), 2.36 (d, *J* = 3.4 Hz, 1 H). Spectral data are in agreement with the literature.[39]

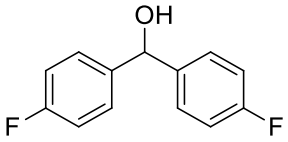

Bis(4-fluorophenyl)methanol (2-35c): Prepared according to **GP2-1** from 4,4'-difluorobenzophenone (872 mg, 4.00 mmol). Purification by flash column chromatography (8:1 hexane/EtOAc) afforded the title compound (784 mg, 89%) as a white solid. **^{1}H NMR** (600 MHz, $CDCl_3$): δ 7.34 – 7.30 (m, 4 H), 7.05 – 7.01 (m, 4 H), 5.81 (s, 1 H), 2.24 (s, 1 H). Spectral data are in agreement with the literature.[40]

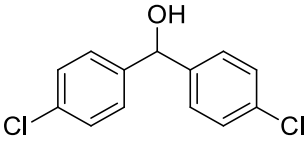

Bis(4-chlorophenyl)methanol (2-35d): Prepared according to **GP2-1** from 4,4'-dichlorobenzophenone (1.00 g, 4.00 mmol). Purification by flash column chromatography (8:1 hexane/EtOAc) afforded the title compound (820 mg, 81%) as a white solid. **^{1}H NMR** (600 MHz, $CDCl_3$): δ 7.32 – 7.30 (m, 4 H), 7.29 – 7.27 (m, 4 H), 5.79 (d, *J* = 2.9 Hz, 1 H), 2.24 (d, *J* = 3.0 Hz, 1 H). Spectral data are in agreement with the literature.[41]

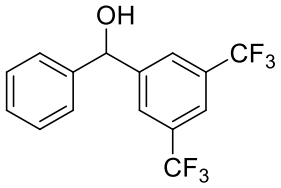

(3,5-Bis(trifluoromethyl)phenyl)(phenyl)methanol (2-35e): A flame dried round bottom flask under nitrogen atmosphere was charged with THF (20 mL) and 1,3-bis(trifluoromethyl)-5-bromobenzene (860 µL, 5.0 mmol). The flask was cooled to −78 °C in a dry ice/acetone bath after which *n*-BuLi (2.5 M solution in hexane, 2.0 mL, 5.0 mmol) was added dropwise. The reaction was stirred for 30 minutes at −78 °C. A solution of benzaldehyde (460 µL, 4.5 mmol) in THF (5 mL) was then added dropwise and the reaction stirred for an additional 30 minutes at −78 °C. The cold bath was removed, and the reaction stirred for 3.5 hours while warming to room temperature. After 3.5 hours, the reaction was cooled to 0 °C in an ice bath and quenched with saturated aqueous NH_4Cl (20 mL). The reaction mixture was extracted with EtOAc (2 × 30 mL) and the combined organic layers were washed with water (2 × 30 mL) and brine (1 × 30 mL). The organic layer was dried with Na_2SO_4, filtered and concentrated under reduced pressure. The resulting oil was purified by flash column chromatography (hexane to 8:1 hexane/EtOAc) to afford the title compound (691 mg, 48%) as an ochre solid. **^{1}H NMR** (500 MHz, $CDCl_3$): δ 7.87 (s, 2 H), 7.79 (s, 1 H), 7.42 – 7.37 (m, 2 H), 7.37 – 7.32 (m, 3 H), 5.92 (d, *J* = 3.0 Hz, 1 H), 2.43 (d, *J* = 3.1 Hz, 1 H). Spectral data are in agreement with the literature.[42]

2.5.3 Optimization of the Friedel-Crafts Benzylation Reaction

General procedure for the Friedel-Crafts Benzylation – NMR Yields (GP2-2)

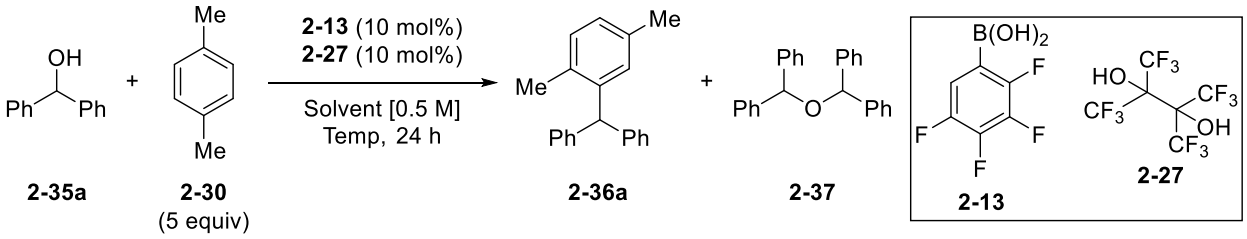

A vial equipped with a stir bar was charged with alcohol **2-35a** (27.6 mg, 0.150 mmol), *p*-xylene **2-30** (92 µL, 0.75 mmol, 5.0 equiv), catalyst **2-13** (3.2 mg, 0.015 mmol, 10 mol%), perfluoropinacol **2-27** (2.7 µL, 0.015 mmol, 10 mol%) and solvent (0.5 M). The vial was capped and stirred at the indicated temperature for 24 hours, after which it was diluted with $CHCl_3$ and filtered through a small silica pipette. The mixture was concentrated by rotary evaporation, and yields were obtained by ^1H NMR relative to 1,3,5-trimethoxybenzene as an internal standard.

2.5.4 Substrate Scope of Friedel-Crafts Benzylation

General procedure for the Friedel-Crafts Benzylation – Isolated Yields (GP2-3)

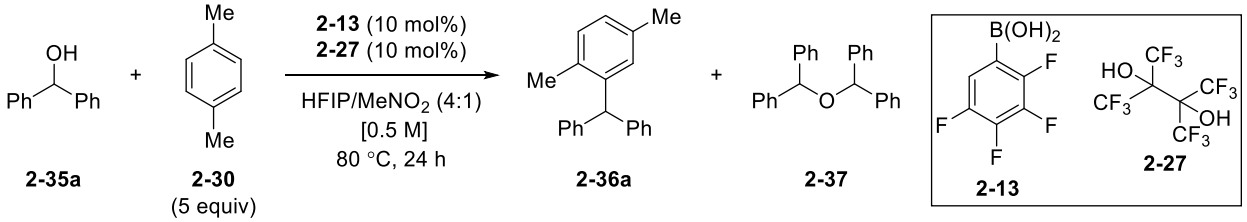

A vial equipped with a stir bar was charged with alcohol **2-35a** (1.0 equiv), *p*-xylene **2-30** (5.0 equiv), catalyst **2-13** (10 mol%), perfluoropinacol **2-27** (10 mol%) and HFIP/$MeNO_2$ (4:1 ratio, 0.5 M). The vial was capped and stirred at 80 °C for 24 hours, after which it was concentrated by rotary evaporation. Purification by column chromatography afforded the desired product.

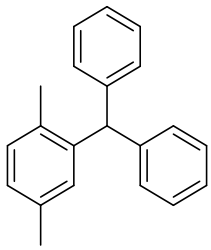

((2,5-Dimethylphenyl)methylene)dibenzene (2-36a): Prepared according to **GP2-3** from alcohol **2-35a** (110 mg, 0.60 mmol) and *p*-xylene (0.37 mL, 3.00 mmol) at 80 °C for 24 hours. Purified by flash chromatography (hexane) and isolated as a colourless oil (without **2-27**: 0%, with **2-27**: 131 mg, 80%). **^{1}H NMR** (500 MHz, $CDCl_3$): δ 7.35 – 7.21 (m, 6 H), 7.12 – 7.05 (m, 5 H), 6.98 (dd, *J* = 7.6, 1.8 Hz, 1 H), 6.68 – 6.63 (m, 1 H), 5.68 (s, 1 H), 2.24 (s, 3 H), 2.20 (s, 3 H); **^{13}C NMR** (101 MHz, $CDCl_3$): δ 143.6, 142.2, 135.2, 133.6, 130.4, 130.3, 129.8, 128.4, 127.2, 126.3, 53.6, 21.4, 19.6; **IR** (Cast Film, cm^{-1}): 3024 (m), 2951 (w), 1599 (m), 1495 (s), 1449 (m), 1290 (w), 1079 (w); **HRMS** (EI) for $C_{21}H_{20}$: Calculated: 272.1565; Found: 272.1564.

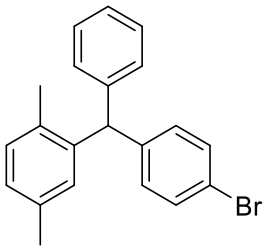

2-((4-Bromophenyl)(phenyl)methyl)-1,4-dimethylbenzene (2-36b): Prepared according to **GP2-3** from alcohol; **2-35b** (157 mg, 0.60 mmol) and *p*-xylene (0.37 mL, 3.00 mmol) at 80 °C for 24 hours. Purified by flash column chromatography (hexane) and isolated as a colorless oil (without **2-27**: 0%, with **2-27**: 164 mg, 78%). **^{1}H NMR** (500 MHz, $CDCl_3$): δ 7.41 (d, *J* = 8.4 Hz, 2 H), 7.29 (dd, *J* = 8.2, 6.7 Hz, 2 H), 7.25 – 7.21 (m, 1 H), 7.08 – 7.02 (m, 3 H), 6.97 (dd, *J* = 7.6, 1.8 Hz, 1 H), 6.94 (d, *J* = 8.4 Hz, 2 H), 6.60 (s, 1 H), 5.60 (s, 1 H), 2.22 (s, 3 H), 2.16 (s, 3 H); **^{13}C NMR** (151 MHz, $CDCl_3$): δ 143.0, 142.8, 141.6, 135.4, 133.5, 131.5 (x 2), 130.6, 130.1, 129.7,

128.5, 127.4, 126.6, 120.3, 53.1, 21.3, 19.6; **IR** (Cast Film, cm^{-1}): 3060 (w), 3024 (w), 2971 (w), 2921 (w), 1486 (s), 1450 (m), 1290 (w), 1195 (w), 1073 (m), 1011 (m), 846 (w), 745 (w); **HRMS** (EI) for $C_{21}H_{19}Br$: Calculated: 350.0670; Found: 350.0668.

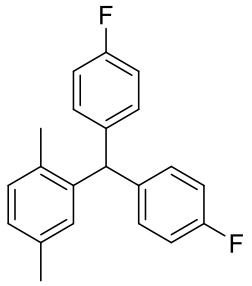

4,4'-((2,5-Dimethylphenyl)methylene)bis(fluorobenzene) (2-36c): Prepared according to **GP2-3** from alcohol **2-35c** (132 mg, 0.60 mmol) and *p*-xylene (0.37 mL, 3.00 mmol) at 80 °C for 24 hours. Purified by flash column chromatography (hexane) and isolated as a white solid (without **2-27**: 0%, with **2-27**: 156 mg, 84%). **^{1}H NMR** (600 MHz, $CDCl_3$): δ 7.08 (d, *J* = 7.6 Hz, 1 H), 7.03 – 6.96 (m, 9 H), 6.57 (s, 1 H), 5.62 (s, 1 H), 2.23 (s, 3 H), 2.11 (s, 3 H); **^{13}C NMR** (151 MHz, $CDCl_3$): δ 161.6 (d, *J* = 244.9 Hz), 141.8, 139.2 (d, *J* = 3.2 Hz), 135.4, 133.5, 131.0 (d, *J* = 7.7 Hz), 130.6, 130.0, 127.5, 115.3 (d, *J* = 21.2 Hz), 52.1, 21.3, 19.5; **^{19}F NMR** (469 MHz, $CDCl_3$): δ –116.8 (app. sept, 2 F); **IR** (Cast Film, cm^{-1}): 3039 (w), 2946 (w), 2923 (w), 1603 (m), 1507 (s), 1460 (w), 1412 (w), 1297 (w), 1225 (s), 1158 (m), 1097 (w), 823 (w); **HRMS** (EI) for $C_{21}H_{18}F_2$: Calculated: 308.1377; Found: 308.1374.

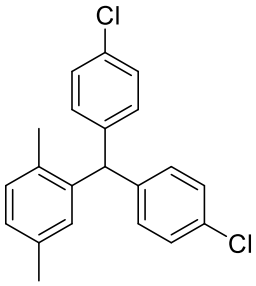

4,4'-((2,5-Dimethylphenyl)methylene)bis(chlorobenzene) (2-36d): Prepared according to **GP2-3** from alcohol **2-35d** (151 mg, 0.60 mmol) and *p*-xylene (0.37 mL, 3.00 mmol) at 80 °C for 24

hours. Purified by flash column chromatography (hexane) and isolated as a white solid (without **2-27**: 0%, with **2-27**: 176 mg, 86%). **^{1}H NMR** (500 MHz, $CDCl_3$): δ 7.29 (d, *J* = 8.5 Hz, 4 H), 7.10 (d, *J* = 7.6 Hz, 1 H), 7.00 – 6.97 (m, 5 H), 6.59 (s, 1 H), 5.61 (s, 1 H), 2.26 (s, 3 H), 2.18 (s, 3 H); **^{13}C NMR** (126 MHz, $CDCl_3$): δ 141.7, 141.2, 135.5, 133.5, 132.4, 131.0, 130.7, 129.9, 128.7, 127.6, 52.4, 21.3, 19.5; **IR** (Cast Film, cm^{-1}): 3022 (w), 2970 (w), 1575 (w), 1489 (s), 1287 (w), 1264 (w), 1091 (s), 1015 (s), 872 (w), 835 (m), 782 (m); **HRMS** (EI) for $C_{21}H_{18}Cl_2$: Calculated: 340.0786; Found: 340.0786.

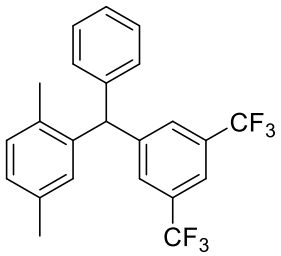

2-((3,5-Bis(trifluoromethyl)phenyl)(phenyl)methyl)-1,4-dimethylbenzene (2-36e): Prepared according to **GP2-3** from alcohol **2-35e** (160 mg, 0.50 mmol) and *p*-xylene (0.31 mL, 2.50 mmol) at 80 °C for 24 hours. Purified by flash column chromatography (hexane) and isolated as a white solid (without **2-27**: 0%, with **2-27**: 74 mg, 36%). **^{1}H NMR** (600 MHz, $CDCl_3$): δ 7.77 (s, 1 H), 7.52 (s, 2 H), 7.33 (t, *J* = 7.4 Hz, 2 H), 7.30 – 7.26 (m, 1 H), 7.10 (d, *J* = 7.7 Hz, 1 H), 7.04 – 7.00 (m, 3 H), 6.52 (s, 1 H), 5.76 (s, 1 H), 2.23 (s, 3 H), 2.17 (s, 3 H); **^{13}C NMR** (151 MHz, $CDCl_3$): δ 146.6, 141.6, 140.3, 135.8, 133.5, 131.7 (q, *J* = 33.0 Hz) 130.9, 129.9, 129.7 (m), 129.6, 128.9, 128.0, 127.2, 123.5 (q, *J* = 271.0 Hz), 120.7 (sept, *J* = 3.7 Hz), 53.3, 21.3, 19.6. **^{19}F NMR** (376 MHz, $CDCl_3$): δ –62.7 (s, 6 F); **IR** (Cast Film, cm^{-1}): 3063 (w), 2982 (w), 1496 (m), 1372 (s), 1278 (s), 1170 (s), 1134 (s), 1109 (m), 899 (m), 701 (m); **HRMS** (EI) for $C_{23}H_{18}F_6$: Calculated: 408.1313; Found: 408.1317.

2.5.5 Characterization of Intermediate Ether and Reaction Kinetics

2.5.5.1 Synthesis of Ether 2-37

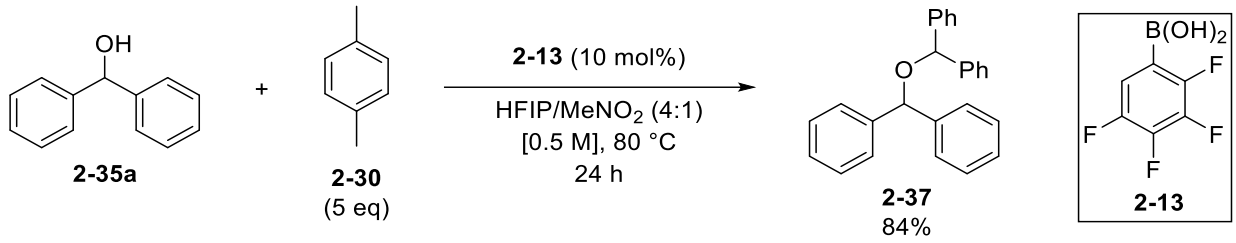

Bis(diphenylmethyl)ether (2-37): A vial was charged with alcohol **2-35a** (184 mg, 1.00 mmol), *p*-xylene (618 µL, 5.00 mmol), catalyst **2-13** (19.4 mg, 0.10 mmol), HFIP (1.6 mL) and $MeNO_2$ (0.4 mL) under air. The vial was capped and stirred at 80 °C for 24 hours. After cooling to room temperature, the reaction was loaded directly onto a silica gel column. Purification by silica gel chromatography (20:1 hexane/EtOAc) afforded Bis(diphenylmethyl)ether (**2-37**) (140 mg, 84% yield) as a white solid. **^{1}H NMR** (600 MHz, $CDCl_3$): δ 7.46 – 7.41 (m, 8 H), 7.38 (dd, J = 8.5, 6.5 Hz, 8 H), 7.33 – 7.28 (m, 4 H), 5.48 (s, 2 H); **^{13}C NMR** (151 MHz, $CDCl_3$): δ 142.3, 128.5, 127.6, 127.4, 80.1. Spectral data are in agreement with the literature.[43]

2.5.5.2 Friedel-Crafts Benzylation with Ether 2-37

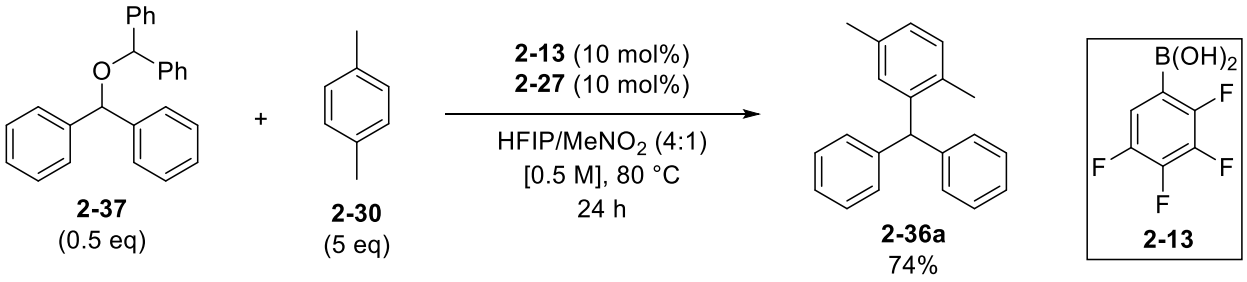

A vial under air was charged with ether **2-37** (27.0 mg, 0.077 mmol), *p*-xylene (95 µL, 0.77 mmol), catalyst **2-13** (2.91 mg, 0.015 mmol), additive **2-27** (2.7 µL, 0.015 mmol), HFIP (240 µL) and $MeNO_2$ (60 µL). The vial was capped and stirred at 80 °C for 24 hours. After cooling to room temperature, the reaction mixture was filtered through a pipette of silica gel and washed with

$CHCl_3$ (12 mL). The filtrate was concentrated under reduced pressure, after which 1,3,5-trimethoxybenzene was added as an internal standard. The yield of **2-36a** was determined by ^1H NMR analysis to be 74%. A yield of greater than 50% indicates that both diphenylmethyl fragments from ether **2-37** can be converted to product.

2.5.5.3 Reaction Monitoring for Friedel-Crafts Benzylation of Alcohol 2-35a

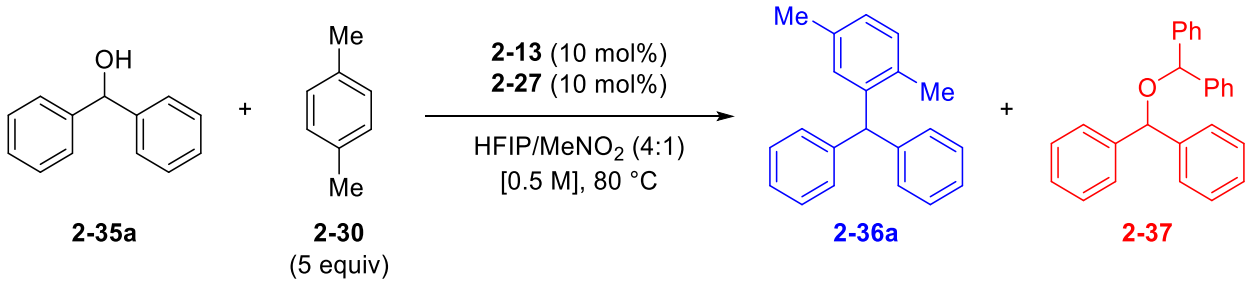

A vial under air was charged with alcohol **2-35a** (185.0 mg, 1.00 mmol), *p*-xylene (620 µL, 5.0 mmol), catalyst **2-13** (20.7 mg, 0.11 mmol), additive **2-27** (19 µL, 0.11 mmol), HFIP (1.6 mL), $MeNO_2$ (0.4 mL) and 1,4-dinitrobenzene (25.9 mg, 0.15 mmol) as an internal standard. The vial was capped and stirred at 80 °C. Over the course of the reaction, aliquots (100 µL) were removed, quenched with $CHCl_3$ (500 µL) and concentrated under reduced pressure. The residue was taken up in $CDCl_3$ and analysed by ^1H NMR analysis. Fast initial formation of bis(diphenylmethyl)ether **2-37** was observed (15 min), which was then consumed over the course of the reaction to form triarylmethane **2-36a** (see Figure 2-2).

A similar procedure was followed where additive **2-27** was only added after 24 hours. The resulting plot is shown in Figure 2-3.

2.5.6 Additive Experiments (*cf.* Table 2-4)

Reactions were performed on 0.10 mmol scale following **GP2-2** along with the addition of 1.0 equivalents of the noted additive. After filtration through a pipette of silica and elution with $CHCl_3$,

1,3,5-trimethoxybenzene was added as an internal standard and yields were determined by ^{1}H NMR analysis of crude unpurified materials.

2.5.7 Mechanistic Studies

2.5.7.1 Effect of 2,6-Di-*tert*-butylpyridine on Friedel-Crafts Benzylation (Table 2-5)

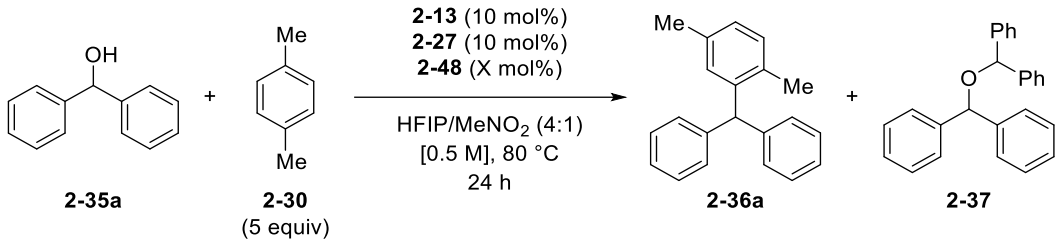

Reactions were performed according to **GP2-2** with varying amounts of 2,6-di-*tert*-butylpyridine **2-48** added to the reaction prior to the addition of solvent.

2.5.7.2 Effect of 2,6-Di-*tert*-butylpyridine on Catalyst Speciation (Figure 2-5)

A vial equipped with a stir bar was charged with boronic acid **2-13** (9.4 mg, 0.050 mmol), co-catalyst **2-27** (8.5 μL, 0.050 mmol, 1.0 equiv) HFIP (400 μL) and $MeNO_2$ (100 μL). If required, 2,6-di-*tert*-butylpyridine (16.2 μL, 0.075 mmol, 1.5 equiv) was added after solvent addition. The vial was capped and stirred at 50 °C for 2 hours in an aluminum heating block. The mixture was allowed to cool to room temperature, at which point an aliquot of 5 μL was removed, diluted with MeCN (1.0 mL) and submitted for low resolution ESI analysis by Hwee Ting Ang. The remainder of the solution was diluted with 0.2 mL CD_3CN and submitted for ^{11}B NMR analysis. The resulting NMR is shown in Figure 2-5.

2.5.7.3 Effect of Molecular Sieves and Anhydrous Solvents on Friedel-Crafts Benzylation

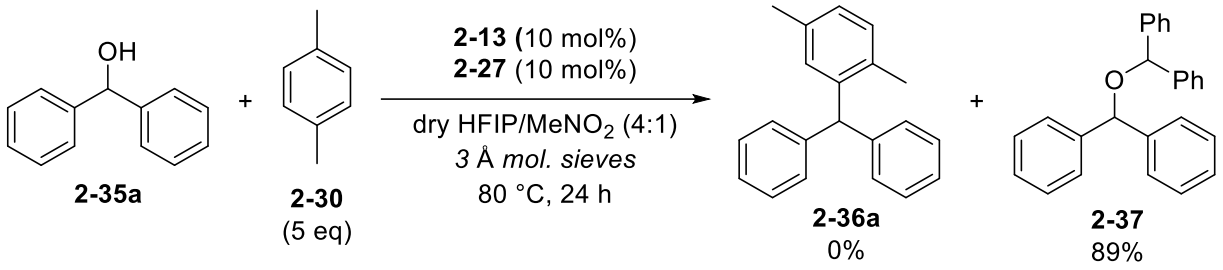

A 15 mL glass reaction tube charged with activated powdered 3 Å molecular sieves (150 mg) was flame-dried and allowed to cool under vacuum four times. After cooling to room temperature the final time, the flask was back-filled with nitrogen and charged with alcohol **2-35a** (27.6 mg, 0.15 mmol), dry *p*-xylene (dried over 3 Å molecular sieves) (92 µL, 0.75 mmol, 5.0 equiv), catalyst **2-13** (2.97 mg, 0.015 mmol, 10 mol%), additive **2-27** (3.0 µL, 0.015 mmol, 10 mol%), anhydrous HFIP (distilled and dried over 3 Å molecular sieves) (240 µL) and anhydrous $MeNO_2$ (distilled from $MgSO_4$ and dried over 3 Å molecular sieves) (60 µL). The flask was sealed with a septum and stirred at 80 °C for 24 hours. After cooling to room temperature, the crude reaction mixture was filtered through a pipette of silica gel with $CHCl_3$ (12 mL). The reaction mixture was concentrated under reduced pressure followed by addition of 1,3,5-trimethoxybenzene and analyzed by ^1H NMR. The Friedel-Crafts product **2-36a** was not observed and ether **2-37** was detected in 89% NMR yield.

2.5.7.4 Effect of Water on Friedel-Crafts Benzylation in Anhydrous Solvents

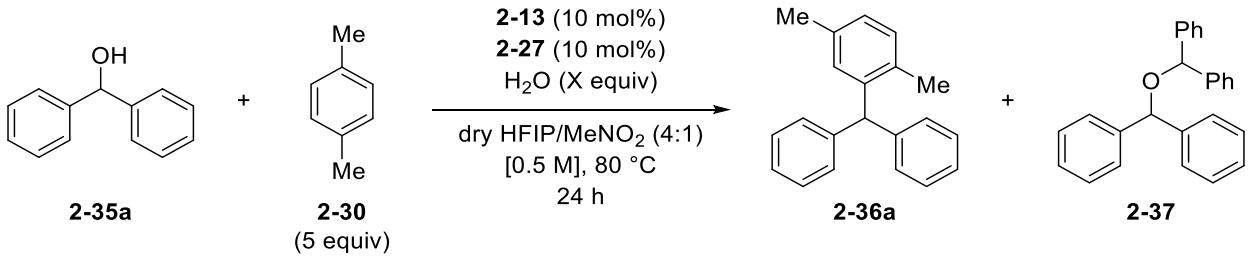

A 15 mL glass reaction tube was flame-dried and allowed to cool under vacuum four times. After cooling to room temperature the final time, the flask was back-filled with nitrogen and charged with alcohol **2-35a** (27.6 mg, 0.15 mmol), dry *p*-xylene (dried over 3 Å molecular sieves) (92 µL, 0.75 mmol, 5.0 equiv), catalyst **2-13** (2.97 mg, 0.015 mmol, 10 mol%), additive **2-27** (3.0 µL, 0.015 mmol, 10 mol%), anhydrous HFIP (distilled and dried over 3 Å molecular sieves) (240 µL), anhydrous $MeNO_2$ (distilled from $MgSO_4$ and dried over 3 Å molecular sieves) (60 µL) and distilled water (0–60 µL, 0–3.3 mmol, 0–22 equiv). The flask was sealed with a septum and stirred at 80 °C for 24 hours. After cooling to room temperature, the crude reaction mixture was filtered through a pipette of silica gel with $CHCl_3$ (12 mL). The reaction mixture was concentrated under reduced pressure followed by addition of 1,3,5-trimethoxybenzene and analyzed by ^1H NMR. Addition of small amounts of water was found to promote the Friedel-Crafts reaction in anhydrous solvents, but excess water ultimately resulted in recovery of starting alcohol **2-35a**.

2.5.7.5 Effect of Molecular Sieves on the Boronic Acid/Boronate Equilibrium (Figure 2-6)

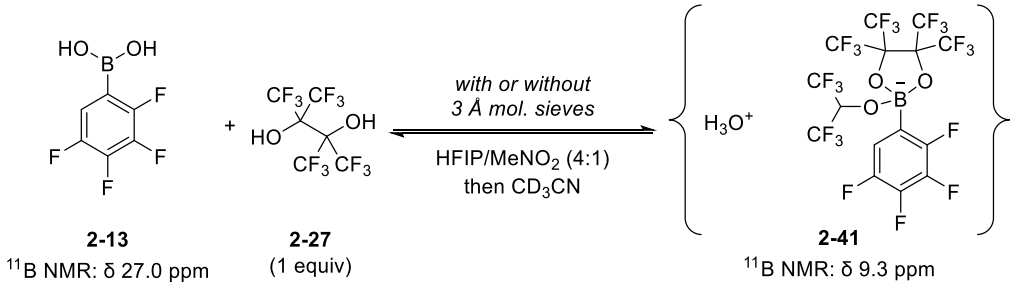

2-13
^{11}B NMR: δ 27.0 ppm

2-27
(1 equiv)

2-41
^{11}B NMR: δ 9.3 ppm

A vial was charged with catalyst **2-13** (10.5 mg, 0.054 mmol), additive **2-27** (10 µL, 0.056 mmol), activated powdered 3 Å molecular sieves (75 mg), dry HFIP (160 µL, distilled and dried over 3 Å molecular sieves) and dry $MeNO_2$ (40 µL, distilled from $MgSO_4$ and dried over 3 Å molecular sieves). The vial was capped and stirred at room temperature for 2 hours. The mixture was diluted with dry CD_3CN (500 µL, dried over 3 Å molecular sieves), filtered through cotton and analyzed

by ^{11}B NMR. An increased fraction of boronate **2-41** was observed in the presence of molecular sieves, consistent with their role as a desiccant in promoting boronic ester formation through condensation.

2.6 References

1) Mondal, S., Panda, G. *RSC Adv.* **2014**, *4*, 28317–28358.
2) Rovner, E. S. *Expert Opin. Pharmacother.* **2005**, *4*, 653–666.
3) Palchaudhuri, R., Nesterenko, V., Hergenrother, P. J. *J. Am. Chem. Soc.* **2008**, *130*, 10274–10281.
4) Ng, C. H., Ohlin, C. A., Winther-Jensen, B. *Dyes and Pigments* **2015**, *115*, 96–101.
5) Kshatriya, R., Jejurkar, V. P., Saha, S. *Eur. J. Org. Chem.* **2019**, *24*, 3818–3841.
6) Rueping, M., Nachtsheim, B. J. *Bellstein J. Org. Chem.* **2010**, *6*, 6.
7) Friedel, C. R., Crafts, J. M. *Compt. Rend.* **1877**, *84*, 1450–1454.
8) Constable, D. J. C., Dunn, P. J., Hayler, J. D., Humphrey, G. R., Leazer Jr., J. L., Linderman, R. J., Lorenz, K. L., Manley, J., Pearlman, B. A., Wells, A., Zaks, A., Zhang, T. Y. *Green Chem.* **2007**, *9*, 411–420.
9) Yamauchi, T., Hattori, K., Mizutaki, S., Tamaki, K., Uemura, S. *Bull. Chem. Soc. Jpn.* **1986**, *59*, 3617–3620.
10) Tsuchimoto, T., Tobita, K., Hiyama, T., Fukuzuma, S.-i. *Synlett* **1996**, 557–559.
11) Isao, S., Meng, K. K., Miki, N., Takayuki, N., Akio, Y. *Chem. Lett.* **1997**, *26*, 851–852.
12) Suzuki, M., Shiina, I. *Tetrahedron Lett.* **2002**, *43*, 6391–6394.
13) Noji, M., Ohno, T., Fuji, K., Futaba, N., Tajima, H., Ishii, K. *J. Org. Chem.* **2003**, *68*, 9340–9347.
14) Sun, H.-B., Li, B. Chen, S., Li, J., Hua, R. *Tetrahedron* **2007**, *63*, 10185–10188.
15) Liu, Y.-L., Liu, L., Wang, Y.-L., Han, Y.-C., Wang, D., Chen, Y-J. *Green Chem.* **2008**, *10*, 635–640.
16) Choudhury, J., Podder, S., Roy, S. *J. Am. Chem. Soc.* **2005**, *127*, 6162–6163.
17) Jaratjaroonphong, J., Sathalalai, S., Techasauvapak, P., Reutrakul, V. *Tetrahedron Lett.* **2009**, *50*, 6012–6015.

18) Mertins, K., Iovel, I., Kischel, J., Zapf, A., Beller, M. *Adv. Synth. Catal.* **2006**, *348*, 691–695.

19) Mertins, K., Iovel, I., Kischel, J., Zapf, A., Beller, M. *Angew. Chem. Int. Ed.* **2005**, *44*, 238–242.

20) Iovel, I., Mertins, K., Kischel, J., Zapf, A., Beller, M. *Angew. Chem. Int. Ed.* **2005**, *44*, 3913–3917.

21) Qin, Q., Xie, Y., Floreancig, P. *Chem. Sci.* **2018**, *9*, 8528–8534.

22) Vuković, V. D., Richmond, E., Wolf, E., Moran, J. *Angew. Chem. Int. Ed.* **2017**, *56*, 3085–3089.

23) Hall, D. G. *Chem. Soc. Rev.* **2019**, *48*, 3475–3496.

24) McCubbin, J. A., Hosseini, H., Krokhin, O. V. *J. Org. Chem.* **2010**, *75*, 959–962.

25) Zheng, H., Ghanbari, S., Nakamura, S., Hall, D. G. *Angew. Chem. Int. Ed.* **2012**, *51*, 6187–6190.

26) Ricardo, C. L., Mo, X., McCubbin, J. A., Hall, D. G. *Chem. Eur. J.* **2015**, *21*, 4218–4223.

27) Colomer, I., Chamberlain, A. E. R., Haughey, M. B., Donohoe, T. J. *Nat. Rev. Chem.* **2017**, *1*, 0088.

28) Bentley, T. W., Carter, G. E. *J. Org. Chem.* **1983**, *48*, 579–584.

29) Mo, X., Yakiwchuk, J., Dansereau, J., McCubbin, J. A., Hall, D. G. *J. Am. Chem. Soc.* **2015**, *137*, 9694–9703.

30) Wolf, E., Richmond, E., Moran, J. *Chem. Sci.* **2015**, *6*, 2501–2505.

31) Mo, X., Morgan, T. D. R., Ang, H. T., Hall, D. G. *J. Am. Chem. Soc.* **2018**, *140*, 5264–5271.

32) Lovering, F., Bikker, J., Humblet, C. *J. Med. Chem.* **2009**, *52*, 6752–6756.

33) Estopiñá-Durán, S., Donnelly, L. J., Mclean, E. B., Hockin, B. M., Slawin, A. M. Z., Taylor, J. E. *Chem. Eur. J.* **2019**, *25*, 3950–3956.

34) Collins, K. D., Glorius, F. *Nat. Chem.* **2013**, *5*, 597–601.

35) Brown, H. C., Kanner, B. *J. Am. Chem. Soc.* **1966**, *88*, 986–992.

36) Li, Y., Xiong, Y., Li, X., Ling, X., Huang, R., Zhang, X., Yang, J. *Green Chem.* **2014**, *16*, 2976–2981.

37) Jin, T., Himuro, M., Yamamoto, Y. *Angew. Chem. Int. Ed.* **2009**, *48*, 5893–5896.

38) Middleton, W. J., Lindsey, R. V. *J. Am. Chem. Soc.* **1964**, *86*, 4948–4952.

39) Padmanaban, M., Biju, A. T., Glorius, F. *Org. Lett.* **2011**, *13*, 98–101.
40) Li, J., He, L., Liu, X., Cheng, X., Li, G. *Angew. Chem. Int. Ed.* **2019**, *58*, 1759–1763.
41) Zhang, X., Xia, A., Chen, H., Liu, Y. *Org. Lett.* **2017**, *19*, 2118–2121.
42) Munoz, S. B., Ni, C., Zhang, Z., Wang, F., Shao, N., Mathew, T., Olah, G. A., Prakash, G. K. S. *Eur. J. Org. Chem.* **2017**, *16*, 2322–2326.
43) Han, F., Yang, L., Li, Z., Yingwei, Z., Xia, C. *Adv. Synth. Catal.* **2014**, *356*, 2506–2516.

Chapter 3 Synthesis, Stability and Reactivity of Boranol-Containing Pseudoaromatic Cyclic Hemiboronic Acids[‡]

3.1 Introduction

3.1.1 Boron-Containing Heterocycles and Pseudoaromaticity

Boron-containing heterocyclic compounds have found wide-ranging applications from functional materials and chemical sensors to catalysts and bioactive compounds (Figure 3-1).[1–6] The replacement of an alkene C=C moiety with a B–O or B–N bond offers a strategy for the synthesis of a variety of isoelectronic analogs, which may demonstrate dramatically different electronic and optical properties than their all-carbon congeners.[7–12] The strategic installation of boron-heteroatom bonds has emerged as a promising strategy for the development of new classes of bioisosteric pharmacophores and offers new areas of chemical space for potential derivatization in medicinal chemistry.[13,14]

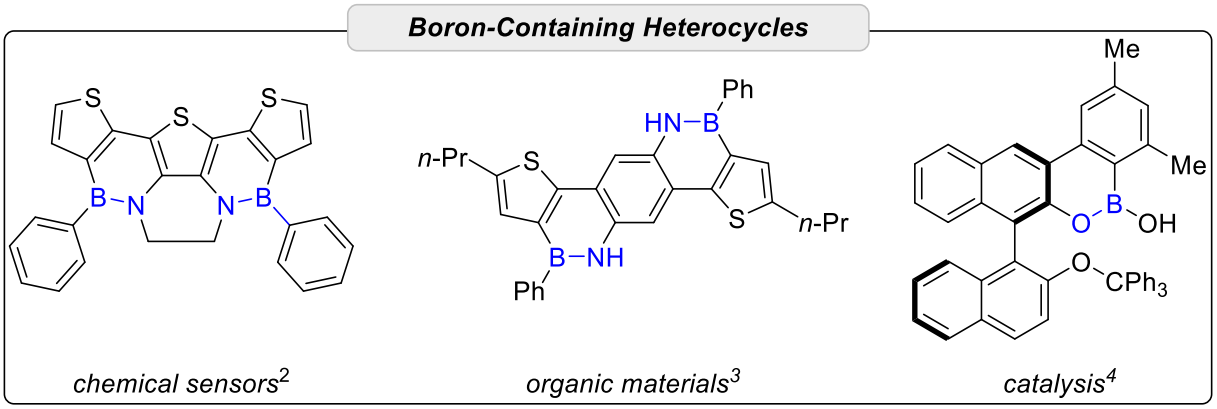

Figure 3-1 Applications of boron-containing heterocycles.

[‡]A version of this chapter has been published as Kazmi, M. Z. H., Rygus, J. P. G., Ang, H. T., Paladino, M., Johnson, M. A., Ferguson, M. J., Hall, D. G. *J. Am. Chem. Soc.* **2021**, *143*, 10143–10156.

Heterocyclic compounds containing boranol (B–OH) units have shown promise as therapeutic agents, with three cyclic non-aromatic hemiboronic acids being commercialized in the past decade (Figure 3-2a).[15–17] Boranol-containing compounds generally demonstrate several desirable properties in the development of medicinal chemistry candidates including hydrogen bonding capabilities and mild acidity in aqueous solution, allowing both trivalent and tetravalent boron coordination spheres to be accessed under physiological conditions. The ability to undergo reversible dative or covalent exchange with nucleophilic residues on biomolecules is essential to the design of new boranol-containing pharmaceutical compounds.[13]

Bioisosterism is an essential concept in drug design in which the rational modification of lead compounds with sterically or electronically similar groups is explored to modify biological activity or attenuate toxicity.[18,19] Arene bioisosterism has been widely explored using saturated carbocycles with comparable C–C distances to benzene,[20] including bicyclo[1.1.1]pentane,[21] bicyclo[2.2.2]octane[22] and cubane.[23] Bioisosteric replacement can dramatically impact compound solubility and lipophilicity,[24] while the use of saturated arene bioisostere disrupts intermolecular π-stacking interactions that may be present in the parent aromatic compound.[25] The development of arene bioisosteres that retain moderate aromaticity would offer new strategies for the rational modification of aromatic drug candidates without necessarily sacrificing π-stacking interactions that may be important towards the desired biological activity. Furthermore, the incorporation of isosteric heteroatom-containing functionality may allow for additional interactions that are not possible in the all-carbon analogs, such as hydrogen bonding or dipole-dipole interactions.

In this context, pseudoaromatic boron-containing heterocycles have emerged as promising bioisosteric arene replacements, with the 1,2-azaborine family being particularly well studied in clinical candidates (Figure 3-2b).[26–28] Interest in azaborine compounds dates back nearly a century

to the 1926 synthesis of borazine, a carbon-free benzene analog containing alternating B–N bonds.[29] The isoelectronic replacement of a C=C unit with a B–N bond has been shown to significantly alter the biologically relevant properties of therapeutic agents, such as their solubility, membrane permeability, and bioavailability.[26] These 1,2-azaborine scaffolds have generally demonstrated diminished aromaticity in computational studies relative to their parent all-carbon analogs based on both experimental and computational methods.[30,31] In view of their somewhat diminished aromaticity, the diene component of 1,2-azaborines has been shown to undergo Diels-Alder reactions with electron-deficient dienophiles on par with other aromatic heterocycles such as furan or thiophene.[32] Improved access to boron-containing heterocycles with new synthetic methods has allowed for deeper interrogation of these compounds and will undoubtedly lead to new applications.[33]

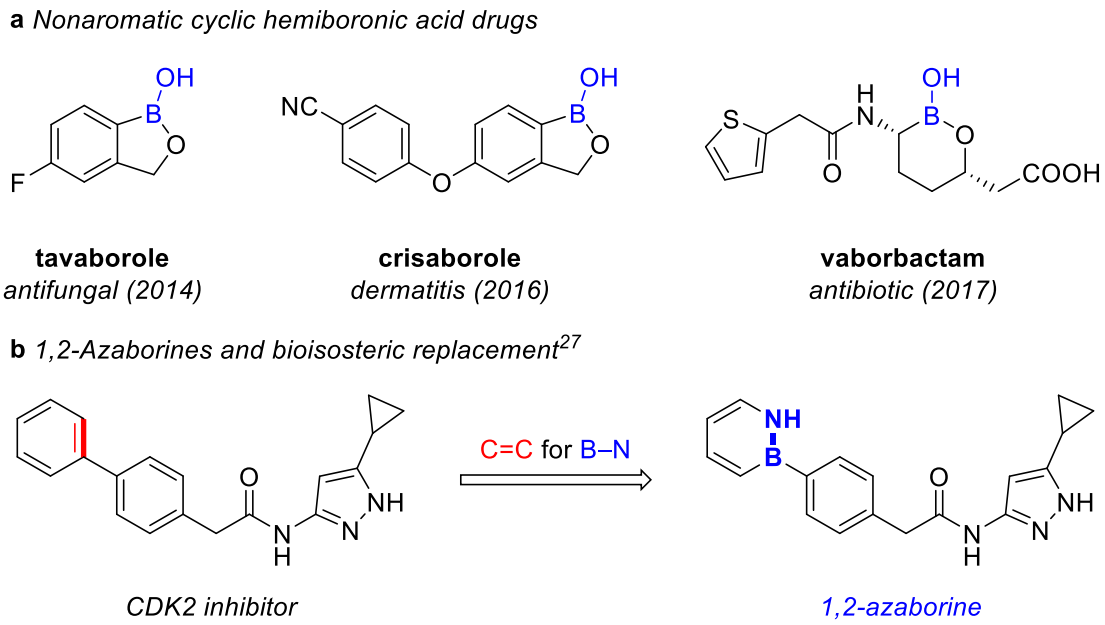

Figure 3-2 a Nonaromatic cyclic hemiboronic acid drugs. **b** 1,2-azaborines and bioisosteric replacement.

Pseudoaromatic cyclic hemiboronic acids, containing both a boranol group and an endocyclic boron-heteroatom bond embedded into an otherwise aromatic core, are a particularly

intriguing class of substructures. The most widely studied motifs within this area are the benzoxazaborine (**3-01**) and benzodiazaborine (**3-02**) scaffolds (Figure 3-3), which are isoelectronic and isosteric analogs of 4-hydroxyquinoline (**3-03**).[1] The benzodiazaborine core has found numerous applications in biological chemistry, including as steroidal mimics,[34] antibacterial agents[35] and antifungal compounds.[36] Since the first reported synthesis of **3-01** by Snyder and co-workers over 60 years ago,[37] these cyclic hemiboronic acids have been the subject of significant debate in the literature regarding their pseudoaromatic and acidic nature, with contradicting views and conclusions being presented.

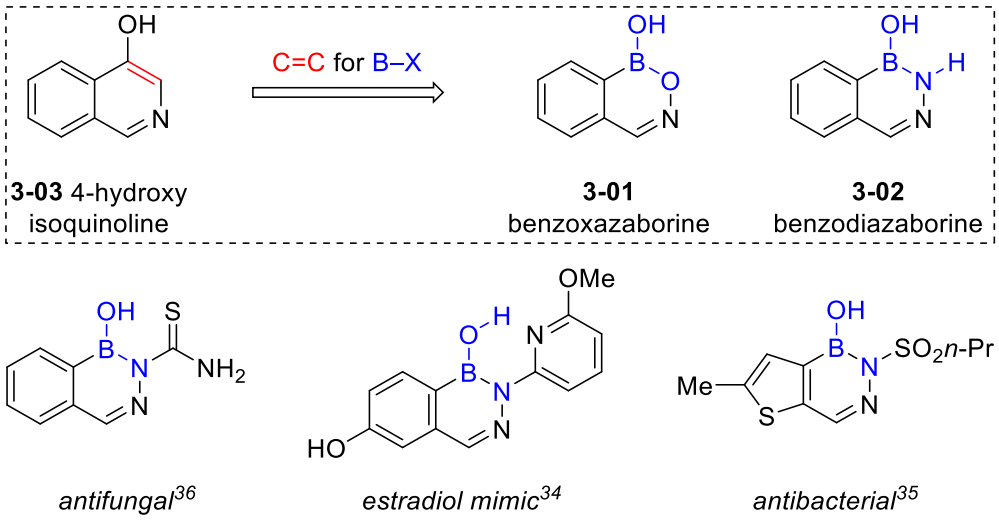

Figure 3-3 Pseudoaromatic hemiboronic acids.

3.1.2 Contrasting Views on the Acidic Nature of Benzoxazaborine and Benzodiazaborines

Arene isosters containing a boron-heteroatom (B–X, X = O or NR) bond retain two alkene units in a cyclic geometry, accounting for four π electrons. An additional contribution to the π system can be considered involving interaction of the lone pair of electrons from the endocyclic heteroatom with the vacant p orbital of boron (X_n–B_p). Provided the boron-containing ring is

sufficiently planar to achieve satisfactory overlap of these orbitals, the heterocyclic ring formally contains six delocalized π electrons and thus obeys Hückel's rule of aromaticity (Scheme 3-1a).[38]

The extent of the aromaticity in pseudoaromatic cyclic hemiboronic acids is intrinsically linked to the nature of their acidity (Scheme 3-1b). Boronic acid derivatives are well established to act as Lewis acids in aqueous solution, reacting with two equivalents of water to form a tetravalent hydroxyboronate anion and associated hydronium cation which conveys indirect Brønsted acidity.[39,40] However, formation of this tetravalent conjugate base entails re-hybridization of the boron center from sp^2 to sp^3. Accordingly, formation of a tetravalent conjugate base (**I**) would disrupt aromaticity in the boron-containing ring. To avoid unfavourable dearomatization, it has been postulated that these heterocycles instead act as direct Brønsted acids through deprotonation of the B–OH moiety to form a boron oxy anion species (**II**) in reactivity that more closely resembles an alcohol.

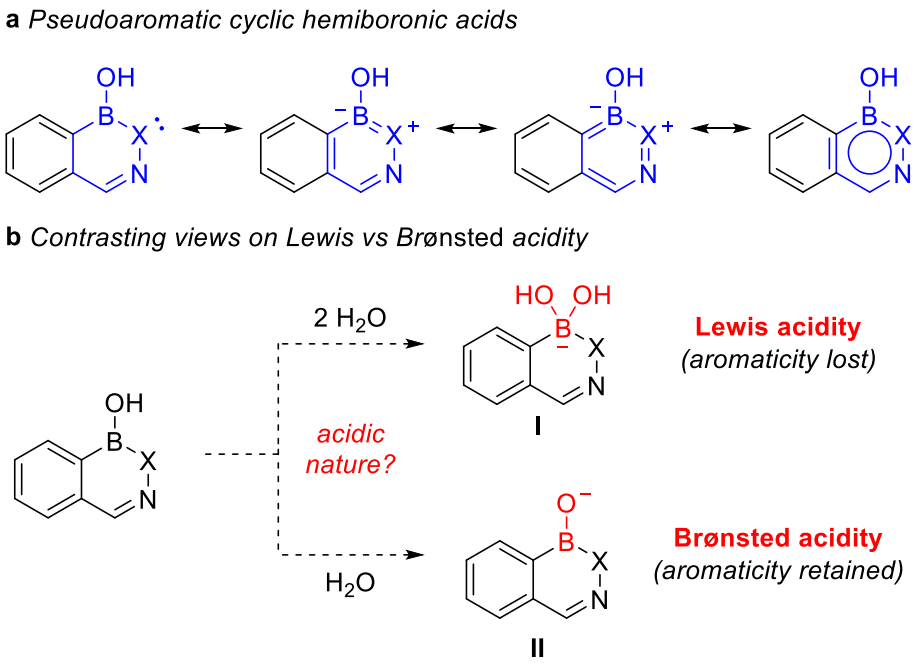

Scheme 3-1 a Pseudoaromaticity in cyclic hemiboronic acids. **b** Uncertainty regarding the acidic nature of these heterocycles.

The first systematic studies on the properties of heterocycles **3-01** and **3-02** were conducted by Dewar and Dougherty in 1962.[41] They demonstrated that unlike typical aromatic hydrazones or boronic acids, compound **3-02** could be successfully recovered after boiling in concentrated hydrochloric acid or potassium hydroxide solution. It was proposed that the unusual hydrolytic stability of **3-02** arises from the aromaticity of the boron-containing ring.[41] Compound **3-01** was examined by UV spectroscopy, where a small bathochromic shift was observed at high pH. Given that Lewis acidic arylboronic acids generally demonstrate a hypsochromic shift under comparable conditions, the observed bathochromic shift for heterocycle **3-01** was taken as evidence for Brønsted acidity, and consequently **3-01** was proposed to contain significant aromaticity in the heterocyclic ring.[41] The same authors later suggested that the N–H stretching mode of heterocycle **3-02** was observed at significantly lower energy than expected, which was rationalized by relatively significant contribution of B=N double bond character.[42] Reaction of heterocycle **3-01**

with 2-ethanolamine led to formation of a new species that was proposed to be adduct **3-04**, while heterocycle **3-02** showed no reaction to form adduct **3-05** under the same conditions (Scheme 3-2). This reactivity was taken as evidence for the greater aromaticity of B–N containing heterocycle **3-02** relative to B–O containing heterocycle **3-01**.[42]

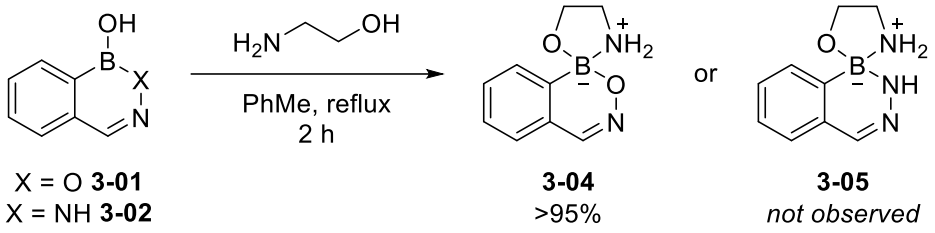

Scheme 3-2 Proposed ethanolamine adduct formation from heterocycle **3-01**.

The emergence of ^{11}B NMR techniques has proven instrumental in the study and elucidation of boron chemical environments and ionization states. Chemical shifts in ^{11}B NMR are highly informative as to the hybridization of boron.[43] Neutral trivalent boronic acid derivatives generally display ^{11}B NMR chemical shifts between 25–30 ppm, while the corresponding tetravalent anionic boronates are found noticeably upfield (0–5 ppm).[44] Heterocycles **3-01** and **3-02** have been studied by ^{11}B NMR over the past several decades in an attempt to elucidate the structure of their conjugate bases, and consequently to resolve the debate regarding their acidic nature.

The ^{11}B NMR analysis of heterocycles **3-01** and **3-02** under basic conditions was first reported by Dewar and Jones in 1967.[45] Upon reaction with potassium hydroxide in ethanol, heterocycle **3-01** displayed a chemical shift of 5.0 ppm, significantly upfield relative to the observed shift in the absence of base (Scheme 3-3). This data was taken as support for formation of tetravalent conjugate base **3-01-I**, suggesting the Lewis acidic nature of heterocycle **3-01** in contrast to previous proposals described above.[45] Conversely, a chemical shift of 29.8 ppm was

reported for heterocycle **3-02** under the same alkaline conditions. The authors claimed that the lack of upfield resonance was conclusive evidence for the Brønsted acidity of **3-02** to form conjugate base **3-02-II**, and thus a reflection of a large energetic penalty for disrupting aromaticity necessary to form a Lewis conjugate base. [45]

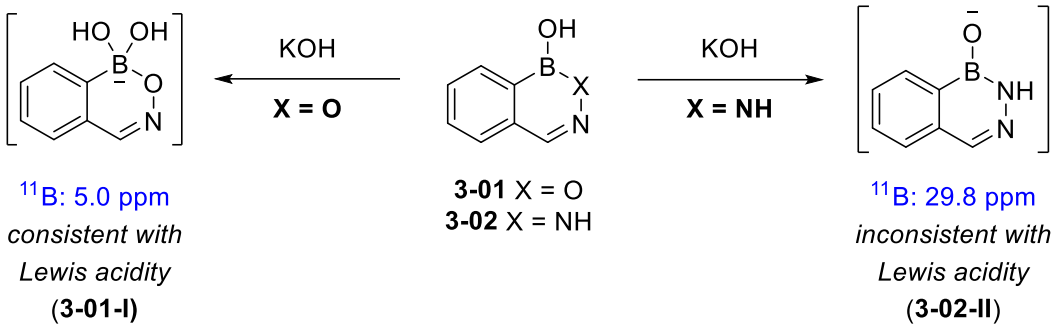

Scheme 3-3 Early ^{11}B NMR studies of heterocycles **3-01** and **3-02** under basic conditions.

The implications of boranol Brønsted acidity on ^{11}B NMR are complicated by the absence of reliable NMR data in aqueous solution for a trivalent boron oxy compound (ie. conjugate base **II** in Scheme 3-1b). Without reference data, it cannot be stated categorically that the absence of an upfield chemical shift under alkaline conditions provides evidence for Brønsted acidity. Solid state ^{11}B NMR analysis of inorganic oxyborate salts has revealed chemical shifts in the range of 16–20 ppm,[46] while a zirconium-bound bis(siloxy)boryloxide displayed a chemical shift of 13.0 ppm in benzene-d_6.[47] This limited data set does not support the formation of a boron-oxy conjugate base **3-01-II** from hemiboronic acid **3-01**.

Further solution state analyses of heterocycles **3-01** and **3-02** were conducted by Groziak and co-workers in 1997 using ^{11}B NMR and ^{18}O-labelling experiments as part of their efforts to develop boron-containing nucleic acid mimics.[48] Incorporation of ^{18}O through reaction with $H_2{}^{18}O$ was believed to occur through an associative addition-elimination mechanism, suggesting that the

rate of ^{18}O-incorporation should be correlated to Lewis acidity (Scheme 3-4a). When ^{11}B NMR analysis was conducted in aqueous NaOH, heterocycle **3-02** displayed a chemical shift of 26.9 ppm, inconsistent with the formation of a tetravalent conjugate base. However, heterocycle **3-02** was found to readily undergo ^{18}O-incorporation through boranol exchange upon reaction with $H_2{}^{18}O$ (Scheme 3-4b).[48] In contrast, heterocycle **3-01** displayed a significant upfield chemical shift by ^{11}B NMR in alkaline solution (2.2 ppm) consistent with Lewis acidic behaviour. Analogous $^{18}OH_2$ exchange experiments, however, demonstrated that ^{18}O-incorporation occurred significantly slower than in heterocycle **3-02** (Scheme 3-4b).[48] Furthermore, pH-dependent potentiometric measurements for both heterocycles revealed estimated pK_a values of 4.8 for heterocycle **3-01** and approximately 8 for heterocycle **3-02**.[48] However, potentiometric titrations provide no insight as to the chemical structure of the species involved in the ionization equilibrium.

To rationalize the seemingly conflicting results of their ^{11}B NMR and ^{18}O-labelling studies, the authors proposed that heterocycles **3-01** and **3-02** are "characterized by a predominant Brønsted acidity, [yet] retain some degree of Lewis acidity".[48] Hemiboronic acid **3-01** was believed to demonstrate primarily Brønsted acidity in water, and it was proposed that little aromaticity was retained in the heterocyclic ring. It was further suggested that oxyanion negative charge in the corresponding Brønsted conjugate base **3-01-II** can readily be delocalized onto boron in accordance with the upfield ^{11}B NMR chemical shift under basic conditions. To rationalize the pH-insensitivity of the ^{11}B NMR chemical shift for hemiboronic acid **3-02**, it was suggested that little delocalization of the oxyanion charge in Brønsted conjugate base **3-02-II** onto boron can occur due to the proposed aromaticity of the boron-containing ring and electrostatic repulsion with the adjacent sp^2-hybridized nitrogen atom.[48] However, the high sensitivity of ^{11}B NMR chemical shifts calls this suggestion into question.[43]

Moreover, boranol exchange experiments described in the study by Groziak and co-workers are difficult to rationalize within their proposed acidic framework (Scheme 3-4c).[48] Heterocycle **3-01** was found to readily undergo exchange with methanol to form the corresponding *B*-methoxy derivative **3-06a**. Conversely, heterocycle **3-02** proved resistant to methanol exchange even under prolonged reflux and *B*-methoxy derivative **3-07a** was not observed. These results directly contrast the ^{18}O-incorporation studies, in which facile ^{18}O-incorporation was observed for heterocycle **3-02**.[48]

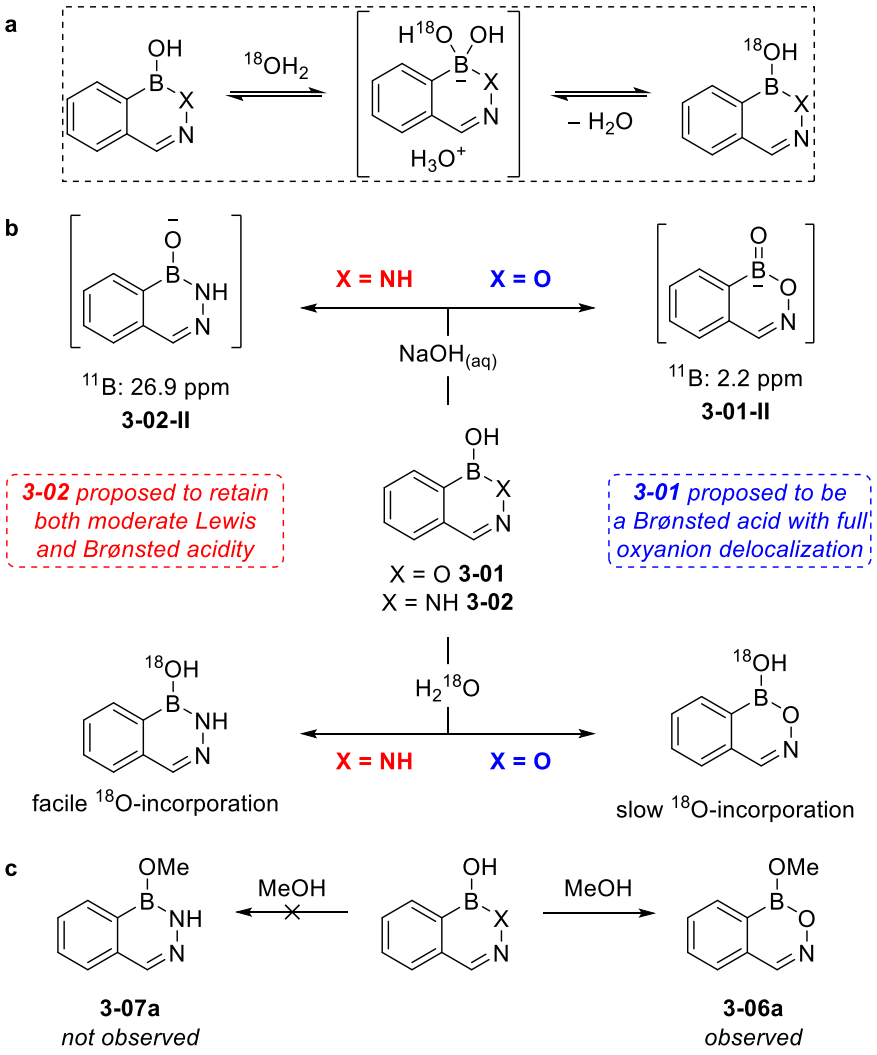

Scheme 3-4 Conclusions of Groziak and co-workers. **a** Postulated mechanism for ^{18}O-incorporation. **b** ^{11}B NMR and ^{18}O-incorporation experiments. **c** Contradictory methanol exchange studies.

3.2 Objectives

Taken together, the above studies on heterocycles **3-01** and **3-02** have failed to fully elucidate the true nature of their acidity. In the absence of unambiguous structural characterization of the conjugate bases, inferences based on indirect evidence have predominated, leading to several ambiguities that have prevented a complete understanding of these important scaffolds. To guide the rational application of these boron heterocycles in catalysis and medicinal chemistry, it is essential to understand their fundamental stability, reactivity, and acidity.

This chapter will describe a systematic experimental study on a series of model benzoxazaborine and benzodiazaborine naphthoid heterocycles. The synthesis of these model compounds will be described, and spectroscopic data will be compared to analogous non-boron-containing compounds. The acidity of the heterocycles will be measured through experimental pK_a measurements, while crystallographic evidence will be presented to unambiguously resolve the question of their acidic nature. The reactivity of the boranol group will be studied through alcohol exchange experiments, while dynamic exchange and crossover experiments will be conducted to gauge the hydrolytic stability of the endocyclic boron-heteroatom bond. Additionally, computational results will be presented to support the conclusions of the experimental studies.

It is important to note that this study was performed in collaboration with several other lab members, and their contributions will be described and noted in this chapter where relevant to my own contribution. Knowledge gathered from this study is directly relevant to the application of cyclic hemiboronic acids in catalysis, which will be described in Chapter 4.

3.3 Results and Discussion

3.3.1 Synthesis of Model Heterocycles

A series of representative boron-containing heterocycles were targeted for our experimental study. In addition to the parent benzoxazaborine (**3-01**) and benzodiazaborine (**3-02**) compounds, a small library of *N*-substituted benzodiazaborines were chosen to gauge the impact of substitution at the boron-bound heteroatom, including *N*-methyl derivative **3-08**, *N*-phenyl derivative **3-09**, and *N*-sulfonyl derivative **3-10**. Synthesis of these compounds proceeded readily by condensation of 2-formylphenylboronic acid **3-11** with hydroxylamine or the requisite hydrazine (Scheme 3-5). The resulting boron heterocycles were obtained on gram-scale as bench-stable solids.

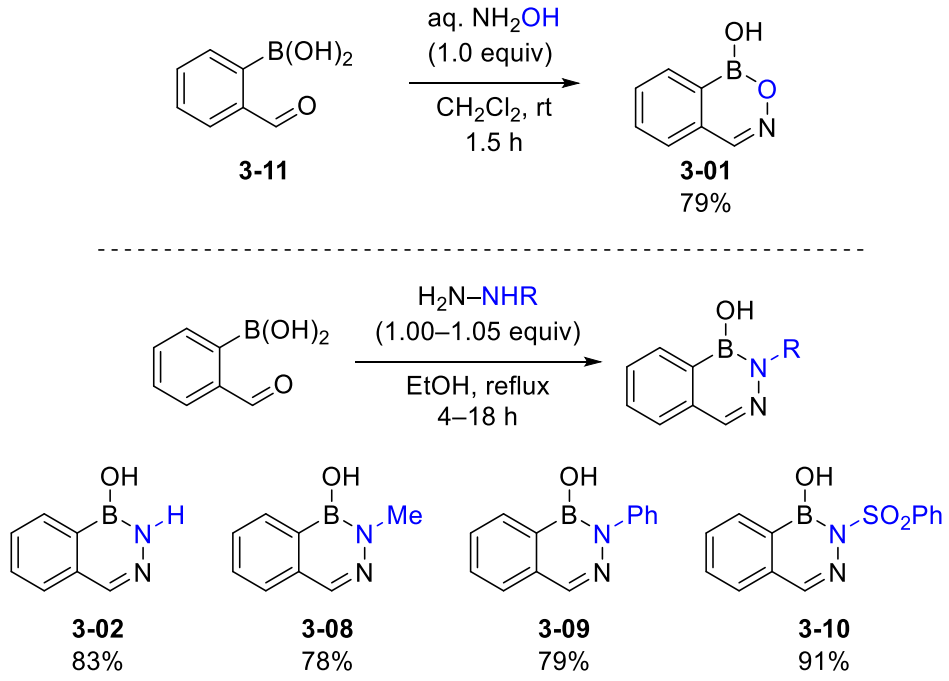

Scheme 3-5 Synthesis of model pseudoaromatic cyclic hemiboronic acids.

Additionally, hemiboronic acid **3-10** was synthesized from pinacol ester **3-12** upon reaction with benzenesulfonyl hydrazide in refluxing ethanol (Scheme 3-6). This result suggests that in the synthesis of other *N*-sulfonyl cyclic hemiboronic acids for future applications, pinacol esters can

be used as starting materials without the need to liberate the free boronic acid, which can be difficult to purify.

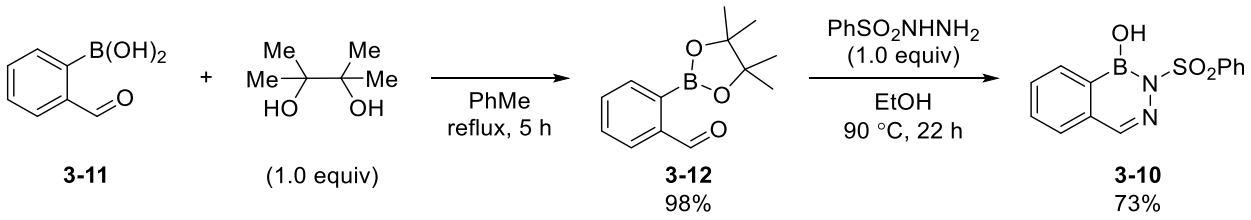

Scheme 3-6 Alternative synthesis of hemiboronic acid **3-10**.

Although the ^{11}B NMR resonances showed little variation across the range of heterocycles, the boranol proton chemical shifts were observed to span a range of nearly 1 ppm (Scheme 3-7). Addition of a drop of D_2O to the acetone-*d*$_6$ NMR solutions, which is commonly done in the analysis of boranol-containing compounds to prevent the formation of B–O–B anhydride dimers,[49] led to disappearance of the boranol proton by ^{1}H NMR, consistent with chemical exchange. The aldimine C–H resonances span a range of roughly 0.5 ppm, and in all cases were significantly upfield of the C=C isostere **3-03**. Interestingly, acyclic oxime (**3-13**) and hydrazone (**3-14**–**3-17**) comparator compounds (prepared by graduate student Zain Kazmi and postdoctoral fellow Dr. Marco Paladino) universally demonstrated C–H chemical shifts upfield of the corresponding hemiboronic acids, though it is unclear whether this can be attributed to anisotropy effects of the pseudoaromatic ring or to the electron-withdrawing effect of the B–X bond.

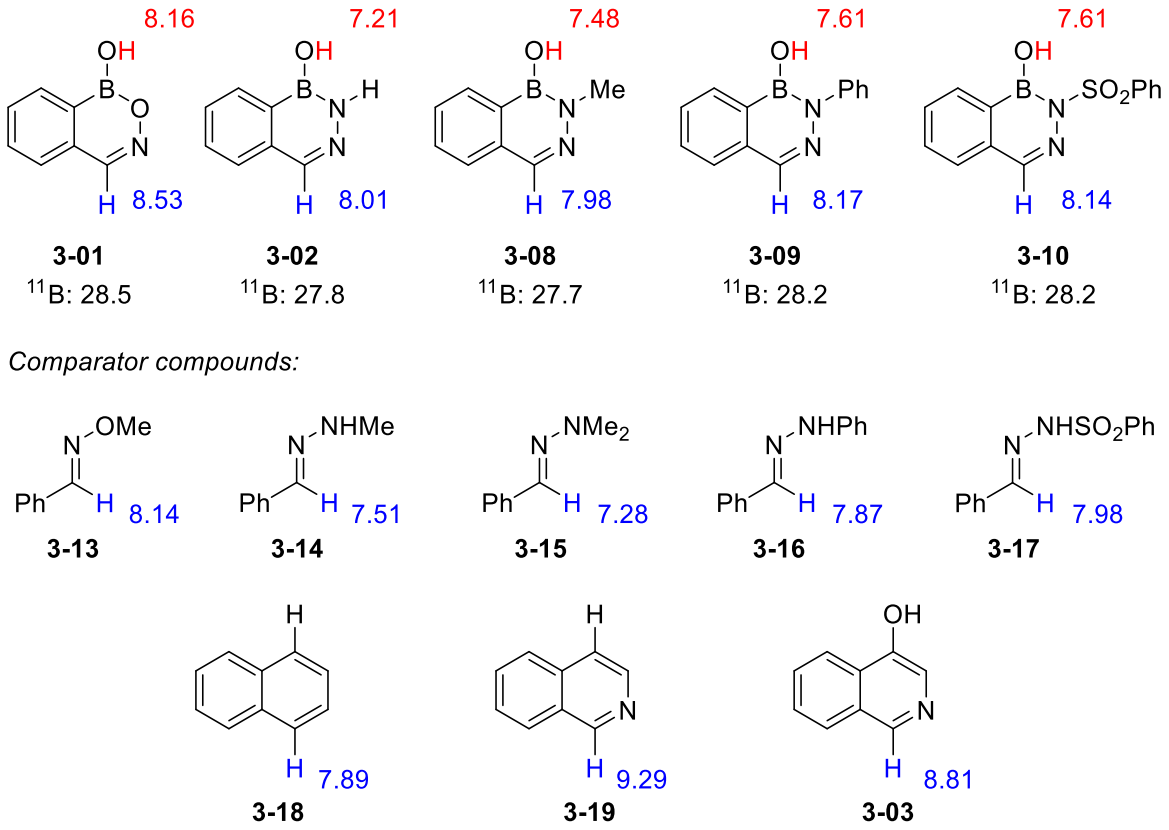

Scheme 3-7 Comparison of NMR data for model cyclic hemiboronic acids with comparator compounds. Chemical shifts are reported in ppm and acetone-d_6 was used as a solvent.

3.3.2 Alcohol Exchange Experiments

With model heterocycles in hand, the exchangeability of the boranol moiety with exogeneous alcohols was examined. Accordingly, methanolysis reactions to form the corresponding methyl esters were investigated following two different procedures. In the first, the heterocycles were dissolved in a large excess of anhydrous methanol for 0.5–24 hours at room temperature prior to concentration under reduced pressure, after which the extent of boranol exchange was quantified by ^{1}H NMR. Additionally, exchange in polar aprotic solvents was monitored by dissolving the heterocycles in CD_3CN along with 5 equivalents of dry methanol. In the latter procedure, the use of rotary evaporation is avoided entirely.

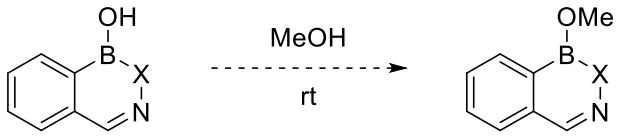

Scheme 3-8 General reaction for methanol exchange of cyclic hemiboronic acids to form the corresponding *B*-methoxy derivatives.

Reaction of heterocycle **3-01** in anhydrous methanol for 30 minutes led to the formation of a new species by ^{1}H NMR, with notable new resonances (marked with an asterisk) in the aromatic region at 8.48 ppm (s, 1 H) and 7.96 ppm (d, J = 7.6 Hz, 1 H), along with a key resonance at 3.88 ppm (s, 3 H) significantly downfield relative to the corresponding resonance in free MeOH (Figure 3-4). Analysis by ^{11}B NMR revealed the appearance of a new resonance slightly upfield of the starting heterocycle at 27.7 ppm (relative to **3-01** at 28.6 ppm). These new signals are consistent with equilibrium formation of *B*-methoxy derivative **3-06a**. The formation of **3-06a** was further supported by HRMS analysis of the reaction mixture. The extent of methanol exchange was calculated from the formula Percent Exchange $= 100\% \times (\text{mmol B–OMe}) \div [(\text{mmol B–OMe}) + (\text{mmol B–OH})]$. After 30 minutes, 38% exchange was observed (Scheme 3-9).

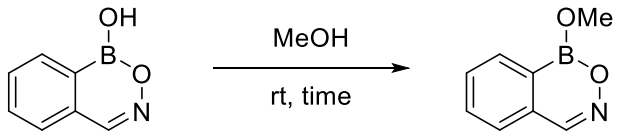

3-01

3-06a
30 min: 38%
24 h: 46%

Scheme 3-9 Methanol exchange of **3-01**.

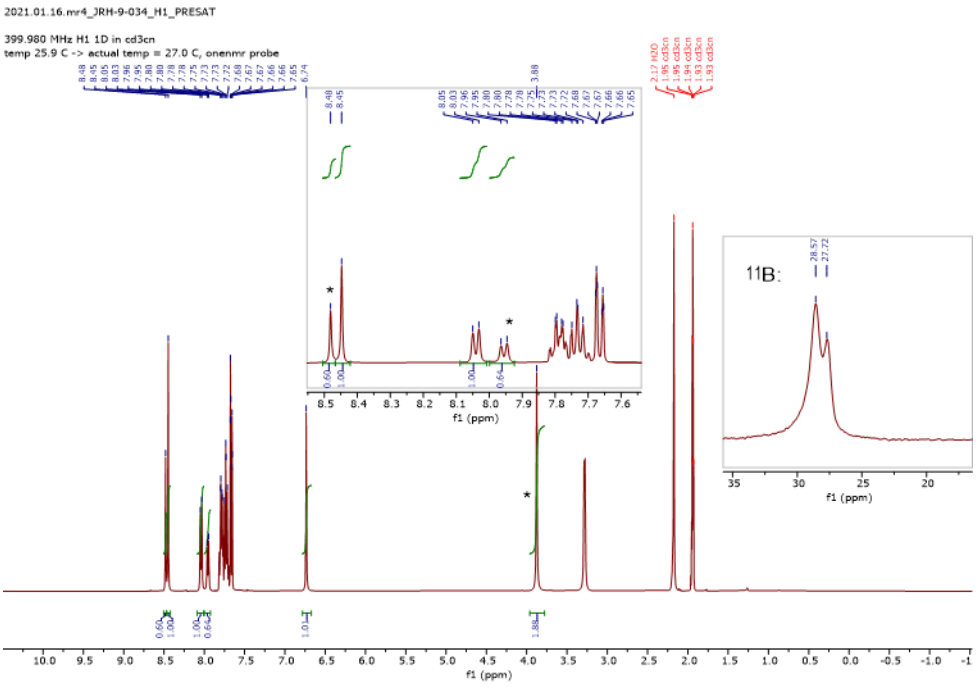

Figure 3-4 ^{1}H (400 MHz, CD_3CN) and ^{11}B (128 MHz) NMR of methanol exchange with **3-01** after 30 minutes. New ^{1}H resonances consistent with formation of **3-06a** are marked with an asterisk.

After 24 hours in methanol, 46% exchange was observed, suggesting that the equilibrium between hemiboronic acid and the corresponding methyl ester is relatively unchanged over prolonged reaction time. When heterocycle **3-01** was reacted with 5 equivalents anhydrous methanol in CD_3CN solution for 30 minutes, a similar analysis demonstrated 56% MeOH exchange, relatively comparable to the results observed in neat methanol. The addition of a drop of D_2O to a mixture of **3-01** and **3-06a** led to full hydrolysis of **3-06a**, and the corresponding B–OD hemiboronic acid was observed by both ^{1}H and ^{11}B NMR (Figure 3-5 & Figure 3-6). Due to H/D exchange with D_2O, the boranol proton was not observed in the hydrolyzed product after addition of D_2O. Facile hydrolysis of **3-06a** is consistent with a previous report by Groziak.[48] Efforts to prepare methyl ester **3-06a** stoichiometrically through azeotropic removal of water were unsuccessful, and **3-06a** was always observed as a mixture with hemiboronic acid **3-01**.

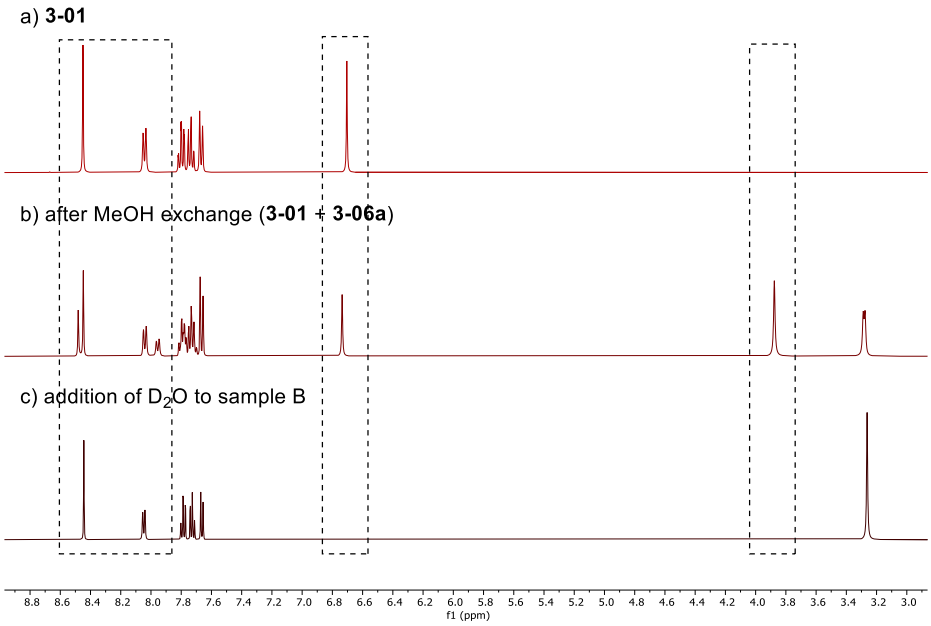

Figure 3-5 ^{1}H (400 MHz, CD_3CN) NMR demonstrating reversible methanol exchange of **3-01** and hydrolysis of **3-06a** upon addition of D_2O.

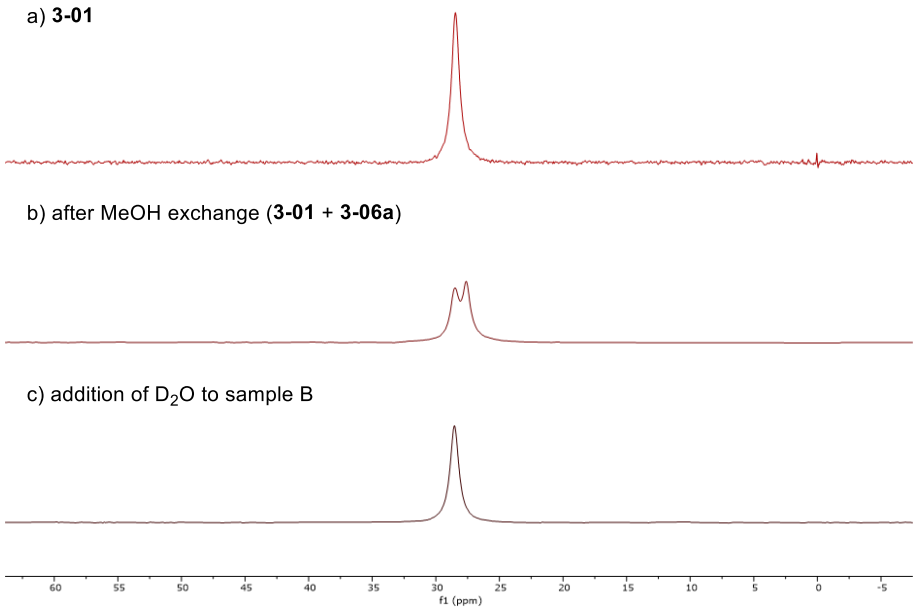

Figure 3-6 ^{11}B (128 MHz, CD_3CN) NMR demonstrating reversible methanol exchange of **3-01** and hydrolysis of **3-06a** upon addition of D_2O.

Alcohol exchange in anhydrous methanol with heterocycle **3-02** was analyzed by a similar procedure. As with heterocycle **3-01**, new resonances were observed by ^{1}H NMR consistent with formation of *B*-methoxy compound **3-07a**, including 9.87 ppm (br s, 1 H) and 3.86 ppm (s, 3 H) (Figure 3-7). Additionally, a new resonance was observed by ^{11}B NMR at 27.5 ppm, slightly upfield of the starting heterocycle (28.0 ppm). Formation of **3-07a** was also supported by HRMS analysis. After 30 minutes in anhydrous methanol, ^{1}H NMR showed 50% methanol exchange. Similar analysis after 24 hours demonstrated 54% exchange, further suggesting that equilibrium is established within the first 30 minutes. Methanol exchange in CD_3CN solution demonstrated 45% exchange (Scheme 3-10).

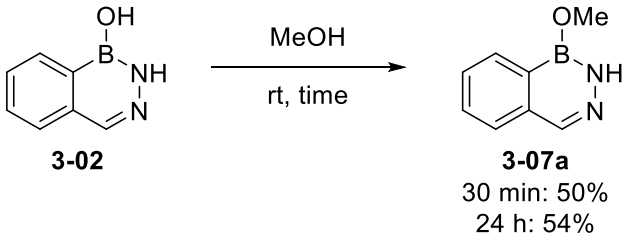

Scheme 3-10 Methanol exchange of **3-02**.

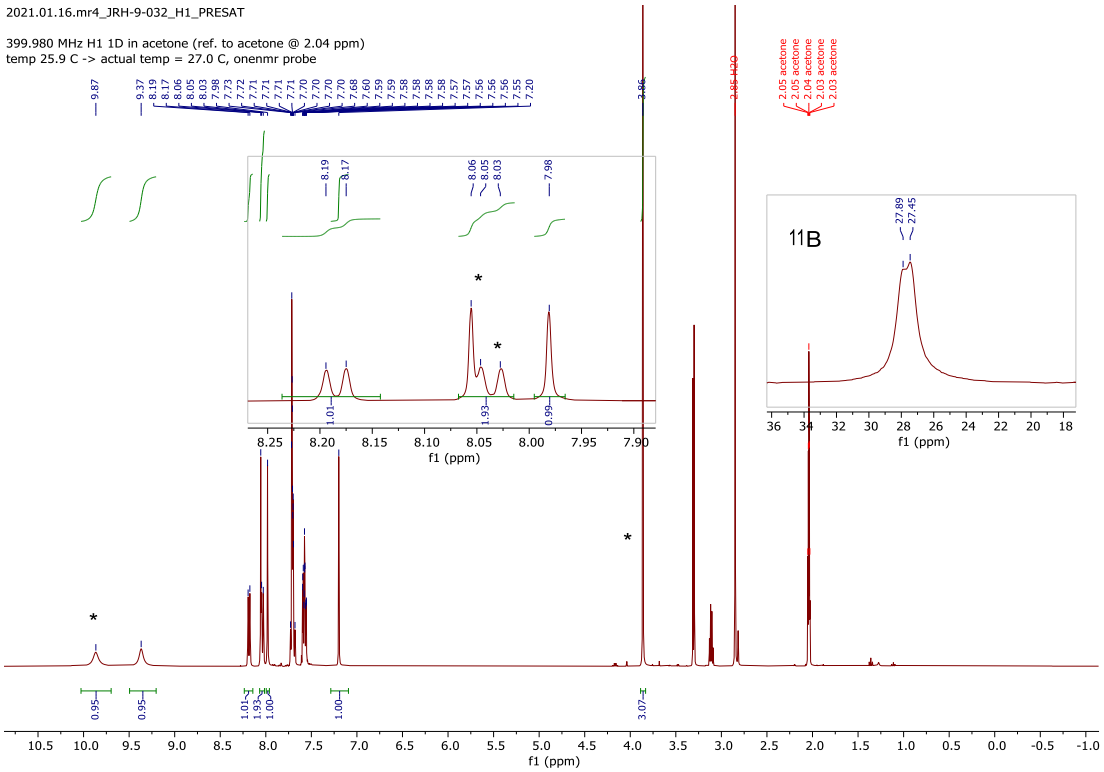

Figure 3-7 ^{1}H (400 MHz, d_6-acetone) and ^{11}B (128 MHz) NMR of methanol exchange with **3-02** after 30 minutes. New ^{1}H resonances consistent with formation of **3-07a** are marked with an asterisk.

As with heterocycle **3-01**, addition of D_2O to a mixture of **3-02** and **3-07a** led to complete hydrolysis of **3-07a** and formation of the corresponding B–OD hemiboronic acid, where the boranol proton was not observed due to chemical exchange (Figures 3-8 & 3-9). Incomplete H/D exchange was observed for the NH resonance. The diminished exchange rate of the NH proton is supported by previous ^{15}N NMR studies of **3-02** which suggested that this motif behaves comparably to a secondary amide, for which incomplete H/D exchange with D_2O has been described.[48,50]

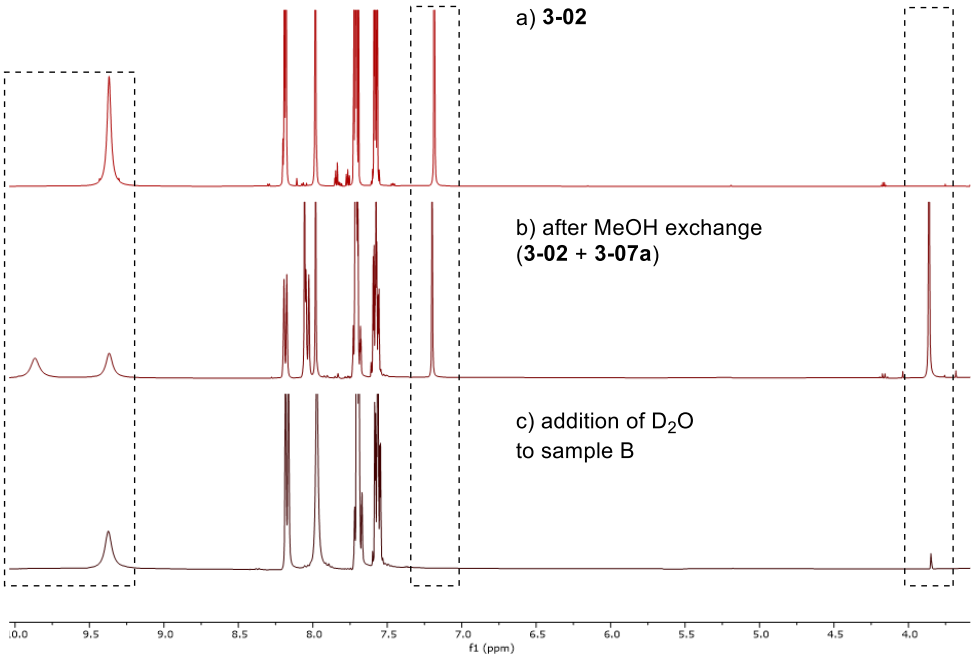

Figure 3-8 ^{1}H (400 MHz, d_6-acetone) NMR demonstrating reversible methanol exchange of **3-02** and hydrolysis of **3-07a** upon addition of D_2O.

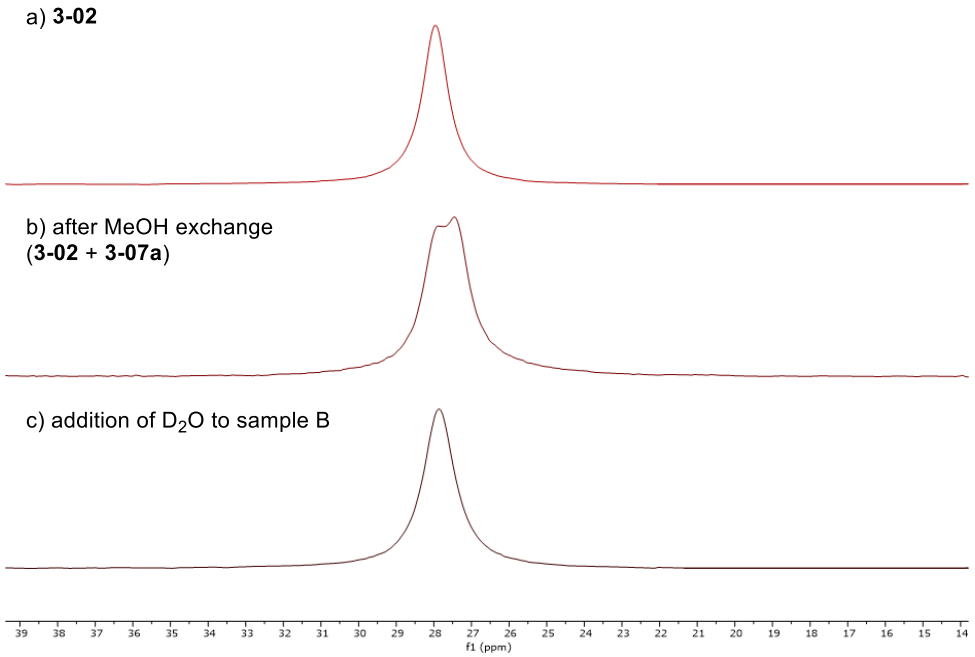

Figure 3-9 ^{11}B (128 MHz, d_6-acetone) NMR demonstrating reversible methanol exchange of **3-02** and hydrolysis of **3-07a** upon addition of D_2O.

When boranol exchange in neat methanol was examined for *N*-methyl derivative **3-08**, no evidence for formation of the corresponding *B*-methoxy derivative **3-20** was observed. Instead, approximately 7% conversion to the B–O–B dimer or other anhydride species was observed by ^{1}H NMR (Scheme 3-11). This process was fully reversible upon addition of D_2O (Figure 3-10). Only trace conversion to the anhydride species was observed in CD_3CN solution. The dehydration of boranol-containing compounds to their corresponding anhydrides is known to be highly solvent dependent.[51,52] Heterocycle **3-08** and the proposed anhydride were indistinguishable by ^{11}B NMR.

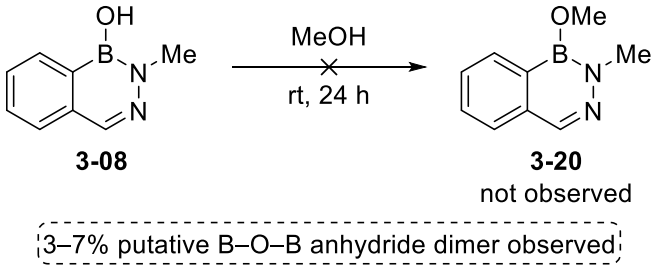

Scheme 3-11 Attempted methanol exchange of heterocycle **3-08**.

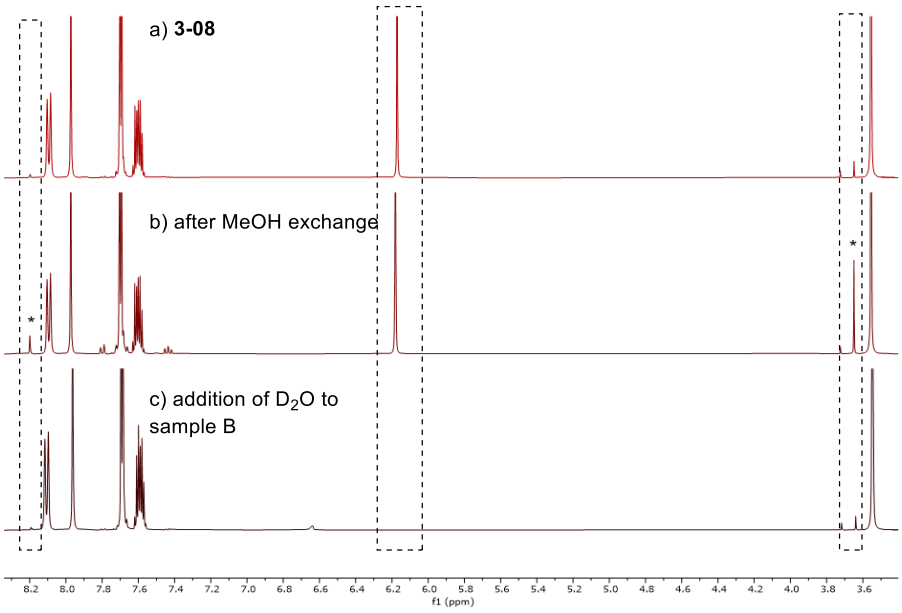

Figure 3-10 ^{1}H (400 MHz, CD_3CN) NMR evidence for anhydride formation from heterocycle **3-08** and reversible hydrolysis upon addition of D_2O.

The behaviour of *N*-phenyl heterocycle **3-09** in MeOH was in stark contrast to that which was observed with heterocycles **3-01**, **3-02** and **3-08**. For compounds **3-01** and **3-02**, methanolysis resulted in new aromatic resonances with the same multiplicity and slightly different chemical shifts, along with the formation of a characteristic B–OCH_3 resonance suggesting formation of the desired *B*-methoxy derivative. When heterocycle **3-09** was exposed to anhydrous methanol, many small new resonances of unclear origin were observed (Figure 3-11).

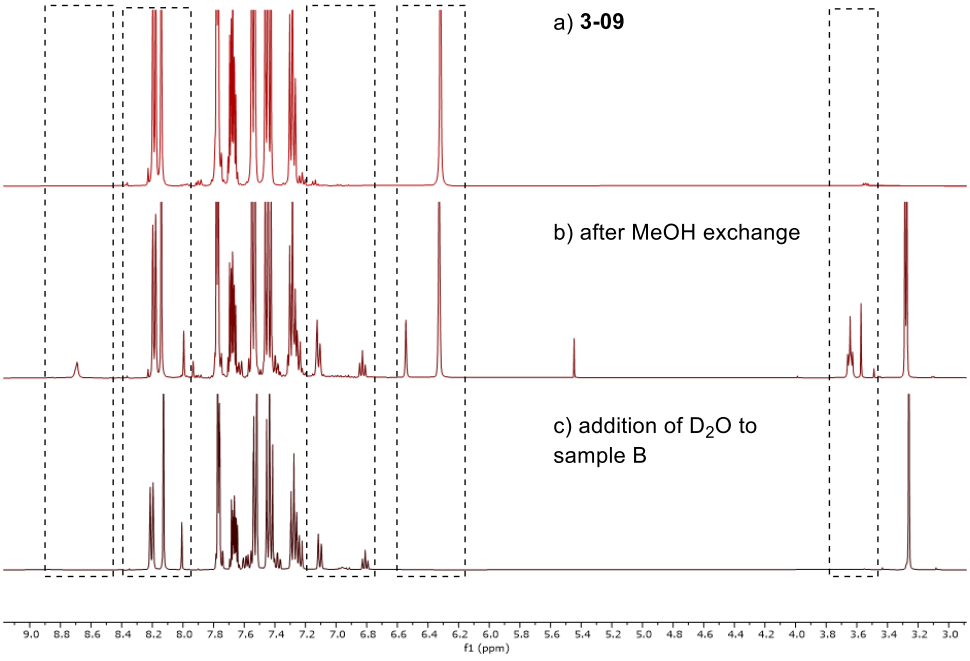

Figure 3-11 ^1H (400 MHz, CD_3CN) NMR evidence for irreversible decomposition of heterocycle **3-09** in methanol.

The characteristic B–OCH_3 resonances were observed noticeably upfield (3.65 and 3.57 ppm) relative to those observed for *B*-methoxy compounds **3-06a** and **3-07a**. Furthermore, an addition resonance was observed with a chemical shift comparable to the boranol proton (6.52 ppm), and a new highly deshielded resonance was observed at 8.70 ppm. Addition of D_2O to the NMR sample resulted in hydrolysis or chemical exchange of these new resonances, but clean

conversion to the B–OD hemiboronic acid was not observed. This suggests that unlike analogous methanol exchange reactions of heterocycles **3-01** and **3-02,** clean conversion of **3-09** to the corresponding *B*-methoxy derivative **3-21** is not occurring (Scheme 3-12a), and that the reaction of **3-09** with methanol is not fully reversible upon addition of water. It was postulated that there may be endocyclic B–N bond cleavage of **3-09** in MeOH, leading to an arylhydrazone derivative with an *ortho* boronic acid substituent, the latter of which could undergo boranol exchange with methanol to form a species such as **3-22**.

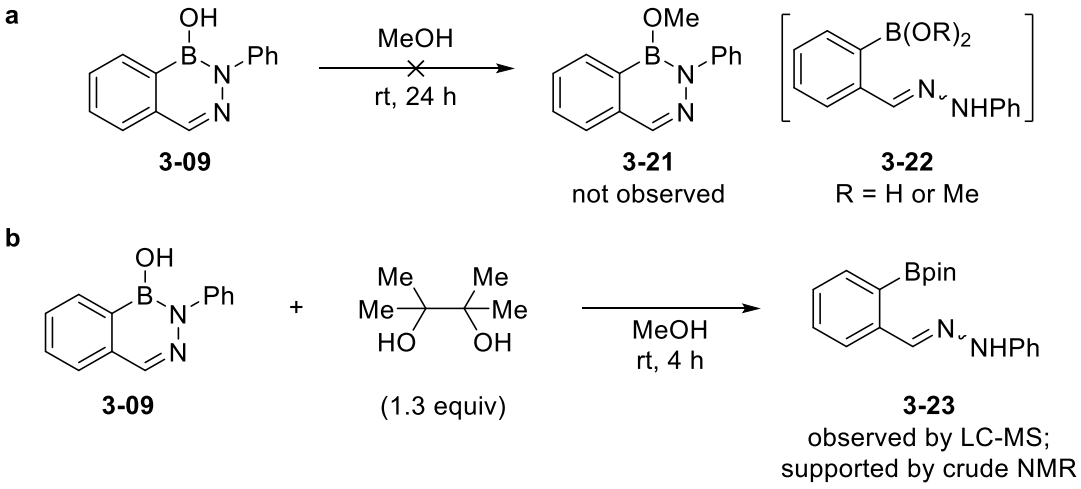

Scheme 3-12 a Attempted methanol exchange of **3-09**. **b** Evidence for B–N bond cleavage of **3-09** in methanol based on detection of **3-23**.

To probe the possibility of B–N bond cleavage, heterocycle **3-09** was treated with excess pinacol in methanol, where ^{1}H and ^{11}B NMR data provided tentative evidence to support the formation of pinacol boronic ester **3-23** under these conditions (Scheme 3-12b). The formation of **3-23** was also supported by LC-MS of the crude reaction mixture, where starting heterocycle **3-09** and boronic ester **3-23** were both detected (see Experimental section for full details). A control reaction between heterocycle **3-09** and pinacol in acetonitrile/water rather than methanol showed no evidence for formation of **3-23**, consistent with the importance of methanol to endocyclic B–N

bond cleavage. The recovery of heterocycle **3-09** in MeOH under exchange conditions was quantified using 1,3,5-trimethoxybenzene as an internal standard. Heterocycle **3-09** was recovered in 58% recovery after 30 minutes, with little change after 24 hours. When methanol exchange was examined using 5 equivalents of alcohol in CD_3CN solvent, the starting heterocycle was recovered quantitatively, with no evidence for either methanol exchange or B–N bond cleavage.

N-Sulfonyl heterocycle **3-10** appeared to demonstrate similar susceptibility to B–N bond cleavage in methanol as was observed for **3-09**, including a lack of complete reversibility upon addition of D_2O (Figure 3-12). After 30 minutes in anhydrous MeOH, only 47% recovery of heterocycle **3-10** was observed, with little change after a further 24 hours. Reaction with 5 equivalents of methanol in CD_3CN afforded the starting hemiboronic acid unchanged, indicating that decomposition or endocyclic B–N bond cleavage occurs more readily in methanol solvent.

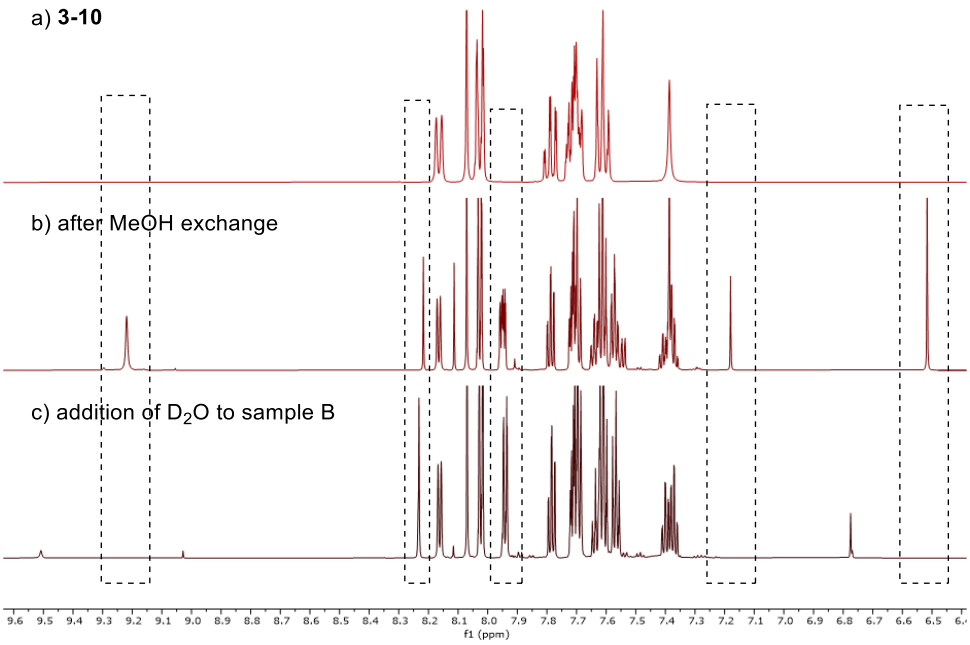

Figure 3-12 ^1H (400 MHz, CD_3CN) evidence for irreversible decomposition of heterocycle **3-10** in methanol.

The appearance of a highly downfield resonance at 9.22 ppm after attempted methanol exchange was suggestive of the NH proton of an acyclic arylhydrazone. Additionally, the appearance of a relatively upfield B–OMe resonance at 3.61 ppm suggested that endocyclic B–N bond cleavage to form hydrazone **3-25** may be occurring (Scheme 3-13a), analogous to the reactivity of heterocycle **3-09**. Reaction of **3-10** with pinacol in anhydrous methanol for 72 hours successfully afforded the ring-opened pinacol boronic ester **3-26**, which was isolated and fully characterized (Scheme 3-13b). The formation of **3-26** provides conclusive evidence for B–N bond cleavage of heterocycle **3-10** in methanol. When the same experiment was performed using acetonitrile/water as a solvent rather than methanol, no evidence for formation of pinacol ester **3-26** was observed.

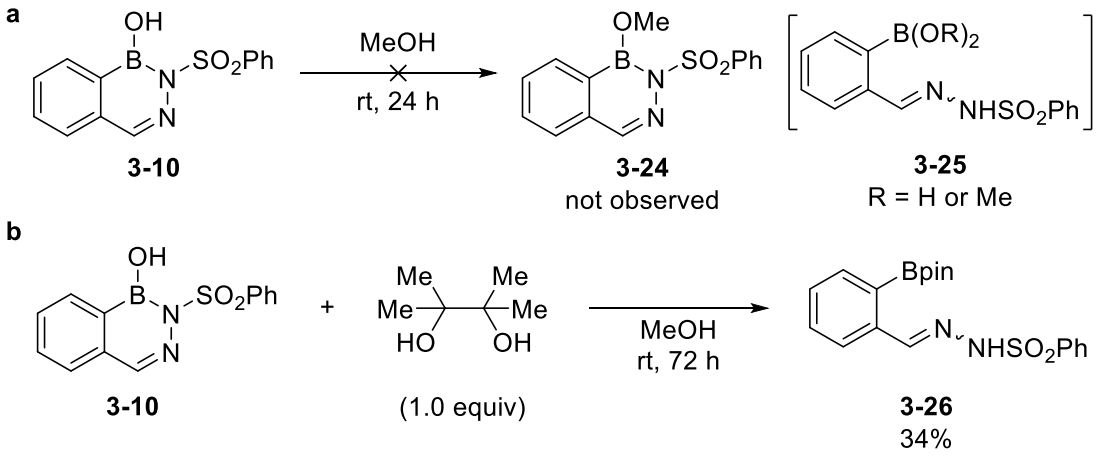

Scheme 3-13 a Unsuccessful methanol exchange of heterocycle **3-10**. **b** Formation of pinacol ester **3-26** to demonstrate endocyclic B–N bond cleavage of **3-10** in methanol.

For hemiboronic acids **3-01** and **3-02**, which readily underwent exchange with methanol, highly comparable reactivity with ethanol and isopropanol was observed for the formation of *B*-ethoxy derivative **3-06b** and *B*-isopropoxy derivative **3-07b** respectively (Scheme 3-14), suggesting that the trends in reactivity with methanol can be extended towards other alcohols.

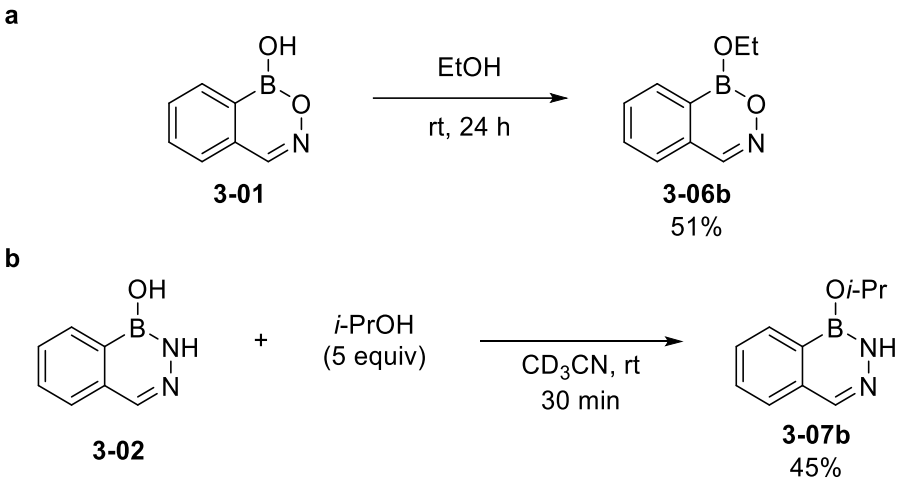

Scheme 3-14 a Exchange of hemiboronic acid **3-01** with ethanol. **b** Exchange of hemiboronic acid **3-02** with isopropanol.

Across the five heterocycles that were examined, universal conclusions cannot be reached regarding the reactivity and stability of cyclic hemiboronic acids in MeOH (Table 3-1). The evidence for substrate-dependent B–N cleavage in methanol led us to further study the stability of these heterocycles towards endocyclic hydrolysis, which will be described in the next section.

Table 3-1 Summary of methanol exchange experiments.

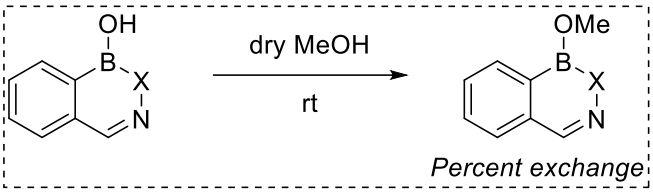

Compound	30 min	24 h	5 equiv MeOH in CD_3CN[a]
3-01 X = O	38	46	56
3-02 X = NH	50	54	45
3-08 X = NMe	<5	<5	<5
3-09 X = NPh	<5 (58% recovery)[b]	<5 (60% recovery)[b]	<5
3-10 X = NSO_2Ph	<5 (47% recovery)[b]	<5 (50% recovery)[b]	<5

[a]Substrate and 5 equiv MeOH mixed in CD_3CN solution. [b]Recovery of starting material was measured by ^1H NMR spectroscopy relative to an internal standard.

3.3.3 Assessment of Heterocycle Stability via Dynamic Crossover Experiments

Substrate decomposition in solution could proceed through hydrolysis or cleavage of both the internal B–X bond and C=N moiety (Scheme 3-15). While this process was never observed in NMR analysis of the purified heterocycles, the possibility of a dynamic equilibrium that dramatically favors the heterocyclic products could not be ruled out.[53]

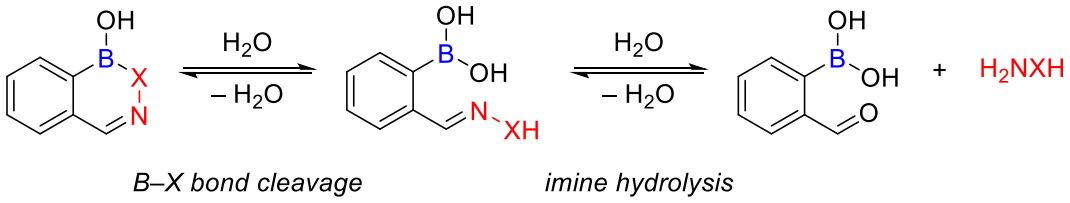

Scheme 3-15 Proposed pathway for reversible heterocycle hydrolysis.

To assess the stability of these heterocycles and probe the possibility of a dynamic equilibrium, crossover experiments were conducted between the model heterocycles and 5-fluoro-

2-formylphenylboronic acid (**3-27**); substrate decomposition to release free hydroxylamine or hydrazine derivative should lead to a mixture of heterocyclic products derived from both aldehydes upon re-condensation. These experiments were conducted in either methanol or acetonitrile/water solvent mixtures and were performed in both directions (i.e., also starting from the fluorinated cyclic hemiboronic acid and non-fluorinated benzaldehyde derivative **3-11**). Experiments in acetonitrile/water were performed by Zain Kazmi.

The corresponding 5-fluoro-substituted cyclic hemiboronic acids **3-28**–**3-32** (Scheme 3-16) were prepared using the same procedure as the non-fluorinated compounds (*cf.* Scheme 3-5). Crossover was quantified using ^{19}F NMR, in which the resonance for each fluorinated hemiboronic acid is distinct from free **3-27**. The extent of crossover was calculated as the relative mole fraction of the crossover product (50% crossover reflects an equimolar mixture of the two fluorinated species).

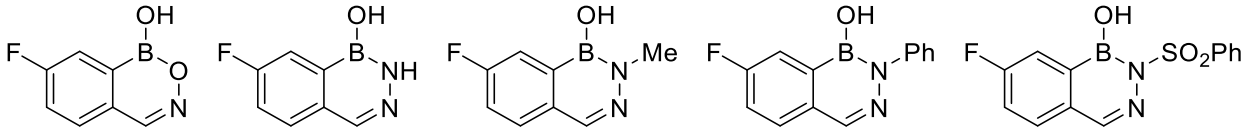

3-28 83% **3-29** 77% **3-30** 79% **3-31** 78% **3-32** 79%

Scheme 3-16 Fluorinated hemiboronic acids prepared for crossover studies. Compound **3-28** was prepared by Zain Kazmi.

Heterocycles **3-01** and **3-08** were found to be highly stable in both solvent systems with little evidence for crossover (Table 3-2). Heterocycle **3-02** showed no evidence for crossover in acetonitrile/water but demonstrated 10–20% crossover in MeOH. Despite the evidence for B–N bond cleavage in MeOH, heterocycle **3-09** showed only trace crossover in the same solvent mixture. This may suggest that after B–N bond cleavage, C=N cleavage does not occur to an extent

sufficient to allow equilibration of the heterocycles. In both solvent systems, *N*-sulfonyl derivative **3-10** demonstrated the most significant crossover.

Table 3-2 Summary of dynamic crossover experiments between cyclic hemiboronic acids and 2-formylarylboronic acids.

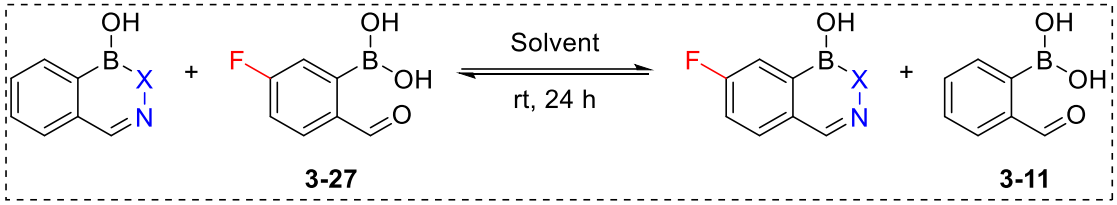

3-27 **3-11**

	Percent Crossover[a]	
Compound	Dry MeOH	MeCN/H_2O (3:1)[b]
3-01 X = O	2%, <2 %	none
3-02 X = NH	18% from left, 8% from right	none
3-08 X = NMe	none	none
3-09 X = NPh	2% from left, 2% from right	none
3-10 X = NSO_2Ph	48% from left, 40% from right	6% from left, 14% from right

[a]Determined by ^{19}F NMR spectroscopy. [b]Measured by Zain Kazmi.

Crossover with *N*-sulfonyl heterocycles was found to occur more readily in methanol, where virtually complete equilibration was observed in both directions. When exchange between hemiboronic acid **3-10** and fluorinated boronic acid **3-27** was examined in different solvent systems, the percent crossover was strongly correlated to the amount of methanol (Table 3-3). The lability of the B–N bond in *N*-sulfonyl heterocycle **3-10** appears to resemble that of *N*-acyl derivatives, which have been shown by Bane and co-workers to exists in equilibrium with their open boronic acid form.[49]

Table 3-3 Solvent-dependent stability and crossover of *N*-sulfonyl heterocycles.

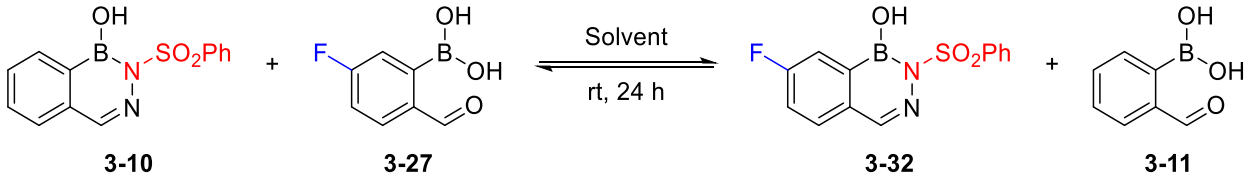

Solvent:	MeCN	H_2O	MeCN/H_2O (3:1)	MeCN/H_2O/MeOH (3:0.5:0.5)	MeOH
% Crossover:	<2	<2	4	11%	48%

An additional series of crossover experiments was conducted between pairs of heterocycles containing distinct substituents on both the aromatic backbone and endocyclic heteroatom substituent (Scheme 3-17). Exchange observed in these experiments must be initiated by breakdown of one of the component heterocycles, with no influence of a free boronic acid or aldehyde moiety that may have affected earlier crossover experiments. As with the previously described crossover experiments, these were conducted in both directions in both methanol and acetonitrile/water solvent systems. Crossover experiments in acetonitrile/water were conducted by Zain Kazmi. Benzoxazaborine heterocycles containing an endocyclic B–O bond (**3-02** and **3-28**) showed no evidence for crossover in either solvent system (Scheme 3-17a). Among the benzodiazaborine heterocycles, crossover was only observed when two inequivalent *N*-sulfonyl heterocycles were used in methanol (Scheme 3-17b). Reaction of fluorinated *N*-sulfonylphenyl hemiboronic acid **3-32** with *N*-*p*-toluenesulfonyl hemiboronic acid **3-33** in methanol led to complete equilibration with the corresponding crossover products **3-34** and **3-10** (Scheme 3-17c & Figure 3-13). This result further supports the instability of these heterocycles in methanol as was observed during the study of boranol exchange.

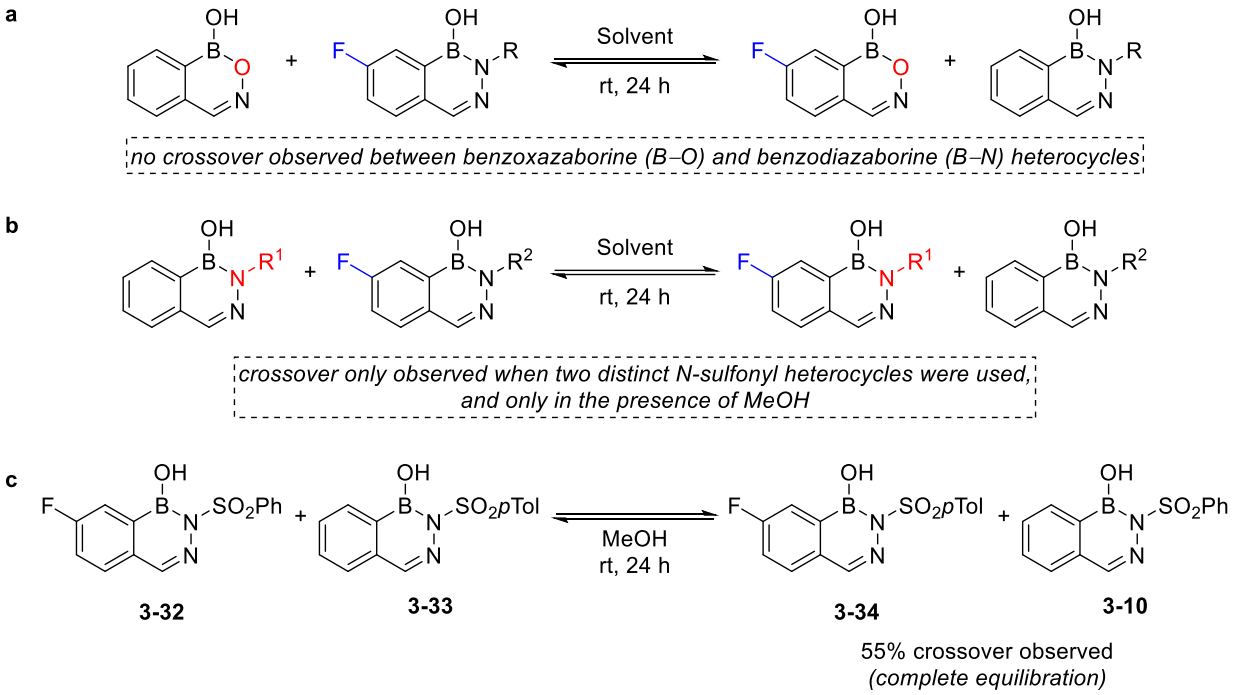

Scheme 3-17 a Dynamic crossover experiments between benzoxazaborine and benzodiazaborine hemiboronic acids. **b** Dynamic crossover experiments between distinct benzodiazaborines. **c** Equilibration of *N*-sulfonyl heterocycles in methanol. Experiments in acetonitrile/water were performed by Zain Kazmi.

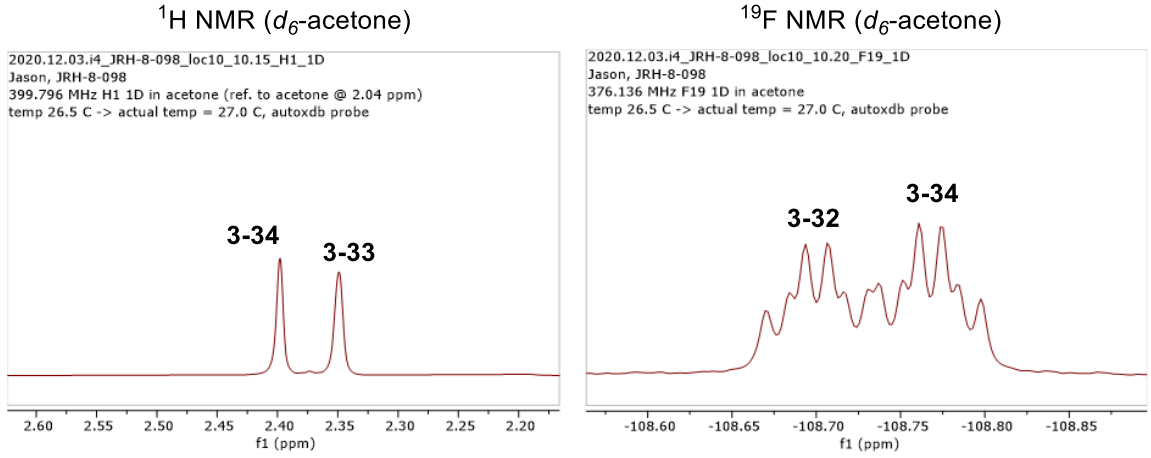

Figure 3-13 ^{1}H (400 MHz, d_6-acetone) and ^{19}F (376 MHz) NMR demonstrating equilibration of *N*-sulfonyl hemiboronic acids in methanol.

3.3.4 Measurement of pK_a Values

The pK_a values of the model heterocycles were measured by ^{11}B NMR in a buffered 1:1 water/acetonitrile solvent mixture.[54] A mixed organic/aqueous mixture was employed to maintain a homogeneous solution across the pH range of interest. Determination of pK_a values by ^{11}B NMR relies on the different chemical shifts of the hemiboronic acid and corresponding conjugate base. The pH at the equivalence point, at which an equimolar mixture of the acid and conjugate bases is present, corresponds to the pK_a. This can be determined graphically by plotting the observed ^{11}B NMR chemical shifts as a function of pH using a modification of the Henderson-Hasselbalch equation.[54] All pK_a measurements and conjugate base syntheses were performed by Zain Kazmi and are described in this thesis to provide context for the exchange and stability studies.

Heterocycles **3-01** and **3-10** displayed a single ^{11}B NMR resonance across the pH range of this study, smoothly transitioning from a downfield resonance at low pH (corresponding to the hemiboronic acid) to an upfield resonance at high pH from the corresponding conjugate base. From these titration curves, pK_a values of 7.1 and 5.5 were calculated for **3-01** and **3-10** respectively (Scheme 3-18). The pK_a of heterocycle **3-01** was also measured in water with minimal DMSO as a co-solvent where a pK_a of 5.5 was calculated, suggesting that pK_a values are increased by roughly 1.5 units in 1:1 water/acetonitrile relative to water alone. The increase in pK_a with the addition of acetonitrile reflects the decreased solvation of the ionic conjugate base with the relative increase in the amount of organic solvent, as poor stabilization of the conjugate base would be expected to decrease the acidity of the corresponding acid.

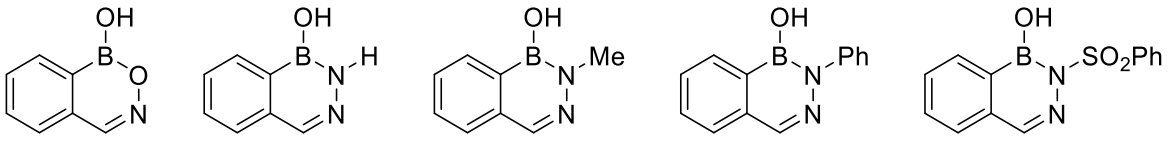

3-01	**3-02**	**3-08**	**3-09**	**3-10**
pK_a 7.1 (5.5)[a]	pK_a >14	pK_a > 14	pK_a 12.2	pK_a 5.5

All pK_a values were measured by ^{11}B NMR titration in 1:1 H_2O/MeCN with a phosphate buffer.
[a]pK_a was measured in H_2O with 4% DMSO.

Scheme 3-18 pK_a values determined by ^{11}B NMR titrations. Titrations and data analysis were performed by Zain Kazmi.

Heterocycles **3-01** and **3-10** demonstrated fast chemical exchange between the trivalent and tetravalent boron species, as evidenced by the single ^{11}B NMR resonance in all titration experiments with a pH-dependent chemical shift reflecting the position of the ionization equilibrium. In contrast, heterocycle **3-09** appeared to demonstrate slow chemical exchange, such that distinct resonances were observed for the acid and conjugate base with former predominating at pH values below the pK_a. Back-titration of a high pH sample revealed this to be a reversible ionization with no evidence for decomposition. The pK_a, at which equimolar amounts of hemiboronic acid and conjugate base are present, was determined to be 12.2.

Consistent with earlier observations by Groziak, heterocycles **3-02** and **3-08** showed no upfield ^{11}B NMR resonances up to pH 13.6 that could be definitively assigned to their corresponding conjugate bases.[48] Back-titration of high pH samples successfully recovered the starting hemiboronic acids, suggesting that there is no irreversible decomposition at high pH. Accordingly, their pK_a values can only be assigned as greater than 14 as they are insufficiently acidic to accurately measure in aqueous solution.

However, formation of the tetramethylammonium conjugate bases of **3-02** and **3-08** proved to be possible under anhydrous conditions (Scheme 3-19). These species displayed upfield ^{11}B

NMR resonances in anhydrous DMSO-d_6 fully consistent with a tetravalent structure (1.3 ppm for **3-02-I**, 2.4 ppm for **3-08-I**). Upon exposure to a pH 13.5 aqueous solution, these species readily reverted to their trivalent acid form, consistent with the previously estimation of their high pK_a (>14).

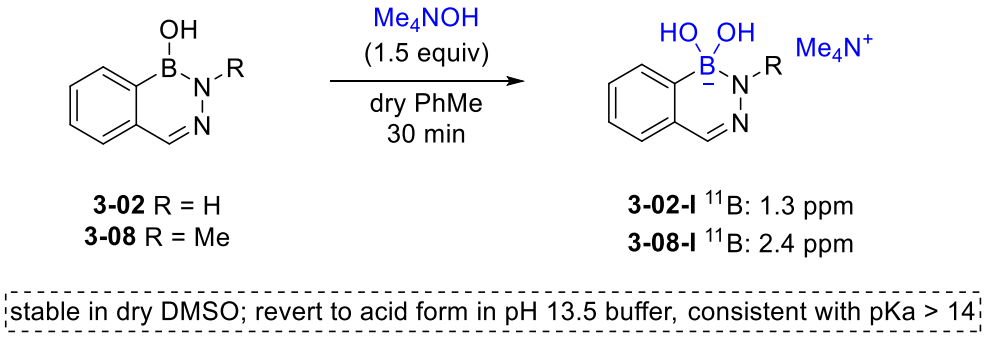

Scheme 3-19 Formation of hygroscopic conjugate bases **3-02-I** and **3-08-I** under anhydrous conditions. Experiments performed by Zain Kazmi.

The experimentally determined pK_a values clearly demonstrate that the acidity of benzodiazaborines is highly dependent on the nitrogen substituent. Across the benzodiazaborines surveyed herein, a pK_a difference of at least 8.5 units was observed, corresponding to a three hundred millionfold difference in acidity in aqueous solution. In previous studies, the lack of upfield ^{11}B NMR resonance for heterocycle **3-02** in basic aqueous solution was taken as evidence for Brønsted acidity.[48] Our results suggest that these claims are mistaken, and the pK_a of heterocycle **3-02** is too high to form appreciable amounts of the conjugate base in water. Accordingly, the observed chemical shifts in these previous studies simply reflect the chemical shift of un-ionized **3-02**.

3.3.5 X-ray Crystallographic Analysis of Tetravalent Conjugate Bases and Diol Adducts

While the ^{11}B NMR methods described in Section 3.3.4 proved effective in assessing the pK_a values of the model heterocycles, they provide no definitive insight as to the true acidic nature (Lewis or Brønsted) of these species. Accordingly, single crystal X-ray analysis was used to obtain unambiguous structural characterization of the conjugate bases and to compare key bond lengths to the starting hemiboronic acids, providing valuable insight into changes in bonding brought about by conjugate base formation. Crystals suitable for X-ray diffraction analysis in this section were prepared by Zain Kazmi, Dr. Hwee Ting Ang, and Dr. Marco Paladino, while X-ray data collection was performed by Dr. Michael Ferguson. Single crystal X-ray structures of heterocycles **3-01** and **3-02** were previously reported by Groziak and co-workers.[48] The results of these experiments are briefly summarized only for their context to the larger study, as they were not performed by the author of this thesis.

Single crystal analysis revealed a tetravalent boron atom in conjugate bases **3-01-I** and **3-10-I,** as well as diol adducts **3-35**–**3-37**, unambiguously establishing the Lewis acidic nature of the parent hemiboronic acids (Figure 3-14). Formation of a tetravalent boron species was found to result in a significant lengthening of the endocyclic B–X bond in all cases, suggesting that an appreciable amount of double bond character to the endocyclic B–X bond exists in the trivalent state and is lost upon ionization. Solution phase ^{11}B NMR spectroscopy of the crystals was fully consistent with their tetravalent nature and suggested that conjugate bases **3-01-I** and **3-10-I** were the same species formed in aqueous solution as described in Section 3.3.4. Adducts **3-35** and **3-36** were found to revert to their parent trivalent acidic form upon exposure to pH 13.5 aqueous solution, further consistent with the high pK_a of heterocycles **3-02** and **3-08**.

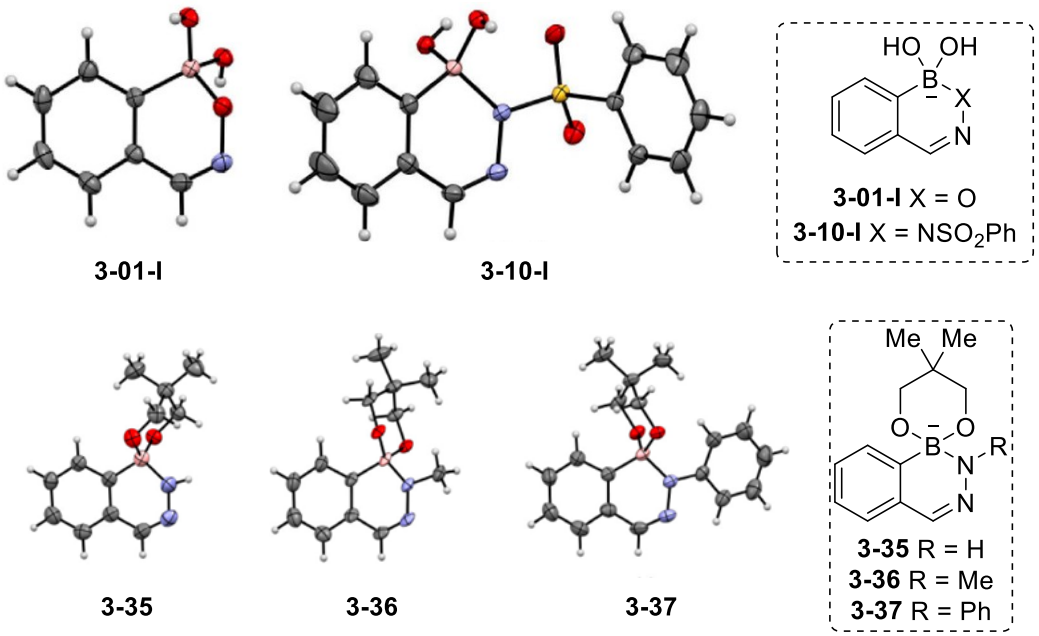

Figure 3-14 ORTEP representations for tetravalent Lewis conjugate bases and diol adducts. Cations have been removed for clarity. Crystals prepared by Dr. Marco Paladino, Dr. Hwee Ting Ang and Zain Kazmi and analyzed by Dr. Mike Ferguson.

The crystallographic data described in this section represents the first unambiguous evidence for the Lewis acidic nature of these hemiboronic acids.

3.3.6 Computational Studies of Aromaticity

The solution-phase NMR and solid-state crystallographic data presented in the previous sections unambiguously demonstrates the Lewis acidic nature of these model benzoxazaborine and benzodiazaborine heterocycles. Historical proposals for Brønsted acidity in these species were largely based on the preservation of pseudoaromaticity in the boron-containing ring. Accordingly, the clear demonstration of their Lewis acidic behaviour calls into question the assumption that the heterocyclic rings display significant aromaticity. To further probe the pseudoaromaticity of these compounds, density functional theory calculations were employed. The calculations in this section

were performed by Professor Dennis Hall with the 6-31G* basis set using the ωB97X-D functional.[56]

Energy minimized structures of heterocycles **3-01**, **3-02** and **3-08**–**3-10** were calculated, along with 4-hydroxyisoquinoline (**3-01)** as an analogous C=C isostere (Table 3-4). The calculated bond lengths and bond angles were in excellent agreement with crystals structures described in Section 3.3.5 and those reported by Groziak.[48] A qualitative assessment of aromaticity can be inferred from computed bond orders. Aromaticity in the boron-containing ring, and subsequent delocalization of electrons in the π system (as depicted by resonance forms **A** and **B**), would be expected to result in fractional C^3–N and C^1–B bond orders between 1.0 and 2.0.

Table 3-4 Computed bond orders of heterocycle **3-03**, benzoxazaborine **3-01** and model benzodiazaborines. Computations were performed by Professor Dennis Hall.

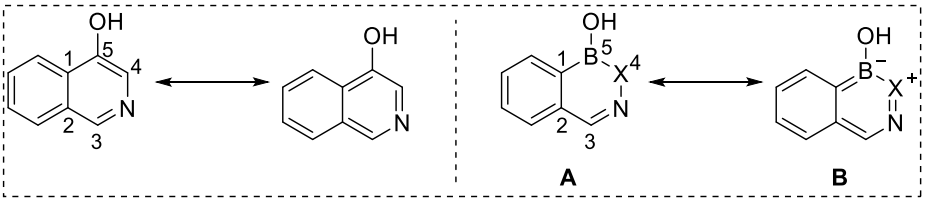

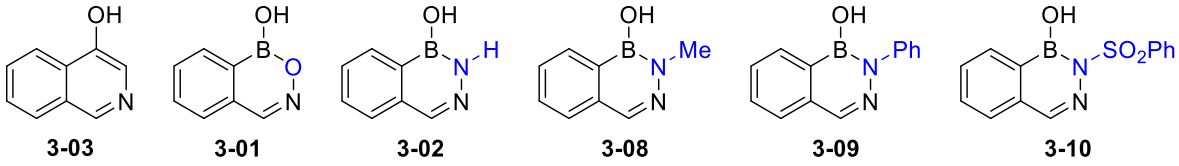

Property	3-03	3-01	3-02	3-08	3-09	3-10
C^1–C^5 or C^1–B bond order	1.231	1.041	1.056	1.062	1.057	1.043
C^4–C^5 or B–X bond order	1.528	1.357	1.325	1.276	1.232	1.172
C^3–N bond order	1.765	2.004	1.931	1.914	1.929	1.951

The effect of delocalization was clearly seen in the bond orders of 4-hydroxyisoquinoline **3-03**, wherein fractional bond orders between 1.23–1.76 were calculated for the C^1–C^5, C^4–C^5 and

C^3–N bonds. In contrast, C^1–B and C^3–N bond orders in the heterocyclic boron-containing rings suggest an alternating series of single and double bonds with little delocalization, consistent with minimal contribution from resonance form **B**. Moderate double bond character was observed in the B–X bond of all hemiboronic acids, suggesting an appreciable amount of B_p–X_n overlap. This effect was most pronounced in the B–O bond of hemiboronic acid **3-01** due to the strength of the B–O bond. Accordingly, the relatively low aromaticity of these heterocycles may originate from an inability of the C–C π bonds to delocalize into the empty p orbital of boron, rather than a lack of π character to the B–X bond. Notably, double bond character in the B–X bond was minimized in heterocycle **3-10**, in which the nitrogen lone pair of electrons can be further delocalized into the sulfonyl moiety.

Heterocycle **3-01** showed a C^1–B bond order of 1.04 and a C^3–N bond order of 2.00, suggesting that extended conjugation is essentially absent from this structure. The B–X bond order in heterocycle **3-01** was larger than that of the benzodiazaborines, but delocalization throughout the π system appears to be minimal. In contrast, boraza-derivatives **3-02** and **3-08** showed increased C^1–B and decreased C^3–N bond orders, suggesting somewhat increased delocalization in these compounds relative to benzoxazaborine **3-01**. While the Lewis acidic nature of hemiboronic acids **3-02** and **3-08** suggests that aromaticity is not sufficiently high to prevent formation of a tetravalent boron, these bond order calculations do suggest that the benzodiazaborines are slightly more aromatic than benzoxazaborine **3-01**.

The aromaticity of these species was further investigated using NICS (nuclear independent chemical shift) calculations performed by graduate student Matthew Johnson. NICS calculations provide an estimation of the induced magnetic field generated from cyclically delocalized electrons in conjugated systems.[57] The strength of this induced field at the center of the ring reflects

the extent of delocalization throughout the cyclic system, where a negative NICS value with larger magnitude reflects increased aromaticity. The results described herein are derived from NICS(1) calculations, where the magnetic field is computed 1 Å above the σ plane of the molecule to maximize the contribution of the π system.[57] The computed NICS(1) value of the non-boron-containing ring (termed the ***A*** ring) is comparable between 4-hydroxyisoquinoline **3-03** and the cyclic hemiboronic acid compounds, suggesting that boron incorporation has little effect on the aromaticity of the all-carbon ring (Table 3-5). However, the heterocyclic ring (***B***) appears to be significantly less aromatic in the hemiboronic acid derivatives than in 4-hydroxyisoquinoline (**3-03**) as judged by a decrease in the magnitude of the negative NICS(1) value. Within the cyclic hemiboronic acids that were examined, compounds **3-02** and **3-08** retain the greatest degree of aromaticity as judged by NICS(1). These conclusions are in line with the decreased Lewis acidity of these two compounds.

Table 3-5 Computed Nuclear Independent Chemical Shift (NICS(1)) values for **3-03** and cyclic hemiboronic acids to assess aromaticity. Computations were performed by graduate student Matthew Johnson.

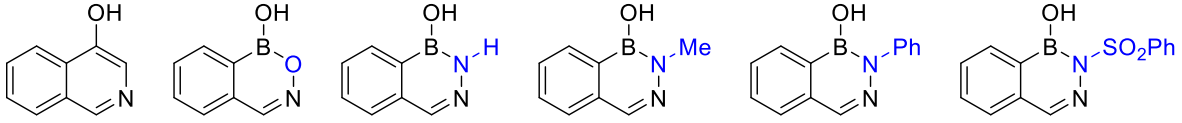

3-03 **3-01** **3-02** **3-08** **3-09** **3-10**

Property	3-03	3-01	3-02	3-08	3-09	3-10
NICS(1) (***A*** ring)	–10.28	–10.25	–10.47	–10.45	–10.23	–10.46
NICS(1) (***B*** ring)	–9.95	–2.75	–4.35	–4.86	–3.75	–3.88

Taken together, these DFT and NICS calculations suggest that pseudoaromaticity is minimal in the boron-containing ring of the model cyclic hemiboronic acids studied herein. Relative to the parent non-borylated scaffold **3-03**, benzoxazaborine **3-01** appears to retain the least aromaticity, while benzodiazaborines **3-02** and **3-08** are more aromatic. NICS(1) values suggest that the heterocyclic ring of all hemiboronic acids examined in this study display significantly less aromaticity than 1,2-oxaborine or 1,2-azaborine derivatives.[58] However, the increased aromaticity of **3-02** and **3-08** relative to **3-01** is in line with precedent for the slightly increased aromaticity of 1,2-azaborines relative to the related 1,2-oxaborines,[58] which similarly differ only in the substitution of a nitrogen and oxygen atom.

3.3.7 Rationalization of Experimental Properties and Relevance to Catalysis

The acidity, aromaticity, stability, and reactivity of the hemiboronic acids discussed in this chapter are inherently linked. The combination of experimental and computational studies described herein conclusively demonstrate that historical claims for the Brønsted acidity of these compounds are incorrect and suggests that the aromaticity of the heterocyclic rings has been overestimated. However, the influence of pseudoaromaticity on the acidity of these heterocycles cannot be ignored. DFT and NICS calculations suggested that hemiboronic acids **3-02** and **3-08** retain a moderate degree of aromaticity. This is consistent with the experimentally determined pK_a values, where these heterocycles showed diminished Lewis acidity. Heterocycles **3-01** and **3-10** appeared to be the least aromatic based on bond orders and NICS(1) values, which was in line with the increased acidity of these species.

The relative acidities of the hemiboronic acids correlates well with the inductive effect and anion-stabilizing ability of the heteroatom in the endocyclic B–X bond, as judged by the pK_a of the corresponding H_2X species which increases in the order $H_2NSO_2Ph < H_2O < H_2NPh < H_2NR$

or H_3N. Upon conjugate base formation, when π bonding character is absent from the B–X bond, the endocyclic oxygen substituent in **3-01** would be expected to offer greater inductive stabilization of the delocalized negative charge. There also appeared to be a correlation between cyclic hemiboronic acid acidity and the chemical shift of the boranol proton (Scheme 3-20); notably, *N*-sulfonyl derivative **3-10** was an exception to this trend as the boranol proton chemical shift is influenced by intramolecular hydrogen bonding to the S=O group.

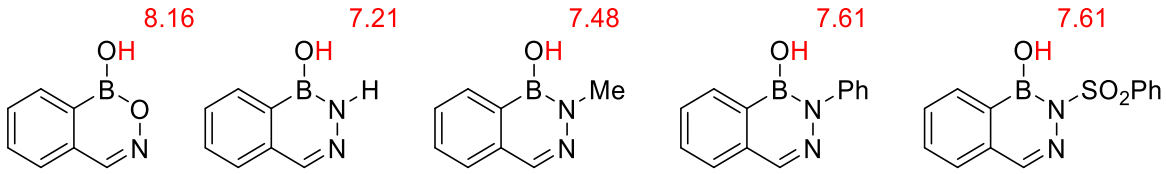

3-01 pK_a 7.1 **3-02** pK_a > 14 **3-08** pK_a > 14 **3-09** pK_a 12.2 **3-10** pK_a 5.5

Scheme 3-20 pK_a values and boranol proton chemical shifts for model cyclic hemiboronic acids.

Trends in reactivity of the heterocycles with methanol cannot be explained by pK_a alone, particularly the dramatic difference in boranol exchangeability of weakly acidic benzodiazaborines **3-02** and **3-08**. Boranol exchange by heterocycle **3-01** can be readily explained through an associative mechanism proceeding through a tetravalent borate intermediate, enabled by the relatively high Lewis acidity of this compound. In contrast, the dramatically reduced acidity of heterocycle **3-02** suggests that a stepwise associative mechanism of alcohol exchange is unlikely. A concerted exchange mechanism may be possible through an intermolecular hydrogen-bonding interaction between the incoming alcohol and neighboring NH unit, enabling alcohol exchange without involvement of an unfavorable tetravalent intermediate, albeit with an unfavorable entropy of activation (Scheme 3-21a). An analogous proton-transfer mechanism has been suggested for the esterification of weakly acidic boronic acids at pH values below their pK_a, conditions at which the

trivalent boronic acid predominates rather than the tetravalent conjugate base.[59] In contrast, an associative mechanism of exchange is similarly disfavored for heterocycle **3-08** due to its low acidity, while the lack of a neighboring hydrogen bond donor fails to enable the concerted mechanism (Scheme 3-21b). Accordingly, hemiboronic acid **3-08** shows no boranol exchange with methanol.

Hemiboronic acid **3-10** was found to be labile in methanol in both alcohol exchange and dynamic crossover studies. Solid state structures of both heterocycle **3-10** and the corresponding conjugate base **3-10-I** demonstrated intramolecular hydrogen bonds between the boranol hydrogen and sulfonyl oxygen groups. Boranol exchange with methanol, which could occur readily through an associative mechanism due to the high Lewis acidity of **3-10**, would result in either a tri- or tetravalent *B*-methoxy derivative (**3-24** or **3-24-I)** lacking the stabilizing internal hydrogen bond (Scheme 3-21c). The absence of this hydrogen bond may facilitate cleavage of the endocyclic B–N bond in methanol. Subsequent breakdown of the imine, as evidenced by the dynamic crossover results, may be facilitated by the electron-withdrawing nature of the sulfonyl group.

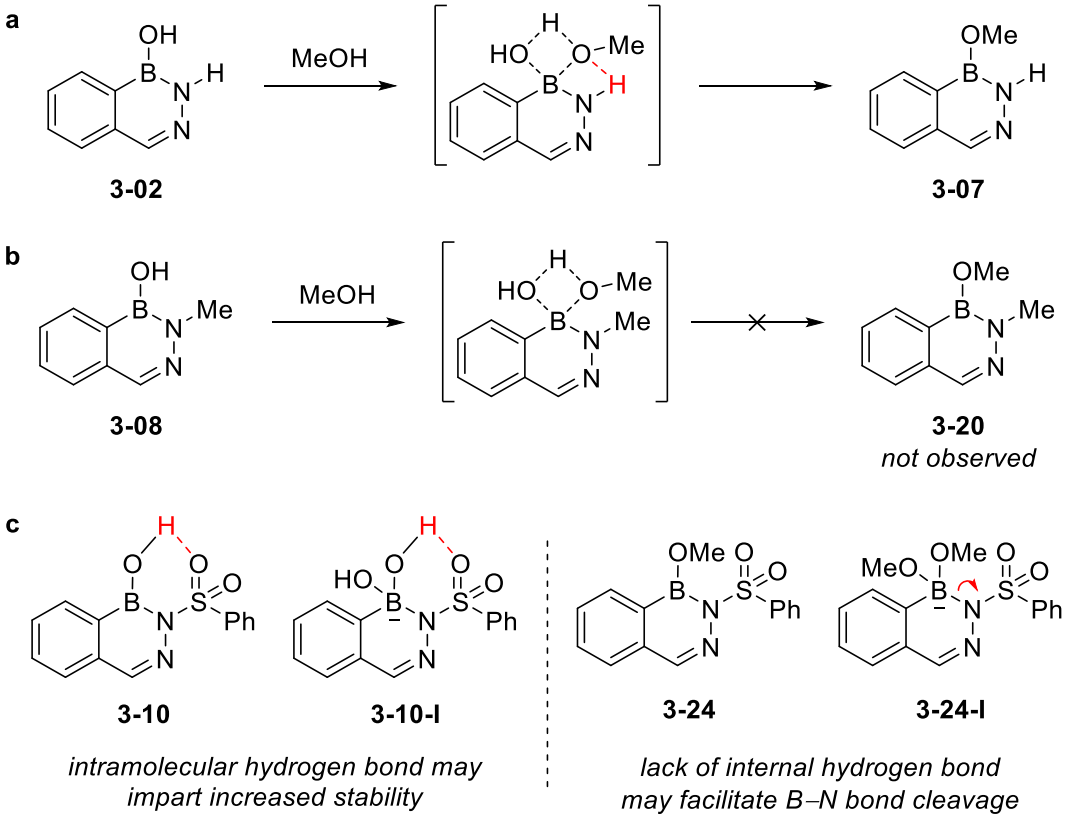

Scheme 3-21 Proposed influence of hydrogen bonding on the contrasting methanol exchange reactivity of heterocycles **3-02** and **3-08** and the instability of heterocycle **3-10** in methanol.

3.4 Summary

This work described in this chapter represents the first systematic study on the acidity, stability, and reactivity of benzoxazaborine and benzodiazaborine hemiboronic acids. The results obtained herein rectify several ambiguous or incorrect conclusions that have previously been reported regarding these compounds, particularly with respect to the extent of their aromaticity and the nature of their acidity. The Lewis acidic nature of the model heterocycles was unambiguously confirmed through X-ray crystallographic analysis of the corresponding tetravalent conjugate bases or diol adducts. Benzoxazaborine **3-01** and *N*-sulfonyl benzodiazaborine **3-10** demonstrated little evidence for aromaticity of the heterocyclic boron-containing ring, and correspondingly were found to be the most acidic heterocycles that were examined. Conversely, computational studies

suggested that a small degree of aromaticity is retained in the heterocyclic ring of benzodiazaborines **3-02** and **3-08**, consistent with the high pK_a of these compounds in aqueous solution. Relative acidity among the hemiboronic acids examined can largely be explained through a combination of the anion-stabilizing effect of the B–X heteroatom and the degree to which aromaticity must be disrupted upon ionization. Dynamic crossover experiments revealed that the heterocycles are largely stable in aqueous solution, with acidities that span greater than 8 orders of magnitude. The highly acidic *N*-sulfonyl derivative **3-10** was found to undergo facile B–N bond cleavage in methanol, while heterocycles **3-01** and **3-02** demonstrated rapid reversible exchange of their boranol moiety with exogenous alcohols.

In addition to providing clear resolution to decades worth of ambiguity regarding these compounds, this study provides a framework to guide the rational application of these hemiboronic acids in medicinal chemistry, bioconjugation and catalysis. Hydrolytically stable *N*-alkyl substituted benzodiazaborines, which retain moderate aromaticity and remain un-ionized well above physiological pH, are well-suited as arene bioisosteres in medicinal chemistry applications. Functionalized *N*-alkyl hydrazine precursors could prove useful in bioconjugation reactions to synthesize hydrolytically stable heterocyclic adducts across a wide pH range. Conversely, hemiboronic acids **3-01** and **3-02** were found to readily undergo covalent exchange with alcohols, suggesting that these scaffolds may have application in the design of covalent enzyme inhibitors or as catalysts for alcohol functionalization reactions. The large difference in acidity between hemiboronic acids **3-01** and **3-02** may be a determining factor in the application of these compounds, particularly in a catalysis context where reasonably facile access to a tetravalent boron species may be desired. With a rigorous understanding of the fundamental properties of benzoxaborine and benzodiazaborine heterocycles, new applications of these heterocycles may yet

emerge. The application of the benzoxazaborine scaffold as a catalyst for the activation of hydroxy-containing compounds will be described in Chapter 4.

3.5 Experimental

3.5.1 General Information

The following section contains representative experimental procedures and details for the isolation of compounds. Partial characterization of known compounds and full characterization of novel compounds presented in this chapter are described. All reactions were performed in regular glassware without any precautions to remove air or moisture, unless otherwise indicated. All chemicals were purchased from commercial sources and used as received unless otherwise noted. All solvents were purchased as ACS reagent grade and were used without further purification. Anhydrous methanol (99.8%) was purchased from Sigma Aldrich and used as received. 2-Formylphenylboronic acid (**3-11**) was purchased from Combi-Blocks and recrystallized from hot H_2O prior to use. Hydroxylamine (50 wt. % solution in water) was purchased from Sigma Aldrich and used as received. Column chromatography was performed on silica gel 60 using ACS grade hexanes and ethyl acetate as eluents. Thin layer chromatography (TLC) analysis was performed on Silicycle silica gel 60 F254 plates, which were visualized under UV light and with phosphomolybdic acid (PMA) or potassium permanganate ($KMnO_4$) stains.

NMR spectra were recorded at ambient temperature using Varian DD2 MR two-channel 400 MHz, Varian INOVA two-channel 400MHz, Varian INOVA four-channel 500 MHz, Varian VNMRS two-channel 500 MHz, Varian VNMRS four-channel 600 MHz and Agilent VNMRS four-channel, dual receiver 700 MHz spectrometers operating at the indicated frequency for ^1H NMR. All NMR chemical shifts are reported in ppm (δ) units with residual solvent peaks (*d*$_6$-acetone, CD_3CN or *d*$_6$-DMSO) as the internal reference. NMR data is reported using the following

abbreviations: s, singlet; br s, broad singlet; d, doublet; t, triplet; q, quartet; h, hextet; dd, doublet of doublets; dt, doublet of triplets; td, triplet of doublets; ddd, doublet of doublet of doublets; dddd, doublet of doublet of doublet of doublets; app, apparent; m, multiplet. The error of coupling constants from ^{1}H NMR spectra is estimated to be approximately 0.3 Hz. The quaternary carbon bound to boron is often not observed due to quadrupolar relaxation of boron, which was the case for all boron-containing compounds described here. A drop of D_2O was typically added to the NMR solution for compounds containing boranol (B–OH) units to prevent the formation of anhydrides.

All pH measurements were performed using an OHAUS ST2100 pH meter with ST350 pH probe. High-resolution mass spectra were recorded by the University of Alberta Mass Spectrometry Services Laboratory using either electrospray (ESI) or electron impact (EI) techniques. LC–MS was performed at the University of Alberta Mass Spectrometry Services Laboratory on an Agilent Technologies 6130 LC–MS using a Phenomenex Luna Omega Polar C18 1.6 μm column. A water/acetonitrile solvent system was used along with 0.1% formic acid according to the following gradient: beginning from 99:1 water/acetonitrile, over 5.00 minutes the ratio was changed to 40:60 water/acetonitrile. Over the next 0.50 minutes, the ratio was changed to 5:95 water/acetonitrile, which was maintained for a further two minutes (total elution time of 7.50 minutes). Melting points were determined in a capillary tube using a melting point apparatus and are uncorrected. Fourier-transform infrared (FTIR) spectra were obtained on a Nicolet Magna-IR instrument.

3.5.2 Synthesis of Hemiboronic Acids

General Procedure for the Synthesis of Benzoxazaborines (GP3-1)

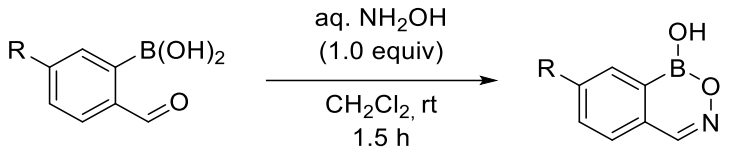

A round bottom flask under air was charged with 2-formylarylboronic acid (1.0 equiv) and CH_2Cl_2 (0.5 M). The resulting mixture was stirred at room temperature for 5 minutes, after which hydroxylamine (50 wt. % solution in water, 1.0 equiv) was added by syringe. The mixture was stirred at room temperature for 1.5 hours, during which time precipitate formation was observed. The precipitate was collected by vacuum filtration and washed thoroughly with H_2O (6 × 50 mL) to remove excess hydroxylamine. After drying under high vacuum overnight, the desired compounds were obtained as solids.

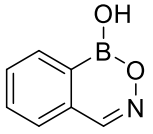

1*H*-Benzo[d][1,2,6]oxazaborinin-1-ol (3-01): Prepared according to **GP3-1** from 2-formylphenylboronic acid (609 mg, 4.06 mmol) and hydroxylamine (50 wt. % in H_2O, 248 µL, 4.06 mmol, 1.00 equiv). The title compound was isolated as a white solid (470 mg, 79%); **mp** = 145.5 – 147.9 °C; **^{1}H NMR** (400 MHz, *d*$_6$-acetone): δ 8.53 (s, 1 H), 8.16 (s, 1 H, exchanges with D_2O), 8.10 (d, *J* = 7.1 Hz, 1 H), 7.84 – 7.80 (m, 1 H), 7.75 (app t, *J* = 7.2 Hz, 2 H); **^{13}C NMR** (176 MHz, *d*$_6$-acetone): δ 150.8, 133.78, 133.74, 132.57, 132.56, 128.1; **^{11}B NMR** (128 MHz, *d*$_6$-acetone): δ 28.5; **FTIR** (cast film, cm^{-1}): 3410 (br, w), 3061 (m), 3015 (m), 1710 (m), 1488 (m), 1402 (s), 1228 (s), 1057 (s), 912 (s), 722 (m); **HRMS** (EI) for $C_7H_6NO_2{}^{11}B$: Calculated: 147.0492; Found: 147.0493.

General Procedure for the Synthesis of Benzodiazaborines (GP3-2)

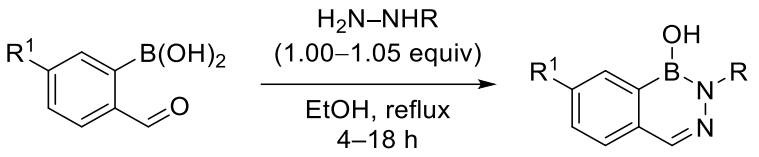

A round bottom flask under air was charged with the corresponding 2-formylarylboronic acid (1.0 equiv) and 95% EtOH (0.5 M). The solution was stirred at room temperature until homogeneous (typically less than 2 minutes), at which time the appropriate hydrazine derivative (1.00–1.05 equiv) was added. The mixture was heated to reflux (92 °C) for 4–18 hours. Upon completion, the reaction was allowed to cool to room temperature, after which it was concentrated by rotary evaporation to remove ethanol. The resulting solid was suspended in cold H_2O, collected by vacuum filtration, and washed thoroughly with cold H_2O (6 × 50 mL). After drying under high vacuum overnight, the desired compounds were obtained as solids.

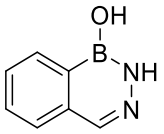

Benzo[*d*][1,2,3]diazaborinin-1(*2H*)-ol (3-02): Prepared according to **GP3-2** from 2-formylphenylboronic acid (1.50 g, 10.0 mmol) and hydrazine monohydrate (509 µL, 10.5 mmol, 1.05 equiv) with a reaction time of 4 hours. The title compound was isolated as a white solid (1.22 g, 83%); **mp** = 219 – 222 °C (turns yellow in color); **^{1}H NMR** (700 MHz, d_6-acetone): δ 9.37 (br s, 1 H), 8.19 (d, J = 7.6 Hz, 1 H), 7.98 (s, 1 H), 7.73 – 7.69 (m, 2 H), 7.58 (ddd, J = 7.6, 6.4, 2.0 Hz, 1 H), 7.18 (s, 1 H, exchanges with D_2O); **^{13}C NMR** (176 MHz, d_6-acetone): δ 140.1, 137.2, 131.9, 131.5, 129.2, 127.6; **^{11}B NMR** (128 MHz, d_6-acetone): δ 28.0; **FTIR** (cast film, cm^{-1}): 3331 (s), 3161 (m), 3066 (br, m), 1560 (m), 1459 (s), 1440 (s), 1345 (m), 1154 (m), 908 (m), 763 (m); **HRMS** (EI) for $C_7H_7N_2O^{11}B$: Calculated: 146.0651; Found: 146.0650.

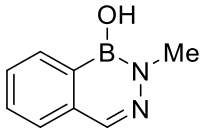

2-Methylbenzo[*d*][1,2,3]diazaborinin-1(*2H*)-ol (3-08): Prepared according to **GP3-2** from 2-formylphenylboronic acid (1.50 g, 10.0 mmol) and monomethylhydrazine (553 µL, 10.5 mmol, 1.05 equiv) with a reaction time of 18 hours. The title compound was isolated as a white solid (1.25 g, 78%); **mp** = 141.5 – 144.1 °C; **^{1}H NMR** (700 MHz, d_6-acetone + 1 drop D_2O): δ 8.24 (d, J = 7.7 Hz, 1 H), 7.96 (s, 1 H), 7.70 (d, J = 7.7 Hz, 1 H), 7.66 (app td, J = 7.4 Hz, 1.4 Hz, 1 H), 7.54 (app td, J = 7.4, 1.4 Hz, 1 H). In d_6-acetone alone without a drop of D_2O, approximately 9% suspected anhydride is observed, and the B–OH resonance is observed at 7.48 ppm (s, 1 H); **^{13}C NMR** (176 MHz, d_6-acetone + 1 drop D_2O): δ 138.5, 136.7, 131.52, 131.51, 129.2, 127.6, 39.1; **^{11}B NMR** (128 MHz, d_6-acetone + 1 drop D_2O): δ 27.6; **FTIR** (cast film, cm^{-1}): 3181 (br, m), 3051 (m), 2955 (m), 2930 (m), 1611 (m), 1418 (m), 1380 (s), 1127 (m), 923 (m), 762 (m); **HRMS** (EI) for $C_8H_9N_2O^{11}B$: Calculated: 160.0808; Found: 160.0805.

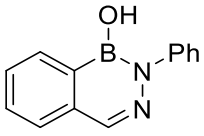

2-Phenylbenzo[*d*][1,2,3]diazaborinin-1(*2H*)-ol (3-09): Prepared according to **GP3-2** from 2-formylphenylboronic acid (2.00 g, 13.3 mmol) and phenylhydrazine (1.38 mL, 14.0 mmol, 1.05 equiv) with a reaction time of 18 hours. The title compound was obtained as an off-white solid (2.34 g, 79%); **mp** = 118.9 – 121.1 °C; **^{1}H NMR** (700 MHz, d_6-acetone + 1 drop D_2O): δ 8.35 (d, J = 7.6 Hz, 1 H), 8.17 (s, 1 H), 7.81 (d, J = 7.8 Hz, 1 H), 7.76 (app td, J = 7.5, 1.2 Hz, 1 H), 7.66 – 7.62 (m, 3 H), 7.41 – 7.38 (m, 2 H), 7.23 – 7.20 (m, 1 H). In d_6-acetone alone without a drop of D_2O, the B–OH resonance is observed at 7.61 ppm (s, 1 H); **^{13}C NMR** (176 MHz, d_6-acetone + 1

drop D_2O): δ 147.5, 140.2, 136.4, 132.3, 132.0, 129.8, 129.0, 127.8, 125.9, 125.7; **^{11}B NMR** (128 MHz, *d_6*-acetone + drop of D_2O): δ 28.3; **FTIR** (cast film, cm^{-1}): 3255 (br, m), 3067 (m), 1598 (s), 1494 (s), 1387 (s), 1291 (m), 1104 (s), 899 (s), 762 (s), 698 (m); **HRMS** (ESI) for $C_{13}H_{12}N_2O^{11}B$ $[M+H]^+$: Calculated: 223.1037; Found: 223.1034.

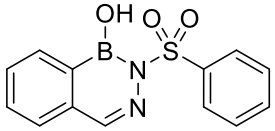

2-(Phenylsulfonyl)benzo[*d*][1,2,3]diazaborinin-1(*2H*)-ol (3-10): Prepared according to **GP3-2** from 2-formylphenylboronic acid (1.20 g, 8.00 mmol) and benzenesulfonyl hydrazide (1.38 g, 8.00 mmol, 1.00 equiv) with a reaction time of 18 hours. The title compound was obtained as a white solid (2.08 g, 91%); **mp** = 154.9 – 157.1 °C; **^{1}H NMR** (700 MHz, *d_6*-acetone): δ 8.18 (d, *J* = 7.7 Hz, 1 H), 8.14 (s, 1 H), 8.10 – 8.08 (m, 2 H), 7.81 (app td, *J* = 7.4 Hz, 1.4Hz, 1 H), 7.77 – 7.71 (m, 3 H), 7.67-7.65 (m, 2 H), 7.61 (br s, 1 H, exchanges with D_2O); **^{13}C NMR** (176 MHz, *d_6*-acetone) δ 144.3, 139.2, 135.3, 135.0, 133.9, 132.6, 131.7, 130.2, 129.2, 128.9; **^{11}B NMR** (128 MHz, *d_6*-acetone): δ 28.3; **FTIR** (cast film, cm^{-1}): 3510 (s), 3068 (w), 3037 (w), 1445 (m), 1348 (m), 1170 (m), 963 (m), 867 (m), 686 (m); **HRMS** (ESI) for $C_{13}H_{12}N_2O_3S^{11}B$ $[M+H]^+$: Calculated: 287.0662; Found: 287.0654.

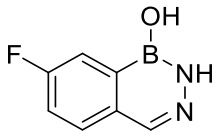

7-Fluorobenzo[*d*][1,2,3]diazaborinin-1(*2H*)-ol (3-29): Prepared according to **GP3-2** from 5-fluoro-2-formylphenylboronic acid (336 mg, 2.00 mmol) and hydrazine monohydrate (102 µL, 0.210 mmol, 1.05 equiv) with a reaction time of 5 hours. The title compound was obtained as an off-white solid (252 mg, 77%); **mp** = 290 – 294 °C (turns dark orange color); **^{1}H NMR** (700 MHz,

d$_6$-acetone): δ 9.43 (br s, 1 H), 8.00 (s, 1 H), 7.84 – 7.82 (m, 2 H), 7.49 (app td, *J* = 9.1, 2.8 Hz, 1 H), 7.30 (s, 1 H, exchanges with D_2O); **^{13}C NMR** (176 MHz, *d*$_6$-acetone): δ 163.3 (d, *J* = 248.6 Hz), 139.1 (d, *J* = 13.9 Hz), 133.9, 130.8 (d, *J* = 8.1 Hz), 120.0 (d, *J* = 23.5 Hz), 116.2 (d, *J* = 19.1 Hz); **^{11}B NMR** (128 MHz, *d*$_6$-acetone): δ 27.6; **^{19}F NMR** (376 MHz, *d*$_6$-acetone): δ –112.4 (app td, *J* = 9.6, 5.2 Hz); **FTIR** (cast film, cm^{-1}): 3325 (m), 3024 (br, m), 1565 (m), 1500 (s), 1345 (m), 1203 (m), 1124 (m), 1018 (m), 902 (m), 807 (w), 717 (m); **HRMS** (EI) for $C_7H_6FN_2O^{11}B$: Calculated: 164.0557; Found: 164.0558.

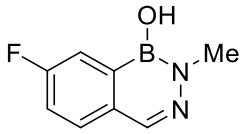

7-Fluoro-2-methylbenzo[*d*][1,2,3]diazaborinin-1(*2H*)-ol (3-30): Prepared according to **GP3-2** from 5-fluoro-2-formylphenylboronic acid (336 mg, 2.00 mmol) and monomethylhydrazine (111 μL, 2.10 mmol, 1.05 equiv) with a reaction time of 18 hours. The title compound was obtained as a yellow solid (281 mg, 79%); **mp** = 159.8 – 162.6 °C; **^{1}H NMR** (700 MHz, *d*$_6$-acetone): δ 8.00 (s 1 H), 7.91 (dd, *J* = 9.4, 2.5 Hz, 1 H), 7.83 (dd, *J* = 8.8, 5.2 Hz, 1 H), 7.55 (s, 1 H, exchanges with D_2O), 7.47 (app td, *J* = 8.8, 2.8 Hz, 1 H), 3.57 (s, 3 H); **^{13}C NMR** (176 MHz, *d*$_6$-acetone): δ 163.3 (d, *J* = 248.5 Hz), 137.6, 133.7, 130.8 (d, *J* = 8.1 Hz), 119.9 (d, *J* = 23.8 Hz), 116.2 (d, *J* = 19.4 Hz), 39.2; **^{11}B NMR** (128 MHz, *d*$_6$-acetone): δ 27.3; **^{19}F NMR** (376 MHz, *d*$_6$-acetone): δ –112.4 (app td, *J* = 9.2, 5.2 Hz); **FTIR** (cast film, cm^{-1}): 3184 (br, m), 3062 (m), 2945 (w), 1490 (m), 1379 (s), 1207 (m), 1082 (w), 911 (m), 829 (m), 721 (m); **HRMS** (EI) for $C_8H_8FN_2O^{11}B$: Calculated: 178.0714; Found: 178.0714.

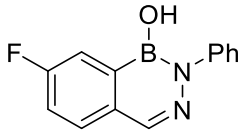

7-Fluoro-2-phenylbenzo[*d*][1,2,3]diazaborinin-1(2*H*)-ol (3-31): Prepared according to **GP3-2** from 5-fluoro-2-formylphenylboronic acid (500 mg, 2.98 mmol) and phenylhydrazine (310 µL, 3.13 mmol, 1.05 equiv) with a reaction time of 18 hours. The title compound was obtained as a white powder (556 mg, 78%); **mp** = 93 – 95 °C; **^{1}H NMR** (500 MHz, *d*$_6$-acetone + 1 drop D_2O): δ 8.17 (s, 1 H), 8.05 (dd, *J* = 9.5, 2.5 Hz, 1 H), 7.91 (dd, *J* = 8.5, 5.0 Hz, 1 H), 7.59 (d, *J* = 8.0 Hz, 2 H), 7.54 (app td, *J* = 9.0, 2.5 Hz, 1 H), 7.39 (app t, *J* = 8.0 Hz, 2 H), 7.21 (t, *J* = 7.5 Hz, 1 H). In *d*$_6$-acetone alone without a drop of D_2O, the B–OH resonance is observed at 7.80 ppm (s, 1 H); **^{13}C NMR** (125 MHz, *d*$_6$-acetone + 1 drop D_2O): δ 163.8 (d, *J* = 248.0 Hz), 147.3, 139.3, 133.3, 131.2 (d, *J* = 8.3 Hz), 129.1, 126.1, 125.8, 120.5 (d, *J* = 23.6 Hz), 117.1 (d, *J* = 19.5 Hz); **^{11}B NMR** (128 MHz, *d*$_6$-acetone + 1 drop D_2O): δ 27.9; **^{19}F NMR** (376 MHz, *d*$_6$-acetone + 1 drop D_2O): δ –111.6 (app td, *J* = 9.0, 5.2 Hz); **FTIR** (KBr pellet, cm^{-1}): 3332 (br, m), 3067 (m), 1594 (s), 1493 (s), 1213 (s), 1110 (s); **HRMS** (EI) for $C_{13}H_{10}N_2O^{11}BF$: Calculated: 240.0870; Found: 240.0868.

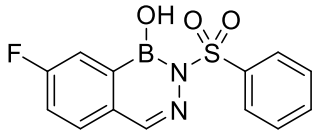

7-Fluoro-2-(phenylsulfonyl)benzo[*d*][1,2,3]diazaborinin-1(*2H*)-ol (3-32): Prepared according to **GP3-2** from 5-fluoro-2-formylphenylboronic acid (336 mg, 2.00 mmol) and benzenesulfonyl hydrazide (344 mg, 2.00 mmol, 1.00 equiv) with a reaction time of 18 hours. The title compound was obtained as a white solid (479 mg, 79%); **mp** = 169.6 – 171.7 °C; **^{1}H NMR** (700 MHz, *d*$_6$-acetone + 1 drop D_2O): δ 8.15 (s, 1 H), 8.10 – 8.08 (m, 2 H), 7.89 (dd, *J* = 8.4, 4.9 Hz, 1 H), 7.80 (dd, *J* = 8.4 Hz, 2.8 Hz, 1 H), 7.75 (app t, *J* = 7.4 Hz, 1 H), 7.66 (app t, *J* = 8.0 Hz, 2 H), 7.58 (td, *J* = 8.8 Hz, 2.8 Hz, 1 H). In *d*$_6$-acetone alone without a drop of D_2O, the B–OH resonance is observed at approximately 7.67 ppm (br s, 1 H); **^{13}C NMR** (176 MHz, *d*$_6$-acetone + 1 drop D_2O): δ 164.7 (d, *J* = 252.6 Hz), 143.2, 139.0, 135.1, 132.2 (d, *J* = 8.6 Hz), 132.0 (d, *J* = 2.3 Hz), 130.2,

129.2, 121.8 (d, J = 23.4 Hz), 117.8 (d, J = 20.2 Hz); **^{11}B NMR** (128 MHz, d_6-acetone + 1 drop D_2O): δ 27.8; **^{19}F NMR** (376 MHz, d_6-acetone + 1 drop D_2O): δ –108.8 (app td, J = 8.6, 5.6 Hz); **FTIR** (cast film, cm^{-1}): 3535 (m), 3511 (s), 3062 (w), 3040 (w), 1493 (m), 1431 (m), 1348 (m), 1224 (m), 1167 (s), 1091 (m), 986 (m), 899 (m), 748 (m); **HRMS** (EI) for $C_{13}H_{10}SFN_2O_3{}^{11}B$: Calculated: 304.0489; Found: 304.0488.

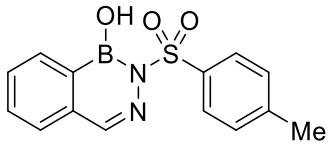

2-Tosylbenzo[*d*][1,2,3]diazaborinin-1(*2H*)-ol (3-33): Prepared according to **GP3-2** from 2-formylphenylboronic acid (600 mg, 4.00 mmol) and *p*-toluenesulfonyl hydrazide (745 mg, 4.00 mmol, 1.00 equiv) with a reaction time of 18 hours. The title compound was obtained as a white solid (917 mg, 76%); **mp** = 151.0 – 153.8 °C; **^{1}H NMR** (700 MHz, d_6-acetone + 1 drop D_2O): δ 8.17 (d, J = 7.7 Hz, 1 H), 8.13 (s, 1 H), 7.95 (d, J = 8.4 Hz, 2 H), 7.80 (app td, J = 7.7, 1.4 Hz, 1 H), 7.76 (d, J = 7.7 Hz, 1 H), 7.72 (app td, J = 7.4, 1.4 Hz, 1 H), 7.45 (d, J = 8.4 Hz, 2 H), 2.41 (s, 3 H). In d_6-acetone alone without a drop of D_2O, the B–OH resonance is observed at 7.59 ppm (s, 1 H); **^{13}C NMR** (176 MHz, d_6-acetone + 1 drop D_2O): δ 146.2, 144.2, 136.2, 135.3, 133.8, 132.6, 131.7, 130.7, 129.2, 128.8, 21.5; **^{11}B NMR** (128 MHz, d_6-acetone + 1 drop D_2O): δ 28.2; **FTIR** (cast film, cm^{-1}): 3489 (s), 3070 (w), 3027 (w), 2987 (w), 2928 (w), 1596 (m), 1491 (m), 1439 (m), 1287 (m), 1092 (m), 884 (m), 763 (m), 707 (m), 682 (m); **HRMS** (ESI) for $C_{14}H_{14}N_2O_3S{}^{11}B$ $[M+H]^+$: Calculated: 301.0818; Found: 301.0813.

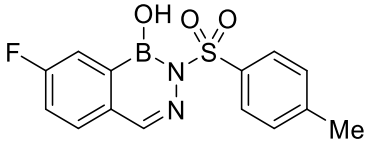

7-Fluoro-2-tosylbenzo[*d*][1,2,3]diazaborinin-1(*2H*)-ol (3-34): Prepared according to **GP3-2** from 5-fluoro-2-formylphenylboronic acid (168 mg, 1.00 mmol) and *p*-toluenesulfonyl hydrazide (196 mg, 1.05 mmol, 1.05 equiv) with a reaction time of 18 hours. The title compound was obtained as a white solid (253 mg, 80%); **mp** = 152.0 – 154.9 °C; **^{1}H NMR** (400 MHz, d_6-acetone): δ 8.15 (s, 1 H), 7.96 (d, J = 8.4 Hz, 2 H), 7.88 (dd, J = 8.6, 5.0 Hz, 1 H), 7.79 (dd, J = 8.6, 2.8 Hz, 1 H), 7.66 (br s, 1 H, exchanges with D_2O), 7.58 (app td, J = 8.8, 2.8 Hz, 1 H), 7.46 (d, J = 7.9 Hz, 2 H), 2.42 (s, 3 H); **^{13}C NMR** (176 MHz, d_6-acetone): δ 164.7 (d, J = 252.5 Hz), 146.3, 143.1, 136.1, 132.2 (d, J = 8.5 Hz), 132.1 (d, J = 2.5 Hz), 130.7, 129.3, 121.8 (d, J = 23.4 Hz), 117.8 (d, J = 20.0 Hz), 21.5; **^{11}B NMR** (128 MHz, d_6-acetone) δ 27.9; **^{19}F NMR** (376 MHz, d_6-acetone): δ –108.8 (app td, J = 8.8, 4.9 Hz); **FTIR** (solid, cm^{-1}): 3502 (s), 3047 (m), 2960 (w), 2928 (w), 1599 (m), 1447 (m), 1354 (m), 1162 (s), 986 (s), 890 (s), 815 (s), 749 (m), 694 (s); **HRMS** (EI) for $C_{14}H_{12}N_2O_3SF^{11}B$: Calculated: 318.0646; Found: 318.0653.

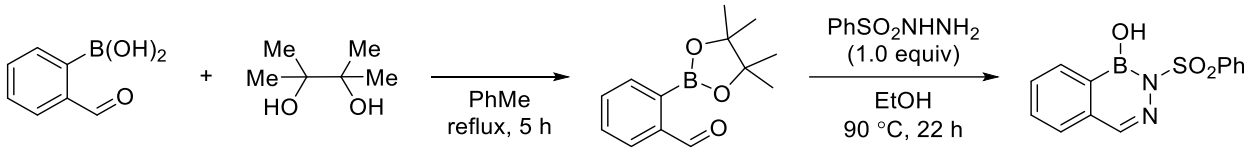

2-(4,4,5,5-Tetramethyl-1,3,2-dioxaborolan-2-yl)benzaldehyde (3-12): A 50 mL flame-dried round bottom flask was cooled under vacuum. Upon reaching room temperature, the flask was backfilled with nitrogen and charged with boronic acid **3-11** (300 mg, 2.00 mmol), pinacol (236 mg, 2.00 mmol, 1.00 equiv) and toluene (10.0 mL). A condenser and Dean-Stark apparatus were attached to the flask and the mixture was heated to reflux (110 °C) for 5 hours. The flask was allowed to cool to room temperature, after which the mixture was filtered through a pad of $MgSO_4$. The $MgSO_4$ was washed thoroughly with CH_2Cl_2. The filtrates were combined and concentrated

by rotary evaporation to yield pinacol ester **3-12** as a thick yellow oil (457 mg, 98%) without further purification; **^{1}H NMR** (500 MHz, d_6-acetone): δ 10.52 (s, 1 H), 7.94 (dd, J = 7.7, 1.4 Hz, 1 H), 7.85 (dd, J = 7.7, 2.0 Hz, 1 H), 7.69 – 7.62 (m, 2 H), 1.40 (s, 12 H); **^{11}B NMR** (128 MHz, d_6-acetone) δ 31.2.

A 10 mL round bottom flask was charged with boronic ester **3-12** (443 mg, 1.91 mmol), 95% EtOH (3.0 mL) and $PhSO_2NHNH_2$ (329 mg, 1.91 mmol, 1.00 equiv). A condenser was attached, and the mixture was heated to reflux (90 °C) for 22 hours. The reaction quickly became homogeneous with heating, after which a white solid began to precipitate as the reaction progressed. After 22 hours, the flask was allowed to cool to room temperature, and was then cooled to 0 °C in an ice bath for 20 minutes. The mixture was filtered and washed with cold 95% EtOH (cooled in a –20 °C freezer). The resulting solid was dried under vacuum to afford hemiboronic acid **3-10** (396 mg, 73%) as a white solid. Spectral data were in agreement with data reported earlier in this section.

3.5.3 Methanol Exchange Experiments (Section 3.3.2)

General Procedure for Methanol Exchange of Hemiboronic Acids in Anhydrous Methanol (GP3-3)

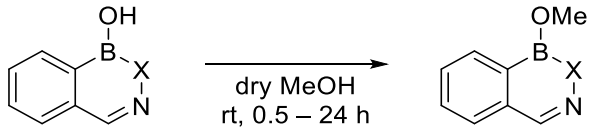

An oven-dried vial was allowed to cool to room temperature under vacuum. The vial was refilled with nitrogen, charged with hemiboronic acid (12.5 mg), and sealed with a septum. The vial was evacuated and backfilled with nitrogen. Dry methanol (0.5 mL) was then added via syringe, and the vial was quickly sealed with a cap and electrical tape. The mixture was stirred for the indicated

time at room temperature, after which it was concentrated by rotary evaporation, dried under vacuum, and analyzed by NMR spectroscopy in CD_3CN.

General Procedure for Methanol Exchange of Hemiboronic Acids with Anhydrous Methanol in CD_3CN solution (GP3-4)

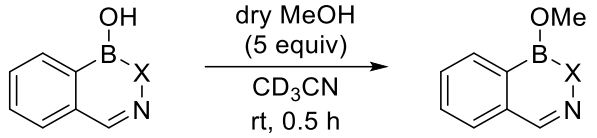

An oven-dried vial was allowed to cool to room temperature under vacuum and then was refilled with nitrogen. The vial was charged with hemiboronic acid (0.07 mmol). The solid was dissolved in CD_3CN (0.6 mL), followed by addition of anhydrous methanol (5.0 equiv). The mixture was transferred to an NMR tube under air, where it was kept at room temperature for 30 minutes prior to NMR spectroscopy.

3.5.3.1 Methanol Exchange of Hemiboronic Acid 3-01

Key resonances in the ^{1}H NMR spectrum of hemiboronic acid **3-01** which were used to quantify the extent of methanol exchange are at 8.46 ppm (s, 1 H), 8.04 ppm (d, J = 7.3 Hz, 1 H) and 6.70 ppm (s, 1 H, B–OH). The ^{11}B NMR spectrum showed a single resonance at 28.6 ppm.

Following **GP3-3**, methanol exchange was examined in anhydrous methanol for 30 minutes.

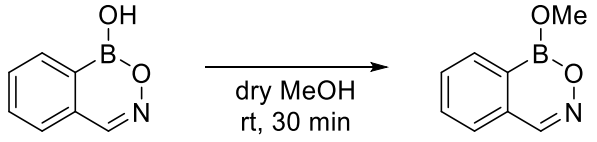

3-01 **3-06a** 38%

New multiplets consistent with formation of methyl ester **3-06a** were observed by ^{1}H NMR, most notably at 8.48 ppm (s, 1 H), 7.96 ppm (d, J = 7.6 Hz, 1 H) and 3.88 ppm (s, 3 H). The ^{11}B NMR

spectrum showed the appearance of a new resonance slightly upfield at 27.7 ppm. The formation of methyl ester **3-06a** was also supported by HRMS of the reaction mixture ($C_8H_8NO_2{}^{11}B$: Calculated: 161.0648; Found: 161.0649).

The extent of methanol exchange was determined by the formula Percent Exchange = 100% × (mmol B–OMe) ÷ [(mmol B–OMe) + (mmol B–OH)], where the mmol of each species are directly proportional to the respective normalized integrals in ^{1}H NMR spectrum. This calculation yields 38% exchange.

Following **GP3-3** with 24-hour reaction time afforded a similar mixture of heterocycle **3-01** and **3-06a**, which showed 46% exchange.

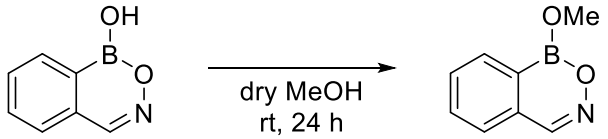

3-01 **3-06a**
46%

Following **GP3-4** for methanol exchange in CD_3CN solution, 56% exchange was observed.

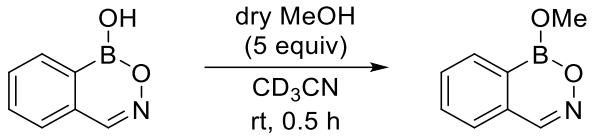

3-01 **3-06a**
56%

Addition of D_2O to a mixture of B–OH (**3-01**) and B–OMe (**3-06a**) was found to promote full conversion to the B–OD hemiboronic acid as evidenced by both ^{1}H and ^{11}B NMR.

3.5.3.2 Methanol Exchange of Hemiboronic Acid 3-02

Key resonances in the ^{1}H NMR spectrum of hemiboronic acid **3-02** which were used to quantify the extent of methanol exchange are at 9.37 ppm (br s, 1 H), 8.18 ppm (d, J = 7.7 Hz, 1 H), 7.98

ppm (s, 1 H) and 7.18 ppm (s, 1 H, B–OH). The ^{11}B NMR spectrum showed a single resonance at 28.0 ppm.

Following **GP3-3**, methanol exchange was examined in anhydrous methanol for 30 minutes. After rotary evaporation, acetone-d_6 was used as the NMR solvent rather than CD_3CN.

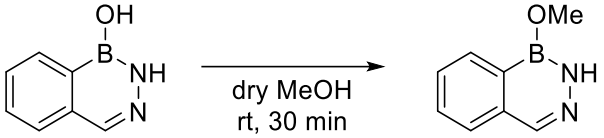

3-02 **3-07a** 50%

New multiplets consistent with formation of methyl ester **3-07a** were observed by ^{1}H NMR, most notably at 9.87 ppm (br s, 1 H), and 3.86 ppm (s, 3 H). A new singlet was also observed at 8.06 ppm which is insufficiently resolved from a new doublet at 8.04 ppm (J =7.8 Hz), although the sum of the two overlapping peaks integrates to 2 H as expected relative to the singlet at 9.87 ppm and 3.86 ppm. ^{11}B NMR showed the appearance of a new resonance slightly upfield at 27.5 ppm. The formation of methyl ester **3-07a** was also supported by HRMS of the reaction mixture ($C_8H_{10}N_2O^{11}B$ $[M+H]^+$: Calculated: 161.0886; Found: 161.0880). The extent of methanol exchange was calculated using the previously described formula and was found to be 50% exchange.

Following **GP3-3** with 24-hour reaction time afforded a similar mixture of heterocycle **3-02** and the corresponding methyl ester **3-07a**, which showed 54% exchange.

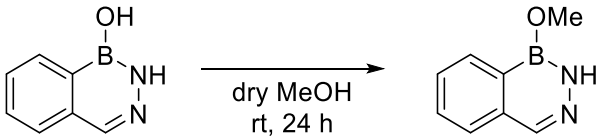

3-02 **3-07a** 54%

Key resonances in the ^{1}H NMR spectrum of **3-02** in CD_3CN which were used to quantify the extent of methanol exchange are at 8.93 ppm (br s, 1 H), 8.09 ppm (d, J = 8.0 Hz, 1 H), 7.98 ppm (s, 1 H) and 5.99 ppm (s, 1 H, B–OH). The ^{11}B NMR spectrum showed a single resonance at 27.9 ppm.

Following **GP3-4**, methanol exchange was examined with anhydrous methanol in CD_3CN solution for 30 minutes.

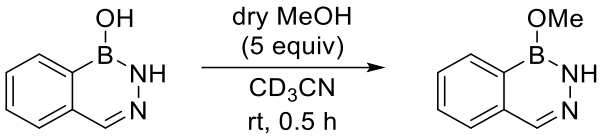

3-02 **3-07a** 45%

New multiplets consistent with formation of methyl ester **3-07a** were observed by ^{1}H NMR, most notably at 9.23 ppm (br s, 1 H), 8.04 ppm (s, 1 H), 8.02 ppm (d, J = 8.0 Hz, 2 H combined with overlapping 8.04 ppm singlet) and 3.80 ppm (s, 3 H). ^{11}B NMR showed the appearance of a new resonance slightly upfield at 27.5 ppm. Using the same calculation described above, 45% exchange was calculated.

Addition of D_2O to a mixture of B–OH (**3-02**) and B–OMe (**3-07a**) compounds was found to promote full hydrolysis to the B–OD hemiboronic acid as evidenced by both ^{1}H and ^{11}B NMR.

3.5.3.3 Methanol Exchange of Hemiboronic Acid 3-08

Key resonances in the ^{1}H NMR spectrum of **3-08** in CD_3CN which were used to quantify the extent of methanol exchange are at 8.09 ppm (d, J = 7.6 Hz, 1 H), 7.97 ppm (s, 1 H), 6.17 ppm (s, 1 H, B–OH) and 3.55 ppm (s, 3 H). The ^{11}B NMR spectrum showed a single resonance at 27.7 ppm. Following **GP3-3**, methanol exchange was examined in anhydrous methanol for 30 minutes.

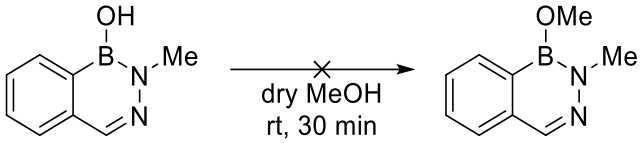

3-08 **3-20**

No evidence for formation of methyl ester **3-20** was observed. A new species was formed with several key resonances including 8.20 ppm (s, 1 H), 7.80 ppm (d, J = 8.0 Hz, 1 H), 7.46 – 7.42 (m, 1 H) and 3.65 (s, 3 H). Notably, no new resonance was observed in the 3.85 – 3.90 ppm region where the B–OCH_3 resonance was detected in methanol exchange experiments of heterocycles **3-01** and **3-02**. Only a single resonance was observed in the ^{11}B NMR spectrum at 27.7 ppm. Addition of D_2O resulted in hydrolysis of the newly formed species and conversion to the B–OD hemiboronic acid as monitored by ^{1}H NMR spectrum, suggesting the new species may be a BOB or other anhydride dimer. The integrations of the new species correspond to approximately 7% conversion, with the starting material largely recovered.

Following **GP3-3** with 24-hour reaction time afforded a similar mixture of heterocycle **3-08** with approximately 8% conversion to the proposed anhydride species, with the starting material making up the remainder of the composition. No evidence for formation of methyl ester **3-20** was observed with the increased reaction time.

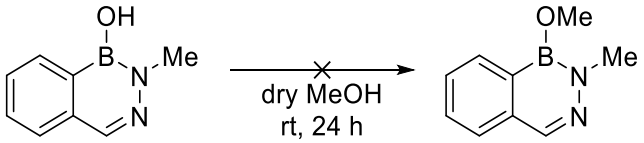

3-08 **3-20**

Following **GP3-4** for methanol exchange in CD_3CN solution, approximately 3% conversion to the proposed anhydride species was observed with no evidence for formation of methyl ester **3-20**.

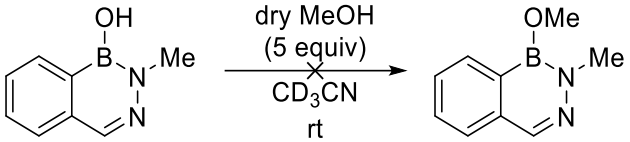

3-08 **3-20**

3.5.3.4 Methanol Exchange of Hemiboronic Acid 3-09

Key resonances in the ^{1}H NMR spectrum of **3-09** which were used to quantify the extent of methanol exchange are at 8.19 ppm (d, J = 7.2 Hz, 1 H), 8.14 ppm (s, 1 H) and 6.32 ppm (s, 1 H, B–OH). The ^{11}B NMR spectrum shows a single resonance at 28.1 ppm.

Following **GP3-3**, methanol exchange was examined in anhydrous methanol for 30 minutes.

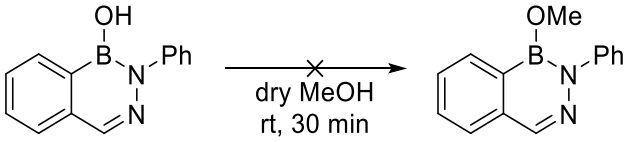

3-09 **3-21**

In heterocycles **3-01** and **3-02**, methanol exchange resulted in new aromatic ^{1}H NMR resonances with indistinguishable multiplicity from the resonances of the starting material and slightly different chemical shifts. In contrast, methanol exchange of heterocycle **3-09** showed many small new resonances of uncertain origin upon incubation in methanol, including a noticeably deshielded singlet at 8.69 ppm. Additionally, the characteristic B–OCH_3 protons were assigned to resonances at 3.88 and 3.86 ppm respectively in exchange reactions of heterocycles **3-01** and **3-02** while an analogous resonance was not observed in the reaction of heterocycle **3-09**, although resonances were observed comparatively upfield at 3.65 and 3.57 ppm.

Furthermore, addition of D_2O was found to hydrolyze the new resonances at 3.65 and 3.57 ppm, as well as many of the small new aryl resonances. However, clean conversion back to the B–OD

hemiboronic acid **3-09** was not observed, suggesting that the reaction of **3-09** with methanol is not entirely reversible upon addition of water, which was the case for methyl ester formation with heterocycles **3-01** and **3-02**.

Heterocycle **3-09** was reacted with pinacol (1.3 equiv) following **GP3-3** for 4 hours, and after the same workup, was analyzed by ^{1}H and ^{11}B NMR in d_6-acetone.

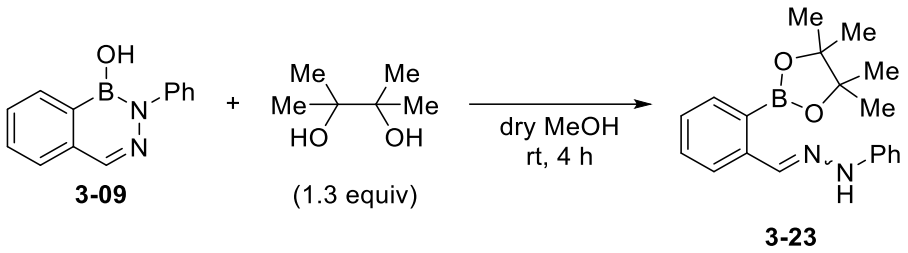

A new downfield singlet at 8.64 ppm was observed, which integrates to 1 H relative to a 12 H singlet at 1.35 ppm that is downfield of residual free pinacol observed at 1.17 ppm. Additionally, deshielded resonances were observed at 9.55 and 10.50 ppm which are consistent with formation of N–H or B–OH functional groups upon B–N bond cleavage. Furthermore, ^{11}B NMR spectrum showed the appearance of a new resonance at 30.9 ppm. Taken together, these observations provide tentative evidence to support formation of pinacol boronic ester **3-23** under these conditions. Formation of **3-23** was also supported by LC–MS of the crude reaction (Figure 3-15), where heterocycle **3-09** (5.176 min) and pinacol ester **3-23** (7.314 min) were both detected.

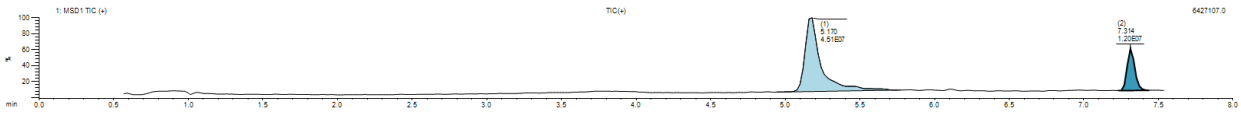

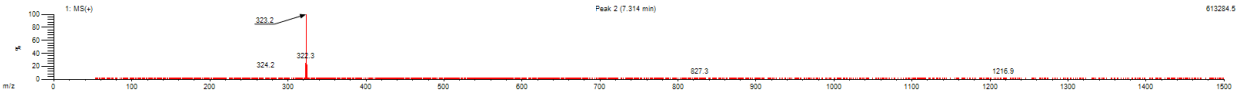

Figure 3-15 LC-MS of the crude reaction mixture indicating a mixture of heterocycle **3-09** and pinacol ester **3-23** (top) and the mass spectrum of the peak at 7.31 minutes corresponding to **3-23** (bottom).

General Procedure for the Determination of Heterocycle Recovery in Anhydrous Methanol by ^{1}H NMR Spectroscopy Using an Internal Standard (GP3-5).

An oven-dried vial was cooled to room temperature under vacuum and charged with hemiboronic acid (approximately 14 mg). The vial was sealed with a septum, evacuated, and backfilled with nitrogen. Dry methanol (0.5 mL) was then added via syringe, and the vial was quickly sealed with a cap and electrical tape. The mixture was stirred for the indicated time at room temperature, after which it was concentrated by rotary evaporation and dried under vacuum. Following addition of 1,3,5-trimethoxybenzene as an internal standard, the mixture was dissolved in CD_3CN or d_6-acetone for NMR.

Methanol exchange was examined in anhydrous methanol for 30 minutes following **GP3-5** with heterocycle **3-09** (14.7 mg, 0.0662 mmol) and 1,3,5-trimethoxybenzene (4.0 mg, 0.024 mmol). The diagnostic peak for the chemically equivalent aryl protons of 1,3,5-trimethoxybenzene was observed at 6.08 ppm in ^{1}H NMR spectrum, and the corresponding integral standardized to 3.00 H. Diagnostic resonances for heterocycle **3-09** were observed at 8.18 ppm (s, 1.69 H) and 8.34 (d, J = 7.6 Hz, 1.56 H), each of which corresponds to one proton in **3-09**. From these integrations, 58% recovery of heterocycle **3-09** was calculated. Percent Conversion was then calculated as 100% – Percent Recovery, or 42% conversion.

Following **GP3-5** with heterocycle **3-09** (13.9 mg, 0.0662 mmol) and 1,3,5-trimethoxybenzene (5.4 mg, 0.032 mmol) with a reaction time of 24 hours, similar calculations as described above showed 40% conversion.

Following **GP3-4** for exchange with 5 equivalents of MeOH in CD_3CN as a solvent, the starting heterocycle **3-09** was recovered in quantitative yield. This is consistent with importance of MeOH towards the breakdown of heterocycle **3-09**, which occurred when MeOH was used as a solvent in large excess but in only trace amounts when MeOH was only present as a reagent in more comparable concentration to heterocycle **3-09**.

3.5.3.5 Methanol Exchange of Hemiboronic Acid 3-10

Key resonances in the ^{1}H NMR spectrum of **3-10** which were used to quantify the extent of methanol exchange are at 8.16 ppm (d, J = 7.2 Hz, 1 H), 8.07 ppm (s, 1 H) and 7.39 ppm (s, 1 H, B–OH). The ^{11}B NMR spectrum shows a single resonance at 28.3 ppm.

Following **GP3-3**, methanol exchange was examined in anhydrous methanol for 30 minutes.

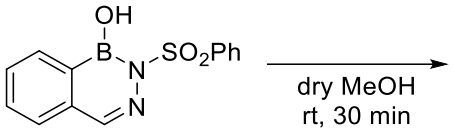

3-10

New singlets were observed at 8.22 ppm and 8.11 ppm, along with a highly deshielded new resonance at 9.22 ppm. A new singlet was observed at 3.61 ppm which integrates to 3 H relative to the singlets at 8.22 and 8.11 ppm, suggesting that there may be a B–OMe moiety with a chemical shift that is noticeably more upfield compared to exchange in heterocycles **3-01** and **3-02**. As was the case with heterocycle **3-09**, ^{1}H NMR of methanol exchange was suggestive of a more complex process than simple B–OH/B–OMe exchange.

This was further supported by addition of D_2O to the MeOH exchange sample. When direct B–OH/B–OMe exchange occurred for compounds **3-01** and **3-02**, addition of D_2O led to full hydrolysis of the methyl ester to form the corresponding deuterated B–OD hemiboronic acid. For heterocycle **3-10**, addition of D_2O resulted in a decrease in intensity for the new singlets at 9.22 ppm, 8.11 ppm and 3.61 ppm, but the new singlet at 8.22 ppm remained as did the new multiplet from 7.96 – 7.94 ppm. All together, these observations suggest that the species which is formed contains a B–OMe moiety capable of hydrolysis by D_2O, but other transformations have occurred which do not revert to the starting heterocycle **3-10** upon hydrolysis.

It was hypothesized that there may be methanol-promoted B–N bond cleavage under the reaction conditions, as was proposed for heterocycle **3-09**, leading to ring-opened hydrazone products containing a free boronic acid moiety that is capable of B–OH/B–OMe exchange. The strongly electron-withdrawing sulfonylphenyl substituent on the boron-bound nitrogen may promote B–N bond cleavage or weaken the B–N bond. To examine this, a pinacol trapping experiment was conducted as was described for heterocycle **3-10**, where pinacol ester **3-26** was isolated from the reaction mixture.

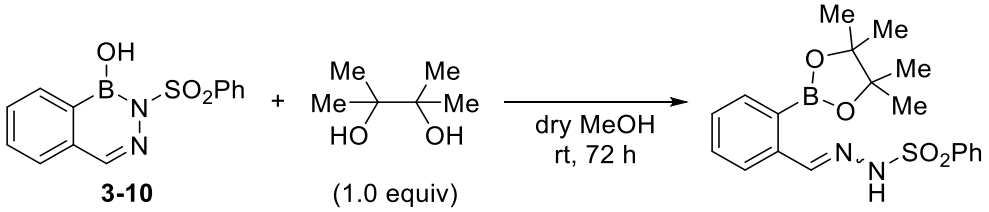

***N*'-(2-(4,4,5,5-Tetramethyl-1,3,2-dioxaborolan-2-yl)benzylidene)benzenesulfonohydrazide (3-26):** An oven-dried vial was charged with boron heterocycle **3-10** (114 mg, 0.400 mmol) and pinacol (47.3 mg, 0.400 mmol, 1.00 equiv). The vial was sealed with a septum, evacuated,

backfilled with nitrogen, and anhydrous methanol (2.00 mL) was added by syringe. The vial was sealed with a cap and electrical tape, and the reaction mixture was stirred at room temperature for 72 hours. The reaction mixture was concentrated under reduced pressure and purified by silica gel chromatography (3:1 hexanes/ethyl acetate). Chloroform was used to combine the column fractions and rinse the test tubes and was unable to be fully removed even with extensive drying under high vacuum. The $CHCl_3$ singlet (8.00 ppm) integrated close to 1.00 H, so the molecular weight and percent yield were calculated based on the chloroform adduct **3-26·CHCl₃** which was isolated as a white solid (68.0 mg, 0.135 mmol, 34% yield); **mp** = 149.4 – 151.3 °C (decomposition, turns dark red color); **^{1}H NMR** (700 MHz, *d*$_6$-acetone): δ 10.30 (s, 1 H, exchanges with D_2O), 8.79 (s, 1 H), 8.00 (s, $CHCl_3$), 7.99 – 7.95 (m, 2 H), 7.94 (app dt, *J* = 7.9, 0.8 Hz, 1 H), 7.77 (dd, *J* = 7.5, 1.5 Hz, 1 H), 7.66 – 7.61 (m, 1 H), 7.62 – 7.57 (m, 2 H), 7.46 (dddd, *J* = 7.9, 7.3, 1.5, 0.6 Hz, 1 H), 7.37 (app td, *J* = 7.4, 1.2 Hz, 1 H), 1.32 (s, 12 H); **^{13}C NMR** (176 MHz, *d*$_6$-acetone): δ 149.2, 140.6, 140.5, 136.9, 133.8, 132.0, 129.9, 129.8, 128.5, 125.7, 84.9, 79.2 ($CHCl_3$), 25.1; **^{11}B NMR** (128 MHz, *d*$_6$-acetone): δ 30.8; **FTIR** (neat solid, cm^{-1}): 3502 (s), 3047 (m), 2960 (w), 2928 (w), 1621 (m), 1492 (m), 1447 (s), 1090 (s), 890 (s), 694 (s); **HRMS** (EI) for $C_{19}H_{23}N_2O_4S^{11}B$: Calculated: 386.1472; Found: 386.1475.

Methanol exchange was examined in anhydrous methanol for 30 minutes following **GP3-5** with heterocycle **3-10** (13.5 mg, 0.0472 mmol) and 1,3,5-trimethoxybenzene (3.9 mg, 0.023 mmol), where 47% recovery (or 53% conversion) was observed. With a reaction time of 24 hours, 50% conversion was observed.

Following **GP3-4** for exchange with 5 equivalents of MeOH in CD_3CN as a solvent, the starting heterocycle **3-10** appeared unchanged. This is consistent with importance of MeOH towards the breakdown of heterocycle **3-10**, which occurred when MeOH was used as a solvent in large excess

but in only trace amounts when MeOH was only present as a reagent in more comparable concentration to heterocycle **3-10**.

3.5.3.6 Exchange with Other Alcohols

Following **GP3-3**, alcohol exchange of hemiboronic acid **3-01** with ethanol was examined. New resonances consistent with the formation of alcohol exchange product **3-06b** were observed by ^{1}H NMR, including 8.49 ppm (s, 1.01 H relative to the imine CH of the starting material), 7.98 ppm (d, J = 7.3 Hz, 1.09 H) and 4.28 ppm (q, J = 7.1 Hz, 2.11 H). A new resonance was observed by ^{11}B NMR with a chemical shift of 27.4 ppm. Using the same formula as described previously, 51% exchange was calculated.

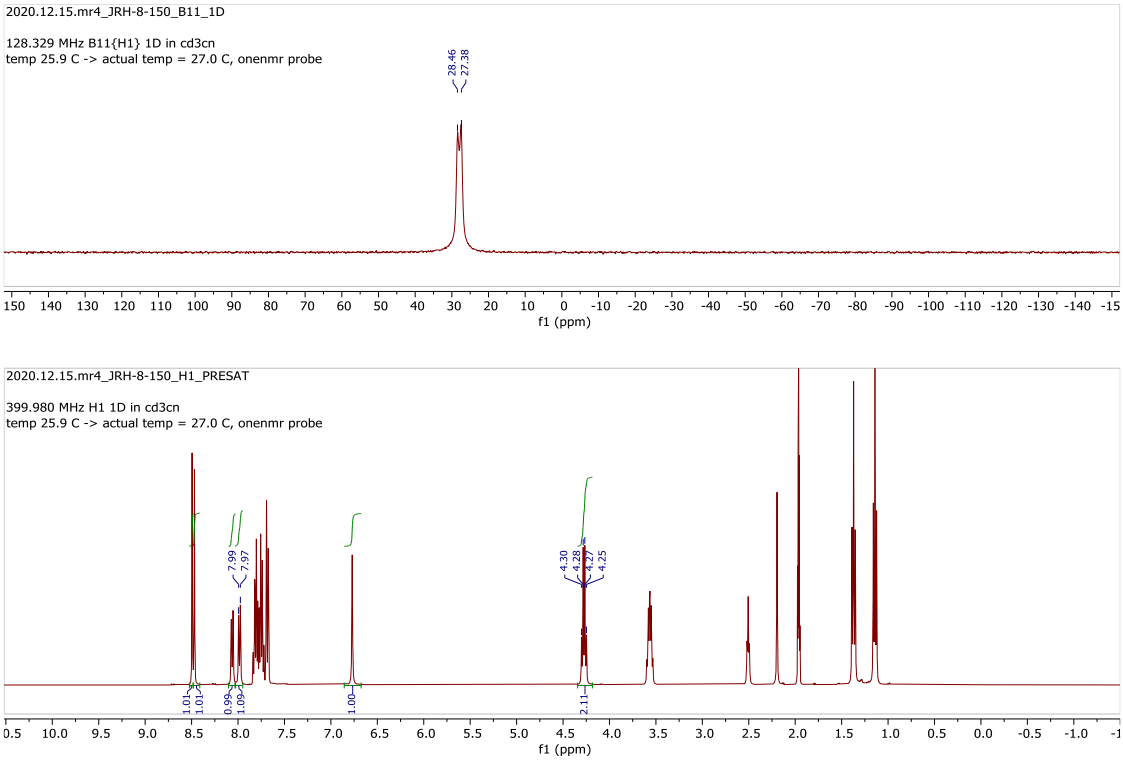

Figure 3-16 ^{11}B (128 MHz, CD_3CN) and ^{1}H (400 MHz) NMR of exchange reaction between **3-01** and ethanol.

Following **GP3-4** for exchange with 5 equivalents of *i*-PrOH in CD_3CN as a solvent, new resonances were observed by ^1H NMR consistent with formation of *B*-isopropoxy ester **3-07b**, including 9.18 ppm (s, 0.86 H relative to the B–OH resonance) and 4.56 ppm (septet, $J = 6.0$ Hz, 0.84 H). A new resonance was observed by ^{11}B NMR at 26.8 ppm. Using the calculation described previously, 45% exchange was calculated.

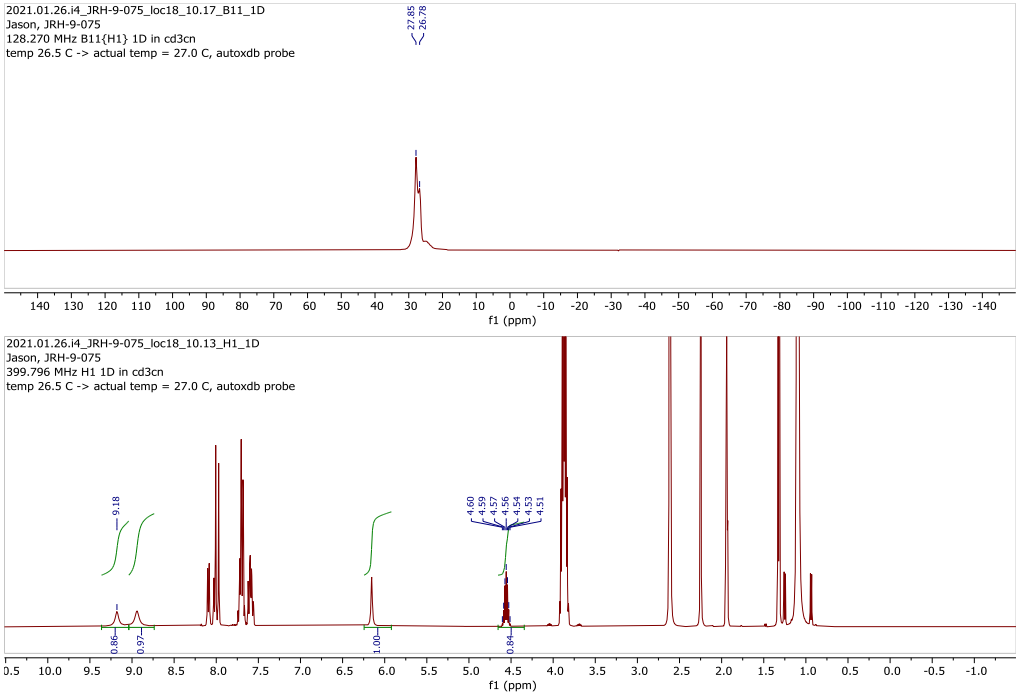

Figure 3-17 ^{11}B (128 MHz, CD_3CN) and ^1H (400 MHz) NMR for exchange of hemiboronic acid **3-02** with isopropanol.

3.5.4 Crossover Experiments

3.5.4.1 Crossover Between Boron Heterocycles and 2-Formylarylboronic Acids

General Procedure for Crossover Reactions Between Hemiboronic Acids and 2-Formylarylboronic Acids in Anhydrous Methanol (GP3-6)

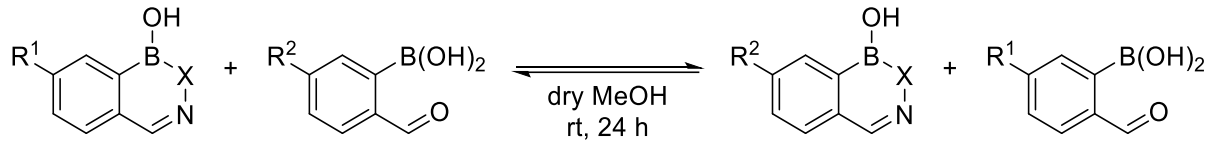

An oven-dried vial was allowed to cool to room temperature under vacuum, after which it was charged with boron heterocycle (0.05 mmol) and 2-formylarylboronic acid (1.0 equiv). The vial was sealed with a septum, evacuated, and backfilled with nitrogen. Dry methanol (0.5 mL) was then added via syringe, and the vial was quickly sealed with a cap and electrical tape. The mixture was stirred for 24 hours at room temperature, after which it was concentrated by rotary evaporation, dried under vacuum, and analyzed by NMR spectroscopy in *d*$_6$-acetone with a drop of D_2O. Unless otherwise noted, crossover was calculated based on integrations from ^{19}F NMR.

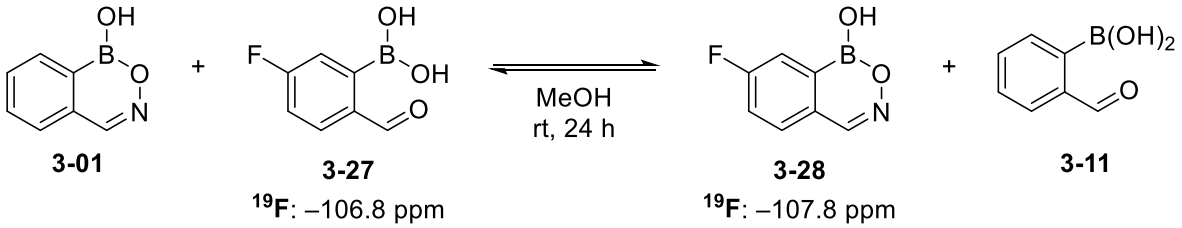

Following **GP3-6**, 6% crossover was observed in anhydrous methanol. However, the resonance for **3-28** overlaps with a side product from reaction of **3-27** in methanol alone, meaning that the extent of crossover is likely being overestimated.

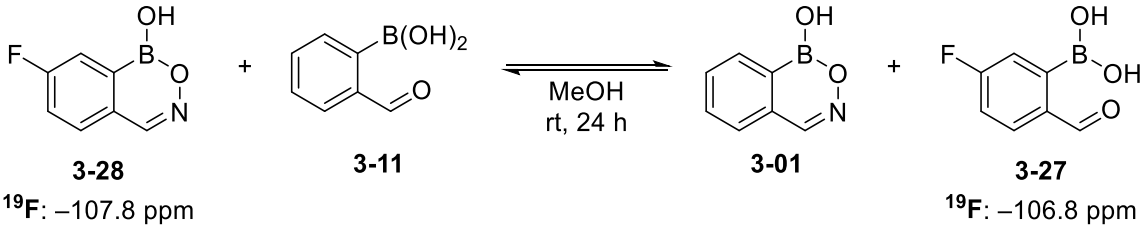

Following **GP3-6**, less than 2% crossover was observed in anhydrous methanol.

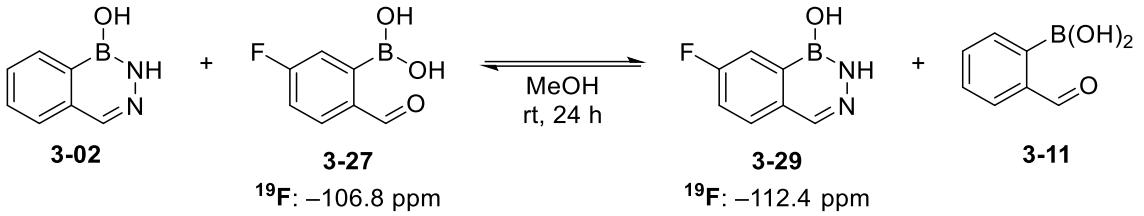

3-02 **3-27** **3-29** **3-11**

^{19}**F**: –106.8 ppm ^{19}**F**: –112.4 ppm

Following **GP3-6** in anhydrous methanol, the ratio of **3-27** to **3-29** was 80:20 (20% crossover), but some decomposition or other side processes were observed to give multiple new species in small amount. These species could originate from nucleophilic attack of the endocyclic secondary amine onto exogenous aldehyde.

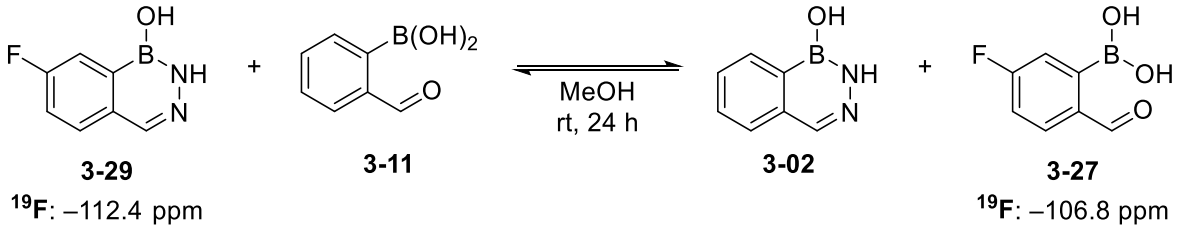

3-29 **3-11** **3-02** **3-27**

^{19}**F**: –112.4 ppm ^{19}**F**: –106.8 ppm

Following **GP3-6** in anhydrous methanol, the ratio of **3-29** to **3-27** was 88:12 (12% crossover). Similar decomposition or side products were observed as when the reaction was run in the reverse direction. The occurrence of these multiple new species appears limited to reactions with heterocycle **3-02** and its fluorinated analog **3-29** as they were not observed with other boron heterocycle crossover reactions.

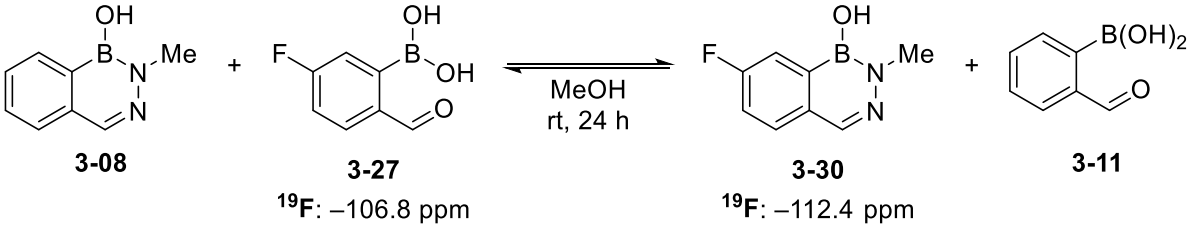

3-08 **3-27** **3-30** **3-11**

^{19}**F**: –106.8 ppm ^{19}**F**: –112.4 ppm

Following **GP3-6,** no crossover was observed in anhydrous methanol.

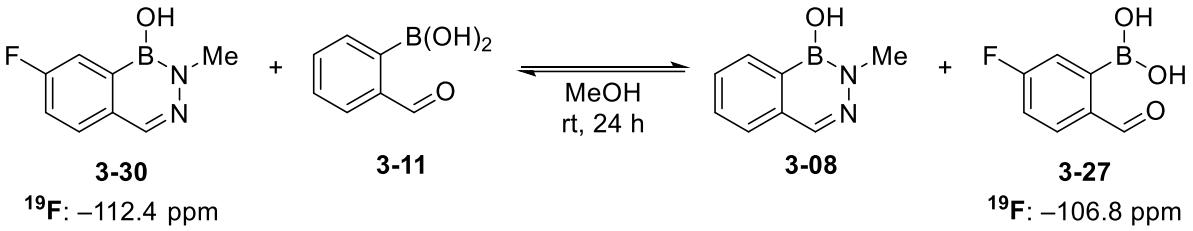

3-30
^{19}**F**: –112.4 ppm

3-11

3-08

3-27
^{19}**F**: –106.8 ppm

Following **GP3-6,** no crossover was observed in anhydrous methanol.

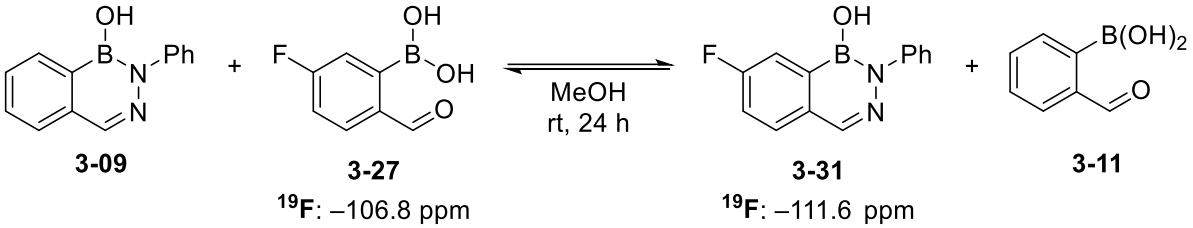

3-09

3-27
^{19}**F**: –106.8 ppm

3-31
^{19}**F**: –111.6 ppm

3-11

Following **GP3-6** in anhydrous methanol, the ratio of **3-27** to **3-31** was 98:2, corresponding to 2% crossover.

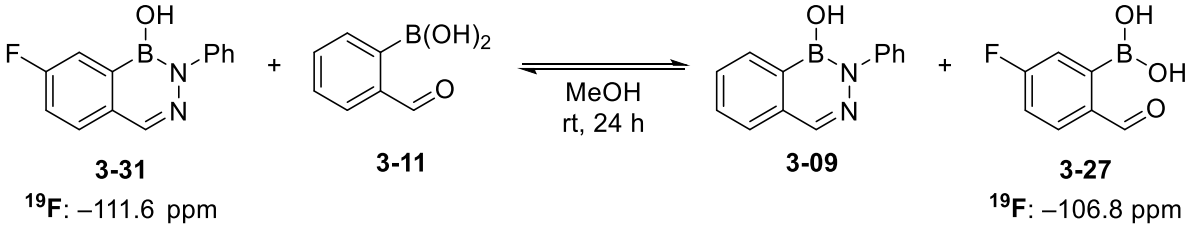

3-31
^{19}**F**: –111.6 ppm

3-11

3-09

3-27
^{19}**F**: –106.8 ppm

Following **GP3-6** in anhydrous methanol, the ratio of **3-31** to **3-27** was approximately 99:1, corresponding to less than 2% crossover.

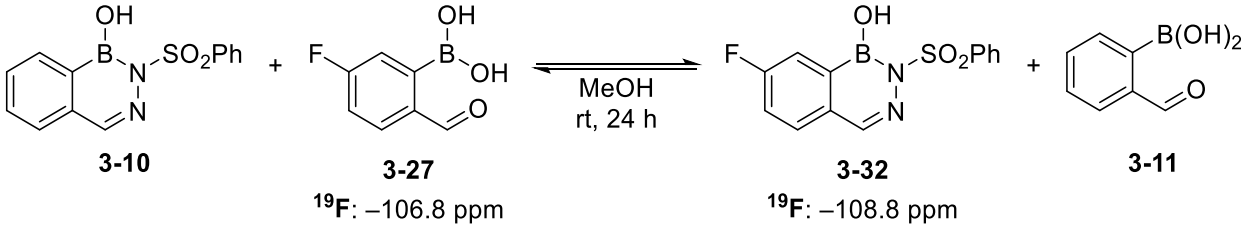

3-10

3-27
^{19}**F**: –106.8 ppm

3-32
^{19}**F**: –108.8 ppm

3-11

Following **GP3-6** in anhydrous methanol, the ratio of **3-27** to **3-32** was 52:48, corresponding to 48% crossover.

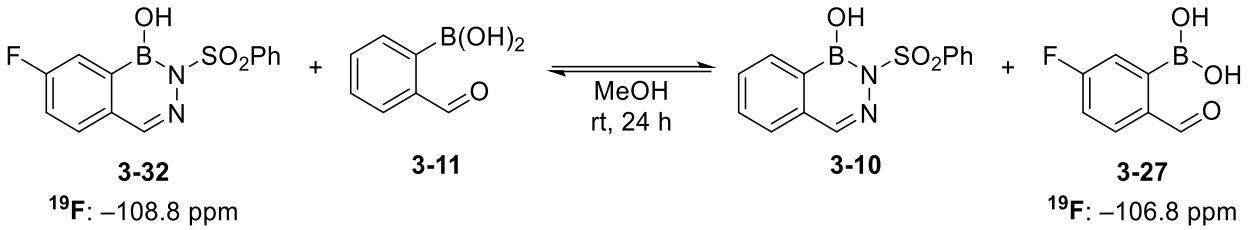

3-32
^{19}F: –108.8 ppm

3-11

3-10

3-27
^{19}F: –106.8 ppm

Following **GP3-6** in anhydrous methanol, the ratio of **3-32** to **3-27** was 60:40, corresponding to 40% crossover.

3.5.4.2 Crossover Between Two Boron Heterocycles

General Procedure for Crossover Reactions Between Two Hemiboronic Acids in Anhydrous Methanol (GP3-7)

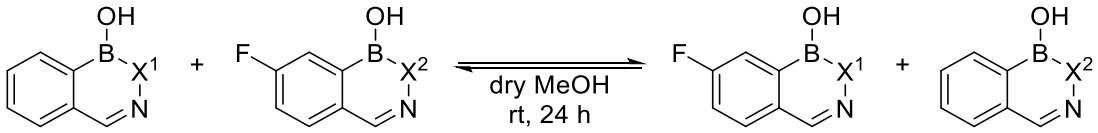

An oven-dried vial was allowed to cool to room temperature under vacuum, after which it was charged with the two respective boron heterocycles (0.05 mmol each). The vial was sealed with a septum, evacuated, and backfilled with nitrogen. Dry methanol (0.5 mL) was then added via syringe, and the vial was quickly sealed with a cap and electrical tape. The mixture was stirred for 24 hours at room temperature, after which it was concentrated by rotary evaporation, dried under vacuum, and analyzed by NMR spectroscopy in *d*$_6$-acetone with a drop of D_2O. Unless otherwise noted, crossover was calculated based on integrations from ^{19}F NMR.

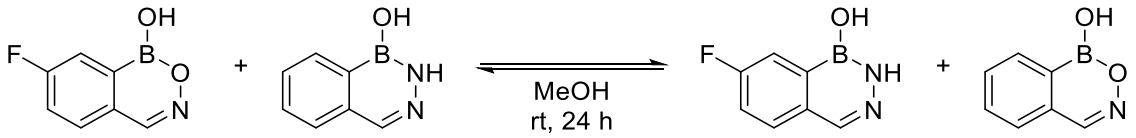

3-28
^{19}F: –107.8 ppm

3-02

3-29
^{19}F: –112.4 ppm

3-01

Following **GP3-7** in anhydrous methanol, no crossover was detected.

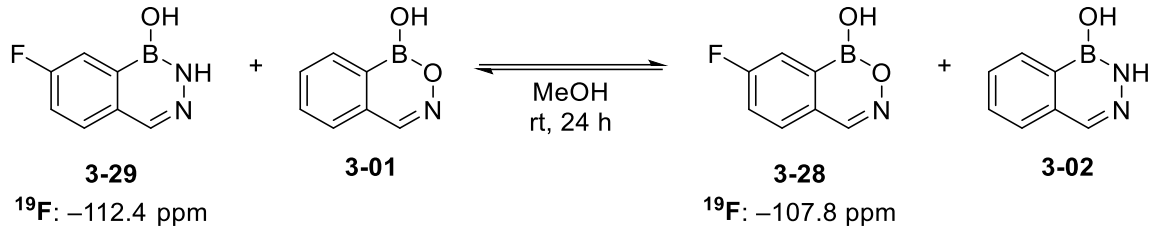

3-29
^{19}**F**: –112.4 ppm

3-01

3-28
^{19}**F**: –107.8 ppm

3-02

Following **GP3-7** in anhydrous methanol, no crossover was detected.

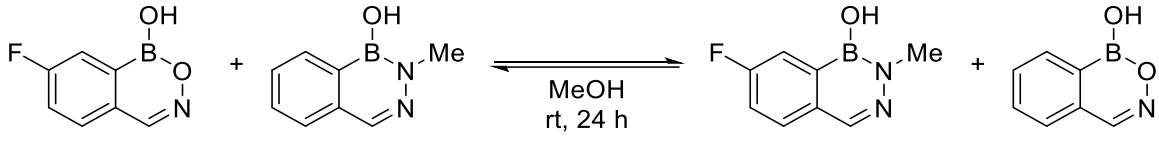

3-28
^{19}**F**: –107.8 ppm

3-08

3-30
^{19}**F**: –112.4 ppm

3-01

Following **GP3-7** in anhydrous methanol, no crossover was detected.

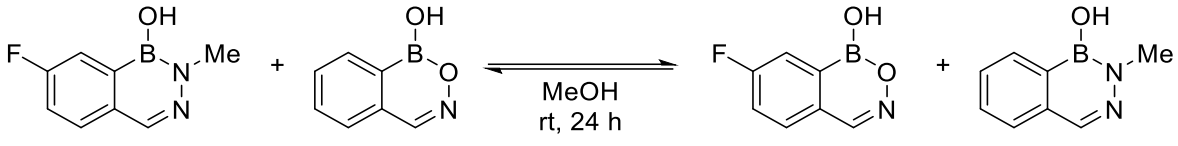

3-30
^{19}**F**: –112.4 ppm

3-01

3-28
^{19}**F**: –107.8 ppm

3-08

Following **GP3-7** in anhydrous methanol, no crossover was detected.

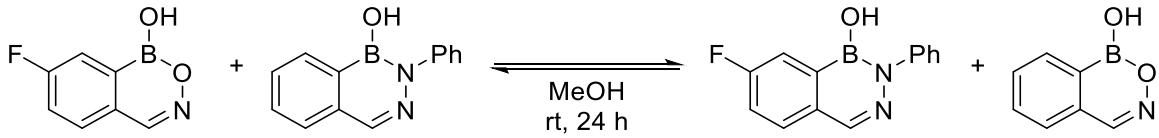

3-28
^{19}**F**: –107.8 ppm

3-09

3-31
^{19}**F**: –111.6 ppm

3-01

Following **GP3-7** in anhydrous methanol, no crossover was detected.

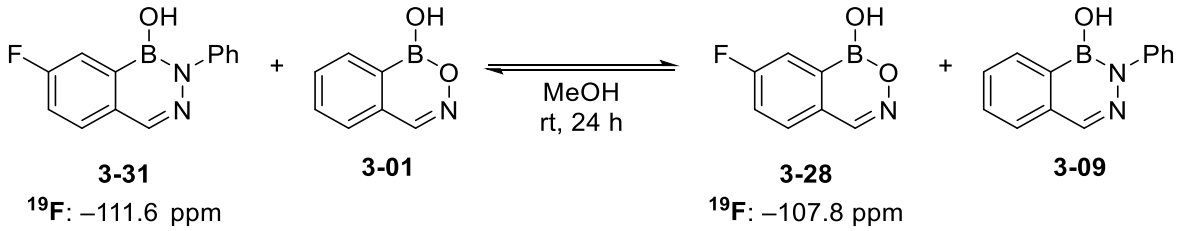

3-31
^{19}**F**: –111.6 ppm

3-01

3-28
^{19}**F**: –107.8 ppm

3-09

Following **GP3-7** in anhydrous methanol, no crossover was detected.

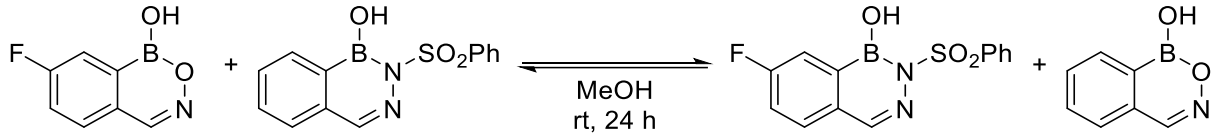

3-28
^{19}**F**: –107.8 ppm

3-10

3-32
^{19}**F**: –108.8 ppm

3-01

Following **GP3-7** in anhydrous methanol, no crossover was detected.

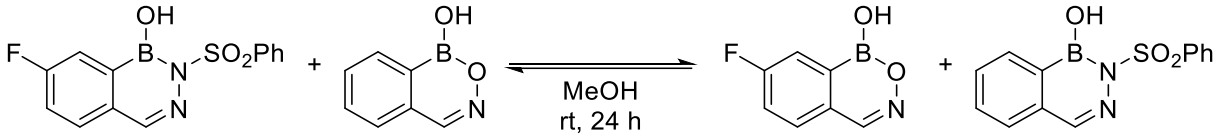

3-32
^{19}**F**: –108.8 ppm

3-01

3-28
^{19}**F**: –107.8 ppm

3-10

Following **GP3-7** in anhydrous methanol, no crossover was detected.

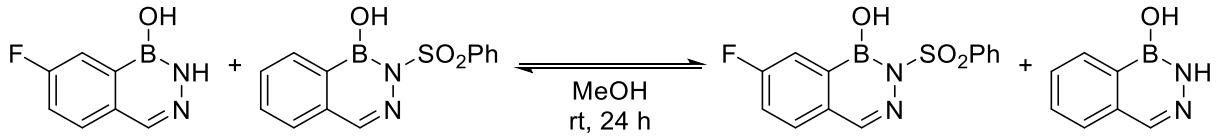

3-29
^{19}**F**: –112.4 ppm

3-10

3-32
^{19}**F**: –108.8 ppm

3-02

Following **GP3-7** in anhydrous methanol, no crossover was detected.

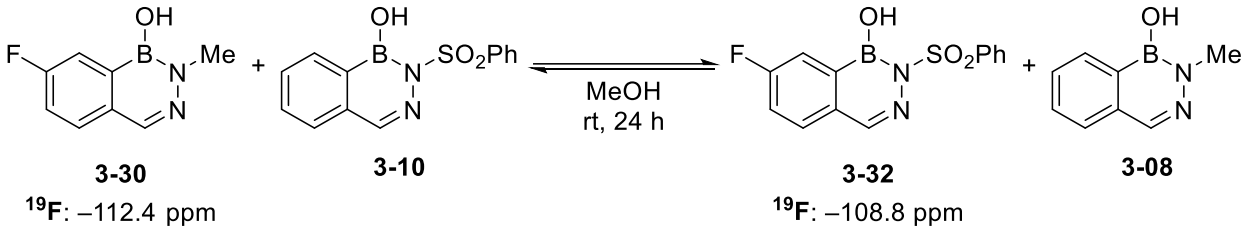

3-30
^{19}**F**: –112.4 ppm

3-10

3-32
^{19}**F**: –108.8 ppm

3-08

Following **GP3-7** in anhydrous methanol, no crossover was detected.

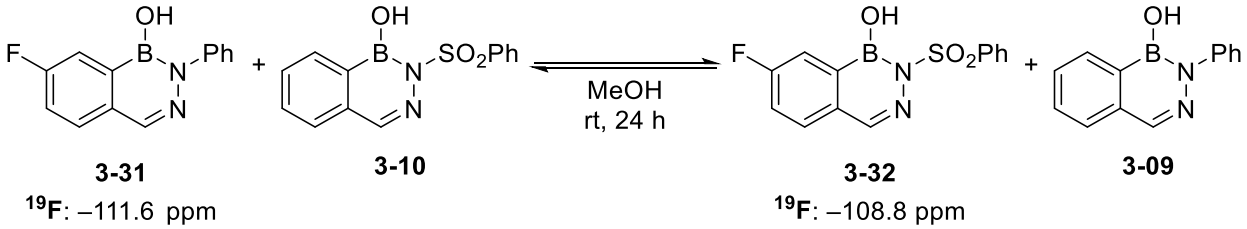

3-31
^{19}**F**: –111.6 ppm

3-10

3-32
^{19}**F**: –108.8 ppm

3-09

Following **GP3-7** in anhydrous methanol, no crossover was detected.

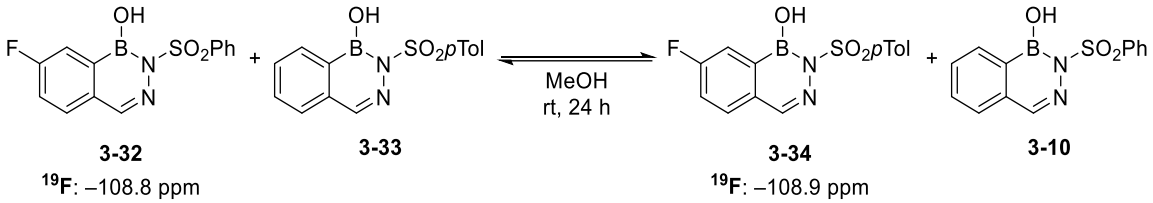

3-32
^{19}**F**: –108.8 ppm

3-33

3-34
^{19}**F**: –108.9 ppm

3-10

Following **GP3-7** in anhydrous methanol, the ratio of **3-32** to **3-34** was approximately 45:55, corresponding to 55% crossover. A similar ratio was observed for the two benzylic methyl resonances in the ^{1}H NMR spectrum (see Figure 3-13).

3.6 References

1) Wang, B. J., Groziak, M. P. *Adv. Heterocycl. Chem.* **2016**, *118*, 47–90.
2) Lepeltier, M., Lukoyanova, O, Jacobsen, A., Jeeva, S., Perepichka, D. F. *Chem. Commun.* **2010**, *46*, 7007–7009.
3) Wang, X., Zhang, F., Liu, J., Tang, R., Fu, Y., Wu, D., Xu, Q., Zhuang, X., He, G., Feng, X. *Org. Lett.* **2013**, *15*, 5714–5717.
4) Estrada, C. D., Ang, H. T., Vetter, K.-M., Ponich, A. A., Hall, D. G. *J. Am. Chem. Soc.* **2021**, *143*, 4162–4167.

5) Jäkle, F. *Coord. Chem. Rev.* **2006**, *250*, 1107–1121.
6) Maitlis, P. M. *Chem. Rev.* **1962**, *62*, 223–245.
7) Matsumi, N., Naka, K., Chujo, Y. *J. Am. Chem. Soc.* **1998**, *120*, 5112–5113.
8) Agou, T., Kobayashi, J., Kawashima, T. *Org. Lett.* **2006**, *8*, 2241–2244.
9) Wang, X.-Y., Wang, J.-Y., Pei, J. *Chem. Eur. J.* **2015**, *21*, 3528–3539.
10) Li, G., Xiong, W.-W., Gu, P.-Y., Cao, J., Zhu, J., Ganguly, R., Li, Y., Grimsdale, A. C., Zhang, Q. *Org. Lett.* **2015**, *17*, 560–563.
11) Li, G., Zhao, Y., Li, J., Cao, J., Zhu, J., Sun, X. W., Zhang, Q. *J. Org. Chem.* **2015**, *80*, 196–203.
12) Marwitz, A. J. V., Jenkins, J. T., Zakharov, L. N., Liu, S.-Y. *Angew. Chem. Int. Ed.* **2010**, *49*, 7444–7447.
13) Fernandes, G. F. S., Denny, W. A., Dos Santos, J. L. *Eur. J. Med. Chem.* **2019**, *179*, 791–804.
14) Baker, S. J., Ding, C. Z., Akama, T., Zhang, Y.-K., Hernandez, V., Xia, Y. *Future Med. Chem.* **2009**, *1*, 1275–1288.
15) Baker, S. J., Zhang, Y.-K., Akama, T., Lau, A., Zhou, H., Hernandez, V., Mao, W., Alley, M. R. K., Sanders, V., Plattner, J. J. *J. Med. Chem.* **2006**, *49*, 4447–4450.
16) Akama, T., Baker, S. J., Zhang, Y.-K., Hernandez, V., Zhou, H., Sanders, V., Freund, Y., Kimura, R., Maples, K. R., Plattner, J. J. *Bioorg. Med. Chem. Let.* **2009**, *19*, 2129–2132.
17) Hecker, S. J., Reddy, K. R., Totrov, M., Hirst, G. C., Lomovskaya, O., Griffith, D. C., King, P., Tsivkovski, R., Sun, D., Sabet, M., Tarazi, Z., Clifton, M. C., Atkins, K., Raymond, A., Potts, K. T., Abendroth, J., Boyer, S. H., Loutit, J. S., Morgan, E. E., Durso, S., Dudley, M. N. *J. Med. Chem.* **2015**, *58*, 3682–3692.
18) Patani, G. A., LaVoie, E. J. *Chem. Rev.* **1996**, *96*, 3147–3176.
19) Lima, L. M., Barreiro, E. J. *Curr. Med. Chem.* **2005**, *12*, 23–49.
20) Mykhailiuk, P. K. *Org. Biomol. Chem.* **2019**, *17*, 2839–2849.
21) Pellicciari, R., Raimondo, M., Marinozzi, M., Natalini, B., Costantino, G., Thomsen, C. *J. Med. Chem.* **1996**, *39*, 2874–2876.
22) Zhong, M., Peng, E., Huang, N., Huang, Q., Huq, A., Lau, M., Colonno, R., Li, L. *Bioorg. Med. Chem. Lett.* **2014**, *24*, 5731–5737.

23) Nicolau, K. C., Vourloumis, D., Totokotsopoulos, S., Papakyriakou, A., Karunsky, H., Fernando, H., Gavriliyuk, J., Webb, D., Stephan, A. *ChemMedChem* **2016**, *11*, 31–37.

24) Stepan, A. F., Subramanyam, C., Efremov, I. V., Dutra, J. K., O'Sullivan, T. J., DiRico, K. J., McDonald, W. S., Won, A., Dorff, P. H., Nolan, C. E. Becker, S. L., Pustilnik, L. R., Riddell, D. R., Kauffman, G. W., Kormos, B. L., Zhang, L., Lu, Y., Capetta, S. H., Green, M. E., Karki, K., Sibley, E., Atchison, K. P., Hallgren, A. J., Oborski, C. E., Robshaw, A. E., Sneed, B., O'Donnell, C. J. *J. Med. Chem.* **2012**, *55*, 3414–3424.

25) Auberson, Y. P., Brocklehurst, C., Furegati, M., Fessard, T. C., Koch, G., Decker, A., La Vecchia, L., Briard, E. *ChemMedChem* **2017**, *12*, 590–598.

26) Giustra, Z. X., Liu, S.-Y. *J. Am. Chem. Soc.* **2018**, *140*, 1184–1194.

27) Zhao, P., Nettleton, D. O., Karki, R. G., Zécri, F. J., Liu, S.-Y. *ChemMedChem* **2017**, *12*, 358–361.

28) Davies, G. H. M. *Chem* **2017**, *2*, 608–609.

29) Stock, A., Pohland, E. *Ber. Dtsch. Chem. Ges.* **1926**, *59*, 2215–2223.

30) Campbell, P. G., Abbey, E. R., Neiner, D., Grant, D. J., Dixon, D. A., Liu, S.-Y. *J. Am. Chem. Soc.* **2010**, *132*, 18048–18050.

31) Baranac-Stojanović, M. *J. Org. Chem.* **2019**, *84*, 13582–13594.

32) Burford, R. J., Li, B., Vasiliu, M, Dixon, D. A., Liu, S.-Y. *Angew. Chem. Int. Ed.* **2015**, *54*, 7823–7827.

33) McConnell, C. R., Haeffner, F., Baggett, A. W., Liu, S.-Y. *J. Am. Chem. Soc.* **2019**, *141*, 9072–9078.

34) Robinson, P. D. Groziak, M. P. *Acta Crystallogr., Sect. C: Cryst. Struct. Commun.* **1999**, C*55*, 1701–1704.

35) Baldock, C., de Boer, G.-J., Rafferty, J. B., Stuitje, A. R., Rice, D. W. *Biochem. Pharmacol.* **1998**, *55*, 1541–1550.

36) Hicks, J. W., Kyle, C. B., Vogels, C. M., Wheaton, S. L., Baerlocher, F. J., Decken, A., Westcott, S. A. *Chem. Biodiversity* **2008**, *5*, 2415–2422.

37) Snyder, H. R., Reedy, A. J., Lennartz, W. J. *J. Am. Chem. Soc.* **1958**, *80*, 835–838.

38) Hückel, E. *Z. Physik* **1931**, *70*, 204–286.

39) Hall, D. G. In *Boronic Acids: Preparation and Application in Organic Synthesis, Medicine, and Materials*. **2011**, Wiley-VCH: Weinheim, Germany; Chapter 1, pp 1–133.

40) Lorand, J. P., Edwards, J. O. *J. Org. Chem.* **1959**, *24*, 769–774.
41) Dewar, M. J. S., Dougherty, R. C. *J. Am. Chem. Soc.* **1962**, *84*, 2648–2649.
42) Dewar, M. J. S., Dougherty, R. C. *J. Am. Chem. Soc.* **1964**, *86*, 433–436.
43) Reed, D. *Chem. Soc. Rev.* **1993**, *22*, 109–116.
44) Gao, P., Wang, X., Huang, Z., Yu, H. *ACS Omega* **2019**, *4*, 12385–12392.
45) Dewar, M. J. S., Jones, R. *J. Am. Chem. Soc.* **1967**, *89*, 2408–2410.
46) Kroeker, S., Stebbins, J. F. *Inorg. Chem.* **2001**, *40*, 6239–6246.
47) Fujdala, K. L., Oliver, A. G., Hollander, F. J., Tilley, T. D. *Inorg. Chem.* **2003**, *42*, 1140–1150.
48) Groziak, M. P., Chen, L., Yi, L., Robinson, P. D. *J. Am. Chem. Soc.* **1997**, *119*, 7817–7826.
49) Gu, H., Chio, T. I., Lei, Z., Staples, R. J., Hirschi, J. S., Bane, S. *Org. Biomol. Chem.* **2017**, *15*, 7543–7548.
50) Whittemore, N. A., Mishra, R., Kheterpal, I., Williams, A. D., Wetzel, R., Serpersu, E. H. *Biochemistry* **2005**, *44*, 4434–4441.
51) Leszczyński, P., Lewandowska, A., Hofman, T., Adamczyk-Woźniak, A., Sporzyński, A. *J. Chem. Eng. Data* **2020**, *65*, 4605–4612.
52) Larkin, J. D., Bhat, K. L., Markham, G. D., Brooks, B. R., Schaefer, H. F., Bock, C. W. *J. Phys. Chem.* **2006**, *110*, 10633–10642.
53) Ang, H. T., Ponich, A. A., Paladino, M., Miskolzie, M., Hall, D. G. *J. Am. Chem. Soc.* **2022**, *144*, 10570–10581.
54) Dowlut, M., Hall, D. G. *J. Am. Chem. Soc.* **2006**, *128*, 4226–4227.
55) Cammidge, A. N., Goddard, V. H. M., Gopee, H., Harrison, N. L., Hughes, D. L., Schubert, C. J., Sutton, B. M., Watts, G. L., Whitehead, A. J. *Org. Lett.* **2006**, *8*, 4071–4074.
56) Shao, Y., et al., *Mol. Phys.* **2015**, *113*, 184–215.
57) Chen, Z., Wannere, C. S., Corminboeuf, C., Puchta, R., Schleyer, P. V. R. *Chem. Rev.* **2005**, *105*, 3842–3888.
58) Yruegas, S., Patterson, D. C., Martin, C. D. *Chem. Commun.* **2016**, *52*, 6658–6661.
59) Watanabe, E., Miyamoto, C., Tanaka, A., Iizuka, K., Iwatsuki, S., Inamo, M., Takagi, H. D., Ishihara, K. *Dalton Trans.* **2013**, *42*, 8446–8453.

Chapter 4 Direct Nucleophilic and Electrophilic Activation of Alcohols using the Benzoxazaborine Catalyst Scaffold

4.1 Introduction

The rational development of new catalytic transformations relies on the ability of chemists to make reasonable predictions regarding the behaviour or reactivity of catalysts under new conditions. Accordingly, the identification of catalyst classes which demonstrate useful levels of reactivity or selectivity across a range of applications can significantly accelerate the process of reaction discovery and optimization. While enzymatic catalysts in biosynthetic processes often display exceptional substrate specificity,[1] many areas of small molecule catalysis have demonstrated remarkable generality of scope. This generality has been most prevalent in the design of chiral secondary amine organocatalysts and chiral ligands for asymmetric transition metal catalysis, where many "privileged scaffolds" have proven to be highly stereoselective in a variety of mechanistically unrelated reactions (Figure 4-1).[2–6]

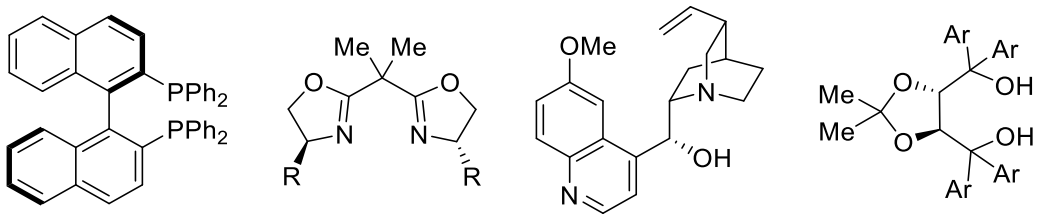

Figure 4-1 Examples of privileged chiral ligand and catalyst scaffolds.

The development of similar privileged catalyst scaffolds in boronic acid catalysis has yet to be successfully realized. As the collection of transformations that have proven amenable to boronic acid catalysis has grown in recent years, new catalyst archetypes have continued to

emerge.[7] Accordingly, the discovery of new transformations often requires bespoke catalyst synthesis or considerable screening and optimization. While this process can be facilitated through Design of Experiments (DOE) strategies or high-throughput experimentation infrastructure,[8,9] the development of broadly applicable scaffolds in boronic acid catalysis could significantly accelerate the discovery of new transformations.

The lack of broadly applicable catalysts likely stems from the significant mechanistic divergence amongst boronic acid-catalyzed reactions. Broadly speaking, substrate activation can be classified as either electrophilic or nucleophilic in nature. The electron-withdrawing effect provided by coordination to boron can provide electrophilic activation of alcohols towards subsequent nucleophilic substitution (Figure 4-2).[7] For activated alcohols, this process can occur via an S_N1 mechanism with complete C–O ionization and a discrete carbocation intermediate. Catalysis within this manifold is largely influenced by the boronic acid pK_a, with increasingly Lewis acidic species generally being more effective catalysts, particularly highly electron-deficient cationic species or heavily fluorinated arylboronic acids.[10–17]

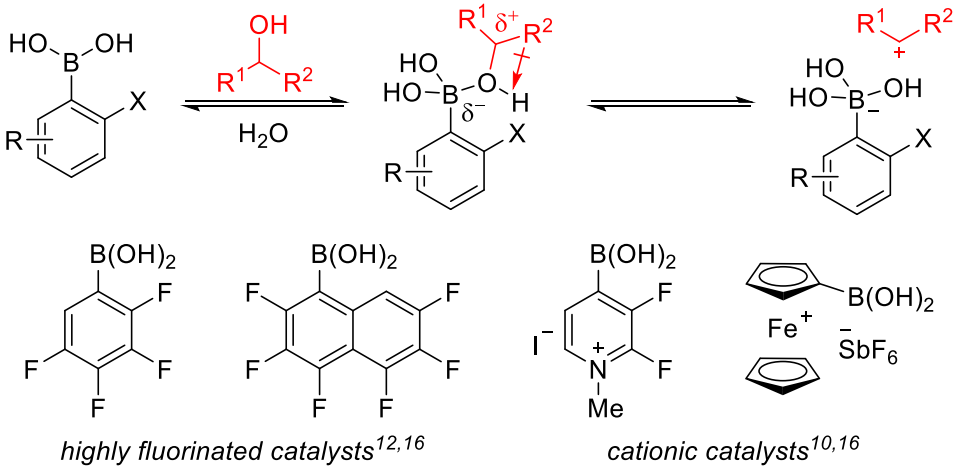

Figure 4-2 Electrophilic activation in boronic acid catalysis and examples of effective catalysts.

Conversely, boron catalysts can also induce nucleophilic activation of polyol substrates by formation of a tetrahedral dialkoxyboronate anion (Figure 4-3).[18] While the formal negative charge lies on the boron atom, significant charge density resides on the oxygen atoms due to their greater electronegativity, which in turn induces nucleophilic activation of the alkoxy groups. The use of borinic acid catalysts (compounds containing two C–B bonds and one B–O bond) in this manifold has been pioneered by the Taylor Group.[19] These species readily form anionic tetravalent adducts upon reaction with diols as they contain only a single exchangeable boranol moiety. Consequently, they have been employed as catalysts in a variety of 1,2- and 1,3-diol monofunctionalization reactions, including benzylation,[20] benzoylation,[20] tosylation,[20] and sulfation.[21] However, borinic acids can be oxidatively unstable, and often require protection as the ethanolamine adduct for storage.[22] When traditional arylboronic acid catalysts are employed, diol exchange occurs readily to form a neutral trivalent boronic ester, and a strong Lewis base is generally required to generate the catalytically active tetravalent boronate species.[23] The Hall Group has recently reported the use of BINOL-derived cyclic hemiboronic acid **4-01** as an efficient catalyst for the enantioselective desymmetrization of 1,3-diols.[24] By combining the oxidative stability of a boronic acid with the single exchangeable boranol moiety of a borinic acid, catalyst **4-01** was found to induce nucleophilic activation of 1,3-diols via a well-defined chair-like tetrahedral dialkoxyboronate anion intermediate.[24]

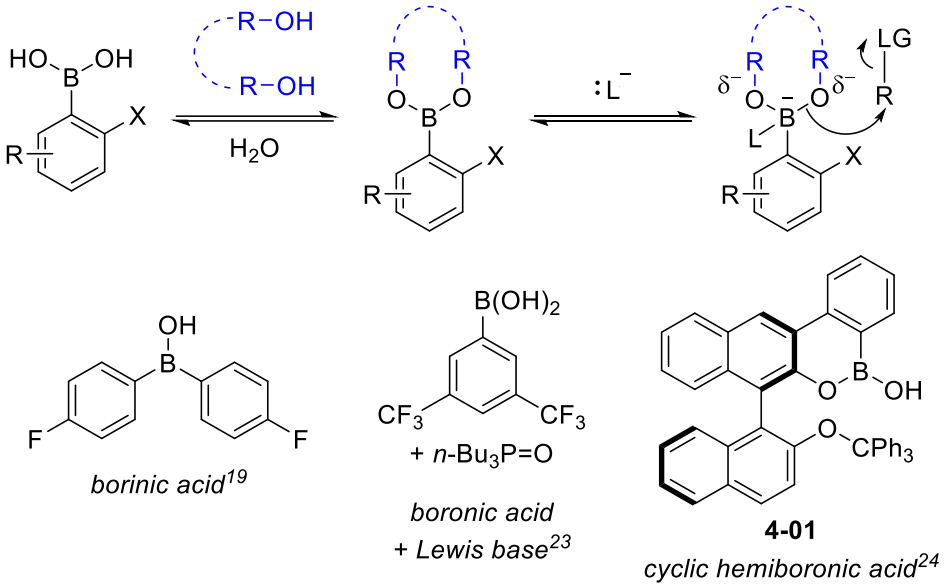

Figure 4-3 Nucleophilic activation of polyols in boronic acid catalysis and examples of catalytic systems.

Given the drastically different mechanisms of activation in electrophilic and nucleophilic pathways, it is perhaps not surprising that considerably different catalysts are often applied for the two classes of reactions (Figure 4-4).[7] Mechanistic details are often substrate dependent, and optimization on a particular model compound is no guarantee of reaction generality. The development of an increasingly universal catalyst framework in boronic acid catalysis represents an appealing prospect, in which mechanistically divergent catalytic transformations could be developed based on well-understood fundamental catalyst reactivity rather than serendipitous optimization. To develop the rigorous mechanistic foundations upon which to build a general catalyst scaffold, it is essential to obtain a systematic understanding of the underlying fundamental properties of boronic acid catalysts, such as their stability, acidity, and exchangeability with hydroxy-containing compounds.

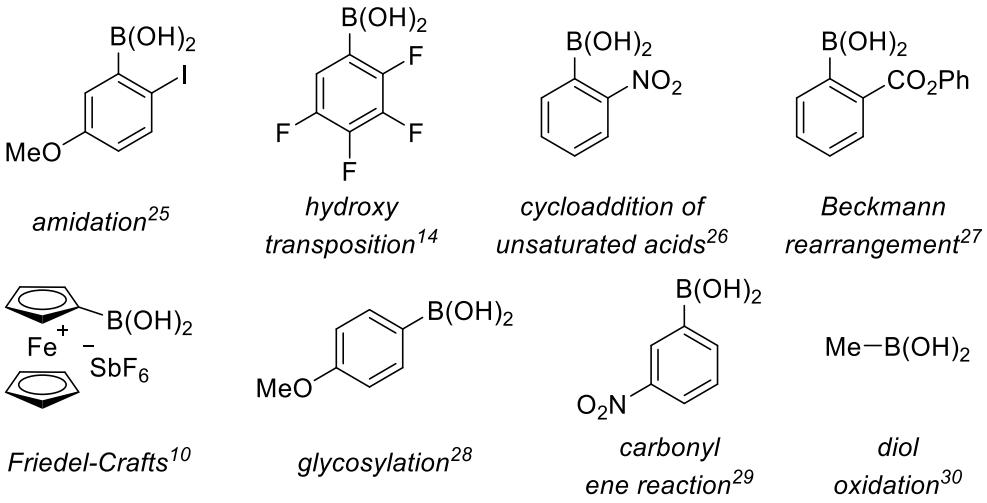

Figure 4-4 Selection of catalysts reported in boronic acid catalysis.

As described in Chapter 3, we recently completed a comprehensive investigation of the acidity and fundamental reactivity of boranol-containing naphthoid heterocycles **4-02** through **4-06**.[31] This library of cyclic hemiboronic acids was examined to assess structure-reactivity relationships between benzoxazaborines and *N*-functionalized benzodiazaborines. While the Lewis acidic character of these hemiboronic acids was unambiguously established by X-ray crystallography, the strength of their acidity was found to vary significantly. Additionally, the exchangeability of their boranol (B–OH) group with alcohols and stability towards endocyclic B–X bond cleavage in methanol was highly substrate dependent.[31] Inspired by the recent successful application of cyclic hemiboronic acid **4-01** in nucleophilic catalysis, it was envisioned that cyclic hemiboronic acids could provide a suitable scaffold from which to develop a broadly applicable catalyst framework.[24]

Among the hemiboronic acids that were examined, the benzoxazaborine scaffold (**4-02**) demonstrated several properties conducive to the development of mechanistically divergent catalysts (Figure 4-5). Hemiboronic acid **4-02** was demonstrated to undergo rapid and reversible

covalent boranol exchange in both protic and aprotic solvents and was found to be highly resistant towards endocyclic B–O hydrolysis. Additionally, heterocycle **4-02** was moderately acidic in both aqueous and mixed aqueous/organic solvent systems, suggesting that both the trivalent and tetravalent species can be reversibly accessed under suitable conditions.[31] It was hypothesized that while the moderate acidity of hemiboronic acid **4-02** could be suitable for nucleophilic activation, the design and synthesis of an increasingly acidic analog for electrophilic activation could enable two mechanistically divergent catalytic strategies for the functionalization of alcohols from a common boron-containing heterocyclic framework.

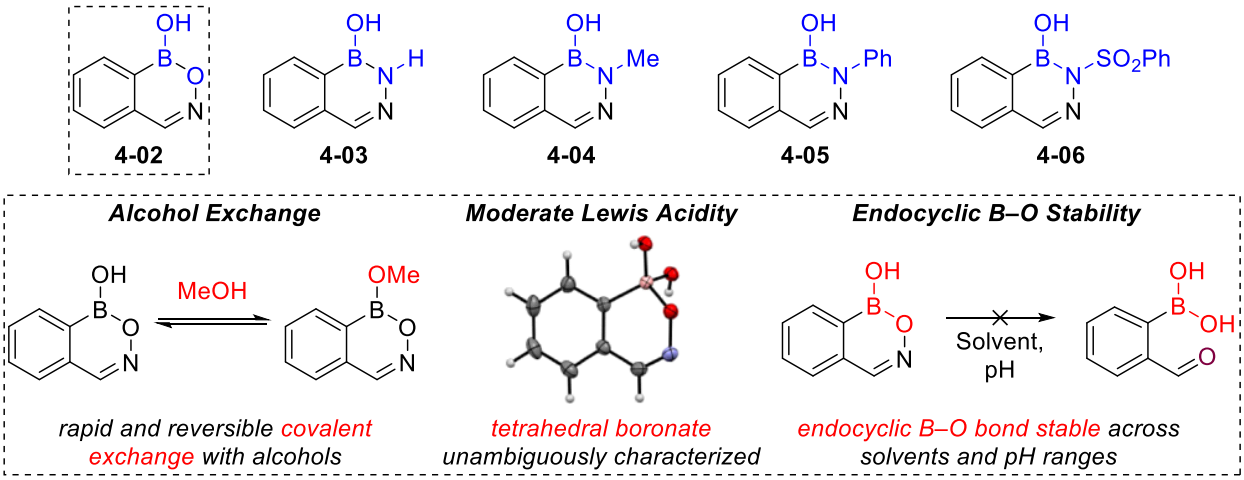

Figure 4-5 Cyclic hemiboronic acid isoquinoline analogs and properties of benzoxazaborine (**4-02**) relevant to catalysis.

4.2 Objectives

The development of a universal catalyst scaffold could accelerate the discovery of new boronic acid-catalyzed transformations by relying on mechanistically guided catalyst selection rather than serendipitous optimization and screening alone. Due to their oxidative and hydrolytic stability, boranol exchangeability, and tunable acidity, cyclic hemiboronic acids show significant potential in boronic acid catalysis, which has been underexplored to date. Drawing from the fundamental

studies described in Chapter 3, this chapter will investigate the use of the benzoxazaborine scaffold as a catalyst framework for the direct nucleophilic and electrophilic activation of diols and alcohols respectively.

Nucleophilic activation using the parent neutral hemiboronic acid **4-02** will be examined, and trends in catalyst reactivity relative to other cyclic hemiboronic acid will be investigated. Additionally, the synthesis of a benzoxazaborine derivative with significantly enhanced acidity will be explored, and its application as a catalyst for electrophilic activation will be examined. Mechanistic studies will be conducted to understand the contrasting mechanisms of activation with the two catalytic species. A clear association will be demonstrated between the fundamental properties and inherent reactivity of cyclic hemiboronic acids and their applications as reaction catalysts.

4.3 Results and Discussion – Nucleophilic Activation

4.3.1 Introduction to Diol Monophosphorylation and Cyclic Hemiboronic Acids as Catalysts for Nucleophilic Activation

The selective phosphorylation of polyhydroxylated compounds is an essential process in many vital biosynthetic pathways.[32] Reversible protein phosphorylation mediated by kinase and phosphatase enzymes plays a crucial role in metabolism, cell division and apoptosis, while many vital biochemical processes are reliant on kinase-mediated ATP- or GTP-dependent pathways.[32–34] The addition of an ionizable phosphate group can be used as a strategy in prodrug modification to increase the water-solubility or oral bioavailability of hydrophobic lead compounds.[35,36] For example, multiple sclerosis medication FTY720, which contains a propan-1,3-diol moiety, was demonstrated to undergo rapid monophosphorylation *in vivo* to form the corresponding monophosphate which is believed to be responsible for its biological activity.[37]

Chemical synthesis of monophosphorylated polyols has paled in comparison to the exquisite activity and selectivity demonstrated in biosynthetic processes. Catalytic enantioselective monophosphorylation of inositol derivative **4-07** using a chiral peptide organocatalyst was reported by Miller and co-workers (Scheme 4-1a).[38] This transformation was proposed to proceed through *N*-phosphorylation of a terminal histidine residue, generating a highly activated phospho-imidazolium intermediate rather than through nucleophilic activation of the diol. The activation of diols for monophosphorylation using metal-based Lewis acids was first demonstrated by Adachi and co-workers using stoichiometric silver(I) oxide (Scheme 4-1b), which was proposed to proceed through a chelated metal alkoxide intermediate.[39] This transformation was highlighted in the synthesis of monophosphate **4-10**, a precursor to S1P receptor agonist FTY720-phosphate.[40] Subsequent studies by the Sculimbrene Group demonstrated that catalytic turnover is possible using titanium Lewis acids (Scheme 4-1c).[41] Unsymmetrical 1,3-diols were found to undergo monophosphorylation with moderate regioselectivity for the least sterically hindered position, while an *in situ* prepared chiral titanium-BINOL complex was later found to catalyze the enantioselective desymmetrization of 1,3-diols with moderate enantioselectivity.[42] A small positive nonlinear effect was observed in the enantiomeric excess of the product relative to that of the catalyst, suggesting that a higher order or oligomeric catalytic species may be active.[42]

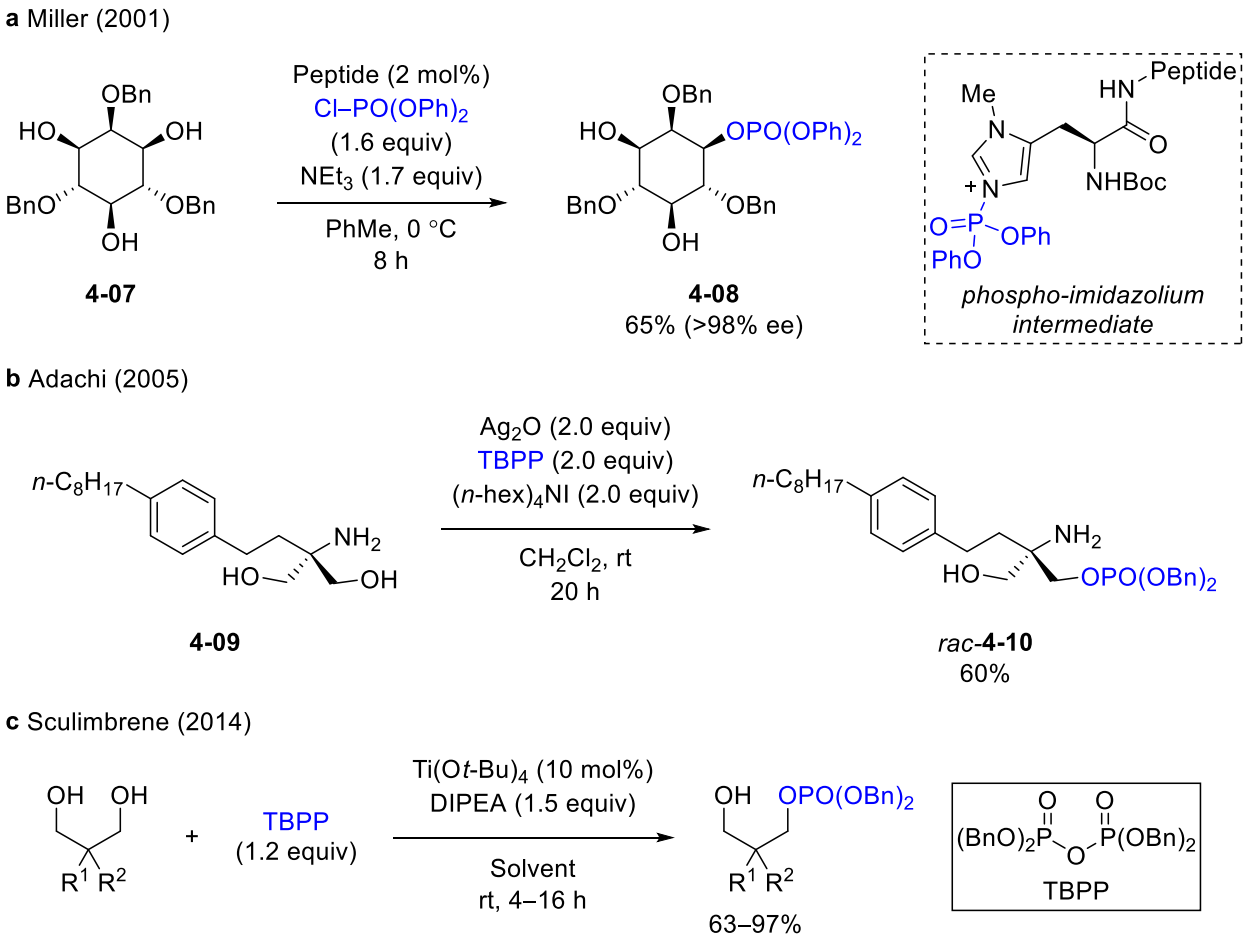

Scheme 4-1 Examples of catalytic diol monophosphorylation reactions.

In recent years, scattered reports have emerged describing the use of cyclic hemiboronic acids as catalysts in nucleophilic activation. Hayashida and co-workers demonstrated the use of benzoxaborole derivative **4-11** to catalyze the site-selective benzylation, tosylation and benzoylation of vicinal diols (Scheme 4-2a).[43] In cyclic diols, high selectivity for *cis*-diol moieties over *trans*-diols was observed, consistent with improved formation of a tetrahedral boronate adduct in the *cis* substrates.[44] Meanwhile, chiral benzazaborole **4-12** was reported by Arai and co-workers to catalyze the enantioselective desymmetrization of cyclic 1,2-diols via sulfonylation (Scheme 4-2b).[45] Lewis basic co-catalyst **4-13** was employed to promote formation of an activated *N*-sulfonylimidazolium electrophile. Acyclic vicinal diols were unsuccessful substrates under

these conditions.[45] Enantioselective desymmetrization of 1,3-diols using chiral boroxarophenanthrene catalyst **4-14** was subsequently reported by Hall and co-workers, who unambiguously demonstrated the formation of a tetravalent substrate-catalyst adduct (Scheme 4-2c).[24]

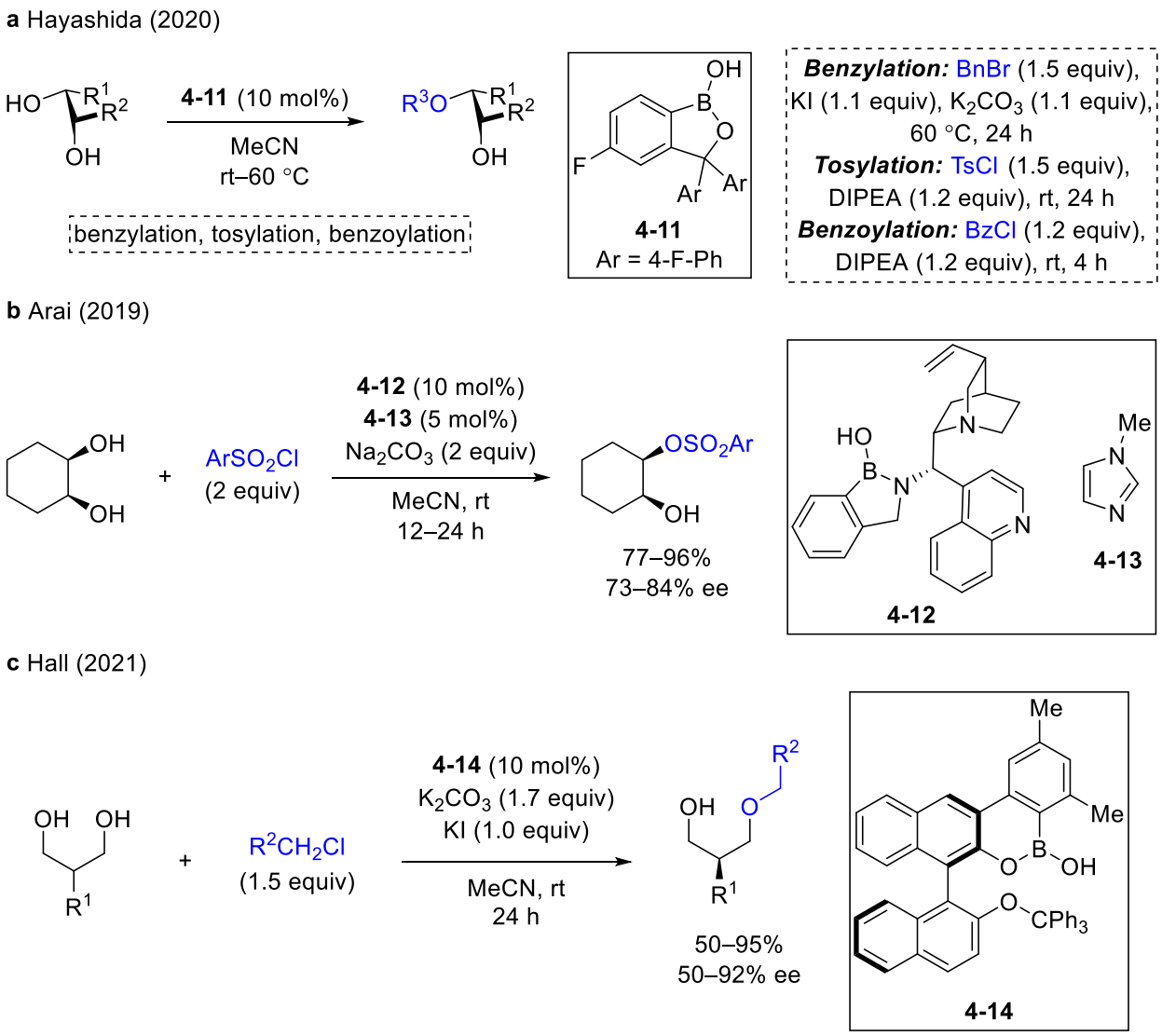

Scheme 4-2 a Monofunctionalization of 1,2-diols using a benzoxaborole catalyst. **b** Enantioselective desymmetrization of cyclic 1,2-diols using a chiral benzazaborole catalyst. **c** Enantioselective desymmetrization of 1,3-diols using a chiral boroxarophenanthrene catalyst.

Compared to the use of inorganic Lewis acid catalysts, the development of a hemiboronic acid-catalyzed monophosphorylation reaction may employ a benign organocatalyst under mild conditions. It was reasoned that reaction of benzoxazaborine (**4-02**) with a vicinal diol under basic conditions could readily induce nucleophilic diol activation through an intermediate tetravalent dialkoxyboronate anion. Provided that the uncatalyzed background reaction is sufficiently slow, high selectivity for monofunctionalization can be achieved due to the enhanced nucleophilicity of the tetravalent boronate. Accordingly, the ability of hemiboronic acid **4-02** to promote monophosphorylation of vicinal diols in the presence of a chlorophosphate electrophile was investigated.

4.3.2 Initial Stoichiometric Studies and Reaction Optimization

The stoichiometric reaction of vicinal diol **4-15a** and hemiboronic acid **4-02** was examined using a combination of ^{1}H and ^{11}B NMR spectroscopy (Scheme 4-3). Initial reaction between diol **4-15a** and hemiboronic acid **4-02** in CD_3CN led to equilibrium generation of boranol exchange product **4-16**, consistent with our previous observations for facile boranol exchange of heterocycle **4-02**.[31] Spectroscopic changes upon boranol exchange with diol **4-15a** were comparable to those observed with methanol, including increasingly deshielded aliphatic protons and a new ^{11}B NMR resonance slightly upfield relative to hemiboronic acid **4-02** (Figure 4-6). New resonances in the ^{1}H NMR consistent with formation of **4-16** were somewhat broadened relative to the free diol, suggesting that there may be a dynamic exchange process between the two regioisomers of the alcohol exchange product. Addition of *N,N*-diisopropylethylamine (DIPEA) led to quantitative formation of proposed tetravalent boronate **4-17** with a corresponding upfield ^{11}B NMR resonance at 7.2 ppm. The formation of intermediates **4-16** and **4-17** was further supported by HRMS analysis. In the absence of hemiboronic acid **4-02**, relative pK_a values would suggest that deprotonation of a

secondary alcohol by DIPEA is thermodynamically unfavourable. Accordingly, the rapid and complete deprotonation observed here suggests that intramolecular coordination to boron is essential to driving the equilibrium.

Subsequent addition of diethyl chlorophosphate (**4-18**) led to rapid quenching of tetravalent boronate **4-17**, restoring free hemiboronic acid **4-02** along with the generation of monophosphorylated alcohol **4-19a**. Phosphorylation occurred with complete regioselectivity for the primary alcohol. The detection of hemiboronic acid **4-02** after electrophile addition suggests that the initially formed trivalent hemiester between secondary alcohol **4-19a** and hemiboronic acid **4-02** is rapidly hydrolyzed by water released in the initial adduct formation. Each step of the reaction occurred rapidly (<5 minutes) at room temperature under ambient conditions.

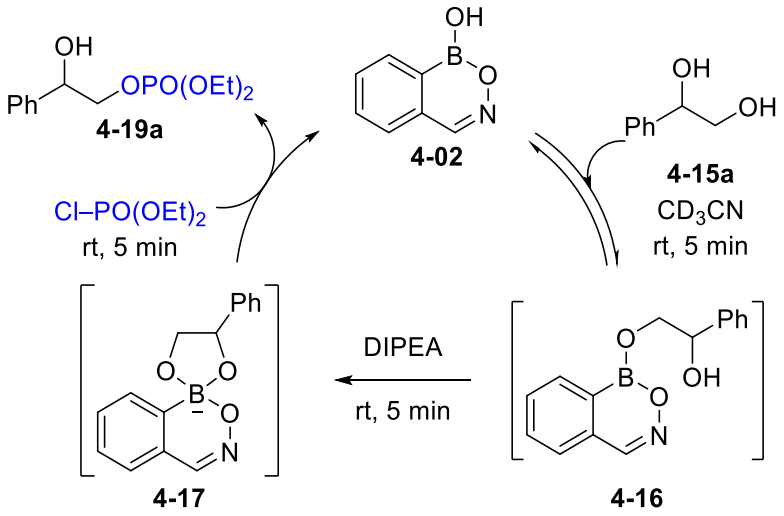

Scheme 4-3 Stoichiometric monophosphorylation of diol **4-15a** promoted by hemiboronic acid **4-02**.

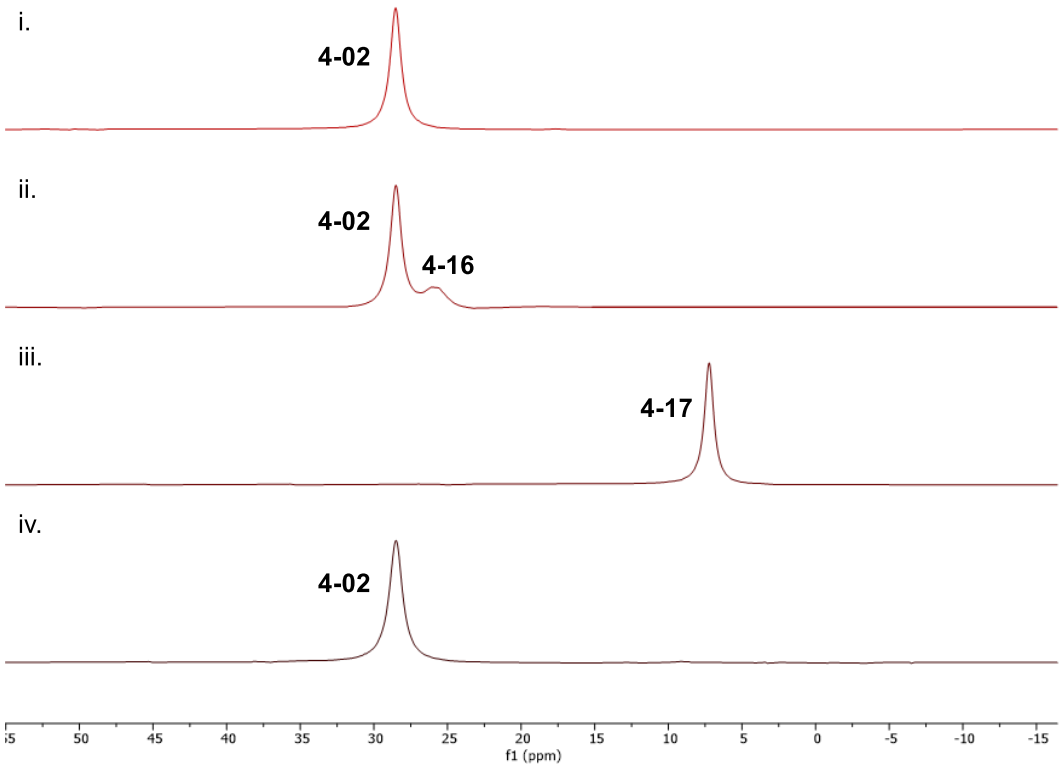

Figure 4-6 ^{11}B NMR (128 MHz, CD_3CN) monitoring of stoichiometric monophosphorylation of diol **4-15a**.

Having established the ability of hemiboronic acid **4-02** to promote monophosphorylation in stoichiometric experiments, a catalytic variant of this reaction was subsequently optimized (Table 4-1). A variety of organic and inorganic bases were examined, where DIPEA was found to give the highest yield (Entries 1–8). The reaction was found to proceed effectively in short reaction time using only slight excesses of base and electrophile (Entries 9–12). Optimized conditions were found using 10 mol% catalyst **4-02**, 1.1 equivalents of DIPEA and $ClPO(OEt)_2$ in acetonitrile at room temperature for 90 minutes.

Table 4-1 Optimization of monophosphorylation catalyzed by hemiboronic acid **4-02**.

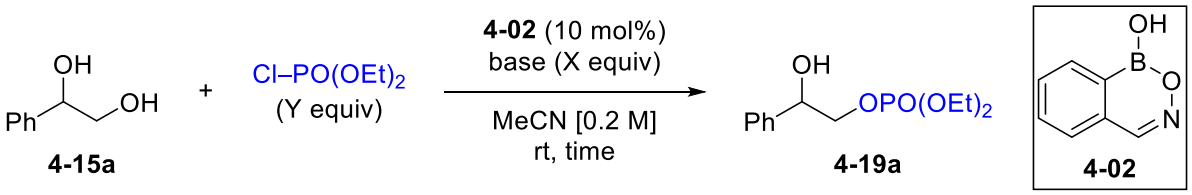

Entry	Base (X equiv)	Cl–PO(OEt)$_2$ (Y equiv)	Time	Yield 4-19a[a]
1	NEt_3 (1.5 equiv)	1.5	18 h	70%
2	Pyridine (1.5 equiv)	1.5	18 h	43%
3	DBU (1.5 equiv)	1.5	18 h	12%
4	DIPEA (1.5 equiv)	1.5	18 h	73%
5	Na_2CO_3 (1.5 equiv)	1.5	18 h	64%
6	K_2HPO_4 (1.5 equiv)	1.5	18 h	34%
7	K_2CO_3 (1.5 equiv)	1.5	18 h	66%
8	Proton Sponge (1.5 equiv)	1.5	18 h	71%
9	DIPEA (1.5 equiv)	1.5	1 h	92%
10	DIPEA (1.5 equiv)	1.0	1 h	85%
11	DIPEA (1.0 equiv)	1.0	1 h	89%
12	DIPEA (1.1 equiv)	1.1	1.5 h	93%

[a]Yields determined by ^{1}H NMR relative to 1,3,5-trimethoxybenzene as an internal standard.

Notably, other naphthoid hemiboronic acids demonstrated significantly reduced catalytic activity relative to hemiboronic acid **4-02** (Table 4-2, Entries 1–3). In the absence of catalyst, only 4% yield of monophosphorylated product **4-19a** was observed, suggesting that the background reaction is minimal under these conditions (Entry 4). A control reaction using primary benzylic alcohol **4-20**, lacking the vicinal diol moiety, showed significantly decreased yield under optimized conditions relative to the reaction of diol **4-15a**, highlighting the nucleophilic activation afforded by tetravalent boronate intermediate **4-17** (Scheme 4-4).

Table 4-2 Comparison of hemiboronic acid catalyst activity in monophosphorylation.

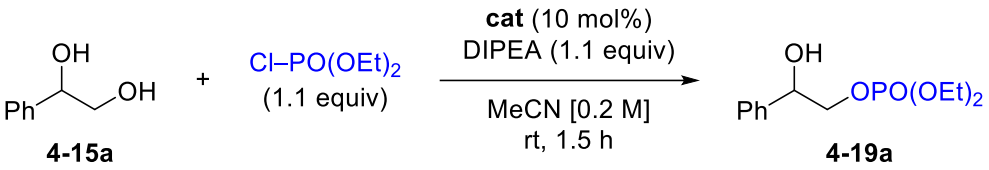

Entry	Catalyst	Yield 4-19[a]
1	**4-04**	6%
2	**4-05**	24%
3	**4-06**	13%
4	-	4%

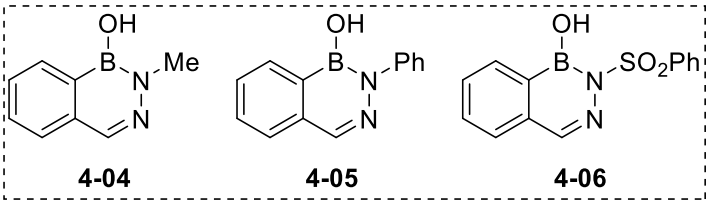

[a]Yields determined by ^{1}H NMR relative to 1,3,5-trimethoxybenzene as an internal standard.

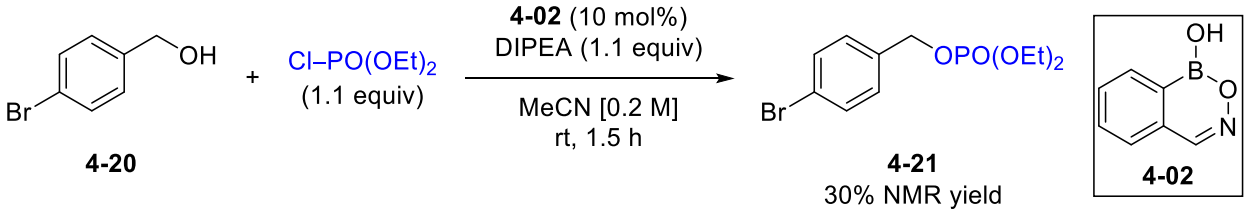

Scheme 4-4 Phosphorylation of a primary benzylic alcohol catalyzed by hemiboronic acid **4-02**.

4.3.3 Substrate Scope of Diol Monophosphorylation

The substrate scope of the monophosphorylation reaction with respect to the diol component **4-15** was examined. Vicinal diols were prepared by osmium-catalyzed dihydroxylation of the corresponding styrene,[46] or through a two-step sequence of selenium dioxide-mediated α-oxidation and borohydride reduction from the corresponding acetophenone (see Experimental section for full details).[47] A variety of vicinal diols **4-15** successfully underwent monophosphorylation with

complete regioselectivity under the optimized conditions (Scheme 4-5). Halogenated substituents were well-tolerated, and *ortho*-substitution did not have a detrimental impact on the yield.

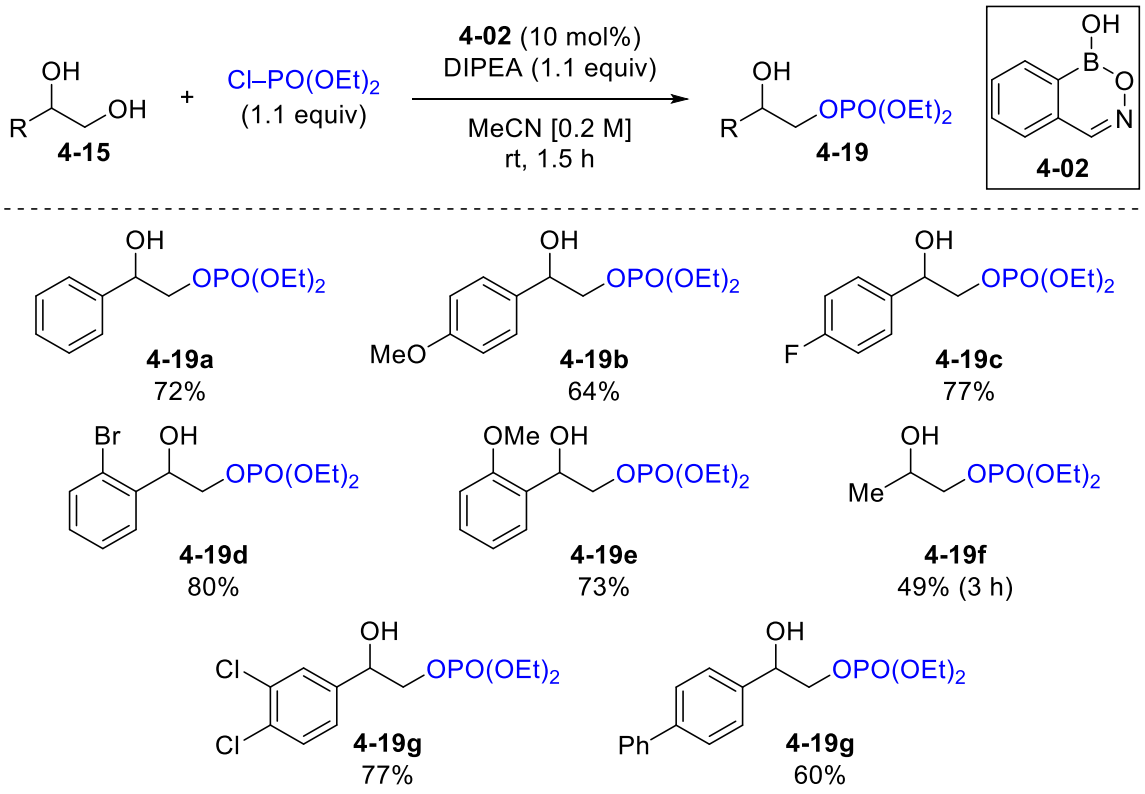

Scheme 4-5 Scope of the monophosphorylation of diols catalyzed by hemiboronic acid **4-02**.

As highlighted in the synthesis of **4-19f**, this methodology was also applicable to aliphatic diols albeit in reduced yield. Stoichiometric reaction of diol **4-15f** with hemiboronic acid **4-02** under basic conditions demonstrated lower conversion to tetrahedral adduct **4-22** relative to the conversion of diol **4-15a** to adduct **4-17** (Figure 4-7). This tentatively suggests that among vicinal diol substrates, relative rates of reaction may be primarily dictated by changes in the rate of adduct formation. However, additional aliphatic diols need to be examined to assess the generality of this observation.

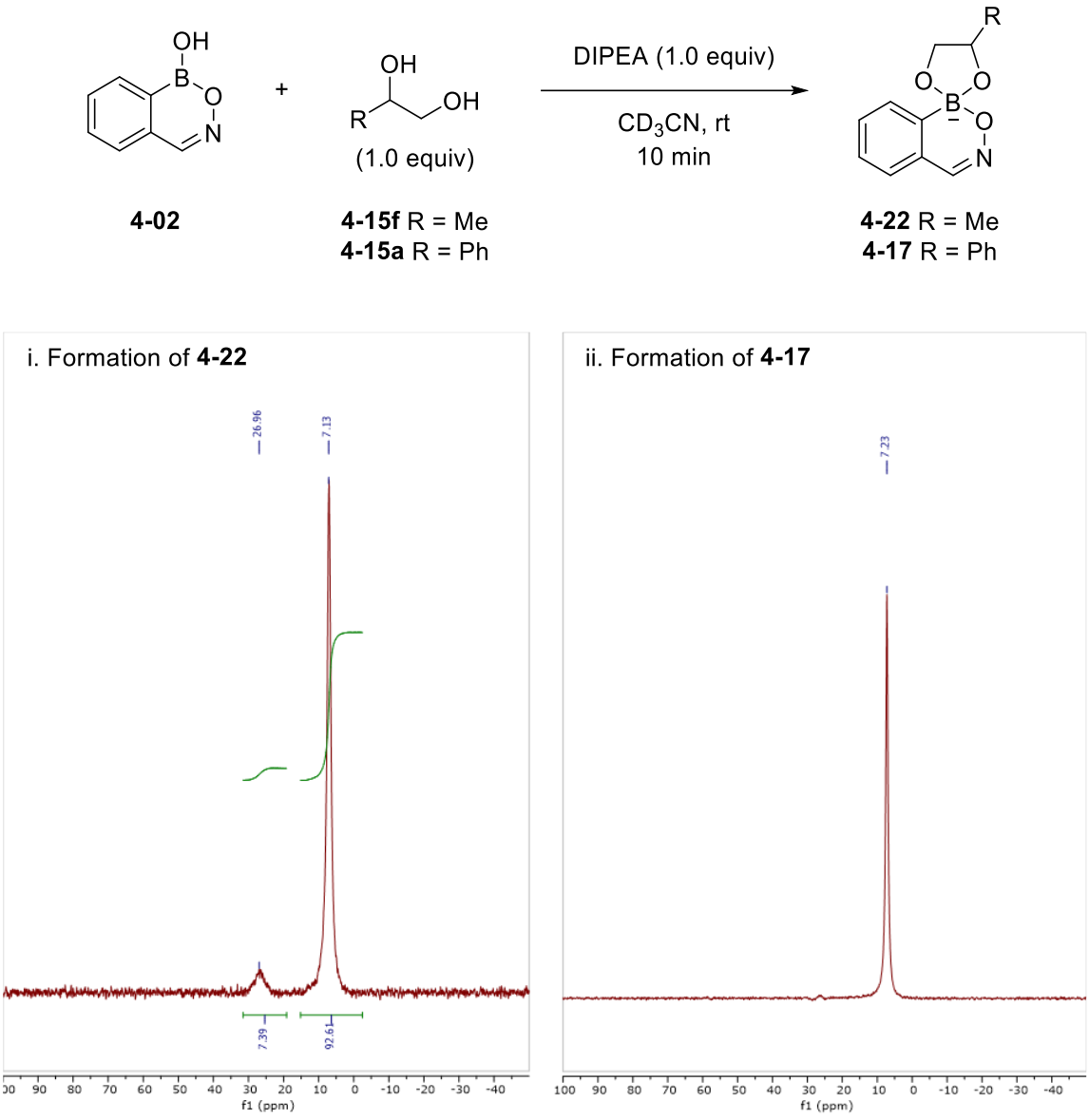

Figure 4-7 ^{11}B NMR (128 MHz, CD_3CN) demonstrating conversion of diols **4-15f** and **4-15a** to the corresponding tetravalent adducts.

4.3.4 Comparison of Hemiboronic Acid Catalytic Activity

As noted in the optimization of catalytic monophosphorylation (*cf.* Table 4-2), benzoxazaborine (**4-02**) displayed significantly greater catalytic activity than other naphthoid hemiboronic acids. In principle, large differences in the rate of reaction could arise from the relative rates of conversion to the corresponding tetravalent boronate adducts, or in the rate of subsequent electrophile

trapping. Stoichiometric reactions between diol **4-15a** and model hemiboronic acids were investigated in an attempt to elucidate the origin of the large differences in catalytic activity of these heterocycles.

Diol complexation in the presence of DIPEA was examined by ^{11}B NMR spectroscopy in the absence of an electrophile. In these stoichiometric experiments, conversion to the corresponding tetravalent adducts was found to be well correlated to the acidity of the parent hemiboronic acids (Table 4-3).[31] Hemiboronic acids **4-06** and **4-02**, with the lowest pK_a values (5.5 and 7.1 respectively in 1:1 water/acetonitrile), demonstrated effectively quantitative conversion to the corresponding tetravalent species (Figure 4-8). Hemiboronic acid **4-05**, with a significantly higher pK_a (12.2), showed relatively low conversion by ^{11}B NMR. In contrast, hemiboronic acid **4-04** (pKa > 14) demonstrated only trace adduct formation under basic conditions. These results demonstrate that acidity and corresponding conversion to a tetravalent diol complex are not directly correlated with catalytic activity. Hemiboronic acids **4-02** and **4-06** afforded the corresponding tetravalent adducts **4-17** and **4-25** in comparable conversion, but benzoxazaborine (**4-02**) showed a sevenfold increase in catalytic activity relative to *N*-sulfonyl benzodiazaborine **4-06**.

Table 4-3 Catalytic activity, acidity, and conversion to a tetrahedral adduct for model hemiboronic acids.

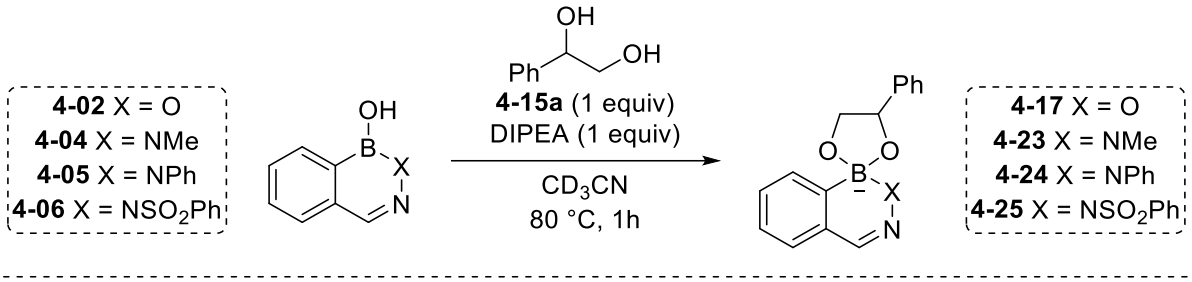

Hemiboronic acid	4-06	4-02	4-05	4-04
Catalytic yield[a]	13%	93%	24%	6%
pK_a (1:1 MeCN/H_2O)	5.5	7.1	12.2	>14
Conversion to tetravalent diol complex[b]	99%	98%	13%	trace

[a]See Table 4-2. [b]Determined by ^{11}B NMR.

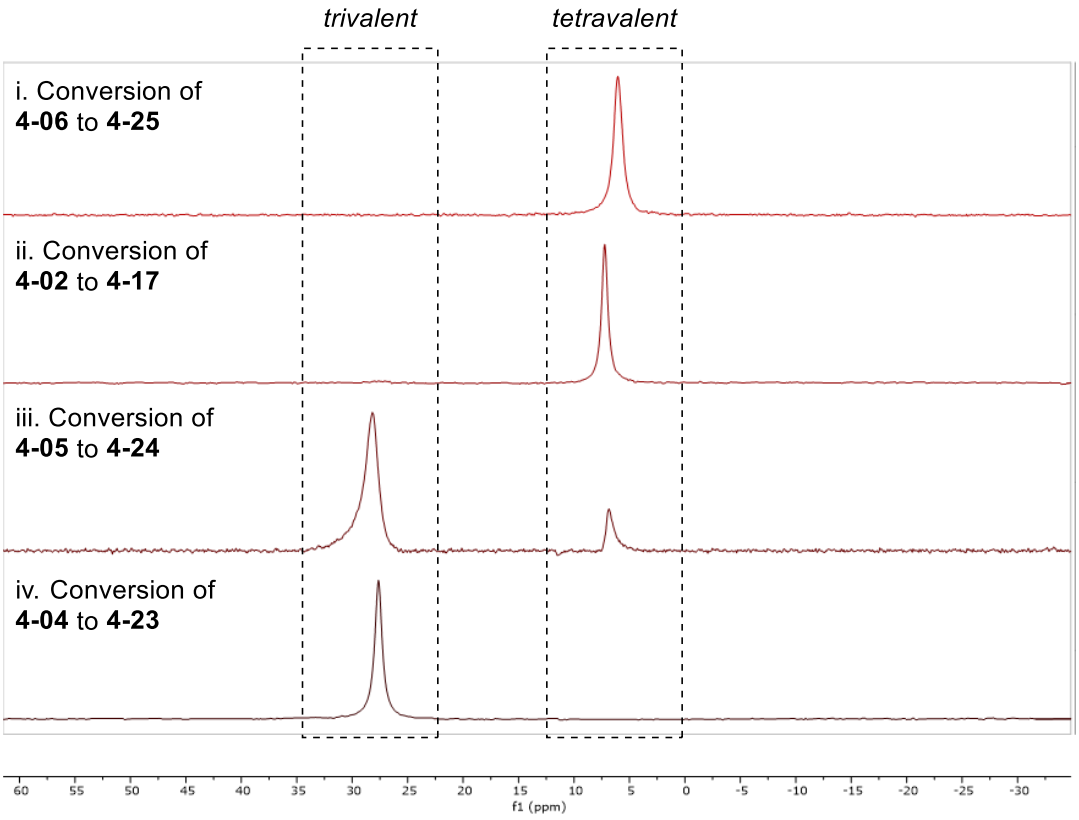

Figure 4-8 ^{11}B NMR (128 MHz, CD_3CN) monitoring of the conversion of cyclic hemiboronic acids to tetravalent diol adducts.

The reaction of diethyl chlorophosphate with *in situ*-generated tetravalent adduct **4-25**, derived from strongly acidic hemiboronic acid **4-06**, was subsequently examined. Reaction of adduct **4-17**, derived from optimal catalyst **4-02**, was previously demonstrated to undergo rapid quenching (<10 minutes) upon addition of the electrophile (*cf.* Scheme 4-3). In contrast, trapping of tetravalent adduct **4-25** proceeded significantly more slowly, requiring greater than 6 hours to reach full conversion as monitored by ^{11}B NMR (Figure 4-9). Given the increased acidity of parent hemiboronic acid **4-06** relative to the optimal catalyst **4-02**, this result suggests that hemiboronic acid acidity is inversely correlated to the nucleophilicity of the corresponding tetravalent adduct.

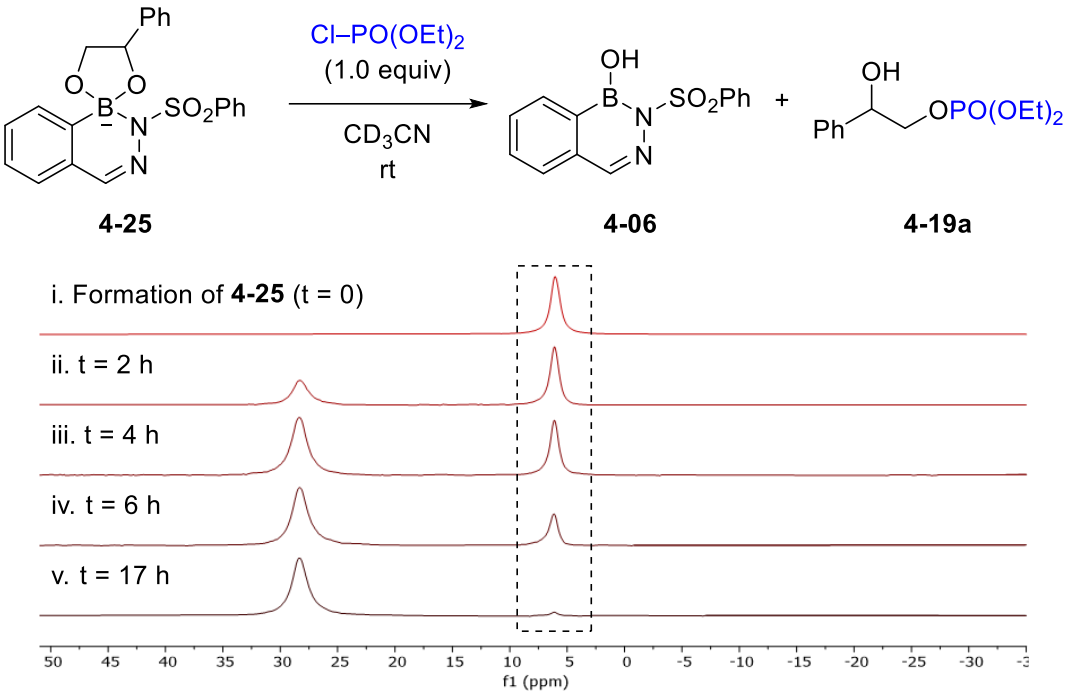

Figure 4-9 ^{11}B NMR (128 MHz, CD_3CN) monitoring of electrophile trapping of tetravalent adduct **4-25**.

The poor catalytic activity of benzodiazaborines **4-04** and **4-05** appears to arise from an inability to form appreciable amounts of the key tetravalent boronate adduct due to insufficient Lewis acidity. In contrast, strongly acidic hemiboronic acid **4-06** is a poor catalyst for

monophosphorylation due to the diminished nucleophilicity of the corresponding tetravalent adduct **4-25**, despite the highly favorable equilibrium for adduct formation. Thus, the unique effectiveness of hemiboronic acid **4-02** as a catalyst likely originates from a balance of being adequately Lewis acidic to promote rapid tetravalent boronate adduct formation, while maintaining sufficient adduct nucleophilicity for rapid reaction with the electrophile.

4.4 Results and Discussion – Electrophilic Activation

4.4.1 Introduction to Reductive Deoxygenation Reactions

Defunctionalization represents a powerful strategy in chemical synthesis for facilitating the transient introduction of reactivity-enabling functional groups that can be selectively removed under mild conditions.[48] Late-stage defunctionalization of bioactive molecules can be used to synthesize novel analogues,[49] while the reduction of lignin or other biomass-derived feedstocks is an increasingly important endeavor to efficiently utilize renewable carbon sources.[50] Deoxygenation reactions afford access to saturated compounds while leveraging the abundance of transformations for the synthesis and functionalization of alcohols and ketones, offering indispensable approaches for converting these readily accessible oxygenated building blocks into less densely functionalized species.

Historical methods for the deoxygenation of alcohols and ketones have often involved the stoichiometric generation of activated intermediates. The Barton-McCombie reaction is widely used in the deoxygenation of alcohols after conversion to the corresponding xanthate (Scheme 4-6a).[51,52] This process typically requires stoichiometric amounts of toxic tin reagents, although alternative methods have been developed which are catalytic in the organotin component.[53] Ketone deoxygenation can be accomplished by means of the Wolff-Kishner reduction via an intermediate hydrazone, often requiring high temperatures and strongly basic conditions (Scheme 4-6b).[54] For

base-sensitive substrates, ketone deoxygenation can also be afforded using zinc-mercury amalgam under strongly acidic conditions in the Clemmensen reduction.[55] Catalytic deoxygenation of activated C–O bonds can be accomplished by transition metal-catalyzed hydrogenolysis, for which a variety of metals have demonstrated high activity (Scheme 4-6c).[56] However, functional group compatibility issues can limit the application of metal-catalyzed hydrogenolysis in synthesis.[57] Electrochemical deoxygenation methods have also been developed based on pioneering work by Shono and co-workers,[58] while formal alcohol deoxygenation has also been reported through two-step sequences of dehydration followed by hydrogenation of the resulting olefin.[59]

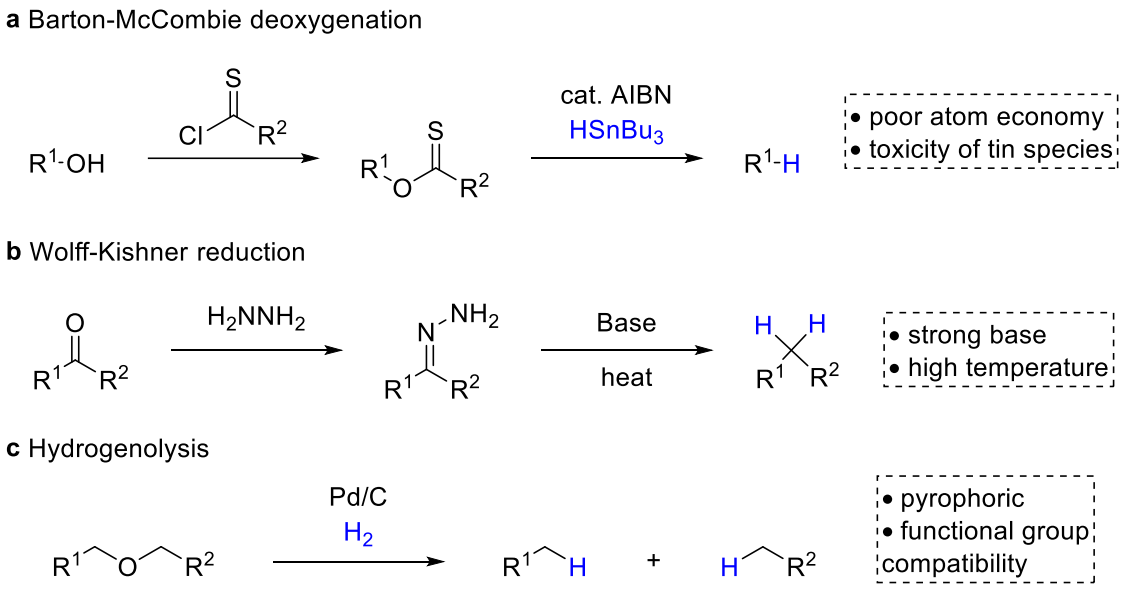

Scheme 4-6 Classical methods for reductive deoxygenation.

In an effort to improve the functional group tolerance and atom economy of reductive deoxygenation reactions, the development of catalytic strategies using silanes as hydride donors has been of significant interest. These strategies avoid the use of hazardous metal reagents or the generation of pyrophoric metal hydrides and aim to promote reductive deoxygenation without stoichiometric pre-activation. The Si–H bond is polarized such that the hydrogen is weakly

hydridic due to the increased electronegativity of hydrogen (2.20) relative to silicon (1.90).[60] Accordingly, organosilane reductants tend to be less reactive than conventional metal hydrides, which can offer improved chemoselectivity in the reduction of complex substrates. The use of organosilane reductants also offers the ability to tune the steric and electronic properties of the reducing agent by modification of the nonreactive groups bound to silicon.[60]

While a number of metal salts have been utilized as catalysts in reductive deoxygenation with silanes,[61] boron-based Lewis acids have emerged as particularly appealing catalysts due to their well-defined structure-acidity relationships and ultimately benign environmental impact upon degradation to boric acid.[62] The silane-mediated deoxygenation of C–O bonds using a boron Lewis acid was first reported by Fry and co-workers in 1976, who demonstrated the deoxygenation of alcohol **4-26** to alkane **4-28** using a silane reductant in the presence of BF_3 (Scheme 4-7).[63] Isomeric product **4-29** was also detected, likely arising from rearrangement of a carbocation intermediate.

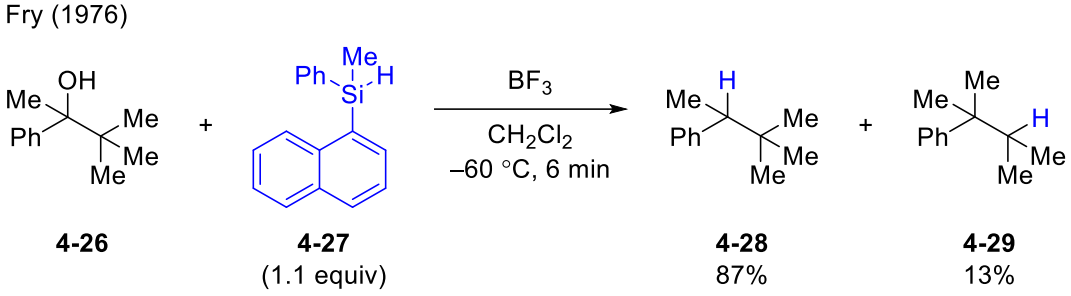

Scheme 4-7 First reported boron-mediated reductive deoxygenation using an organosilane reductant.

In recent decades, trispentafluorophenylborane ($B(C_6F_5)_3$) has proven to be an active catalyst for a variety of reductive deoxygenation reactions.[62] A pioneering report by Piers and co-workers in 1996 established that this highly acidic borane is an effective catalyst for the hydrosilylation of aromatic esters, ketones and aldehydes (Scheme 4-8a).[64] Kinetic studies led the

authors to propose a mechanism in which the Lewis acid catalyst polarizes the Si–H bond, rather than directly activating the carbonyl. This catalyst system was subsequently applied to the deoxygenation of alcohols and ethers by Gevorgyan, Yamamoto and co-workers in 1999 (Scheme 4-8b).[65] Interestingly, deoxygenation of primary alcohols was found to proceed more rapidly than secondary or tertiary alcohols, in stark contrast to the predicted trend based on carbocation stability. Subsequent mechanistic investigations on the deoxygenation of ethers led to two proposed mechanisms.[66] Activated secondary or tertiary substrates were believed to undergo C–O activation directly to form intermediate carbenium borate ion pair **A**, followed by hydride ion abstraction from the silane. Conversely, deoxygenation of primary alcohols or ethers was proposed to proceed through oxonium borohydride ion pair **B** after Lewis acid-promoted Si–H bond activation, followed by borohydride reduction.[66]

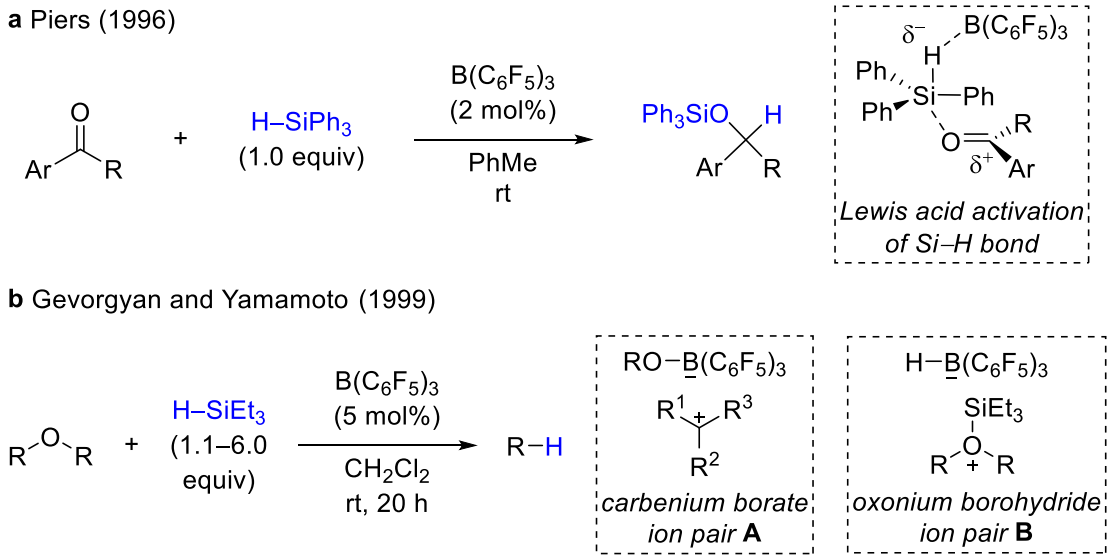

Scheme 4-8 Early reports on the $B(C_6F_5)_3$-catalyzed hydrosilylation and reductive deoxygenation.

Since these initial reports, $B(C_6F_5)_3$ has revealed remarkable catalytic activity in the deoxygenation of a variety of carbon-oxygen moieties, including alcohols, ethers, aldehydes, ketones, esters, carboxylic acids, acid chlorides and amides.[67–71] In addition to applications of the

parent perfluorotriarylborane as a Lewis acid, the water adduct $B(C_6F_5)_3 \cdot H_2O$ is a strong Brønsted acid of comparable strength to HCl.[72] Additionally, other fluorinated arylborane catalysts have been reported as well with varying air- and moisture-sensitivity.[73] The development of new boron catalysts for reductive deoxygenation under ambient conditions is highly desirable to afford practical reactivity under mild conditions.[74]

4.4.2 Synthesis of an Increasingly Acidic Benzoxazaborine Heterocycle

As discussed in Section 4.3.4, an effective boronic acid catalyst for nucleophilic diol activation requires a balancing of rapid substrate binding, thermodynamically driven adduct formation, and nucleophilicity of the tetravalent adduct. Consequently, a moderate pK_a is generally desired for catalysts in nucleophilic activation. In contrast, boronic acid-catalyzed electrophilic activation of alcohols involves partial or complete ionization of the C–O bond to form a carbocation intermediate, with a lifetime that is inversely related to the nucleophilicity of the resulting hydroxyboronate anion.[10] Many different mechanisms of activation have been proposed in these processes including direct Lewis acidity, Lewis acid-assisted Brønsted acidity, or hydrogen bonding activation.[15] Across these mechanistic manifolds, the activity of boronic acid catalysts in electrophilic activation is often correlated to their acidity, where more acidic catalysts (lower pK_a) lead to the formation of a more stable hydroxyboronate anion upon C–O activation.[16]

Several strategies have been demonstrated to increase the acidity of arylboronic acids. The introduction of fluorine substituents can have a dramatic impact on boronic acid acidity, where the effect is dependent on the regiochemistry of fluorine incorporation (Figure 4-10a).[17,75,76] Fluorine substituents in the *para*-position cause the smallest increase in acidity due to a combination of resonance effects and the diminished inductive effect with increasing distance from the boron atom, while *ortho*-substitution can impact acidity through the formation of intramolecular BOH–

F hydrogen bonds.[75] However, heavily fluorinated aryl boronic acid derivatives are highly susceptible to protodeboronation in acidic media, particularly those with *ortho*-fluorine substituents which stabilize negative charge build-up on the *ipso* carbon upon C–B heterolysis.[77] The formation of intramolecular hydrogen bonds in *ortho*-substituted arylboronic acids can have a significant impact on acidity, particularly in "Wulff-type" boronic acids containing an *ortho*-(aminoalkyl)-substituent.[44]

An alternative strategy to increase catalytic activity in electrophilic alcohol activation is the use of cationic boronic acid catalysts (Figure 4-10b). Upon C–O bond cleavage, the resulting tetravalent hydroxyboronate species is formally zwitterionic, affording a reactive carbocation and slowing the rate of C–O bond recombination relative to the carbocation/hydroxyboronate anion ion pair that is formed upon ionization with a neutral catalyst. This strategy has been demonstrated previously by the Hall Group in Friedel-Crafts benzylation with deactivated alcohols, where ferrocenium boronic acid hexafluoroantimonate salt was an exceptionally active catalyst relative to the neutral ferrocene analog.[10]

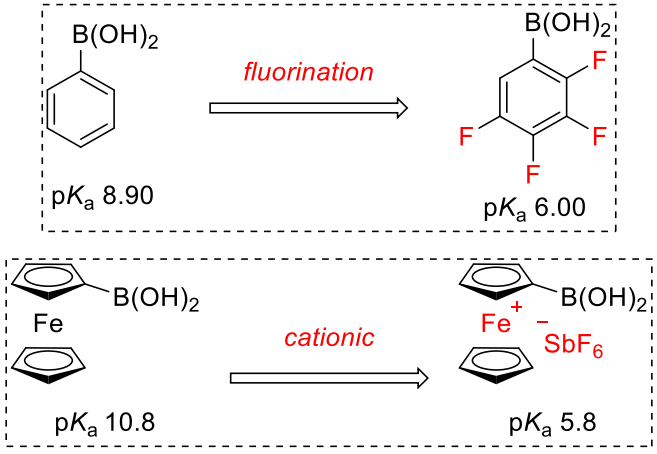

Figure 4-10 Strategies to decrease the pK_a of boronic acids.

Accordingly, it was reasoned that a cationic benzoxazaborine derivative may provide sufficient acidity for high catalytic activity in electrophilic alcohol activation. In a procedure adapted from the synthesis of hemiboronic acid **4-02**, condensation of 2-formylphenylboronic acid with *N*-methylhydroxylamine hydrochloride in dichloromethane readily afforded benzoxazaborinium chloride salt **4-30** (Scheme 4-9).[78] Heterocycle **4-30** was readily purified by precipitation on gram scale and was stable to storage under ambient conditions for prolonged periods with no evidence for decomposition.

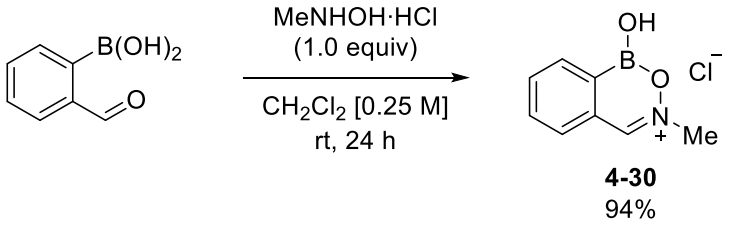

Scheme 4-9 Synthesis of cationic benzoxazaborine derivative **4-30**.

The pK_a of heterocycle **4-30** was assessed using an ^{11}B NMR titration as described in Chapter 3. Compound **4-30** was poorly soluble in organic solvents such as acetone, chloroform, or acetonitrile, so the titration was performed in D_2O. The ^{11}B NMR chemical shift in D_2O was found to be essentially pH-independent and was observed between 4.1–4.6 ppm across a pH range of 0.8–13.0 (Figure 4-11). These chemical shifts are consistent with a tetravalent boron species, suggesting that the pK_a of compound **4-30** in water is less than 1 and cannot be accurately measured using this technique. This value represents a minimum thirty thousandfold increase in acidity relative to the parent neutral heterocycle **4-02** (pK_a 5.5).[31]

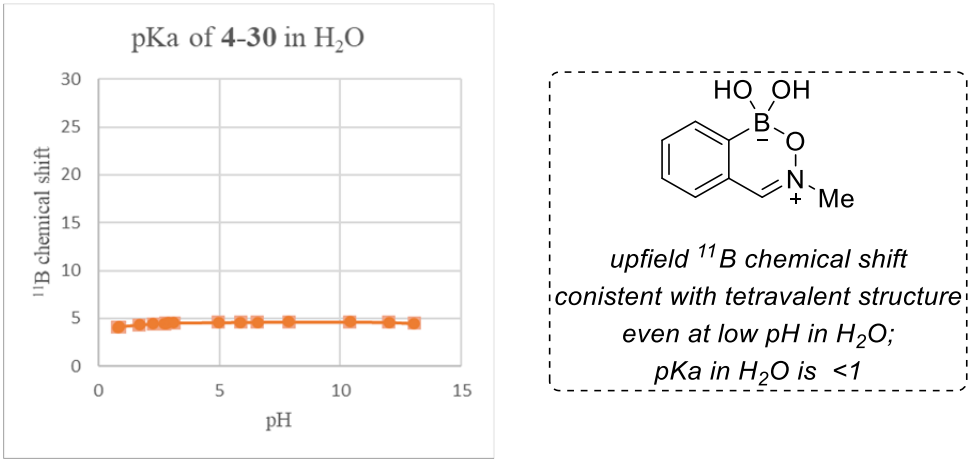

Figure 4-11 ^{11}B NMR titration of heterocycle **4-30** in aqueous solution.

To demonstrate the ability of heterocycle **4-30** to promote catalytic electrophilic activation of alcohols, the reductive deoxygenation reaction of carbon-oxygen bonds was examined. Encouraged by the low pK_a of compound **4-30**, it was hypothesized that C–O bond activation of a π-activated alcohol could occur upon reaction with catalyst **4-30**. Trapping of the resulting carbocation by silane would lead to the desired deoxygenation product, while Si–O bond formation could regenerate the catalyst (Scheme 4-10).

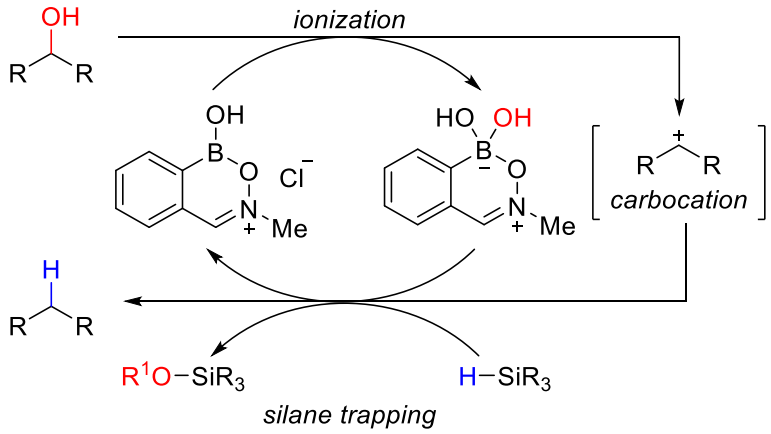

Scheme 4-10 Proposal for reductive deoxygenation catalyzed by heterocycle **4-30**.

4.4.3 Reductive Deoxygenation of Alcohols – Optimization

The reductive deoxygenation of diphenylmethanol (**4-31a**) to afford diphenylmethane (**4-32a**) using triethylsilane as a reducing agent was examined as an initial model reaction (Table 4-4). A mixture of 1,1,1,3,3,3-hexafluoroisopropanol (HFIP) and nitromethane was employed as an initial solvent system based on related reports from the Hall Group on Friedel-Crafts benzylation.[10] HFIP is a widely used solvent in the reaction of carbocations due to its high dielectric constant, low nucleophilicity, and enhanced acidity and hydrogen bond donor ability in comparison to other alcohols.[79] Nitromethane can provide improved solubility to afford homogeneous reaction mixtures and has been reported to enhance reactivity in acid-catalyzed reactions by acting as a hydrogen bond acceptor.[80] Reduction product **4-32a** was obtained in high yield using hemiboronic acid **4-30** as a catalyst when this mixture of HFIP and nitromethane was employed (Entry 1). Full conversion was observed with only 1 mol% catalyst in 1.5 hours (Entry 4). A reduction in yield was observed upon decreasing the proportion of HFIP (Entry 5), while solvent mixtures lacking HFIP were ineffective (Entries 6–10). The failure of other solvents likely stems from their inability to effectively promote C–O activation and stabilize the corresponding intermediate. The reaction proceeded effectively at concentrations up to 2.0 M, providing efficient solvent economy (Entries 11–13). Reduction product **4-32a** was not observed in the absence of catalyst **4-30**, demonstrating that the Brønsted acidic HFIP solvent alone does not catalyze the reaction (Entry 15). Optimized conditions were found using 1 mol% catalyst **4-30** in HFIP/nitromethane (4:1) at room temperature for 90 minutes at a concentration of 2.0 M.

Table 4-4 Optimization of alcohol reductive deoxygenation catalyzed by hemiboronic acid **4-30**.

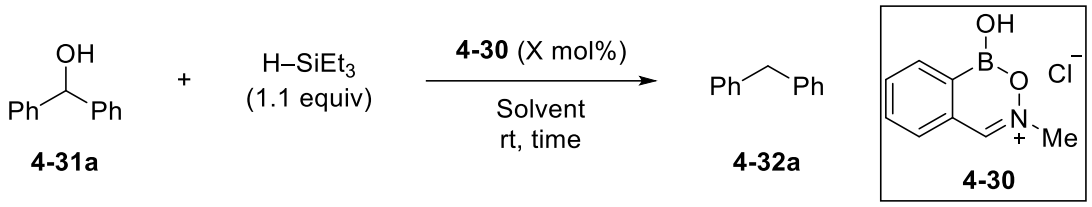

Entry	Catalyst (X mol%)	Solvent	Concentration	Time	Yield 4-32a[a]
1	10 mol%	HFIP/$MeNO_2$ 4:1	0.5 M	18 h	96%
2	5 mol%	HFIP/$MeNO_2$ 4:1	0.5 M	18 h	98%
3	1 mol%	HFIP/$MeNO_2$ 4:1	0.5 M	18 h	97%
4	1 mol%	HFIP/$MeNO_2$ 4:1	0.5 M	1.5 h	98%
5	1 mol%	HFIP/$MeNO_2$ 1:4	0.5 M	1.5 h	68%
6	1 mol%	$MeNO_2$	0.5 M	1.5 h	0%
7	1 mol%	MeCN	0.5 M	1.5 h	0%
8	1 mol%	CH_2Cl_2	0.5 M	1.5 h	0%
9	1 mol%	PhMe	0.5 M	1.5 M	0%
10	1 mol%	TFE/$MeNO_2$ 4:1	0.5 M	1.5 h	38%
11	1 mol%	HFIP/$MeNO_2$ 4:1	1.0 M	1.5 h	95%
12	1 mol%	HFIP/$MeNO_2$ 4:1	1.5 M	1.5 h	96%
13	1 mol%	HFIP/$MeNO_2$ 4:1	2.0 M	1.5 h	98%
14	1 mol%	HFIP	2.0 M	1.5 h	90%
15	-	HFIP/$MeNO_2$ 4:1	2.0 M	1.5 h	0%

[a]Yield determined by ^1H NMR relative to 1,3,5-trimethoxybenzene as an internal standard.

4.4.4 Reductive Deoxygenation of Alcohols – Substrate Scope

A wide scope of diarylmethanol derivatives were successfully deoxygenated under the optimized conditions (Scheme 4-11). Synthesis of diphenylmethane (**4-32a**) could be performed on gram scale with no reduction in yield. A variety of halogenated aromatic rings were well tolerated (**4-32b**–**4-32g**) with no evidence for hydrodehalogenation, which may occur in transition metal-catalyzed hydrogenolysis reactions. Reduction of alcohol **4-31h**, containing both a primary and secondary benzylic alcohol, occurred chemoselectively at the secondary alcohol to afford diarylmethane **4-32h**. Tolyl derivatives **4-32i** and **4-32j** were successfully prepared, and a 2,6-

disubstituted alcohol gave the corresponding diarylmethane **4-32k** in good yield. Substrates containing Lewis basic heteroatoms, including *N,N*-dimethylamine and methoxy substituted alcohols, were successfully transformed into the corresponding diarylmethanes **4-32l** and **4-32m**, while no competing reduction of a benzoate ester was observed in the synthesis of **4-32n**. A heteroaryl thiophene moiety was well-tolerated to afford product **4-32o**, while deoxygenation of an allylic alcohol proceeded without competing reduction of the alkene to afford styrene derivative **4-32p**. Diarylethane **4-32q** was prepared in good yield from the corresponding tertiary benzylic alcohol, while the synthesis of triphenylmethane (**4-32r**) was conducted on multigram-scale with reduced catalyst loading. Compound **4-32s**, which has shown preliminary cytotoxic activity against the HCT-116 colon cancer cell line,[81] was successfully synthesized via reduction of the corresponding tertiary alcohol. Furthermore, cardiovascular drug cloridarol[82] was smoothly deoxygenated to afford heteroaryl substrate **4-32t**.

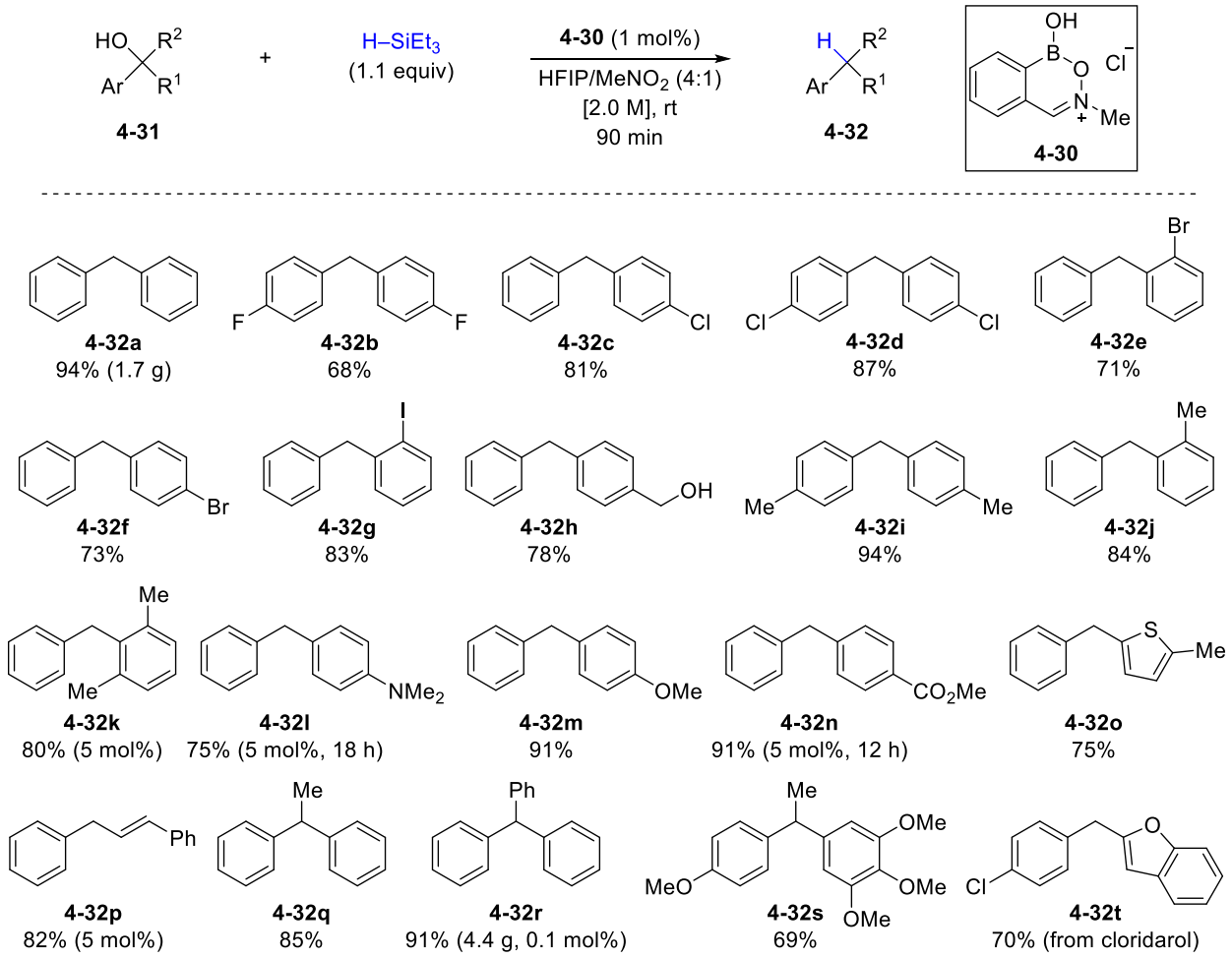

Scheme 4-11 Substrate scope of alcohol reductive deoxygenation catalyzed by heterocycle **4-30**.

Secondary alcohols containing only a single activating arene substituent could also be successfully deoxygenated using increased catalyst loading (5 mol%) and reaction time (3 hours), consistent with an increased barrier for C–O activation with decreasing substitution on the proposed carbocation intermediate. Biphenyl derivatives **4-32u** and **4-32v** were prepared in good yield, while ortho-substituted **4-32w** was formed in reduced yield, suggesting that a bulky *ortho*-biphenyl substituent may slow the reaction (Scheme 4-12). Synthesis of compound **4-32x** was achieved without reduction of the isolated terminal alkene, while an α-cyclopropyl substituent was well tolerated to afford benzylated cyclopropane **4-32y** with no evidence for ring opening.

Secondary alcohol **4-31z**, prepared through reduction of the corresponding acetophenone with $NaBD_4$, was successfully deoxygenated to provide mono-deuterated product **4-32z**.

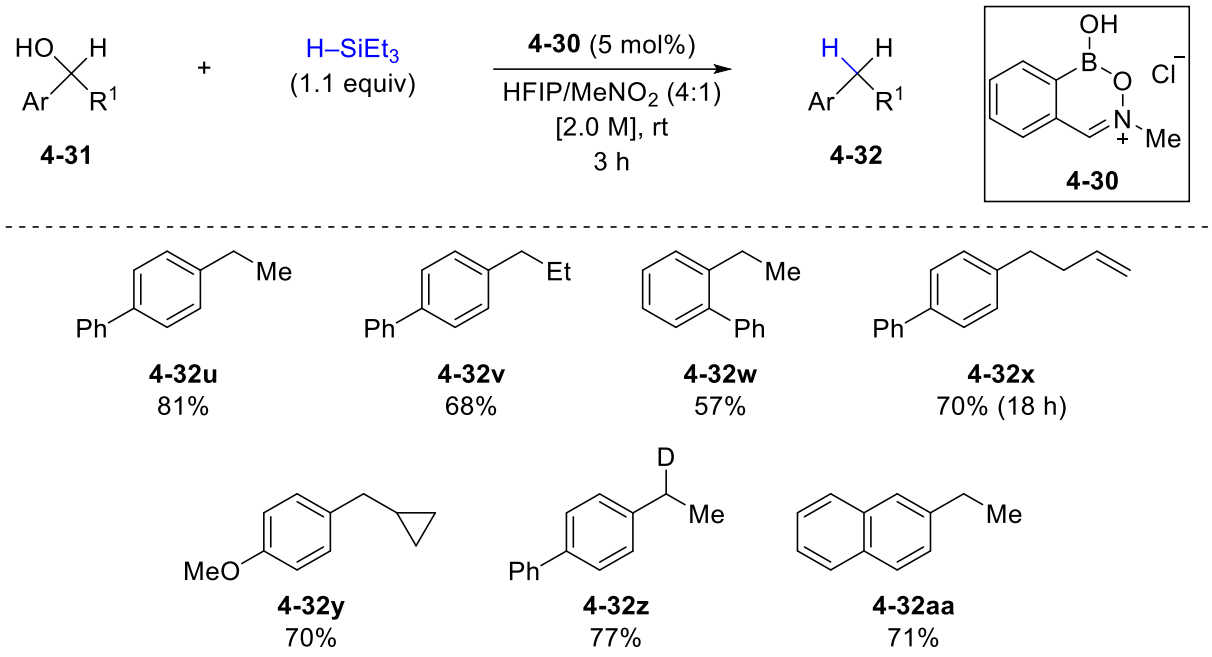

Scheme 4-12 Continued substrate scope of alcohol reductive deoxygenation catalyzed by **4-30**.

While investigating the substrate scope of the deoxygenation reaction, several unsuccessful substrates were identified (Figure 4-12). Highly electron-deficient alcohols were poor substrates, presumably due to the decreased stability of the putative carbocation intermediate and corresponding increase in the barrier for C–O bond activation. Propargylic or allylic substrates containing a terminal unsaturation appeared to decompose under the reaction conditions, leading to a rapid color change and intractable by-products. Heteroaryl substrates containing furan, pyridine or *N*-methyl pyrrole groups were unsuccessful. When a highly activated diol substrate was subjected to alcohol deoxygenation conditions, the pinacol rearrangement product was observed in good yield.

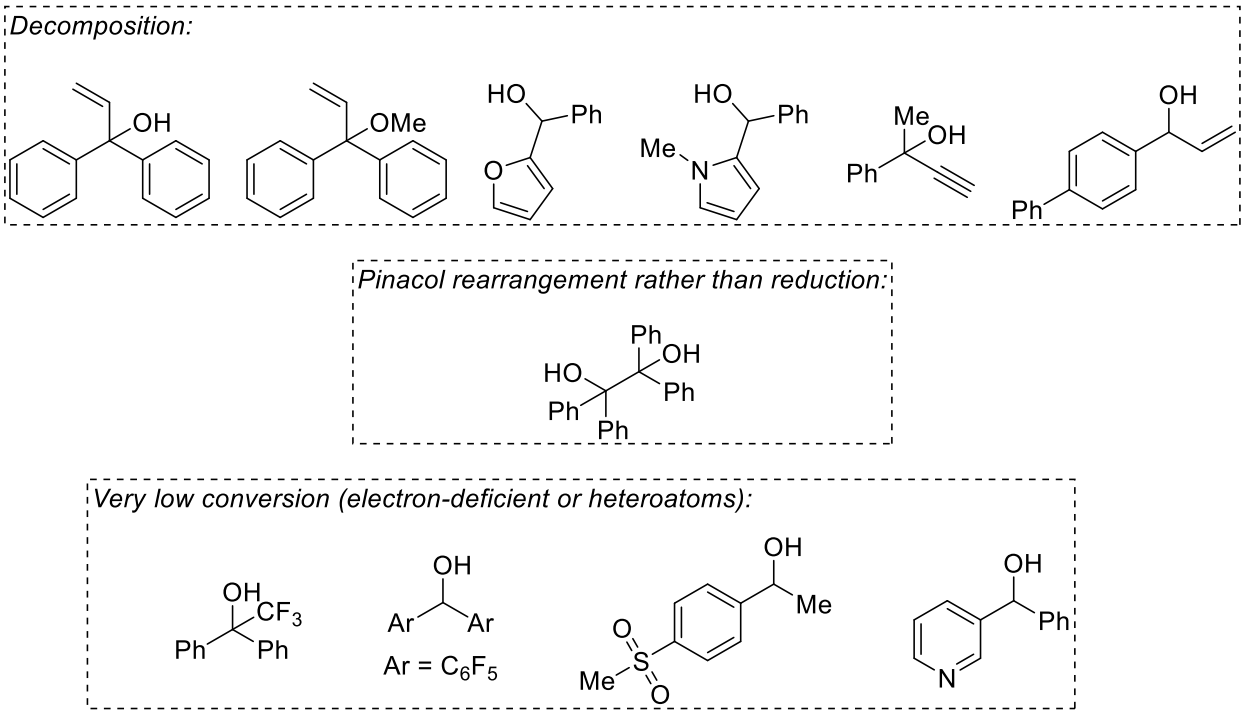

Figure 4-12 Unsuccessful reductive deoxygenation substrates.

The synthesis of diphenylmethane (**4-32a**) was examined using other C–O containing precursors to further examine the scope of the reaction with respect to the oxygenated partner (Scheme 4-13). Benzylic acetate **4-33** successfully afforded reduction product **4-32a** in comparable yield to the reaction of alcohol **4-31a**. Symmetrical ether **4-34** was also a viable deoxygenation substrate, but lower yield was obtained relative to the alcohol and acetate substrates. This observation is fully consistent with the results described in Chapter 2 on Friedel-Crafts chemistry, where symmetrical ethers were found to undergo C–O activation at a rate slower than that of the free alcohols.[83]

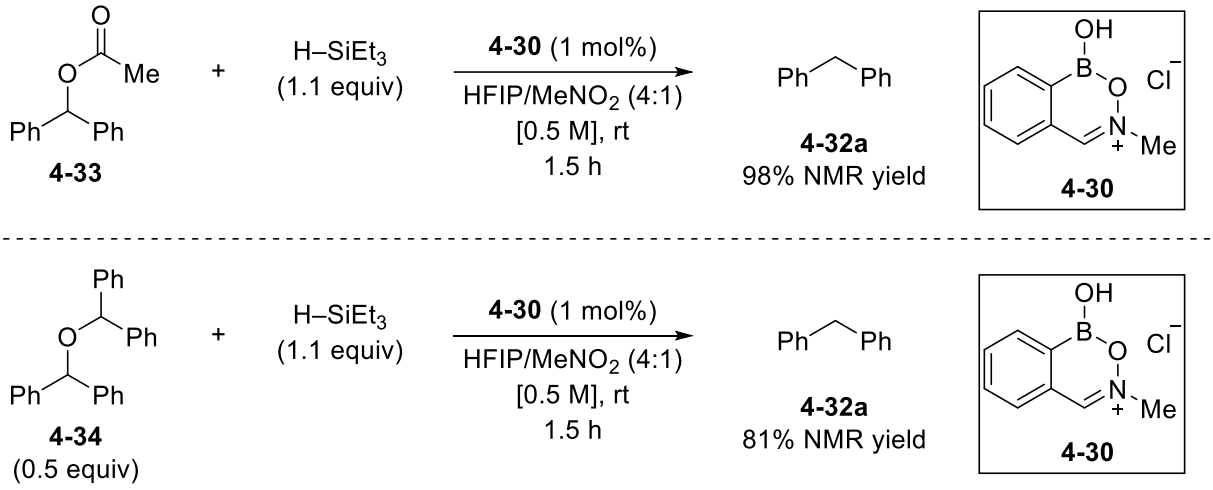

Scheme 4-13 Comparison of acetate and ether substrates in reductive deoxygenation catalyzed by **4-30**.

To assess the mildness of the deoxygenation conditions using catalyst **4-30**, the reduction of alcohol **4-31h** (containing both a secondary and primary benzylic alcohol) was also examined using a $pTsOH \cdot H_2O$ as a conventional Brønsted acid catalyst. Additionally, gallium(III) trifluoromethanesulfonate was examined as a catalyst using conditions reported previously for ketone deoxygenation by Olah and co-workers.[84] Deoxygenation using catalyst **4-30** gave a significantly cleaner crude reaction mixture for the reaction of alcohol **4-31h** than other catalysts, which appeared to form undesired ethers or other side-products based on analysis of the crude ^1H NMR (Figure 4-13). Thus, the catalyst system using hemiboronic acid **4-30** may offer milder conditions or improved chemoselectivity relative to existing deoxygenation methods.

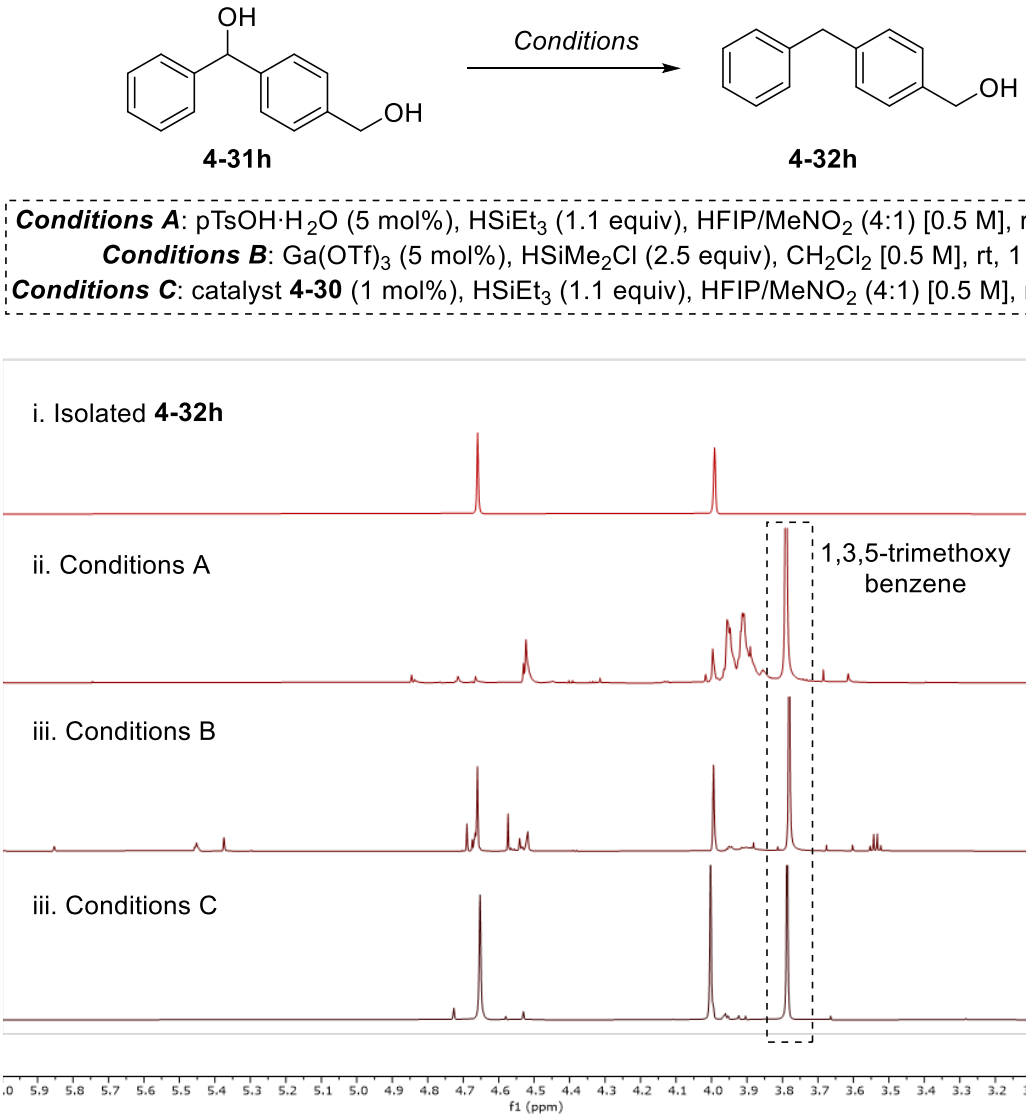

Figure 4-13 Comparison of reductive deoxygenation conditions for alcohol **4-31h** based on crude ^{1}H NMR (600 MHz, $CDCl_3$).

In a preliminary effort to extend the deoxygenation protocol beyond π-activated alcohols, it was found that conversion of 1-adamantanol (**4-35**) to adamantane (**4-36**) proceeded smoothly at room temperature catalyzed by hemiboronic acid **4-30** (Scheme 4-14). A putative carbocation intermediate formed from C–O bond activation of alcohol **4-35** is unlikely to undergo elimination to form the severely distorted anti-Bredt olefin adamantene, which may inhibit a possible side reaction with this tertiary aliphatic alcohol substrate.[85]

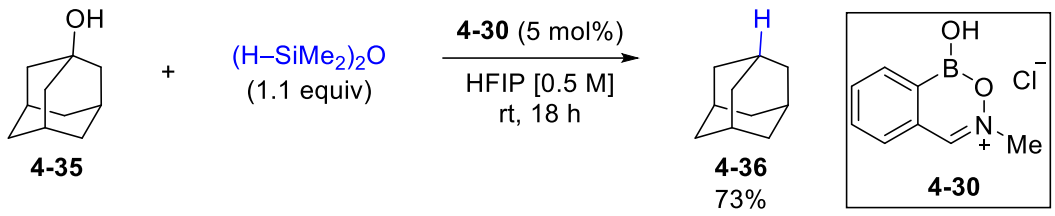

Scheme 4-14 Reductive deoxygenation of 1-adamantanol catalyzed by hemiboronic acid **4-30**.

4.4.5 Reductive Deoxygenation of Ketones – Optimization

To expand the synthetic utility of deoxygenation reactions catalyzed by hemiboronic acid **4-30**, the use of this catalyst in the reductive deoxygenation of aromatic ketones was subsequently examined (Table 4-5). Using the previously employed solvent system of HFIP/$MeNO_2$ (4:1) at room temperature, triethylsilane was found to be only moderate effective in the deoxygenation of ketone **4-37a** (Entry 1), although increased yield was observed using a large excess of the reducing agent at elevated temperature (Entries 2–4). When other silanes were examined, phenyldimethylsilane was found to show significantly greater activity (Entries 5–8). Attempts to lower the equivalents of silane while increasing the reaction time led to lower yield of reduction product **4-32a** (Entries 9–12). Subsequently, 1,1,3,3-tetramethyldisiloxane (TMDSO)[60] was identified as a highly active silane for this reaction, allowing for a decrease in catalyst loading to 5 mol% and improved chromatographic purification from silicon-containing by-products (Entry 13). The reaction was found to proceed effectively without the addition of nitromethane as a co-solvent using 2.2 equivalents of TMDSO (Entry 14). Decreasing the amount of silane led to a noticeable decrease in yield (Entries 15–16). Thus, optimized conditions were found employing 5 mol% catalyst **4-30**, 2.2 equivalents TMDSO in HFIP at room temperature for 24 hours. Ketone deoxygenation proceeds under ambient conditions with no exclusion of air or moisture.

Table 4-5 Optimization of ketone reductive deoxygenation catalyzed by hemiboronic acid **4-30**.

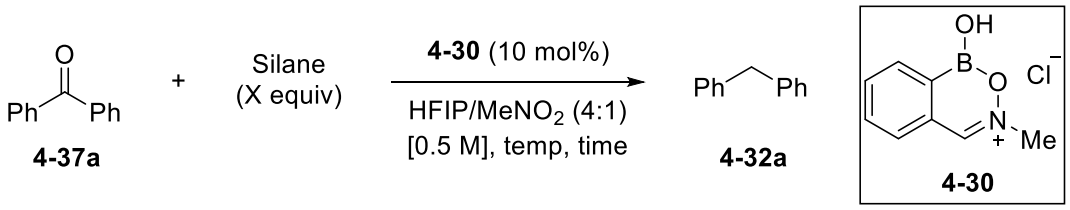

Entry	Silane (equiv)	Time	Temp	Yield 4-32a[c]
1	$HSiEt_3$ (3.0 equiv)	18 h	rt	54%
2	$HSiEt_3$ (5.0 equiv)	18 h	80 °C	84%
3	$HSiEt_3$ (5.0 equiv)	18 h	rt	43%
4	$HSiEt_3$ (5.0 equiv)	6 h	rt	20%
5	PMHS (5.0 equiv)	6 h	rt	3%
6	$HSi(OEt)_3$ (5.0 equiv)	6 h	rt	11%
7	$PhSiH_3$ (5.0 equiv)	6 h	rt	7%
8	$HSiMe_2Ph$ (3.0 equiv)	6 h	rt	88%
9	$HSiMe_2Ph$ (5.0 equiv)	18 h	rt	94%
10	$HSiMe_2Ph$ (3.0 equiv)	18 h	rt	90%
11	$HSiMe_2Ph$ (2.0 equiv)	18 h	rt	70%
12	$HSiMe_2Ph$ (2.0 equiv)	48 h	rt	83%
13	$(HSiMe_2)_2O$ (2.2 equiv)	24 h	rt	95%[a]
14	$(HSiMe_2)_2O$ (2.2 equiv)	24 h	rt	97%[a,b]
15	$(HSiMe_2)_2O$ (1.1 equiv)	24 h	rt	56%[a,b]
16	$(HSiMe_2)_2O$ (2.0 equiv)	24 h	rt	84%[a,b]

[a]5 mol% catalyst. [b]HFIP used as solvent without $MeNO_2$. [c]Yields determined by ^1H NMR relative to 1,3,5-trimethoxybenzene as an internal standard.

4.4.6 Reductive Deoxygenation of Ketones – Substrate Scope

Ketone deoxygenation catalyzed by hemiboronic acid **4-30** demonstrated similar functional group tolerance to the analogous alcohol deoxygenation protocol (Scheme 4-15). A variety of benzophenone and acetophenone derivatives were deoxygenated in comparable yields to the corresponding alcohols (**4-37a, b, e**, **u** and **aa**). Benzophenone derivatives containing allyloxy (**4-**

37ab) or benzyloxy (**4-37ac**) substituents were smoothly deoxygenated without competing alkene hydrogenation, debenzylation or sp^2 C–O bond cleavage. Aryl acetate derivative **4-32ad** was formed through selective benzophenone deoxygenation without competing ester reduction or hydrolysis, while a pendant aliphatic ester was also well tolerated to afford γ-arylated product **4-32ae** in good yield. Reduction of 4-chromanone to cyclic ether **4-32af** proceeded in reduced yield relative to acyclic compounds. This could arise from either decreased carbocation stabilization due to restricted rotation of the sp^2-C–O bond, or an increased energy barrier for rehybridization of the benzylic carbon from sp^3 to sp^2 upon C–O activation if the cyclic structure restricts the corresponding increase in bond angles. Deoxygenation of dibenzosuberenone proceeded on gram-scale with excellent yield to afford tricyclic **4-32ag** with reduced catalyst loading. Two benzophenone-containing bioactive compounds, fenofibrate and ketoprofen, underwent deoxygenation in good yields to afford the corresponding diarylmethanes **4-32ai** and **4-32aj**.

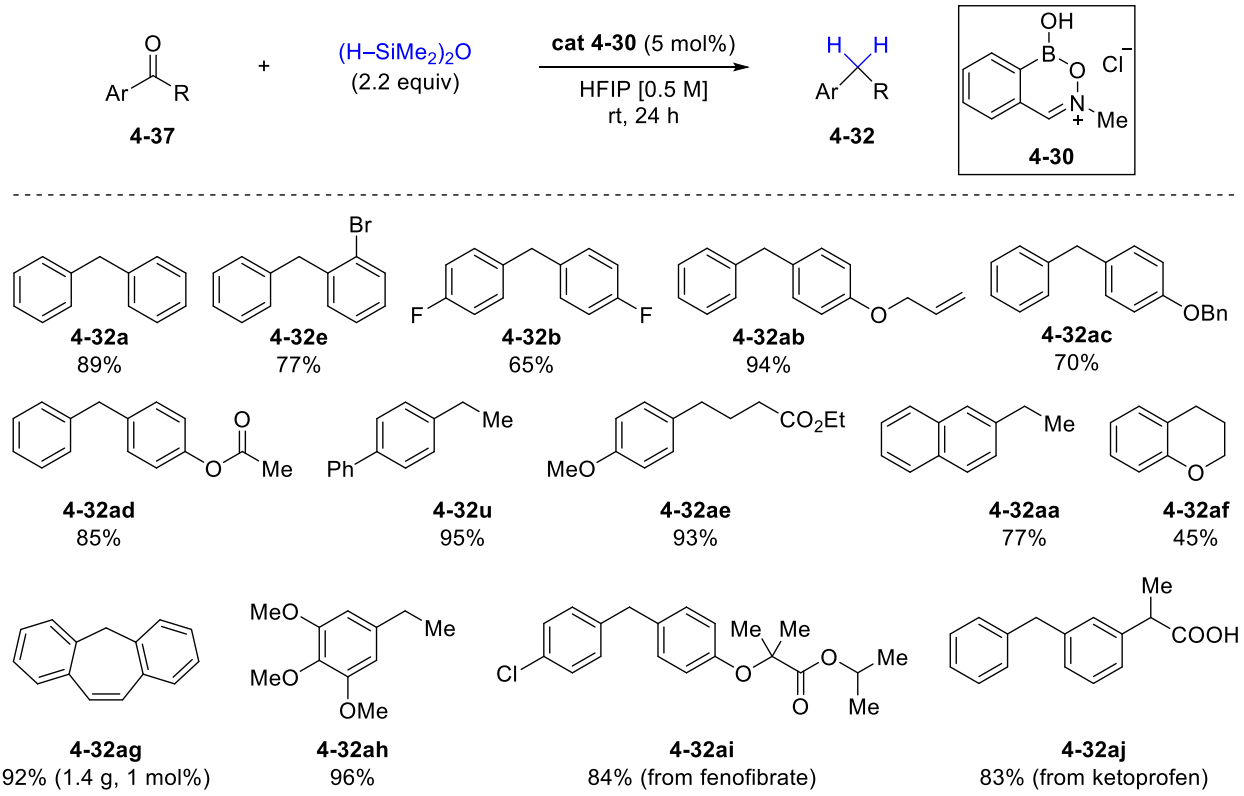

Scheme 4-15 Scope of ketone reductive deoxygenation catalyzed by hemiboronic acid **4-30**.

Reduction of electron-deficient acetophenone derivative **4-37ak** afforded alcohol **4-31ak** in excellent NMR yield with no evidence for the fully deoxygenated product **4-32ak** (Scheme 4-16). This result is consistent with destabilization of a putative carbocation intermediate due to the electron-deficient aromatic ring, and correspondingly an increased barrier for C–O activation.

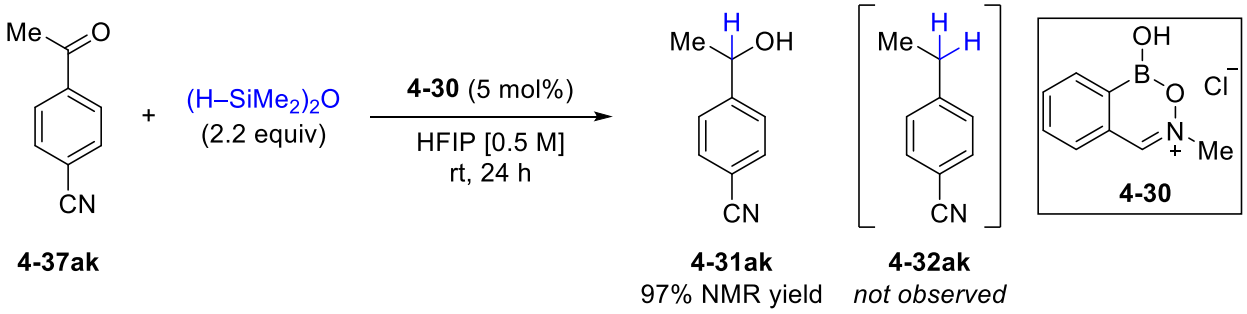

Scheme 4-16 Incomplete reduction of ketone **4-37ak** under deoxygenation conditions.

In a two-step sequence of HFIP-mediated acylation[86] followed by ketone deoxygenation with hemiboronic acid catalyst **4-30**, 1,3,5-trimethoxybenzene (**4-38**) was converted to arene **4-39** in excellent yield through a formal Friedel-Crafts primary alkylation (Scheme 4-17). Previously reported syntheses of **4-39** from **4-38** include the use of a triruthenium cluster-catalyzed hydrosilylation using esters as alkyl sources under strictly inert conditions,[87] or a multi-step sequence – in which the lithiated arene is reacted with ethylene oxide, followed by Appel bromination and Mg-mediated reduction – that requires three reactions heated to reflux under anhydrous conditions and three chromatographic purifications.[88] Conversely, the two-step sequence described here occurs under ambient conditions at room temperature and requires only a single purification.

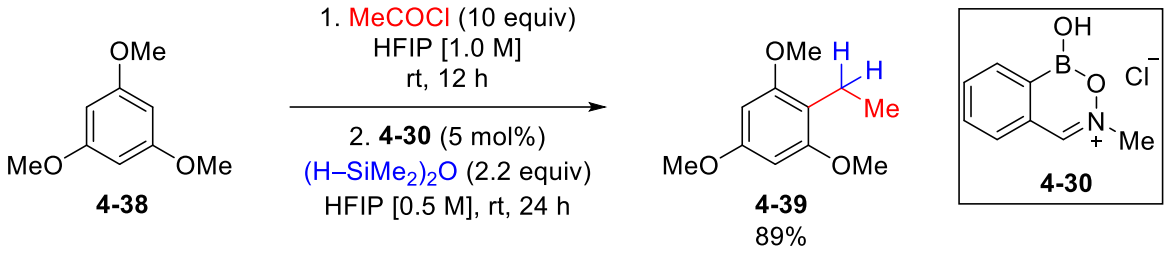

Scheme 4-17 Two-step formal Friedel-Crafts alkylation of 1,3,5-trimethoxybenzene.

4.4.7 Mechanistic Studies of Reductive Deoxygenation

By analogy to previous reports on the reduction of carbonyl derivatives using organoboron catalysts,[64] it was hypothesized that ketone deoxygenation of benzophenone (**4-37a**) catalyzed by hemiboronic acid **4-30** may proceed through an initial hydrosilylation to generate the corresponding secondary silyl ether **4-40**, or alcohol **4-31a** upon *in situ* desilylation. Subsequent C–O bond activation and trapping of the resulting carbocation by the hydridic Si–H bond would afford deoxygenation product **4-32a**. The conversion of ketone **4-37a** to reduction product **4-32a** was monitored by ^{1}H NMR analysis of a series of reaction aliquots (Figure 4-14). Clean conversion

to diphenylmethane (**4-32a**) was observed with no evidence for intermediates **4-40** or **4-31a**. While this result could suggest that an alternative mechanism is operative in which neither of these species are reaction intermediates, it cannot be ruled out that a rate-determining hydrosilylation is followed by rapid C–O bond activation such that the intermediates are not detected.

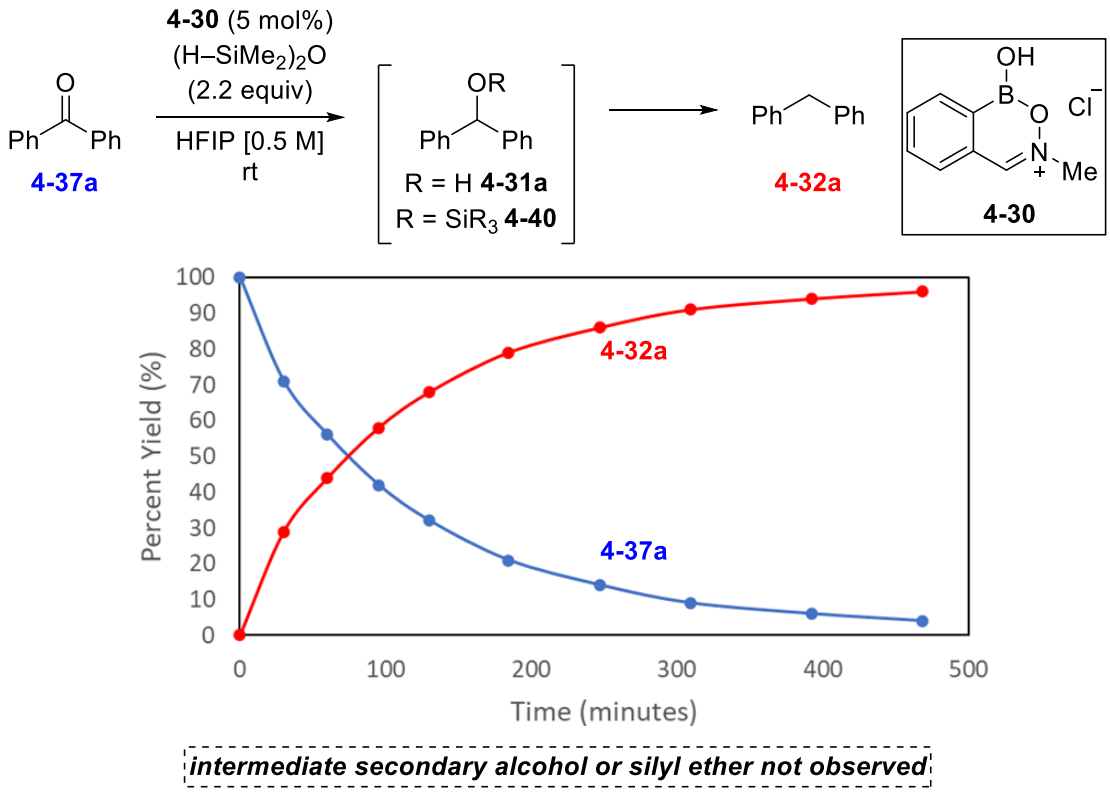

Figure 4-14 Reaction monitoring for the deoxygenation of benzophenone.

To further probe the possibility of a silyl ether intermediate, benzaldehyde derivative **4-41** was subjected to modified deoxygenation conditions using triethylsilane along with catalyst **4-30**. Triethylsilane was used in this experiment such that a putative silyl ether intermediate would contain a well defined triethylsiloxy group. Ketone reduction with TMDSO, which contains two Si–H bonds, could lead to a mixture of silyl ether species that would make unambiguous characterization difficult. It was hypothesized that deoxygenation of aldehyde **4-41** may not

proceed to the fully reduced product due to the increased barrier for C–O bond activation of the resulting primary alcohol relative to their more substituted secondary or tertiary analogs, facilitating detection of the intermediates. When aldehyde **4-41** was subjected to these modified deoxygenation conditions, both silyl ether **4-42** and free alcohol **4-20** were observed by crude ^{1}H NMR analysis (Scheme 4-18).

The stability of silyl ether **4-42** under the reaction conditions was examined with respect to *in situ* desilylation to afford alcohol **4-20**. When silyl ether **4-42** was incubated in HFIP alone, no evidence for desilylation was observed. However, reaction of silyl ether **4-42** with catalyst **4-30** in HFIP led to formation of alcohol **4-20** in excellent conversion. Furthermore, deoxygenation of ether **4-43**, which contains both a secondary and primary benzylic C–O bond, was found to occur with complete chemoselectivity for the secondary position. The liberated primary benzyl group was observed as a mixture of silyl ether **4-42** and free alcohol **4-20** by crude ^{1}H NMR. Taken together, these results are consistent with the formation of silyl ether intermediates in deoxygenation reactions catalyzed by heterocycle **4-30**.

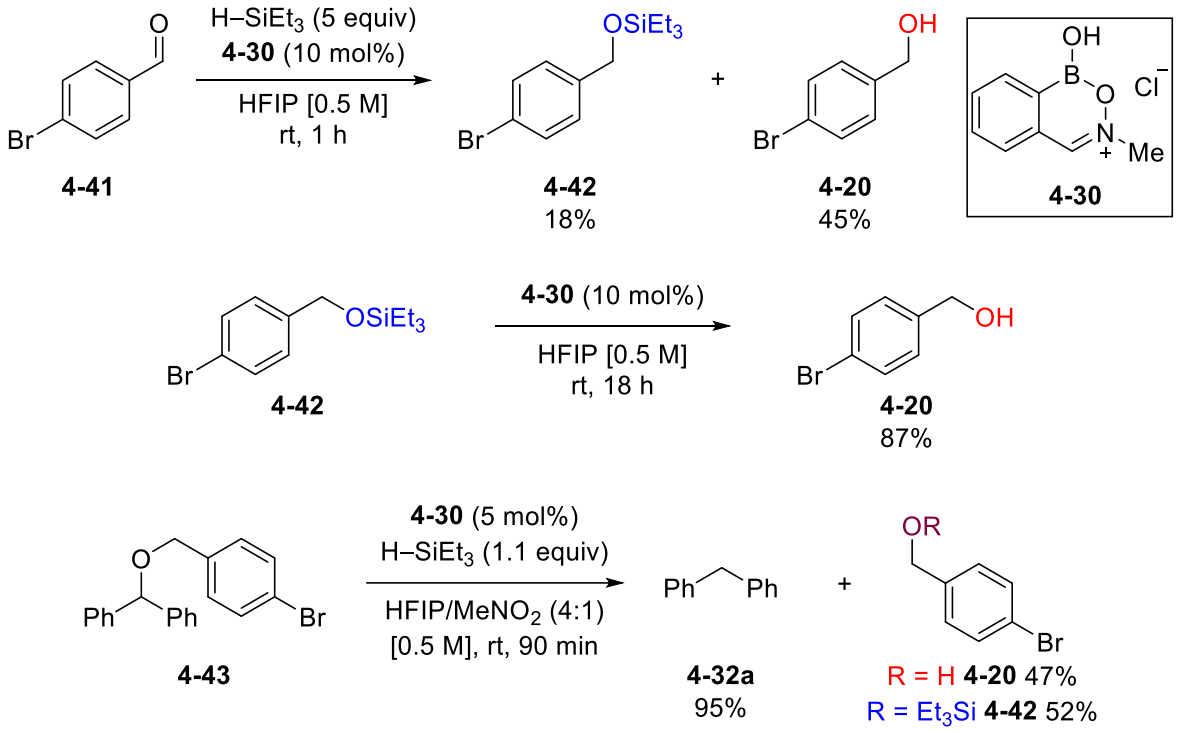

Scheme 4-18 Evidence for formation of silyl ether intermediates.

The rate of deoxygenation for several aromatic ketones was examined, where consumption of benzophenone (**4-37a**) was found to occur at a rate slower than that of acetophenone derivative **4-37u** (Figure 4-15). This trend is in stark contrast to the reactivity order observed in alcohol deoxygenation, where reduction of diphenylmethanol **4-31a** proceeds using lower catalyst loading and shorter reaction time relative to secondary alcohol **4-31u** (*cf.* Section 4.4.4). This result would seem to suggest that the rate of alcohol deoxygenation is largely controlled by the stability of the putative carbocation intermediate, while the rate of ketone deoxygenation is primarily influenced by the electrophilicity of the carbonyl carbon. A decrease in the relative rate of deoxygenation in the order aldehyde **4-41** > acetophenone **4-37u** > benzophenone **4-37a** is consistent with the trend observed for borohydride reduction.[89] Furthermore, the relative rate of reduction for fused diarylketones was found to be highly sensitive to the degree of aromaticity of the carbonyl-

containing ring. Reduction of 9-fluorenone (**4-37ak**), in which the central ring contains four π electrons and the resulting carbocation intermediate would display anti-aromaticity,[90] occurs at a rate significantly slower than benzophenone (**4-37a**). Conversely, deoxygenation of 5-dibenzosuberenone (**4-37ag**), in which the central ring contains six π electrons, proceeded rapidly under the standard conditions.

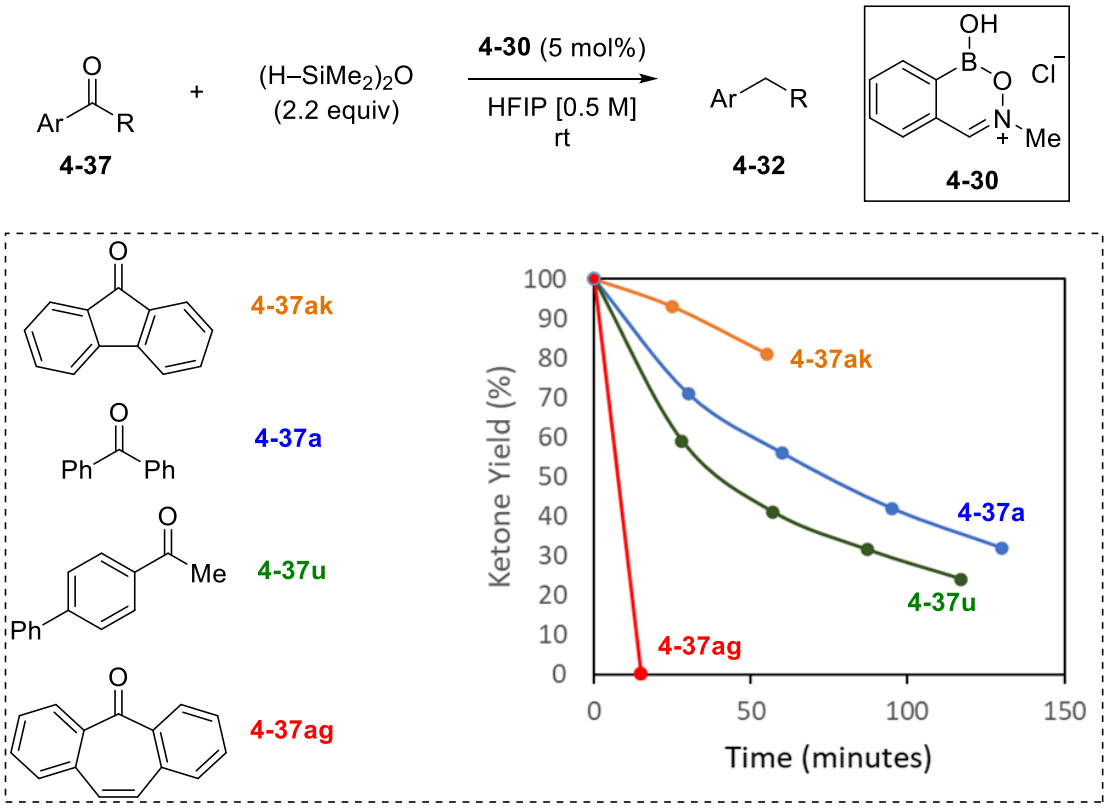

Figure 4-15 Substrate-dependent ketone deoxygenation kinetics.

The deoxygenation of alcohol **4-31a** catalyzed by hemiboronic acid **4-30** was further examined by ^{11}B NMR to gain additional understanding regarding changes in boron speciation and hybridization during the reaction. Analysis of heterocycle **4-30** in a mixture of HFIP/CD_3CN (10:1) revealed only one aromatic species by ^{1}H NMR, along with a single ^{11}B NMR resonance at 26.2 ppm suggestive of a trivalent boron environment (Figure 4-16). This data is consistent with

formation of boranol exchange ester **4-44**, which was further supported by ESI analysis in positive mode.

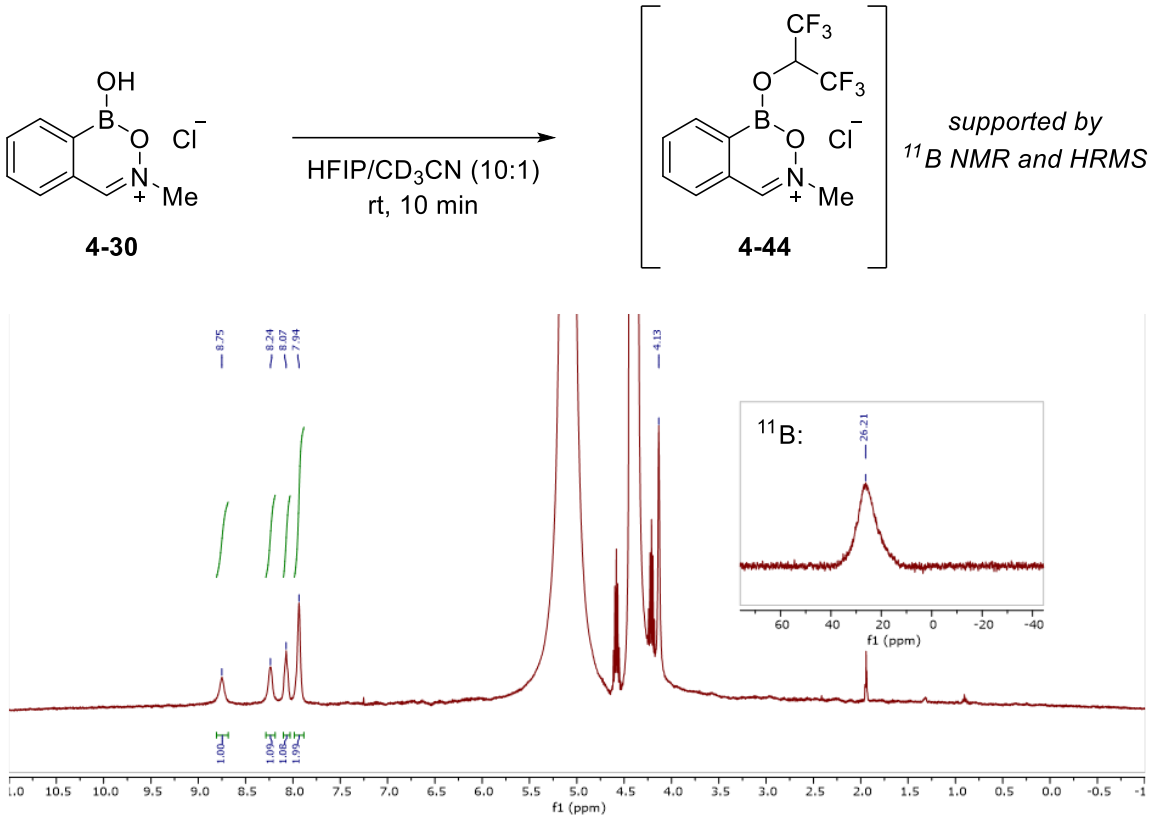

Figure 4-16 Proposed catalytic intermediate **4-44** and corresponding ^{1}H (400 MHz, HFIP/CD_3CN 10:1) and ^{11}B (128 MHz) NMR.

Upon addition of 2.0 equivalents of alcohol **4-31a**, ^{11}B NMR revealed a single resonance at 6.0 ppm, suggesting full conversion to a tetravalent boron species. This result is consistent with formation of zwitterionic boronate **4-45** and resulting ion pair **4-46**, formed by C–O ionization of alcohol **4-31a** (Scheme 4-19). Addition of excess TMDSO to the mixture rapidly (<10 minutes) led to full consumption of the tetravalent boronate, along with formation of a new ^{11}B NMR resonance at 24.9 ppm, suggesting that a trivalent boron species has been restored (Figure 4-17). Additionally, reductive deoxygenation product **4-32a** was observed by ^{1}H NMR after addition of

the silane. These observations are consistent with hydride ion abstraction or Si–H bond activation by proposed ion pair **4-46** to ultimately form the reduction product **4-32a**.

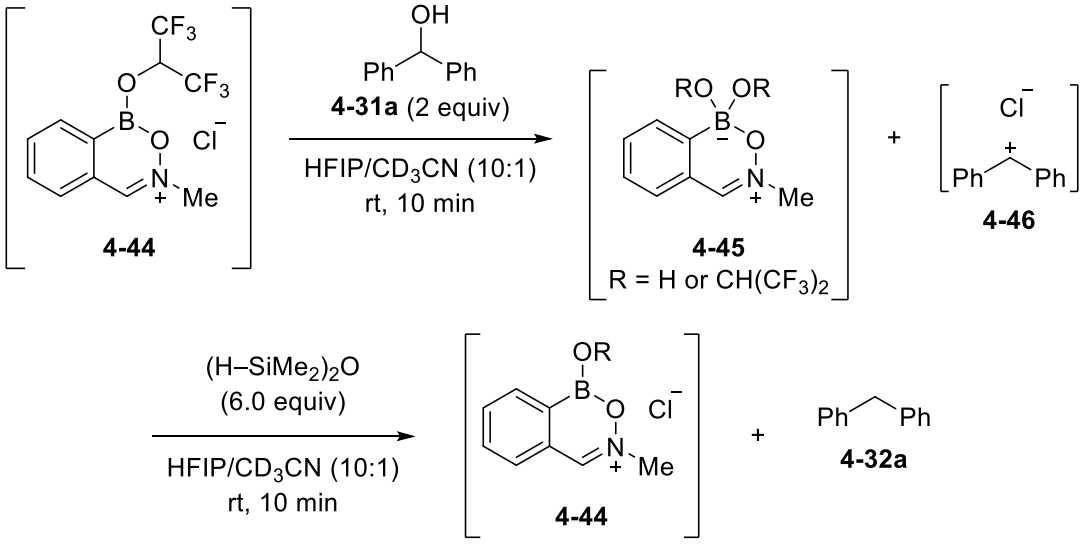

Scheme 4-19 Proposed intermediates during alcohol deoxygenation.

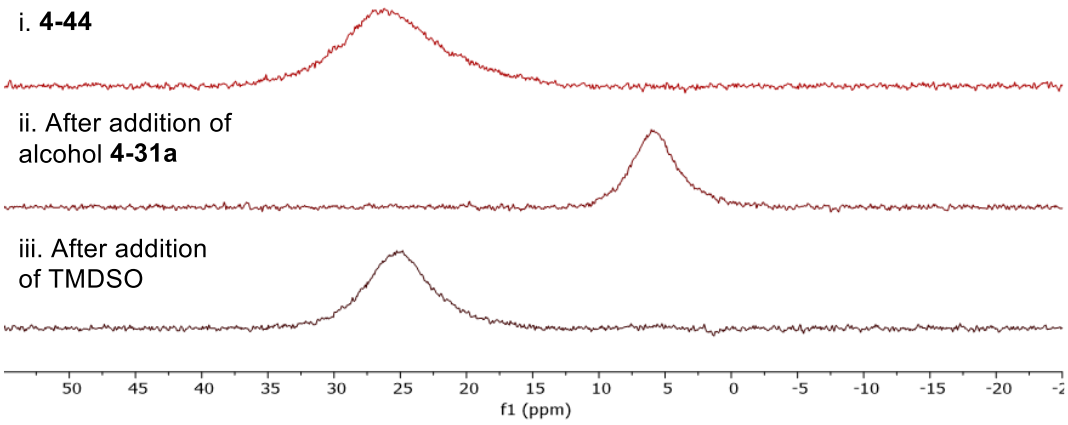

Figure 4-17 ^{11}B NMR (128 MHz, 10:1 HFIP/CD_3CN) spectra supporting the proposed intermediates.

Reaction of heterocycle **4-30** with two equivalents of nonactivated alcohol **4-47** in HFIP/CD_3CN solution resulted in a single ^{11}B NMR resonance at 26.2 ppm, with no evidence for the formation of a tetravalent boron species. This result contrasts with the reactivity observed with alcohol **4-31a** described above and suggests that the upfield ^{11}B NMR resonance upon reaction

with activated alcohol **4-31a** originates from catalytically productive C–O activation, rather than covalent boranol exchange alone. The deshielded methylene resonance of alcohol **4-47** showed significant broadening by ^{1}H NMR upon reaction with heterocycle **4-30**, suggesting that a dynamic exchange process may be operating for alcohols which are not readily ionized (Figure 4-18).

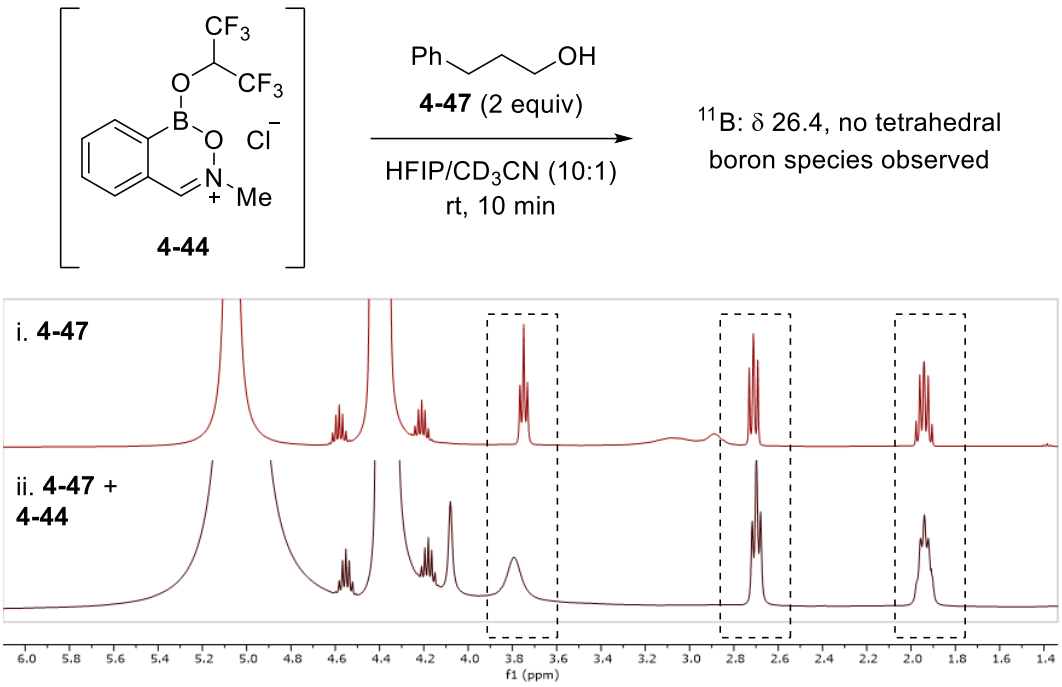

Figure 4-18 Reaction of catalyst **4-30** with a nonactivated alcohol and corresponding ^{1}H NMR (400 MHz, 10:1 HFIP/CD_3CN).

These NMR studies converge to a relatively consistent mechanistic picture for alcohol deoxygenation catalyzed by hemiboronic acid **4-30** (Figure 4-19). In HFIP solvent, the catalytically active species is believed to be hexafluoroisopropoxy boronic ester **4-44**. Reaction with an activated benzylic alcohol leads to C–O ionization to afford zwitterionic boronate **4-45**, along with stabilized carbenium ion pair **4-46**. Finally, subsequent reaction with silane affords the reduction product **4-32**, and concomitant Si–O bond formation regenerates the active trivalent boron species. Further studies are required in order to elucidate the precise mechanisms of ketone

activation and C–O ionization by catalyst **4-30**, which may involve a combination of Brønsted acid, Lewis acid, or silylium ion catalysis.[91,92]

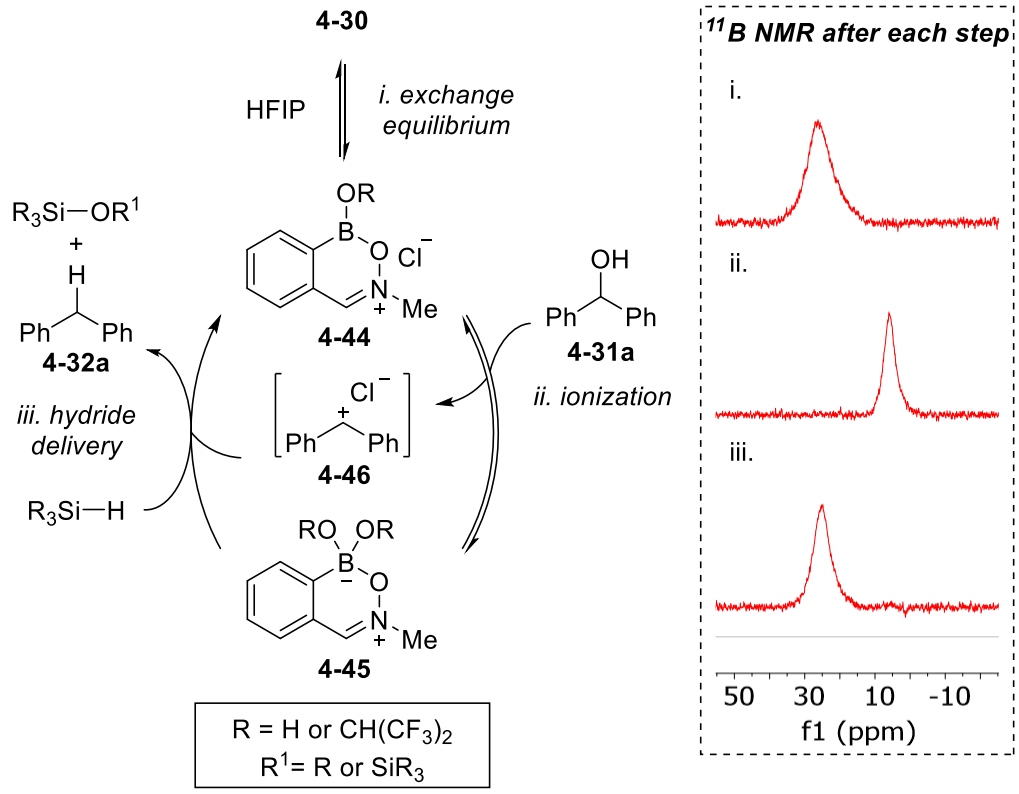

Figure 4-19 Proposed mechanism of alcohol deoxygenation and supporting ^{11}B NMR (128 MHz, 10:1 HFIP/CD_3CN).

4.4.8 Crystallization and Study of a Bis(hexafluoroisopropoxy)boronate Zwitterion

X-ray crystallography was employed to further study the atom connectivity and bonding of heterocycle **4-30** and its derivatives. When heterocycle **4-30** was dissolved in a mixture of HFIP and acetonitrile (10:1), concentration by rotary evaporation afforded white plate-shaped crystals which were demonstrated by X-ray crystallographic analysis to be zwitterionic bis(hexafluoroisopropoxy)boronate **4-48** (Figure 4-20).[93] Zwitterion **4-48** displayed an endocyclic B–O bond length of 1.559(6) Å, significantly longer than the endocyclic B–O bond length reported for neutral benzoxazaborine **4-02** by Groziak (1.388(6) Å)[78] and comparable to that of the

corresponding tetravalent dihydroxy conjugate base (1.537(3) Å).[25] The C–N bond length of zwitterion **4-48** (1.290(2) Å) was comparable to that of the neutral heterocycle **4-02** (1.283(5) Å).[78] A decreased N–O bond length was observed for the zwitterionic species relative to the parent heterocycle (1.3474(19) vs 1.419(6) Å), while the N–O and two N–C bonds of zwitterion **4-48** were highly coplanar.

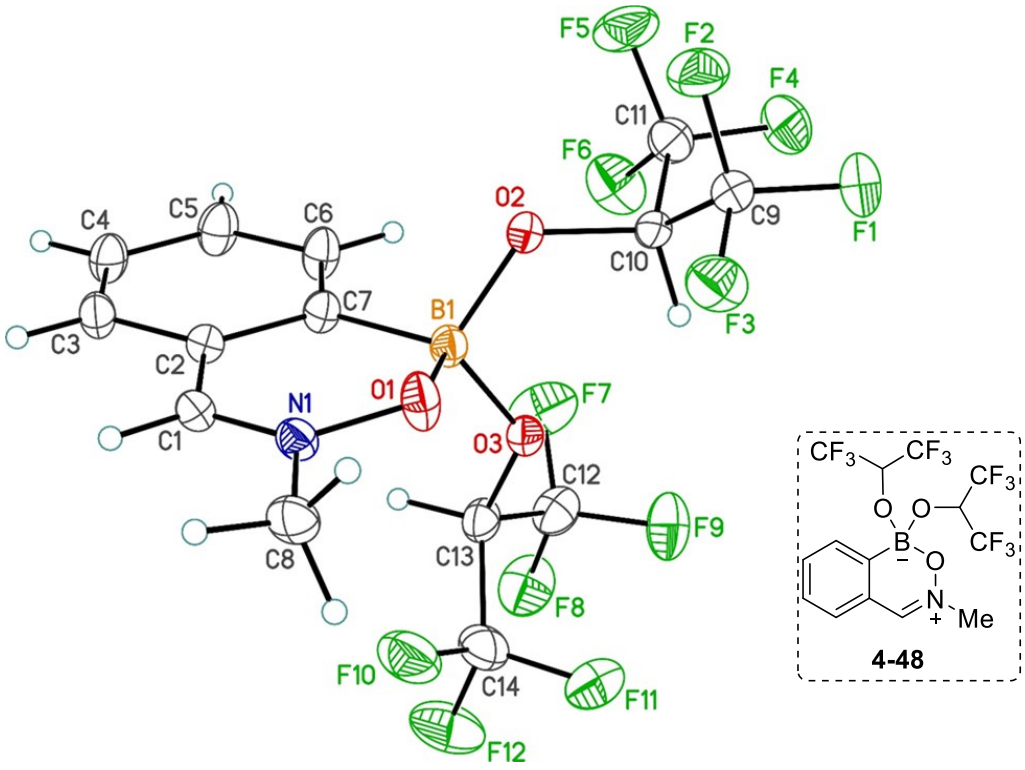

Figure 4-20 ORTEP representation of zwitterionic boronate **4-48**.

Zwitterion **4-48** was fully soluble in CD_3CN solution, in stark contrast to hemiboronic acid **4-30**. A single ^{11}B NMR resonance was observed at 4.9 ppm, consistent with the tetravalent boron environment. Analysis by ^{19}F NMR spectroscopy showed two distinct doublets of quartets with equivalent integration, suggesting that the two trifluoromethyl groups on the same hexafluoroisopropoxy unit are diastereotopic. The tetravalent structure of zwitterion **4-48**, obtained from concentration of an HFIP/acetonitrile solution by rotary evaporation, is in contrast

with NMR experiments described earlier (*cf.* Section 4.4.7) in which heterocycle **4-30** in HFIP/CD_3CN displayed a single ^{11}B NMR resonance at 26.2, consistent with trivalent boron species **4-44**. Accordingly, additional experiments were performed to clarify the impact of rotary evaporation on boron speciation of heterocycle **4-30**, and to determine whether zwitterionic species **4-48** is catalytically active in deoxygenation reactions.

When boron heterocycle **4-30** was analyzed by ^{11}B NMR in 10:1 HFIP/CD_3CN, a single resonance was observed at 26.2 ppm. Solutions of **4-30** in three different solvents were prepared and concentrated by rotary evaporation, and the resulting solids were each analyzed by ^{11}B NMR in 10:1 HFIP/CD_3CN (Figure 4-21). When concentrated from HFIP/CD_3CN (10:1), a single ^{11}B NMR resonance was observed at 5.9 ppm, fully consistent with the tetravalent boron species **4-48** that was characterized by X-ray crystallography under these conditions. Rotary evaporation from HFIP (without CD_3CN) gave a mixture of trivalent (15%) and tetravalent (85%) species. Finally, concentration from CD_3CN (without HFIP) showed only a trivalent boron species as is typically observed when no rotary evaporation is performed.

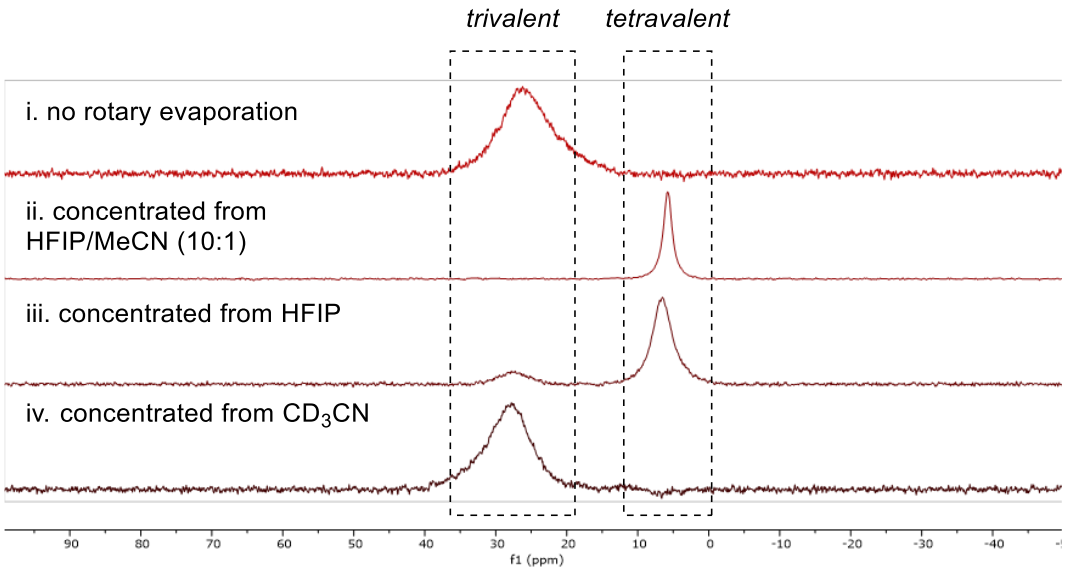

Figure 4-21 Effect of rotary evaporation on the speciation of boron heterocycle **4-30** as determined by ^{11}B NMR (128 MHz, 10:1 HFIP/CD_3CN).

Concentration of an HFIP/CD_3CN solution by rotary evaporation is expected to increase the fraction of CD_3CN (boiling point 81 °C) over time owing to the lower boiling point of HFIP (59 °C). As the polarity of the solvent mixture decreases along with the evaporation of HFIP, zwitterion **4-48** may be more effectively solubilized than heterocycle **4-30** in the remaining CD_3CN solution due to the internal charge neutralization of the zwitterion. Rotary evaporation from an HFIP/CD_3CN solution may thus have a significant impact on boron speciation and a potential equilibrium between zwitterion **4-48** and ionic species **4-30** or **4-44**.

Zwitterionic species **4-48** was examined as a catalyst in the reductive deoxygenation of alcohol **4-31u** and ketone **4-37a** (Scheme 4-20). In both cases, near quantitative recovery of the starting materials was observed. The lack of catalytic activity for zwitterion **4-48** is consistent with mechanistic studies (*cf.* Figure 4-19) which suggested that trivalent boron species **4-44** may be the active catalyst in solution. Furthermore, the lack of reactivity for zwitterion **4-48** suggests that

tetravalent and trivalent boron species do not appreciably interconvert in solution prior to substrate activation.

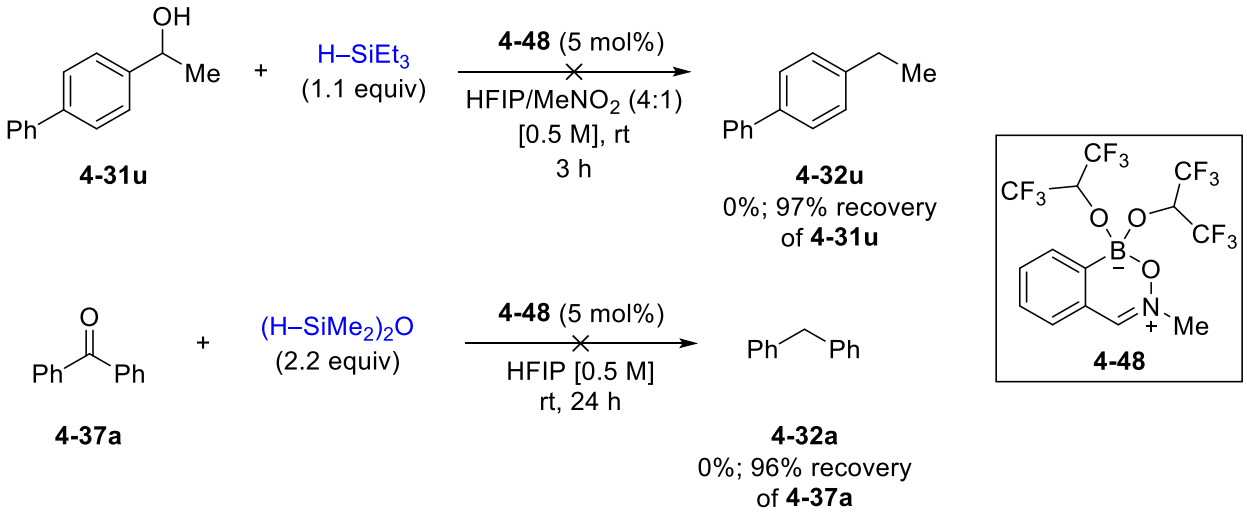

Scheme 4-20 Examination of zwitterion **4-48** as a catalyst in reductive deoxygenation.

4.4.9 Comparison of Catalysts for Nucleophilic and Electrophilic Activation

While benzoxazaborines **4-02** and **4-30** show significant structural similarity, their catalytic applications are founded upon mechanistically divergent modes of activation. When cationic catalyst **4-30** was applied in the monophosphorylation of diol **4-15a**, a tenfold decrease in activity was observed relative to neutral catalyst **4-02** (Scheme 4-21). This result is likely a reflection of the dramatic decrease in nucleophilicity for a zwitterionic tetravalent diol complex derived from heterocycle **4-30** relative to an anionic tetravalent boronate formed from catalyst **4-02**. Conversely, benzoxazaborine **4-02** was entirely inactive as a catalyst under optimized conditions for the reductive deoxygenation of alcohol **4-31a**, demonstrating the dramatic improvement in electrophilic activation that is afforded with catalyst **4-30**.

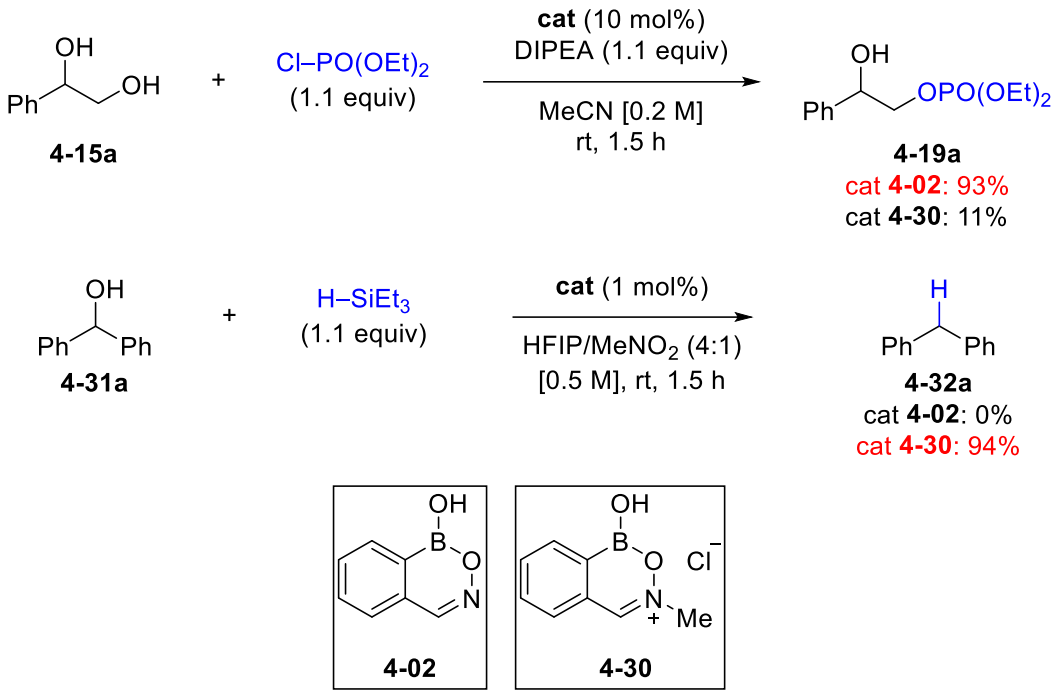

Scheme 4-21 Comparison of the two benzoxazaborine catalysts in the two model reactions.

4.5 Summary

The work described in this chapter has recognized the benzoxazaborine scaffold as a versatile platform for the development of hemiboronic acid-catalyzed transformations. Catalysts within this framework can be employed for the direct activation or functionalization of hydroxy-containing compounds under mild, ambient conditions. The parent heterocycle **4-02** was demonstrated to be an active catalyst for the selective monophosphorylation of vicinal diols. Mechanistic studies revealed that the exceptional activity of this catalyst relative to other naphthoid hemiboronic acids arises from a balancing of effective substrate binding and Lewis acidity-driven conversion to a highly nucleophilic tetravalent adduct. Conversely, cationic derivative **4-30** was found to be a highly active catalyst for the reductive deoxygenation of alcohols and ketones under ambient conditions employing silanes as reducing agents. Ketone deoxygenation was demonstrated to

occur through an initial hydrosilylation reaction, followed by C–O activation upon reaction with a trivalent catalytic boron species.

These results establish a clear association between the fundamental properties of boron-containing heterocycles and their application in catalysis. Rational modifications to the core scaffold can be employed to tailor catalytic activity towards a given application, while the use of bench-stable catalysts under ambient conditions facilitates analysis of the reactions and catalytic intermediates by conventional NMR spectroscopic techniques. The results described herein constitute an encouraging starting point for the design of new cyclic hemiboronic acid catalysts and may lead to the development of new hemiboronic acid-catalyzed transformations.

4.6 Experimental

4.6.1 General Information

The following section contains representative experimental procedures and details for the isolation of compounds. Partial characterization of known compounds and full characterization of novel compounds presented in this chapter are described. All reactions were performed in regular glassware without any precautions to remove air or moisture, unless otherwise indicated. All chemicals were purchased from commercial sources and used as received unless otherwise noted. 2-formylphenylboronic acid was purchased from Combi-Blocks and recrystallized from hot H_2O prior to use. Hydroxylamine (50 wt. % solution in water) was purchased from Sigma Aldrich and used as received. *N*-methylhydroxylamine hydrochloride was purchased from Combi-Blocks and used as received. 1,1,1,3,3,3-hexafluoroisopropanol (HFIP) was purchased from Oakwood Chemical and used as received. All other solvents were purchased as ACS reagent grade and were used as received. Column chromatography was performed on silica gel 60 using ACS grade hexanes and ethyl acetate as eluents. Thin layer chromatography (TLC) analysis was performed

on Silicycle silica gel 60 F254 plates, which were visualized under UV light and with phosphomolybdic acid (PMA) or potassium permanganate ($KMnO_4$) stains.

NMR spectra were recorded at ambient temperature using Varian DD2 MR two-channel 400 MHz, Varian INOVA two-channel 400MHz, Varian INOVA four-channel 500 MHz, Varian VNMRS two-channel 500 MHz, Varian VNMRS four-channel 600 MHz and Agilent VNMRS four-channel, dual receiver 700 MHz spectrometers operating at the indicated frequency for ^1H NMR. All NMR chemical shifts are reported in ppm (δ) units with residual solvent peaks ($CDCl_3$, CD_3CN or D_2O) as the internal reference. NMR data is reported using the following abbreviations: s, singlet; br s, broad singlet; d, doublet; t, triplet; q, quartet; h, hextet; dd, doublet of doublets; dt, doublet of triplets; td, triplet of doublets; ddd, doublet of doublet of doublets; dddd, doublet of doublet of doublet of doublets; app, apparent; m, multiplet. The error of coupling constants from ^1H NMR spectra is estimated to be approximately 0.3 Hz. The quaternary carbon bound to boron is often not observed due to quadrupolar relaxation of boron, which was the case for all boron-containing compounds described here.

All pH measurements were performed using an OHAUS ST2100 pH meter with ST350 pH probe. High-resolution mass spectra were recorded by the University of Alberta Mass Spectrometry Services Laboratory using either electrospray (ESI) or electron impact (EI) techniques. Melting points were determined in a capillary tube using a melting point apparatus and are uncorrected. Fourier-transform infrared (FTIR) spectra were obtained on a Nicolet Magna-IR instrument.

4.6.2 Synthesis and Characterization of Boron Heterocycles

The synthesis and pK_a values of heterocycles **4-02**, **4-04**, **4-05** and **4-06** were described previously in Chapter 3.[31]

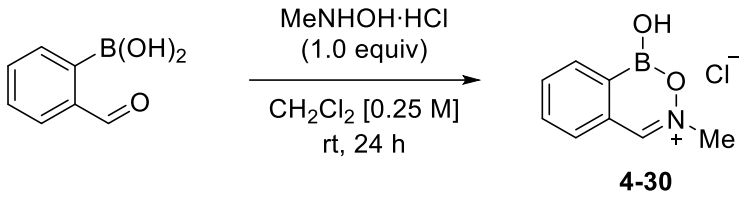

4-30

1-Hydroxy-3-methyl-1H-benzo[d][1,2,6]oxazaborinin-3-ium chloride (4-30): A round bottom flask under air was charged with 2-formylphenylboronic acid (1.20 g, 8.00 mmol) and CH_2Cl_2 (32 mL). The resulting solution was stirred at room temperature for 10 minutes, after which *N*-methylhydroxylamine hydrochloride (668 mg, 8.00 mmol, 1.00 equiv) was added in one portion. The mixture was stirred at room temperature for 24 hours, during which time a precipitate was observed. Upon completion, the precipitate was collected by vacuum filtration, washed with CH_2Cl_2 (6 × 15 mL), and dried under vacuum to afford the title compound as a white solid (1.48 g, 94%). **mp** = 234 – 237 °C (sweating and change in morphology observed at 145.6 – 148.1 °C); **^{1}H NMR** (500 MHz, D_2O): δ 8.59 (s, 1 H), 7.78 (t, *J* = 7.4 Hz, 1 H), 7.70 (d, *J* = 7.4 Hz, 1 H), 7.62 (d, *J* = 7.7 Hz, 1 H), 7.55 (t, *J* = 7.6 Hz, 1 H), 3.94 (s, 3 H); **^{13}C NMR** (126 MHz, D_2O): δ 148.9, 136.8, 131.0, 130.9, 129.5, 127.6, 49.6; **^{11}B NMR** (128 MHz, D_2O): δ 4.5; **FTIR** (microscope, cm^{-1}): 3362 (br, s), 3324 (m), 3062 (w), 2980 (m), 1648 (m), 1560 (m), 1392 (m), 1158 (m), 1101 (m), 998 (w), 769 (m), 708 (w); **HRMS** (ESI Positive Mode) for $C_8H_9BNO_2^+$: Calculated: 162.0721; Found: 162.0722.

To determine the pK_a of heterocycle **4-30**, an ^{11}B NMR titration was conducted according to the following procedure: Boron heterocycle **4-30** (49.4 mg, 0.250 mmol) was dissolved in 5.0 mL D_2O. The solution was then diluted to a total volume of 25 mL using a phosphate buffer solution, which was prepared by dissolving 690.0 mg sodium phosphate monobasic monohydrate in 50.0 mL deionized water. Aliquots of 2.0 mL from the boron heterocycle stock solution were transferred to 3-dram vials, where the pH of the solutions was then adjusted using 0.1 M NaOH,

1.0 M NaOH or 1.0 M HCl and measured using a pH meter. After a stable pH reading was observed, approximately 700 μL of each aliquot was transferred to an NMR tube and analyzed by ^{11}B NMR spectroscopy, using D_2O as the solvent for locking and shimming.

No significant change in ^{11}B NMR chemical shift was observed between pH 0.81–13.04. Across this entire range, a chemical shift between 4.1–4.6 ppm was observed corresponding to a tetravalent boron environment. Thus, the pK_a of heterocycle **4-30** in H_2O can be estimated to be less than 1.

4.6.3 Synthesis and Characterization of Vicinal Diols

Diols **4-15a** and **4-15f** were purchased from commercial suppliers and used as received.

General Procedure for the synthesis of 1-aryl-1,2-diols from acetophenones (GP4-1)

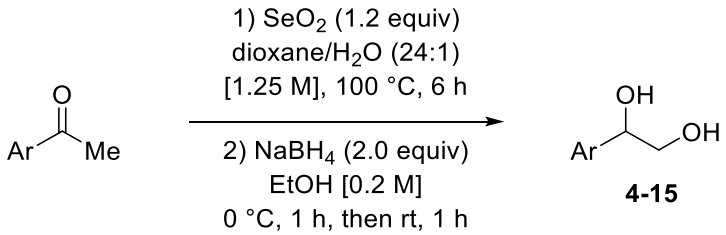

A 10 mL round bottom flask was charged with SeO_2 (1.2 equiv), dioxane and H_2O (24:1 ratio, 1.25 M in limiting reagent). The resulting suspension was heated to 55 °C until fully soluble (approximately 5 minutes), at which time it was allowed to cool to room temperature. The corresponding acetophenone (1.0 equiv) was then added in a single portion. The mixture was heated to reflux at 100 °C for 6 hours. Upon heating, a color change to a dark red solution was observed, followed by a dark green solution over time along with precipitation of a black solid. After 6 hours, the reaction was allowed to cool to room temperature and filtered through fluted filter paper (caution: the filter paper contains selenium waste and must be disposed of accordingly)

to yield a pale green/yellow solution, which was concentrated by rotary evaporation. The crude mixture was passed through a short column of silica gel using hexanes/ethyl acetate (2:1) and concentrated by rotary evaporation, after which it was dissolved in ethanol (0.2 M) and cooled to 0 °C. $NaBH_4$ (2.0 equiv) was added in two portions approximately 5 minutes apart. The reaction was stirred for 1 hour at 0 °C, and then stirred for an additional 1 hour after removing the ice bath. The reaction was quenched with 1M $HCl_{(aq)}$ and concentrated by rotary evaporation to remove EtOH. The resulting mixture was extracted with ethyl acetate (3 × 25 mL). The combined organic phases were washed with water (30 mL) and brine (30 mL), dried over Na_2SO_4 and filtered. After removal of the solvent by rotary evaporation, purification by column chromatography afforded the diol **4-15**.

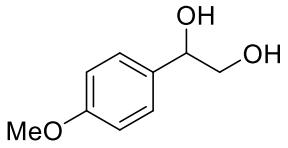

1-(4-Methoxyphenyl)ethane-1,2-diol (4-15b): Prepared according to **GP4-1** from 4-methoxyacetophenone (751 mg, 5.00 mmol). Purification by column chromatograph (1:2 hexane/EtOAc) afforded the title compound as a white solid (145 mg, 17%). **^{1}H NMR** (500 MHz, $CDCl_3$): δ 7.29 (d, *J* = 8.7 Hz, 2 H), 6.90 (d, *J* = 8.6 Hz, 2 H), 4.77 (dd, *J* = 8.2, 3.7 Hz, 1 H), 3.80 (s, 3 H), 3.72 (dd, *J* = 11.3, 3.7 Hz, 1 H), 3.65 (dd, *J* = 11.3, 8.2 Hz, 1 H), 2.53 (br s, 1 H), 2.15 (br s, 1 H); **^{13}C NMR** (126 MHz, $CDCl_3$): δ 159.6, 132.8, 127.5, 114.1, 74.4, 68.2, 55.5. Spectral data were in agreement with the literature.[94]

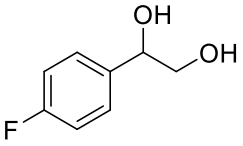

1-(4-Fluorophenyl)ethane-1,2-diol (4-15c): Prepared according to **GP4-1** from 4-fluoroacetophenone (607 μL, 5.00 mmol) and obtained as a white solid (390 mg, 50%) without further purification. **^{1}H NMR** (500 MHz, $CDCl_3$): δ 7.37 (dd, *J* = 8.6, 5.5 Hz, 2 H), 7.08 (app t, *J* = 8.7 Hz, 2 H), 4.84 (dd, *J* = 8.3, 3.5 Hz, 1 H), 3.77 (dd, *J* = 11.3, 3.5 Hz, 1 H), 3.66 (dd, *J* = 11.3, 8.2 Hz, 1 H), 2.78 (s, 1 H), 2.29 (s, 1 H); **^{13}C NMR** (126 MHz, $CDCl_3$): δ 162.6 (d, *J* = 246.2 Hz), 136.3 (d, *J* = 3.1 Hz), 127.9 (d, *J* = 8.3 Hz), 115.6 (d, *J* = 21.4 Hz), 74.2, 68.2; **^{19}F NMR** (376 MHz, $CDCl_3$): δ –114.3 (app tt, *J* = 8.8, 5.2 Hz). Spectral data were in agreement with the literature.[94]

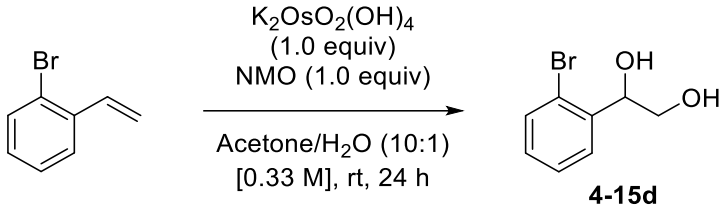

1-(2-Bromophenyl)ethane-1,2-diol (4-15d): Under nitrogen, a 25 mL round bottom flask was charged with $K_2OsO_2(OH)_4$ (12.1 mg, 0.03 mmol, 1 mol%) and *N*-methylmorpholine *N*-oxide (352 mg, 3.00 mmol, 1.00 equiv). The solids were suspended in acetone (8.20 mL) and H_2O (0.820 mL). 4-bromostyrene (376 μL, 3.00 mmol, 1.00 equiv) was added via syringe and the mixture was stirred for 24 hours at room temperature. The reaction was then diluted with H_2O (25 mL) and extracted with ethyl acetate (3 × 25 mL). The combined organic phases were washed with brine (25 mL), dried over Na_2SO_4 and filtered. The solvent was removed by rotary evaporation, and purification by column chromatography (2:1 hexane/EtOAc) afforded the title compound as a white solid (169 mg, 26%). **^{1}H NMR** (500 MHz, $CDCl_3$): δ 7.63 (dd, *J* = 7.8, 1.7 Hz, 1 H), 7.57 (dd, *J* = 8.0, 1.2 Hz, 1 H), 7.39 (td, *J* = 7.6, 1.2 Hz, 1H), 7.20 (td, *J* = 7.7, 1.8 Hz, 1 H), 5.24 (dt, *J* = 8.1, 3.0 Hz, 1 H), 3.96 (ddd, *J* = 10.7, 6.9, 3.1 Hz, 1 H), 3.61 (ddd, *J* = 11.6, 7.8, 4.2 Hz, 1 H),

2.67 (d, *J* = 3.3 Hz, 1 H), 2.08 – 2.02 (m, 1 H); **^{13}C NMR** (126 MHz, $CDCl_3$): δ 139.5, 132.9, 129.5, 128.0, 127.9, 122.1, 73.7, 66.4. Spectral data were in agreement with the literature.[95]

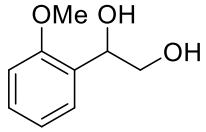

1-(2-Methoxyphenyl)ethane-1,2-diol (4-15e): Prepared according to **GP4-1** from 2-methoxyacetophenone (827 μL, 6.00 mmol). Purification by column chromatography (1:1 hexane/EtOAc) afforded the title compound as a white solid (403 mg, 40%). **^{1}H NMR** (500 MHz, $CDCl_3$): δ 7.38 (dd, *J* = 7.5, 1.7 Hz, 1 H), 7.31 – 7.25 (m, 1 H), 6.98 (td, *J* = 7.5, 1.0 Hz, 1 H), 6.89 (dd, *J* = 8.3, 1.0 Hz, 1 H), 5.05 (dd, *J* = 8.0, 3.6 Hz, 1 H), 3.85 (s, 3 H), 3.81 (dd, *J* = 11.2, 3.6 Hz, 1 H), 3.69 (dd, *J* = 11.2, 8.0 Hz, 1 H), 2.92 (br s, 1 H), 2.20 (br s, 1 H); **^{13}C NMR** (126 MHz, $CDCl_3$): δ 156.7, 129.0, 128.5, 127.4, 121.0, 110.6, 71.4, 66.6, 55.4. Spectral data were in agreement with the literature.[96]

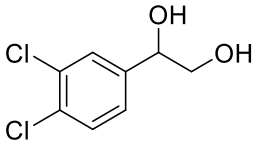

1-(3,4-Dichlorophenyl)ethane-1,2-diol (4-15g): Prepared according to **GP4-1** from 3,4-dichloroacetophenone (1.13 g, 6.00 mmol). Purification by column chromatography (gradient 1:1 to 1:2 hexane/EtOAc) afforded the title compound as a clear oil (1.04 g, 83%). **^{1}H NMR** (500 MHz, $CDCl_3$): δ 7.48 (d, *J* = 2.0 Hz, 1 H), 7.42 (d, *J* = 8.2 Hz, 1 H), 7.19 (dd, *J* = 8.3, 2.1 Hz, 1 H), 4.78 (dd, *J* = 8.1, 3.5 Hz, 1 H), 3.76 (dd, *J* = 11.3, 3.4 Hz, 1 H), 3.60 (dd, *J* = 11.3, 8.0 Hz, 1 H), 2.82 (br s, 1 H), 2.20 (br s, 1 H); **^{13}C NMR** (126 MHz): δ 140.8, 132.9, 132.1, 130.6, 128.3, 125.5, 73.6, 67.9. Spectral data were in agreement with the literature.[97]

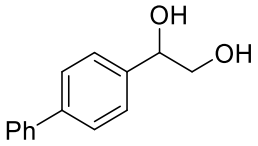

1-([1,1'-Biphenyl]-4-yl)ethane-1,2-diol (4-15h): Prepared according to **GP4-1** from 4-acetylbiphenyl (1.17 g, 6.00 mmol) and obtained as a white solid (583 mg, 45%) without further purification. **^{1}H NMR** (500 MHz, $CDCl_3$): δ 7.62 – 7.56 (m, 4 H), 7.50 – 7.39 (m, 4 H), 7.39 – 7.32 (m, 1 H), 4.89 (dd, *J* = 8.1, 3.6 Hz, 1 H), 3.83 (dd, *J* = 11.3, 3.6 Hz, 1 H), 3.73 (dd, *J* = 11.3, 8.1 Hz, 1 H), 1.58 (br s, 2 H); **^{13}C NMR** (126 MHz, $CDCl_3$): δ 141.2, 140.9, 139.6, 129.0, 127.6, 127.5, 127.2, 126.7, 74.6, 68.2. Spectral data were in agreement with the literature.[97]

4.6.4 Monophosphorylation – Initial Stoichiometric Study and Reaction Optimization

4.6.4.1 Initial Stoichiometric Study

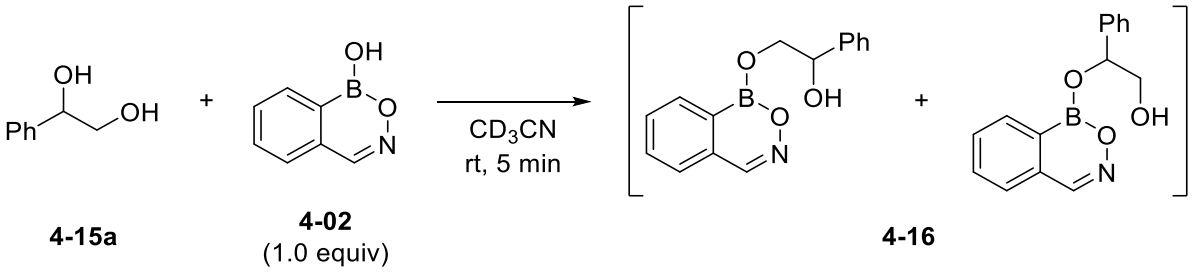

A half-dram vial was charged with diol **4-15a** (10.4 mg, 0.0750 mmol) and boron heterocycle **4-02** (10.9 mg, 0.0750 mmol, 1.00 equiv). The solids were dissolved in CD_3CN (0.7 mL) to give a homogeneous solution, which was transferred to an NMR tube. Two new multiplets were observed in the 4.0–5.5 ppm region downfield from the corresponding resonances in free **4-15a**, consistent with formation of hemiboronic ester **4-16**. The broadness of these new resonances suggests a dynamic exchange process and may indicate that both regioisomers of **4-16** exist in equilibrium. The ^{11}B NMR spectrum displayed a new resonance slightly upfield relative to the starting heterocycle, also consistent with boranol exchange. The formation of ester **4-16** was also supported

by HRMS of the reaction mixture ($C_{15}H_{14}NO_3{}^{11}BNa$ $[M+Na]^+$: Calculated: 290.0964; Found: 290.0960).

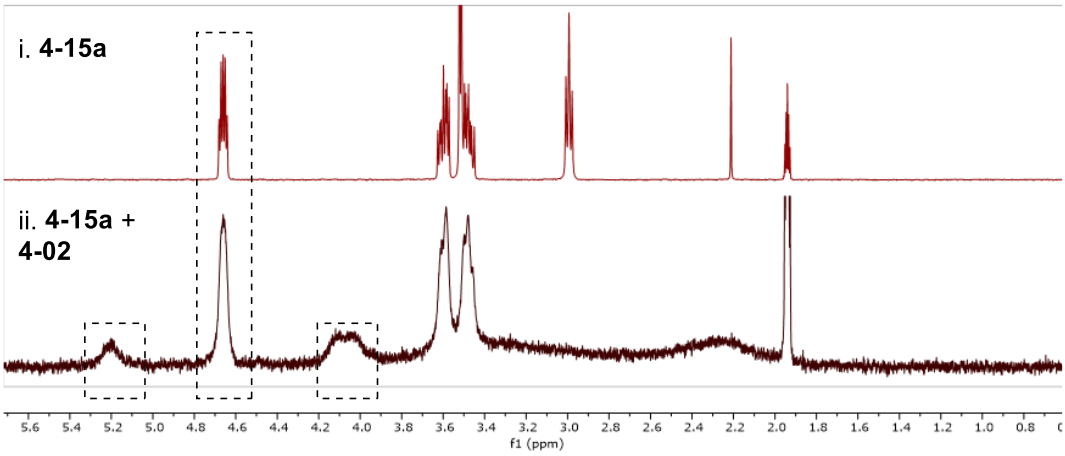

Figure 4-22 ^{1}H NMR (400 MHz, CD_3CN) of formation of boranol exchange product **4-16**.

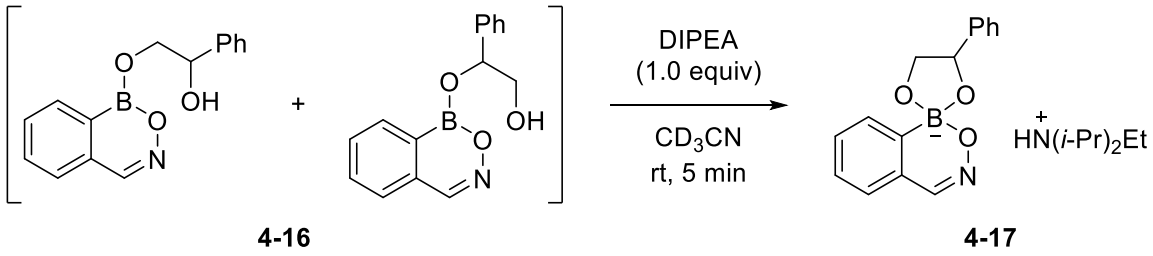

4-16 **4-17**

N,*N*-diisopropylethylamine (13.1 µL, 0.0750 mmol, 1.0 equiv) was then added to the NMR tube and the solution mixed thoroughly. ^{11}B NMR displayed greater than 95% conversion to a tetrahedral boronate (7.2 ppm), consistent with formation of adduct **4-17.** The formation of adduct **4-17** was also supported by HRMS of the reaction mixture in negative mode ($C_{15}H_{13}NO_3{}^{11}B^-$: Calculated: 266.0994; Found: 266.090).

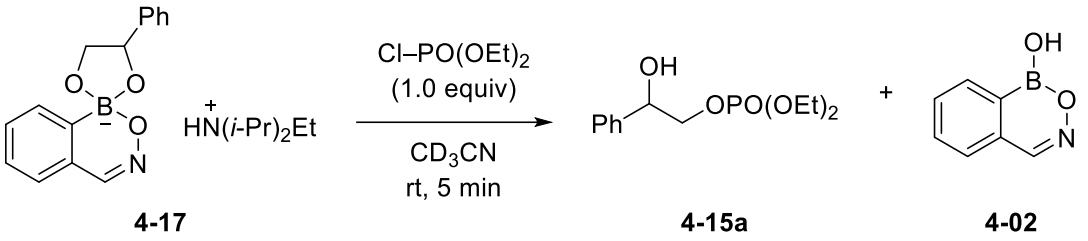

4-17 **4-15a** **4-02**

Diethyl chlorophosphate (10.8 μL, 1.00 equiv) was then added to the NMR tube and the solution mixed thoroughly. ^{11}B NMR showed complete consumption of tetrahedral adduct **4-17** and regeneration of heterocycle **4-02**. ^{1}H NMR also demonstrated formation of a multiplet (4.87 ppm, t, J = 5.4 Hz) consistent with an authentic sample of **4-15a** isolated from subsequent catalytic experiments.

4.6.4.2 Optimization of Catalytic Monophosphorylation

General Procedure for the monophosphorylation of diols using NMR yields (GP4-2)

A vial equipped with a stir bar was charged with diol **4-15a** (13.8 mg, 0.100 mmol), catalyst (10 mol%), MeCN (0.5 mL), base (X equiv) and diethyl chlorophosphate (Y equiv). The vial was capped and stirred at room temperature for the indicated time. Upon completion, the mixture was diluted with $CHCl_3$ and filtered through a small pipette of silica (approximately 1 cm high) with $CHCl_3$ washings to remove insoluble components. The mixture was concentrated by rotary evaporation, and yields were obtained by ^{1}H NMR relative to 1,3,5-trimethoxybenzene as an internal standard.

4.6.5 Monophosphorylation – Substrate Scope

General Procedure for the monophosphorylation of vicinal diols (GP4-3)

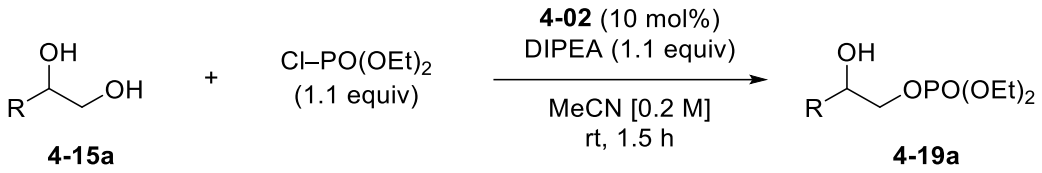

A two-dram vial with a stir bar was charged with diol **4-15a** (1.0 equiv), catalyst **4-02** (10 mol%) and MeCN (0.2 M). The reaction was stirred at room temperature for thirty seconds until fully dissolved, at which point DIPEA (1.1 equiv) and $ClPO(OEt)_2$ (1.1 equiv) were added (caution: addition of the electrophile is mildly exothermic). The vial was capped and stirred at room temperature for 1.5 hours. Upon completion, the reaction mixture was diluted with ethyl acetate (20 mL) and washed successively with 1 M $HCl_{(aq)}$ (10 mL), saturated $NaHCO_{3(aq)}$ (10 mL) and brine (10 mL). The organic layer was dried over Na_2SO_4, filtered, and concentrated by rotary evaporation. Purification by column chromatography afforded the desired product.

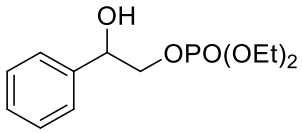

Diethyl (2-hydroxy-2-phenylethyl) phosphate (4-19a): Prepared according to **GP4-3** from diol **4-15a** (83.0 mg, 0.600 mmol), catalyst **4-02** (8.8 mg, 0.060 mmol, 10 mol%), MeCN (3.0 mL), DIPEA (115 µL, 0.660 mmol, 1.10 equiv) and $ClPO(OEt)_2$ (96 µL, 0.66 mmol, 1.1 equiv). Purification by column chromatography (1:2 hexane/EtOAc) afforded the title compound as a clear oil (118 mg, 72%). **^{1}H NMR** (500 MHz, $CDCl_3$): δ 7.39 (dd, *J* = 8.4, 1.7 Hz, 2 H), 7.36 (td, *J* = 7.6 Hz, 1.4 Hz, 2 H), 7.30 (tt, *J* = 7.4, 1.6 Hz, 1 H), 4.98 (dd, *J* = 8.3, 3.0 Hz, 1 H), 4.21 – 4.05 (m 6 H), 3.55 (br s, 1 H), 1.33 (tdd, *J* = 7.1, 6.1, 1.1 Hz, 6 H); **^{13}C NMR** (126 MHz, $CDCl_3$): δ 139.3, 128.6, 128.3, 126.4, 73.2 (d, *J* = 5.4 Hz), 72.8 (d, *J* = 6.0 Hz), 64.3 (d, *J* = 5.9 Hz), 16.2 (d, *J* = 6.6 Hz); **^{31}P NMR** (161 MHz, $CDCl_3$): δ – 0.1 (s); **FTIR** (Cast film, cm^{-1}): 3365 (br, m), 3031 (w),

2985 (w), 1454 (w), 1258 (m), 1030 (s), 984 (m), 702 (m); **HRMS** (ESI) for $C_{12}H_{19}PO_5Na$ $[M+Na]^+$: Calculated: 297.0868; Found: 297.0861.

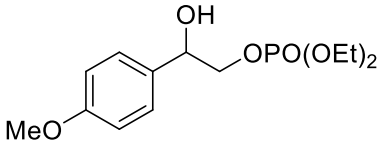

Diethyl (2-hydroxy-2-(4-methoxyphenyl)ethyl) phosphate (4-19b): Prepared according to **GP4-3** from diol **4-15b** (84.0 mg, 0.500 mmol), catalyst **4-02** (7.3 mg, 0.050 mmol, 10 mol%), MeCN (2.5 mL), DIPEA (96 μL, 0.55 mmol, 1.1 equiv) and $ClPO(OEt)_2$ (80 μL, 0.55 mmol, 1.1 equiv). Purification by column chromatography (1:2 hexane/EtOAc) afforded the title compound as a clear oil (97 mg, 64%). **^{1}H NMR** (500 MHz, $CDCl_3$): δ 7.31 (d, *J* = 8.5 Hz, 2 H), 6.89 (d, *J* = 8.7 Hz, 2 H), 4.93 (dd, *J* = 8.4, 3.2 Hz, 1 H), 4.16 – 4.03 (m, 6 H), 3.80 (s, 3 H), 3.40 (br s, 1 H), 1.34 (tdd, *J* = 7.1, 4.3, 1.0 Hz, 6 H); **^{13}C NMR** (126 MHz, $CDCl_3$): δ 159.7, 131.3, 127.6, 114.1, 72.8 (d, *J* = 5.7 Hz), 72.7 (d, *J* = 6.5 Hz), 64.3 (d, *J* = 5.9 Hz), 55.4, 16.2 (d, *J* = 6.7 Hz); **^{31}P NMR** (162 MHz, $CDCl_3$): δ – 0.1 (s) (note: sample contains approximately 4% excess $ClPO(OEt)_2$, observed at –13.2 ppm); **FTIR** (Cast film, cm^{-1}): 3367 (br, m), 2985 (w), 2946 (w), 1613 (w), 1515 (m), 1250 (s), 1031 (s), 833 (w); **HRMS** (ESI) for $C_{13}H_{21}PO_6Na$ $[M+Na]^+$: Calculated: 327.0973; Found: 327.0969.

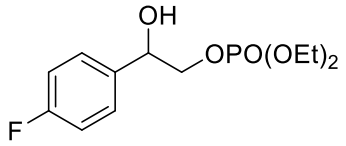

Diethyl (2-(4-fluorophenyl)-2-hydroxyethyl) phosphate (4-19c): Prepared according to **GP4-3** from diol **4-15c** (93.8 mg, 0.600 mmol), catalyst **4-02** (8.8 mg, 0.060 mmol, 10 mol%), MeCN (3.0 mL), DIPEA (116 μL, 0.660 mmol, 1.10 equiv) and $ClPO(OEt)_2$ (96 μL, 0.66 mmol, 1.1

equiv). Purification by column chromatography (1:2 hexane/EtOAc) afforded the title compound as a clear oil (134 mg, 77%). **^{1}H NMR** (500 MHz, $CDCl_3$): δ 7.40 – 7.34 (dd, *J* = 8.2, 5.3 Hz, 2 H), 7.04 (app t, *J* = 8.7 Hz, 2 H), 4.97 (dt, *J* = 8.1, 3.1 Hz, 1 H), 4.20 – 4.03 (m, 6 H), 3.69 (d, *J* = 3.3 Hz, 1 H), 1.34 (tdd, *J* = 7.2, 6.2, 1.0 Hz, 6 H); **^{13}C NMR** (126 MHz, $CDCl_3$): δ 162.7 (d, *J* = 246.0 Hz), 135.1 (d, *J* = 3.0 Hz), 128.1 (d, *J* = 8.1 Hz), 115.5 (d, *J* = 21.5 Hz), 72.6 (d, *J* = 6.3 Hz), 72.58 (d, *J* = 5.0 Hz), 64.4 (d, *J* = 5.9 Hz), 16.2 (d, *J* = 6.5 Hz); **^{31}P NMR** (202 MHz, $CDCl_3$): δ – 0.02 (s) (contains trace excess $ClPO(OEt)_2$ at –13.2 ppm); **^{19}F NMR** (376 MHz, $CDCl_3$): δ – 114.2 (tt, *J* = 11.6, 5.7 Hz) ; **FTIR** (Cast film, cm^{-1}): 3357 (br, m), 3066 (w), 2985 (w), 1442 (w), 1256 (s), 1033 (s), 757 (w) ; **HRMS** (ESI) for $C_{12}H_{18}PO_5FNa$ $[M+Na]^+$: Calculated: 315.0774; Found: 315.0767.

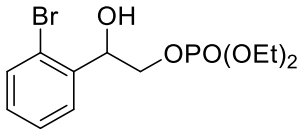

2-(2-Bromophenyl)-2-hydroxyethyl diethyl phosphate (4-19d): Prepared according to **GP4-3** from diol **4-15d** (109 mg, 0.500 mmol), catalyst **4-02** (7.3 mg, 0.050 mmol, 10 mol%), MeCN (2.5 mL), DIPEA (96 μL, 0.55 mmol, 1.1 equiv) and $ClPO(OEt)_2$ (80 μL, 0.55 mmol, 1.1 equiv). Purification by column chromatography (1:2 hexane/EtOAc) afforded the title compound as a clear oil (142 mg, 80%). **^{1}H NMR** (500 MHz, $CDCl_3$): δ 7.66 (dd, *J* = 7.8, 1.7 Hz, 1 H), 7.52 (dd, *J* = 8.0, 1.2 Hz, 1 H), 7.35 (td, *J* = 7.6, 1.3 Hz, 1 H), 7.17 (td, *J* = 7.7, 1.8 Hz, 1 H), 5.33 (dt, *J* = 8.0, 3.0 Hz, 1 H), 4.29 (td, *J* = 11.0, 2.5 Hz, 1 H), 4.22 – 4.08 (m, 4 H), 4.01 (ddd, *J* = 11.4, 9.2, 8.0 Hz, 1 H), 3.97 (d, *J* = 3.5 Hz, 1 H), 1.35 (ddd, *J* = 14.8, 7.6, 6.6 Hz, 6 H); **^{13}C NMR** (126 MHz, $CDCl_3$): δ 138.3, 132.8, 129.7, 128.5, 127.9, 122.1, 72.4 (d, *J* = 4.7 Hz), 71.2 (d, *J* = 6.0 Hz), 64.5 (d, *J* = 3.9 Hz), 64.4 (d, *J* = 4.0 Hz), 16.3 (d, *J* = 2.5 Hz), 16.2 (d, *J* = 2.6 Hz); **^{31}P NMR** (162 MHz, $CDCl_3$): δ 0.3 (s); **FTIR** (Cast film, cm^{-1}): 3363 (br, m), 2985 (m), 1605 (m), 1510 (s), 1395

(w), 1253 (s), 1221 (s), 1022 (s), 836 (m), 739 (w) ; **HRMS** (ESI) for $C_{12}H_{18}PO_5BrNa$ $[M+Na]^+$: Calculated: 374.9973; Found: 374.9969.

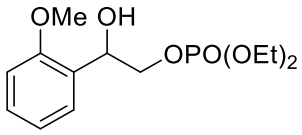

Diethyl (2-hydroxy-2-(2-methoxyphenyl)ethyl) phosphate (4-19e): Prepared according to **GP4-3** from diol **4-15e** (101 mg, 0.600 mmol), catalyst **4-02** (8.8 mg, 0.060 mmol, 10 mol%), MeCN (3.0 mL), DIPEA (116 µL, 0.660 mmol, 1.10 equiv) and $ClPO(OEt)_2$ (96 µL, 0.66 mmol, 1.1 equiv). Purification by column chromatography (1:2 hexane/EtOAc) afforded the title compound as a clear oil (133 mg, 73%). **^{1}H NMR** (500 MHz, $CDCl_3$): δ 7.48 (dd, *J* = 7.6, 1.7 Hz, 1 H), 7.27 (td, *J* = 7.8 Hz, 1 H (integral inflated by overlap with $CHCl_3$ residual signal), 6.98 (td, *J* = 7.5, 1.1 Hz, 1 H), 6.86 (dd, *J* = 8.3, 1.0 Hz, 1 H), 5.23 (dd, *J* = 7.9, 2.9 Hz, 1 H), 4.25 (ddd, *J* = 10.9, 9.5, 3.0 Hz, 1 H), 4.16 – 4.05 (m, 5 H), 3.84 (s, 3 H), 3.61 (br s, 1 H), 1.33 (dtd, *J* = 11.8, 7.1, 1.0 Hz, 7 H); **^{13}C NMR** (126 MHz, $CDCl_3$): δ 156.3, 129.1, 127.6, 127.3, 120.9, 110.3, 71.4 (d, *J* = 6.0 Hz), 69.2 (d, *J* = 5.6 Hz), 64.21 (d, *J* = 2.4 Hz), 64.16 (d, *J* = 2.5 Hz), 55.4, 16.3 (d, *J* = 1.6 Hz), 16.2 (d, *J* = 1.6 Hz); **^{31}P NMR** (162 MHz, $CDCl_3$): δ 0.03 (s) ; **FTIR** (Cast film, cm^{-1}): 3375 (br, m), 2985 (m), 1602 (w), 1491 (m), 1241 (s), 1026 (s), 985 (m), 756 (w); **HRMS** (ESI) for $C_{13}H_{21}PO_6Na$ $[M+Na]^+$: Calculated: 327.0973; Found: 327.0970.

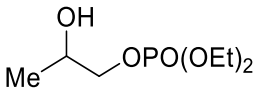

Diethyl (2-hydroxypropyl) phosphate (4-19f): Prepared according to **GP4-3** from diol **4-15f** (114 mg, 1.50 mmol), catalyst **4-02** (21.8 mg, 0.150 mmol, 10 mol%), MeCN (7.5 mL), DIPEA (288 µL, 1.65 mmol, 1.10 equiv) and $ClPO(OEt)_2$ (240 µL, 1.65 mmol, 1.10 equiv) with a reaction

time of 3 hours. Purification by column chromatography (EtOAc) afforded the title compound as a clear oil (155 mg, 49%). **^{1}H NMR** (500 MHz, $CDCl_3$): δ 4.17 – 4.11 (m, 4 H), 4.06 – 3.99 (m, 2 H), 3.87 (ddd, *J* = 10.7, 8.8, 7.5 Hz, 1 H), 2.90 (d, *J* = 3.7 Hz, 1 H), 1.35 (tt, *J* = 7.1, 1.1 Hz, 6 H), 1.19 (d, *J* = 6.4 Hz, 3 H) ; **^{13}C NMR** (126 MHz, $CDCl_3$): δ 73.0 (d, *J* = 6.0 Hz), 66.8 (d, *J* = 5.6 Hz), 64.2 (d, *J* = 5.9 Hz), 18.5, 16.3 (d, *J* = 6.6 Hz); **^{31}P NMR** (202 MHz, $CDCl_3$): δ – 0.1 (s) (trace contamination at – 0.4 ppm); **FTIR** (Cast film, cm^{-1}): 3410 (br, w), 2983 (w), 1262 (m), 1165 (w), 1035 (s), 980 (w), 820 (w); **HRMS** (ESI) for $C_7H_{17}PO_5Na$ $[M+Na]^+$: Calculated: 235.0711; Found: 235.0708.

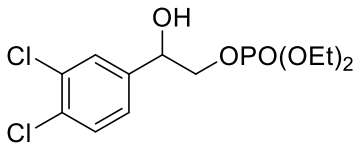

2-(3,4-Dichlorophenyl)-2-hydroxyethyl diethyl phosphate (4-19g): Prepared according to **GP4-3** from diol **4-15g** (123 mg, 0.600 mmol), catalyst **4-02** (8.8 mg, 0.060 mmol, 10 mol%), MeCN (3.0 mL), DIPEA (116 μL, 0.660 mmol, 1.10 equiv) and $ClPO(OEt)_2$ (96 μL, 0.66 mmol, 1.1 equiv). Purification by column chromatography (1:2 hexane/EtOAc) afforded the title compound as a clear oil (159 mg, 77%). **^{1}H NMR** (500 MHz, $CDCl_3$): δ 7.53 (d, *J* = 2.0 Hz, 1 H), 7.43 (d, *J* = 8.3 Hz, 1 H), 7.23 (dd, *J* = 8.2, 2.0 Hz, 1 H), 4.95 (dt, *J* = 7.1, 3.3 Hz, 1 H), 4.18 – 4.02 (m, 6 H), 3.97 (d, *J* = 3.6 Hz, 1 H), 1.34 (dtd, *J* = 8.2, 7.1, 1.0 Hz, 6 H); **^{13}C NMR** (126 MHz, $CDCl_3$): δ 139.7, 132.9, 132.2, 130.6, 128.5, 125.7, 72.3 (d, *J* = 5.9 Hz), 72.1 (d, *J* = 4.6 Hz), 64.6 (d, *J* = 6.0 Hz), 16.3 (d, *J* = 1.6 Hz), 16.2 (d, *J* = 1.7 Hz); **^{31}P NMR** (202 MHz, $CDCl_3$): δ 0.2 (s); **FTIR** (Cast film, cm^{-1}): 3349 (br, m), 2984 (w), 1565 (w), 1469 (m), 1393 (m), 1249 (m), 1024 (s), 819 (w); **HRMS** (ESI) for $C_{12}H_{17}PO_5Cl_2Na$ $[M+Na]^+$: Calculated: 365.0088; Found: 365.0081.

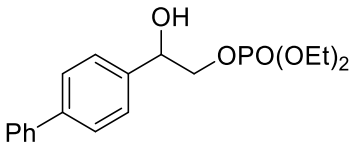

2-([1,1'-Biphenyl]-4-yl)-2-hydroxyethyl diethyl phosphate (4-19h): Prepared according to **GP4-3** from diol **4-15h** (107 mg, 0.500 mmol), catalyst **4-02** (7.3 mg, 0.050 mmol, 10 mol%), MeCN (2.5 mL), DIPEA (96 μL, 0.55 mmol, 1.1 equiv) and $ClPO(OEt)_2$ (80 μL, 0.55 mmol, 1.1 equiv). Purification by column chromatography afforded the title compound as a viscous clear oil (105 mg, 60%). **^{1}H NMR** (500 MHz, $CDCl_3$): δ 7.61 – 7.57 (t, *J* = 8.0 Hz, 4 H), 7.48 (d, *J* = 8.2 Hz, 2 H), 7.44 (t, *J* = 7.7 Hz, 2 H), 7.35 (tt, *J* = 7.5, 1.2 Hz, 1 H), 5.04 (dt, *J* = 8.1, 3.2 Hz, 1 H), 4.22 (ddd, *J* = 11.1, 9.7, 3.1 Hz, 1 H), 4.18 – 4.09 (m, 5 H), 3.63 (d, *J* = 3.3 Hz, 1 H), 1.35 (qd, *J* = 7.0, 1.0 Hz, 6 H); **^{13}C NMR** (126 MHz, $CDCl_3$): δ 141.2, 140.8, 138.3, 128.9, 127.5, 127.4, 127.2, 126.8, 73.0 (d, *J* = 5.2 Hz), 72.7 (d, *J* = 6.0 Hz), 64.4 (d, *J* = 5.9 Hz), 16.2 (d, *J* = 6.6 Hz); **^{31}P NMR** (202 MHz, $CDCl_3$): δ – 0.02 (s); **FTIR** (Cast film, cm^{-1}): 3377 (br, m), 3029 (w), 2984 (w), 1601 (w), 1487 (w), 1444 (w), 1258 (m), 1029 (s), 767 (w); **HRMS** (ESI) for $C_{18}H_{23}PO_5Na$ $[M+Na]^+$: Calculated: 373.1181; Found: 373.1174.

4.6.6 Diol Complexation Studies

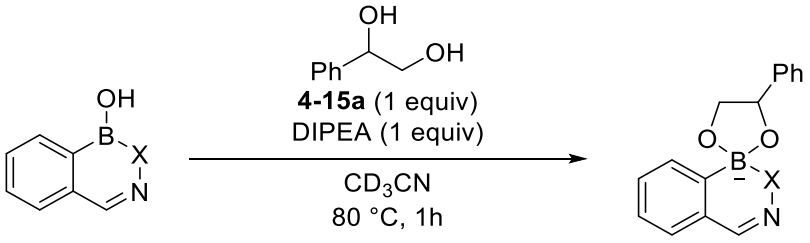

A vial was charged with diol **4-15a** (6.9, 0.050 mmol), boron heterocycle (1.0 equiv), DIPEA (9.6 μL, 1.0 equiv) and CD_3CN (0.70 mL). The vial was capped and heated to 80 °C in an aluminum heating block for one hour. After cooling to room temperature, the solution was transferred to a

quartz NMR tube for ^{11}B NMR analysis. Conversion to the corresponding tetrahedral adduct was determined using relative integrations.

4.6.7 Synthesis and Characterization of Reductive Deoxygenation Substrates

4.6.7.1 Synthesis and Characterization of Benzylic Alcohols, Ethers and Acetates

General Procedure for the synthesis of benzylic alcohols from ketones via reduction (GP4-4)

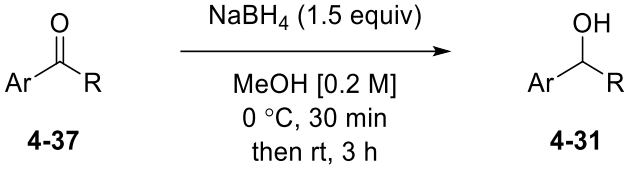

A round bottom flask equipped with a stir bar was charged with a solution of ketone (1.0 equiv) in MeOH (0.2 M). The flask was cooled in an ice bath to 0 °C, after which $NaBH_4$ (1.5 equiv) was added in two portions. The reaction mixture was stirred at 0 °C for 30 minutes, at which point the ice bath was removed and the mixture was stirred for an additional 3 hours. The reaction was quenched by addition of saturated $NH_4Cl_{(aq)}$ and concentrated by rotary evaporation to remove methanol. The mixture was extracted with EtOAc (3 × 25 mL). The combined organic phases were washed with H_2O (35 mL) and brine (35 mL), dried over Na_2SO_4, filtered, and concentrated by rotary evaporation. If necessary, purification by column chromatography was conducted to afford the desired alcohol.

General Procedure for the synthesis of benzylic alcohols via Grignard addition of PhMgBr (GP4-5)

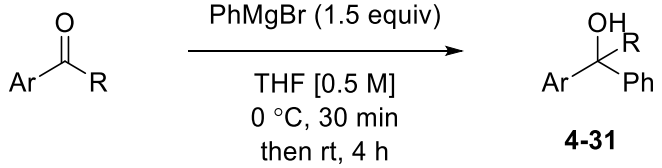

Under nitrogen, a flame-dried round bottom flask equipped with stir bar was charged with carbonyl compound (1.0 equiv) and THF (0.5 M). The solution was cooled in an ice bath to 0 °C, after which PhMgBr (1.5 equiv, 3.0 M solution in Et_2O) was added dropwise. When the addition was complete, the reaction was stirred at 0 °C for an additional 30 minutes, at which point the ice bath was removed and stirring continued for an additional 4 hours. The reaction was quenched by addition of saturated $NH_4Cl_{(aq)}$. The mixture was extracted with EtOAc (3 × 25 mL). The combined organic phases were washed with H_2O (35 mL) and brine (35 mL), dried over Na_2SO_4, filtered, and concentrated by rotary evaporation. Purification by column chromatography was conducted to afford the desired alcohol.

Benzylic alcohols **4-31a**, **4-31p** and **4-31r** were purchased from commercial suppliers and used as received. The synthesis of ether **4-34** was described in Chapter 2.

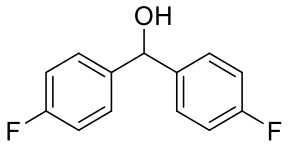

Bis(4-Fluorophenyl)methanol (4-31b): Prepared according to **GP4-4** from 4,4'-difluorobenzophenone (873 mg, 4.00 mmol). Purification by column chromatography (8:1 hexane/EtOAc) afforded the title compound as a white solid (865 mg, 99%). **^{1}H NMR** (500 MHz, $CDCl_3$): δ 7.32 (dd, *J* = 8.6, 5.5 Hz, 4 H), 7.03 (app t, *J* = 8.7 Hz, 4 H), 5.82 (d, *J* = 3.5 Hz, 1 H), 2.20 (d, *J* = 3.5 Hz, 1 H); **^{13}C NMR** (126 MHz, $CDCl_3$): δ 162.4 (d, *J* = 246.4 Hz), 139.6 (d, *J* = 3.1 Hz), 128.3 (d, *J* = 8.3 Hz), 115.6 (d, *J* = 21.4 Hz), 75.1; **^{19}F NMR** (469 MHz, $CDCl_3$): δ –114.7 (ddd, *J* = 13.8, 8.9, 5.3 Hz). Spectral data were in agreement with the literature.[98]

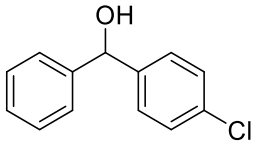

(4-Chlorophenyl)(phenyl)methanol (4-31c): Prepared according to **GP4-4** from 4-chlorobenzophenone (867 mg, 4.00 mmol). Purification by column chromatography (5:1 hexane/EtOAc) afforded the title compound as a white solid (756 mg, 86%). **^{1}H NMR** (500 MHz, $CDCl_3$): δ 7.35 (d, *J* = 4.4 Hz, 4 H), 7.33 – 7.27 (m, 5 H), 5.81 (d, *J* = 3.5 Hz, 1 H), 2.25 (d, *J* = 3.5 Hz, 1 H); **^{13}C NMR** (126 MHz, $CDCl_3$): δ 143.6, 142.4, 133.4, 128.80, 128.75, 128.0 (according to literature data, there are two overlapping carbon resonances here separated by 0.01 ppm, but separation was not observed here), 126.7, 75.8. Spectral data were in agreement with the literature.[99]

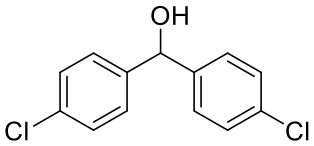

Bis(4-Chlorophenyl)methanol (4-31d): Prepared according to **GP4-4** from 4,4'-dichlorobenzophenone (1.00 g, 4.00 mmol). Purification by column chromatography (8:1 hexane/EtOAc) afforded the title compound as a white solid (820 mg, 81%). **^{1}H NMR** (600 MHz, $CDCl_3$): δ 7.32 (d, *J* = 8.6 Hz, 4 H), 7.29 (d, *J* = 8.6 Hz, 4 H), 5.79 (d, *J* = 2.9 Hz, 1 H), 2.24 (d, *J* = 3.1 Hz, 1 H); **^{13}C NMR** (151 MHz): δ 142.0, 133.8, 128.9, 128.0, 75.1. Spectral data were in agreement with the literature.[100]

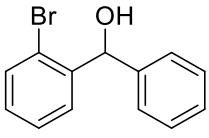

(2-Bromophenyl)(phenyl)methanol (4-31e): Prepared according to **GP4-4** from 2-bromobenzophenone (1.04 g, 4.00 mmol). Purification by column chromatography (5:1 hexane/EtOAc) afforded the title compound as a white solid (838 mg, 80%). **^{1}H NMR** (600 MHz, $CDCl_3$): δ 7.59 (dd, *J* = 7.8, 1.7 Hz, 1 H), 7.54 (dd, *J* = 8.0, 1.3 Hz, 1 H), 7.42 – 7.40 (m, 2 H), 7.36 – 7.33 (m, 3 H), 7.29 (tt, *J* = 7.3, 1.2 Hz 1 H), 7.15 (td, *J* = 7.7, 1.7 Hz, 1 H), 6.21 (d, *J* = 3.8 Hz, 1 H), 2.38 (d, *J* = 3.9 Hz, 1 H); **^{13}C NMR** (126 MHz, $CDCl_3$): δ 142.7, 142.3, 133.0, 129.2, 128.64, 128.62, 127.91, 127.86, 127.2, 123.0, 74.9. Spectral data were in agreement with the literature.[101]

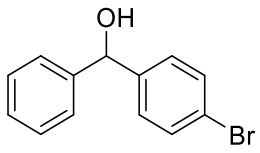

(4-Bromophenyl)(phenyl)methanol (4-31f): Prepared according to **GP4-4** from 4-bromobenzophenone (2.61 g, 10.0 mmol). Purification by column chromatography (5:1 hexane/EtOAc) afforded the title compound as a white solid (2.21 g, 84%). **^{1}H NMR** (600 MHz, $CDCl_3$): δ 7.46 (d, *J* = 8.5 Hz, 2 H), 7.36 – 7.33 (m, 4 H), 7.31 – 7.28 (m, 1 H), 7.25 (d, *J* = 8.3 Hz, 2 H), 5.76 (d, *J* = 3.2 Hz, 1 H), 2.42 (d, *J* = 3.4 Hz, 1 H); **^{13}C NMR** (151 MHz, $CDCl_3$): δ 143.5, 142.8, 131.7, 128.8, 128.3, 128.0, 126.6, 121.5, 75.7. Spectral data were in agreement with the literature.[102]

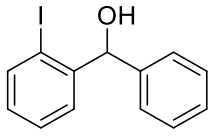

(2-Iodophenyl)(phenyl)methanol (4-31g): Prepared according to **GP4-4** from 2-iodobenzophenone (2.46 g, 8.00 mmol) afforded the title compound as a yellow oil (2.13 g, 86%).

^{1}H NMR (600 MHz, $CDCl_3$): δ 7.84 (dd, *J* = 7.9, 1.3 Hz, 1 H), 7.53 (dd, *J* = 7.8, 1.7 Hz, 1 H), 7.42 – 7.34 (m, 5 H), 7.29 (tt, *J* = 7.4, 1.4 Hz, 1 H), 7.00 (td, *J* = 7.6, 1.7 Hz, 1 H), 6.06 (d, *J* = 3.7 Hz, 1 H), 2.47 (br s, 1 H); **^{13}C NMR** (151 MHz, $CDCl_3$): δ 145.5, 142.2, 139.7, 129.6, 128.7, 128.6, 128.5, 127.9, 127.3, 98.8, 79.1. Spectral data were in agreement with the literature.[103]

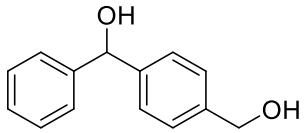

(4-(Hydroxymethyl)phenyl)(phenyl)methanol (4-31h): Under nitrogen, a flame-dried round bottom flask equipped with stir bar was charged with 4-bromobenzyl alcohol **4-20** (1.12 g, 6.00 mmol, 1.00 equiv) and THF (18 mL). The flask was cooled in a dry ice/acetone bath to – 78 °C, at which point *n*-butyllithium (4.9 mL, 2.6 M in hexanes, 13 mmol, 2.1 equiv) was added dropwise. The reaction was stirred at – 78 °C for an additional one hour, at which point a solution of benzaldehyde (735 μL, 7.20 mmol, 1.20 equiv) in THF (15 mL) was added dropwise. The reaction was stirred at – 78 °C for an additional one hour, after which the cooling bath was removed, and the reaction was stirred for an additional 2 hours while warming to room temperature. The reaction was then cooled to 0 °C and quenched with saturated $NH_4Cl_{(aq)}$ (30 mL) and extracted with EtOAc (3 × 25 mL). The combined organic layers were washed with brine (35 mL), dried over Na_2SO_4, filtered, and concentrated by rotary evaporation. Recrystallization from CH_2Cl_2/hexane afforded the title compound as a white solid (530 mg, 68%). **^{1}H NMR** (600 MHz, $CDCl_3$): δ 7.37 – 7.36 (m, 4 H), 7.34 – 7.30 (m, 4 H), 7.26 (tt, *J* = 6.5, 1.5 Hz, 1 H), 5.83 (s, 1 H), 4.64 (s, 2 H), 1.76 (br s, 2 H); **^{13}C NMR** (151 MHz): δ 143.9, 143.4, 140.3, 128.7, 127.8, 127.3, 126.9, 126.6, 76.2, 65.2. Spectral data were in agreement with the literature.[99]

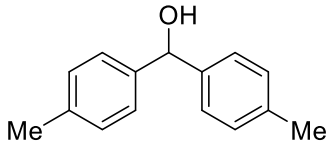

Di-p-tolylmethanol (4-31i): Prepared according to **GP4-4** from 4,4'-dimethylbenzophenone (841 mg, 4.00 mmol). Purification by column chromatography (4:1 hexane/EtOAc) afforded the title compound as a white solid (504 mg, 59%). **^{1}H NMR** (500 MHz, $CDCl_3$): δ 7.26 (d, *J* = 8.0 Hz, 4 H), 7.14 (d, *J* = 7.8 Hz, 4 H), 5.79 (d, *J* = 3.0 Hz, 1 H), 2.33 (s, 6 H), 2.14 (d, *J* = 3.3 Hz, 1 H); **^{13}C NMR** (126 MHz, $CDCl_3$): δ 141.3, 137.3, 129.3, 126.6, 76.1, 21.2. Spectral data were in agreement with the literature.[104]

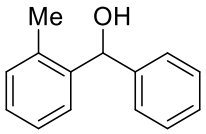

Phenyl(o-tolyl)methanol (4-31j): Prepared according to **GP4-4** from 2-methylbenzophenone (1.81 mL, 10.0 mmol). Purification by column chromatography (8:1 hexane/EtOAc) afforded the title compound as a white solid (1.53 g, 77%). **^{1}H NMR** (500 MHz, $CDCl_3$): δ 7.53 (dd, *J* = 7.6, 1.6 Hz, 1 H), 7.34 (d, *J* = 4.4 Hz, 4 H), 7.30 – 7.24 (m, 2 H), 7.22 (td, *J* = 7.4, 1.6 Hz, 1 H), 7.16 (d, *J* = 6.8 Hz, 1 H), 6.02 (d, *J* = 3.3 Hz, 1 H), 2.27 (s, 3 H), 2.15 (d, *J* = 3.6 Hz, 1 H); **^{13}C NMR** (126 MHz, $CDCl_3$): δ 143.0, 141.6, 135.5, 130.7, 128.6, 127.71, 127.68, 127.2, 126.4, 126.3. Spectral data were in agreement with the literature.[99]

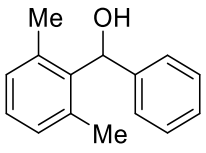

(2,6-Dimethylphenyl)(phenyl)methanol (4-31k): Prepared according to **GP4-5** from 2,6-dimethylbenzaldehyde (537 mg, 4.00 mmol). Purification by column chromatography (10:1

hexane/EtOAc) afforded the title compound as a white solid (734 mg, 86%). **^{1}H NMR** (500 MHz, $CDCl_3$): δ 7.33 – 7.22 (m, 5 H), 7.14 (dd, *J* = 8.1, 6.9 Hz, 1 H), 7.05 (d, *J* = 7.5 Hz, 2 H), 6.38 (d, *J* = 4.2 Hz, 1 H), 2.29 (s, 6 H), 2.19 (d, *J* = 4.2 Hz, 1 H); **^{13}C NMR** (126 MHz, $CDCl_3$): δ 143.0, 139.5, 137.3, 129.5, 128.3, 127.9, 126.7, 125.6, 71.4, 20.8. Spectral data were in agreement with the literature.[105]

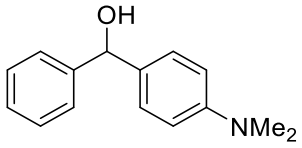

(4-(Dimethylamino)phenyl)(phenyl)methanol (4-31l): Prepared according to **GP4-5** from 4-(dimethylamino)benzaldehyde (597 mg, 4.00 mmol). Purification by column chromatography (gradient 7:1 to 4:1 hexane/EtOAc) afforded the title compound as a yellow oil that solidifies in the freezer to a white solid (795 mg, 88%). **^{1}H NMR** (600 MHz, $CDCl_3$): δ 7.40 (d, *J* = 7.7 Hz, 2 H), 7.33 (td, *J* = 7.6, 1.6 Hz, 2 H), 7.26 – 7.20 (m, 3 H), 6.70 (d, *J* = 8.8 Hz, 2 H), 5.78 (s, 1 H), 2.93 (s, 2 H), 2.10 (br s, 1 H); **^{13}C NMR** (151 MHz, $CDCl_3$): δ 150.3, 144.4, 132.1, 128.4, 127.9, 127.3, 126.5, 112.6, 76.1, 40.7. Spectral data were in agreement with the literature.[106]

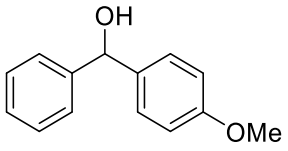

(4-Methoxyphenyl)(phenyl)methanol (4-31m): Prepared according to **GP4-4** from 4-methoxybenzophenone (1.27 g, 6.0 mmol). Purification by column chromatography (2:1 hexane/EtOAc) afforded the title compound as a white solid (1.02 g, 78%). **^{1}H NMR** (500 MHz, $CDCl_3$): δ 7.39 – 7.32 (m, 4 H), 7.31 – 7.25 (m, 3 H), 6.87 (d, *J* = 8.7 Hz, 2 H), 5.81 (d, *J* = 3.5

Hz, 1 H), 3.80 (s, 3 H), 2.17 (d, *J* = 3.5 Hz, 1 H); **^{13}C NMR** (126 MHz): δ 159.2, 144.2, 136.3, 128.6, 128.0, 127.6, 126.5, 114.0, 76.0, 55.4. Spectral data were in agreement with the literature.[99]

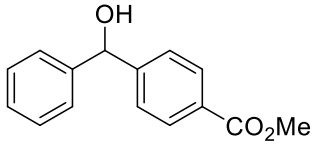

Methyl 4-(hydroxy(phenyl)methyl)benzoate (4-31n): Prepared according to **GP4-5** from methyl 4-formylbenzoate (657 mg, 4.00 mmol). Purification by column chromatography (4:1 hexane/EtOAc) afforded the title compound as a white solid (727 mg, 75%). **^{1}H NMR** (500 MHz, $CDCl_3$): δ 8.00 (d, *J* = 8.3 Hz, 2 H), 7.46 (d, *J* = 8.2 Hz, 2 H), 7.37 – 7.27 (m, 5 H), 5.87 (d, *J* = 3.1 Hz, 1 H), 3.89 (d, *J* = 0.5 Hz, 3 H), 2.42 (d, *J* = 3.3 Hz, 1 H); **^{13}C NMR** (126 MHz, $CDCl_3$): δ 167.0, 148.8, 143.4, 129.9, 129.4, 128.8, 128.1, 126.8, 126.5, 76.1, 52.2. Spectral data were in agreement with the literature.[107]

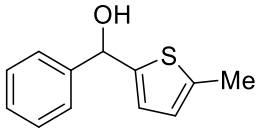

(5-Methylthiophen-2-yl)(phenyl)methanol (4-31o): Prepared according to **GP4-5** from 5-methyl-2-thiophenecarboxaldehyde (430 μL, 4.00 mmol). Purification by column chromatography (9:1 hexane/EtOAc) afforded the title compound as a white solid (693 mg, 85%). **^{1}H NMR** (500 MHz, $CDCl_3$): δ 7.46 – 7.44 (m, 2 H), 7.39 – 7.35 (m, 2 H), 7.30 (tt, *J* = 7.3, 1.3 Hz, 1 H), 6.68 (dd, *J* = 3.5, 0.9 Hz, 1 H), 6.58 (dq, *J* = 3.4, 1.1 Hz, 1 H), 5.97 (d, *J* = 3.7 Hz, 1 H), 2.44 (d, *J* = 1.0 Hz, 3 H), 2.32 (d, *J* = 3.9 Hz, 1 H); **^{13}C NMR** (126 MHz, $CDCl_3$): δ 145.8, 143.3, 140.4, 128.6, 128.0, 126.3, 125.1, 124.8, 72.6, 15.5. Spectral data were in agreement with the literature.[108]

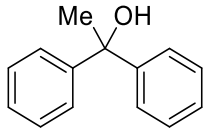

1,1-Diphenylethanol (4-31q): Under nitrogen, a flame-dried round bottom flask equipped with stir bar was charged with benzophenone (728 mg, 4.00 mmol) and THF (12 mL). The solution was cooled to 0 °C in an ice bath, after which MeLi (5.0 mL, 1.6 M solution in Et_2O, 8.0 mmol, 2.0 equiv) was added dropwise. The resulting orange solution was stirred for 2 hours at 0 °C, at which point the ice bath was removed and stirring continued for an additional 18 hours. The reaction was cooled back to 0 °C and quenched by slow addition of saturated $NH_4Cl_{(aq)}$ (30 mL). The mixture was extracted with EtOAc (3 × 25 mL). The combined organic phases were washed with H_2O (35 mL) and brine (35 mL), dried over Na_2SO_4, filtered, and concentrated by rotary evaporation. Purification by column chromatography (7:1 hexane/EtOAc) afforded the title compound as a white solid (620 mg, 78%). **^{1}H NMR** (500 MHz, $CDCl_3$): δ 7.45 – 7.43 (m, 4 H), 7.34 (t, *J* = 7.6 Hz, 4 H), 7.26 (tt, *J* = 6.7, 1.3 Hz, 2 H), 2.19 (s, 1 H), 1.98 (s, 3 H); **^{13}C NMR** (126 MHz, $CDCl_3$): δ 148.1, 128.3, 127.1, 126.0, 76.4, 31.0. Spectral data were in agreement with the literature.[109]

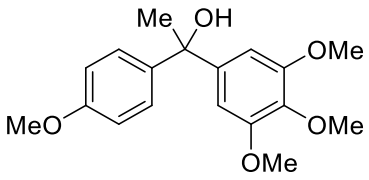

1-(4-Methoxyphenyl)-1-(3,4,5-trimethoxyphenyl)ethanol (4-31s): Under nitrogen, a flame-dried 50 mL round bottom flask equipped with stir bar was charged with 4-iodoanisole (1.12 g, 4.80 mmol, 1.20 equiv) and THF (8 mL). To this solution was added *i*-PrMgCl (2.4 mL, 2.0 M solution in THF, 4.8 mmol, 1.2 equiv) dropwise at room temperature, which caused a color change from purple to yellow. After addition was complete the mixture was stirred at room temperature

for an additional 1 hour, at which point a solution of 3,4,5-trimethoxyacetophenone (841 mg, 4.00 mmol, 1.00 equiv) in THF (5 mL) was added dropwise. The resulting solution was stirred at room temperature for 14 hours, during which time it turned orange in color. The reaction was then cooled in an ice bath to 0 °C and quenched by slow addition of saturated $NH_4Cl_{(aq)}$ (30 mL). The mixture was extracted with EtOAc (3 × 25 mL). The combined organic phases were washed with H_2O (35 mL) and brine (35 mL), dried over Na_2SO_4, filtered, and concentrated by rotary evaporation. Purification by column chromatography (2:1 hexane/EtOAc) afforded the title compound as a clear oil (337 mg, 27%); **^{1}H NMR** (600 MHz, $CDCl_3$): δ 7.33 (d, *J* = 8.9 Hz, 2 H), 6.85 (d, *J* = 8.9 Hz, 2 H), 6.62 (s, 2 H), 3.83 (s, 3 H), 3.80 (s, 6 H), 3.80 (s, 3 H), 2.18 (s, 1 H), 1.91 (s, 3 H); **^{13}C NMR** (151 MHz, $CDCl_3$): δ 158.7, 152.9, 144.2, 140.2, 137.0, 127.2, 113.6, 103.4, 76.2, 60.9, 56.3, 55.4, 31.3; **FTIR** (cast film, cm^{-1}): 3474 (br, m), 2936 (m), 1590 (m), 1510 (s), 1413 (m), 1247 (m), 1125 (s), 1031 (w), 835 (w); **HRMS** (ESI) for $C_{18}H_{22}O_5Na$ $[M+Na]^+$: Calculated 341.1365; Found: 341.1363.

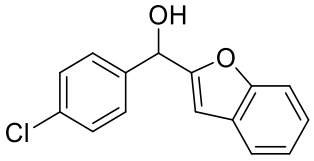

Benzofuran-2-yl(4-chlorophenyl)methanol (Cloridarol) (4-31t): Under nitrogen, a flame-dried 50 mL round bottom flask equipped with stir bar was charged with 1-chloro-4-iodobenzene (1.33 g, 5.60 mmol, 1.40 equiv) and THF (20 mL). The solution was cooled to –78 °C in a dry ice/acetone bath, after which *n*-BuLi (2.1 mL, 1.3 equiv, 2.5 M solution in hexanes) was added dropwise. When addition was complete, the reaction was stirred at –78 °C for 1 hour, at which point a solution of 2-benzofurancarboxaldehyde (585 mg, 4.00 mmol, 1.00 equiv) in THF (6.6 mL) was added dropwise. Following addition of the aldehyde solution, the reaction was stirred at –78 °C for an

additional 15 minutes, at which point the cooling bath was removed and stirring continued for an additional 3 hours. The reaction was then cooled to 0 °C and quenched by slow addition of saturated $NH_4Cl_{(aq)}$ (30 mL). The mixture was extracted with EtOAc (3 × 25 mL). The combined organic phases were washed with H_2O (35 mL) and brine (35 mL), dried over Na_2SO_4, filtered, and concentrated by rotary evaporation. Purification by column chromatography (5:1 hexane/EtOAc) afforded the title compound as a thick yellow oil (696 mg, 67%). **^{1}H NMR** (700 MHz, $CDCl_3$): δ 7.52 (app d, *J* = 8.5 Hz, 3 H), 7.44 (d, *J* = 8.5 Hz, 2 H), 7.27 (td, *J* = 7.2, 1.3 Hz, 1 H), 7.21 (td, *J* = 7.5, 1.1 Hz, 1 H), 6.53 (s, 1 H), 5.94 (d, *J* = 4.5 Hz, 1 H), 2.50 (d, *J* = 4.5 Jz, 1 H); **^{13}C NMR** (151 MHz, $CDCl_3$): δ 158.1, 155.2, 138.8, 134.3, 128.9, 128.3, 128.0, 124.7, 123.1, 121.4, 111.5, 104.4, 70.1. Spectral data were in agreement with the literature.[110]

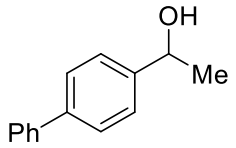

1-([1,1'-Biphenyl]-4-yl)ethanol (4-31u): Prepared according to **GP4-4** from 4-acetylbiphenyl (1.96 g, 10.0 mmol). Purification by column chromatography (6:1 hexane/EtOAc) afforded the title compound as a white solid (1.61 g, 81%). **^{1}H NMR** (500 MHz, $CDCl_3$): δ 7.60 – 7.57 (m, 4 H), 7.47 – 7.43 (m, 4 H), 7.35 (tt, *J* = 7.4, 1.2 Hz, 1 H), 4.96 (q, *J* = 6.5 Hz, 1 H), 1.80 (br s, 1 H), 1.55 (d, *J* = 6.4 Hz, 3 H); ^{13}C NMR (126 MHz, $CDCl_3$): δ 145.0, 141.0, 140.6, 128.9, 127.4, 127.2, 126.0, 70.3, 25.3. Spectral data were in agreement with the literature, which also observed only seven aromatic ^{13}C resonances due to overlap.[111]

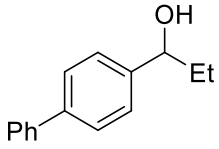

1-([1,1'-Biphenyl]-4-yl)propan-1-ol (4-31v): Under nitrogen, a flame-dried 50 mL round bottom flask equipped with stir bar was charged with 4-biphenylcarboxaldehyde (728 mg, 4.00 mmol) and THF (8 mL). The solution was cooled to 0 °C in an ice bath, at which point EtMgBr (2.0 mL, 1.5 equiv, 3.0 M solution in Et_2O) was added dropwise. The reaction was stirred at 0 °C for 30 minutes, at which point the ice bath was removed and stirring continued for an additional 3 hours. The reaction was quenched by addition of saturated $NH_4Cl_{(aq)}$. The mixture was extracted with EtOAc (3 × 25 mL). The combined organic phases were washed with H_2O (35 mL) and brine (35 mL), dried over Na_2SO_4, filtered, and concentrated by rotary evaporation. Purification by column chromatography (9:1 hexane/EtOAc) afforded the title compound as a white solid (619 mg, 73%). **^{1}H NMR** (500 MHz, $CDCl_3$): δ 7.61 – 7.58 (m, 4 H), 7.46 – 7.41 (m, 4 H), 7.35 (tt, *J* = 7.4, 1.3 Hz, 1 H), 4.66 (td, *J* = 6.6, 3.3 Hz, 1 H), 1.92 – 1.76 (m, 3 H), 0.97 (t, 7.4 Hz, 3 H); **^{13}C NMR** (126 MHz, $CDCl_3$): δ 143.8, 141.0, 140.6, 128.9, 127.4, 127.3, 127.2, 126.6, 75.9, 32.0, 10.3. Spectral data were in agreement with the literature.[112]

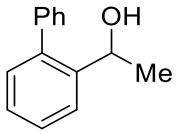

1-([1,1'-Biphenyl]-2-yl)ethanol (4-31w): Under nitrogen, a flame-dried 50 mL round bottom flask equipped with stir bar was charged with 2-biphenylcarboxaldehyde (645 µL, 4.00 mmol) and THF (8 mL). The solution was cooled to 0 °C in an ice bath, after which MeMgCl (2.0 mL, 1.5 equiv, 3.0 M solution in THF) was added dropwise. When the addition was complete, the reaction was stirred at 0 °C for 30 minutes, at which point the cooling bath was removed and stirring continued for an additional 3 hours. The reaction was quenched by addition of saturated $NH_4Cl_{(aq)}$. The mixture was extracted with EtOAc (3 × 25 mL). The combined organic phases were washed

with H_2O (35 mL) and brine (35 mL), dried over Na_2SO_4, filtered, and concentrated by rotary evaporation. Purification by column chromatography (10:1 hexane/EtOAc) afforded the title compound as am off-white solid (571 mg, 72%). **^{1}H NMR** (500 MHz, $CDCl_3$): δ 7.68 (dd, *J* = 7.9, 1.4 Hz, 1 H), 7.44 – 7.41 (m, 3 H), 7.39 – 7.35 (m, 1 H),7.34 – 7.30 (m, 3 H), 7.22 (dd, *J* = 7.6, 1.4 Hz, 1 H), 4.99 (q, *J* = 6.4 Hz, 1 H), 1.70 (s, 1 H), 1.42 (d, *J* = 6.4 Hz, 3 H); **^{13}C NMR** (126 MHz, $CDCl_3$): δ 143.2, 141.1, 140.5, 130.1, 129.4, 128.3, 127.3, 127.2, 125.5, 66.6, 25.0. Spectral data were in agreement with the literature.[113]

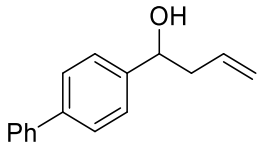

1-([1,1'-Biphenyl]-4-yl)but-3-en-1-ol (4-31x): Under nitrogen, a flame-dried 50 mL round bottom flask equipped with stir bar was charged with 4-biphenylcarboxaldehyde (728 mg, 4.00 mmol) and THF (12 mL). The solution was cooled to 0 °C in an ice bath, after which allylmagnesium chloride (3.0 mL, 1.5 equiv, 2.0 M solution in THF) was added dropwise. When the addition was complete, the reaction was stirred at 0 °C for 30 minutes, at which point the cooling bath was removed and stirring continued for an additional 3 hours. The reaction was quenched by addition of saturated $NH_4Cl_{(aq)}$. The mixture was extracted with EtOAc (3 × 25 mL). The combined organic phases were washed with H_2O (35 mL) and brine (35 mL), dried over Na_2SO_4, filtered, and concentrated by rotary evaporation. Purification by column chromatography (9:1 hexane/EtOAc) afforded the title compound as a white solid (592 mg, 66%). **^{1}H NMR** (500 MHz, $CDCl_3$): δ 7.61 – 7.58 (m, 4 H), 7.46 – 7.43 (m, 4 H), 7.35 (tt, *J* = 6.8, 1.2 Hz, 1 H), 5.86 (dddd, *J* = 16.9, 10.2, 7.6, 6.5 Hz, 1 H), 5.23 – 5.16 (m, 2 H), 4.80 (ddd, *J* = 8.1, 5.0, 3.2 Hz, 1 H), 2.62 – 2.51 (m, 2 H), 2.07 (d, *J* = 3.2 Hz, 1 H); **^{13}C NMR** (126 MHz, $CDCl_3$): δ 143.0, 141.0,

140.6, 134.6, 128.9, 127.4, 127.3, 127.2, 126.4, 118.7, 73.2, 44.0. Spectral data were in agreement with the literature.[114]

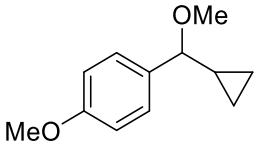

1-(Cyclopropyl(methoxy)methyl)-4-methoxybenzene (4-31y): Prepared according to **GP4-4** from cyclopropyl 4-methoxyphenyl ketone (705 mg, 4.0 mmol), where 1M $HCl_{(aq)}$ was used to quench the reaction rather than $NH_4Cl_{(aq)}$. Purification by column chromatography (7:1 hexane/EtOAc) afforded the title compound as a clear oil (613 mg, 80%). **^{1}H NMR** (500 MHz, $CDCl_3$): δ 7.24 (d, *J* = 8.4 Hz, 2 H), 6.89 (d, *J* = 8.7 Hz, 2 H), 3.81 (s, 3 H), 3.50 (d, 7.9 Hz, 1 H), 3.23 (s, 3 H), 1.19 – 1.12 (m, 1 H), 0.66 – 0.61 (m, 1 H), 0.46 – 0.40 (m, 2 H), 0.25 – 0.19 (m, 1 H); **^{13}C NMR** (126 MHz, $CDCl_3$): δ 159.2, 134.0, 128.1, 113.8, 87.4, 56.0, 55.4, 17.7, 4.4, 1.9. Spectral data were in agreement with the literature.[115]

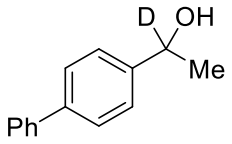

(92% D incorporation)

1-([1,1'-Biphenyl]-4-yl)-1-deuteroethanol (4-31z): Prepared according to **GP4-4** from 4-acetylbiphenyl (785 mg, 4.00 mmol) and $NaBD_4$ (252 mg, 6.00 mmol, 1.50 equiv). Purification by column chromatography (3:1 hexane/EtOAc) afforded the title compound as a white solid (669 mg, 84%). **^{1}H NMR** (500 MHz, $CDCl_3$): δ 7.61 – 7.57 (m, 4 H), 7.47 – 7.43 (m, 4 H), 7.35 (tt, *J* = 6.8, 1.2 Hz, 1 H), 1.80 (s, 1 H), 1.54 (s, 3 H); **^{13}C NMR** (126 MHz, $CDCl_3$): δ 144.9, 141.0, 140.6, 128.9, 127.4, 127.3, 127.2, 126.0, 69.9 (1:1:1 t, *J* = 21.9 Hz), 25.2. Additional resonances are observed from the 8% of non-deuterium labelled analog **4-31u** in ^{1}H NMR (4.96 ppm, q, *J* =

6.5 Hz, 0.09 H corresponding to the benzylic proton) and ^{13}C NMR (25.3 ppm and 70.3 ppm, corresponding to the methyl and benzylic carbons respectively). Spectral data were in agreement with the literature.[116]

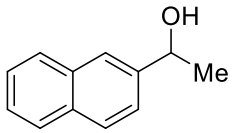

1-(Naphthalen-2-yl)ethanol (4-31aa): Prepared according to **GP4-4** from 2-acetylnaphthalene (851 mg, 5.00 mmol). Purification by column chromatography (5:1 hexane/EtOAc) afforded the title compound as a white solid (759 mg, 88%). **^{1}H NMR** (500 MHz, $CDCl_3$): δ 7.85 – 7.81 (m, 4 H), 7.51 (dd, *J* = 8.7, 1.8 Hz, 1 H), 7.49 – 7.45 (m, 2 H), 5.07 (qd, *J* = 6.5, 2.3 Hz, 1 H), 1.94 (d, *J* = 2.4 Hz, 1 H), 1.59 (d, *J* = 6.5 Hz, 3 H); **^{13}C NMR** (126 MHz, $CDCl_3$): δ 143.3, 133.5, 133.1, 128.5, 128.1, 127.8, 126.3, 125.9, 123.96, 123.95, 70.7, 25.3. Spectral data were in agreement with the literature.[106]

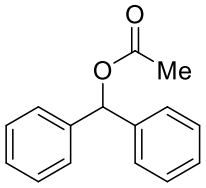

Benzhydryl acetate (4-33): Under nitrogen, a flame-dried 50 mL round bottom flask equipped with a stir bar was charged with diphenylmethanol (921 mg, 5.00 mmol), CH_2Cl_2 (5 mL) and triethylamine (1.40 mL, 10.0 mmol, 2.00 equiv). The solution was cooled to 0 °C in an ice bath, after which acetic anhydride (0.500 mL, 5.25 mmol, 1.05 equiv) was added dropwise. After addition was complete, 4-(dimethylamino)pyridine (30.5 mg, 0.250 mmol, 5 mol%) was added in one portion. The reaction was stirred at 0 °C for 30 minutes, at which point the cooling bath was removed and stirring continued for an additional 16 hours. The reaction was diluted with additional

CH_2Cl_2 and washed with saturated $NaHCO_{3(aq)}$ (3 × 25 mL), H_2O (35 mL) and brine (35 mL), dried over Na_2SO_4, filtered, and concentrated by rotary evaporation. Purification by column chromatography (4:1 hexane/EtOAc) afforded the title compound as a white solid (796 mg, 70%). **^{1}H NMR** (600 MHz, $CDCl_3$): δ 7.37 – 7.34 (m, 8 H), 7.31 – 7.28 (m, 2 H), 6.91 (s, 1 H), 2.18 (s, 3 H). Spectral data were in agreement with the literature.[117]

4.6.7.2 Synthesis and Characterization of Benzylic Ketones

Ketones **4-37a**, **4-37b**, **4-37e**, **4-37u**, **4-37aa**, **4-37ae**, **4-37af**, **4-37ag**, **4-37ah**, **4-37ai** (fenofibrate) and **4-37aj** (ketoprofen) were purchased from commercial suppliers and used as received.

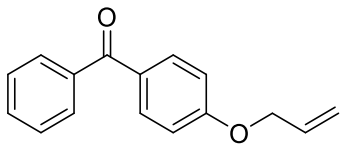

(4-(Allyloxy)phenyl)(phenyl)methanone (4-37ab): Under nitrogen, a flame-dried 50 mL round bottom flask equipped with stir bar was charged with 4-hydroxybenzophenone (991 mg, 5.00 mmol), K_2CO_3 (1.38 g, 10.0 mmol, 2.00 equiv), KI (41 mg, 0.25 mmol, 5 mol%) and acetone (20 mL). The resulting suspension was stirred at room temperature for 5 minutes, after which allyl bromide (866 μL, 10.0 mmol, 2.00 equiv) was added via syringe. The mixture was then heated to reflux (66 °C) for 4 hours. The reaction was then cooled to room temperature and concentrated by rotary evaporation. The mixture was taken up in 30 mL CH_2Cl_2 and washed with H_2O (15 mL), 1 M $NaOH_{(aq)}$ (3 × 10 mL) and brine (20 mL). The organic phase was dried over Na_2SO_4, filtered, and concentrated by rotary evaporation. Purification by column chromatography (gradient 1:3 to 1:10 hexane/CH_2Cl_2) afforded the title compound as a white solid (862 mg, 72%). **^{1}H NMR** (500 MHz, $CDCl_3$): δ 7.82 (d, J = 9.0 Hz, 2 H), 7.77 – 7.75 (m, 2 H), 7.56 (tt, J = 6.7, 1.3 Hz, 1 H), 7.49 – 7.46 (m, 2 H), 6.98 (d, J = 8.9 Hz, 2 H), 6.07 (ddt, J = 17.2, 10.5, 5.3 Hz, 1 H), 5.44 (dq, J =

17.3, 1.6 Hz, 1 H), 5.33 (dq, *J* = 10.5, 1.4 Hz, 1 H), 4.62 (dt, *J* = 5.3, 1.5 Hz, 2 H); **^{13}C NMR** (126 MHz): δ 195.6, 162.4, 138.4, 132.68. 132.66, 132.0, 130.4, 129.9, 128.3, 118.3, 114.4, 69.1. Spectral data were in agreement with the literature.[118]

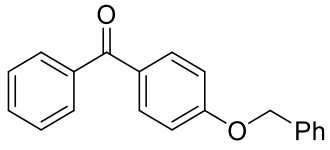

(4-(Benzyloxy)phenyl)(phenyl)methanone (4-37ac): Under nitrogen, a flame-dried 50 mL round bottom flask equipped with stir bar was charged with 4-hydroxybenzophenone (793 mg, 4.00 mmol), K_2CO_3 (1.11 g, 8.0 mmol, 2.00 equiv), KI (33 mg, 0.20 mmol, 5 mol%) and acetone (16 mL). The resulting suspension was stirred at room temperature for 5 minutes, after which benzyl bromide (950 μL, 8.0 mmol, 2.00 equiv) was added via syringe. The mixture was heated to reflux (66 °C) for 4 hours. The reaction was then cooled to room temperature and concentrated by rotary evaporation. The mixture was taken up in 30 mL CH_2Cl_2 and washed with H_2O (15 mL), 1 M $NaOH_{(aq)}$ (3 × 10 mL) and brine (20 mL). The organic phase was dried over Na_2SO_4, filtered, and concentrated by rotary evaporation. Purification by column chromatography (gradient 1:3 to 1:10 hexane/CH_2Cl_2) afforded the title compound as a white solid (667 mg, 58%). **^{1}H NMR** (500 MHz, $CDCl_3$): δ 7.83 (d, *J* = 9.0 Hz, 2 H), 7.77 – 7.75 (m, 2 H), 7.57 (tt, *J* = 7.5, 1.3 Hz, 1 H), 7.49 – 7.39 (m, 6 H), 7.35 (tt, *J* = 7.2, 1.6 Hz, 1 H), 7.04 (d, *J* = 8.9 Hz, 2 H), 5.16 (s, 2 H); **^{13}C NMR** (126 MHz, $CDCl_3$) δ 195.7, 162.5, 138.4, 136.4, 132.7, 132.0, 130.5, 129.9, 128.9, 128.4, 128.3, 127.6, 114.6, 70.3. Spectral data were in agreement with the literature.[119]

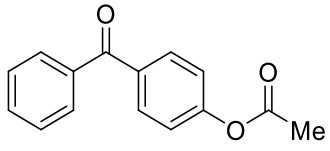

4-Benzoylphenyl acetate (4-37ad): Under nitrogen, a flame-dried 100 mL round bottom flask equipped with stir bar was charged with 4-hydroxyphenol (968 mg, 4.80 mmol), CH_2Cl_2 (25 mL), triethylamine (1.4 mL, 9.6 mmol, 2.0 equiv) and acetyl chloride (512 μL, 7.2 mmol, 1.5 equiv). The mixture was heated to reflux (39 °C) for 12 hours. The reaction was then cooled to room temperature and diluted with CH_2Cl_2 (20 mL). The reaction was washed with H_2O (2 × 20 mL), saturated $NaHCO_{3(aq)}$ (2 × 25 mL) and brine (25 mL). The organic phase was dried over Na_2SO_4, filtered, and concentrated by rotary evaporation. Purification by column chromatography (5:1 hexane/EtOAc) afforded the title compound as a white solid (976 mg, 85%). **^{1}H NMR** (500 MHz, $CDCl_3$): δ 7.86 (d, *J* = 8.9 Hz, 2 H), 7.81 – 7.79 (dd, *J* = 8.3, 1.4 Hz, 2 H), 7.59 (tt, *J* = 7.5, 1.84 Hz, 1 H), 7.49 (t, *J* = 7.7 Hz, 2 H), 7.22 (d, *J* = 8.7 Hz, 2 H), 2.34 (s, 3 H); **^{13}C NMR** (126 MHz, $CDCl_3$): δ 195.7, 169.1, 154.0, 137.7, 135.2, 132.6, 131.8, 130.1, 128.5, 121.7, 21.3. Spectral data were in agreement with the literature.[120]

4.6.8 Reductive Deoxygenation – Optimization

4.6.8.1 Optimization of Reductive Deoxygenation of Benzylic Alcohols

General Procedure for the reductive deoxygenation of alcohols using NMR yields (GP4-6)

A vial equipped with a stir bar was charged with alcohol **4-31a** (27.6 mg, 0.150 mmol), catalyst **4-30** (X mol%), triethylsilane (26 μL, 0.16 mmol, 1.1 equiv) and solvent. The vial was capped and stirred at room temperature for the indicated time, after which it was diluted with $CHCl_3$ and filtered through a small pipette of silica (approximately 1 cm high) with $CHCl_3$ washings to remove insoluble components. The mixture was concentrated by rotary evaporation, and yields were obtained by ^{1}H NMR relative to 1,3,5-trimethoxybenzene as an internal standard.

4.6.8.2 Optimization of Reductive Deoxygenation of Benzylic Ketones

General Procedure for the reductive deoxygenation of ketones using NMR yields (GP4-7)

A vial equipped with a stir bar was charged with ketone **4-37a** (27.6 mg, 0.150 mmol), catalyst **4-30** (X mol%), silane (Y equiv) and solvent. The vial was capped and stirred at room temperature for the indicated time, after which it was diluted with $CHCl_3$ and filtered through a small pipette of silica (approximately 1 cm high) with $CHCl_3$ washings to remove insoluble components. The mixture was concentrated by rotary evaporation, and yields were obtained by ^1H NMR relative to 1,3,5-trimethoxybenzene as an internal standard.

4.6.9 Reductive Deoxygenation – Substrate Scope

4.6.9.1 Reductive Deoxygenation of Benzylic Alcohols

General Procedure for the reductive deoxygenation of benzylic alcohols (GP4-8)

A vial equipped with a stir bar was charged with alcohol **4-31**, catalyst **4-30** (0.1–5 mol%), triethylsilane (1.1 equiv), HFIP and $MeNO_2$ (4:1 ratio, 2.0 M in alcohol **4-31**). The reaction was stirred at room temperature for the indicated time, after which it was concentrated by rotary evaporation. Purification by column chromatography afforded the reduction product **4-32**.

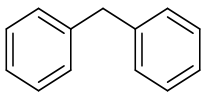

Diphenylmethane (4-32a): Prepared according to **GP4-8** from alcohol **4-31a** (2.02 g, 11.0 mmol), catalyst **4-30** (22.0 mg, 0.110 mmol, 1 mol%) and triethylsilane (1.94 mL, 12.1 mmol, 1.10 equiv) for 90 minutes. Purification by column chromatography (hexane) afforded the title compound as a clear oil (1.73 g, 94%). **^{1}H NMR** (500 MHz, $CDCl_3$): δ 7.32 – 7.28 (m, 4 H), 7.23 – 7.20 (m, 6

H), 4.00 (s, 2 H); **^{13}C NMR** (126 MHz, $CDCl_3$): δ 141.3, 129.1, 128.6, 126.2, 42.1. Spectral data were in agreement with the literature.[121]

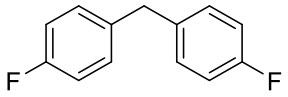

Bis(4-fluorophenyl)methane (4-32b): Prepared according to **GP4-8** from alcohol **4-31b** (220 mg, 1.00 mmol), catalyst **4-30** (2.0 mg, 0.010 mmol, 1 mol%) and triethylsilane (176 μL, 1.10 mmol, 1.10 equiv) for 90 minutes. Purification by column chromatography (hexane) afforded the title compound as a clear oil (138 mg, 68%). **^{1}H NMR** (500 MHz, $CDCl_3$): δ 7.12 (dd, *J* = 8.8, 5.4 Hz, 4 H), 6.98 (app t, *J* = 8.7 Hz, 4 H), 3.93 (s, 2 H); **^{13}C NMR** (126 MHz, $CDCl_3$): δ 161.6 (d, *J*= 244.2 Hz), 136.7 (d, *J* = 3.5 Hz), 130.3 (d, *J* = 8.1 Hz), 115.4 (d, *J* = 21.0 Hz), 40.4; **^{19}F NMR** (376 MHz, $CDCl_3$): δ – 117.1 (tt, *J* = 9.1, 5.3 Hz). Spectral data were in agreement with the literature.[122]

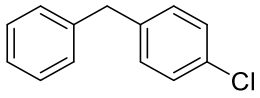

1-Benzyl-4-chlorobenzene (4-32c): Prepared according to **GP4-8** from alcohol **4-31c** (218 mg, 1.00 mmol), catalyst **4-30** (2.0 mg, 0.010 mmol, 1 mol%) and triethylsilane (176 μL, 1.10 mmol, 1.10 equiv) for 90 minutes. Purification by column chromatography (hexane) afforded the title compound as a clear oil (164 mg, 81%). **^{1}H NMR** (500 MHz, $CDCl_3$): δ 7.33 (t, *J* = 7.2 Hz, 2 H), 7.29 (d, *J* = 8.6 Hz, 2 H), 7.25 (tt, *J* = 7.5, 1.4 Hz, 1 H), 7.20 (dd, *J* = 7.6, 0.7 Hz, 2 H), 7.16 (d, *J* = 8.4 Hz, 2 H), 3.99 (s, 2 H); **^{13}C NMR** (126 MHz, $CDCl_3$): δ 140.7, 139.7, 132.0, 130.4, 129.0, 128.7, 126.4, 41.4. Spectral data were in agreement with the literature.[121]

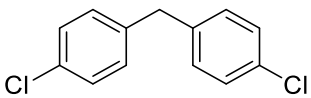

Bis(4-chlorophenyl)methane (4-32d): Prepared according to **GP4-8** from alcohol **4-31d** (253 mg, 1.00 mmol), catalyst **4-30** (2.0 mg, 0.010 mmol, 1 mol%) and triethylsilane (176 μL, 1.10 mmol, 1.10 equiv) for 90 minutes. Purification by column chromatography (hexane) afforded the title compound as a white solid (206 mg, 87%). **^{1}H NMR** (500 MHz, $CDCl_3$): δ 7.29 (d, *J* = 8.5 Hz, 4 H), 7.12 (d, *J* = 8.6 Hz, 4 H), 3.94 (s, 2 H); **^{13}C NMR** (126 MHz, $CDCl_3$): δ 139.2, 132.3, 130.3, 128.8. Spectral data were in agreement with the literature.[122]

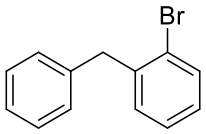

1-Benzyl-2-bromobenzene (4-32e): Prepared according to **GP4-8** from alcohol **4-31e** (263 mg, 1.00 mmol), catalyst **4-30** (2.0 mg, 0.010 mmol, 1 mol%) and triethylsilane (176 μL, 1.10 mmol, 1.10 equiv) for 90 minutes. Purification by column chromatography (hexane) afforded the title compound as a clear oil (174 mg, 71%). **^{1}H NMR** (500 MHz, $CDCl_3$): δ 7.58 (dd, *J* = 8.0, 1.4 Hz, 1 H), 7.30 (t, *J* = 7.3 Hz, 2 H), 7.25 – 7.19 (m, 4 H), 7.14 (dd, *J* = 7.8, 1.8 Hz, 1 H), 7.09 (td, *J* = 7.8, 1.8 Hz, 1 H), 4.13 (s, 2 H); **^{13}C NMR** (126 MHz, $CDCl_3$): δ 140.5, 139.6, 133.0, 131.2, 129.2, 128.6, 128.0, 127.6, 126.4, 125.0, 41.9. Spectral data were in agreement with the literature.[123]

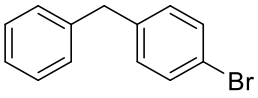

1-Benzyl-4-bromobenzene (4-32f): Prepared according to **GP4-8** from alcohol **4-31f** (263 mg, 1.00 mmol), catalyst **4-30** (2.0 mg, 0.010 mmol, 1 mol%) and triethylsilane (176 μL, 1.10 mmol, 1.10 equiv) for 90 minutes. Purification by column chromatography (hexane) afforded the title compound as a clear oil (180 mg, 73%). **^{1}H NMR** (500 MHz, $CDCl_3$): δ 7.41 (d, *J* = 8.4 Hz, 2 H), 7.30 (t, *J* = 7.2 Hz, 2 H), 7.22 (tt, *J* = 7.4, 2.2 Hz, 1 H), 7.17 (d, *J* = 7.5 Hz, 2 H), 7.07 (d, *J* = 8.7

Hz, 2 H), 3.94 (s, 2 H); **^{13}C NMR** (126 MHz, $CDCl_3$): δ 140.6, 140.2, 131.7, 130.8, 129.0, 128.7, 126.4, 120.1, 41.5. Spectral data were in agreement with the literature.[121]

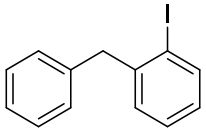

1-Benzyl-2-iodobenzene (4-32g): Prepared according to **GP4-8** from alcohol **4-31g** (310 mg, 1.00 mmol), catalyst **4-30** (2.0 mg, 0.010 mmol, 1 mol%) and triethylsilane (176 μL, 1.10 mmol, 1.10 equiv) for 90 minutes. Purification by column chromatography (hexane) afforded the title compound as a clear oil (244 mg, 83%). **^{1}H NMR** (500 MHz, $CDCl_3$): δ 7.87 (dd, *J* = 7.9, 1.3 Hz, 1 H), 7.32 – 7.28 (m, 2 H), 7.27 – 7.21 (m, 2 H), 7.20 – 7.18 (m, 2 H), 7.12 (d, *J* = 7.7, 1.7 Hz, 1 H), 6.92 (td, *J* = 7.6, 1.7 Hz, 1 H), 4.12 (s, 2 H); **^{13}C NMR** (126 MHz, $CDCl_3$): δ 143.8, 139.7, 130.5, 129.2, 128.6, 128.5, 128.2, 126.4, 101.4, 46.6. Spectral data were in agreement with the literature.[124]

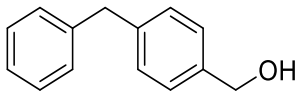

(4-Benzylphenyl)methanol (4-32h): Prepared according to **GP4-8** from alcohol **4-31h** (193 mg, 0.900 mmol), catalyst **4-30** (1.8 mg, 0.0090 mmol, 1 mol%) and triethylsilane (159 μL, 0.990 mmol, 1.10 equiv) for 90 minutes. Purification by column chromatography (7:1 hexane/EtOAc) afforded the title compound as a white solid (138 mg, 78%). **^{1}H NMR** (500 MHz, $CDCl_3$): δ 7.30 – 7.28 (m, 4 H), 7.22 – 7.18 (m 5 H), 4.66 (s, 2 H), 3.99 (s, 2 H), 1.61 (br s, 1 H); **^{13}C NMR** (126 MHz, $CDCl_3$): δ 141.2, 140.8, 138.8, 129.3, 129.0, 128.6, 127.4, 126.2, 65.4, 41.8. Spectral data were in agreement with the literature.[125]

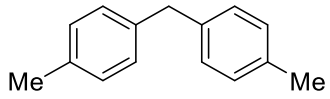

Di-p-tolylmethane (4-32i): Prepared according to **GP4-8** from alcohol **4-31i** (212 mg, 1.00 mmol), catalyst **4-30** (2.0 mg, 0.010 mmol, 1 mol%) and triethylsilane (176 μL, 1.10 mmol, 1.10 equiv) for 90 minutes. Purification by column chromatography (hexane) afforded the title compound as a clear oil (184 mg, 94%). **^{1}H NMR** (500 MHz, $CDCl_3$): δ 7.12 – 7.08 (m, 8 H), 3.93 (s, 2 H), 2.33 (s, 6 H); **^{13}C NMR** (126 MHz, $CDCl_3$): δ 138.5, 135.6, 129.3, 128.9, 41.2, 21.1. Spectral data were in agreement with the literature.[122]

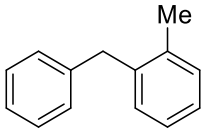

1-Benzyl-2-methylbenzene (4-32j): Prepared according to **GP4-8** from alcohol **4-31j** (198 mg, 1.00 mmol), catalyst **4-30** (2.0 mg, 0.010 mmol, 1 mol%) and triethylsilane (176 μL, 1.10 mmol, 1.10 equiv) for 90 minutes. Purification by column chromatography (hexane) afforded the title compound as a clear oil (154 mg, 84%). **^{1}H NMR** (500 MHz, $CDCl_3$): δ 7.33 – 7.30 (m, 2 H), 7.25 – 7.14 (m, 7 H), 4.04 (s, 2 H), 2.29 (s, 3 H); **^{13}C NMR** (126 MHz, $CDCl_3$): δ 140.5, 139.1, 136.8, 130.4, 130.1, 128.9, 128.5, 126.6, 126.13, 126.06, 39.6, 19.8. Spectral data were in agreement with the literature.[121]

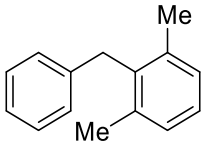

2-Benzyl-1,3-dimethylbenzene (4-32k): Prepared according to **GP4-8** from alcohol **4-31k** (159 mg, 0.750 mmol), catalyst **4-30** (7.5 mg, 0.0375 mmol, 5 mol%) and triethylsilane (135 μL, 0.825

mmol, 1.10 equiv) for 90 minutes. Purification by column chromatography (hexane) afforded the title compound as a clear oil (117 mg, 80%). **^{1}H NMR** (500 MHz, $CDCl_3$): δ 7.29 (t, *J* = 7.2 Hz, 2 H), 7.21 (t, *J* = 7.5 Hz, 1 H), 7.17 – 7.11 (m, 3 H), 7.07 (d, *J* = 7.8 Hz, 2 H), 4.12 (s, 2 H), 2.30 (s, 6 H); **^{13}C NMR** (126 MHz, $CDCl_3$): δ 139.9, 137.3, 137.0, 128.5, 128.3, 128.0, 126.5, 125.9, 35.2, 20.4. Spectral data were in agreement with the literature.[126]

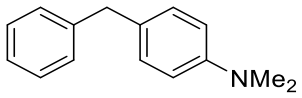

4-Benzyl-*N*,*N*-dimethylaniline (4-32l): Prepared according to **GP4-8** from alcohol **4-32l** (227 mg, 1.00 mmol), catalyst **4-30** (10.0 mg, 0.050 mmol, 5 mol%) and triethylsilane (176 μL, 1.10 mmol, 1.10 equiv) with a reaction time of 18 hours. Purification by column chromatography (20:1 hexane/EtOAc) afforded the title compound as a clear oil (158 mg, 75%). **^{1}H NMR** (500 MHz, $CDCl_3$): δ 7.31 – 7.27 (m, 2 H), 7.22 – 7.18 (m, 3 H), 7.09 (d, *J* = 8.8 Hz, 2 H), 6.72 (d, *J* = 8.8 Hz, 2 H), 3.92 (s, 2 H), 2.94 (s, 6 H); **^{13}C NMR** (126 MHz, $CDCl_3$): δ 149.3, 142.2, 129.7, 129.4, 129.0, 128.5, 125.9, 113.1, 41.1, 41.0. Spectral data were in agreement with the literature.[127]

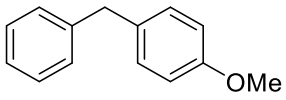

1-Benzyl-4-methoxybenzene (4-32m): Prepared according to **GP4-8** from alcohol **4-31m** (214 mg, 1.00 mmol), catalyst **4-30** (2.0 mg, 0.010 mmol, 1 mol%) and triethylsilane (176 μL, 1.10 mmol, 1.10 equiv) for 90 minutes. Purification by column chromatography (200:1 hexane/EtOAc) afforded the title compound as a clear oil (181 mg, 91%). **^{1}H NMR** (600 MHz, $CDCl_3$): δ 7.29 (t, *J* = 7.1 Hz, 2 H), 7.21 – 7.18 (m, 3 H), 7.12 (d, *J* = 8.6 Hz, 2 H), 6.84 (d, *J* = 8.8 Hz, 2 H), 3.94 (s, 2 H), 3.79 (s, 3 H); **^{13}C NMR** (151 MHz, $CDCl_3$): δ 158.1, 141.7, 133.4, 130.0, 128.9, 128.6, 126.1, 114.0, 55.4, 41.2. Spectral data were in agreement with the literature.[121]

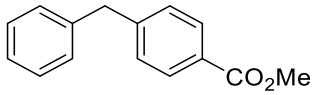

Methyl 4-benzylbenzoate (4-32n): Prepared according to **GP4-8** from alcohol **4-31n** (182 mg, 0.750 mmol), catalyst **4-30** (7.5 mg, 0.038 mmol, 5 mol%) and triethylsilane (134 μL, 0.825 mmol, 1.10 equiv) for 12 hours. Purification by column chromatography (gradient 19:1 to 9:1 hexane/EtOAc) afforded the title compound as a clear oil (144 mg, 85%). **^{1}H NMR** (500 MHz, $CDCl_3$): δ 8.00 (dd, *J* = 8.4, 2.5 Hz, 2 H), 7.34 (td, *J* = 8.0, 1.6 Hz, 2 H), 7.31 – 7.24 (m, 3 H), 7.22 (d, *J* = 6.8 Hz, 2 H), 4.07 (s, 2 H), 3.94 (s, 3 H); **^{13}C NMR** (126 MHz, $CDCl_3$): δ 167.2, 146.7, 140.3, 130.0, 129.1, 128.8, 128.3, 126.5, 52.1, 42.1. Spectral data were in agreement with the literature.[128]

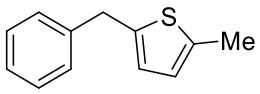

2-Benzyl-5-methylthiophene (4-32o): Prepared according to **GP4-8** from alcohol **4-31o** (204 mg, 1.00 mmol), catalyst **4-30** (2.0 mg, 0.010 mmol, 1 mol%) and triethylsilane (176 μL, 1.10 mmol, 1.10 equiv) for 90 minutes. Purification by column chromatography (hexane) afforded the title compound as a clear oil (142 mg, 75%). **^{1}H NMR** (600 MHz, $CDCl_3$): δ 7.35 (tt, *J* = 6.1, 1.6 Hz, 2 H), 7.30 – 7.25 (m, 3 H), 6.63 – 6.62 (m, 1 H), 6.60 (dq, *J* = 3.4, 1.2 Hz, 1 H), 4.12 (s, 2 H), 2.46 (s, 3 H); **^{13}C NMR** (176 MHz, $CDCl_3$): δ 141.9, 140.7, 138.5, 128.7, 126.5, 125.0, 124.9, 36.4, 15.4. Spectral data were in agreement with the literature.[129]

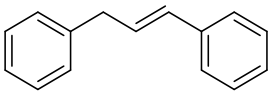

(E)-Prop-1-ene-1,3-diyldibenzene (4-32p): Prepared according to **GP4-8** from alcohol **4-31p** (210 mg, 1.00 mmol), catalyst **4-30** (10.0 mg, 0.050 mmol, 5 mol%) and triethylsilane (176 μL,

1.10 mmol, 1.10 equiv) for 90 minutes. Purification by column chromatography (hexane) afforded the title compound as a clear oil (158 mg, 82%). **^{1}H NMR** (600 MHz, $CDCl_3$): δ 7.41 (d, *J* = 7.3 Hz, 2 H), 7.38 – 7.33 (m, 4 H), 7.31 – 7.24 (m, 4 H), 6.51 (dt, *J* = 15.8, 1.6 Hz, 1 H), 6.41 (dt, *J* = 15.8, 6.8 Hz, 1 H), 3.61 (d, 6.6 Hz, 2 H); **^{13}C NMR** (151 MHz, $CDCl_3$): δ 140.3, 137.6, 131.2, 129.4, 128.8, 128.64, 128.63, 127.2, 126.32, 126.27, 39.5. Spectral data were in agreement with the literature.[130]

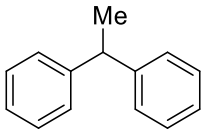

Ethane-1,1-diyldibenzene (4-32q): Prepared according to **GP4-8** from alcohol **4-31q** (198 mg, 1.00 mmol), catalyst **4-30** (2.0 mg, 0.010 mmol, 1 mol%) and triethylsilane (176 μL, 1.10 mmol, 1.10 equiv) for 90 minutes. Purification by column chromatography (hexane) afforded the title compound as a clear oil (154 mg, 85%). **^{1}H NMR** (500 MHz, $CDCl_3$): δ 7.30 (t, *J* = 7.7 Hz, 4 H), 7.25 – 7.23 (m, 4 H), 7.20 (tt, *J* = 7.2, 1.5 Hz, 2 H), 4.17 (q, *J* = 7.2 Hz, 1 H), 1.66 (d, *J* = 7.3 Hz, 3 H); **^{13}C NMR** (125 MHz, $CDCl_3$): δ 146.5, 128.5, 127.8, 126.2, 44.9, 22.0. Spectral data were in agreement with the literature.[121]

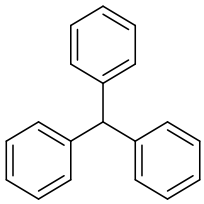

Triphenylmethane (4-32r): Prepared according to **GP4-8** from alcohol **4-31r** (5.21 g, 20.0 mmol), catalyst **4-30** (4.0 mg, 0.020 mmol, 0.1 mol%) and triethylsilane (3.50 mL, 22.0 mmol, 1.10 equiv) for 90 minutes. Purification by column chromatography (hexane) afforded the title compound as a white solid (4.44 g, 91%). **^{1}H NMR** (500 MHz, $CDCl_3$): δ 7.29 (t, *J* = 7.4 Hz, 6

H), 7.22 (tt, *J* = 7.5, 2.2 Hz, 3 H), 7.13 (d, *J* = 7.2 Hz, 6 H), 5.57 (s, 1 H); **^{13}C NMR** (125 MHz, $CDCl_3$): δ 144.1, 129.6, 128.4, 126.4, 57.0. Spectral data were in agreement with the literature.[131]

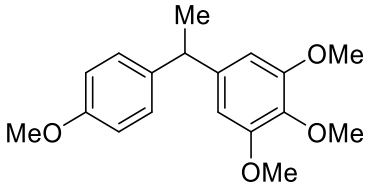

1,2,3-Trimethoxy-5-(1-(4-methoxyphenyl)ethyl)benzene (4-32s): Prepared according to **GP4-8** from alcohol **4-31s** (136 mg, 0.430 mmol), catalyst **4-30** (0.9 mg, 0.043 mmol, 1 mol%) and triethylsilane (84 μL, 0.47 mmol, 1.10 equiv) for 90 minutes. Purification by column chromatography (6:1 hexane/EtOAc) afforded the title compound as a clear oil (89 mg, 69%). **^{1}H NMR** (600 MHz, $CDCl_3$): δ 7.15 (d, *J* = 8.8 Hz, 2 H), 6.84 (d, *J* = 8.8 Hz, 2 H), 6.42 (s, 2 H), 4.04 (q, *J* = 7.2 Hz, 1 H), 3.82 (s, 3 H), 3.81 (s, 6 H), 3.79 (s, 3 H), 1.60 (d, *J* = 7.2 Hz, 3 H); **^{13}C NMR** (151 MHz, $CDCl_3$): δ 158.0, 153.2, 142.6, 138.5, 136.4, 128.5, 113.9, 104.8, 60.9, 56.2, 55.4, 44.3, 22.3; **FTIR** (Cast film, cm^{-1}): 2962 (w), 2835 (w), 1589 (m), 1511 (m), 1244 (m), 1128 (s), 1009 (m), 832 (w); **HRMS** (ESI) for $C_{18}H_{22}O_4Na$ $[M+Na]^+$: Calculated: 325.1416; Found: 325.1412. Spectral data were in agreement with the literature.[121]

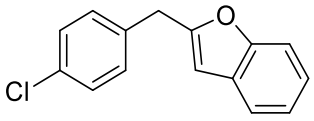

2-(4-Chlorobenzyl)benzofuran (4-32t): Prepared according to **GP4-8** from alcohol **4-31t** (161 mg, 0.62 mmol), catalyst **4-30** (1.2 mg, 0.0062 mmol, 1 mol%) and triethylsilane (109 μL, 0.682 mmol, 1.10 equiv) for 90 minutes. Purification by column chromatography (hexane) afforded the title compound as a white solid (106 mg, 70%). **mp** = 68.6 – 70.1 °C; **^{1}H NMR** (500 MHz, $CDCl_3$): δ 7.48 (dd, *J* = 7.2, 1.8 Hz, 1 H), 7.41 (d, *J* = 7.7 Hz, 1 H), 7.30 (d, *J* = 8.6 Hz, 2 H), 7.25 – 7.21

(m, 3 H), 7.19 (td, *J* = 7.2, 1.2 Hz, 1 H), 6.38 (dd, *J* = 2.0, 1.0 Hz, 1 H), 4.08 (s, 2 H); **^{13}C NMR** (126 MHz, $CDCl_3$): δ 157.2, 155.1, 135.8, 132.8, 130.4, 128.9, 128.8, 123.8, 122.8, 120.6, 111.1, 103.7, 34.5; **FTIR** (Cast film, cm^{-1}): 3054 (w), 2919 (w), 1587 (w), 1491 (s), 1454 (s), 1253 (m), 1105 (m), 1016 (m), 796 (s), 751 (s); **HRMS** (ESI) for $C_{15}H_{11}OCl$: Calculated: 242.0498; Found: 242.0492. Spectral data were in agreement with the literature.[132]

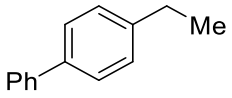

4-Ethyl-1,1'-biphenyl (4-32u): Prepared according to **GP4-8** from alcohol **4-31u** (198 mg, 1.00 mmol), catalyst **4-30** (10.0 mg, 0.050 mmol, 5 mol%) and triethylsilane (176 µL, 1.10 mmol, 1.10 equiv) with a reaction time of 3 hours. Purification by column chromatography (hexane) afforded the title compound as a white solid (147 mg, 81%). **^{1}H NMR** (500 MHz, $CDCl_3$): δ 7.59 (dd, *J* = 7.2, 1.2 Hz, 2 H), 7.53 (d, *J* = 8.4 Hz, 2 H), 7.44 (t, *J* = 7.7 Hz, 2 H), 7.33 (tt, *J* = 7.4, 1.3 Hz, 1 H), 7.29 (d, *J* = 8.4 Hz, 2 H), 2.71 (q, *J* = 7.6 Hz, 1 H), 1.29 (t, *J* = 7.6 Hz, 3 H); **^{13}C NMR** (126 MHz, $CDCl_3$): δ 143.5, 141.3, 138.8, 128.8, 128.4, 127.23, 127.16, 127.11, 28.7, 15.7. Spectral data were in agreement with the literature.[133]

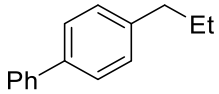

4-Propyl-1,1'-biphenyl (4-32v): Prepared according to **GP4-8** from alcohol **4-31v** (212 mg, 1.00 mmol), catalyst **4-30** (10.0 mg, 0.050 mmol, 5 mol%) and triethylsilane (176 µL, 1.10 mmol, 1.10 equiv) with a reaction time of 3 hours. Purification by column chromatography (hexane) afforded the title compound as a clear oil (142 mg, 68%). **^{1}H NMR** (500 MHz, $CDCl_3$): δ 7.63 (dd, *J* = 8.4, 1.1 Hz, 2 H), 7.56 (d, *J* = 8.4 Hz, 2 H), 7.47 (t, *J* = 7.4 Hz, 2 H), 7.37 (tt, *J* = 7.4, 1.3 Hz, 1 H), 7.30 (d, *J* = 7.6 Hz, 2 H), 2.68 (t, *J* = 7.7 Hz, 2 H), 1.73 (h, *J* = 7.4 Hz, 2 H), 1.03 (t, *J* = 7.3 Hz, 3

H) ; **^{13}C NMR** (126 MHz, $CDCl_3$): δ 142.0, 141.4, 138.7, 129.0, 128.8, 127.14, 127.11, 127.09, 37.8, 24.7, 14.0. Spectral data were in agreement with the literature.[134]

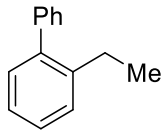

2-Ethyl-1,1'-biphenyl (4-32w): Prepared according to **GP4-8** from alcohol **4-31w** (198 mg, 1.00 mmol), catalyst **4-30** (10.0 mg, 0.050 mmol, 5 mol%) and triethylsilane (176 µL, 1.10 mmol, 1.10 equiv) with a reaction time of 3 hours. Purification by column chromatography (hexane) afforded the title compound as a clear oil (107 mg, 59%). **^{1}H NMR** (500 MHz, $CDCl_3$): δ 7.42 (tt, *J* = 6.9 Hz, 2.8 Hz, 2 H), 7.37 – 7.2 (m, 5 H), 7.25 – 7.20 (m, 2 H), 2.61 (q, *J* = 7.6 Hz, 2 H), 1.11 (t, *J* = 7.6 Hz, 3 H); **^{13}C NMR** (126 MHz, $CDCl_3$): δ 142.1, 141.79, 141.76, 130.1, 129.4, 128.7, 128.1, 127.6, 126.9, 125.7, 26.3, 15.8. Spectral data were in agreement with the literature.[133]

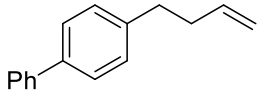

4-(But-3-en-1-yl)-1,1'-biphenyl (4-32x): Prepared according to **GP4-8** from alcohol **4-31x** (224 mg, 1.00 mmol), catalyst **4-30** (10.0 mg, 0.050 mmol, 5 mol%) and triethylsilane (176 µL, 1.10 mmol, 1.10 equiv) with a reaction time of 18 hours. Purification by column chromatography (hexane) afforded the title compound as a clear oil (145 mg, 70%). **^{1}H NMR** (500 MHz, $CDCl_3$): δ 7.60 (dd, *J* = 8.4, 1.2 Hz, 2 H), 7.54 (d, *J* = 8.4 Hz, 2 H), 7.44 (t, *J* = 7.7 Hz, 2 H), 7.34 (tt, *J* = 7.3, 1.3 Hz, 1 H), 7.28 (d, *J* = 8.4 Hz, 2 H), 5.91 (ddt, *J* = 16.9, 10.3, 6.6 Hz, 1 H), 5.09 (dq, *J* = 17.1, 1.7 Hz, 1 H), 5.04 – 5.01 (m, 1 H), 2.78 (t, *J* = 7.8 Hz, 2 H), 2.44 (tdt, *J* = 7.9, 6.6, 1.5 Hz, 2 H); **^{13}C NMR** (126 MHz, $CDCl_3$): δ 141.2, 141.1, 138.9, 138.2, 129.0, 128.9, 127.19, 127.15 (x 2), 115.2, 35.6, 35.2. Spectral data were in agreement with the literature.[135]

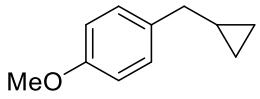

1-(Cyclopropylmethyl)-4-methoxybenzene (4-32y): Prepared according to **GP4-8** from ether **4-31y** (192 mg, 1.00 mmol), catalyst **4-30** (10.0 mg, 0.050 mmol, 5 mol%) and triethylsilane (176 μL, 1.10 mmol, 1.10 equiv) with a reaction time of 3 hours. Purification by column chromatography (hexane) afforded the title compound as a clear oil (114 mg, 70%). **^{1}H NMR** (700 MHz, $CDCl_3$): δ 7.19 (d, *J* = 8.8 Hz, 2 H), 6.85 (d, *J* = 8.7 Hz, 2 H), 3.80 (s, 3 H), 2.50 (d, *J* = 6.9 Hz, 2 H), 0.99 – 0.92 (m, 1 H), 0.53 – 0.50 (m, 2 H), 0.20 – 0.18 (m, 2 H) ; **^{13}C NMR** (125 MHz, $CDCl_3$): δ 158.0, 134.4, 129.4, 113.8, 55.4, 39.6, 12.2, 4.7. Spectral data were in agreement with the literature.[136]

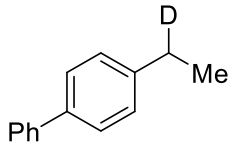

4-(1-Deuteroethyl)-1,1'-biphenyl (4-32z): Prepared according to **GP4-8** from alcohol **4-31z** (199 mg, 1.00 mmol), catalyst **4-30** (10.0 mg, 0.050 mmol, 5 mol%) and triethylsilane (176 μL, 1.10 mmol, 1.10 equiv) with a reaction time of 3 hours. Purification by column chromatography (hexane) afforded the title compound as a white solid (141 mg, 77%). **^{1}H NMR** (500 MHz, $CDCl_3$): δ 7.61 (dd, *J* = 8.4, 1.4 Hz, 2 H), 7.54 (d, *J* = 8.3 Hz, 2 H), 7.45 (t, *J* = 7.8 Hz, 2 H), 7.34 (tt, *J* = 7.4, 1.3 Hz, 1 H), 7.30 (d, *J* = 8.0 Hz, 2 H), 2.74 – 2.67 (m, 1 H), 1.29 (d, *J* = 7.6 Hz, 3 H); **^{13}C NMR** (126 MHz, $CDCl_3$): δ 143.5, 141.4, 138.8, 128.8, 128.4, 127.22, 127.16, 127.1, 28.31 (1:1:1 triplet, *J* = 19.3 Hz), 15.6. Traces of the non-deuterated product are observed (15.7 ppm, 28.7 ppm). Spectral data were in agreement with the literature.[137]

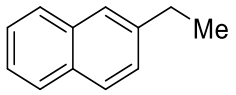

2-Ethylnaphthalene (4-32aa): Prepared according to **GP4-8** from alcohol **4-31aa** (172 mg, 1.00 mmol), catalyst **4-30** (10.0 mg, 0.050 mmol, 5 mol%) and triethylsilane (176 μL, 1.10 mmol, 1.10 equiv) with a reaction time of 3 hours. Purification by column chromatography (100:1 hexane/EtOAc) afforded the title compound as a clear oil (111 mg, 71%). **^{1}H NMR** (600 MHz, $CDCl_3$): δ 7.82 – 7.78 (m, 3 H), 7.64 (s, 1 H), 7.46 (td, *J* = 7.4, 1.3 Hz, 1 H), 7.43 (td, *J* = 7.4, 1.5 Hz, 1 H), 7.37 (dd, *J* = 8.3, 1.7 Hz, 1 H), 2.34 (q, *J* = 7.6 Hz, 2 H), 1.35 (t, *J* = 7.6 Hz, 3 H); **^{13}C NMR** (151 MHz, $CDCl_3$): δ 141.9, 133.9, 132.1, 127.9, 127.7, 127.6, 127.2, 126.0, 125.7, 125.2, 29.2, 15.7. Spectral data were in agreement with the literature.[138]

4.6.9.2 Comparison of C–O Substrates

The use of benzylic acetate **4-33** or benzylic ether **4-34** in reductive deoxygenation was done according to **GP4-6** using acetate **4-33** (33.9 mg, 0.150 mmol, 1.00 equiv) or ether **4-34** (26.2 mg, 0.0750 mmol, 0.500 equiv), triethylsilane (28 μL, 0.16 mmol, 1.1 equiv), catalyst **4-30** (0.3 mg, 0.002 mmol, 1 mol%), HFIP (240 μL) and $MeNO_2$ (60 μL). Yields were determined by ^{1}H NMR relative to 1,3,5-trimethoxybenzene as an internal standard.

4.6.9.3 Comparison of Reduction Methods for Alcohol 4-31h

The reduction of alcohol **4-31h** was performed according to **GP4-6** using alcohol **4-31h** (21.4 mg, 0.100 mmol, 1.00 equiv). In Conditions A, $pTsOH \cdot H_2O$ (0.9 mg, 0.005 mmol, 5 mol%) was used as a catalyst. In Conditions C, hemiboronic acid **4-30** (0.2 mg, 0.001 mmol, 1 mol%) was used as a catalyst. In Conditions B, the alcohol was reacted with $Ga(OTf)_3$ (2.5 mg, 0.005 mmol, 5 mol%), $HSiMe_2Cl$ (28 μL, 0.25 mmol, 2.5 equiv) and CH_2Cl_2 (0.2 mL) at room temperature for 1 hour. The reaction was worked up following **GP4-6**.

4.6.9.4 Synthesis of Adamantane

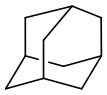

Adamantane (4-36): A vial equipped with a stir bar was charged with 1-adamantol (**4-35**) (114 mg, 0.750 mmol), catalyst **4-30** (7.5 mg, 0.038 mmol, 5 mol%), TMDSO (146 μL, 0.825 mmol, 1.10 equiv) and HFIP (1.5 mL). The reaction was stirred at room temperature for 18 hours, after which it was concentrated by rotary evaporation. Purification by column chromatography (hexane) afforded the title compound as a white solid (75 mg, 73%). **^{1}H NMR** (500 MHz, $CDCl_3$): δ 1.89 – 1.86 (m, 4 H), 1.76 (t, *J* = 3.2 Hz, 12 H); **^{13}C NMR** (126 MHz, $CDCl_3$): δ 37.9, 28.5 Spectral data were in agreement with the literature.[139]

4.6.9.5 Reductive Deoxygenation of Benzylic Ketones

General Procedure for the reductive deoxygenation of benzylic ketones (GP4-9)

A vial equipped with a stir bar was charged with ketone **4-37**, catalyst **4-30** (5 mol%), 1,1,3,3-tetramethyldisiloxane (TMDSO) (2.2 equiv) and HFIP (0.5 M in ketone). The reaction was stirred at room temperature for 24 hours, after which it was concentrated by rotary evaporation. Purification by column chromatography afforded the reduction product **4-32**.

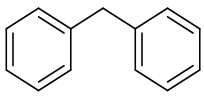

Diphenylmethane (4-32a): Prepared according to **GP4-9** from ketone **4-37a** (164 mg, 0.900 mmol), catalyst **4-30** (9.0 mg, 0.045 mmol, 5 mol%) and TMDSO (348 μL, 1.98 mmol, 2.20 equiv). Purification by column chromatography (hexane) afforded the title compound as a clear oil (135 mg, 89%). Spectral data match that reported in section 4.6.9.1.

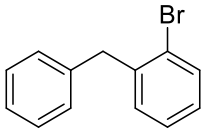

1-Benzyl-2-bromobenzene (4-32e): Prepared according to **GP4-9** from ketone **4-37e** (196 mg, 0.750 mmol), catalyst **4-30** (7.5 mg, 0.038 mmol, 5 mol%) and TMDSO (292 μL, 1.65 mmol, 2.20 equiv). Purification by column chromatography (hexane) afforded the title compound as a clear oil (142 mg, 77%). Spectral data match that reported in section 4.6.9.1.

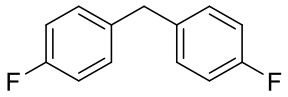

Bis(4-fluorophenyl)methane (4-32b): Prepared according to **GP4-9** from ketone **4-37b** (165 mg, 0.750 mmol), catalyst **4-30** (7.5 mg, 0.038 mmol, 5 mol%) and TMDSO (292 μL, 1.65 mmol, 2.20 equiv). Purification by column chromatography (hexane) afforded the title compound as a clear oil (101 mg, 65%). Spectral data match that reported in section 4.6.9.1.

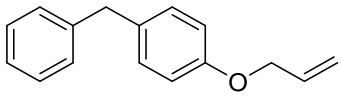

1-(Allyloxy)-4-benzylbenzene (4-32ab): Prepared according to **GP4-9** from ketone **4-37ab** (178 mg, 0.750 mmol), catalyst **4-30** (7.5 mg, 0.038 mmol, 5 mol%) and TMDSO (292 μL, 1.65 mmol, 2.20 equiv). Purification by column chromatography (gradient 200:1 to 50:1 hexane/EtOAc) afforded the title compound as a clear oil (157 mg, 94%). **^{1}H NMR** (600 MHz, $CDCl_3$): δ 7.29 (t, *J* = 7.4 Hz, 2 H), 7.22 – 7.18 (m, 3 H), 7.11 (d, *J* = 8.9 Hz, 2 H), 6.86 (d, *J* = 8.8 Hz, 2 H), 6.06 (ddt, *J* = 17.2, 10.5, 5.3 Hz, 1 H), 5.42 (dq, *J* = 17.2, 1.6 Hz, 1 H), 5.29 (dq, *J* = 10.5, 1.4 Hz, 1 H), 4.52 (dt, *J* = 5.3, 1.6 Hz, 2 H), 3.94 (s, 2 H); **^{13}C NMR** (151 MHz, $CDCl_3$): δ 157.2, 141.7, 133.60,

133.58, 130.0, 129.0, 128.6, 126.1, 117.7, 114.9, 69.0, 41.2. Spectral data were in agreement with the literature.[140]

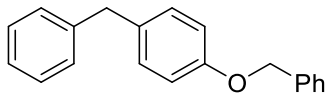

1-Benzyl-4-(benzyloxy)benzene (4-32ac): Prepared according to **GP4-9** from ketone **4-37ac** (216 mg, 0.750 mmol), catalyst **4-30** (7.5 mg, 0.038 mmol, 5 mol%) and TMDSO (292 μL, 1.65 mmol, 2.20 equiv). Purification by column chromatography (gradient 100:1 to 20:1 hexane/EtOAc) afforded the title compound as a white solid (144 mg, 70%). **^{1}H NMR** (600 MHz, $CDCl_3$): δ 7.45 (d, *J* = 6.7 Hz, 2 H), 7.40 (t, *J* = 7.5 Hz, 2 H), 7.35 (tt, *J* = 7.4, 1.4 Hz, 1 H), 7.30 (t, *J* = 7.5 Hz, 2 H), 7.22 – 7.19 (m, 3 H), 7.12 (d, *J* = 8.8 Hz, 2 H), 6.93 (d, *J* = 8.8 Hz, 2 H), 5.06 (s, 2 H), 3.95 (s, 2 H); **^{13}C NMR** (151 MHz, $CDCl_3$): δ 157.4, 141.7, 137.3, 133.7, 130.0, 129.0, 128.7, 128.6, 128.0, 127.6, 126.1, 115.0, 70.2, 41.2. Spectral data were in agreement with the literature.[141]

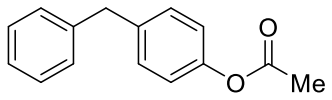

4-Benzylphenyl acetate (4-32ad): Prepared according to **GP4-9** from ketone **4-37ad** (180 mg, 0.750 mmol), catalyst **4-30** (7.5 mg, 0.038 mmol, 5 mol%) and TMDSO (292 μL, 1.65 mmol, 2.20 equiv). Purification by column chromatography (40:1 hexane/EtOAc) afforded the title compound as a clear oil (145 mg, 85%). **^{1}H NMR** (500 MHz, $CDCl_3$): δ 7.30 (t, *J* = 7.6 Hz, 2 H), 7.23 – 7.19 (m, 5 H), 7.01 (d, *J* = 8.5 Hz, 2 H), 3.98 (s, 2 H), 2.29 (s, 3 H); **^{13}C NMR** (126 MHz): δ 169.7, 149.1, 140.9, 138.8, 130.0, 129.1, 128.7, 126.3, 121.6, 41.4, 21.3. Spectral data were in agreement with the literature.[142]

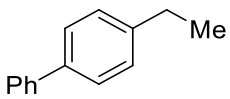

4-Ethyl-1,1'-biphenyl (4-32u): Prepared according to **GP4-9** from ketone **4-37u** (195 mg, 1.00 mmol), catalyst **4-30** (10.0 mg, 0.050 mmol, 5 mol%) and TMDSO (388 μL, 2.20 mmol, 2.20 equiv). Purification by column chromatography (hexane) afforded the title compound as a white solid (145 mg, 95%). Spectral data match that reported in section 4.6.9.1.

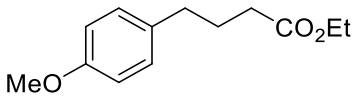

Ethyl 4-(4-methoxyphenyl)butanoate (4-32ae): Prepared according to **GP4-9** from ketone **4-37ae** (177 mg, 0.750 mmol), catalyst **4-30** (7.5 mg, 0.038 mmol, 5 mol%) and TMDSO (292 μL, 1.65 mmol, 2.20 equiv). Purification by column chromatography (40:1 hexane/EtOAc) afforded the title compound as a clear oil (155 mg, 93%). **^{1}H NMR** (500 MHz, $CDCl_3$): δ 7.09 (d, *J* = 8.7 Hz, 2 H), 6.83 (d, *J* = 8.7 Hz, 2 H), 4.12 (q, *J* = 7.2 Hz, 2 H), 3.79 (s, 3 H), 2.59 (t, *J* = 7.6 Hz, 2 H), 2.30 (t, *J* = 7.5 Hz, 2 H), 1.92 (p, *J* = 7.6 Hz, 2 H), 1.25 (t, *J* = 7.2 Hz, 3 H); **^{13}C NMR** (126 MHz, $CDCl_3$): δ 173.7, 158.0, 133.7, 129.5, 113.9, 60.4, 55.4, 34.4, 33.8, 26.9, 14.4. Spectral data were in agreement with the literature.[143]

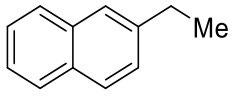

2-Ethylnaphthalene (4-32aa): Prepared according to **GP4-9** from ketone **4-37aa** (170 mg, 1.00 mmol), catalyst **4-30** (10.0 mg, 0.050 mmol, 5 mol%) and TMDSO (388 μL, 2.20 mmol, 2.20 equiv). Purification by column chromatography (hexane) afforded the title compound as a clear oil (121 mg, 77%). Spectral data match that reported in section 4.6.9.1.

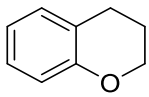

Chromane (4-32af): Prepared according to **GP4-9** from ketone **4-37af** (111 mg, 0.750 mmol), catalyst **4-30** (7.5 mg, 0.038 mmol, 5 mol%) and TMDSO (292 μL, 1.65 mmol, 2.20 equiv). Purification by column chromatography (35:1 hexane/EtOAc) afforded the title compound as a clear oil (45 mg, 45%). **^{1}H NMR** (500 MHz, $CDCl_3$): δ 7.09 (t, *J* = 8.2 Hz, 1 H), 7.04 (d, *J* = 7.8 Hz, 1 H), 6.84 (td, *J* = 7.1, 1.0 Hz, 1 H), 6.81 (d, *J* = 8.2 Hz, 1 H), 4.19 (t, *J* = 5.2 Hz, 2 H), 2.80 (t, *J* = 6.6 Hz, 2 H), 2.04 – 2.00 (m, 2 H); **^{13}C NMR** (126 MHz, $CDCl_3$): δ 155.1, 129.9, 127.3, 122.4, 120.2, 116.8, 66.6, 25.0, 22.5. Spectral data were in agreement with the literature.[144]

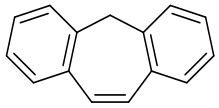

5H-Dibenzo[a,d][7]annulene (4-32ag): Prepared according to **GP4-9** from ketone **4-37ag** (1.65 g, 8.00 mmol), catalyst **4-30** (16.0 mg, 0.400 mmol, 5 mol%) and TMDSO (3.1 mL, 17.6 mmol, 2.20 equiv). Purification by column chromatography (hexane) afforded the title compound as a white solid (1.41 g, 92%). **^{1}H NMR** (600 MHz, $CDCl_3$): δ 7.34 – 7.29 (m, 6 H), 7.22 (td, *J* = 6.6, 1.7 Hz, 2 H), 3.76 (s, 2 H); **^{13}C NMR** (151 MHz, $CDCl_3$): δ 138.3, 135.3, 131.7, 128.6, 128.2, 128.0, 126.2, 41.8. Spectral data were in agreement with the literature.[145]

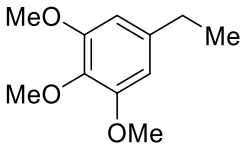

5-Ethyl-1,2,3-trimethoxybenzene (4-32ah): Prepared according to **GP4-9** from ketone **4-37ah** (158 mg, 0.750 mmol), catalyst **4-30** (7.5 mg, 0.038 mmol, 5 mol%) and TMDSO (292 μL, 1.65 mmol, 2.20 equiv). Purification by column chromatography (6:1 hexane/EtOAc) afforded the title compound as a clear oil (142 mg, 96%). **^{1}H NMR** (600 MHz, $CDCl_3$): δ 6.42 (s, 2 H), 3.86 (s, 6 H), 3.82 (s, 3 H), 2.60 (q, *J* = 7.6 Hz, 2 H), 1.24 (t, *J* = 7.6 Hz, 3 H); **^{13}C NMR** (151 MHz, $CDCl_3$):

153.2, 140.2, 136.1, 104.9, 61.0, 56.2, 29.4, 15.8. Spectral data were in agreement with the literature.[146]

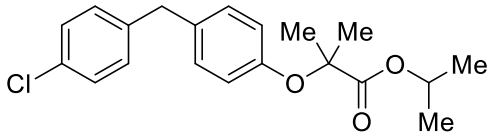

Isopropyl 2-(4-(4-chlorobenzyl)phenoxy)-2-methylpropanoate (4-32ai): Prepared according to **GP4-9** from ketone **4-37ai** (271 mg, 0.750 mmol), catalyst **4-30** (7.5 mg, 0.038 mmol, 5 mol%) and TMDSO (292 μL, 1.65 mmol, 2.20 equiv). Purification by column chromatography (hexane to 25:1 hexane/EtOAc) afforded the title compound as a clear oil (219 mg, 84%). **^{1}H NMR** (600 MHz, $CDCl_3$): δ 7.24 (d, *J* = 8.4 Hz, 2 H), 7.08 (d, *J* = 8.5 Hz, 2 H), 7.00 (d, *J* = 8.7 Hz, 2 H), 6.78 (d, *J* = 8.7 Hz, 2 H), 5.07 (hept, *J* = 6.3 Hz, 1 H), 3.87 (s, 2 H), 1.56 (s, 6 H), 1.21 (d, *J* = 6.2 Hz, 6 H); **^{13}C NMR** (151 MHz, $CDCl_3$): δ 173.9, 154.2, 140.0, 134.2, 132.0, 130.3, 129.6, 128.6, 119.4, 79.2, 69.0, 40.5, 25.5, 21.7; **FTIR** (Cast film, cm^{-1}): 2983 (w), 2939 (w), 1728 (s), 1610 (w), 1508 (s), 1383 (w), 1238 (m), 1179 (m), 1153 (m), 1104 (s), 1015 (w), 812 (w); **HRMS** (ESI) for $C_{20}H_{23}O_3ClNa$ $[M+Na]^+$: Calculated: 369.1233; Found: 369.1227.

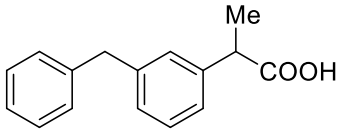

2-(3-Benzylphenyl)propanoic acid (4-32aj): Prepared according to **GP4-9** from ketone **4-37aj** (127 mg, 0.500 mmol), catalyst **4-30** (5.0 mg, 0.025 mmol, 5 mol%) and TMDSO (194 μL, 2.20 mmol, 2.20 equiv). Purification by column chromatography (2:1 hexane/EtOAc) afforded the title compound as a clear oil (99 mg, 83%). **^{1}H NMR** (500 MHz, $CDCl_3$): δ 7.29 (tt, *J* = 7.0, 1.8 Hz, 2.0 H), 7.24 – 7.16 (m, 6 H), 7.08 (d, *J* = 7.8 Hz, 1 H), 3.98 (s, 2 H), 3.71 (q, *J* = 7.2 Hz, 1 H), 1.50 (d, *J* = 7.2 Hz, 3 H); **^{13}C NMR** (126 MHz, $CDCl_3$): δ 180.2, 141.7, 140.1, 129.1, 128.9, 128.6,

128.5, 128.2, 126.3, 125.4, 45.4, 42.0, 18.3; **FTIR** (Cast film, cm^{-1}): 3063 (m), 3027 (m), 3000 (br, m), 2631 (w), 1708 (s), 1601 (w), 1453 (w), 1240 (w), 1074 (w), 935 (w), 699 (m); **HRMS** (ESI) for $C_{16}H_{15}O_2$ $(M-H)^-$: Calculated: 239.1078; Found: 239.1079.

Partial reduction of ketone **4-37ak** was performed following **GP4-7** using ketone **4-37ak** (21.8 mg, 0.150 mmol), catalyst **4-30** (1.5 mg, 0.0075 mmol, 5 mol%), TMDSO (58 μL, 0.33 mmol, 2.2 equiv) and HFIP (0.30 mL). The yield of alcohol **4-31ak** was determined by crude NMR relative to 1,3,5-trimethoxybenzene as an internal standard in accordance with literature spectral data.[147]

4.6.9.6 Formal Friedel-Crafts Alkylation of 1,3,5-Trimethoxybenzene

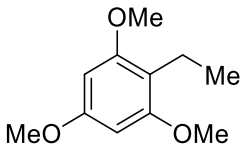

2-Ethyl-1,3,5-trimethoxybenzene (4-39): A vial equipped with a stir bar was charged with 1,3,5-trimethoxybenzene **4-38** (126 mg, 0.750 mmol), acetyl chloride (535 μL, 7.50 mmol, 10.0 equiv) and HFIP (0.75 mL). The reaction was stirred for 12 hours at room temperature, during which time it turned a dark red color. The reaction was then concentrated by rotary evaporation, after which the vial was charged with catalyst **4-30** (7.5 mg, 0.038 mmol, 5 mol%), TMDSO (292 μL, 1.65 mmol, 2.20 equiv) and HFIP (1.5 mL). The reaction was stirred at room temperature for 24 hours, after which it was concentrated by rotary evaporation. Purification by column chromatography (10:1 hexane/EtOAc) afforded the title compound as a clear oil (131 mg, 89%). **^{1}H NMR** (500 MHz, $CDCl_3$): δ 6.14 (s, 2 H), 3.81 (s, 3 H), 3.80 (s, 6 H), 2.59 (q, J = 7.5 Hz, 2 H), 1.05 (t, J = 7.4 Hz, 3 H); **^{13}C NMR** (126 MHz, $CDCl_3$): δ 159.2, 158.8, 113.6, 90.8, 55.9, 55.5, 16.1, 14.3; **FTIR** (Cast film, cm^{-1}): 2999 (w), 2996 (w), 2837 (w), 1611 (m), 1437 (w), 1226 (m), 1140 (m), 1058 (w), 811 (w); **HRMS** (ESI) for $C_{11}H_{16}O_3$: Calculated: 196.1099; Found: 196.1099.

4.6.10 Kinetic and Mechanistic Studies of Reductive Deoxygenation

4.6.10.1 Ketone Deoxygenation Kinetics

General Procedure for kinetic studies of ketone deoxygenation (GP4-10)

A vial equipped with a stir bar was charged with ketone **4-37** (1.00 mmol), catalyst **4-30** (10.0 mg, 0.050 mmol, 5 mol%), TMDSO (388 µL, 2.20 mmol, 2.20 equiv), HFIP (2.0 mL) and 1,4-dinitrobenzene (21.8 mg, 0.130 mmol) as an internal standard. The reaction was stirred at room temperature, and aliquots of 160 µL were taken periodically. These aliquots were diluted with $CHCl_3$ (1.0 mL), concentrated by rotary evaporation, and analyzed by ^1H NMR in $CDCl_3$.

When the deoxygenation of ketone **4-37a** was monitored following **GP4-10**, clean conversion to diphenylmethane (**4-32a**) was observed. No evidence for intermediates **4-40** or **4-31a** was observed (Figure 4-23, 1,4-DNB = 1,4-dinitrobenzene used as an internal standard).

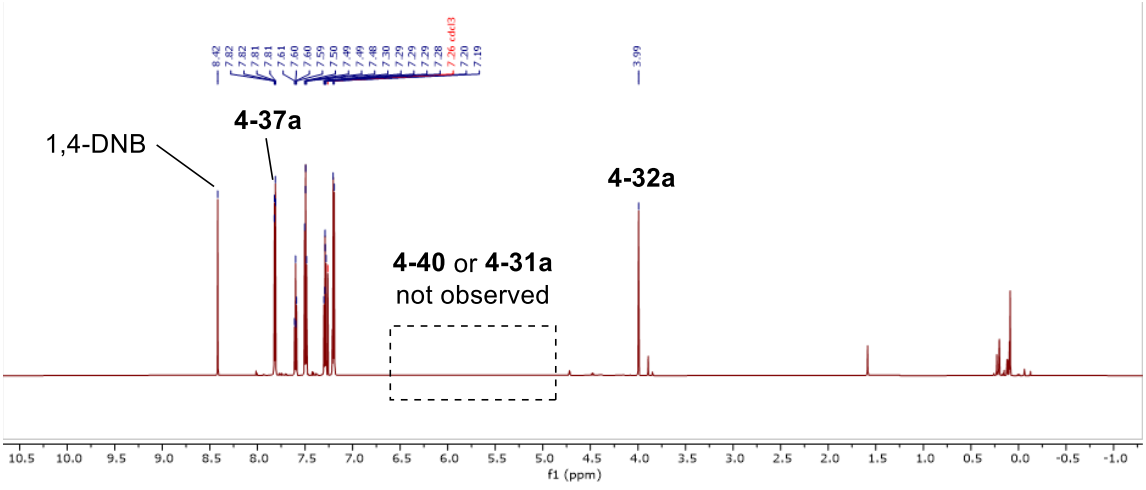

Figure 4-23 Representative ^1H NMR (600 MHz, $CDCl_3$) from a reaction aliquot for the deoxygenation of benzophenone.

4.6.10.2 Evidence for Silyl Ether Intermediates

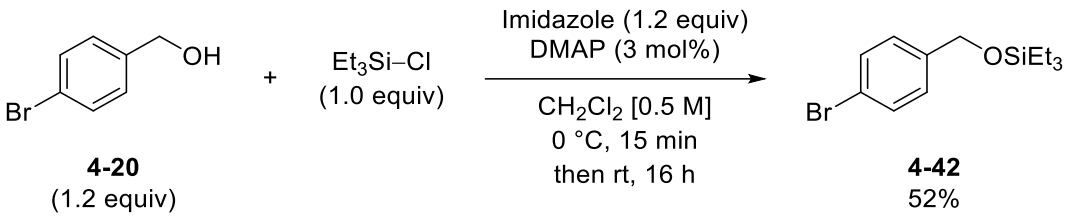

((4-Bromobenzyl)oxy)triethylsilane (4-42): Under nitrogen, a flame-dried 50 mL round bottom flask equipped with a stir bar was charged with alcohol **4-20** (673 mg, 3.60 mmol, 1.20 equiv), imidazole (245 mg, 3.60 mmol, 1.20 equiv), DMAP (10.0 mg, 0.090 mmol, 3 mol%) and CH_2Cl_2 (10 mL). The flask was cooled in an ice bath to 0 °C, at which point chlorotriethylsilane (508 µL, 3.00 mmol, 1.00 equiv) was added dropwise. The reaction was stirred at 0 °C for an additional 15 minutes, at which point the cooling bath was removed and the reaction was stirred for an additional 16 hours. The mixture was then diluted with CH_2Cl_2 (15 mL) and H_2O (15 mL). The phases were separated, and the aqueous phase was extracted with an additional 10 mL CH_2Cl_2. The combined organic phases were washed with H_2O (15 mL) and brine (15 mL). The organic layer was dried over Na_2SO_4, filtered, and concentrated by rotary evaporation. Purification by column chromatography (15:1 hexane/EtOAc) afforded the desired product as a clear oil (465 mg, 1.56 mmol, 52%). **^{1}H NMR** (600 MHz, $CDCl_3$): δ 7.45 (d, *J* = 8.4 Hz, 2 H), 7.21 (d, *J* = 8.7 Hz, 2 H), 4.68 (s, 2 H), 0.97 (t, *J* = 7.9 Hz, 9 H), 0.65 (q, *J* = 7.9 Hz, 6 H); **^{13}C NMR** (151 MHz, $CDCl_3$): δ 140.5, 131.4, 128.0, 120.8, 64.2, 6.9, 4.6. Spectral data were in agreement with the literature.[148]

Reduction of 4-bromobenzaldehyde (**4-41**) was performed following **GP4-7** using 5 equivalents triethylsilane as a reductant and analyzed after 1 hour, where both silyl ether **4-42** and alcohol **4-20** were observed based on crude ^{1}H NMR analysis. Yields were determined by ^{1}H NMR relative to 1,3,5-trimethoxybenzene as an internal standard (18% **4-42**, 45% **4-20**).

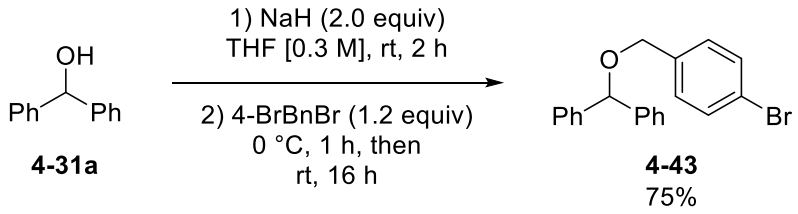

(((4-Bromobenzyl)oxy)methylene)dibenzene (4-43): Under nitrogen, a flame-dried 100 mL round bottom flask was charged with NaH (240 mg, 60% dispersion in mineral oil, 6.00 mmol, 2.00 equiv) and THF (4 mL). A solution of diphenylmethanol **4-31a** (552 mg, 3.00 mmol, 1.00 equiv) in THF (6 mL) was added dropwise at room temperature, after which the reaction was stirred for 2 hours. The flask was then cooled to 0 °C in an ice bath, after which a solution of 4-bromobenzyl bromide (900 mg, 3.60 mmol, 1.20 equiv) in THF (6 mL) was added dropwise. The reaction was stirred at 0 °C for 1 hour, at which point the cooling bath was removed and the reaction was stirred for an additional 16 hours. The reaction was quenched with saturated $NH_4Cl_{(aq)}$ (25 mL) and extracted with EtOAc (3 × 30 mL). The combined organic phases were washed with water (3 × 25 mL), brine (2 × 25 mL), dried over Na_2SO_4 and filtered. After removal of the solvent by rotary evaporation, purification by column chromatography (gradient 15:1 to 3:1 hexane/CH_2Cl_2) afforded the title compound as a white solid (791 mg, 75%). **^{1}H NMR** (500 MHz, $CDCl_3$): δ 7.50 (d, J = 8.4 Hz, 2 H), 7.41 – 7.35 (m, 8 H), 7.31 – 7.27 (m, 4 H), 5.45 (s, 1 H), 4.52 (s, 2 H); **^{13}C NMR** (126 MHz, $CDCl_3$): δ 142.0, 137.6, 131.6, 129.5, 128.6, 127.7, 127.2, 121.5, 82.8, 69.9. Spectral data were in agreement with the literature.[149]

Reductive deoxygenation of ether **4-43** was performed following **GP4-6**. Yields were determined by ^{1}H NMR relative to 1,3,5-trimethoxybenzene as an internal standard (95% **4-32a**, 47% **4-20**, 52% **4-42**)

4.6.11 ^{11}B NMR Study of Alcohol Deoxygenation

A vial was charged with heterocycle **4-30** (5.0 mg, 0.025 mmol), HFIP (600 μL) and CD_3CN (60 μL). The solution was transferred to an NMR tube for analysis. ^{1}H NMR, ^{11}B NMR and HRMS were consistent with formation of boranol exchange ester **4-44** ($C_{11}H_9BF_6NO_2^+$: Calculated: 312.0625; Found: 312.0626). After NMR spectra were recorded, the solution was charged with alcohol **4-31a** (9.2 mg, 0.050 mmol, 2.0 equiv). The solution turned pale yellow in color and was analyzed by ^{11}B NMR approximately 10 minutes later, which suggested the formation of zwitterionic boronate **4-45**. After the NMR was recorded, the solution was charged with TMDSO (53 μL, 0.30 mmol, 6.0 equiv). The solution was mixed thoroughly and analyzed by ^{1}H and ^{11}B NMR approximately 10 minutes later. ^{11}B NMR showed full consumption of the tetravalent boron species, while ^{1}H NMR revealed the formation of reduction product **4-32a**.

4.6.12 Crystallization of Bis(hexafluoroisopropoxy)boronate Zwitterion 4-48

Crystallization was performed as follows: Heterocycle **4-30** (7.0 mg) was dissolved in a mixture of HFIP (600 μL) and MeCN (60 μL). After standing at room temperature for 10 minutes, the mixture was concentrated by rotary evaporation (water bath temperature 30 °C). Upon evaporation, white plate shaped crystals were obtained and used for X-ray crystallography, which revealed the zwitterionic structure **4-48**.

The crystals were subsequently dissolved in CD_3CN, where they were fully soluble.

1,1-Bis[(1,1,1,3,3,3-hexafluoropropan-2-yl)oxy]-3-methyl-1*H*-2,3,1-benzoxazaborinin-1-uide (4-48): mp = 95.3 – 99.0 °C; **^{1}H NMR** (500 MHz, CD_3CN): δ 8.41 (m, 1 H), 7.72 (td, *J* = 7.4, 1.3 Hz, 1 H), 7.64 (d, *J* = 7.2 Hz, 1 H), 7.59 (d, *J* = 7.7 Hz, 1 H), 7.53 (td, *J* = 7.6, 1.3 Hz, 1 H), 4.65 (heptet, *J* = 6.5 Hz, 2 H), 3.85 (d, *J* = 0.7 Hz, 3 H); **^{13}C NMR** (126 MHz, CD_3CN): δ 147.8, 136.3, 132.6, 130.5, 129.6, 128.3, 123.7 (q, *J* = 283.2 Hz), 70.1 (heptet, *J* = 32.0 Hz), 49.5; **^{11}B NMR**

(128 MHz, CD_3CN): δ 4.9; **^{19}F NMR** (376 MHz, CD_3CN): δ – 75.2 (dq, *J* = 9.5, 6.6 Hz, 6 F), – 75.4 (dq, *J* = 8.9, 6.5 Hz, 6 F) (sample contains 2% free HFIP, – 76.4 (d, *J* = 6.5 Hz)); **FTIR** (microscope, cm^{-1}): 2956 (w), 2911 (w), 1375 (m), 1233 (s), 1187 (s), 1149 (m), 1105 (m), 1007 (w), 894 (w), 672 (w); **HRMS** (ESI) for $C_{14}H_{10}{}^{11}BF_{12}NO_3Na$ $[M+Na]^+$: Calculated: 502.0454; Found: 502.0450.

The catalytic activity of zwitterion **4-48** was examined following **GP4-6** and **GP4-7** for the deoxygenation of alcohol **4-31u** and ketone **4-37a** respectively, where virtually quantitative recovery of starting material was observed in both cases.

4.7 References

1) Hedstrom, L. *Enzyme Specificity and Selectivity; eLS;* John Wiley & Sons, Ltd.: Chichester, UK, 2010.
2) Yoon, T. P., Jacobsen, E. N. *Science* **2003**, *299*, 1691–1693.
3) Berthod, M., Mignani, G., Woodward, G., Lemaire, M. *Chem. Rev.* **2005**, *105*, 1801–1836.
4) Ghosh, A. K., Mathivanan, P., Cappiello, J. *Tetrahedron: Asymmetry* **1998**, *9*, 1–45.
5) Kacprzak, K., Gawroński, J. *Synthesis* **2001**, *7*, 961–998.
6) Seebach, D., Beck, A. K., Heckel, A. *Angew. Chem. Int. Ed.* **2001**, *40*, 92–138.
7) Hall, D. G. *Chem. Soc. Rev.* **2019**, *48*, 3475–3496.
8) Weissman, S. A., Anderson, N. G. *Org. Process Res. Dev.* **2015**, *19*, 1605–1633.
9) Shevlin, M. *ACS Med. Chem. Lett.* **2017**, *8*, 601–607.
10) Mo, X., Yakiwchuk, J., Dansereau, J., McCubbin, J. A., Hall, D. G. *J. Am. Chem. Soc.* **2015**, *137*, 9694–9703.
11) Estopiñá-Durán, S., Mclean, E. B., Donnelly, L. J., Hockin, B. M., Taylor, J. E. *Org. Lett.* **2020**, *22*, 7547–7551.
12) Mo, X., Hall, D. G. *J. Am. Chem. Soc.,* **2016**, *138*, 10762–10765.
13) Estopiñá-Durán, S., Donnelly, L. J., Mclean, E. B., Hockin, B. M., Slawin, A. M. Z., Taylor, J. E. *Chem. Eur. J.* **2019**, *25*, 3950–3956.
14) Verdelet, T., Ward, R. M., Hall, D. G. *Eur. J. Org. Chem.* **2017**, *38*, 5729–5738.

15) Zhang, S., Leboeuf, D., Moran, J. *Chem. Eur. J.* **2020**, *26*, 9883–9888.

16) Zheng, H., Ghanbari, S., Nakamura, S., Hall, D. G. *Angew. Chem. Int. Ed.* **2012**, *51*, 6187–6190.

17) Ricardo, C. L., Mo, X., McCubbin, J. A., Hall, D. G. *Chem. Eur. J.* **2015**, *21*, 4128–4223.

18) Oshima, K., Aoyama, Y. *J. Am. Chem. Soc.* **1999**, *121*, 2315–2316.

19) Taylor, M. S. *Acc. Chem. Res.* **2015**, *48*, 295–305.

20) Lee, D., Williamson, C. L., Chan, L., Taylor, M. S. *J. Am. Chem. Soc.* **2012**, *134*, 8260–8267.

21) Gorelik, D., Lin, Y. C., Briceno-Strocchia, A. I., Taylor, M. S. *J. Org. Chem.* **2019**, *84*, 900–908.

22) D'Angelo, K. A., Taylor, M. S. *J. Am. Chem. Soc.* **2016**, *138*, 11058–11066.

23) Lee, D., Taylor, M. S. *Org. Biomol. Chem.* **2013**, *11*, 5409–5412.

24) Estrada, C. D., Ang, H. T., Vetter, K.-M., Ponich, A. A., Hall, D. G. *J. Am. Chem. Soc.* **2021**, *143*, 4162–4167.

25) Fatemi, S., Gernigon, N., Hall, D. G. *Green Chem.* **2015**, *17*, 4016–4028.

26) Zheng, H., McDonald, R., Hall, D. G. *Chem. Eur. J.* **2010**, *16*, 5454–5460.

27) Mo, X., Morgan, T. D. R., Ang, H. T., Hall, D. F. *J. Am. Chem. Soc.* **2018**, *140*, 5264–5271.

28) Tanaka, M., Nakagawa, A., Nishi, N., Ijima, K., Sawa, R., Takahashi D., Toshima, K. *J. Am. Chem. Soc.* **2018**, *140*, 3644–3651.

29) Li, M., Yang, T., Dixon, D. J. *Chem. Commun.* **2010**, *46*, 2191–2193.

30) William, J. M., Kuriyama, M., Onomura, O. *Adv. Synth. Catal.* **2014**, *356*, 934–940.

31) Kazmi, M. Z. H., Rygus, J. P. G., Ang, H. T., Paladino, M., Johnson, M. A., Ferguson, M. J., Hall, D. G. *J. Am. Chem. Soc.* **2021**, *143*, 10143–10156.

32) Tasnádi, G., Lukesch, M., Zechner, M., Jud, W., Hall, M., Ditrich, K., Baldenius, K., Hartog, A. F., Wever, R., Faber, K. *Eur. J. Org. Chem.* **2016**, *1*, 45–50.

33) Bilbrough, T., Piemontese, E., Seitz, O. *Chem. Soc. Rev.* **2022**, *51*, 5691–5730.

34) Kyriakis, J. M. *J. Biol. Chem.* **2014**, *289*, 9460–9462.

35) Rautio, J., Kumpulainen, H., Heimbachm T., Oliyai, R., Oh, D., Järvinen, T., Savolainen, J. *Nat. Rev. Drug Discov.* **2008**, *7*, 255–270.

36) Stella, V. J., Nti-Addae, K. W. *Adv. Drug Deliv. Rev.* **2007**, *59*, 677–694.

37) Mandala, S., Hajdu, R., Bergstrom, J., Quackenbush, E., Xie, J., Milligan, J., Thornton, R., Shei, G.-J., Card, D., Keohane, C., Rosenbach, M., Hale, J., Lynch, C. L., Rupprecht, K., Parsons, W., Rosen, H. *Science* **2002**, *296*, 346–349.

38) Sculimbrene, B. R., Miller, S. J. *J. Am. Chem. Soc.* **2001**, *123*, 10125–10126.

39) Takeda, S., Chino, M., Kiuchi, M., Adachi, K. *Tetrahedron Lett.* **2005**, *46*, 5169–5172.

40) Kiuchi, M., Adachi, K., Tomatsu, A., Chino, M., Takeda, S., Tanaka, Y., Maeda, Y., Sato, N., Mitsutomi, N., Sugahara, K., Chiba, K. *Bioorg. Med. Chem.* **2005**, *13*, 425–432.

41) Coppola, K. A., Testa, J. W., Allen, E. E., Sculimbrene, B. R. *Tetrahedron Lett.* **2014**, *55*, 4203–4206.

42) Ouellette, E. T., Lougee, M. G., Bucknam, A. R., Endres, P. J., Kim, J. Y., Lynch, E. J., Sisko, E. J., Sculimbrene, B. R. *J. Org. Chem.* **2021**, *86*, 7450–7459.

43) Kusano, S., Miyamoto, S., Matsuoka, A., Yamada, Y., Ishikawa, R., Hayashida, O. *Eur. J. Org. Chem.* **2020**, *11*, 1598–1602.

44) Li, H., Liu, Y., Liu, J., Liu, Z. *Chem. Commun.* **2011**, *47*, 8169–8171.

45) Kuwano, S., Hosaka, Y., Arai, T. *Org. Biomol. Chem.* **2019**, *17*, 4475–4482.

46) Kolb, H. C., VanNieuwenhze, M. S., Sharpless, B. K. *Chem. Rev.* **1994**, *94*, 2483–2547.

47) Mahajabeen, P., Chadha, A. *Tetrahedron: Asymmetry* **2011**, *22*, 2156–2160.

48) Modak, A., Maiti, D. *Org. Biomol. Chem.* **2016**, *14*, 21–35.

49) Hong, B., Luo, T., Lei, X. *ACS Cent. Sci.* **2020**, *6*, 622–635.

50) Sun, Z., Fridrich, B., de Santi, A., Elangovan, S., Barta, K. *Chem. Rev.* **2018**, *118*, 614–678.

51) Barton, D. H. R., McCombie, S. W. *J. Chem. Soc., Perkin Trans. 1* **1975**, 1574–1585.

52) McCombie, S., Motherwell, W. B., Tozer, M. J. *Org. React.* **2012**, *77*, 161–591.

53) Lopez, R. M., Hays, D. S., Fu, G. C. *J. Am. Chem. Soc.* **1997**, *119*, 6949–6950.

54) Minlon-H. *J. Am. Chem. Soc.* **1946**, *68*, 2487–2488.

55) Clemmensen, E. *Chem. Ber.* **1913**, *46*, 1837–1843.

56) Ooi, X. Y., Gao, W., Ong, H. C., Lee, H. V., Juan, J. C., Chen, W. H., Lee, K. T. *Renew. Sust. Energ. Rev.* **2019**, *112*, 834–852.

57) Yoneda, T., Aoyama, T., Koizumi, K., Takido, T. *Chem. Lett.* **2014**, *43*, 1604–1606.

58) Shono, T., Matsumura, Y., Tsubata, K., Yoshihiro, S. *Tetrahedron Lett.* **1979**, *20*, 2157–2160.

59) Schwob, T., Kunnas, P., De Jonge, N., Papp, C., Streinrück, H.-P., Kempe, R. *Sci. Adv.* **2019**, *5*, eeav3680.

60) Pesti, J., Larson, G. L. *Org. Process Res. Dev.* **2016**, *20*, 1164–1181.

61) Herrmann, J. M., König, B. *Eur. J. Org. Chem.* **2013**, *31*, 7017–7027.

62) Fang, H., Oestreich, M. *Chem. Sci.* **2020**, *11*, 12604–12615.

63) Adlington, M. G., Orfanopoulos, M., Fry, J. L. *Tetrahedron Lett.* **1976**, *17*, 2955–2958.

64) Parks, D. J., Piers, W. E. *J. Am. Chem. Soc.* **1996**, *118*, 9440–9441.

65) Gevorgyan, V., Liu, J.-X., Rubin, M., Benson, S., Yamamoto, Y. *Tetrahedron Lett.* **1999**, *40*, 8919–8922.

66) Gevorgyan, V., Rubin, M., Benson, S., Liu, J.-X., Yamamoto, Y. *J. Org. Chem.* **2000**, *65*, 6179–6186.

67) Mahdi, T., Stephan, D. W. *Angew. Chem. Int. Ed.* **2015**, *54*, 8511–8514.

68) Chandrasekhar, S., Reddy, C. R., Babu, B. N. *J. Org. Chem.* **2002**, *67*, 9080–9082.

69) Chadwick, R. C., Kardelis, V., Lim, P., Adronov, A. *J. Org. Chem.* **2014**, *79*, 7728–7733.

70) Bajracharya, G. B., Nogami, T., Jin, T., Matsuda, K., Gevorgyan, V., Yamamoto, Y. *Synthesis* **2004**, *2*, 308–311.

71) Gevorgyan, V., Rubin, M., Liu, J.-X., Yamamoto, Y. *J. Org. Chem.* **2001**, *66*, 1672–1675.

72) Bergquist, C., Bridgewater, B. M., Harlan. C. J., Norton, J. R., Friesner, R. A., Parkin, G. *J. Am. Chem. Soc.* **2000**, *122*, 10581–10590.

73) Bender, T. A., Payne, R. R., Gagné, M. R. *Nat. Chem.* **2018**, *10*, 85–90.

74) Li, Y., de la Torre, J. A. M., Grabow, K., Bentrup, U., Junge, K., Zhou, S., Brückner, A., Beller, M. *Angew. Chem. Int. Ed.* **2013**, *52*, 11577–11580.

75) Yan, J., Springsteen, G., Deeter, S., Wang, B. *Tetrahedron* **2004**, *60*, 11205–11209.

76) Axthelm, J., Askes, S. H. C., Elstner, M., Reddy G, U., Görls, H., Bellstedt, P., Schiller, A. *J. Am. Chem. Soc.* **2017**, *139*, 11413–11420.

77) Budiman, Y. P., Westcott, S. A., Radius, U., Marder, T. B. *Adv. Synth. Catal.* **2021**, *363*, 2224–2255.

78) Groziak, M. P., Chen, L., Yi, L., Robinson, P. D. *J. Am. Chem. Soc.* **1997**, *119*, 7817–7826.

79) Colomer, I., Chamberlain, A. E. R., Haughey, M. B., Donohoe, T. J. *Nat. Rev. Chem.* **2017**, *1*, 0088.

80) Dryzhavok, M., Hellal, M., Wolf, E., Falk, F. C., Moran, J. *J. Am. Chem. Soc.* **2015**, *137*, 9555–9558.

81) Cheltsov, A. V., Aoyagi, M., Aleshin, A., Yu, E. C.-W., Gilliland, T., Zhai, D., Bobkov, A. A., Reed, J. C., Liddington, R. C., Abagyan, R. *J. Med. Chem.* **2010**, *53*, 3899–3906.

82) Tang, Y., Liu, Y., Zhang, Y., Zhang, D., Gong, X., Zheng, J. *ACS Chem. Neurosci.* **2021**, *12*, 1419–1427.

83) Ang, H. T., Rygus, J. P. G., Hall, D. G. *Org. Biomol. Chem.* **2019**, *17*, 6007–6014.

84) Surya Prakash, G. K., Do, C., Mathew, T., Olah, G. A. *Catal. Lett.* **2011**, *141*, 507–511.

85) Conlin, R. T., Miller, R. D., Michl, J. *J. Am. Chem. Soc.* **1979**, *101*, 7637–7638.

86) Vekariya, R. H., Aubé, J. *Org. Lett.* **2016**, *18*, 3534–3537.

87) Nagashima, H., Kubo, Y., Kawamura, M., Nishikata, T., Motoyama, Y. *Tetrahedron* **2011**, *67*, 7667–7672.

88) Lal, K., Ghosh, S., Salomon, R. G. *J. Org. Chem.* **1987**, *52*, 1072–1078.

89) Brown, H. C., Wheeler, O. H., Ichikawa, K. *Tetrahedron* **1957**, *1*, 214–220.

90) Duvinage, D., Mebs, S., Beckman, J. *Chem. Eur. J.* **2021**, *27*, 8105–8109.

91) Müther, K., Mohr, J., Oestreich, M. *Organometallics* **2013**, *32*, 6643–6646.

92) Yata, T., Nishimoto, Y., Yasuda, M. *Chem. Eur. J.* **2022**, *28*, e202103852.

93) Kliegel, W., Nanninga, D. *J. Organomet. Chem.* **1983**, *247*, 247–252.

94) Farre, A., Soares, K., Briggs, R. A., Balanta, A., Benoit, D. M., Bonet, A. *Chem. Eur. J.* **2016**, *22*, 17552–17556.

95) Inada, H., Shibuya, M., Yamamoto, Y. *J. Org. Chem.* **2020**, *85*, 11047–11059.

96) Cao, Y.-X., Zhu, G., Li, Y., Le Breton, N., Gourlaouen, G., Choua, S., Boixel, J., Jacquot de Rouville, H.-P., Soulé, J-F. *J. Am. Chem. Soc.* **2002**, *144*, 5902–5909.

97) Zhang, Y., He, L., Shi, L. *Adv. Synth. Catal.* **2018**, *360*, 1926–1931.

98) Li, J., He, L., Liu, X., Cheng, X., Li, G. *Angew. Chem. Int. Ed.* **2019**, *58*, 1759–1763.

99) Garcia, K. J., Gilbert, M. M., Weix, D. J. *J. Am. Chem. Soc.* **2019**, *141*, 1823–1827.

100) Shinohara, K., Tsurugi, H., Anwander, R., Mashima, K. *Chem. Eur. J.* **2020**, *26*, 14130–14136.

101) Uchiyama, M., Kobayashi, Y., Furuyama, T., Nakamura, S., Kajihara, Y., Miyoshi, T., Sakamoto, T., Kondo, Y., Morokuma, K. *J. Am. Chem. Soc.* **2008**, *130*, 472–480.

102) Lerebours, R., Wolf, C. *J. Am. Chem. Soc.* **2006**, *128*, 13052–13053.

103) Caspers, L. D., Spils, J., Damrath, M., Lork, E., Nachtsheim, B. J. *J. Org. Chem.* **2020**, *85*, 9161–9178.

104) Zhang, G., Scott, B. L., Hanson, S. K. *Angew. Chem. Int. Ed.* **2012**, *51*, 12102–12106.

105) Yu, J-Y., Kuwano, R. *Org. Lett.* **2008**, *10*, 973–976.

106) Balakrishnan, V., Murugesan, V., Chindan, B., Rasappan, R. *Org. Lett.* **2021**, *23*, 1333–1338.

107) Zhang, X., Yang, C., Gao, H., Wang, L., Guo, L., Xia, W. *Org. Lett.* **2021**, *23*, 3472–3476.

108) Dhiman, S., Ramasastry, S. S. V. *Org. Biomol. Chem.* **2013**, *11*, 8030–8035.

109) Lei, C., Yip, Y. J., Zhou, J. S. *J. Am. Chem. Soc.* **2017**, *139*, 6086–6089.

110) Isbrandt, E. S., Nasim, A., Zhao, K., Newman, S. G. *J. Am. Chem. Soc.* **2021**, *143*, 14646–14656.

111) Xi, Z.-W., Yang, L., Wang, D.-Y., Feng, C.-W., Qin,Y., Shen, Y.-M., Pu, C., Peng, X. *J. Org. Chem.* **2021**, *86*, 2474–2488.

112) Heijnen, D., Helbert, H., Luurtsema, G., Elsinga, P. H., Feringa, B. L. *Org. Lett.* **2019**, *21*, 4087–4091.

113) Kourist, R., González-Sabin, J., Liz, R., Rebolledo, F. *Adv. Synth. Catal.* **2005**, *347*, 695–702.

114) Potenti, S., Gualandi, A., Puggoli, A., Fermi, A., Bergamini, G., Cozzi, P. G. *Eur. J. Org. Chem.* **2021**, *11*, 1624–1627.

115) Kirmse, W., Krzossa, B., Steenken, S. *J. Am. Chem. Soc.* **1996**, *118*, 7473–7477.

116) Stridfeldt, E., Lindstedt, E., Reitti, M., Blid, J., Norrby, P.-O., Olofsson, B. *Chem. Eur. J.* **2017**, *23*, 13249–13258

117) Mamidi, N., Manna, D. *J. Org. Chem.* **2013**, *78*, 2386–2396.

118) Ai, J.-J., Liu, B.-B., Li, J., Wang, F., Huang, C-M., Rao, W., Wang, S.-Y. *Org. Lett.* **2021**, *23*, 4705–4709.

119) Meng, M., Yang, L., Cheng, K., Qi, C. *J. Org. Chem.* **2018**, *83*, 3275–3284.

120) Yu, C., Huang, R., Patureau, F. W. *Angew. Chem. Int. Ed.* **2022**, *61*, e202201142.

121) Vasilopoulos, A., Zultanski, S. L., Stahl, S. S. *J. Am. Chem. Soc.* **2017**, *139*, 7705–7708.

122) Wang, X., Liu, L.-H., Shi, J.-H., Peng, J., Tu, H.-Y., Zhang, A.-D. *Eur. J. Org. Chem.* **2013**, *30*, 6870–6877.

123) Zhao, G., Yuan, L.-Z., Alami, M., Provot, O. *Adv. Synth. Catal.* **2018**, *360*, 2522–2536.

124) Song, J., Li, Y., Sun, W., Yi, C., Wu, H., Wang, H., Ding, K., Xiao, K., Liu, C. *New. J. Chem.* **2016**, *40*, 9030–9033.

125) Bernhardt, S., Shen, Z.-L., Knochel, P. *Chem. Eur. J.* **2013**, *19*, 828–833.

126) Wang, X.-X., Xu, B.-B., Song, W.-T., Sun, K.-X., Lu, J.-M. *Org. Biomol. Chem.* **2015**, *13*, 4925–4930.

127) Suga, T., Ukaji, Y. *Org. Lett.* **2018**, *20*, 7846–7850.

128) Yoon, S., Hong, M. C., Rhee, H. *J. Org. Chem.* **2014**, *79*, 4206–4211.

129) Yuguchi, M., Tokuda, M., Orito, K. *J. Org. Chem.* **2004**, *69*, 908–914.

130) Aguila, M. J. B., Badiei, Y. M., Warren, T. H. *J. Am. Chem. Soc.* **2013**, *135*, 9399–9406.

131) Sai, M. *Adv. Synth. Catal.* **2018**, *360*, 4330–4335.

132) Udagawa, T., Kogawa, M., Tsuchi, Y., Watanabe, H., Yamamoto, M., Kawatsura, M. *Tetrahedron Lett.* **2017**, *58*, 227–230.

133) Liu, H., Yin, B., Gao, Z., Li, Y., Jiang, H. *Chem. Commun.* **2012**, *48*, 2033–2035.

134) Tsubouchi, A., Muramatsu, D., Takeda, T. *Angew. Chem. Int. Ed.* **2013**, *52*, 12719–12722.

135) Kariofillis, S. K., Jiang, S., Żurański, A. M., Gandhi, S. S., Martinez Alvarado, J. I., Doyle, A. G. *J. Am. Chem. Soc.* **2022**, *144*, 1045–1055.

136) Jana, S. K., Maiti, M., Dey, P., Maji, B. *Org. Lett.* **2002**, *24*, 1298–1302.

137) Meng, Q.-Y., Schirmer, T. E., Berger, A. L., Donabauer, K., König, B. *J. Am. Chem. Soc.* **2019**, *141*, 11393–11397.

138) Leow, D., Chen, Y.-H., Hung, T.-Z., Lin, Y.-Z. *Eur. J. Org. Chem.* **2014**, *33*, 7347–7352.

139) Fukuyama, T., Fujita, Y., Miyoshi, H., Ryu, I., Kao, S.-C., Wu, Y.-K. *Chem. Commun.* **2018**, *54*, 5582–5585.

140) Sun, Y.-Y., Yi, J., Lu, X., Zhang, Z.-Q., Xiao, B., Fu, Y. *Chem. Commun.* **2014**, *50*, 11060–11062.

141) Zhao, C., Zha, G.-F., Fang, W.-Y., Rakesh, K. P., Qin, H.-L. *Eur. J. Org. Chem.* **2019**, *8*, 1801–1807.

142) Chen, C.-R., Zhou, S., Biradar, D. B., Gau, H.-M. *Adv. Synth. Catal.* **2010**, *352*, 1718–1727.

143) Perkins, R. J., Pedro, D. J., Hansen, E. C. *Org. Lett.* **2017**, *19*, 3755–3758.

144) Mikhael, M., Guo, W., Tantillo, D. J., Wengryniuk, S. E. *Adv. Synth. Catal.* **2021**, *363*, 4867–4875.

145) Jereb, M., Vražič, D. *Org. Biomol. Chem.* **2013**, *11*, 1978–1999.

146) Pincock, J. A., Wedge, P. J. *J. Org. Chem.* **1994**, *59*, 5587–5595.

147) Schiltz, P., Casaretto, N., Auffrant, A., Gosmini, C. *Chem. Eur. J.* **2022**, *28*, e202200437.

148) Chan, Y.-C., Bai, Y., Chen, W.-C., Chen, H.-Y., Li, C.-Y., Wu, Y.-Y., Tseng, M.-C., Yap, G. A. P., Zhao, L., Chen, H.-Y., Ong, T.-G. *Angew. Chem. Int. Ed.* **2021**, *60*, 19949–19956.

149) Xu, Q., Xie, H., Chen, P., Yu, L., Chen, J., Hu, X. *Green Chem.* **2015**, *17*, 2774–2779.

Chapter 5 Conclusions and Future Perspectives

5.1 Conclusions and Future Perspectives

Innovative new strategies in catalysis are vital to the discovery of new chemical transformations. An improved understanding of the mechanisms through which catalysts operate can allow for the design of new reactions, which in turn can be further enabled by the design of new catalysts. In particular, innovations in organocatalysis can facilitate new chemical processes with decreased chemical waste and improved sustainability. While organocatalytic strategies for the direct activation of hydroxy-containing compounds have largely paled in comparison to those which are applicable to carbonyl compounds, boronic acid catalysis has begun to emerge as a promising solution to this problem. By avoiding the need for wasteful stoichiometric pre-activation processes, boronic acid catalysis has been successfully applied in a wide variety of transformations of hydroxy-containing compounds, including alcohols, polyols, and carboxylic acids. However, the development of new boronic acid-catalyzed reactions can be limited by a poor understanding of the underlying mechanisms of activation, an inability to modulate catalyst activity with suitable additives, and a reluctance towards exploring new classes of catalysts. The research described in this thesis documents a series of approaches towards the use of reactivity-enabling additives, as well as the implementation of cyclic hemiboronic acids as a new catalyst scaffold in boronic acid-catalyzed transformations.

Chapter 2 described the successful use of perfluoropinacol as a diol additive to enable Friedel-Crafts alkylations with electronically deactivated benzylic alcohols. Mechanistic studies revealed that condensation of perfluoropinacol with the boronic acid catalyst affords a transient boronic ester. The latter is sufficiently Lewis acidic to promote deprotonation of HFIP solvent, leading to the generation of a hydronium boronate species that appears to be the active catalyst in

solution through a Brønsted acid-dependent mechanism. Ionization was proposed to occur through an S_N1 mechanism with a carbocation intermediate. Accordingly, the development of a stereoconvergent Friedel-Crafts transformation to generate enantiomerically-enriched products from racemic alcohols may be possible.

The stereochemistry-determining step in boronic acid-catalyzed Friedel-Crafts benzylation occurs during nucleophilic addition of the arene to an intermediate carbocation/hydroxyboronate ion pair. Thus, the formation of a chiral hydroxyboronate anion may induce facial selectivity in the nucleophilic addition. Using a two-component catalyst system as described in Chapter 2, two possible strategies for the introduction of chirality could be envisioned (Scheme 5-1). The use of a chiral boronic acid could be pursued along with perfluoropinacol as an additive for increased reactivity. Alternatively, an achiral electron-deficient boronic acid could be used along with a chiral diol additive. It is anticipated that significant optimization of the solvent system will be necessary to minimize the formation of solvent-separated ion pairs, as a tight ion pair would be expected to afford an increasingly stereoconvergent process.

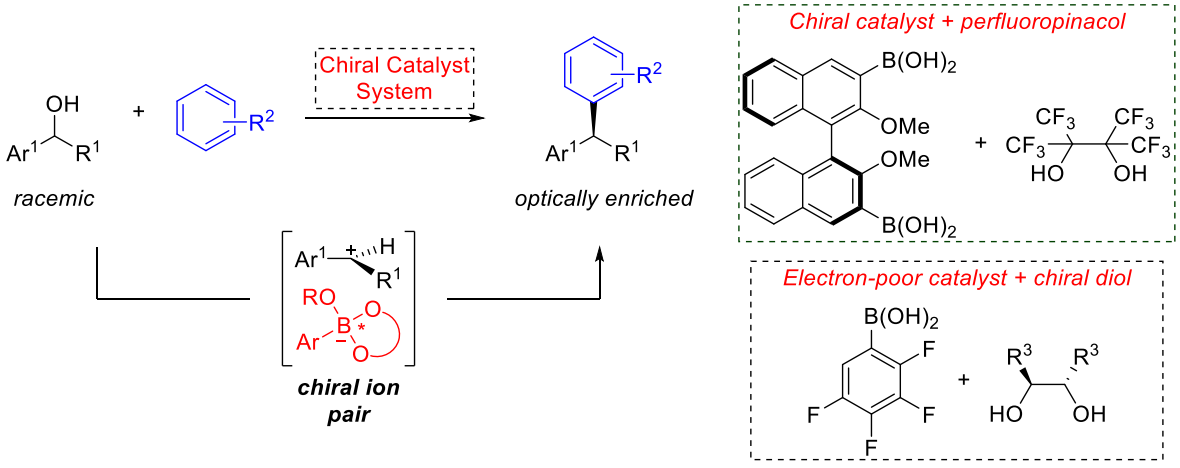

Scheme 5-1 Proposal for stereoconvergent Friedel-Crafts benzylation reactions using boronic acid catalysis via a two-component catalyst system.

Furthermore, the use of heavily fluorinated catalysts in these reactions raises questions as to the scalability and environmental impact of these methods. Highly fluorinated compounds are resistant to environmental degradation, leading to bioaccumulation which may have toxicological implications.[1] Accordingly, the development of electron-deficient boronic acids or diols lacking extensive fluorination should be investigated as these may offer catalytic systems with reduced environmental impact.

In Chapter 3, systematic studies on the acidity, stability, and reactivity of pseudoaromatic cyclic hemiboronic acid naphthalene analogs were described. The identity and substitution of the boron-bound heteroatom was found to have a dramatic influence on molecular properties. Among the parent benzoxazaborine (B–O) and model benzodiazaborine (B–N) heterocycles, pK_a values were found to span a range greater than nine units, corresponding to a 10^9-fold change in acidity. Some hemiboronic acids were found to cleanly undergo boranol exchange in the presence of methanol, while others demonstrated B–N bond cleavage under the same conditions. Additionally, dynamic crossover experiments revealed that *N*-sulfonyl benzodiazaborines are susceptible to solvent-dependent hydrolysis and ring-opening. Computational studies revealed that retention of aromaticity in these cyclic hemiboronic acids is minimal.

The effect of pseudoaromaticity in cyclic hemiboronic acids could be further explored by incorporating B–X units into systems that would display formal antiaromaticity in their all-carbon congeners (provided they are sufficiently planar). This may result in an increasingly Lewis acidic boron center, providing a driving force for disruption of conjugation upon formation of a tetravalent conjugate base (Scheme 5-2a). Alternatively, these systems may adopt geometries that are significantly less planar than the naphthoid isosteres studied in Chapter 3, which may have an impact on their hydrolytic stability. Furthermore, the synthesis of benzodiazaborines with pendant

hydroxy groups would allow for the examination of intramolecular boranol exchange, which may be more facile than the intermolecular variant (Scheme 5-2b). A dynamic equilibrium between open and closed forms may also have an impact on the acidity or hydrolytic stability of the resulting compounds.

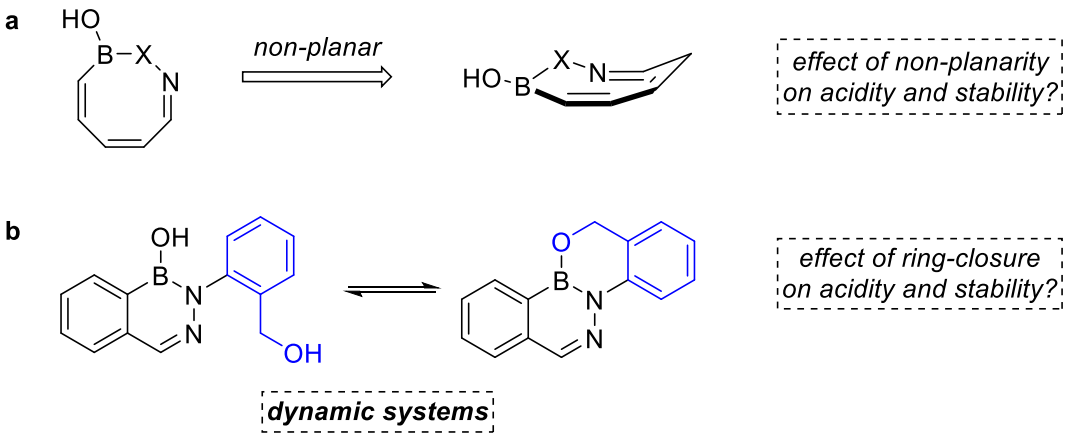

Scheme 5-2 a Extension of cyclic pseudoaromatic hemiboronic acids towards non-planar or anti-aromatic structures. **b** Intramolecular boranol exchange in a dynamic benzodiazaborine system.

Guided by the fundamental reactivity studied in Chapter 3, the results described in Chapter 4 illustrate a systematic application of the benzoxazaborine scaffold in boronic acid catalysis. The parent hemiboronic acid was found to be an effective catalyst for the monophosphorylation of vicinal diols, which was demonstrated to occur through a tetravalent boronate intermediate. Conversely, a cationic derivative of this heterocycle was found to be a highly active catalyst for the reductive deoxygenation of alcohols and ketones using silane reductants. Despite the structural similarity of the two catalysts, minimal overlap in catalytic activity was observed between the two hemiboronic acids.

These results may enable the development of new hemiboronic acid-catalyzed transformations through a mechanistically guided approach. In particular, the cationic catalytic

system for electrophilic activation may be applicable to other types of bond-forming processes for the synthesis of ketones, which could be deoxygenated using the same catalyst. Building on well-established precedents for the electrophilic activation of carboxylic acids, the development of a hemiboronic acid-catalyzed Friedel-Crafts acylation protocol could allow for sequential acylation and deoxygenation, enabling a formal catalytic Friedel-Crafts alkylation under mild conditions (Scheme 5-3a). Alternatively, dual-catalytic strategies can be pursued, such as the direct alkylation of aldehydes using alcohols as electrophiles with a carbene co-catalyst. In these ways, the use of deoxygenation in tandem with other hemiboronic acid-catalyzed bond forming processes may enable the installation of unactivated primary alkyl substituents to aromatic rings under mild conditions (Scheme 5-3b).

Additionally, further derivatization of the benzoxazaborine scaffold could be investigated to design new cationic hemiboronic acid catalysts. In particular, the effect of different counter anions on the reactivity of these cationic species should also be examined, particularly the use of weakly coordinating anions such as SbF_6, PF_6 or tetrakis[3,5-bis(trifluoromethyl)phenyl]borate to generate a more reactive carbocation (Scheme 5-3c). Studies on other anions may also facilitate the development of enantioselective transformations when catalysts with chiral anions are employed. Furthermore, the effect of electron-withdrawing substituents on nitrogen should be examined for their impact on the electrophilicity of the iminium carbon and the stability of the endocyclic B–O bond, as an increasingly electron-deficient nitrogen atom may facilitate these possible catalyst decomposition pathways.

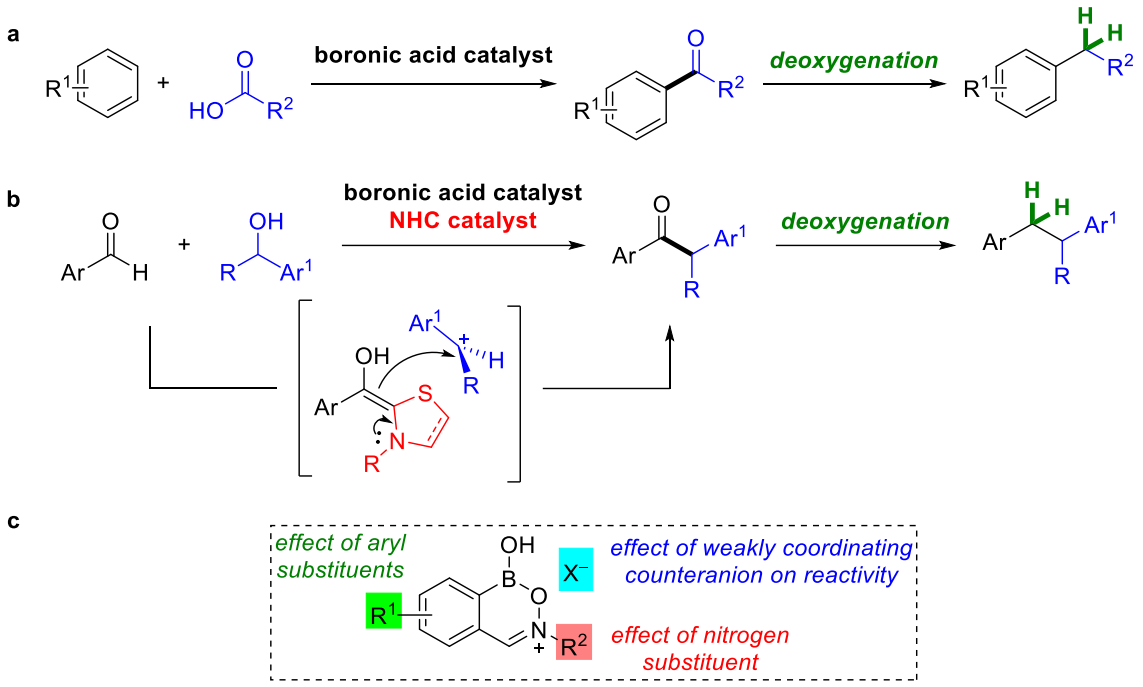

Scheme 5-3 a Tandem acylation/deoxygenation sequence via BAC. **b** Dual catalytic benzylation and deoxygenation strategy using boronic acid and carbene catalysis. **c** New benzoxazaborine derivatives.

Although the toolbox of transformations that have proven amenable to boronic acid catalysis has continued to grow, new strategies in the design of catalytic systems are essential to unlocking new boronic acid-catalyzed processes. The research described herein represents a contribution to the development of co-catalytic systems using diol additives, and to the mechanistically guided application of cyclic hemiboronic acids as a new catalyst scaffold. With an improved understanding of the underlying mechanisms of boronic acid catalysis, as well as innovations in the synthesis of boron-containing heterocycles, new advances in catalytic hydroxy-group activation may be achieved to offer sustainable new strategies in synthesis.

5.2 References

1) Evich, M. G., Davis, M. J. B., Mccord, J. P., Acrey, B., Awkerman, J. A., Knappe, D. R. U., Lindstrom, A. B., Speth, T. F., Tebes-Stevens, C., Strynar, M. J., Wang, Z., Weber, E. J., Henderson, W. M., Washington, J. W. *Science* **2022**, *375*, 6580.

Bibliography

1) Catlow, C. R., Davidson, M., Hardacre, C., Hutchings, G. J. *Phil. Trans. R. Soc. A* **2016**, *374*, 20150089.

2) Hartwig, J. *Organotransition Metal Chemistry: From Bonding to Catalysis*; University Science Books: Sausalito, CA, **2010**.

3) Clark, J. H. *Green Chem.* **1999**, *1*, 1–8.

4) Constable, D. J. C., Dunn, P. J., Hayler, J. D., Humphrey, G. R., Leazer Jr., J. L., Linderman, R. J., Lorenz, K. L., Manley, J., Pearlman, B. A., Wells, A., Zaks, A., Zhang, T. Y. *Green Chem.* **2007**, *9*, 411–420.

5) Trader, D. J., Carlson, E. E. *Mol. Biosyst.* **2012**, *8*, 2484–2493.

6) Henkel, T., Brunne, R. M., Müller, H., Reichel, F. *Angew. Chem. Int. Ed.* **1999**, *38*, 643–647.

7) Appel, R. *Angew. Chem. Int. Ed.* **1975**, *14*, 801–811.

8) Kumara Swamy, K. C., Bhuvan Kumar, N. N., Balaraman, E., Pavan Kumar, K. V. P. *Chem. Rev.* **2009**, *109*, 2551–2561.

9) Grieco, P. A., Gilman, S., Nishizawa, M. *J. Org. Chem.* **1976**, *41*, 1485–1486.

10) Carey, J. S., Laffan, D., Thomson, C., Williams, M. T. *Org. Biomol. Chem.* **2006**, *4*, 2337–2347.

11) Hall, D. G. *Chem. Soc. Rev.* **2019**, *48*, 3475–3496.

12) Hall, D. G., Ed. *Boronic Acids: Preparation and Applications in Organic Synthesis,* 2nd edn., Wiley-VCH: Weinheim, **2011**.

13) Frankland, E., Duppa, B. F. *Liebigs Ann.* **1860**, *115*, 319–322.

14) Michaelis, A., Becker, P. *Ber. Dtsch. Chem. Ges.* **1880**, *13*, 58–61.

15) Michaelis, A. *Liebigs Ann. Chen.* **1901**, *315*, 19–43.

16) Partyka, D. V. *Chem. Rev.* **2011**, *111*, 1529–1595.

17) Miyaura, N., Yamada, K., Suzuki, A. *Tetrahedron Lett.* **1979**, *20*, 3437–3440.

18) Suzuki, A. *Angew. Chem. Int. Ed.* **2011**, *50*, 6722–6737.

19) Chan, D., Monaco, K., Wang, R., Winter, M. *Tetrahedron Lett.* **1998** *39*, 2933–2936.

20) Evans, D., Katz, J., West, T. *Tetrahedron Lett.* **1998**, *39*, 2937–2940.

21) Lam, P., Clark, C., Saubern, S., Adams, J., Winters, M., Chan, D., Combs, A. *Tetrahedron Lett.* **1998**, *39*, 2941–2944.

22) Liebeskind, L., Srogl, J. *J. Am. Chem. Soc.* **2000**, *122*, 11260–11261.

23) Hayashi, T., Takahashi, M., Takaya, Y., Ogasawara, M. *J. Am. Chem. Soc.* **2002**, *124*, 5052–5058.

24) Petasis, N. A., Akritopoulou, I. *Tetrahedron Lett.* **1993**, *34*, 583–586.

25) Matteson, D. S., Mah, R. W. H. *J. Am. Chem. Soc.* **1963**, *85*, 2599–2603.

26) Lachance, H., Hall, D. G. Allylboration of Carbonyl Compounds. In *Organic Reactions*, **2009**, 1–574.

27) Armstrong, R. J., Aggarwal, V. K. *Synthesis* **2017**, *49*, 3323–3336.

28) Xu, L., Wang, G., Zhang, S., Wang, H., Wang, L., Liu, L., Jiao, J., Li, P. *Tetrahedron* **2017**, *73*, 7123–7157.

29) Yadagiri, B., Daipule, K., Singh, S. P. *Asian J. Chem.* **2020**, *10*, 7–37.

30) Hu, J., Ferger, M., Shi, Z., Marder, T. B. *Chem. Soc. Rev.* **2021**, *50*, 13129–13188.

31) Neeve, E. C., Geier, S. J., Mkhalid, I. A. I., Westcott, S. A., Marder, T. B. *Chem. Rev.* **2016**, *116*, 9091–9161.

32) Chow, W. K., Yuen, O. Y., Choy, P. Y., So, C. M., Lau, C. P., Wong, W. T., Kwong, F. Y. *RSC Adv.* **2013**, *3*, 12518–12539.

33) Silva, M. P., Saraiva, L., Pinto, M., Sousa, M. E. *Molecules* **2020**, *25*, 4323–4362.

34) Messner, K., Vuong, B., Tranmer, G. K. *Pharmaceuticals* **2022**, *15*, 2, 264–296.

35) Cadahía, J. P., Previtali, V., Troelsen, N. S., Clausen, M. H. *Med. Chem. Commun.* **2019**, *10*, 1531–1549.

36) António, J. P. M., Russo, R., Carvalho, C. P., Cal, P. M. S. D., Gois, P. M. P. *Chem. Soc. Rev.* **2019**, *48*, 3513–3536.

37) Cho, S., Hwang, S. Y., Oh, D. X., Park, J. *J. Mater. Chem. A.* **2021**, *9*, 14630–14655.

38) Brooks, W. L. A., Sumerlin, B. S. *Chem. Rev.* **2016**, *116*, 1375–1397.

39) Williams, G. T., Kedge, J. L., Fossey, J. S. *ACS Sens.* **2021**, *6*, 1508–1528.

40) Wu, X., Chen, X.-X., Song, B.-N., Huang, Y.-J., Ouyang, W.-J., Li, Z., James, T. D., Jiang, Y.-B. *Chem. Commun.* **2014**, *50*, 13987–13989.

41) Aung, Y.-Y., Kristani, A. N., Lee, H. V., Fahmi, M. Z. *ACS Omega,* **2021**, *6*, 17750–17765.

42) Li, H., Zhang, X., Zhang, L., Wang, X., Kong, F., Fan, D., Li, L., Wang, W. *Anal. Chim. Acta.* **2017**, *15*, 104–113.

43) Frey, L., Jarju, J. J., Salonen, L. M., Medina, D. D. *New J. Chem.* **2021**, *45*, 14879–14907.

44) Rettig, S. J., Trotter, T. *Can. J. Chem.* **1997**, *55*, 3071–3075.

45) Soundararajan, S., Duesler, E. N., Hageman, J. H. *Acta Crystallogr.* **1993**, *C49*, 690–693.

46) Lorand, J. P., Edwards, J. O. *J. Org. Chem.* **1959**, *24*, 769–774.

47) Letsinger, R. L., Dandegaonker, S., Vullo, W. J., Morrison, J. D. *J. Am. Chem. Soc.* **1963**, *85*, 2223–2227.

48) Rao, G., Philipp, M. *J. Org. Chem.* **1991**, *56*, 1505–1512.

49) Taylor, M. S. *Acc. Chem. Res.* **2015**, *48*, 295–305.

50) Carey, J. S., Laffan, D., Thomson, C., Williams, M. T. *Org. Biomol. Chem.* **2006**, *4*, 2337–2347.

51) Dugger, R. W., Ragan, J. A., Ripin, D. H. B. *Org. Process Res. Dev.* **2005**, *9*, 253–258.

52) Ishihara, K., Ohara, S., Yamamoto, H. *J. Org. Chem.* **1996**, *61*, 4196–4197.

53) Arkhipenko, S., Sabatini, M. T., Batsanov, A. S., Karaluka, V., Sheppard, T. D., Rzepa, H. S., Whiting, A. *Chem. Sci.* **2018**, *9*, 1058–1072.

54) Tale, R. H., Patil, K. M. *Tetrahedron Lett.* **2002**, *43*, 9715–9716.

55) Tale, R. H., Patil, K. M., Dapurkar, S. E. *Tetrahedron Lett.* **2003**, *44*, 3427–3428.

56) Maki, T., Ishihara, K., Yamamoto, H. *Synlett* **2004**, 1355–1358.

57) Maki, T., Ishihara, K., Yamamoto, H. *Org. Lett.* **2005**, *7*, 5047–5050.

58) Sakakura, A., Ohkubo, T., Yamashita, R., Akakura, M., Ishihara, K. *Org. Lett.* **2011**, *13*, 892–895.

59) Al-Zoubi, R. M., Marion, O., Hall, D. G. *Angew. Chem. Int. Ed.* **2008**, *47*, 2876–2879.

60) Zheng, H., McDonald, R., Hall, D. G. *Chem. Eur. J.***2010**, *16*, 5454–5460.

61) Azuma, T., Murata, A., Kobayashi, Y., Inokuma, T., Takemoto, Y. *Org. Lett.* **2014**, *16*, 4256–4259.

62) Ayama, N., Azuma, T., Kobayashi, Y., Takemoto, Y. *Chem. Pharm. Bull.* **2016**, *64*, 704–717.

63) McCubbin, J. A., Hosseini, H., Krokhin, O. V. *J. Org. Chem.* **2010**, *75*, 959–962.

64) Zheng, H., Lejkowski, M., Hall, D. G. *Chem. Sci.* **2011**, *2*, 1305–1310.

65) Zheng, H., Ghanbari, S., Nakamura, S., Hall, D. G. *Angew. Chem. Int. Ed.* **2012**, *51*, 6187–6190.

66) Zheng, H., Lejkowski, M., Hall, D. G. *Tetrahedron Lett.* **2013**, *54*, 91–94.

67) Tang, W.-B., Cao, K.-S., Meng, S.-S., Zheng, W.-H. *Synthesis* **2017**, *49*, 3670–3675.

68) Debache, A., Boumoud, B., Armimour, M., Belfaitah, A., Rhouati, S., Carboni, B. *Tetrahedron Lett.* **2006**, *47*, 5697–5699.

69) Aelvoet, K., Batsanov, A. S., Blatch, A. J., Grosjean, C., Patrick, L. G. F., Smethurst, C. A., Whiting, A. *Angew. Chem. Int. Ed.* **2008**, *47*, 768–770.

70) Lee, D., Taylor, M. S. *Org. Biomol. Chem.* **2013**, *11*, 5409–5412.

71) Tanaka, M., Nakagawa, A., Nishi, N., Ijima, K., Sawa, R., Takahashi, D., Toshima, K. *J. Am. Chem. Soc.* **2018**, *140*, 3644–3651.

72) William, J. M., Kuriyama, M., Onomura, O. *Adv. Synth. Catal.* **2014**, *356*, 934–940.

73) Zhang, S., Leboeuf, D., Moran, J. *Chem. Eur. J.* **2020**, *26*, 9883–9888.

74) Pires, E., Fraile, J. S. *Phys. Chem. Chem. Phys.* **2020**, *22*, 24351–24358.

75) Diemoz, K. M., Franz, A. K. *J. Org. Chem.* **2019**, *84*, 1126–1138.

76) Tatina, M. B., Moussa, Z., Xia, M., Judeh, Z. M. A. *Chem. Commun.* **2019** *55*, 12204–12207.

77) Cao, K.-S., Bian, H.-X., Zheng, W.-H. *Org. Biomol. Chem.* **2015**, *13*, 6449–6452.

78) Arnold, K., Batsanov, A. S., Davies, B., Grosjean, C., Schütz, T., Whiting, A., Zawatsky, K. *Chem. Commun.* **2008**, *33*, 3879–3881.

79) Estopiñá-Durán, S., Donnelly, L. J., Mclean, E. B., Hockin, B. M., Slawin, A. M. Z., Taylor, J. E. *Chem. Eur. J.* **2019**, *25*, 3950–3956.

80) Verdelet, T., Ward, R. M., Hall, D. G. *Eur. J. Org. Chem.* **2017**, *38*, 5729–5738.

81) Wolf, E., Richmond, E., Moran, J. *Chem. Sci.* **2015**, *6*, 2501–2505.

82) Torssell, K. *Arkiv foer Kemi* **1957**, *10*, 507–511.

83) Baker, S. J., Zhang, Y.-K., Akama, T., Lau, A., Zhou, H., Hernandez, V., Mao, W., Alley, M. R. K., Sanders, V., Plattner, J. J. *J. Med. Chem.* **2006**, *49*, 4447–4450.

84) Liu, C. T., Tomsho, J. W., Benkovic, S. J. *Bioorg***.** *Med. Chem.* **2014**, *22*, 4462–4473.

85) Adamczyk-Woźniak, A., Borys, K. M., Sporzyński, A. *Chem. Rev.* **2015**, *115*, 5224–5247.

86) Dowlut, M., Hall, D. G. *J. Am. Chem. Soc.* **2006**, *128*, 4226–4227.

87) Adamczyk-Woźniak, A., Borys, K. M., Madura, I. D., Pawełko, A., Tomecka, E., Żukowski, K. *New J. Chem.* **2013**, *37*, 188–194.

88) Vshyvenko, S., Clapson, M. L., Suzuki, I., Hall, D. G. *ACS Med. Chem. Lett.* **2016**, *7*, 1097–1101.

89) Shimada, N., Hirata, M., Koshizuka, M., Ohse, N., Kaito, R., Makino, K. *Org. Lett.* **2019**, *21*, 4303–4308.

90) Koshizuka, M., Makino, K., Shimada, N. *Org. Lett.* **2020**, *22*, 8658–8664.

91) Michigami, K., Sakaguchi, T., Takemoto, Y. *ACS Catal.* **2020**, *10*, 683–688.

92) Wang, K., Lu, Y., Ishihara, K. *Chem. Commun.* **2018**, *54*, 5410–5413.

93) Kusano, S., Miyamoto, S., Matsuoka, A., Yamada, Y., Ishikawa, R., Hayashida, O. *Eur. J. Org. Chem.* **2020**, *11*, 1598–1602.

94) Kuwano, S., Hosaka, Y., Arai, T. *Org. Biomol. Chem.* **2019**, *17*, 4475–4482.

95) Mondal, S., Panda, G. *RSC Adv.* **2014**, *4*, 28317–28358.

96) Rovner, E. S. *Expert Opin. Pharmacother.* **2005**, *4*, 653–666.

97) Palchaudhuri, R., Nesterenko, V., Hergenrother, P. J. *J. Am. Chem. Soc.* **2008**, *130*, 10274–10281.

98) Ng, C. H., Ohlin, C. A., Winther-Jensen, B. *Dyes and Pigments*, **2015**, *115*, 96–101.

99) Kshatriya, R., Jejurkar, V. P., Saha, S. *Eur. J. Org. Chem.* **2019**, *24*, 3818–3841.

100) Rueping, M., Nachtsheim, B. J. *Bellstein J. Org. Chem.* **2010**, *6*, 6.

101) Friedel, C. R., Crafts, J. M. *Compt. Rend.* **1877**, *84*, 1450–1454.

102) Yamauchi, T., Hattori, K., Mizutaki, S., Tamaki, K., Uemura, S. *Bull. Chem. Soc. Jpn.* **1986**, *59*, 3617–3620.

103) Tsuchimoto, T., Tobita, K., Hiyama, T., Fukuzuma, S.-i. *Synlett* **1996**, 557–559.

104) Isao, S., Meng, K. K., Miki, N., Takayuki, N., Akio, Y. *Chem. Lett.* **1997**, *26*, 851–852.

105) Suzuki, M., Shiina, I. *Tetrahedron Lett.* **2002**, *43*, 6391–6394.

106) Noji, M., Ohno, T., Fuji, K., Futaba, N., Tajima, H., Ishii, K. *J. Org. Chem.* **2003**, *68*, 9340–9347.

107) Sun, H.-B., Li, B. Chen, S., Li, J., Hua, R. *Tetrahedron* **2007**, *63*, 10185–10188.

108) Liu, Y.-L., Liu, L., Wang, Y.-L., Han, Y.-C., Wang, D., Chen, Y-J. *Green Chem.* **2008**, *10*, 635–640.

109) Choudhury, J., Podder, S., Roy, S. *J. Am. Chem. Soc.* **2005**, *127*, 6162–6163.

110) Jaratjaroonphong, J., Sathalalai, S., Techasauvapak, P., Reutrakul, V. *Tetrahedron Lett.* **2009**, *50*, 6012–6015.

111) Mertins, K., Iovel, I., Kischel, J., Zapf, A., Beller, M. *Adv. Synth. Catal.* **2006**, *348*, 691–695.

112) Mertins, K., Iovel, I., Kischel, J., Zapf, A., Beller, M. *Angew. Chem. Int. Ed.* **2005**, *44*, 238–242.

113) Iovel, I., Mertins, K., Kischel, J., Zapf, A., Beller, M. *Angew. Chem. Int. Ed.* **2005**, *44*, 3913–3917.

114) Qin, Q., Xie, Y., Floreancig, P. *Chem. Sci.* **2018**, *9*, 8528–8534.

115) Vuković, V. D., Richmond, E., Wolf, E., Moran, J. *Angew. Chem. Int. Ed.* **2017**, *56*, 3085–3089.

116) Ricardo, C. L., Mo, X., McCubbin, J. A., Hall, D. G. *Chem. Eur. J.* **2015**, *21*, 4218–4223.

117) Colomer, I., Chamberlain, A. E. R., Haughey, M. B., Donohoe, T. J. *Nat. Rev. Chem.* **2017**, *1*, 0088.

118) Bentley, T. W., Carter, G. E. *J. Org. Chem.* **1983**, *48*, 579–584.

119) Mo, X., Yakiwchuk, J., Dansereau, J., McCubbin, J. A., Hall, D. G. *J. Am. Chem. Soc.* **2015**, *137*, 9694–9703.

120) Wolf, E., Richmond, E., Moran, J. *Chem. Sci.* **2015**, *6*, 2501–2505.

121) Mo, X., Morgan, T. D. R., Ang, H. T., Hall, D. G. *J. Am. Chem. Soc.* **2018**, *140*, 5264–5271.

122) Lovering, F., Bikker, J., Humblet, C. *J. Med. Chem.* **2009**, *52*, 6752–6756.

123) Collins, K. D., Glorius, F. *Nat. Chem.* **2013**, *5*, 597–601.

124) Brown, H. C., Kanner, B. *J. Am. Chem. Soc.* **1966**, *88*, 986–992.

125) Li, Y., Xiong, Y., Li, X., Ling, X., Huang, R., Zhang, X., Yang, J. *Green Chem.* **2014**, *16*, 2976–2981.

126) Jin, T., Himuro, M., Yamamoto, Y. *Angew. Chem. Int. Ed.* **2009**, *48*, 5893–5896.

127) Middleton, W. J., Lindsey, R. V. *J. Am. Chem. Soc.* **1964**, *86*, 4948–4952.

128) Padmanaban, M., Biju, A. T., Glorius, F. *Org. Lett.* **2011**, *13*, 98–101.

129) Li, J., He, L., Liu, X., Cheng, X., Li, G. *Angew. Chem. Int. Ed.* **2019**, *58*, 1759–1763.

130) Zhang, X., Xia, A., Chen, H., Liu, Y. *Org. Lett.* **2017**, *19*, 2118–2121.

131) Munoz, S. B., Ni, C., Zhang, Z., Wang, F., Shao, N., Mathew, T., Olah, G. A., Prakash, G. K. S. *Eur. J. Org. Chem.* **2017**, *16*, 2322–2326.

132) Han, F., Yang, L., Li, Z., Yingwei, Z., Xia, C. *Adv. Synth. Catal.* **2014**, *356*, 2506–2516.

133) Wang, B. J., Groziak, M. P. *Adv. Heterocycl. Chem.* **2016**, *118*, 47–90.

134) Lepeltier, M., Lukoyanova, O, Jacobsen, A., Jeeva, S., Perepichka, D. F. *Chem. Commun.* **2010**, *46*, 7007–7009.

135) Wang, X., Zhang, F., Liu, J., Tang, R., Fu, Y., Wu, D., Xu, Q., Zhuang, X., He, G., Feng, X. *Org. Lett.* **2013**, *15*, 5714–5717.

136) Estrada, C. D., Ang, H. T., Vetter, K.-M., Ponich, A. A., Hall, D. G. *J. Am. Chem. Soc.* **2021**, *143*, 4162–4167.

137) Jäkle, F. *Coord. Chem. Rev.* **2006**, *250*, 1107–1121.

138) Maitlis, P. M. *Chem. Rev.* **1962**, *62*, 223–245.

139) Matsumi, N., Naka, K., Chujo, Y. *J. Am. Chem. Soc.* **1998**, *120*, 5112–5113.

140) Agou, T., Kobayashi, J., Kawashima, T. *Org. Lett.* **2006**, *8*, 2241–2244.

141) Wang, X.-Y., Wang, J.-Y., Pei, J. *Chem. Eur. J.* **2015**, *21*, 3528–3539.

142) Li, G., Xiong, W.-W., Gu, P.-Y., Cao, J., Zhu, J., Ganguly, R., Li, Y., Grimsdale, A. C., Zhang, Q. *Org. Lett.* **2015**, *17*, 560–563.

143) Li, G., Zhao, Y., Li, J., Cao, J., Zhu, J., Sun, X. W., Zhang, Q. *J. Org. Chem.* **2015**, *80*, 196–203.

144) Marwitz, A. J. V., Jenkins, J. T., Zakharov, L. N., Liu, S.-Y. *Angew. Chem. Int. Ed.* **2010**, *49*, 7444–7447.

145) Fernandes, G. F. S., Denny, W. A., Dos Santos, J. L. *Eur. J. Med. Chem.* **2019**, *179*, 791–804.

146) Baker, S. J., Ding, C. Z., Akama, T., Zhang, Y.-K., Hernandez, V., Xia, Y. *Future Med. Chem.* **2009**, *1*, 1275–1288.

147) Akama, T., Baker, S. J., Zhang, Y.-K., Hernandez, V., Zhou, H., Sanders, V., Freund, Y., Kimura, R., Maples, K. R., Plattner, J. J. *Bioorg. Med. Chem. Let.* **2009**, *19*, 2129–2132.

148) Hecker, S. J., Reddy, K. R., Totrov, M., Hirst, G. C., Lomovskaya, O., Griffith, D. C., King, P., Tsivkovski, R., Sun, D., Sabet, M., Tarazi, Z., Clifton, M. C., Atkins, K., Raymond, A., Potts, K. T., Abendroth, J., Boyer, S. H., Loutit, J. S., Morgan, E. E., Durso, S., Dudley, M. N. *J. Med. Chem.* **2015**, *58*, 3682–3692.

149) Patani, G. A., LaVoie, E. J. *Chem. Rev.* **1996**, *96*, 3147–3176.

150) Lima, L. M., Barreiro, E. J. *Curr. Med. Chem.* **2005**, *12*, 23–49.

151) Mykhailiuk, P. K. *Org. Biomol. Chem.* **2019**, *17*, 2839–2849.

152) Pellicciari, R., Raimondo, M., Marinozzi, M., Natalini, B., Costantino, G., Thomsen, C. *J. Med. Chem.* **1996**, *39*, 2874–2876.

153) Zhong, M., Peng, E., Huang, N., Huang, Q., Huq, A., Lau, M., Colonno, R., Li, L. *Bioorg. Med. Chem. Lett.* **2014**, *24*, 5731–5737.

154) Nicolau, K. C., Vourloumis, D., Totokotsopoulos, S., Papakyriakou, A., Karunsky, H., Fernando, H., Gavriliyuk, J., Webb, D., Stephan, A. *ChemMedChem* **2016**, *11*, 31–37.

155) Stepan, A. F., Subramanyam, C., Efremov, I. V., Dutra, J. K., O'Sullivan, T. J., DiRico, K. J., McDonald, W. S., Won, A., Dorff, P. H., Nolan, C. E. Becker, S. L., Pustilnik, L. R., Riddell, D. R., Kauffman, G. W., Kormos, B. L., Zhang, L., Lu, Y., Capetta, S. H., Green, M. E., Karki, K., Sibley, E., Atchison, K. P., Hallgren, A. J., Oborski, C. E., Robshaw, A. E., Sneed, B., O'Donnell, C. J. *J. Med. Chem.* **2012**, *55*, 3414–3424.

156) Auberson, Y. P., Brocklehurst, C., Furegati, M., Fessard, T. C., Koch, G., Decker, A., La Vecchia, L., Briard, E. *ChemMedChem* **2017**, *12*, 590–598.

157) Giustra, Z. X., Liu, S.-Y. *J. Am. Chem. Soc.* **2018**, *140*, 1184–1194.

158) Zhao, P., Nettleton, D. O., Karki, R. G., Zécri, F. J., Liu, S.-Y. *ChemMedChem* **2017**, *12*, 358–361.

159) Davies, G. H. M. *Chem* **2017**, *2*, 608–609.

160) Stock, A., Pohland, E. *Ber. Dtsch. Chem. Ges.* **1926**, *59*, 2215–2223.

161) Campbell, P. G., Abbey, E. R., Neiner, D., Grant, D. J., Dixon, D. A., Liu, S.-Y. *J. Am. Chem. Soc.* **2010**, *132*, 18048–18050.

162) Baranac-Stojanović, M. *J. Org. Chem.* **2019**, *84*, 13582–13594.

163) Burford, R. J., Li, B., Vasiliu, M, Dixon, D. A., Liu, S.-Y. *Angew. Chem. Int. Ed.* **2015**, *54*, 7823–7827.

164) McConnell, C. R., Haeffner, F., Baggett, A. W., Liu, S.-Y. *J. Am. Chem. Soc.* **2019**, *141*, 9072–9078.

165) Robinson, P. D. Groziak, M. P. *Acta Crystallogr., Sect. C: Cryst. Struct. Commun.* **1999**, C*55*, 1701–1704.

166) Baldock, C., de Boer, G.-J., Rafferty, J. B., Stuitje, A. R., Rice, D. W. *Biochem. Pharmacol.* **1998**, *55*, 1541–1550.

167) Hicks, J. W., Kyle, C. B., Vogels, C. M., Wheaton, S. L., Baerlocher, F. J., Decken, A., Westcott, S. A. *Chem. Biodiversity* **2008**, *5*, 2415–2422.

168) Snyder, H. R., Reedy, A. J., Lennartz, W. J. *J. Am. Chem. Soc.* **1958**, *80*, 835–838.

169) Hückel, E. *Z. Physik* **1931**, *70*, 204–286.

170) Dewar, M. J. S., Dougherty, R. C. *J. Am. Chem. Soc.* **1962**, *84*, 2648–2649.

171) Dewar, M. J. S., Dougherty, R. C. *J. Am. Chem. Soc.* **1964**, *86*, 433–436.

172) Reed, D. *Chem. Soc. Rev.* **1993**, *22*, 109–116.

173) Gao, P., Wang, X., Huang, Z., Yu, H. *ACS Omega*, **2019**, *4*, 12385–12392.

174) Dewar, M. J. S., Jones, R. *J. Am. Chem. Soc.* **1967**, *89*, 2408–2410.

175) Kroeker, S., Stebbins, J. F. *Inorg. Chem.* **2001**, *40*, 6239–6246.

176) Fujdala, K. L., Oliver, A. G., Hollander, F. J., Tilley, T. D. *Inorg. Chem.* **2003**, *42*, 1140–1150.

177) Groziak, M. P., Chen, L., Yi, L., Robinson, P. D. *J. Am. Chem. Soc.* **1997**, *119*, 7817–7826.

178) Gu, H., Chio, T. I., Lei, Z., Staples, R. J., Hirschi, J. S., Bane, S. *Org. Biomol. Chem.* **2017**, *15*, 7543–7548.

179) Whittemore, N. A., Mishra, R., Kheterpal, I., Williams, A. D., Wetzel, R., Serpersu, E. H. *Biochemistry* **2005**, *44*, 4434–4441.

180) Leszczyński, P., Lewandowska, A., Hofman, T., Adamczyk-Woźniak, A., Sporzyński, A. *J. Chem. Eng. Data* **2020**, *65*, 4605–4612.

181) Larkin, J. D., Bhat, K. L., Markham, G. D., Brooks, B. R., Schaefer, H. F., Bock, C. W. *J. Phys. Chem.* **2006**, *110*, 10633–10642.

182) Ang, H. T., Ponich, A. A., Paladino, M., Miskolzie, M., Hall, D. G. *J. Am. Chem. Soc.* **2022**, *144*, 10570–10581.

183) Cammidge, A. N., Goddard, V. H. M., Gopee, H., Harrison, N. L., Hughes, D. L., Schubert, C. J., Sutton, B. M., Watts, G. L., Whitehead, A. J. *Org. Lett.* **2006**, *8*, 4071–4074.

184) Shao, Y., et al., *Mol. Phys.* **2015**, *113*, 184–215.

185) Chen, Z., Wannere, C. S., Corminboeuf, C., Puchta, R., Schleyer, P. V. R. *Chem. Rev.* **2005**, *105*, 3842–3888.

186) Yruegas, S., Patterson, D. C., Martin, C. D. *Chem. Commun.* **2016**, *52*, 6658–6661.

187) Watanabe, E., Miyamoto, C., Tanaka, A., Iizuka, K., Iwatsuki, S., Inamo, M., Takagi, H. D., Ishihara, K. *Dalton Trans.* **2013**, *42*, 8446–8453.

188) Hedstrom, L. *Enzyme Specificity and Selectivity; eLS;* John Wiley & Sons, Ltd.: Chichester, UK, 2010.

189) Yoon, T. P., Jacobsen, E. N. *Science* **2003**, *299*, 1691–1693.

190) Berthod, M., Mignani, G., Woodward, G., Lemaire, M. *Chem. Rev.* **2005**, *105*, 1801–1836.

191) Ghosh, A. K., Mathivanan, P., Cappiello, J. *Tetrahedron: Asymmetry* **1998**, *9*, 1–45.

192) Kacprzak, K., Gawroński, J. *Synthesis* **2001**, 961–998.

193) Seebach, D., Beck, A. K., Heckel, A. *Angew. Chem. Int. Ed.* **2001**, *40*, 92–138.

194) Weissman, S. A., Anderson, N. G. *Org. Process Res. Dev.* **2015**, *19*, 1605–1633.

195) Shevlin, M. *ACS Med. Chem. Lett.* **2017**, *8*, 601–607.

196) Estopiñá-Durán, S., Mclean, E. B., Donnelly, L. J., Hockin, B. M., Taylor, J. E. *Org. Lett.* **2020**, *22*, 7547–7551.

197) Mo, X., Hall, D. G. *J. Am. Chem. Soc.,* **2016**, *138*, 10762–10765.

198) Oshima, K., Aoyama, Y. *J. Am. Chem. Soc.* **1999**, *121*, 2315–2316.

199) Lee, D., Williamson, C. L., Chan, L., Taylor, M. S. *J. Am. Chem. Soc.* **2012**, *134*, 8260–8267.

200) Gorelik, D., Lin, Y. C., Briceno-Strocchia, A. I., Taylor, M. S. *J. Org. Chem.* **2019**, *84*, 900–908.

201) D'Angelo, K. A., Taylor, M. S. *J. Am. Chem. Soc.* **2016**, *138*, 11058–11066.

202) Li, M., Yang, T., Dixon, D. J. *Chem. Commun.* **2010**, *46*, 2191–2193.

203) Kazmi, M. Z. H., Rygus, J. P. G., Ang, H. T., Paladino, M., Johnson, M. A., Ferguson, M. J., Hall, D. G. *J. Am. Chem. Soc.* **2021**, *143*, 10143–10156.

204) Tasnádi, G., Lukesch, M., Zechner, M., Jud, W., Hall, M., Ditrich, K., Baldenius, K., Hartog, A. F., Wever, R., Faber, K. *Eur. J. Org. Chem.* **2016**, *1*, 45–50.

205) Bilbrough, T., Piemontese, E., Seitz, O. *Chem. Soc. Rev.* **2022**, *51*, 5691–5730.

206) Kyriakis, J. M. *J. Biol. Chem.* **2014**, *289*, 9460–9462.

207) Rautio, J., Kumpulainen, H., Heimbachm T., Oliyai, R., Oh, D., Järvinen, T., Savolainen, J. *Nat. Rev. Drug Discov.* **2008**, *7*, 255–270.

208) Stella, V. J., Nti-Addae, K. W. *Adv. Drug Deliv. Rev.* **2007**, *59*, 677–694.

209) Mandala, S., Hajdu, R., Bergstrom, J., Quackenbush, E., Xie, J., Milligan, J., Thornton, R., Shei, G.-J., Card, D., Keohane, C., Rosenbach, M., Hale, J., Lynch, C. L., Rupprecht, K., Parsons, W., Rosen, H. *Science* **2002**, *296*, 346–349.

210) Sculimbrene, B. R., Miller, S. J. *J. Am. Chem. Soc.* **2001**, *123*, 10125–10126.

211) Takeda, S., Chino, M., Kiuchi, M., Adachi, K. *Tetrahedron Lett.* **2005**, *46*, 5169–5172.

212) Kiuchi, M., Adachi, K., Tomatsu, A., Chino, M., Takeda, S., Tanaka, Y., Maeda, Y., Sato, N., Mitsutomi, N., Sugahara, K., Chiba, K. *Bioorg. Med. Chem.* **2005**, *13*, 425–432.

213) Coppola, K. A., Testa, J. W., Allen, E. E., Sculimbrene, B. R. *Tetrahedron Lett.* **2014**, *55*, 4203–4206.

214) Ouellette, E. T., Lougee, M. G., Bucknam, A. R., Endres, P. J., Kim, J. Y., Lynch, E. J., Sisko, E. J., Sculimbrene, B. R. *J. Org. Chem.* **2021**, *86*, 7450–7459.

215) Li, H., Liu, Y., Liu, J., Liu, Z. *Chem. Commun.* **2011**, *47*, 8169–8171.

216) Kolb, H. C., VanNieuwenhze, M. S., Sharpless, B. K. *Chem. Rev.* **1994**, *94*, 2483–2547.

217) Mahajabeen, P., Chadha, A. *Tetrahedron: Asymmetry* **2011**, *22*, 2156–2160.

218) Modak, A., Maiti, D. *Org. Biomol. Chem.* **2016**, *14*, 21–35.

219) Hong, B., Luo, T., Lei, X. *ACS Cent. Sci.* **2020**, *6*, 622–635.

220) Sun, Z., Fridrich, B., de Santi, A., Elangovan, S., Barta, K. *Chem. Rev.* **2018**, *118*, 614–678.

221) Barton, D. H. R., McCombie, S. W. *J. Chem. Soc., Perkin Trans. 1* **1975**, 1574–1585.

222) McCombie, S., Motherwell, W. B., Tozer, M. J. *Org. React.* **2012**, *77*, 161–591.

223) Lopez, R. M., Hays, D. S., Fu, G. C. *J. Am. Chem. Soc.* **1997**, *119*, 6949–6950.

224) Minlon-H. *J. Am. Chem. Soc.* **1946**, *68*, 2487–2488.

225) Clemmensen, E. *Chem. Ber.* **1913**, *46*, 1837–1843.

226) Ooi, X. Y., Gao, W., Ong, H. C., Lee, H. V., Juan, J. C., Chen, W. H., Lee, K. T. *Renew. Sust. Energ. Rev.* **2019**, *112*, 834–852.

227) Yoneda, T., Aoyama, T., Koizumi, K., Takido, T. *Chem. Lett.* **2014**, *43*, 1604–1606.

228) Shono, T., Matsumura, Y., Tsubata, K., Yoshihiro, S. *Tetrahedron Lett.* **1979**, *20*, 2157–2160.

229) Schwob, T., Kunnas, P., De Jonge, N., Papp, C., Streinrück, H.-P., Kempe, R. *Sci. Adv.* **2019**, *5*, eeav3680.

230) Pesti, J., Larson, G. L. *Org. Process Res. Dev.* **2016**, *20*, 1164–1181.

231) Herrmann, J. M., König, B. *Eur. J. Org. Chem.* **2013**, *31*, 7017–7027.

232) Fang, H., Oestreich, M. *Chem. Sci.* **2020**, *11*, 12604–12615.

233) Adlington, M. G., Orfanopoulos, M., Fry, J. L. *Tetrahedron Lett.* **1976**, *17*, 2955–2958.

234) Parks, D. J., Piers, W. E. *J. Am. Chem. Soc.* **1996**, *118*, 9440–9441.

235) Gevorgyan, V., Liu, J.-X., Rubin, M., Benson, S., Yamamoto, Y. *Tetrahedron Lett.* **1999**, *40*, 8919–8922.

236) Gevorgyan, V., Rubin, M., Benson, S., Liu, J.-X., Yamamoto, Y. *J. Org. Chem.* **2000**, *65*, 6179–6186.

237) Mahdi, T., Stephan, D. W. *Angew. Chem. Int. Ed.* **2015**, *54*, 8511–8514.

238) Chandrasekhar, S., Reddy, C. R., Babu, B. N. *J. Org. Chem.* **2002**, *67*, 9080–9082.

239) Chadwick, R. C., Kardelis, V., Lim, P., Adronov, A. *J. Org. Chem.* **2014**, *79*, 7728–7733.

240) Bajracharya, G. B., Nogami, T., Jin, T., Matsuda, K., Gevorgyan, V., Yamamoto, Y. *Synthesis* **2004**, *2*, 308–311.

241) Gevorgyan, V., Rubin, M., Liu, J.-X., Yamamoto, Y. *J. Org. Chem.* **2001**, *66*, 1672–1675.

242) Bergquist, C., Bridgewater, B. M., Harlan. C. J., Norton, J. R., Friesner, R. A., Parkin, G. *J. Am. Chem. Soc.* **2000**, *122*, 10581–10590.

243) Bender, T. A., Payne, R. R., Gagné, M. R. *Nat. Chem.* **2018**, *10*, 85–90.

244) Li, Y., de la Torre, J. A. M., Grabow, K., Bentrup, U., Junge, K., Zhou, S., Brückner, A., Beller, M. *Angew. Chem. Int. Ed.* **2013**, *52*, 11577–11580.

245) Yan, J., Springsteen, G., Deeter, S., Wang, B. *Tetrahedron* **2004**, *60*, 11205–11209.

246) Axthelm, J., Askes, S. H. C., Elstner, M., Reddy G, U., Görls, H., Bellstedt, P., Schiller, A. *J. Am. Chem. Soc.* **2017**, *139*, 11413–11420.

247) Budiman, Y. P., Westcott, S. A., Radius, U., Marder, T. B. *Adv. Synth. Catal.* **2021**, *363*, 2224–2255.

248) Dryzhavok, M., Hellal, M., Wolf, E., Falk, F. C., Moran, J. *J. Am. Chem. Soc.* **2015**, *137*, 9555–9558.

249) Cheltsov, A. V., Aoyagi, M., Aleshin, A., Yu, E. C.-W., Gilliland, T., Zhai, D., Bobkov, A. A., Reed, J. C., Liddington, R. C., Abagyan, R. *J. Med. Chem.* **2010**, *53*, 3899–3906.

250) Tang, Y., Liu, Y., Zhang, Y., Zhang, D., Gong, X., Zheng, J. *ACS Chem. Neurosci.* **2021**, *12*, 1419–1427.

251) Ang, H. T., Rygus, J. P. G., Hall, D. G. *Org. Biomol. Chem.* **2019**, *17*, 6007–6014.

252) Surya Prakash, G. K., Do, C., Mathew, T., Olah, G. A. *Catal. Lett.* **2011**, *141*, 507–511.

253) Conlin, R. T., Miller, R. D., Michl, J. *J. Am. Chem. Soc.* **1979**, *101*, 7637–7638.

254) Vekariya, R. H., Aubé, J. *Org. Lett.* **2016**, *18*, 3534–3537.

255) Nagashima, H., Kubo, Y., Kawamura, M., Nishikata, T., Motoyama, Y. *Tetrahedron* **2011**, *67*, 7667–7672.

256) Lal, K., Ghosh, S., Salomon, R. G. *J. Org. Chem.* **1987**, *52*, 1072–1078.

257) Brown, H. C., Wheeler, O. H., Ichikawa, K. *Tetrahedron* **1957**, *1*, 214–220.

258) Duvinage, D., Mebs, S., Beckman, J. *Chem. Eur. J.* **2021**, *27*, 8105–8109.

259) Müther, K., Mohr, J., Oestreich, M. *Organometallics* **2013**, *32*, 6643–6646.

260) Yata, T., Nishimoto, Y., Yasuda, M. *Chem. Eur. J.* **2022**, *28*, e202103852.

261) Kliegel, W., Nanninga, D. *J. Organomet. Chem.* **1983**, *247*, 247–252.

262) Farre, A., Soares, K., Briggs, R. A., Balanta, A., Benoit, D. M., Bonet, A. *Chem. Eur. J.* **2016**, *22*, 17552–17556.

263) Inada, H., Shibuya, M., Yamamoto, Y. *J. Org. Chem.* **2020**, *85*, 11047–11059.

264) Cao, Y.-X., Zhu, G., Li, Y., Le Breton, N., Gourlaouen, G., Choua, S., Boixel, J., Jacquot de Rouville, H.-P., Soulé, J-F. *J. Am. Chem. Soc.* **2002**, *144*, 5902–5909.

265) Zhang, Y., He, L., Shi, L. *Adv. Synth. Catal.* **2018**, *360*, 1926–1931.

266) Li, J., He, L., Liu, X., Cheng, X., Li, G. *Angew. Chem. Int. Ed.* **2019**, *58*, 1759–1763.

267) Garcia, K. J., Gilbert, M. M., Weix, D. J. *J. Am. Chem. Soc.* **2019**, *141*, 1823–1827.

268) Shinohara, K., Tsurugi, H., Anwander, R., Mashima, K. *Chem. Eur. J.* **2020**, *26*, 14130–14136.

269) Uchiyama, M., Kobayashi, Y., Furuyama, T., Nakamura, S., Kajihara, Y., Miyoshi, T., Sakamoto, T., Kondo, Y., Morokuma, K. *J. Am. Chem. Soc.* **2008**, *130*, 472–480.

270) Lerebours, R., Wolf, C. *J. Am. Chem. Soc.* **2006**, *128*, 13052–13053.

271) Caspers, L. D., Spils, J., Damrath, M., Lork, E., Nachtsheim, B. J. *J. Org. Chem.* **2020**, *85*, 9161–9178.

272) Zhang, G., Scott, B. L., Hanson, S. K. *Angew. Chem. Int. Ed.* **2012**, *51*, 12102–12106.

273) Yu, J-Y., Kuwano, R. *Org. Lett.* **2008**, *10*, 973–976.

274) Balakrishnan, V., Murugesan, V., Chindan, B., Rasappan, R. *Org. Lett.* **2021**, *23*, 1333–1338.

275) Zhang, X., Yang, C., Gao, H., Wang, L., Guo, L., Xia, W. *Org. Lett.* **2021**, *23*, 3472–3476.

276) Dhiman, S., Ramasastry, S. S. V. *Org. Biomol. Chem.* **2013**, *11*, 8030–8035.

277) Lei, C., Yip, Y. J., Zhou, J. S. *J. Am. Chem. Soc.* **2017**, *139*, 6086–6089.

278) Isbrandt, E. S., Nasim, A., Zhao, K., Newman, S. G. *J. Am. Chem. Soc.* **2021**, *143*, 14646–14656.

279) Xi, Z.-W., Yang, L., Wang, D.-Y., Feng, C.-W., Qin,Y., Shen, Y.-M., Pu, C., Peng, X. *J. Org. Chem.* **2021**, *86*, 2474–2488.

280) Heijnen, D., Helbert, H., Luurtsema, G., Elsinga, P. H., Feringa, B. L. *Org. Lett.* **2019**, *21*, 4087–4091.

281) Kourist, R., González-Sabin, J., Liz, R., Rebolledo, F. *Adv. Synth. Catal.* **2005**, *347*, 695–702.

282) Potenti, S., Gualandi, A., Puggoli, A., Fermi, A., Bergamini, G., Cozzi, P. G. *Eur. J. Org. Chem.* **2021**, *11*, 1624–1627.

283) Kirmse, W., Krzossa, B., Steenken, S. *J. Am. Chem. Soc.* **1996**, *118*, 7473–7477.

284) Stridfeldt, E., Lindstedt, E., Reitti, M., Blid, J., Norrby, P.-O., Olofsson, B. *Chem. Eur. J.* **2017**, *23*, 13249–13258

285) Mamidi, N., Manna, D. *J. Org. Chem.* **2013**, *78*, 2386–2396.

286) Ai, J.-J., Liu, B.-B., Li, J., Wang, F., Huang, C-M., Rao, W., Wang, S.-Y. *Org. Lett.* **2021**, *23*, 4705–4709.

287) Meng, M., Yang, L., Cheng, K., Qi, C. *J. Org. Chem.* **2018**, *83*, 3275–3284.

288) Yu, C., Huang, R., Patureau, F. W. *Angew. Chem. Int. Ed.* **2022**, *61*, e202201142.

289) Vasilopoulos, A., Zultanski, S. L., Stahl, S. S. *J. Am. Chem. Soc.* **2017**, *139*, 7705–7708.

290) Wang, X., Liu, L.-H., Shi, J.-H., Peng, J., Tu, H.-Y., Zhang, A.-D. *Eur. J. Org. Chem.* **2013**, *30*, 6870–6877.

291) Zhao, G., Yuan, L.-Z., Alami, M., Provot, O. *Adv. Synth. Catal.* **2018**, *360*, 2522–2536.

292) Song, J., Li, Y., Sun, W., Yi, C., Wu, H., Wang, H., Ding, K., Xiao, K., Liu, C. *New. J. Chem.* **2016**, *40*, 9030–9033.

293) Bernhardt, S., Shen, Z.-L., Knochel, P. *Chem. Eur. J.* **2013**, *19*, 828–833.

294) Wang, X.-X., Xu, B.-B., Song, W.-T., Sun, K.-X., Lu, J.-M. *Org. Biomol. Chem.* **2015**, *13*, 4925–4930.

295) Suga, T., Ukaji, Y. *Org. Lett.* **2018**, *20*, 7846–7850.

296) Yoon, S., Hong, M. C., Rhee, H. *J. Org. Chem.* **2014**, *79*, 4206–4211.

297) Yuguchi, M., Tokuda, M., Orito, K. *J. Org. Chem.* **2004**, *69*, 908–914.

298) Aguila, M. J. B., Badiei, Y. M., Warren, T. H. *J. Am. Chem. Soc.* **2013**, *135*, 9399–9406.

299) Sai, M. *Adv. Synth. Catal.* **2018**, *360*, 4330–4335.

300) Udagawa, T., Kogawa, M., Tsuchi, Y., Watanabe, H., Yamamoto, M., Kawatsura, M. *Tetrahedron Lett.* **2017**, *58*, 227–230.

301) Liu, H., Yin, B., Gao, Z., Li, Y., Jiang, H. *Chem. Commun.* **2012**, *48*, 2033–2035.

302) Tsubouchi, A., Muramatsu, D., Takeda, T. *Angew. Chem. Int. Ed.* **2013**, *52*, 12719–12722.

303) Kariofillis, S. K., Jiang, S., Żurański, A. M., Gandhi, S. S., Martinez Alvarado, J. I., Doyle, A. G. *J. Am. Chem. Soc.* **2022**, *144*, 1045–1055.

304) Jana, S. K., Maiti, M., Dey, P., Maji, B. *Org. Lett.* **2002**, *24*, 1298–1302.

305) Meng, Q.-Y., Schirmer, T. E., Berger, A. L., Donabauer, K., König, B. *J. Am. Chem. Soc.* **2019**, *141*, 11393–11397.

306) Leow, D., Chen, Y.-H., Hung, T.-Z., Lin, Y.-Z. *Eur. J. Org. Chem.* **2014**, *33*, 7347–7352.

307) Fukuyama, T., Fujita, Y., Miyoshi, H., Ryu, I., Kao, S.-C., Wu, Y.-K. *Chem. Commun.* **2018**, *54*, 5582–5585.

308) Sun, Y.-Y., Yi, J., Lu, X., Zhang, Z.-Q., Xiao, B., Fu, Y. *Chem. Commun.* **2014**, *50*, 11060–11062.

309) Zhao, C., Zha, G.-F., Fang, W.-Y., Rakesh, K. P., Qin, H.-L. *Eur. J. Org. Chem.* **2019**, *8*, 1801–1807.

310) Chen, C.-R., Zhou, S., Biradar, D. B., Gau, H.-M. *Adv. Synth. Catal.* **2010**, *352*, 1718–1727.

311) Perkins, R. J., Pedro, D. J., Hansen, E. C. *Org. Lett.* **2017**, *19*, 3755–3758.

312) Mikhael, M., Guo, W., Tantillo, D. J., Wengryniuk, S. E. *Adv. Synth. Catal.* **2021**, *363*, 4867–4875.

313) Jereb, M., Vražič, D. *Org. Biomol. Chem.* **2013**, *11*, 1978–1999.

314) Pincock, J. A., Wedge, P. J. *J. Org. Chem.* **1994**, *59*, 5587–5595.

315) Schiltz, P., Casaretto, N., Auffrant, A., Gosmini, C. *Chem. Eur. J.* **2022**, *28*, e202200437.

316) Chan, Y.-C., Bai, Y., Chen, W.-C., Chen, H.-Y., Li, C.-Y., Wu, Y.-Y., Tseng, M.-C., Yap, G. A. P., Zhao, L., Chen, H.-Y., Ong, T.-G. *Angew. Chem. Int. Ed.* **2021**, *60*, 19949–19956.

317) Xu, Q., Xie, H., Chen, P., Yu, L., Chen, J., Hu, X. *Green Chem.* **2015**, *17*, 2774–2779.

318) Evich, M. G., Davis, M. J. B., Mccord, J. P., Acrey, B., Awkerman, J. A., Knappe, D. R. U., Lindstrom, A. B., Speth, T. F., Tebes-Stevens, C., Strynar, M. J., Wang, Z., Weber, E. J., Henderson, W. M., Washington, J. W. *Science* **2022**, *375*, 6580.

Appendices

Appendix 1: Selected Copies of NMR Spectra

^{1}H (500 MHz) and ^{13}C (101 MHz) NMR of compound 2-36a ($CDCl_3$)

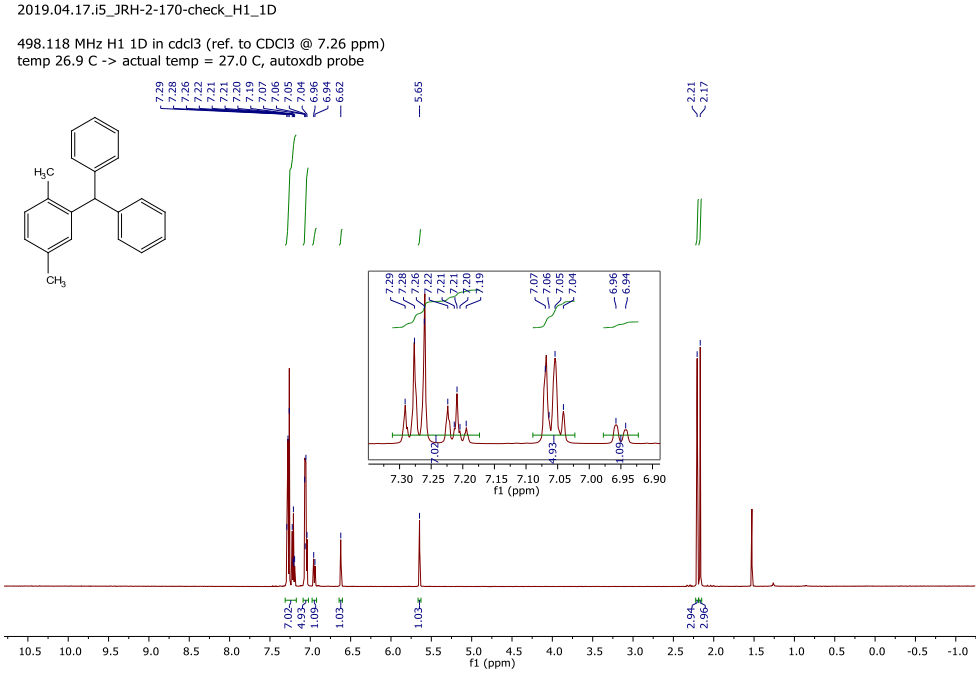

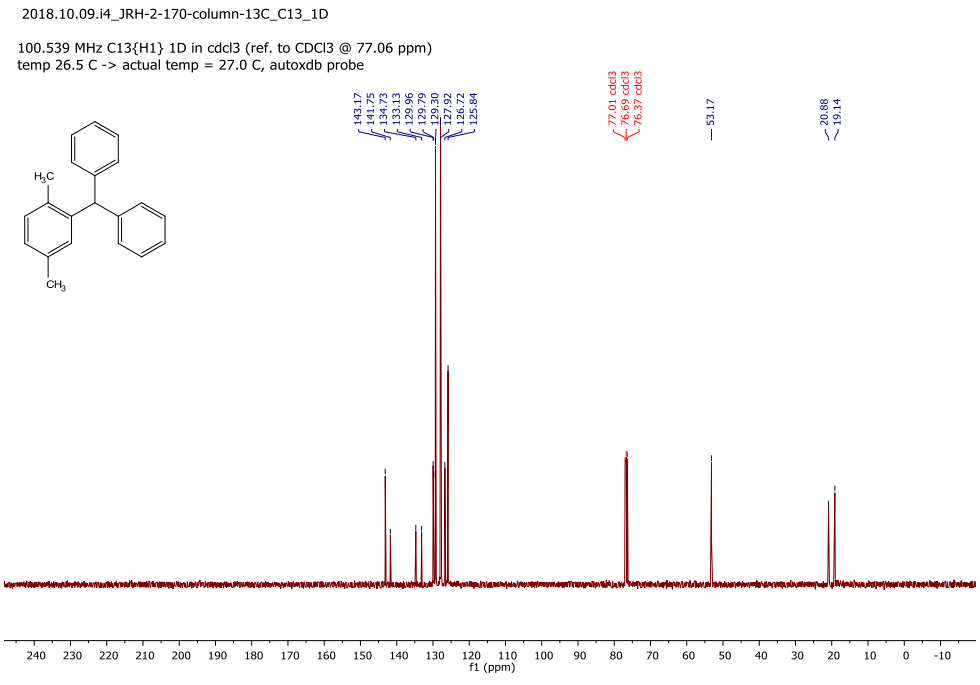

^{1}H (400 MHz), ^{13}C (176 MHz) and ^{11}B (128 MHz) NMR of compound 3-01 (*d*$_6$-acetone)

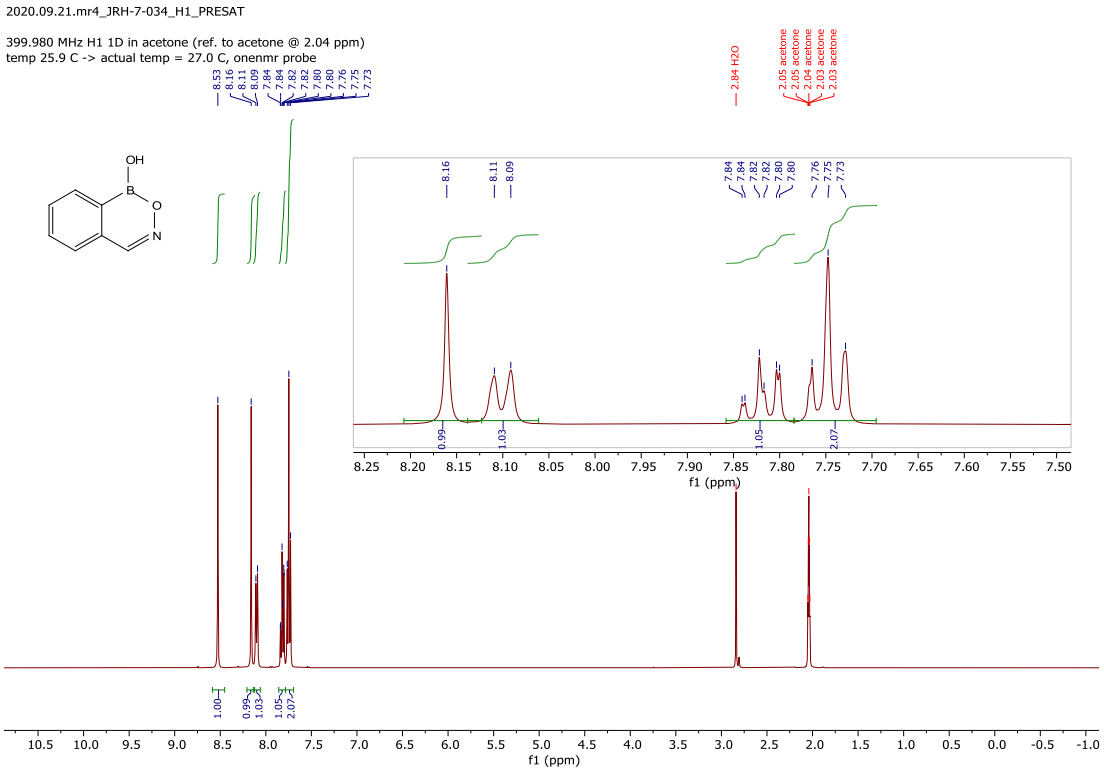

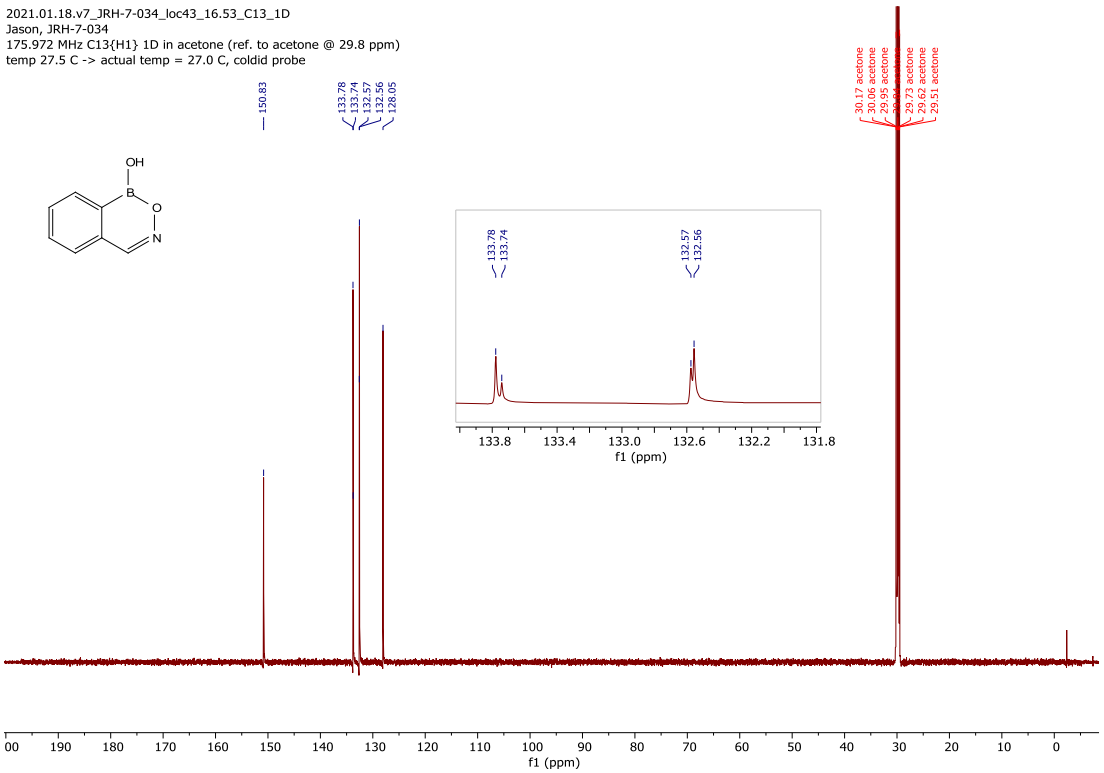

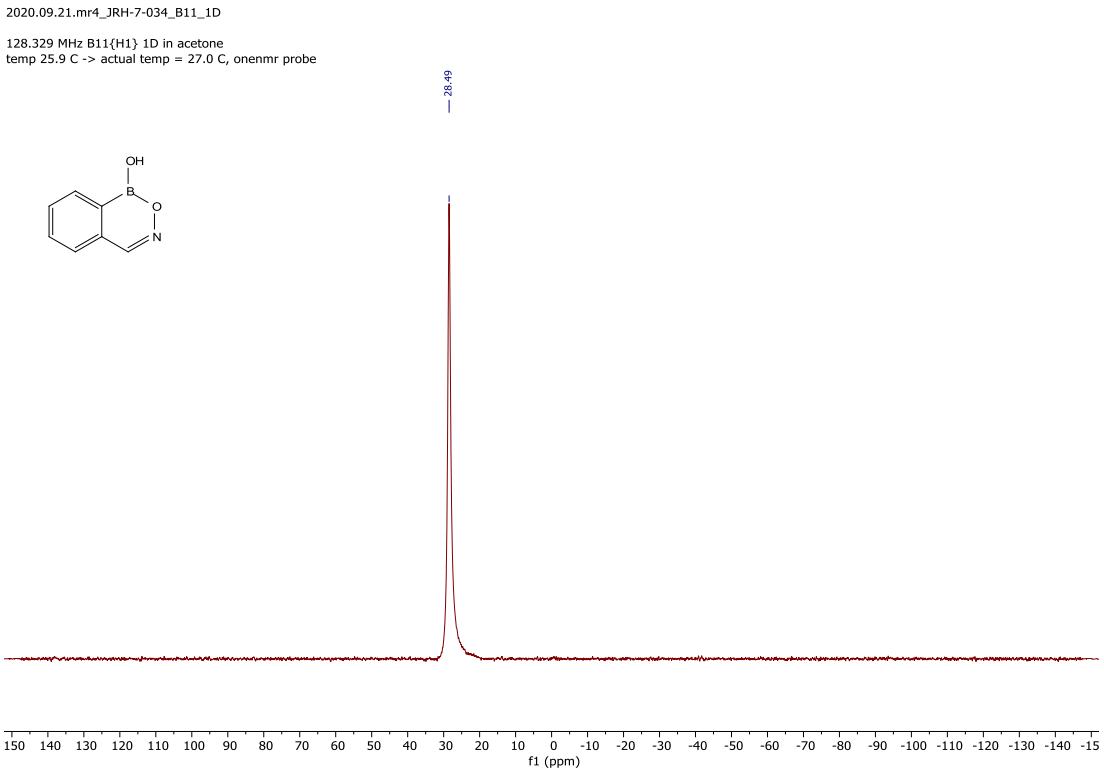

^{1}H (700 MHz), ^{13}C (176 MHz) and ^{11}B (128 MHz) NMR of compound 3-02 (*d*$_6$-acetone)

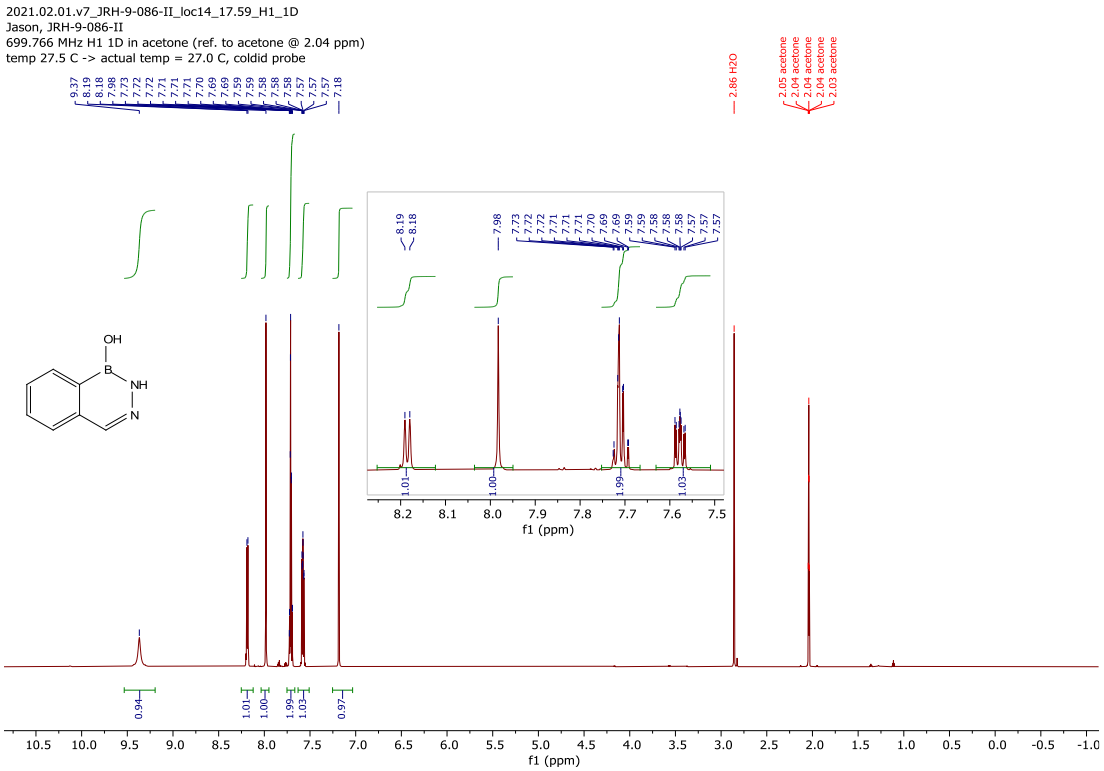

2021.02.01.v7_JRH-9-086-II_loc14_18.00_C13_1D
Jason, JRH-9-086-II
175.972 MHz C13{H1} 1D in acetone (ref. to acetone @ 29.8 ppm)
temp 27.5 C -> actual temp = 27.0 C, coldid probe

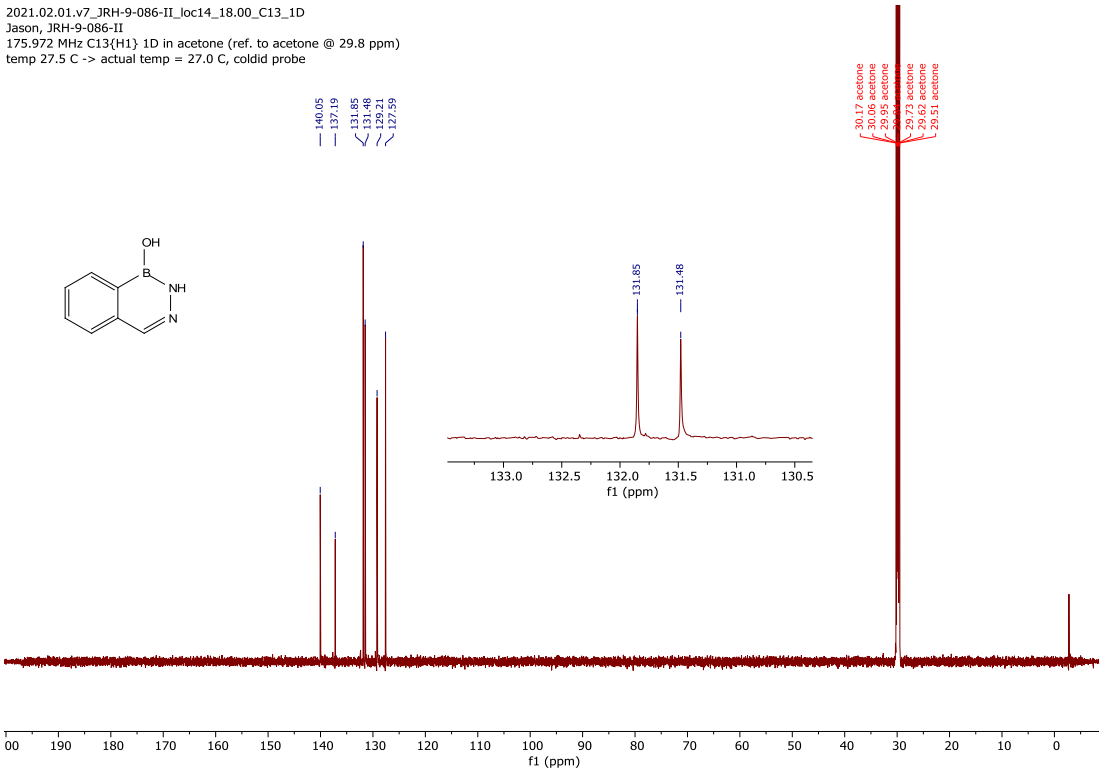

2021.02.01.i4_JRH-9-086-II_loc24_10.53_B11_1D
Jason, JRH-9-086-II
128.270 MHz B11{H1} 1D in acetone
temp 26.5 C -> actual temp = 27.0 C, autoxdb probe

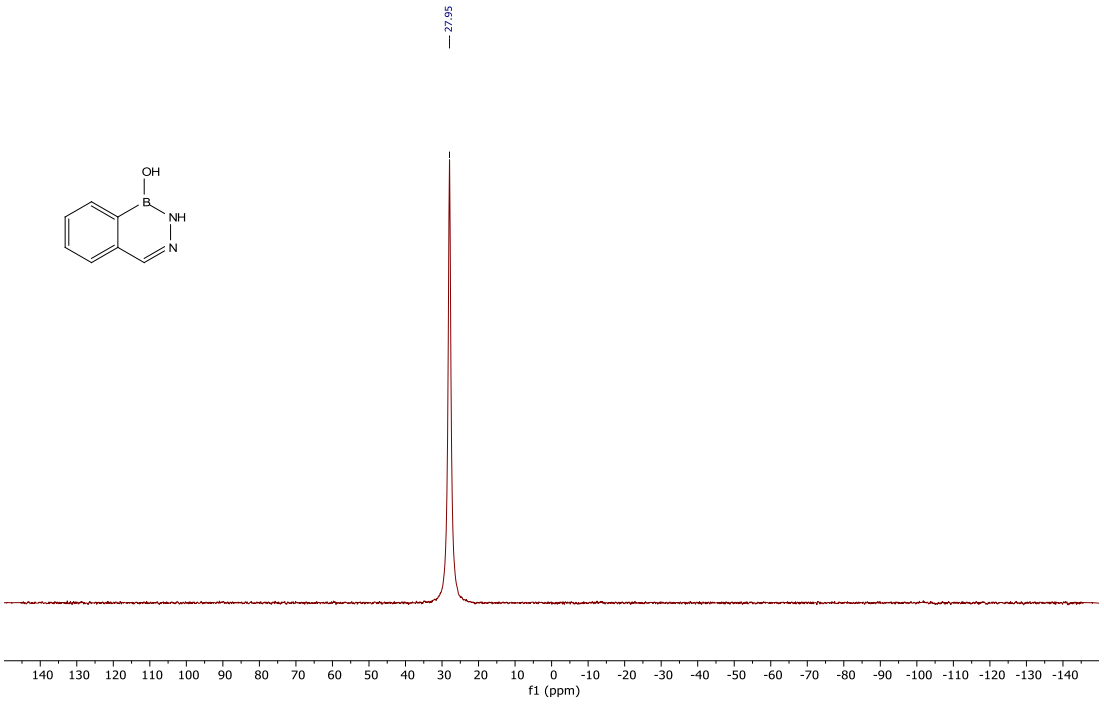

^{1}H (700 MHz), ^{13}C (176 MHz) and ^{11}B (128 MHz) NMR of compound 3-08 (*d*$_6$-acetone + one drop D$_2$O)

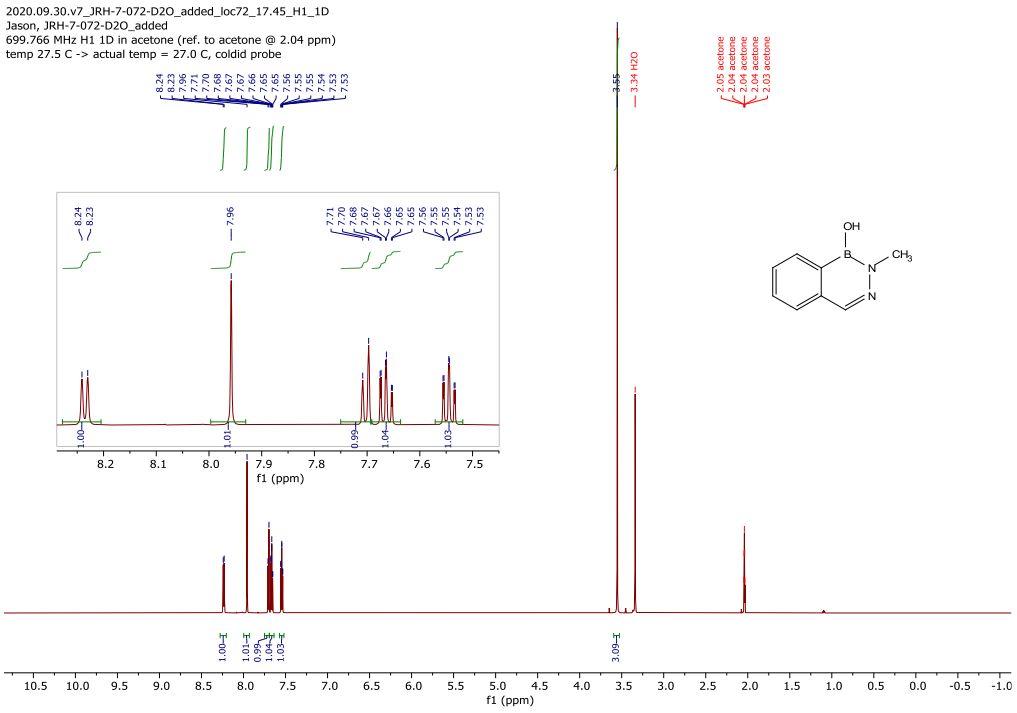

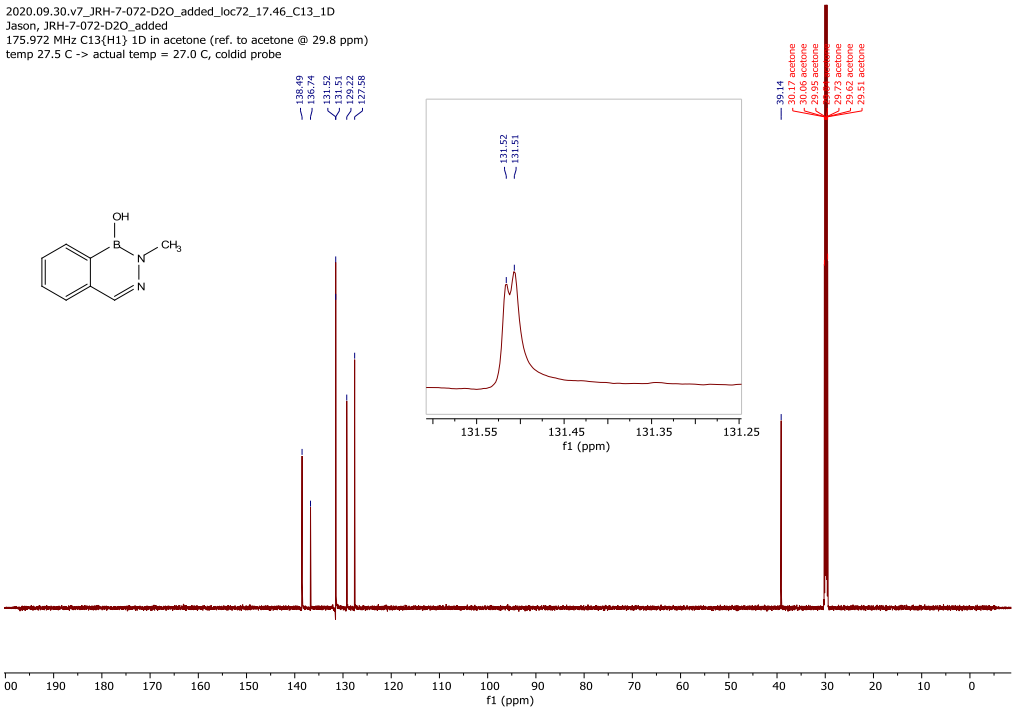

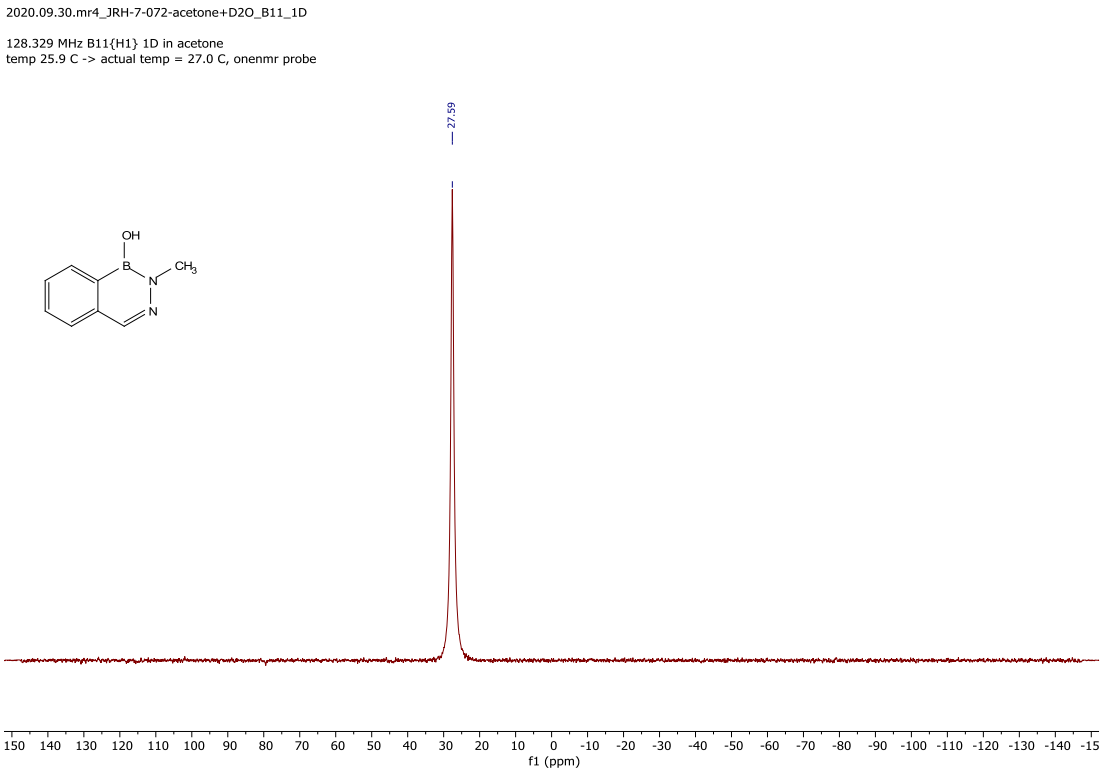

^{1}H (600 MHz), ^{13}C (176 MHz) and ^{11}B (128 MHz) NMR of compound 3-09 (*d*$_6$-acetone)

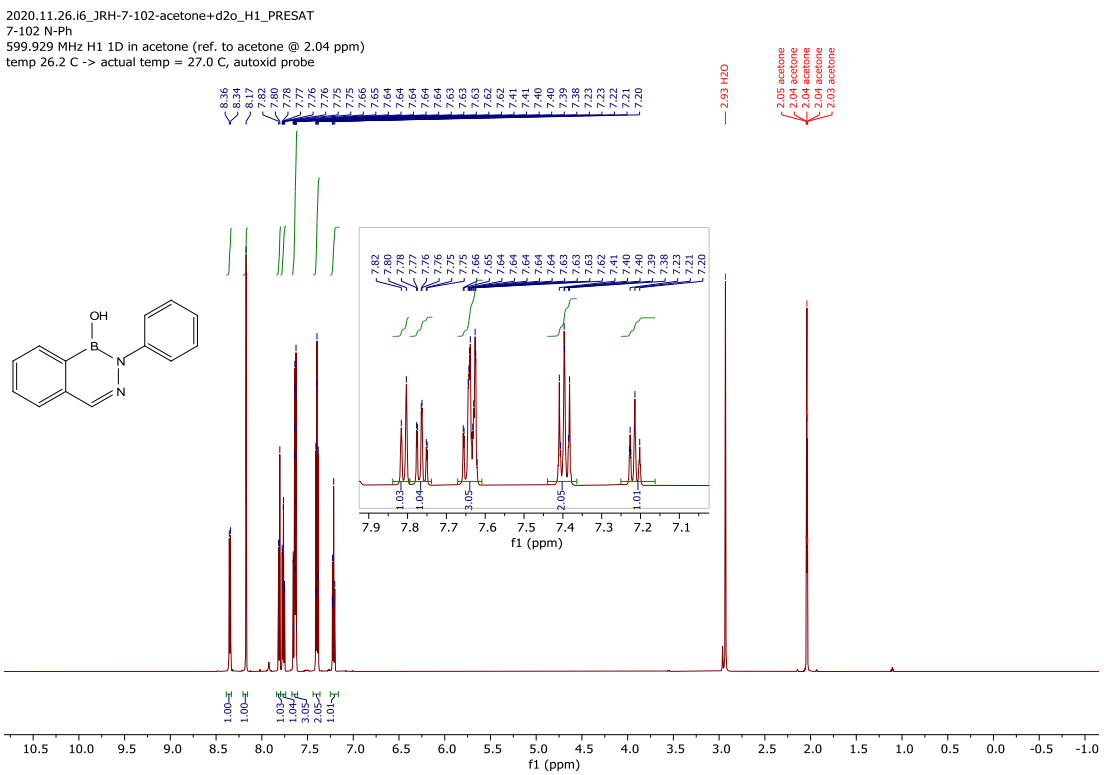

2021.02.01.v7_JRH-7-102-acetone_d2o_loc13_17.52_C13_1D
Jason, JRH-7-102-acetone_d2o
175.972 MHz C13{H1} 1D in acetone (ref. to acetone @ 29.8 ppm)
temp 27.5 C -> actual temp = 27.0 C, coldid probe

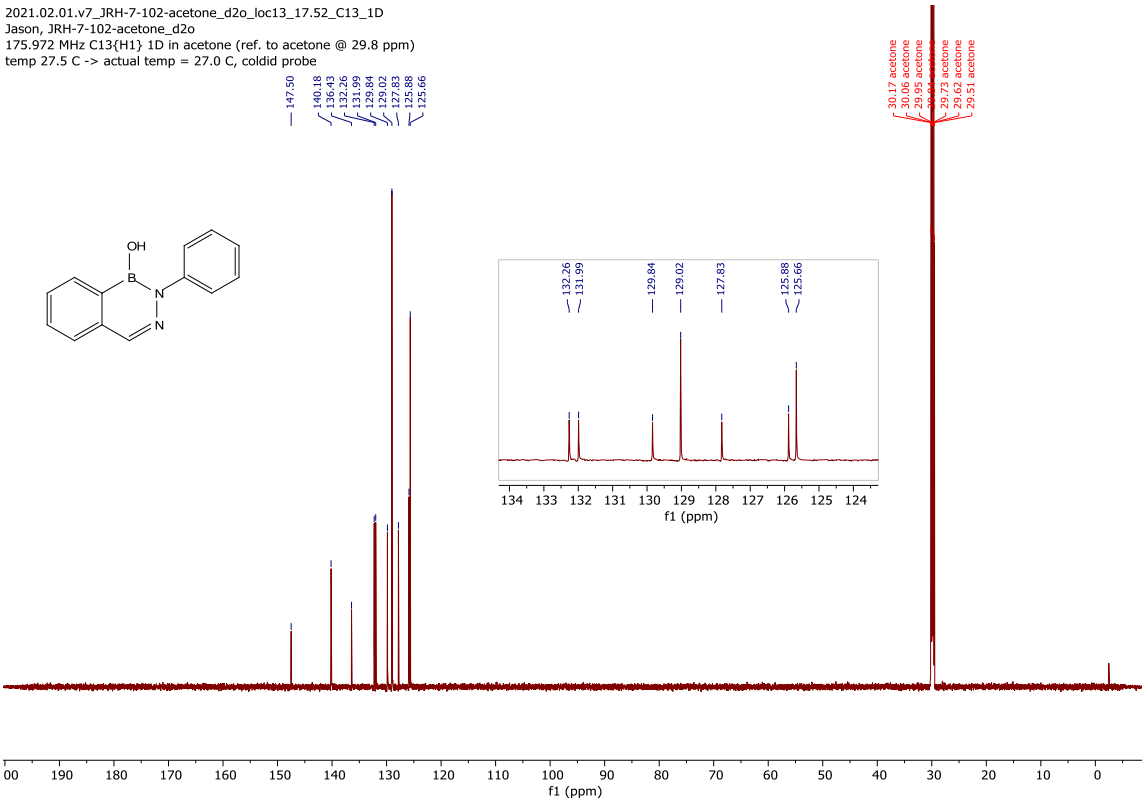

2021.01.26.mr4_JRH-7-102-check-acetone+d2O_B11_1D

128.329 MHz B11{H1} 1D in acetone
temp 25.9 C -> actual temp = 27.0 C, onenmr probe

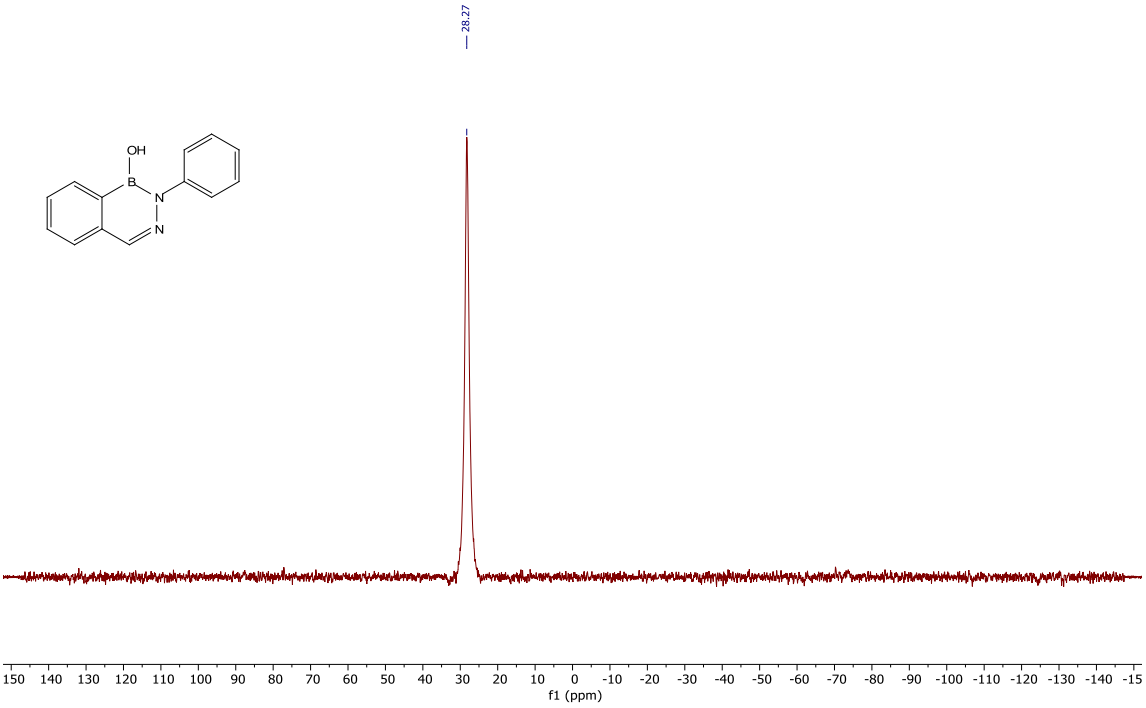

^{1}H (700 MHz), ^{13}C (176 MHz) and ^{11}B (128 MHz) NMR of compound 3-10 (*d*$_6$-acetone)

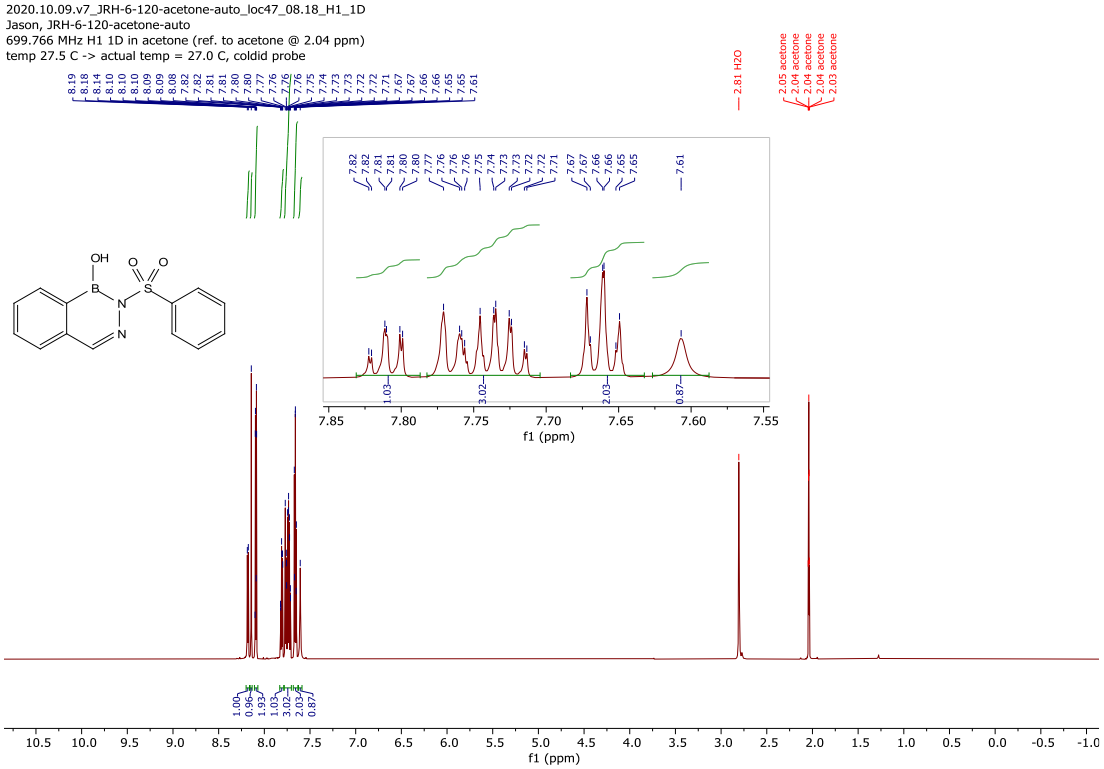

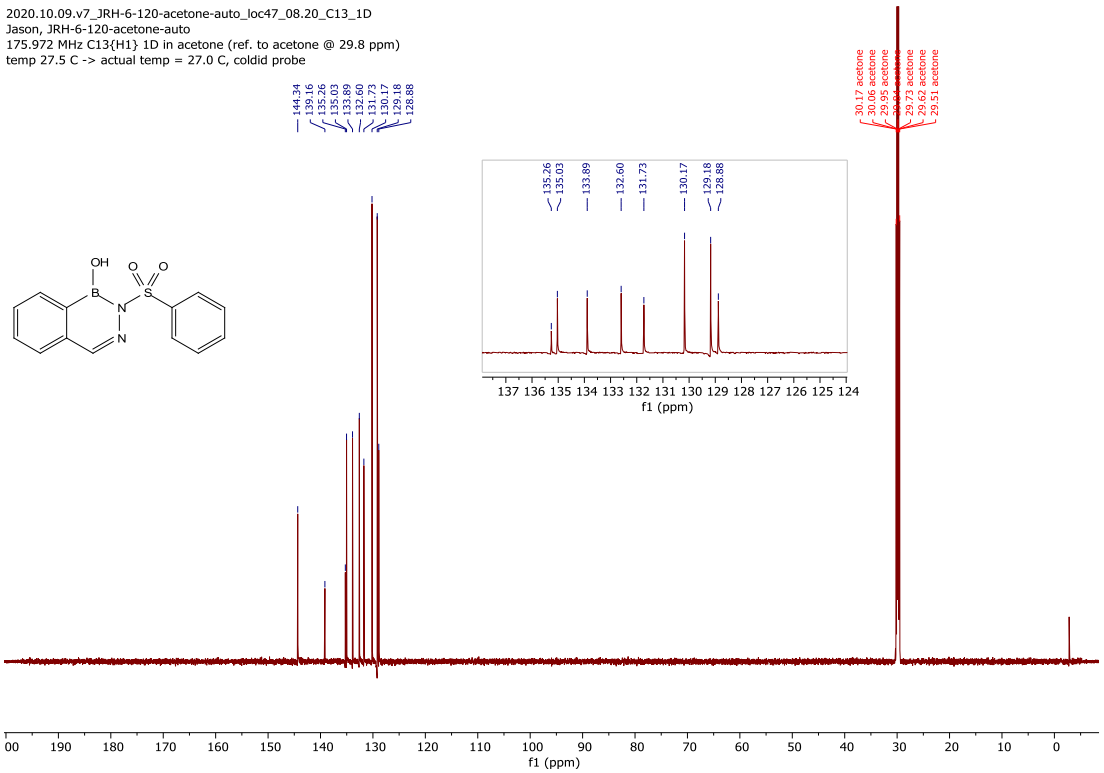

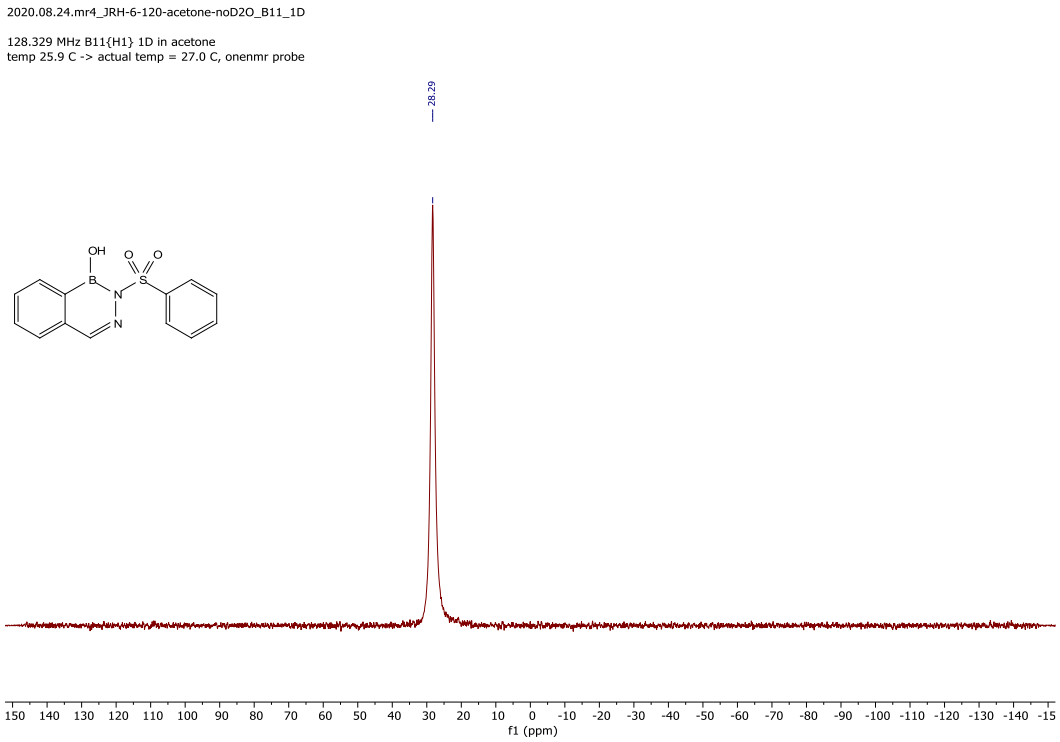

^{1}H (400 MHz), ^{13}C (176 MHz), ^{11}B (128 MHz) and ^{19}F (376 MHz) NMR of compound 3-34 (*d*$_6$-acetone)

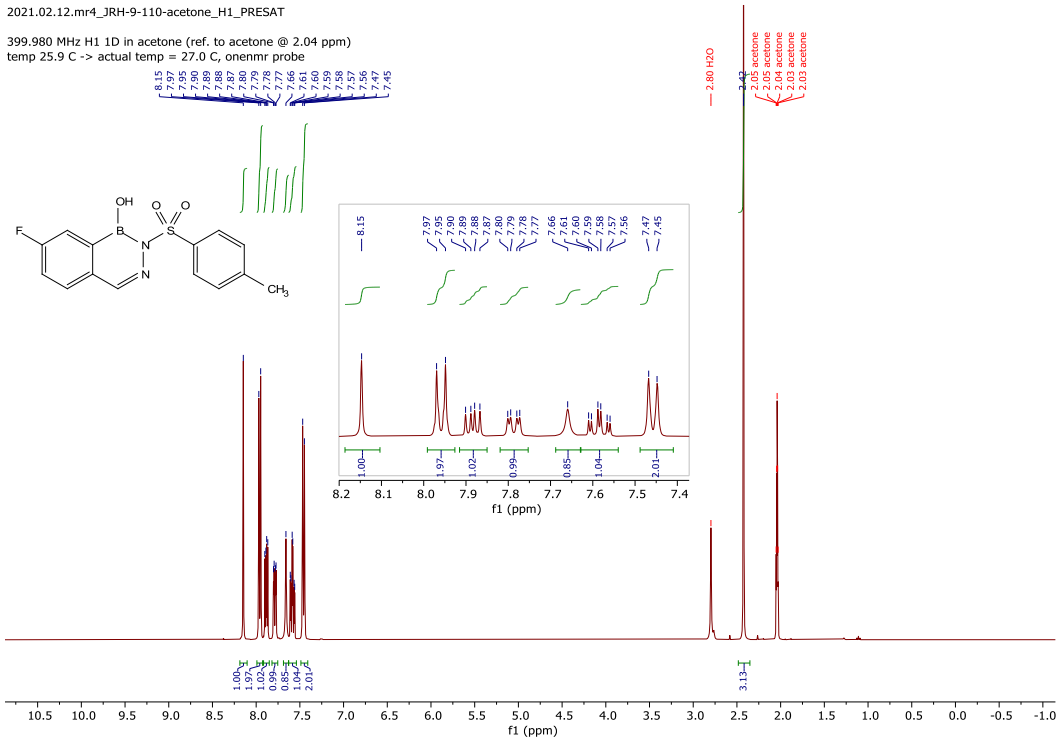

2021.02.12.v7_JRH-9-110-acetone_loc25_10.53_C13_1D
Jason, JRH-9-110-acetone
175.972 MHz C13{H1} 1D in acetone (ref. to acetone @ 29.8 ppm)
temp 27.5 C -> actual temp = 27.0 C, coldid probe

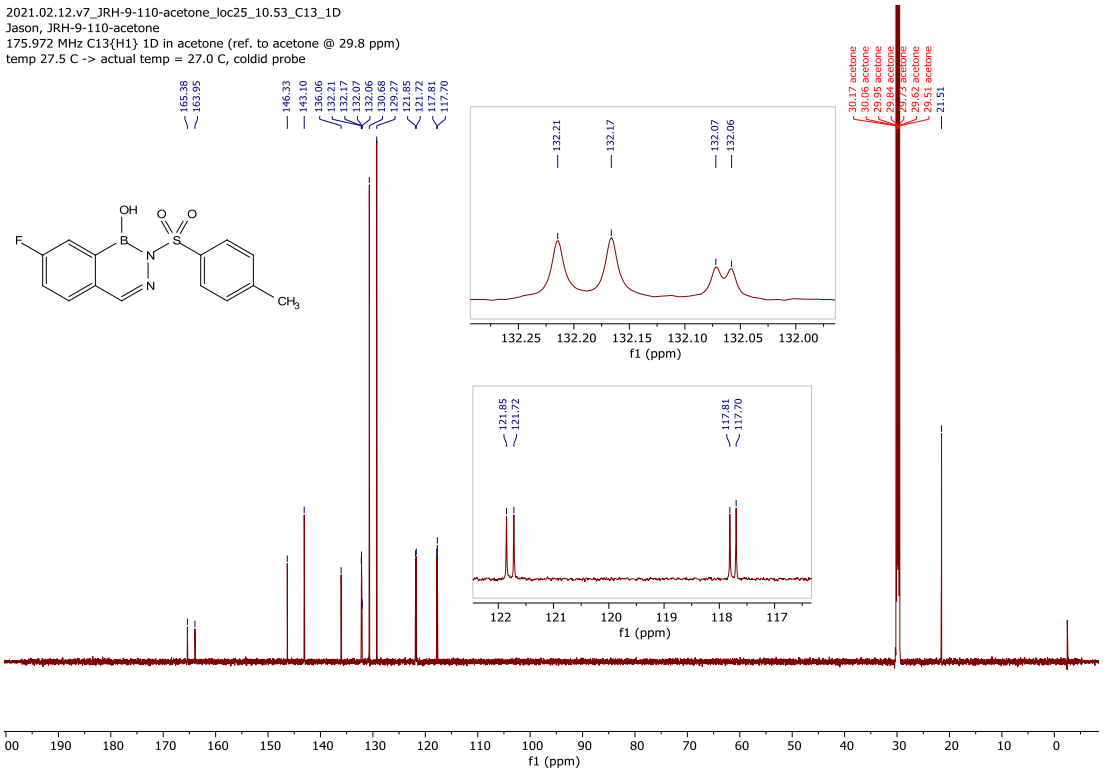

2021.02.12.mr4_JRH-9-110-acetone_B11_1D

128.329 MHz B11{H1} 1D in acetone
temp 25.9 C -> actual temp = 27.0 C, onenmr probe

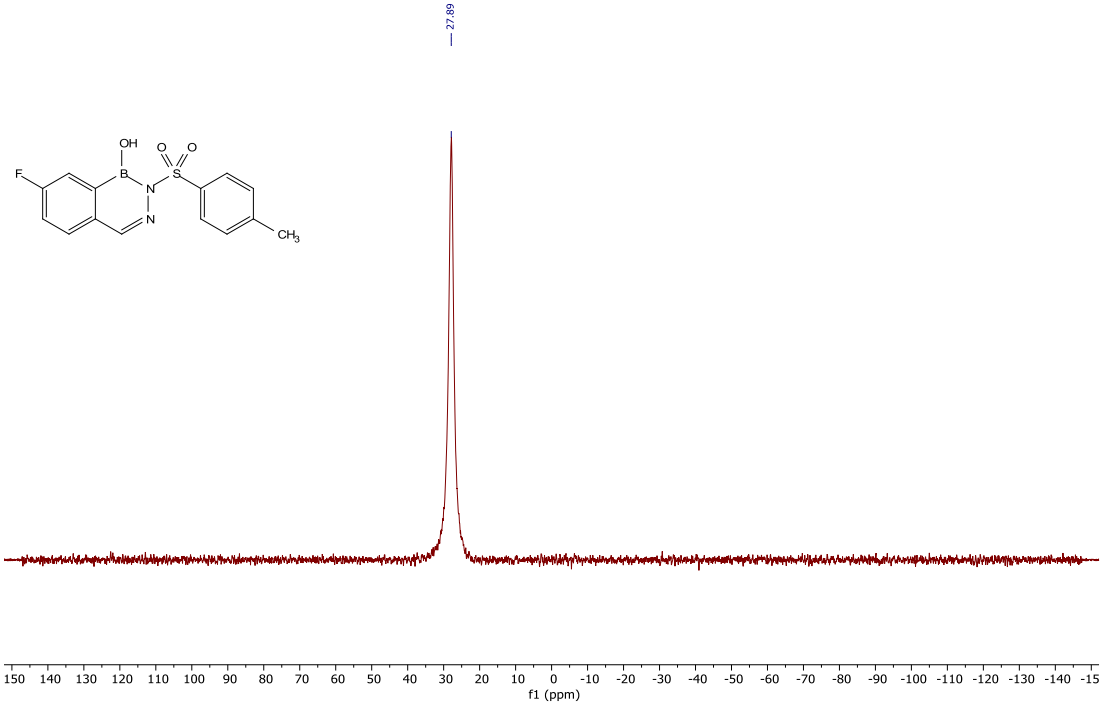

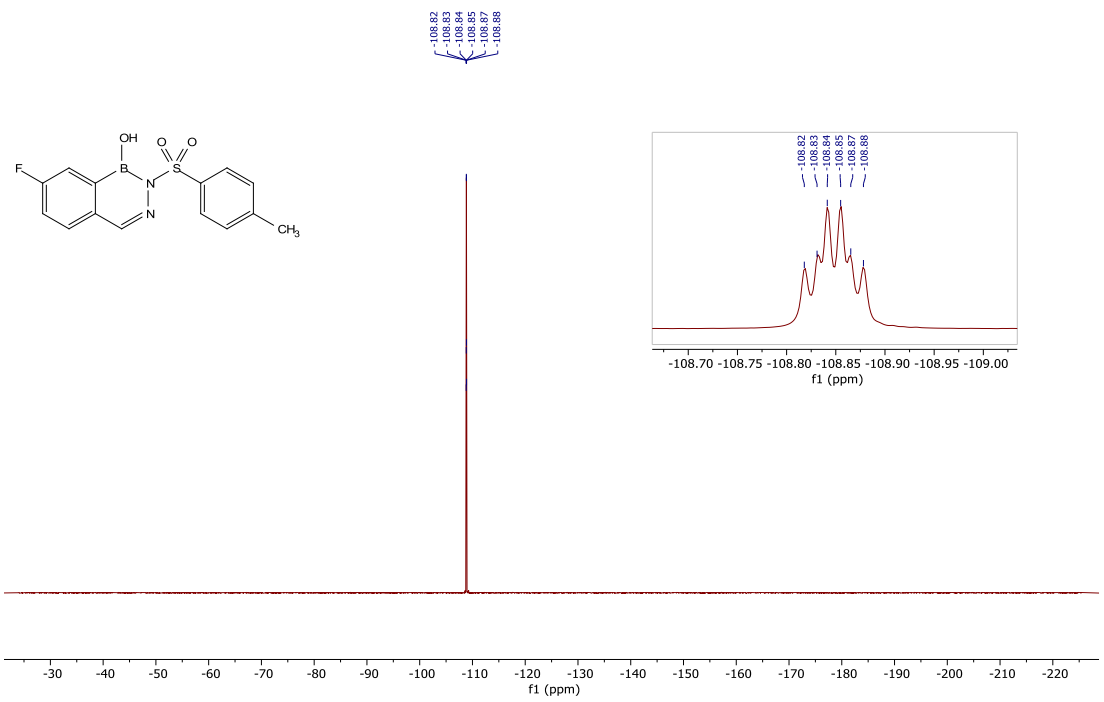

^{1}H (700 MHz), ^{13}C (176 MHz) and ^{11}B (128 MHz) NMR of compound 3-26 (*d*$_6$-acetone)

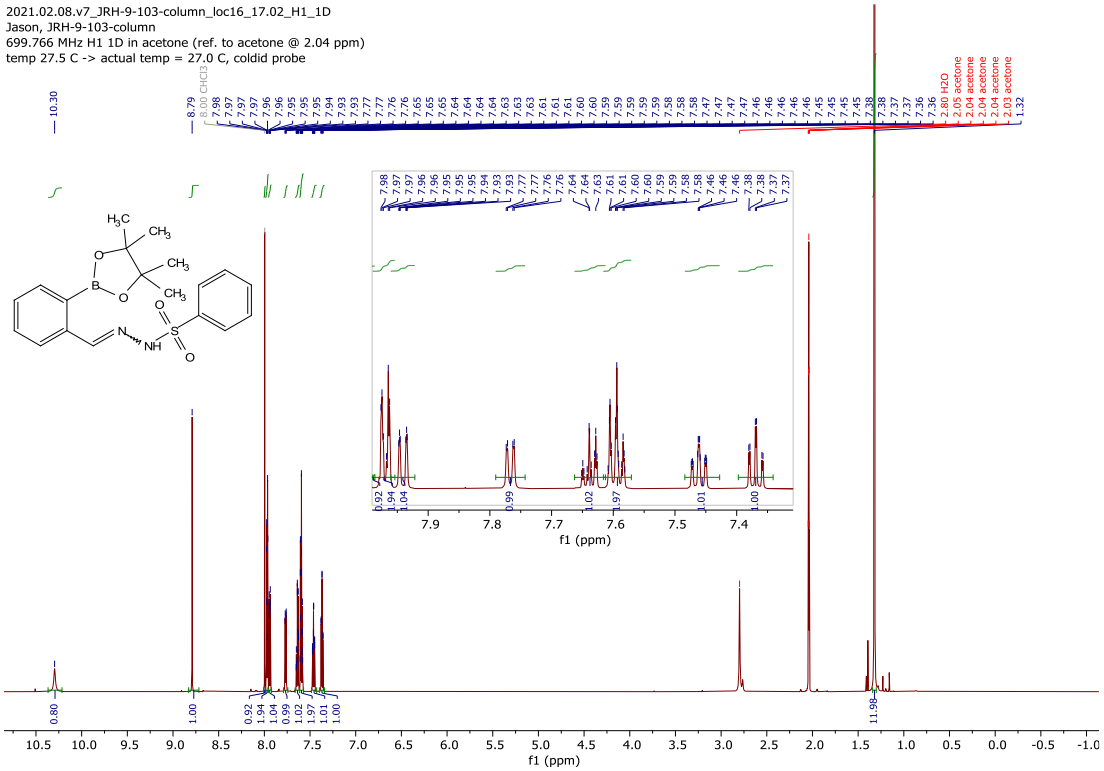

2021.02.08.v7_JRH-9-103-column_loc16_17.04_C13_1D
Jason, JRH-9-103-column
175.972 MHz C13{H1} 1D in acetone (ref. to acetone @ 29.8 ppm)
temp 27.5 C -> actual temp = 27.0 C, coldid probe

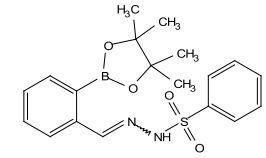

2021.02.08.mr4_JRH-9-103-column_B11_1D

128.329 MHz B11{H1} 1D in acetone
temp 25.9 C -> actual temp = 27.0 C, onenmr probe

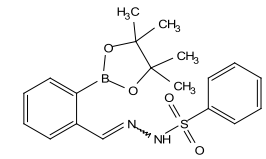

^{1}H (500 MHz), ^{13}C (126 MHz) and ^{19}F (376 MHz) NMR of compound 4-15c ($CDCl_3$)

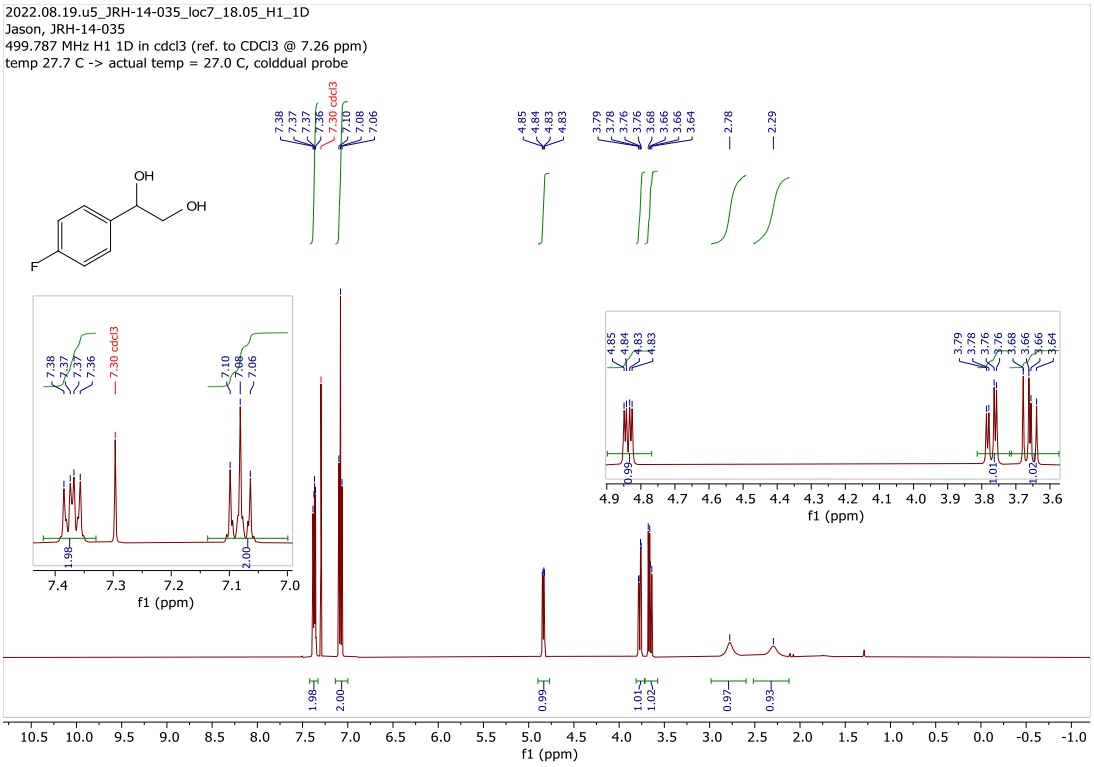

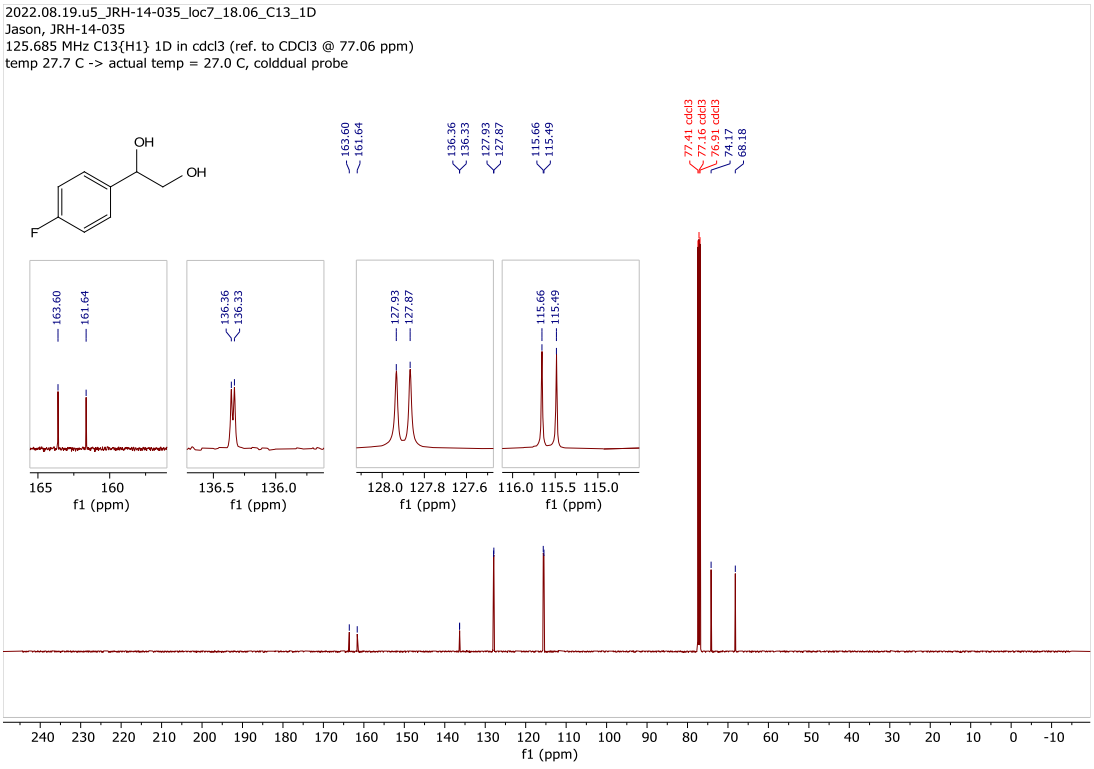

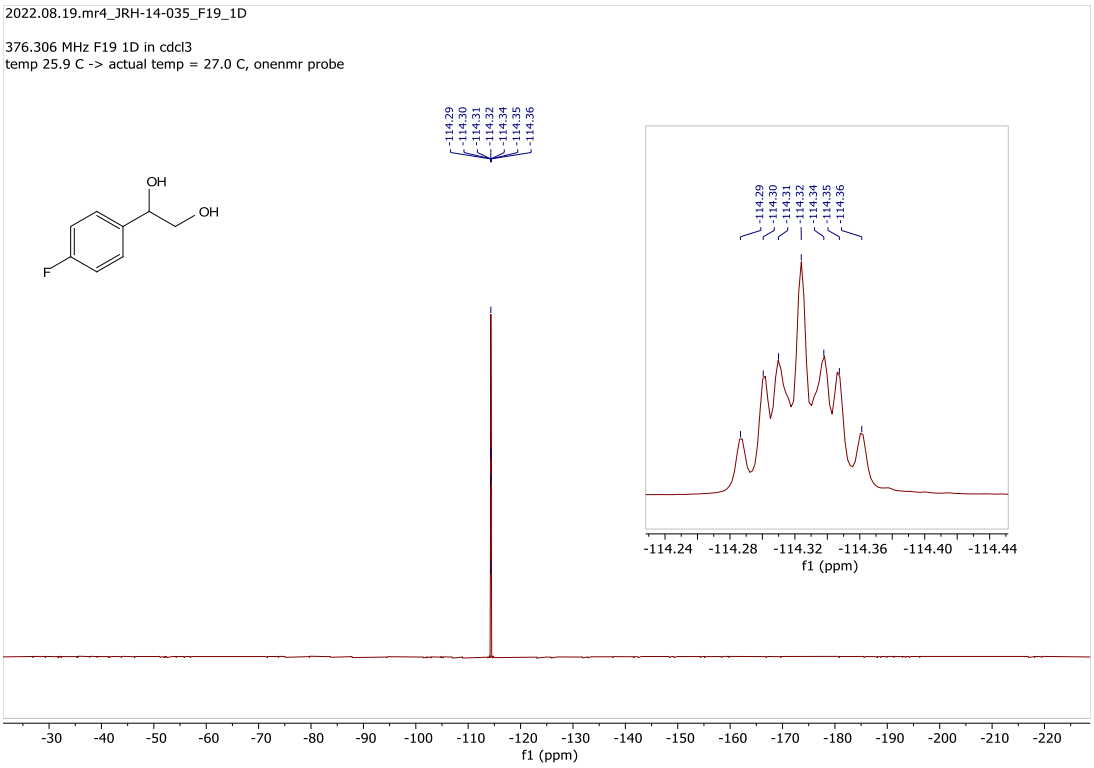

^{1}H (500 MHz), ^{13}C (126 MHz) and ^{31}P (162 MHz) NMR of compound 4-19a ($CDCl_3$)

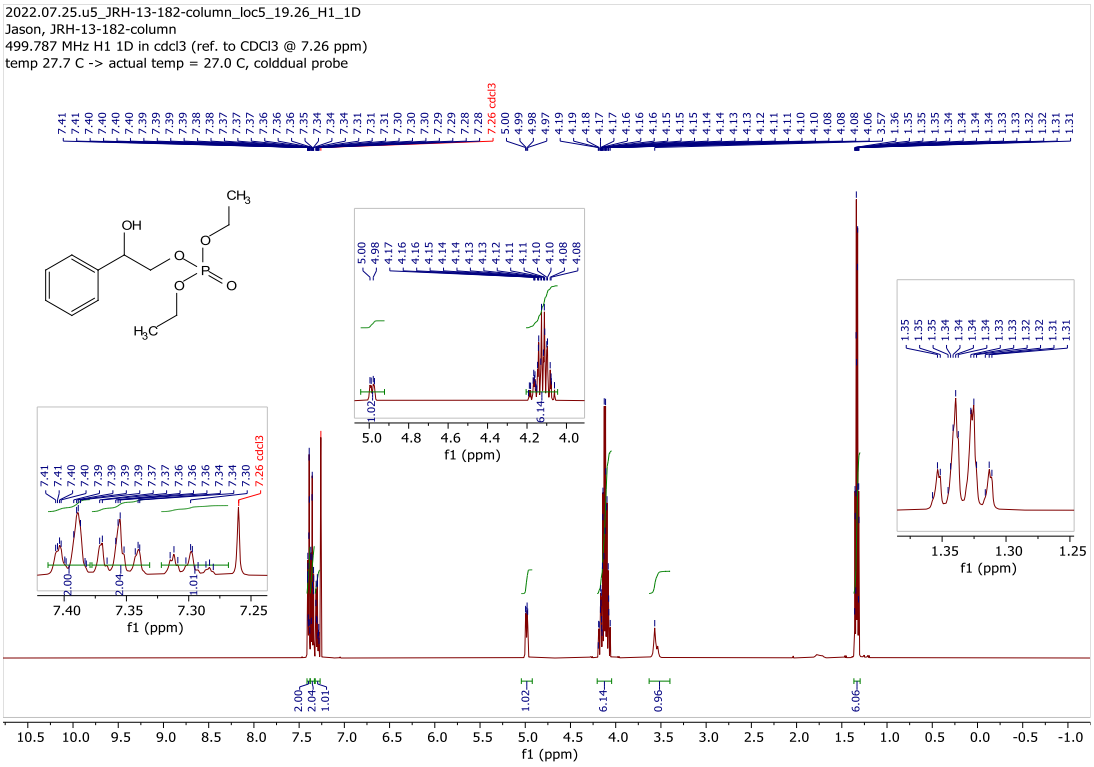

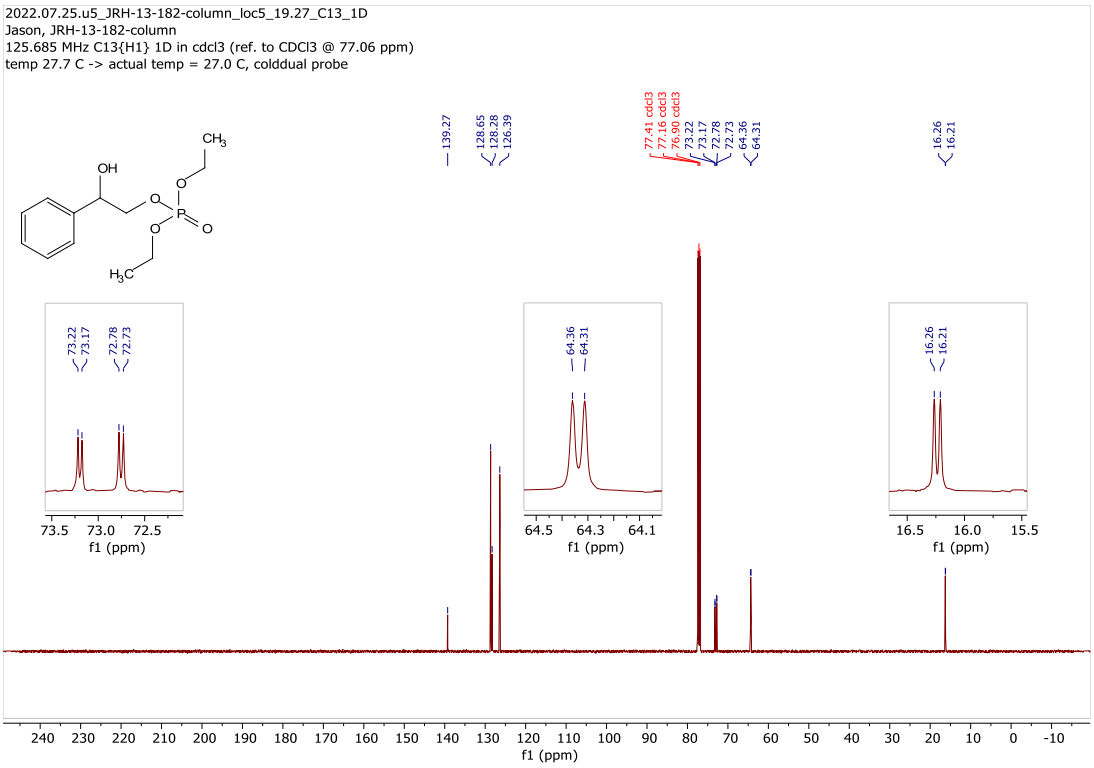
2022.07.25.u5_JRH-13-182-column_loc5_19.27_C13_1D
Jason, JRH-13-182-column
125.685 MHz C13{H1} 1D in cdcl3 (ref. to CDCl3 @ 77.06 ppm)
temp 27.7 C -> actual temp = 27.0 C, colddual probe
139.27
128.65
128.28
126.39
77.41 cdcl3
77.16 cdcl3
76.90 cdcl3
73.22
73.17
72.78
72.73
64.36
64.31
16.26
16.21
f1 (ppm)

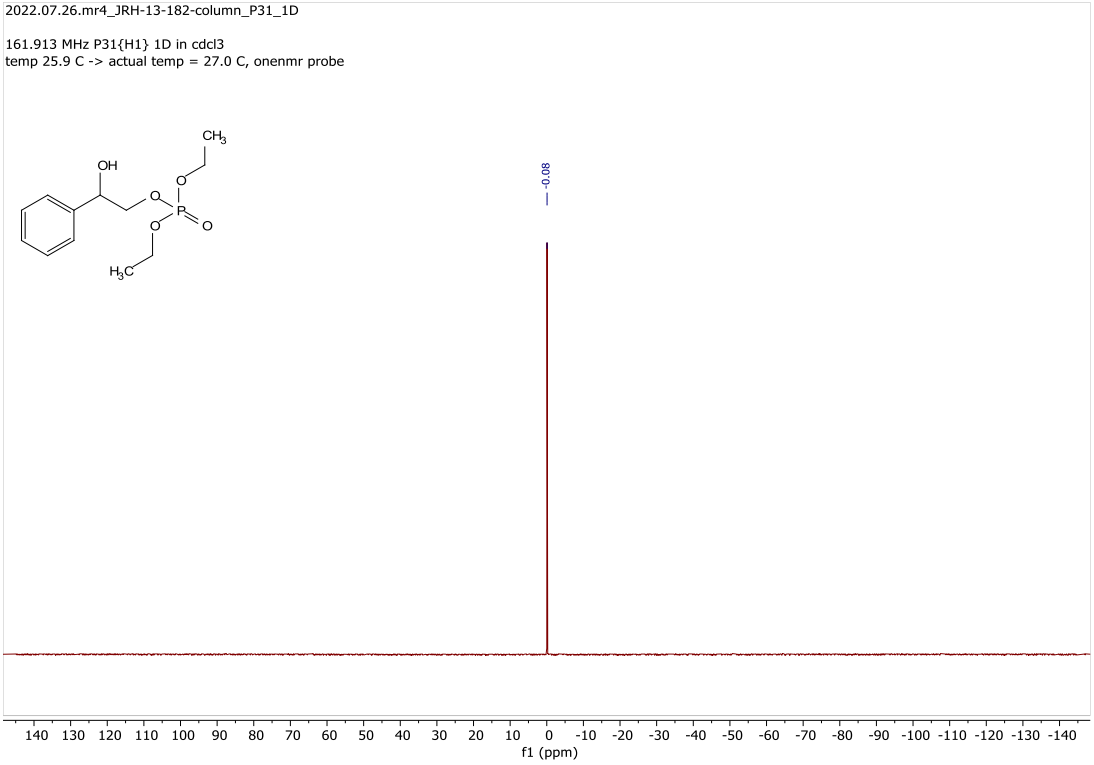
2022.07.26.mr4_JRH-13-182-column_P31_1D
161.913 MHz P31{H1} 1D in cdcl3
temp 25.9 C -> actual temp = 27.0 C, onenmr probe
-0.08
f1 (ppm)

^{1}H (500 MHz), ^{13}C (126 MHz) and ^{11}B (128 MHz) NMR of compound 4-30 (D_2O)

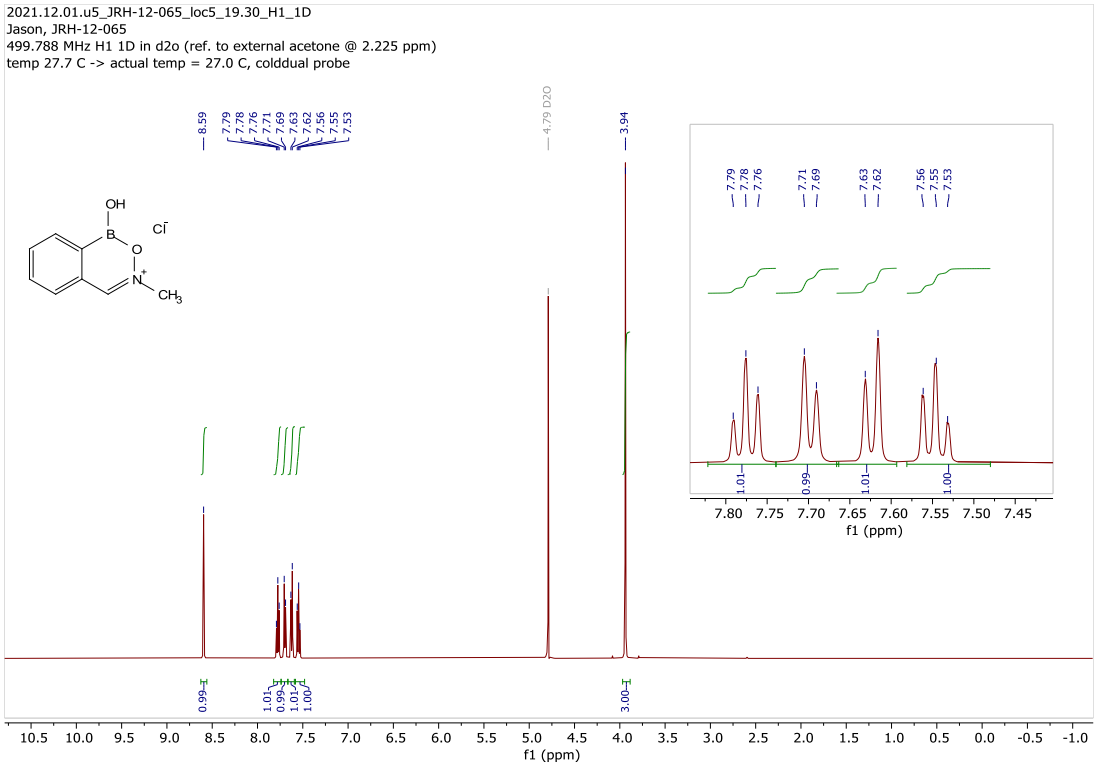

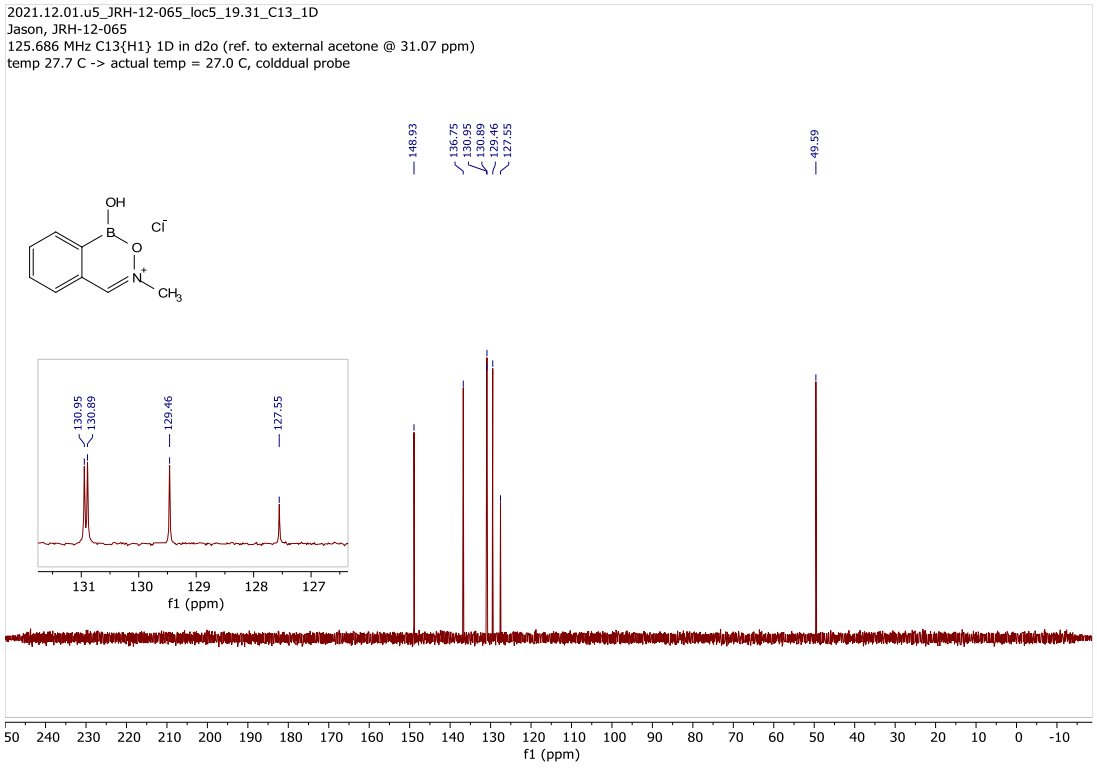

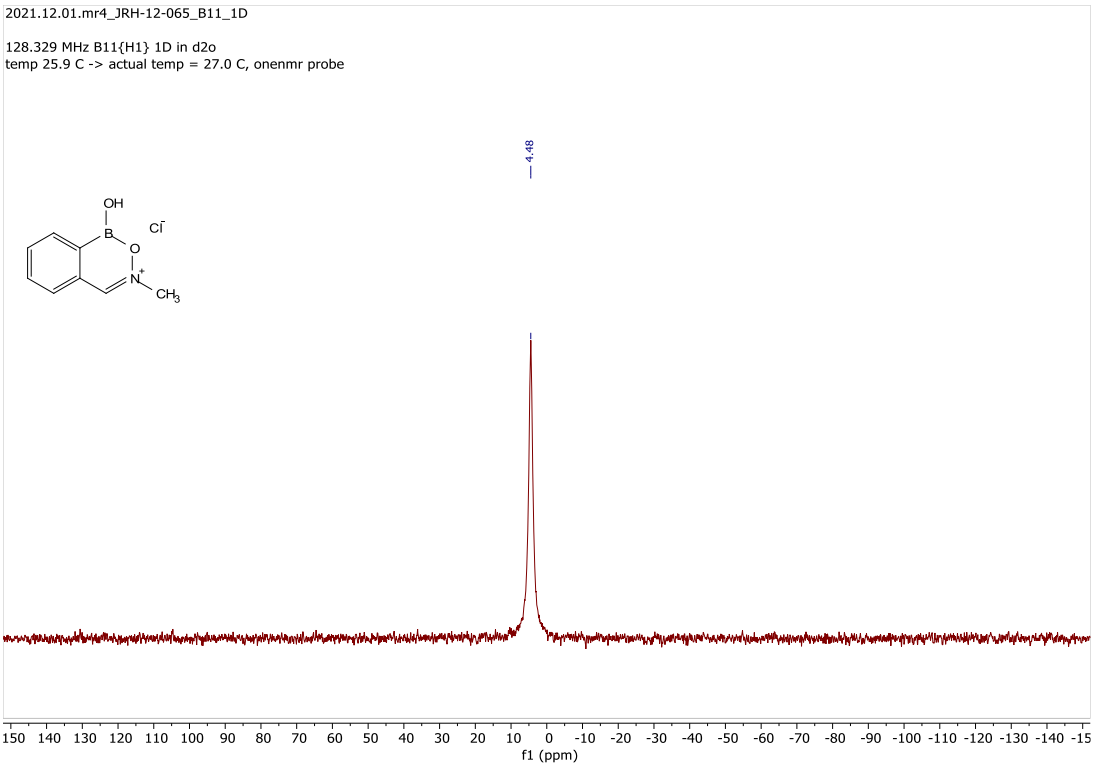

^{1}H (600 MHz) and ^{13}C (151 MHz) NMR of compound 4-31s ($CDCl_3$)

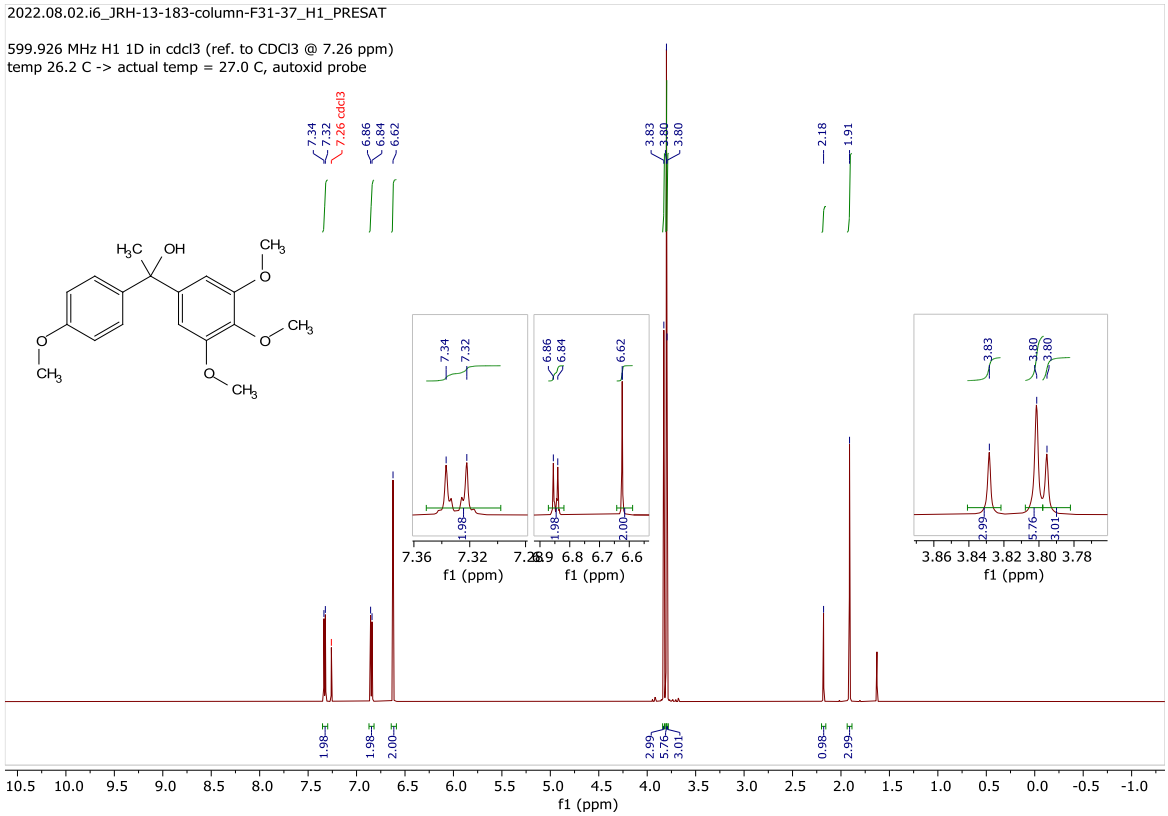

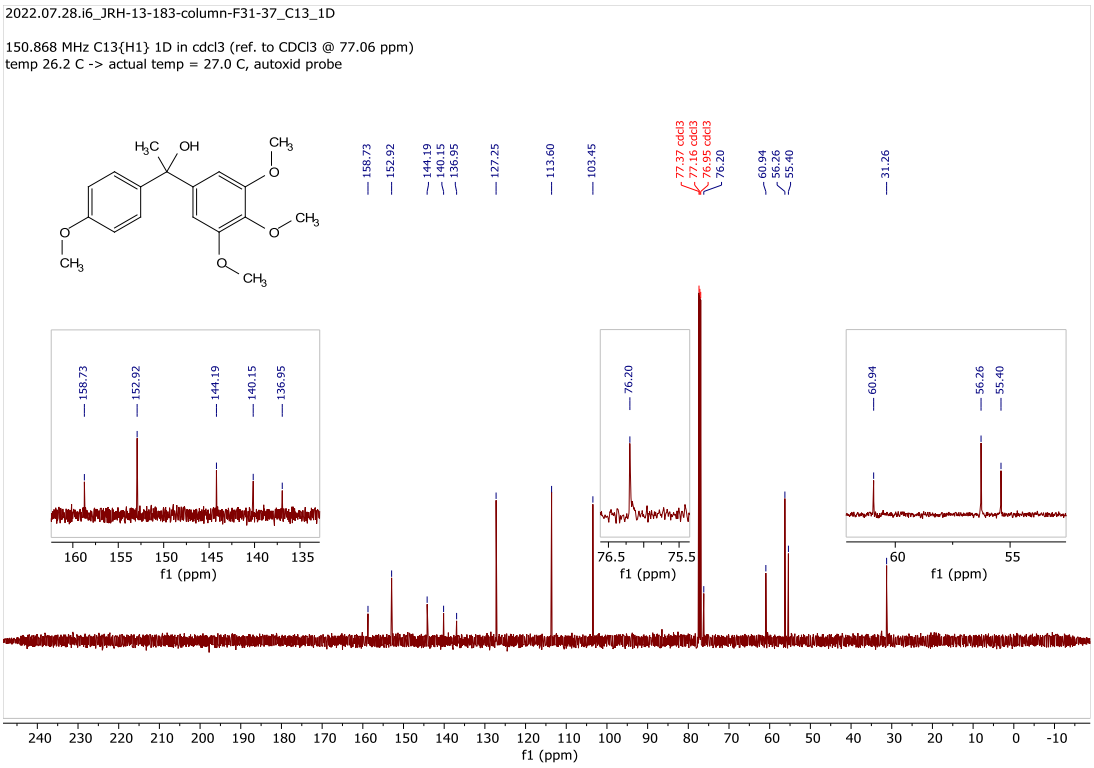

^{1}H (600 MHz) and ^{13}C (151 MHz) NMR of compound 4-32s ($CDCl_3$)

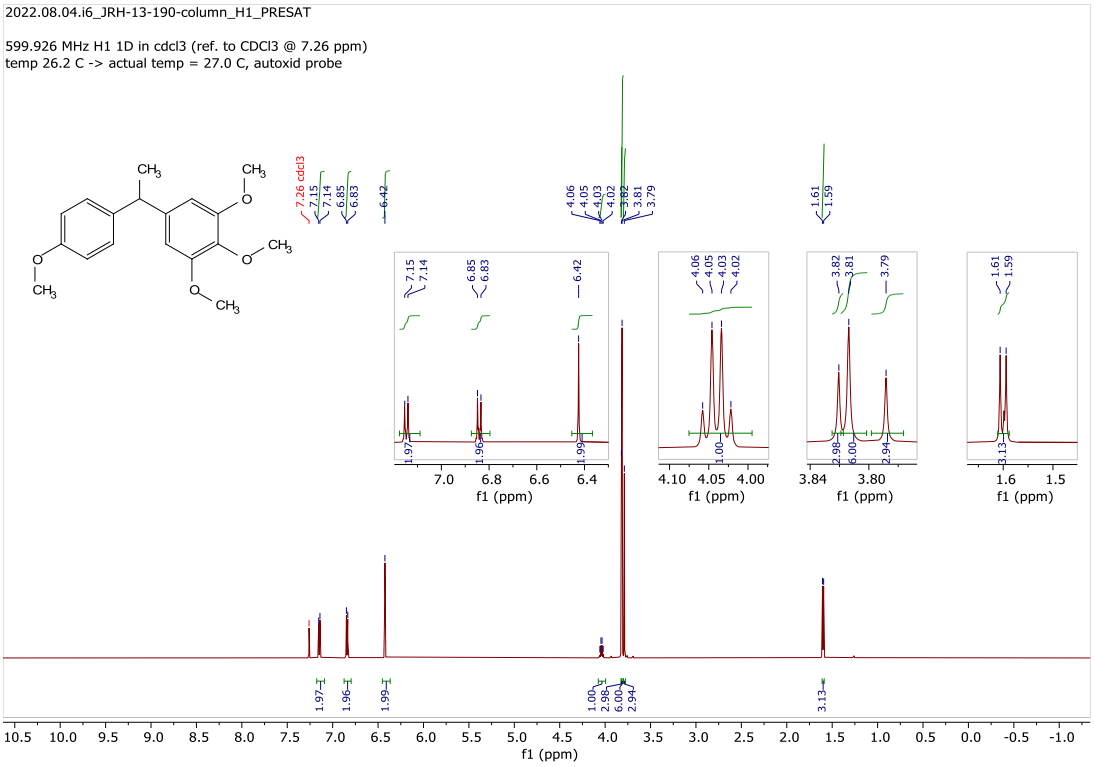

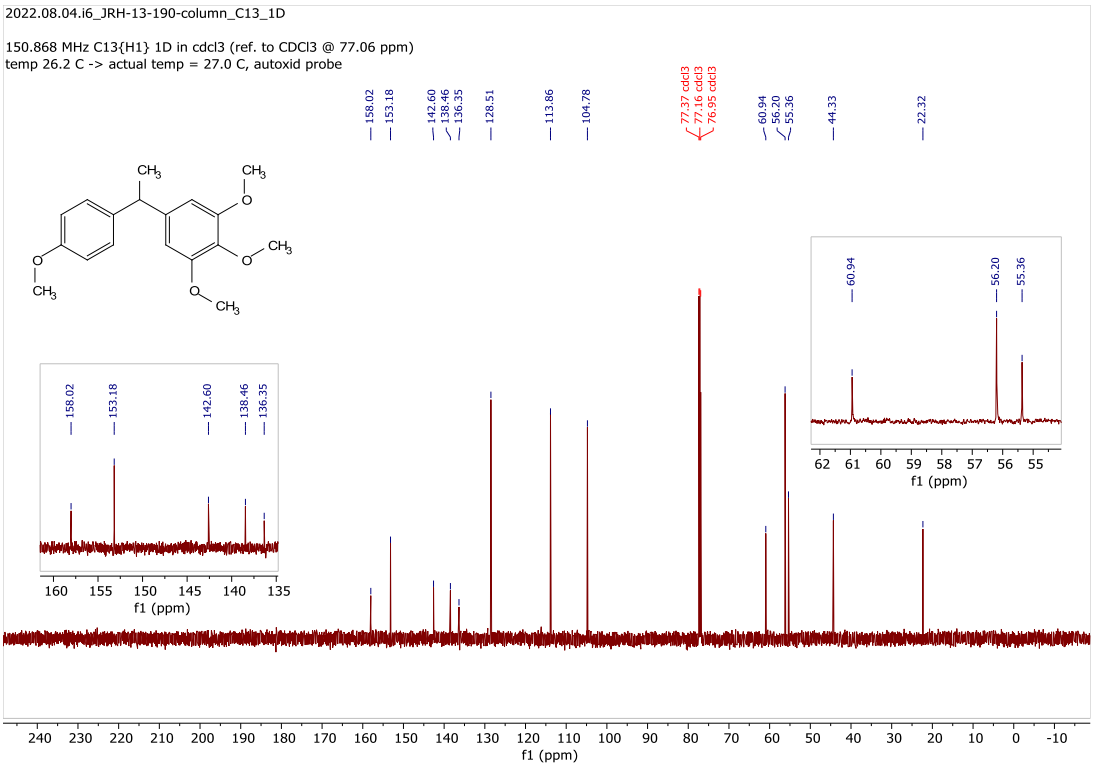

^{1}H (500 MHz) and ^{13}C (126 MHz) NMR of compound 4-32t ($CDCl_3$)

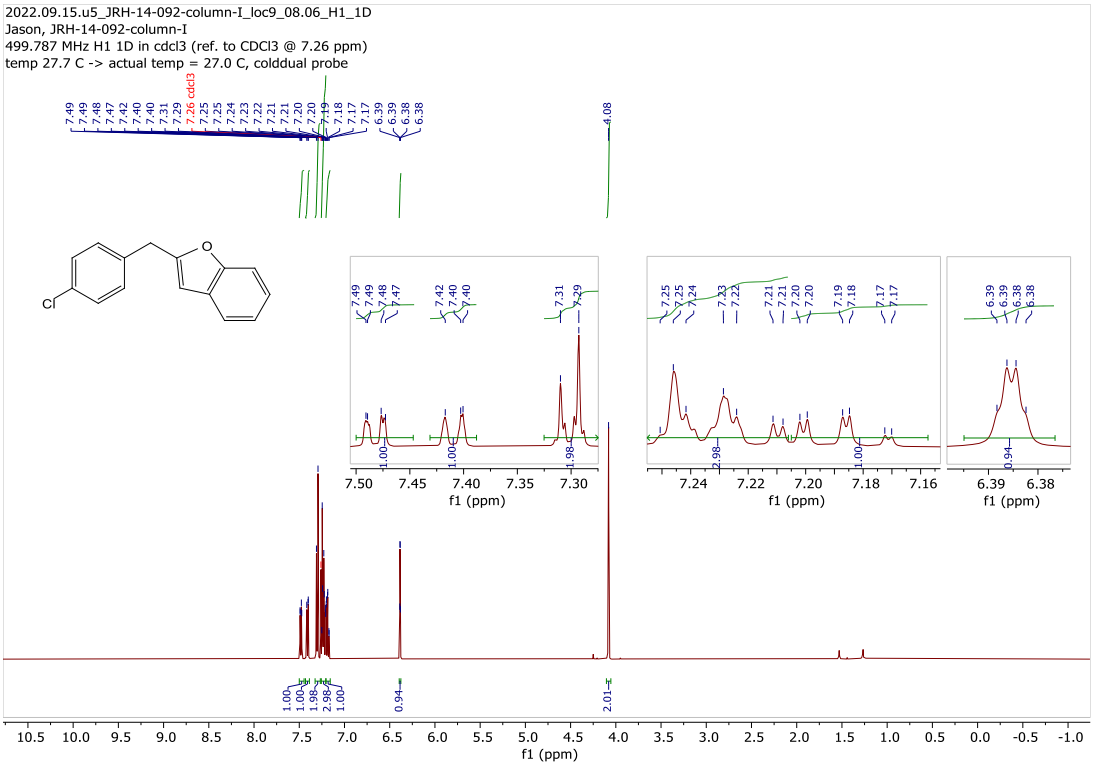

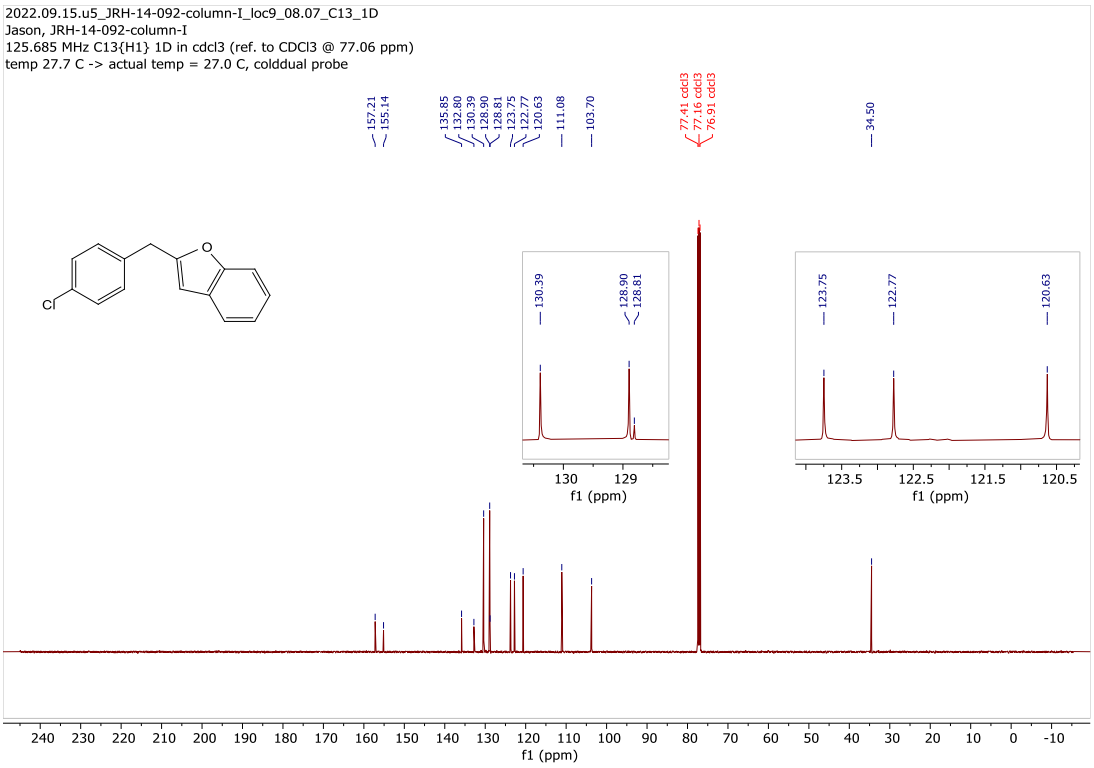

^{1}H (600 MHz) and ^{13}C (151 MHz) NMR of compound 4-32ai

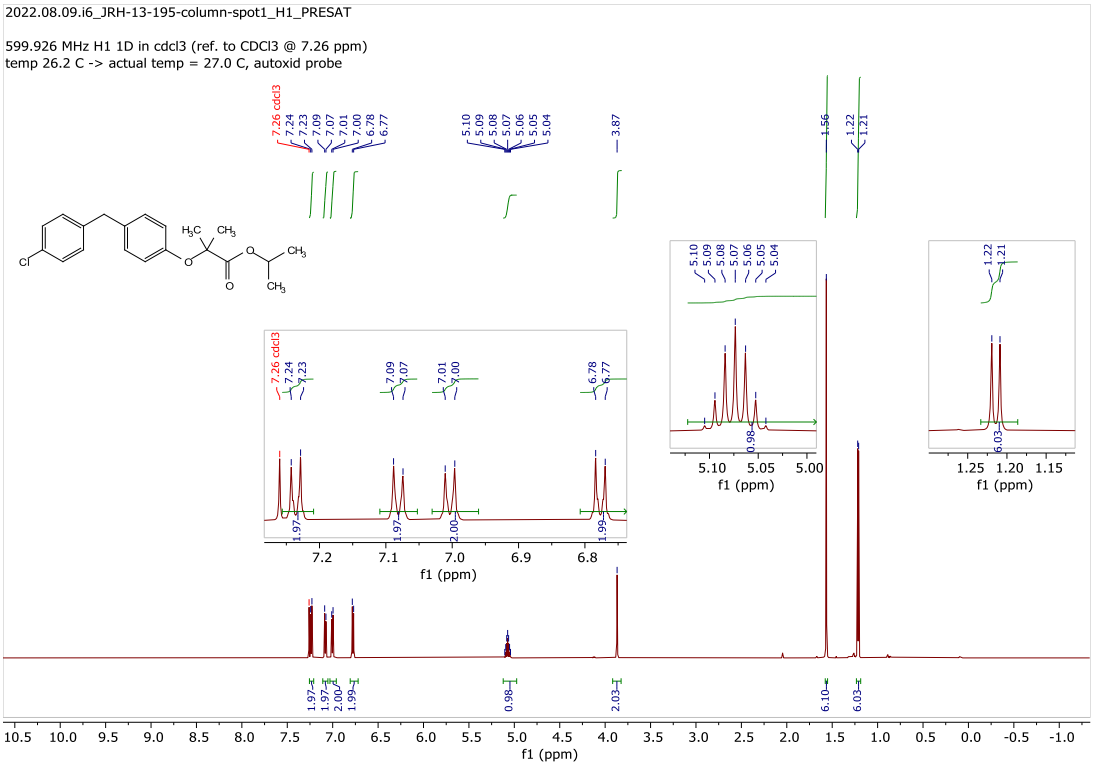

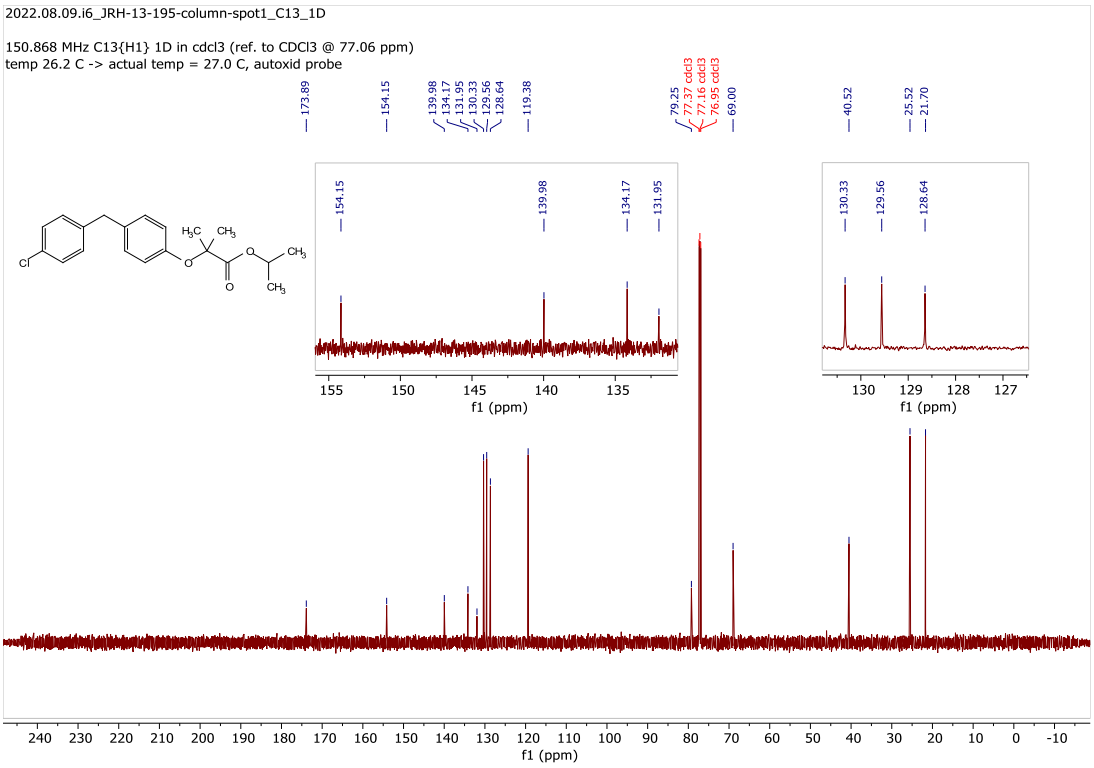

^{1}H (500 MHz) and ^{13}C (126 MHz) NMR of compound 4-39 ($CDCl_3$)

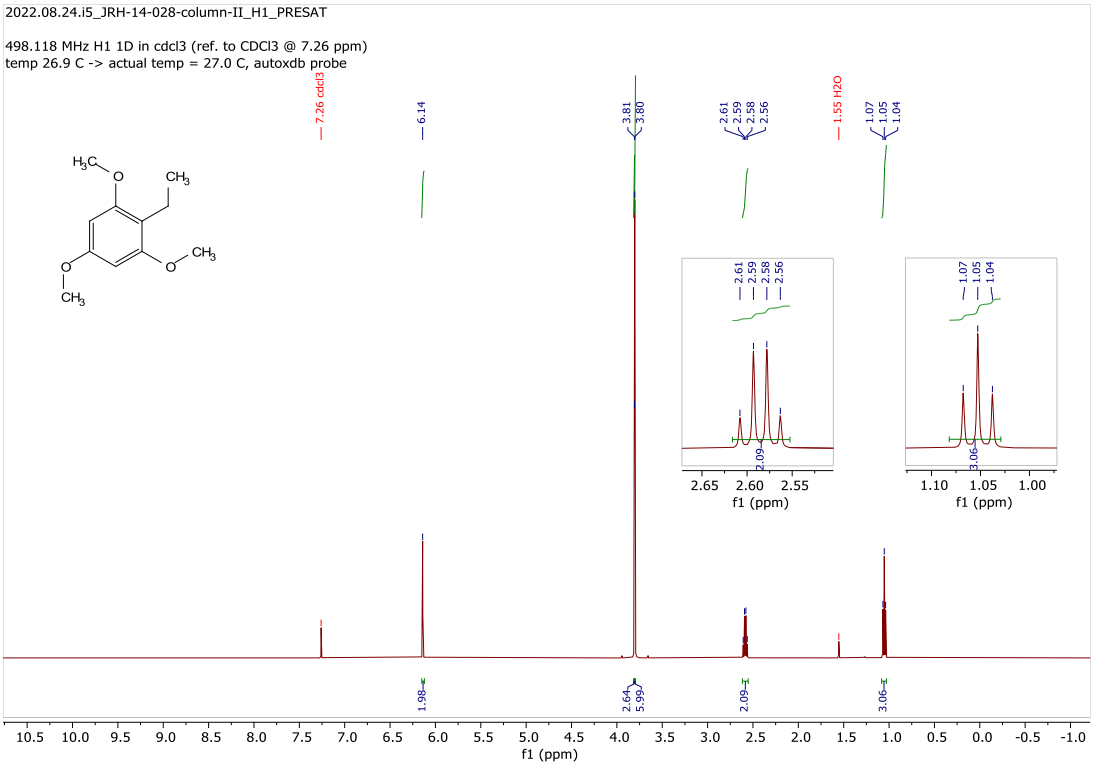

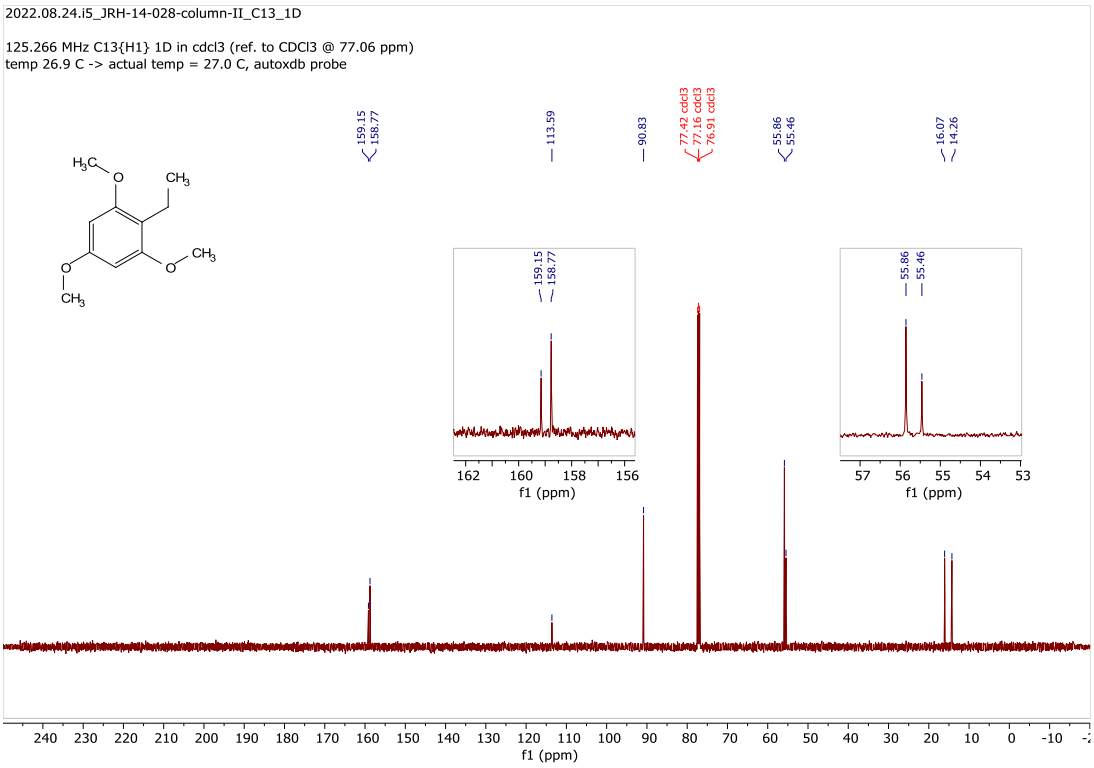

^{1}H (500 MHz) and ^{13}C (126 MHz) NMR of compound 4-43 ($CDCl_3$)

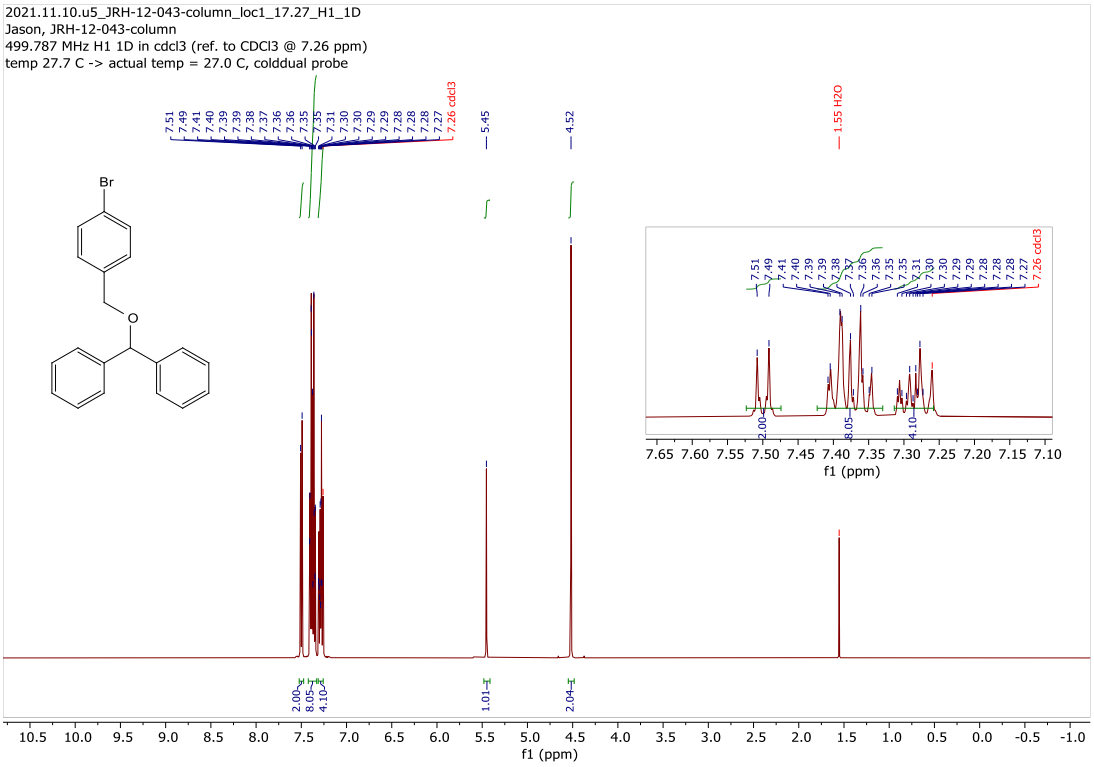

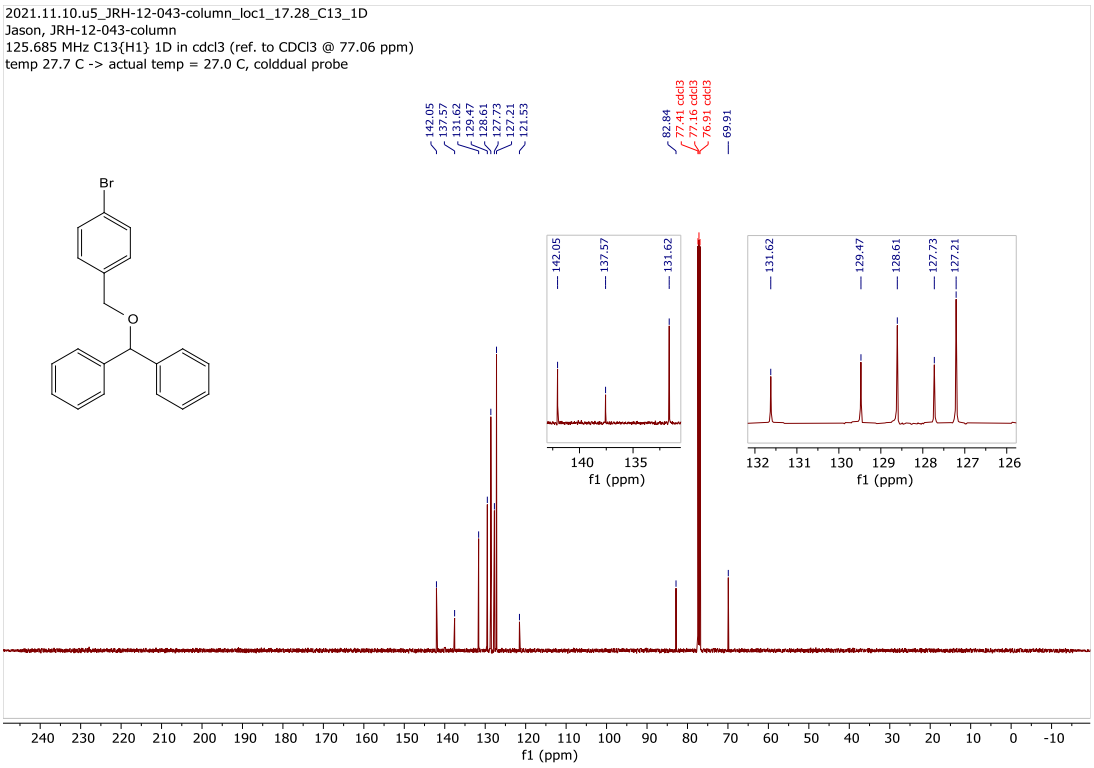

^{1}H (500 MHz), ^{13}C (126 MHz), ^{11}B (128 MHz) and ^{19}F (376 MHz) NMR of compound 4-48 (CD_3CN)

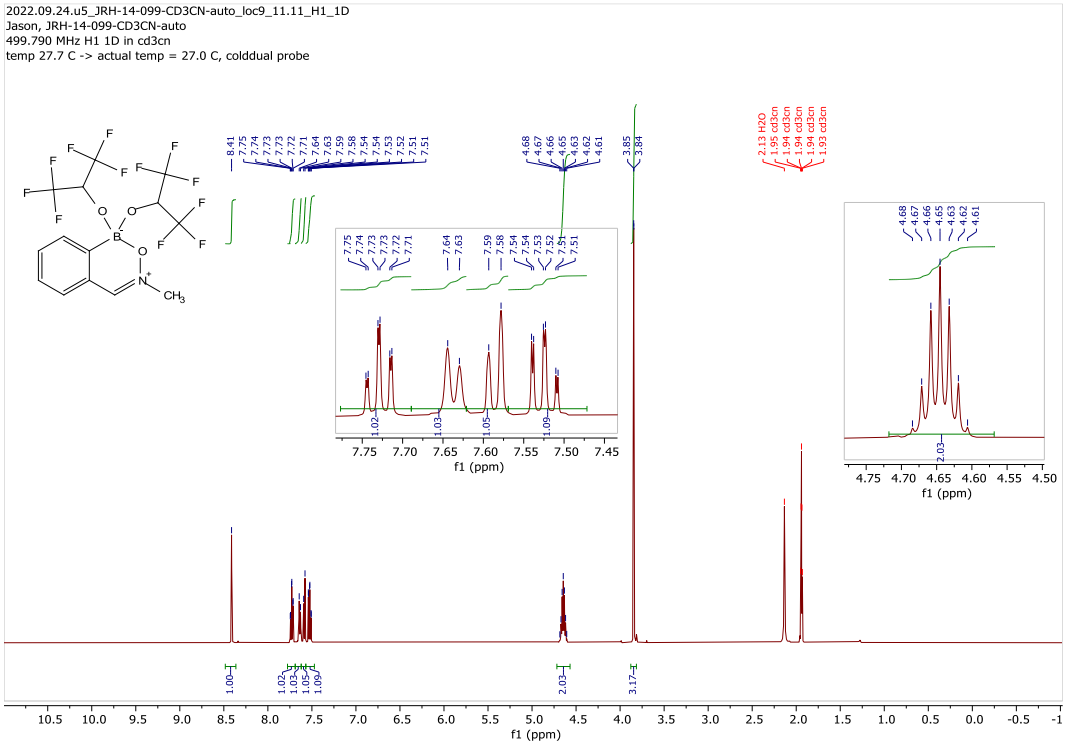

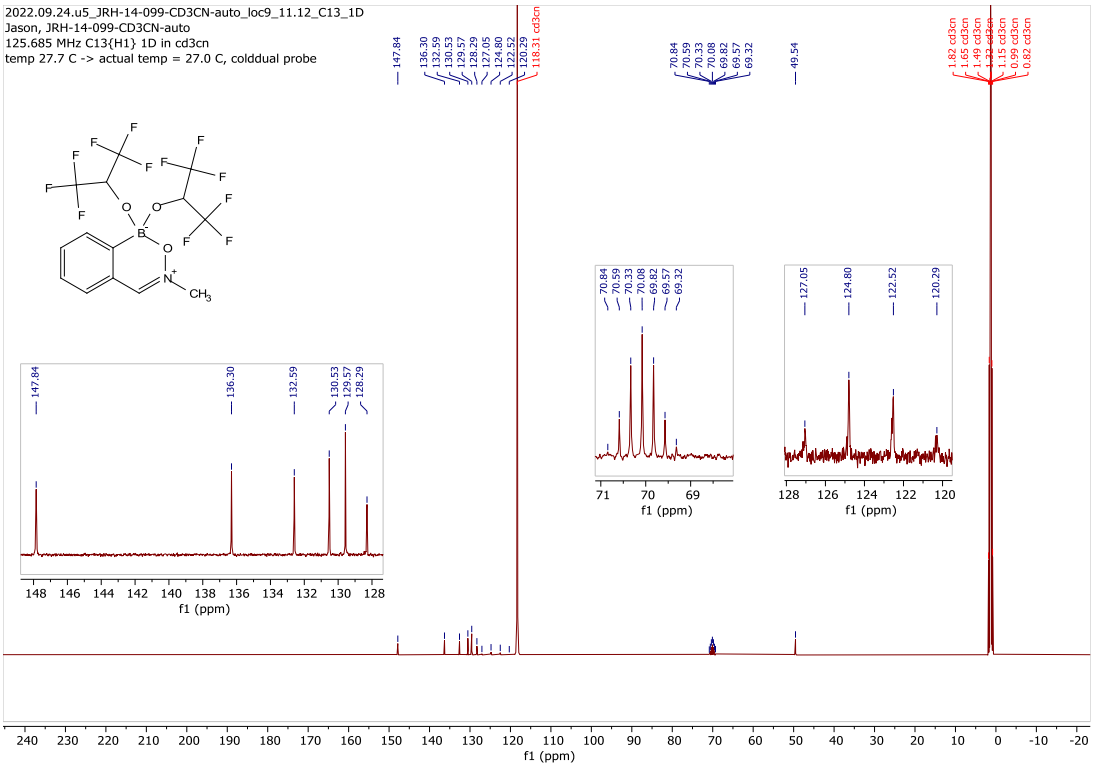
2022.09.24.u5_JRH-14-099-CD3CN-auto_loc9_11.12_C13_1D
Jason, JRH-14-099-CD3CN-auto
125.685 MHz C13{H1} 1D in cd3cn
temp 27.7 C -> actual temp = 27.0 C, colddual probe
147.84
136.30
132.59
130.53
129.57
128.29
127.05
124.80
122.52
120.29
118.31 cd3cn
70.84
70.59
70.33
70.08
69.82
69.57
69.32
49.54
1.82 cd3cn
1.65 cd3cn
1.49 cd3cn
1.32 cd3cn
1.15 cd3cn
0.99 cd3cn
0.82 cd3cn
f1 (ppm)

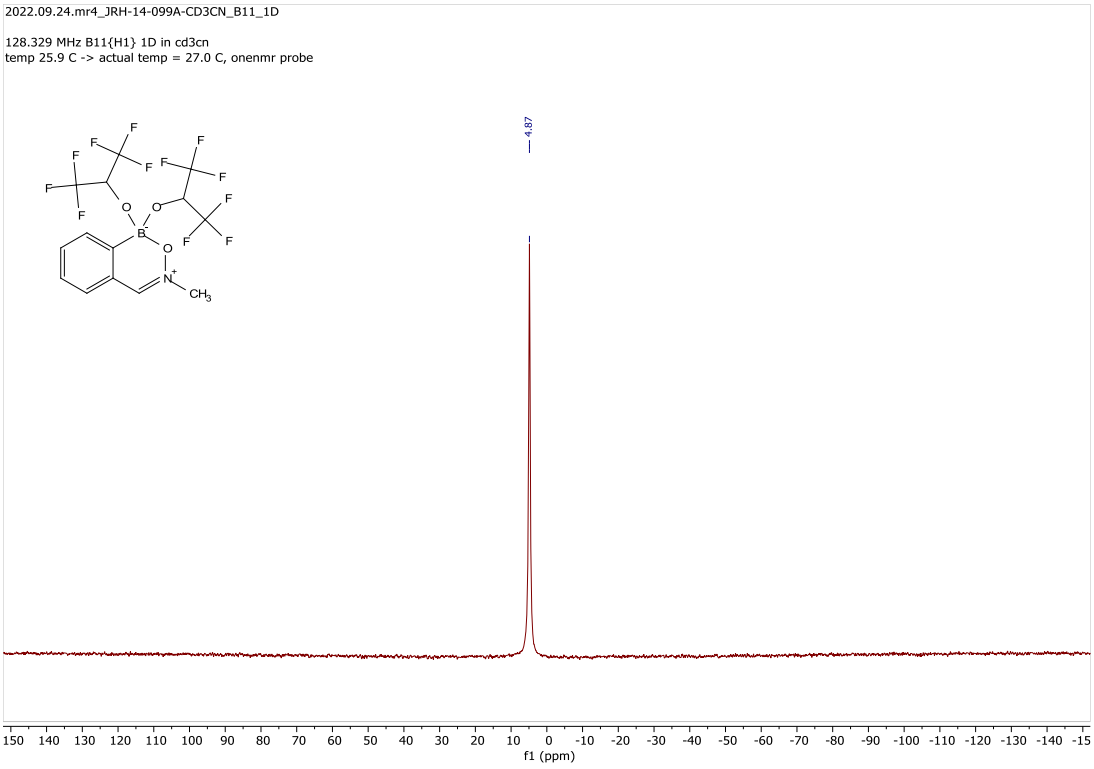
2022.09.24.mr4_JRH-14-099A-CD3CN_B11_1D
128.329 MHz B11{H1} 1D in cd3cn
temp 25.9 C -> actual temp = 27.0 C, onenmr probe
4.87
f1 (ppm)

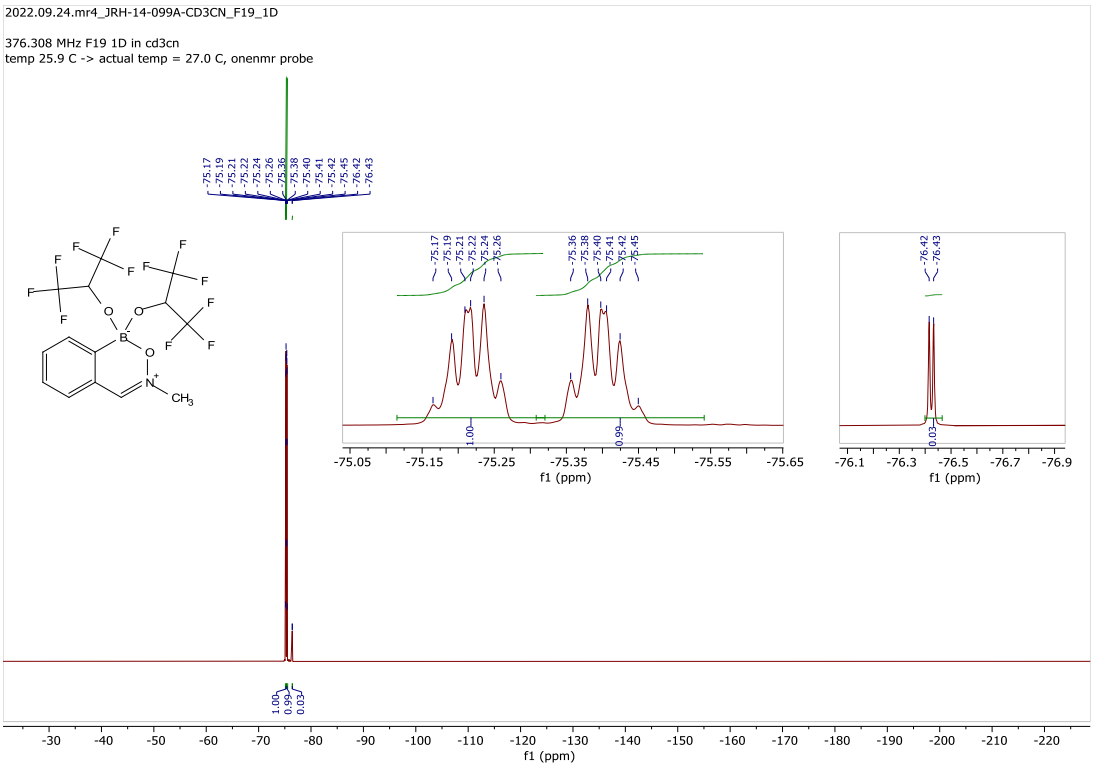
2022.09.24.mr4_JRH-14-099A-CD3CN_F19_1D
376.308 MHz F19 1D in cd3cn
temp 25.9 C -> actual temp = 27.0 C, onenmr probe
-75.17
-75.19
-75.21
-75.22
-75.24
-75.26
-75.36
-75.38
-75.40
-75.41
-75.42
-75.45
-76.42
-76.43
1.00
0.99
0.03
f1 (ppm)

Appendix 2: X-ray Crystallography Report

X-ray Structure Report of Compound 4-48

CCDC 2210073 (compound **4-48**) contains the supplementary crystallographic data for this thesis. This data can be obtained free of charge from the Cambridge Crystallographic Data Center.

XCL Code: DGH2206 **Date:** 23 September 2022

Compound: 1,1-bis[(1,1,1,3,3,3-hexafluoropropan-2-yl)oxy]-3-methyl-1*H*-2,3,1-benzoxazaborinin-1-uide

Formula: $C_{14}H_{10}BF_{12}NO_3$

Supervisor: D. G. Hall **Crystallographer:** M. J. Ferguson

Perspective view of the 1,1-bis[(1,1,1,3,3,3-hexafluoropropan-2-yl)oxy]-3-methyl-1*H*-2,3,1-benzoxazaborinin-1-uide molecule showing the atom labelling scheme. Non-hydrogen atoms are represented by Gaussian ellipsoids at the 30% probability level. Hydrogen atoms are shown with arbitrarily small thermal parameters.